Development and Application of Advanced Mass Spectrometry Techniques for Determination of Reactive Aerosol Constituents

by

Tania Gautam

A thesis submitted in partial fulfillment of the requirements for the degree of

Doctor of Philosophy

Department of Chemistry
University of Alberta

Abstract

Reactive aerosol constituents, including organic peroxides (H_2O_2, ROOR and ROOH), organosulfates (OS), and organonitrates (ON), are integral components of atmospheric chemistry, climate dynamics, and human health. However, their intricate chemical compositions and dynamic behaviours present formidable challenges for accurate identification and quantification. These reactive species emerge from complex photochemical reactions involving volatile organic compounds (VOCs), nitrogen oxides (NO_x), and various other precursors emitted from both biogenic and anthropogenic sources. Peroxides, as reactive oxygen species, significantly contribute to respiratory illnesses, while OS and ON, derivatives of sulfur and nitrate species, influence climate dynamics by altering water uptake properties and facilitating cloud formation. Collectively, these reactive aerosol constituents exacerbate air quality issues by promoting the formation of secondary organic aerosols (SOA) and imposing health burdens on human populations. Despite extensive research, several aspects of their formation, transformation, and atmospheric fate remain ambiguous. Challenges in their characterization stem from the lack of sensitive techniques offering molecular specificity, biases prone to matrix effects, and the chemical complexity arising from structural diversity. In this thesis, we employ advanced mass spectrometry techniques to delve into the fundamental mechanisms underlying the formation of peroxides in aqueous environments and to identify sulfur/nitrate enriched species in ambient samples under the influence of meteorological conditions.

Chapter 2 introduces a novel pathway to investigate the occurrence of aqueous-phase autoxidation as a crucial reaction mechanism facilitating the formation of hydroper-

oxides (ROOHs). Leveraging linear unsaturated organic acids, a selective chemical-assay assisted (i.e., iodometry) liquid chromatography-mass spectroscopy (LC-MS) technique is utilized to systematically study the formation of highly oxygenated molecules (HOMs) containing up to two - OOH groups. The empirical dependence of these ROOHs on wavelengths (UVA, UVB and UVC) and oxidant/precursor concentrations is explored to discern the conditions favourable to their formation. While our findings support the feasibility of aqueous ROOHs from various water-soluble organic precursors, distinguishing the specific mechanism solely from offline iodometry-assisted LC-MS technique remains challenging due to lack of online measurements for rapid formation of intermediate compounds.

In Chapter 3, I have investigated the experimental limits of the conventional iodometry method, which is known to undergo interferences from reducing agents such as olefins. This halogen chemistry has been widely used in food chemistry to determine the degree of unsaturation. Our results show that linear unsaturated compounds can react with halogen species such as I_2 - a key intermediate in iodometry. However, this underestimation in peroxide content will occur during extended periods of bench reaction and relatively higher concentrations (>500 μM) of olefinic compounds. I have determined that in the case of atmospheric samples including complex mixtures of SOA, it is unlikely that olefinic concentrations will reach the level of causing interference with the conventional iodometry approach.

In Chapter 4, I have adopted a broader approach to understanding the role of ROS and sulfate/nitrate enriched particle-bound species in ambient aerosol samples. Compared to separation-based techniques utilized in Chapters 2 and 3, here I have adopted a far more robust analytical approach, i.e., nano-DESI-HRMS. Through this study, I have determined that sulfate/nitrate enriched species are more episodic during day-to-day comparisons, with meteorological factors such as wind direction playing a determining role in the emergence of OSs. Furthermore, photochemical processing may be alluding to the dominance of ONs. There could likely be potential CHO compounds with

peroxy functionality, however, the application of chemical derivatization techniques (e.g., iodometry) to resolve the molecular ambiguity is difficult in complex matrices with high salt concentrations.

Overall, this thesis adopts a complementary functional approach and robust analytical methodology to pursue investigation into elusive reactive aerosol constituents, thereby providing crucial insights into their formation and critical dependence on meteorological parameters.

Preface

Chapter 1 Introduction

Contributions: The conclusion was written by Tania Gautam with review and feedback by Dr. Ran Zhao.

Chapter 2

Photooxidation initiated aqueous-phase formation of organic peroxides: delving into formation mechanisms T. Gautam, E. Kim, L. Ng, V. Choudhary, J.Lima Amorim, M.Loebel Roson, R. Zhao,"Photooxidation initiated aqueous-phase formation of organic peroxides: delving into formation mechanisms," *Environmental Science & Technology*, vol 58, no. 15, pp: 6564-6574

Chapter 3

Potential matrix effects in iodometry determination of peroxides induced by olefins T. Gautam, S.Wu, J. Ma, R. Zhao,"Potential Matrix Effects in Iodometry Determination of Peroxides Induced by Olefins," *Journal of Physical Chemistry A*, vol 126, no.17, pp: 2632-2644, 2022

Chapter 4

Chemical insights into molecular composition of organic aerosols in the urban region of Houston, Texas T. Gautam, G.W. Vandergrift, N.N. Lata, Z. Cheng, A. Rahman, A. Minke, Z. Lai, D.N. Dexheimer, D. Zhang, M. A. Marcus, M. A. Zawadowicz, C. Kuang, R. Zhao, A.L. Steiner, S. China, "Chemical insights into molecular composition of organic aerosols in the urban region of Houston, Texas," *Environmental Science & Technology-Air*, Submitted December 22 2023

Chapter 5

Conclusions and Future Work

Contributions: The conclusion was written by Tania Gautam with review and feedback by Dr. Ran Zhao.

Acknowledgements

I am deeply grateful to my supervisor, Dr. Ran Zhao for their invaluable guidance, encouragement, and unwavering support throughout the journey of this thesis. Their expertise, patience, and constructive feedback have been instrumental in shaping the trajectory of my research and academic growth. I am truly fortunate to have had the opportunity to work under their mentorship.

I extend my heartfelt appreciation to the members of Zhao group members including former and current graduate/undergraduate researchers: Shuang Wu, Xinyang Guo, Shakiba Talebian, Amanda Hanashiro Moraes, Mst Rowshon Afroz, Anastasia Kim, Jessica Lima Amorim, Max Loebel Roson, Erica Kim, Lisa Ng, Vikram Choudhary and many more. I want to sincerely give gratitude to those who took part in this journey with me. Additionally, I want to express my gratitude to my best friend: I Teng Cheong, who was always willing to listen and support me throughout my undergraduate and graduate career.

I would also like to give special appreciation goes to Daniel R. Aldrich, whose expertise in LaTeX formatting streamlined the presentation of this thesis, enhancing its clarity and professionalism. I am indebted to the Department of Chemistry at University of Alberta for providing the resources and environment conducive to research and learning. Their ongoing support has been invaluable in facilitating this study. I extend my heartfelt thanks to the members of the research committee: Dr X. Chris Le, Dr. Gabriel Hanna and Dr. Sarah S. Styler for their valuable feedback and constructive criticism, which have played a crucial role in refining this work and pushing it to new heights.

Finally, I would like to express my deepest gratitude to my mother-Anju Anju and sister-Deeksha Gautam for their unwavering love, encouragement, and understanding throughout this journey. Their endless support and sacrifices have been the cornerstone of my success, and I am forever grateful for their presence in my life.

Table of Contents

List of Tables

List of Figures

Abbreviations

1-OA 1-octanoic acid.

2-FA 2-Furoic acid.

3-OE 3-octenoic acid.

4-NG 4-nitroguaiacol.

7-OE 7-octenoic acid.

AA Acetic acid.

ACN Acetonitrile.

ACSM Aerosol chemical speciation monitor.

AGC Automatic gain control.

AI Aromaticity index.

ALS Advanced light source.

AMS Aerosol mass spectrometer.

AOCS American oil chemists' society.

ARM Atmospheric radiation measurement.

AZA Azelaic acid.

BNA Benzoic acid.

CCN Cloud condensation nuclei.

CCSEM Computer controlled scanning electron microscope.

CIMS Chemical ionization mass spectrometry.

CPA *cis*-pinonic acid.

DBE Double bond equivalent.

DBE-O Double bond equivalents minus oxygen.

DMSO Dimethyl sulfoxide.

DOE Department of energy.

DTT Dithiothreitol.

EDX Energy-dispersive X-ray.

EI Electron impact.

EIC Extracted ion chromatogram.

ELVOC Extreme low volatility organic compound.

EPR Electron paramagnetic resonance.

ESI Electrospray ionization.

FA Formic acid.

HILIC Hydrophilic interaction liquid chromatography.

HOM Highly oxygenated molecule.

HR High resolution.

In Inorganic substances.

IV Iodine value.

IVOC Intermediate volatile organic compound.

K_H Henry's law constant.

KAZR Ka-band arm zenith radar.

KI Potassium iodide.

LC Liquid chromatography.

LMA Limononic acidl.

LVOC Low volatile organic compound.

MCA Methacrylic acid.

MF Molecular feature.

MS Mass spectrometry.

NANO-DESI Nanospray desorption electrospray ionization.

NEXFAS Near-edge x-ray absorption fine structure spectroscopy.

NMR Nuclear magnetic resonance.

OA Organic aerosol.

OAc Organic acid.

OC Organic carbon.

OCIn Inorganic substances infused with organic carbon.

OCInEC Mixtures of organic carbon, elemental carbon, and inorganic inclusions.

OD Optical density.

OE Olefin.

ON Organonitrates.

OOA Oxidized organic aerosol.

OS Organosulfates.

OS_C Oxidation state of carbon.

OVF Organic volume fraction.

PAH Polycyclic aromatic hydrocarbon.

PAN Peroxyacetyl nitrate.

$PM_{2.5}$ Particulate matter below 2.5 μm in diameter.

PMA Pimelic acid.

PNA Pinic acid.

PTFE Polytetrafluoroethylene.

PUFA Polyunsaturated fatty acid.

PV Peroxide value.

RH Relative humidity.

ROOH Organic hydroperoxide.

ROOR Organic peroxide.

ROS Reactive oxygen species.

RPC Reverse phase column.

Rt Retention time.

SIM Selective ion monitoring.

SOA Secondary organic aerosol.

STXM Scanning transmission x-ray microscopy.

SVOC Semi volatile organic compound.

T Temperature.

t-BP tert-butyl hydroperoxide.

Tg Glass transition temperature.

TMI Transition metal ion.

ToF Time of flight.

TPP Triphenylphosphine.

TPPO Triphenylphosphine oxide.

TRACER Tracking aerosol convention interactions experiment.

TX Texas.

UV UltraViolet.

VK Van krevelen.

VOC Volatile organic compound.

WHO World health organization.

WSOC Water soluble organic compound.

Chapter 1

Introduction

Contributions: The introduction was written by Tania Gautam with review and feedback by Dr. Ran Zhao.

1.1 Air Pollution

In 1999, the World Health Organization (WHO) defined air pollution as "substances laid by human activities with enough concentration to cause detrimental influences to health, vegetation, yield of crops, properties, or to interfere with the enjoyment of properties."[1] Air pollution has had a long and complex history throughout human civilization. Initial alarms were sounded by inhabitants of ancient Athens but urban-industrial developments largely undermined the concerns regarding ill-effects of air pollution and the implementation of environmental laws.[2, 3] One pivotal moment in the history of air pollution awareness came about in 1948, Donora Pennsylvania, USA. In this small industrial town, atmospheric inversion trapped pollutants from local steel and zinc smelting operations, leading to the deaths of 20 people and thousands sick by October 30 1948.[3] Four years later, the Great Smog of London-another landmark event - led to a suspension of thick black coal smoke, rendering the populace helpless and resulting in 4000 deaths.[3]

Throughout the 20th and 21st centuries, there has been a notable escalation in the frequency and intensity of air pollution related incidents, spurred by rapid urbanization.[2, 4] While the aforementioned specific historical events serve as poignant examples, the broader trend underscores strategies needed to mitigate air pollution. Discussions revolving air pollution predominantly stem from apprehension and frequently focus on how air quality deviates from norm in the stratosphere or troposhere.[5, 6] This process is a leading environmental problem observed indoors and outdoors, recognizable in various forms of visible particles of soot/smoke to invisible gases such as sulfur dioxide (SO_2).

1.1.1 Atmospheric Burden of Particulate Matter

When considering the impact of air pollution, aerosols are major drivers in implicating human health and imposing a significant climate burden.[7] Generally, aerosols are defined as stable suspensions of solid or liquid particles in a gas. Common usage of aerosols typically refers to particular matter i.e., fine particles of aerodynamic size ≤ 2.5 μm.[3, 7] Atmospheric aerosols can originate from natural or anthropogenic sources. Major natural sources include sea spray, volcanic and mineral dust emissions,

while anthropogenic sources include industry and combustion emissions.[7] Figure 1.1 reveals estimated global concentrations of $PM_{2.5}$ in 2015 via Goddard Earth Observing System chemical transport model.[8] $PM_{2.5}$ concentrations in North America and Middle East are potentially driven by dust storms, while elevated levels in East Asia and South Asia are likely originating from biomass burning (e.g., Pearl River Delta region)[9, 10] or industrial and transportation emissions.[11]

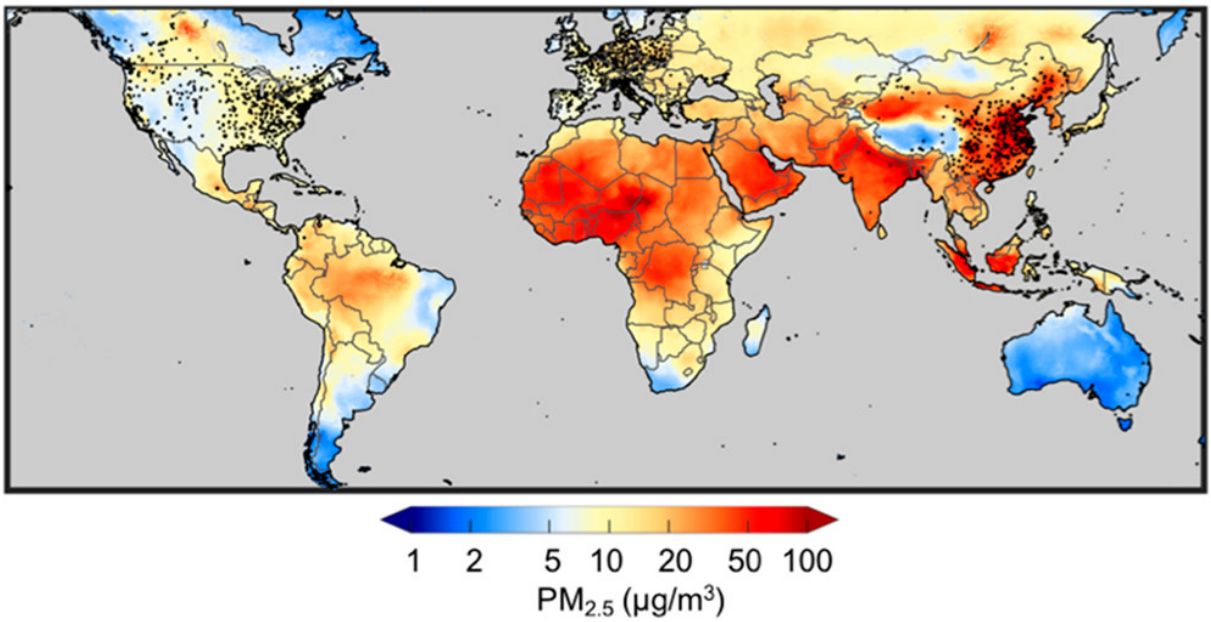

Figure 1.1: Estimated global concentrations of fine PM in 2015. Black dots represent monitor locations. Color scale indicates the concentration of $PM_{2.5}$.[8] Reprinted (adapted) with permission from Hammer et al.[8] Copyright 2024 American Chemical Society.

1.1.1.1 PM constituents-Health Effects

Ambient PM is a chemically complex mixture of organic and inorganic constituents which are ultimate drivers to oxidative stress.[3, 12] In particular, reactive oxygen species (ROS) represented in Figure 1.2 are key contributors to the cytotoxicity of $PM_{2.5}$.[13–15] Generally, ROS refers to oxidants derived from molecular oxygen (O_2) which includes hydrogen peroxide (H_2O_2), organic peroxides (ROOH and ROOR), superoxide ion ($O_2^{-\cdot}$), hydroxyl (OH) radical and others.[16] Furthermore, ROS belong to a family of reactive species including nitrogen and sulfur, which are capable of undergoing redox reactions. ROS can be either transported or catalytically generated

thereby causing injurious cellular responses.[17] In addition to ROS, organosulfates (OS) belong to a highly complex and unresolved fraction of aerosol and demonstrate a strong correlation with the oxidative potential of dithiothreitol (DTT) and as such, OSs may pose significant health risks.[18, 19]

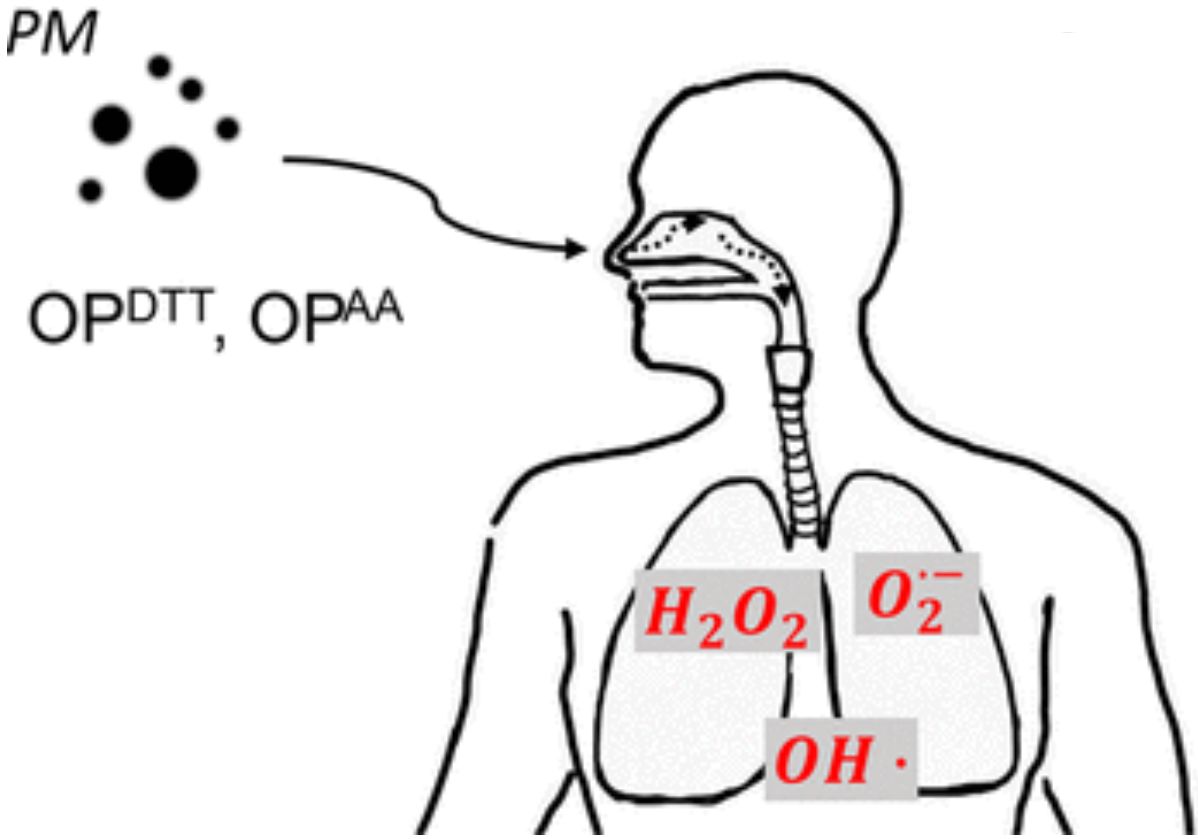

Figure 1.2: $PM_{2.5}$ and oxidative stress. Reprinted (adapted) with permission from Fang et al.[15] Copyright 2024 American Chemical Society.

Note, while ROS are imperative to determine the mechanisms on the induced cellular toxicity,[20] their oxidative chemistry is also essential in the formation of organic aerosol (OA) which can constitute up to 90% of submicron mass.[21] It is known that ROS can facilitate particle growth and alter particle morphology via oxidation of biogenic and anthropogenic volatile organic compounds (VOCs) by participating in photolysis, daytime OH radical chemistry, nighttime nitrate (NO_3) radical processing, ozonolysis and other mechanisms.[22]

1.1.1.2 Climate Effects

Under the climate burden of PM, aerosol-cloud interactions bear a large burden of uncertainty.[23] Under supersaturation conditions, OAs can act as cloud condensation nuclei (CCN) activating into cloud droplets thereby influencing cloud microphysical properties and regional precipitation.[24] Aerosol-cloud interactions are important to understand the climate burden of atmospheric PM. Several studies have shown that hygroscopicity of OAs can be influenced by their chemical composition,[25, 26] molecular weight[27, 28] and functional groups (e.g., carboxyl, carbonyl).[23, 29, 30] The oxygen to carbon (O:C) ratio of OAs, representing the abundance of oxygen containing functional groups relative the number of carbon atoms, plays crucial role in modifying hygroscopic properties. Studies have shown that organic compounds with higher O:C ratios tend to be more hygroscopic due to the presence of polar functional groups that readily interact with water molecules.[31, 32] Conversely, hydrophobic compounds such as hydrocarbons, possess lower O:C ratios and hence, exhibit lower hygroscopicity. In general, hygroscopicity of OAs influences cloud optical properties and precipitation patterns, thereby impacting Earth's radiative budget. Highly hygroscopic OAs can enhance cloud droplet activation, leading to increased cloud albedo and indirect cooling effects.[33, 34]

1.2 Oxidative Chemistry of the Atmosphere

Oxidative processing in the atmosphere refers to the intricate network of chemical reactions involving oxygen-containing species such as ozone (O_3), organics (e.g., VOCs) and inorganics (e.g., trace gases).[3, 35] These reactions often lead to the formation of secondary pollutants, which can implicate air quality and climate as well as the overall chemistry of the atmosphere.[36] In the following sections, I will briefly describe the role of certain aerosol constituents and the radical chemistry governing their formation as well as degradation.

1.2.1 Atmosphere-A Slow-Burning Flame

Earth's atmosphere is comprised of 20% O_2, an essential component in biosphere and combustion processes.[37] The high content of O_2, along with solar radiation, makes

Earth's atmosphere a highly oxidizing environment. Given the fact that the majority of chemical species undergo oxidation at variable rates in the atmosphere, the oxidation process is often related to a slow burning flame.[38] Atmospheric oxidative processing of VOCs can occur in gas-phase, condensed-phase and at the air-liquid interface.[39] Figure 1.3 illustrates general gas-phase reactions that VOCs tend to undergo in the troposphere, generating secondary pollutants such as ozone (O_3), peroxyacetyl nitrate (PAN) and secondary organic aerosol (SOA).[40, 41] These reaction pathways lead to oxidized products that are vastly different from their parent compounds,[42] facilitating their atmospheric removal through wet and dry deposition processes.[43] Overall, the oxidative processing outlined in Figure 1.3 alters the fate, lifetime and reactivity of oxidized matter with atmospheric oxidants.[41, 44]

1.2.2 Oxidation, Volatility and and Emerging Reaction Intermediates

In the atmosphere, the oxidation of organic compounds can continue to occur until organic carbon is either fully converted to CO_2 or removed from the atmosphere through dry or wet deposition.[36, 46] During oxidation, multiple reactions often yield products that are far less volatile and more polar than parent compounds.[47] The formation of intermediate compounds with different functional groups (e.g., carboxylic acids, aldehydes etc.) can affect the solubility of oxidized matter- affecting their atmospheric transport and alter cloud formation processes by enhancing aerosol hygroscopicity.[29, 48–50] Gas-phase oxidation of VOCs leads to the formation of species with sufficiently low vapor pressure to be condensable and generate SOA with volatilities often higher than their parent compounds.[51] Vapor pressure of oxidized matter is determined by molecular particle size and polarity, wherein specific polar functional groups can be determinant for controlling volatility.[51] In particular, an increase in carbon atom is not as impactful as the increase in oxygen-containing functional groups such as hydroperoxy (OOH), nitrate and carboxylic acid. Addition of these functional group to a VOC can lower its vapor pressure by two orders of magnitude.[51, 52]

The oxidative degradation of VOCs influences the climatic impact of aerosols as organics transition from the hydrophobic to hydrophilic phase gaining more oxygen

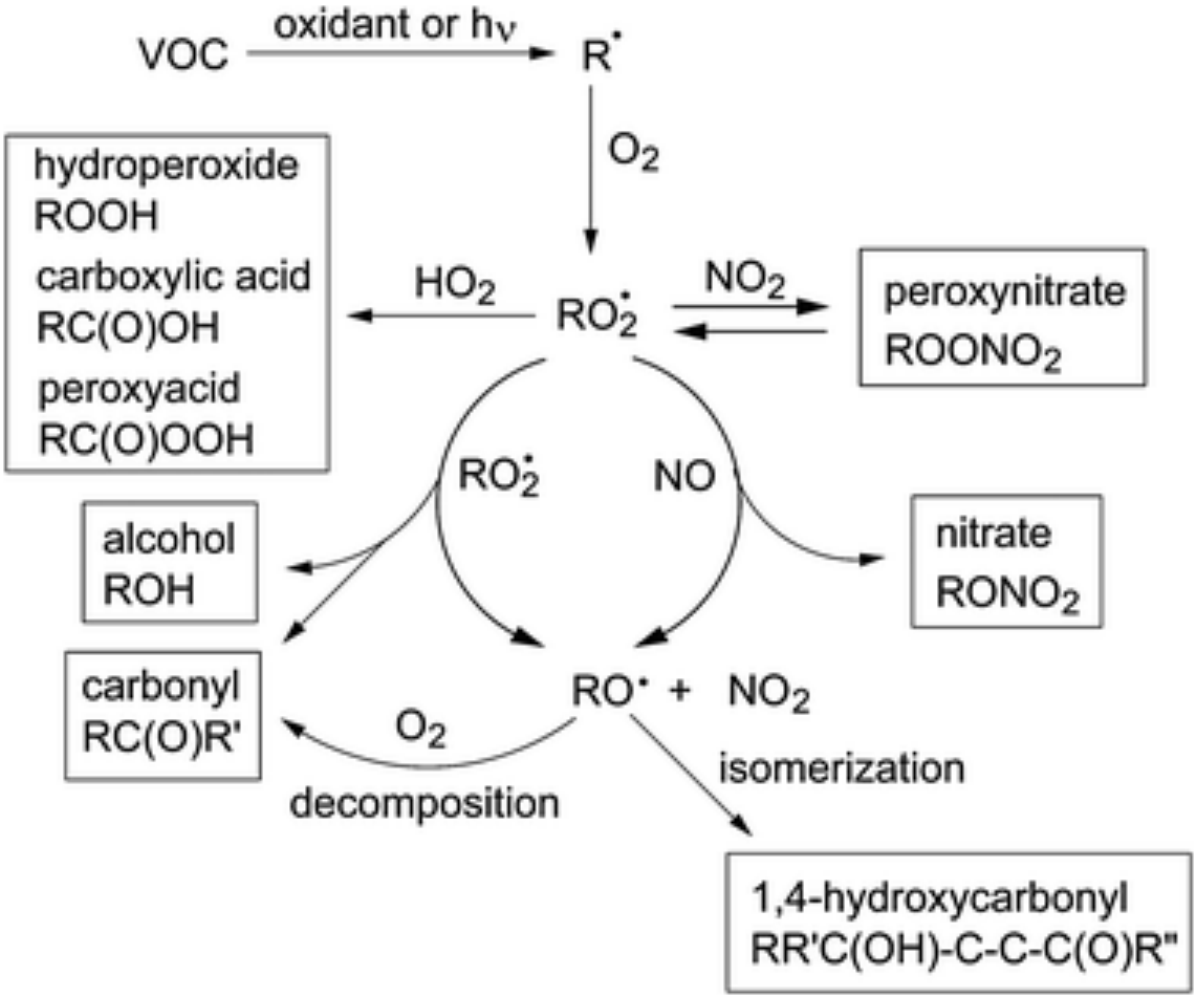

Figure 1.3: Atmospheric degradation mechanism of VOCs.[41, 45] Reproduced from Ref. Ziemann et al[45] with permission from the Royal Society of Chemistry.

during this process.[31, 53] Volatility can be indirectly estimated by measuring OA responses during equilibrium shifts due to variation in gas-phase concentrations or temperature (T).[31] Volatility parameterization of the oxidized matter is determined by experimentally derived logarithmic saturation mass concentration ($\log_{10}C_0$), where C_0 is the sum of condensed-phase concentrations of all compounds (eq-1.1).[31] Based on the work of Li et al,[54] using eq-1.1, vapor pressure can be converted to C_0, where M is molar mass (g.mol^{-1}), p_0 is saturation vapor pressure (mmHg), R is the ideal gas constant (8.205 x 10^{-5} atm K^{-1} mol^{-1} m^3) and T (K). From calculated C_0 (eq-1.1), VOC is defined as: $C_0 > 3$ x 10^{-4} μg.m^{-3}, semI$^-$VOC (SVOC): $0.3 < C_0 < 300$ μg.m−3, intermediate-VOC (IVOC): $300 < C_0 < 3$ x 10^6 μg.m^{-3}, low-VOC (LVOC):

3 x 10^4 < C0 < 0.3 μg.m^3 and extremely low-VOC: C_0 < 3 x 10^{-4} μg.m^{-3}.

$$C_0 = \frac{M \times 10^6 \times p_0}{760 \times RT} \quad \text{(eq-1.1)}$$

More recently, novel intermediates such as organic peroxides, OSs and organonitrates (ONs) have been found to be crucial in propagating the formation of highly oxygenated molecules (HOMs) and extremely low volatile organic compounds (ELVOCs).[55–60] Peroxides, OSs and ONs contribute to the formation of HOMs by propagating radical chain and oligomerization or functionalization reactions.[60–64] Despite extensive knowledge, these elusive compounds remain a poorly understood fraction in OAs.[65, 66] This is due to: (i) chemical complexity, wherein these compounds can involve multiple precursors and reaction pathways alluding to their formation, and (ii) varying precursor emissions due to seasonal differences (i.e., summer, winter), leading to their dynamic tranformation regionally and globally, further making it difficult to accurately estimate their concentration through model pedictions.[32, 42, 67, 68] Since their formation pathways and lifetimes can be widely influenced by radical initiation or photochemistry in gas- and condensed-phase,[60, 65, 69, 70] the next few sections will briefly outline their fate and chemistry.

1.2.2.1 Organic Peroxides

Peroxides play an important role in atmospheric processes, serving as oxidants and reservoirs of HO_x species leading to the perpetual evolution of HOMs in the atmosphere.[71, 72] Peroxides represent a significant fraction of SOA constituting up to 80% of the aerosol mass.[66, 72] Peroxides are crucial intermediates in facilitating the formation of HOMs adding multiple O atoms.[71] It is well known that H_2O_2 and organic peroxides can catalyze S (IV) to S (VI) resulting in OSs.[73] Peroxides are ubiquitous in atmospheric matrices including air, water, precipitation, cloud and fog water.[74] Despite considerable attention to gas-phase processes involving peroxides, there is ambiguity associated with their formation in the condensed-phase and the relative influence of competing radical species. The role of RO_2/HO_2 radicals in the gas-and condensed-phase is briefly discussed in Sections 1.3.1 and 1.3.2.

1.2.2.2 Organosulfates and Organonitrates

The oxidation of VOCs is often dependent on gas-and condensed-phase radicals leading to the subsequent changes in oxidized particle morphology including size, phase state, volatility and viscosity.[53] ONs are integral components of SOA and contribute to regional O_3 formation, subsequently affecting air quality.[75] OSs are important SOA constituents which contribute up to 30% of the SOA mass.[76] Despite considerable attention, ONs and OSs remain elusive due to their physicochemical complexity and lack of sensitive analytical methods, thereby remaining as a poorly understood fraction of SOA.[66] OSs are important SOA species,[77] which contribute significantly to SOA mass and influence cloud formation properties of OAs.[49, 76] Their water uptake and growth factors can be dependent on their structures. Hansen et al[78] have shown that pure limonene-derived OS is weakly hygroscopic with growth factors of 1.0 and 1.2 at 80% and 90% relative humidity (RH) respectively. However, the hygroscopicity of OS may be dependent on their structural factors such as degree of unsaturation, aromaticity and oxygenation, which can further govern the thermodynamic and kinetic properties of absorption and desorption of OS.[49] This indicates that OS can further impact the aqueous-phase chemistry of HOMs.[79] Their radical chemistry is briefly outlined in Sections 1.3.1 and 1.3.2.

1.3 Radical Chemistry

It is well established that free radicals play an important role in the stratosphere, troposphere, cloud droplets and gas phase.[80] Amongst these radicals, O_3, NO_3 and OH are are some of the dominant oxidants initiating VOC degradation.[81] Within these oxidants, OH radical is an important daytime oxidant, which facilitates the formation of RO_2/HO_2 radicals and O_3.[81–84] Radical chemistry occurs in multiple phases (gas, aqueous, and particle phases) and is often heterogeneous (gas-phase radical can oxidize particle-phase constitutents.[84, 85] The intricate role that these oxidants play in atmospheric matrices is detailed below.

1.3.1 Gas-Phase Radical Chemistry

Atmospheric photochemistry produces a wide range of radicals which exert significant influence on the composition of the atmosphere.[86] The initial oxidant generation is accompanied by the chemical process of photolysis at wavelengths > 290 nm.[66] OH radical, which is a major initiator of radical-chain oxidation, is formed via photolysis of O_3 by ultraviolet (UV) light in the presence of water vapor.[86] The inherent reactivity of OH radicals, characterized by its short lifetime ($\tau = 1.01$ μs),[87] allows for their indiscriminate reactions with most organic species.[81] Figure 1.3 outlines major reactions of OH radicals, wherein the production of RO_2/HO_2 radicals is essential to understanding the oxidative degradation of VOCs.[86]

1.3.1.1 Sources of Radicals

OH radicals initiate chain reactions in clean and polluted environments, with their production in the atmosphere governed by photolysis of gaseous O_3 (Figure 1.4, reaction 1). Under polluted conditions with high NO_x concentrations (< 10 ppb), OH radicals are consumed by reacting with carbon monoxide, methane or other VOCs to generate HO_2/RO_2 radicals (Figure 1.4, reactions 3-6). The newly formed HO_2 radicals can further recycle the production of OH radicals (Figure 1.4, reaction 7).[88] Another particularly known pathway for the daytime generation of OH radicals is the photolytic decomposition of HONO.[88] On the other hand, RO_2 radicals can be generated via combination reactions with O_2, H-abstraction, photolysis, decomposition of organonitrates (RO_2NO_2) and abstraction from hydroperoxides (ROOHs).[89]

$$O_3 + h\nu\ (< 320\ nm) \longrightarrow O(^1D) + O_2\ (\Delta_g) \quad (1)$$

$$O(^1D) + H_2O \longrightarrow OH + OH \quad (2)$$

$$OH + RH \longrightarrow R + H_2O \quad (3)$$

$$R + O_2 + M \longrightarrow RO_2 + M \quad (4)$$

$$RO_2 + NO \longrightarrow RO + NO_2 \quad (5)$$

$$RO \longrightarrow Carbonyls + HO_2 \quad (6)$$

$$HO_2 + NO \longrightarrow OH + NO_2 \quad (7)$$

Figure 1.4: Reactions of OH radicals in the atmosphere leading to generation of RO_2/HO_2 radicals.[86] Reproduced from Ref. Monks et al[86] with permission from the Royal Society of Chemistry

1.3.1.2 Reactions of Radicals

The reaction of OH radicals with alcohols, ethers (poly, cyclic, aliphatic), alkanes generally proceeds with H-abstraction. Some additional mechanisms include hydrogen-bonded complex and addition on the C=C bond.[88] The mechanisms pertaining to aqueous-phase reactions are more complex and briefly described in the following sections. The RO_2 and HO_2 radical intermediates can either terminate the chain reaction by forming stable products or propagate the chain reactions via complex channels.[70] Under atmospheric conditions, peroxy radicals tend to react slowly with alkenes and SO_2, while reacting quite rapidly with other free radicals such as NO and NO_2 in the troposphere.[89] It is likely that alkyl group in alkylperoxy radical (RO_2) may

weaken the O-O bond leading to subsequent transfer to NO and yielding NO_2.[89] The remaining alkoxy (RO) radical may isomerize, dissociate or further react with O_2, with all these pathways leading to more RO_2 species.[89] Despite their reactions with organics, literature has shown that radical chemistry is further compounded by self- and cross-reactions of RO_2 radicals.[70] Reactions of RO_2 + HO_2 radicals typically lead to ROOH products,[90] while self- and cross-reactions of RO_2 radical proceed with a tetroxide intermediate, which can subsequently dissociate to an intermediate (RO) or products (ROH, ROOR).[91] The unimolecular H-shifts occurring during RO_2 reactions is widely known as "autoxidation" which often leads to rapid formation of HOMs with as many as 10 O atoms.[91, 92]

1.3.2 Aqueous-Phase Radical Chemistry

Atmospheric radical chemistry can occur when organic compounds partition from gas to aqueous-phase (e.g., cloud and-,fog water) or condensed-phase (e.g., aerosol liquid water, organic-phase).[93–95] This transfer can be often dependent on their chemical composition and oxidation processes occurring at the air-liquid interface.[96, 97] While the particle phase is prone to excess salts and organics,[98] the aqueous-phase (e.g., cloud water) is far more diluted and ideal to pursue fundamental laboratory analysis to understand radical-initiated mechanisms. Thus, the majority of the current discussion will refer to radical processing in aqueous-phase. We will briefly describe the radical sources and highlight their reactions in the following section.

1.3.2.1 Sources of Radicals

Early efforts in tropospheric aqueous-phase chemistry were pursued to understand the evolution of species during California fog.[99] During the late 1980s, detailed aqueous-phase chemistry studies of inorganic systems, specifically radicals as oxidants were also undertaken.[99] Photochemical processing of water-soluble content in aqueous media such as cloud water, and fog droplets is dependent on pH, temperature and solar flux.[100] Atmospheric aqueous media can be comprised of inorganic ions (Cl^-, Na^+, ${SO_4}^{2-}$, ${NH_4}^+$), antioxidants (e.g., phenols), water-soluble organic compounds (WSOCs) (e.g., carboxylic acids, aldehydes), dissolved anthropogenic gaseous components (e.g., SO_2, NO_x) and photosensitizers (e.g., excited triplet state or $^3C^*$). Ionic

radicals (e.g., $Cl_2^{-\cdot}$, $Br_2^{-\cdot}$, $O_2^{-\cdot}$ etc.) are photochemically produced while neutral radicals (e.g., OH, NO_2, NO_3, $HO_2^{\cdot}$, $RO_2^{\cdot}$) can either diffuse from gas-phase (gas to liquid transfer) or directly produced in aqueous-phase.[101] OH radicals are electrophilic species and are hence, not very selective in their reactivity. Typical OH concentrations in cloud droplets can be 3.5 x 10^{-15} M and 2.2 x 10^{-14} M in urban and remote areas respectively.[99] Aside from photolytic decomposition of H_2O_2, some other sources of OH radicals include Fenton-type reactions between H_2O_2 and transition metal ions (TMIs) (e.g., Fe^{2+}, Cu^{+}), gas-phase uptake of OH and iron complexation.[99] NO_3 radical is an important nighttime oxidant which is primarily formed via gas-phase reaction between O_3 and NO_2.[99] Given that gas-to-aqueous partitioning is often governed by Henry's Law coefficient (K_H),[102] aqueous chemistry of NO_3 is negligible due to low K_H of NO_2 (1.4 x 10^{-2} M atm^{-1})[103] However, NO_2 induced oxidation at the surface of deliquesced aerosol particles can be important to consider sulfate formation during haze episodes.[104]

Sulfur-oxy radicals (e.g., $SO_4^{-\cdot}$) are additional radical species formed through oxidation of S(IV), which can interact with atmospheric reactants besides OH radicals.[99] On average, $SO_4^{-\cdot}$ radical concentrations in cloud droplets can be 1.1 x 10^{-14} M and 2.4 x 10^{-14} M in urban and remote environments respectively. In deliquescent particles, their average concentrations can be 9.3 x 10^{-15} M and 3.6 x 10^{-13} M in urban and remote environments respectively.[99] Aside from the aforementioned radicals, HO_2/RO_2 radicals have also been found in cloud water, fog droplets. Aqueous concentrations of peroxy radicals (i.e., RO_2+HO_2) can be 2.0-32.0 nM.[105] The two main sources of these radicals are: (i) gas-to-droplet partitioning, and (ii) aqueous-phase photochemical processing.[105] In the aqueous-phase HO_2 radicals can establish equilibrium with $O_2^{-\cdot}$, which is a powerful oxidizing agent with a lifetime of 1 min and an initiator of radical reactions.[106]

1.3.2.2 Reactions of Radicals

Radicals in aqueous-phase tend to react preferentially depending on the reactants in their vicinity.[105, 107] Photochemical oxidation of WSOCs can be induced by oxidants as shown in Figure 1.5.[47, 108, 109] There is extensive data available on the kinetics of OH radicals, investigating their reactivity with wide range of WSOCs.[99,

110] For the sake of the current discussion, the reactivity of RO_2/HO_2 radicals will be of primary focus. TMIs are ubiquitous in atmospheric waters, with metals such as iron (Fe), copper (Cu) and manganese (Mn) being the most prevalent. Aqueous concentrations of these metals are >6000 nM in cloud and fog waters.[110] TMIs such as Fe^{2+}, Cu^{+} are known to play crucial roles in facilitating HOx and sulfur chemistry. For instance, smaller RO_2 radicals (e.g., CH_3COO) during the oxidation of Fe^{2+} form an intermediate complex (RO_2Fe^{2+}) which decomposes to Fe^{3+} and ROOH.[111, 112] In urban regions, TMIs can facilitate S (IV) to S (VI) oxidation either via direct production through oxidation of H_2O_2, HNO_4 or indirect oxidation initiated by halogen ions (e.g., Cl^{-}), OH.[112, 113] This pathway is known to generate particle-bound sulfate species.[114] Additional pathways leading to OSs can be OH initiated H-abstraction from H_2SO_4 or bisulfate anions (HSO_4^{-}), addition of sulfur-oxy radical ions (e.g., $SO_2^{-\cdot}$, $SO_3^{-\cdot}$) to C=C in VOCs (e.g., isoprene, methyl vinyl ketone) and reaction between sulfate and alkyl radicals.[115]

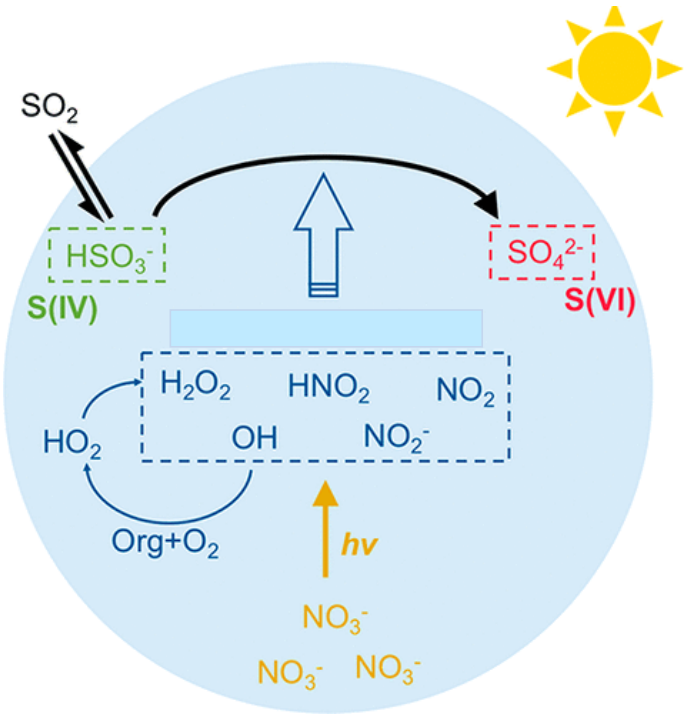

Figure 1.5: Aqueous-phase chemical processing via radical chemistry.[116] Reprinted (adapted) with permission from Gen et al.[116] Copyright 2024 American Chemical Society

RO_2 radicals possess oxidizing properties and react with electron rich donors via electron transfer mechanisms. Another reaction pathway that RO_2 radicals undergo is chain reaction or autoxidation via successive H-abstraction of unsaturated fatty acids and esters.[117] To this day, there is no evidence of aqueous-phase autoxidation initiated by RO_2 radicals in the atmosphere. This could be due to the slow reaction rate and three or four orders of magnitude of concentrations needed in the molar range which are often not found in the atmospheric aqueous-phase. Kinetic parameters acquired from the organic-phase are not transferable to aqueous solutions due to their dependence on the polarity of the medium.[117] On the other hand, HO_2 radicals represent a special case within the peroxyl radical family. HO_2 radicals have a pKa value of 4.8 and as such, in neutral solutions $O_2^{-\cdot}$ dominates. Bimolecular termination involves a disproportionation reaction between HO_2 and $O_2^{-\cdot}$, thereby yielding H_2O_2 and O_2. While HO_2 radicals undergo self-reaction, no such case has been observed for $O_2^{-\cdot}$ which is known to further react with RO_2 radicals under an acidic medium to yield ROOHs via electron transfer mechanism. Usually, RO_2 radicals can form tetroxide intermediate via head-to-head termination reaction, but this intermediate has never been observed in an aqueous solution. Interestingly, RO_2 radicals can form six-membered rings via the inclusion of additional water molecules (Figure 1.6); this reaction pathway may be of interest in aqueous solutions.[117]

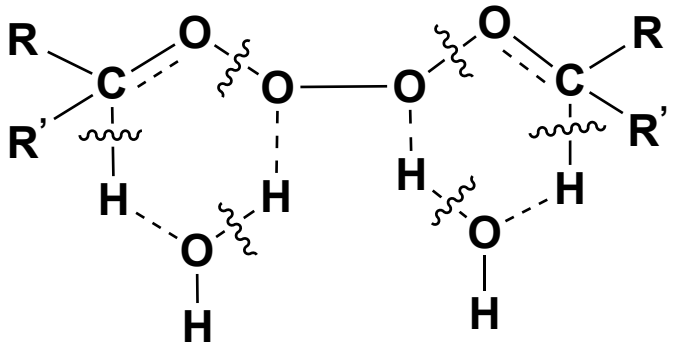

Figure 1.6: Transition state involving RO_2 radicals with inclusion of water molecules.[117] Copyright © 1991 by VCH Verlagsgesellschaft mbH, Germany. Reproduced with permission of Wiley via Copyright Clearance Center.

In addition to the aqueous-phase, oxidative processing of WSOCs at the micro-droplet surface can also be vital to generate HOMs and facilitate aqSOA.[118–121] Cloud droplet size can vary from 5-50 μm which is favorable for interfacial chemistry to dominate.[122] Microdroplet surfaces can accommodate a wide spectrum of organic compounds such as VOCs, PAHs, dicarboxylic acids and many other surface-active compounds.[119, 123, 124] It is understood that the the hydrophobic alkyl backbone at the cloud droplet surface would be exposed to potential oxidants (e.g., O_3),[120, 121] facilitating the formation of ROOHs[125] and contribution to aqSOA.[121] The formation of reactive intermediates such as organic peroxides via RO_2/HO_2 radical chemistry can occur both in aqueous-phase and at the air-water interface.[126–128]

A decade earlier, aqueous chemistry of H_2O_2 was known to be a major in-cloud SO_2 oxidant.[129–134] However, recently it has been shown that aquoeus peroxides can oxidize bisulfite ions,[135] formed via aqueous dissolution of SO_2 (g) thereby generating OS.[73] While considerable attention has been paid to aqueous chemistry of H_2O_2 and SO_2 (g), recent studies shed light on organic peroxide catalyzed formation of OS on water droplet and aqueous solutions.[73, 136] Li et al have experimentally determined that isoprene hydroxyl hydroperoxides tend to react with HSO_3^- to form OS on a water nanodroplet.[136] In a study conducted by Ye et al,[137] bimolecular reaction between OS and peroxides is found to be dependent on pH, aerosol liquid water content and ionic strength. In highly polluted regions, peroxides can further catalyze the SO_2 (g) absorption leading to OS formation and impacting climate.[138]

1.4 Analysis of Reactive Compounds

Chemical speciation and structural determination of organics in airborne PM is often challenging due to complex environmental matrices, which are further compounded by an array of formation mechanisms.[84, 139, 140] In particular, identification of particle-bound peroxides and sulfates is arduous due to: (i) lability of the peroxide bond, (ii) lack of selective methods for molecular-level speciation, and (iii) lack of appropriate surrogate or standards for quantification.[66, 71, 115, 141, 142] A large body of literature divides characterization of ROS and OS/ON in online and offline detection approaches.[66, 143] While online methods provide real-time evolution of particle-bound organic species bypassing physico-chemical losses,[66] offline targeted analysis can help resolves molecular ambiguity associated with labile species such as peroxides and offer molecular-level analysis of OS/ON.[144]

1.4.1 Online Measurements

Amongst many available analytical methodologies, mass spectrometry (MS) has emerged as a versatile tool for the sensitive determination of peroxides and OS.[145] In the past decade, a variety of mass spectrometric methods including combinations of separation techniques (i.e., liquid chromatography, LC) have been applied for selective identification and quantification of bulk aerosol properties (e.g., O:C ratios).[66, 146]

1.4.1.1 Aerosol Mass Spectrometry (AMS)

AMS is one of the highly sought-after analytical techniques in aerosol research for characterizing OA in both field and laboratory samples.[147, 148] Briefly, ambient particles are introduced into the aerodynamic lens, followed by particle volatilization in the evaporation unit under high T. The evaporated compounds are ionized by electron impact (EI) at 70 eV for subsequent analysis by MS.[148] While AMS allows analysis of a wide range of chemical species and provides quantitative information on non-refractory -aerosol-components, high degree of fragmentation during EI impedes the identification of individual particle-phase organics such as OS and peroxides.[144, 148, 149] Note, despite several attempts made to utilize AMS for labile

species, there has been limited success. As such, researchers have probed into novel approaches for the selective determination of peroxides and OSs. Recently, Weloe at el have demonstrated real-time bulk analysis of peroxides in SOA via chemical assay of triphenylphosphine (TPP) coupled with AMS.[66, 148] Similar to other derivatization methods,[130] TPP chemistry utilizes the oxidizing capability of peroxides such that TPP is chemically oxidized to triphenylphosphine oxide (TPPO) via either nucleophilic displacement of TPP on the O-O bond of peroxides or cyclic peroxide intermediate formation. Conventionally, TPP-TPPO can be detected spectrophotometrically and is often insensitive to moisture and O_2.[148]

1.4.1.2 CIMS

Chemical ionization mass spectrometry (CIMS) is a fast and versatile technique with detection limits within 10 pptv[150–152] for a wide variety of trace atmospheric gases through ionization of reactive ions such as H_3O^+, CF_3O^-, acetate and iodide (I^-).[66, 142, 150, 153] CIMS has been revolutionary in providing high time resolution data of many stable atmospherically relevant compounds such as carbonyls and carboxylic acids. Ng et al have demonstrated the application of CIMS for sensitive determination of labile species such as ROOHs and multifunctional nitrates.[43, 142] In principle, CIMS uses ion-molecule reaction that induces soft ionization in contrast to EI, thereby lessening fragmentation losses.[152] To initiate ion formation, reagent ions such as NO_3^-, I^-, acetate and fluoride are introduced into the source of the mass spectrometer.[154] The ion-molecular reaction can proceed through several pathways, which include proton transfer, hydride abstraction, electron attachment, electron transfer (Figure 1.7, reaction 4) and adduct or ion cluster formation.[155] While recent studies have utilized ToF-CIMS coupled to atmospheric or low-pressure ionization source for gas-phase oxygenated organics such as HOMs, much of the molecular identification is based on O:C ratios which don't assist in determining peroxy functionality.[66, 156, 157] However, the clustering chemistry (Figure 1.7) between CF_3O^- and peroxides/OS has been particularly advantageous for molecular level speciation than bulk analysis.[66, 158] However, the reagent gas (CF_3OOCF_3) is not commercially available, and the synthesis of which requires special expertise. As such, CF_3O^--CIMS is currently used in only a few research groups.[159–161]

$$e + CF_3COOCF_3 \longrightarrow CF_3O^- + \dot{C}F_3O \quad (1)$$

$$CF_3O^- + ROOH + M \longrightarrow CF_3O^-.\ ROOH + M \quad (2)$$

$$CF_3O^-.\ H_2O + ROOH \longrightarrow CF_3O^-.\ ROOH + H_2O \quad (3)$$

Figure 1.7: Clustering ion reactions during CIMS analysis of peroxides.[66] Reprinted (adapted) with permission from Wang et al.[66] Copyright 2024 American Chemical Society.

1.4.2 Offline Techniques

Offline analytical methods employed for the analysis of peroxides and OS generally involve sample collection and pre-treatment before instrumental detection.[144] Conventionally bulk-phase total peroxide content has been achieved via spectrophotometric methods such as chemiluminescence with luminol, fluorescence with p-hydroxyphenyl acetic acid or dichlorofluorescein assay, absorbance with iodometry or fenton-xylenol assay.[130, 162–164] While these conventional methods have been advantageous for quantification of peroxide content, many of them are also prone to interferences such as O_2, olefins (OEs), TMIs, steric hindrances by alkyl substituents.[66] Additionally, obtaining the total peroxide content does not offer any information regarding individual peroxide species. As such, recent modifications of chemical assay-assisted separation techniques coupled with MS have been demonstrated to assist in molecular-level information of peroxides/sulfates which is essential for understanding their formation, transformation and thereby impacts on the atmosphere.[66]

1.4.2.1 Nano-DESI-HRMS

In the early 2000s, desorption electrospray ionization (DESI) was introduced for sample analysis under ambient conditions.[165] DESI was initially developed for in-vivo sampling and crude MS imaging, proving advantageous in comparison to other MS imaging tools due to its non-destructive nature.[166] A slight modification adopted

in DESI is nanospray (nano)-DESI with targeted approach towards molecular characterization in SOA.[167, 168] DESI utilizes solvent spray on sample substrate at a distance leading to unstable MS signal,[167] on the other hand, nano-DESI (Figure 1.8) employs a liquid micro-junction between primary and secondary capillary leading to hybrid liquid extraction surface analysis.[165, 166] Herein, the primary capillary is used to create and maintain charged solvent droplets while the secondary capillary creates a self-aspirating nanospray of solvent containing dissolved analyte which is then directed into a high resolution (HR) MS inlet. Nano-DESI allows efficient collection, ionization and transfer of analytes resulting in significantly improved detection limits, thereby preserving samples without required pre-treatment and maintaining analysis speed.[167]

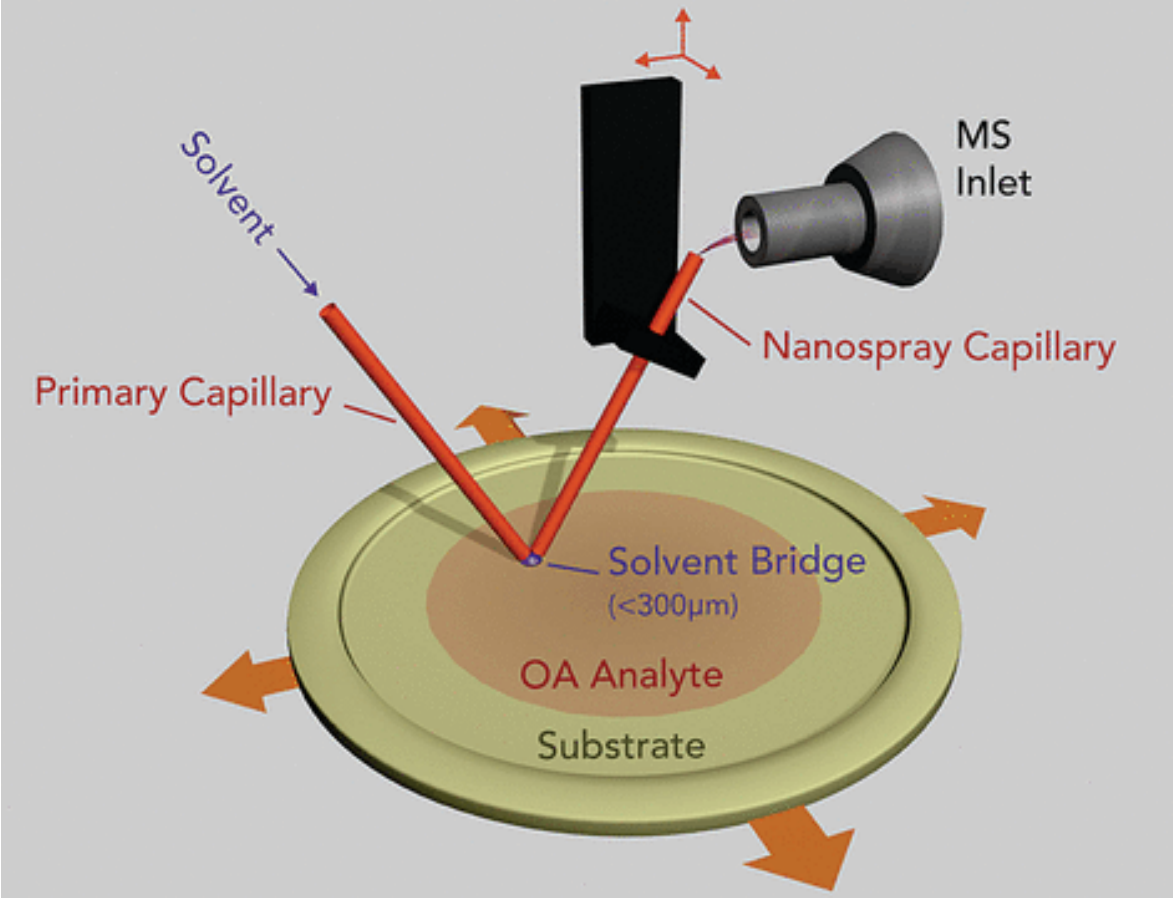

Figure 1.8: Nano-DESI-HRMS sampling interface and analysis representation.[167] Reprinted (adapted) with permission from Roach et al.[167] Copyright 2024 American Chemical Society.

1.4.2.2 Chemical Assay Assisted Liquid Chromatography-MS

The most commonly applied technique for the detection of particle-bound OS and peroxides is the use of quartz filter extracts analysis by liquid chromatography (LC) coupled with electrospray ionization (ESI)-MS. Given the likely presence of acidic protons of sulfate functional groups, high ionization efficiency is achievable through the generation of deprotonated molecular ions ($[M\text{-}H]^-$) in the negative ionization mode without derivatization of OSs.[144] Collision-induced dissociation ions (CID) have been utilized for the identification of OSs including bisulfite ions for aliphatic OSs, and sulfite and sulfate ions for aromatic OSs.[144] Apart from varying separation methods (e.g., ultra-high performance LC, reverse-phase LC), several MS based approaches (e.g., quadrupole time-of-flight, orbitrap) with high resolving power (>105) and greater mass accuracies (< 5 ppm) have been used to identify OSs.[144] While LC-MS based methods have been crucial for the qualitative determination of OSs, there are still many OSs requiring further confirmation in their identification during targeted and non-targeted analysis. This is due to lack of authentic standards, which have been attempted to be synthesized during fundamental laboratory studies but often pose time and quality constraints.[144] In contrast to OSs, peroxides lack acidic protons which can be utilized for their identification during LC-MS based approaches. As a result, chemical assays such as TPP and iodometry coupled with MS have been demonstrated to be useful.[148, 169, 170] The American Oil Chemists' Society (AOCS) modified and adapted the iodometry method developed by Lea and Wheeler to provide an accurate estimate of peroxide value (PV) which is used to gauge rancidity in fats and edible oils.[171, 172] Briefly, the iodometric determination of peroxides relies on the oxidation of I^- to corresponding molecular iodine (I_2) (Figure 1.9) under acidic conditions.[173, 174] I_2 generated will further recombine with excess I^- to lead to the formation of triiodide ion ($I_3{}^-$), which is measured at 253 nm via UV-Vis spectroscopy.[175] Following Beer's law, with a 1:1 stoichiometry between peroxides and $I_3{}^-$, the quantitative estimation can be achieved.[175] Though powerful, iodometric reduction of peroxides is widely prone to principal sources of errors: (i) reaction of I_2 with unsaturated fatty acids (Figure 1.9, reaction 3), and (ii) liberation of I^- from potassium iodide (KI) by the O_2 present in the matrix.[172] While the latter

is referred to as the O_2 error leading to overestimation and is treatable by bubbling nitrogen (N_2) gas,[176] the former leads to underestimation in peroxide quantification but the magnitude of underestimation has never been evaluated. Aside from these errors, easily oxidizable agents such as TMIs and mercaptans can also induce negative bias by leading to the decomposition of ROOHs.[177] While many of these errors have been countered to some extent, conventional approaches via absorbance-based methods such as UV-Vis spectroscopy and titration, still need to adopt cautious measures to counter matrix effects. Amongst the conventional derivatization assays for peroxide determination,[178, 179] recent modifications in iodometry-assisted LC-MS approach has been found be quite versatile in resolving molecular ambiguity of peroxy compounds in atmospheric samples.[180] During iodometry, peroxides are converted to their corresponding alcohols (Figure 1.9, reaction 1) indicating likely disappearance of peroxides. The comparison between control (no addition of I^-) and iodometry applied sampled during chromatographic separation prior to introduction in MS inlet demonstrated the versatility of this technique which selectively reacts with peroxy groups.[180]

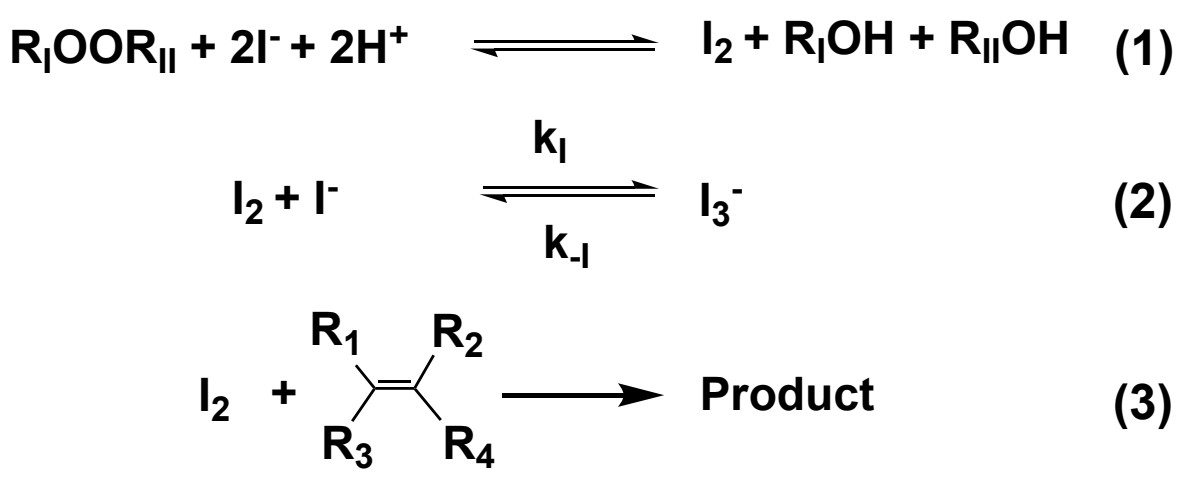

Figure 1.9: Iodometric reduction of organic peroxides and reaction of molecular iodine.[174, 181, 182] Reprinted (adapted) with permission from Gautam et al.[183] Copyright 2024 American Chemical Society.

While this modification in iodometry has been far more advantageous than the conventional version,[184] there are still some downsides that should be noted. Conventionally, iodometry coupled to LC-MS has opted with a reverse phase column (RPC), which is optimum for the majority of polar and water-soluble organics.[184] But highly polar analytes such HOMs with multiple OOH groups are not retained well on RPCs leading to poor peak shapes and co-elution. To compensate for this, hydrophilic interaction liquid chromatography (HILIC) can be useful to allow optimum separation and retention of highly polar analytes such as isoprene-epoxydiol (IEPOX)-OS.[185] Lastly, ion suppression effects are quite prone to iodometry assisted LC-MS. Specifically, to allow reduction of peroxide in 1 hour, I^- is maintained at concentrations 60 times higher than any other analytes in a given matrix.[180] With such high salt concentrations, ion intensity of peaks with peroxy functional groups can be suppressed to the level of noise.[186] While the concentration of I^- can be reduced, there will be a compromise either to increasing reaction time leading to additional matrix interferences or decreasing ion signal intensities of possible alcohol products.

1.5 Motivation

Particle-bound aerosol constituents such as ROS and sulfates/nitrates impose a tremendous burden on health and air quality.[187, 188] While significant advances have been made in deconvoluting the mechanisms and allowing sensitive detection of ROS and OS/ON in the atmosphere,[187] comprehensive understanding on molecular diversity and abundance of these species is still lacking.[66] ROS such as peroxides serve as important source of radicals and tend to be short-lived due to their accelerated degradation under thermolytic and photolytic conditions.[66] OS/ON are major contributors to SOA and accelerate haze formation episodes within metropolitan cities.[189, 190] A large body of literature divides characterization of ROS and OS/ON in online and offline detection approaches.[66, 143]

Fundamental laboratory approaches can assist in deconvoluting reaction mechanisms and acquire quantitative analysis on reactive SOA constituents such as peroxides and OS/ON. For instance, while the gas-phase formation of HOMs has been extensively studied, the mechanisms on the aqueous-phase formation of peroxides are often lacking in the current literature. Specifically, the conditions adopted within fundamental laboratory studies may be neglecting the impact of the choice of UV wavelength. It is essential to apply a robust and selective analytical method to elucidate the formation mechanisms of peroxides as a way to replicate their atmospheric photochemical evolution. Secondly, offline methods can be prone to known biases which can compromise their applicability for diverse analysis. Lastly, while laboratory studies can be utilized to demonstrate the physico-chemical properties of oxygenated molecules, advanced analytical approaches with direct MS can be useful for bulk characterization of particle-bound ROS and OS/ON.

Overall, we believe that synergetic fundamental laboratory and field studies can assist in unraveling the intricacies associated with the emergence of HOMs such as peroxides, OS/ON. Fundamental laboratory techniques provide invaluable insights into the conditions that impede or foster the formation of HOMs. This knowledge lays the foundation for understanding ambient samples, which are often more convoluted than the controlled laboratory settings. By bridging the gap between laboratory experiments and field observations, we can assess how meteorological parameters such as

solar flux, RH and T would influence the reaction pathways involved in the formation of peroxides, OS/ON. In general, this dual approach allows us to evaluate whether the reaction mechanisms elucidated through targeted laboratory investigations hold under ambient conditions.

1.6 Thesis Objectives

The overall goal of this thesis is threefold:

- Firstly, explore novel aqueous-phase formation mechanisms of HOMs (e.g., peroxides) which may be overlooked during conventional laboratory studies via the application of chemical assay-assisted LC-MS method
- Secondly, experimentally explore matrix effects occurring during the application of chemical assay method for the quantitative determination of oxidizing agents.
- And thirdly, probe in the emergence of ROS, sulfate/nitrate enriched species in ambient aerosols using advanced analytical direct MS approach.

1.7 Thesis Outline

This thesis consists of 5 chapters. In Chapter 1, the intricate role of ROS and OS-/ON is described to understand their burden on climate and air quality. This chapter further delves into oxidative reaction pathways involving RO_2, and OH radicals alluding to the transformation of VOCs in the atmosphere. We further address key knowledge gaps in the current understanding on the formation of HOMs such as peroxides in atmospheric aqueous media (e.g., cloud water). In Chapter 2, we elucidate the formation mechanisms of aqueous HOMs, probing the experimental conditions favourable to their formation through fundamental laboratory studies. Specifically, a novel mechanism alluding to the formation of ROOHs in the aqueous-phase is investigated via the application of iodometry-assisted LC-MS. Continuing in Chapter 3, the conventional derivatization technique adopted for the quantification of peroxides is examined for potential matrix effects under the deliberate introduction of known artifacts (e.g., OEs). This is the first-ever systematically designed experimental study

to understand the matrix-induced bias which could impact the application of this method in atmospheric matrices. Chapter 4 delves into the application of a more robust and versatile direct MS analytical technique to characterize a wide range of organic compounds such as ROS, OSs/ONs in ambient aerosol samples acquired during an active field campaign. This study provides a comprehensive understanding on the impact of meteorological conditions such as wind direction on the emergence of reactive aerosol constituents (e.g., ROS, OS) which can alter the air quality in urban environments.

References

[1] A. A. Almetwally, M. Bin-Jumah, and A. A. Allam, "Ambient air pollution and its influence on human health and welfare: An overview," en, *Environmental Science and Pollution Research*, vol. 27, no. 20, pp. 24 815–24 830, Jul. 2020, ISSN: 0944-1344, 1614-7499. DOI: 10.1007/s11356-020-09042-2.

[2] S. Mosley, "Environmental History of Air Pollution and Protection," en, in *The Basic Environmental History*, M. Agnoletti and S. Neri Serneri, Eds., vol. 4, Cham: Springer International Publishing, 2014, pp. 143–169, ISBN: 978-3-319-09179-2 978-3-319-09180-8. DOI: 10.1007/978-3-319-09180-8_5.

[3] J. H. Seinfeld, "Air pollution A half century of progress," en, *AIChE Journal*, vol. 50, no. 6, pp. 1096–1108, Jun. 2004, ISSN: 0001-1541, 1547-5905. DOI: 10.1002/aic.10102.

[4] J. Fenger, "Air pollution in the last 50 years From local to global," en, *Atmospheric Environment*, vol. 43, no. 1, pp. 13–22, Jan. 2009, ISSN: 13522310. DOI: 10.1016/j.atmosenv.2008.09.061.

[5] D. Vallero, "The State of the Atmosphere," en, in *Fundamentals of Air Pollution*, Elsevier, 2014, pp. 3–22, ISBN: 978-0-12-401733-7. DOI: 10.1016/B978-0-12-401733-7.00001-3.

[6] B. Brunekreef and S. T. Holgate, "Air pollution and health," en, *The Lancet*, vol. 360, no. 9341, pp. 1233–1242, Oct. 2002, ISSN: 01406736. DOI: 10.1016/S0140-6736(02)11274-8.

[7] I. Colbeck and M. Lazaridis, "Aerosols and environmental pollution," *Naturwissenschaften*, vol. 97, pp. 117–131, 2010.

[8] M. S. Hammer *et al.*, "Global Estimates and Long-Term Trends of Fine Particulate Matter Concentrations (1998 to 2018)," en, *Environmental Science & Technology*, vol. 54, no. 13, pp. 7879–7890, Jul. 2020, ISSN: 0013-936X, 1520-5851. DOI: 10.1021/acs.est.0c01764.

[9] H. Deng *et al.*, "Daytime SO_2 chemistry on ubiquitous urban surfaces as a source of organic sulfur compounds in ambient air," en, *Science Advances*, vol. 8, no. 39, eabq6830, Sep. 2022, ISSN: 2375-2548. DOI: 10.1126/sciadv.abq6830.

[10] M. Zhang, Y. Wang, Y. Ma, L. Wang, W. Gong, and B. Liu, "Spatial distribution and temporal variation of aerosol optical depth and radiative effect in south china and its adjacent area," *Atmospheric Environment*, vol. 188, pp. 120–128, 2018.

[11] R Timmermans *et al.*, "Source apportionment of pm2. 5 across china using lotos-euros," *Atmospheric Environment*, vol. 164, pp. 370–386, 2017.

[12] M. Pandolfi *et al.*, "Long-range and local air pollution: What can we learn from chemical speciation of particulate matter at paired sites?" en, *Atmospheric Chemistry and Physics*, vol. 20, no. 1, pp. 409–429, Jan. 2020, ISSN: 1680-7324. DOI: 10.5194/acp-20-409-2020.

[13] X. Shan, L. Liu, G. Li, K. Xu, B. Liu, and W. Jiang, "$PM_{2.5}$ and the typical components cause organelle damage, apoptosis and necrosis: Role of reactive oxygen species," en, *Science of The Total Environment*, vol. 782, p. 146 785, Aug. 2021, ISSN: 00489697. DOI: 10.1016/j.scitotenv.2021.146785. (visited on 01/29/2024).

[14] H. Hong *et al.*, "Cytotoxicity induced by iodinated haloacetamides via ROS accumulation and apoptosis in HepG-2 cells," en, *Environmental Pollution*, vol. 242, pp. 191–197, Nov. 2018, ISSN: 02697491. DOI: 10.1016/j.envpol.2018.06.090.

[15] T. Fang, P. S. J. Lakey, R. J. Weber, and M. Shiraiwa, "Oxidative Potential of Particulate Matter and Generation of Reactive Oxygen Species in Epithelial Lining Fluid," en, *Environmental Science & Technology*, vol. 53, no. 21, pp. 12 784–12 792, Nov. 2019, ISSN: 0013-936X, 1520-5851. DOI: 10.1021/acs.est.9b03823.

[16] A. Valavanidis, T. Vlachogianni, K. Fiotakis, and S. Loridas, "Pulmonary Oxidative Stress, Inflammation and Cancer Respirable Particulate Matter, Fibrous Dusts and Ozone as Major Causes of Lung Carcinogenesis through Reactive Oxygen Species Mechanisms," en, *International Journal of Environmental Research and Public Health*, vol. 10, no. 9, pp. 3886–3907, Aug. 2013, ISSN: 1660-4601. DOI: 10.3390/ijerph10093886.

[17] J. T. Bates *et al.*, "Reactive Oxygen Species Generation Linked to Sources of Atmospheric Particulate Matter and Cardiorespiratory Effects," en, *Environmental Science & Technology*, vol. 49, no. 22, pp. 13 605–13 612, Nov. 2015, ISSN: 0013-936X, 1520-5851. DOI: 10.1021/acs.est.5b02967.

[18] L. Guo *et al.*, "Comprehensive characterization of hygroscopic properties of methanesulfonates," *Atmospheric Environment*, vol. 224, p. 117 349, 2020, Publisher: Elsevier.

[19] W. Wang *et al.*, "Influence of covid-19 lockdown on the variation of organic aerosols: Insight into its molecular composition and oxidative potential," *Environmental Research*, vol. 206, p. 112 597, 2022.

[20] P. H. Chowdhury, Q. He, R. Carmieli, C. Li, Y. Rudich, and M. Pardo, "Connecting the Oxidative Potential of Secondary Organic Aerosols with Reactive Oxygen Species in Exposed Lung Cells," en, *Environmental Science & Technology*, vol. 53, no. 23, pp. 13 949–13 958, Dec. 2019, ISSN: 0013-936X, 1520-5851. DOI: 10.1021/acs.est.9b04449.

[21] P. Liu *et al.*, "Lability of secondary organic particulate matter," en, *Proceedings of the National Academy of Sciences*, vol. 113, no. 45, pp. 12 643–12 648, Nov. 2016, ISSN: 0027-8424, 1091-6490. DOI: 10.1073/pnas.1603138113.

[22] P. J. Ziemann and R. Atkinson, "Kinetics, products, and mechanisms of secondary organic aerosol formation," *Chemical Society Reviews*, vol. 41, no. 19, pp. 6582–6605, 2012.

[23] Y. Kuang, W. Xu, J. Tao, N. Ma, C. Zhao, and M. Shao, "A Review on Laboratory Studies and Field Measurements of Atmospheric Organic Aerosol Hygroscopicity and Its Parameterization Based on Oxidation Levels," en, *Current Pollution Reports*, vol. 6, no. 4, pp. 410–424, Dec. 2020, ISSN: 2198-6592. DOI: 10.1007/s40726-020-00164-2.

[24] C. Zhao, X. Tie, and Y. Lin, "A possible positive feedback of reduction of precipitation and increase in aerosols over eastern central china," *Geophysical Research Letters*, vol. 33, no. 11, 2006.

[25] M Song, P. Liu, S. Hanna, Y. Li, S. Martin, and A. Bertram, "Relative humidity-dependent viscosities of isoprene-derived secondary organic material and atmospheric implications for isoprene-dominant forests," *Atmospheric Chemistry and Physics*, vol. 15, no. 9, pp. 5145–5159, 2015.

[26] A. P. Bateman, A. K. Bertram, and S. T. Martin, "Hygroscopic influence on the semisolid-to-liquid transition of secondary organic materials," *The Journal of Physical Chemistry A*, vol. 119, no. 19, pp. 4386–4395, 2015.

[27] T. Koop, J. Bookhold, M. Shiraiwa, and U. Poschl, "Glass transition and phase state of organic compounds: Dependency on molecular properties and implications for secondary organic aerosols in the atmosphere," *Physical Chemistry Chemical Physics*, vol. 13, no. 43, pp. 19 238–19 255, 2011.

[28] J. H. Slade and D. A. Knopf, "Multiphase oh oxidation kinetics of organic aerosol: The role of particle phase state and relative humidity," *Geophysical Research Letters*, vol. 41, no. 14, pp. 5297–5306, 2014.

[29] S. Han *et al.*, "Hygroscopicity of organic compounds as a function of organic functionality, water solubility, molecular weight, and oxidation level," en, *Atmospheric Chemistry and Physics*, vol. 22, no. 6, pp. 3985–4004, Mar. 2022, ISSN: 1680-7324. DOI: 10.5194/acp-22-3985-2022. [Online]. Available: https://acp.copernicus.org/articles/22/3985/2022/.

[30] M. D. Petters and S. M. Kreidenweis, "A single parameter representation of hygroscopic growth and cloud condensation nucleus activity," en, *Atmospheric Chemistry and Physics*, vol. 7, no. 8, pp. 1961–1971, Apr. 2007, ISSN: 1680-7324. DOI: 10.5194/acp-7-1961-2007.

[31] N. M. Donahue, S. A. Epstein, S. N. Pandis, and A. L. Robinson, "A two-dimensional volatility basis set: 1. organic-aerosol mixing thermodynamics," en, *Atmospheric Chemistry and Physics*, vol. 11, no. 7, pp. 3303–3318, Apr. 2011, ISSN: 1680-7324. DOI: 10.5194/acp-11-3303-2011. [Online]. Available: https://acp.copernicus.org/articles/11/3303/2011/.

[32] Q. Zhang *et al.*, "Ubiquity and dominance of oxygenated species in organic aerosols in anthropogenically influenced Northern Hemisphere midlatitudes," en, *Geophysical Research Letters*, vol. 34, no. 13, 2007GL029979, Jul. 2007, ISSN: 0094-8276, 1944-8007. DOI: 10.1029/2007GL029979.

[33] A. Clarke *et al.*, "Indoex aerosol: A comparison and summary of chemical, microphysical, and optical properties observed from land, ship, and aircraft," *Journal of Geophysical Research: Atmospheres*, vol. 107, no. D19, INX2–32, 2002.

[34] T. M. VanReken *et al.*, "Toward aerosol/cloud condensation nuclei (ccn) closure during crystal-face," *Journal of Geophysical Research: Atmospheres*, vol. 108, no. D20, 2003.

[35] C. Ronneau, "Atmospheric Chemistry: Fundamentals and Experimental Techniques," en, *Eos, Transactions American Geophysical Union*, vol. 68, no. 49, pp. 1643–1643, Dec. 1987, ISSN: 0096-3941, 2324-9250. DOI: 10.1029/EO068i049p01643-01.

[36] G. Isaacman-VanWertz *et al.*, "Chemical evolution of atmospheric organic carbon over multiple generations of oxidation," en, *Nature Chemistry*, vol. 10, no. 4, pp. 462–468, Apr. 2018, ISSN: 1755-4330, 1755-4349. DOI: 10.1038/s41557-018-0002-2.

[37] H. Akimoto, *Atmospheric Reaction Chemistry* (Springer Atmospheric Sciences). Tokyo: Springer Japan, 2016, ISBN: 978-4-431-55868-2 978-4-431-55870-5. DOI: 10.1007/978-4-431-55870-5.

[38] V. P. Barber, W. H. Green, and J. H. Kroll, "Screening for New Pathways in Atmospheric Oxidation Chemistry with Automated Mechanism Generation," en, *The Journal of Physical Chemistry A*, vol. 125, no. 31, pp. 6772–6788, Aug. 2021, ISSN: 1089-5639, 1520-5215. DOI: 10.1021/acs.jpca.1c04297.

[39] V. F. McNeill, "Aqueous Organic Chemistry in the Atmosphere: Sources and Chemical Processing of Organic Aerosols," en, *Environmental Science & Technology*, vol. 49, no. 3, pp. 1237–1244, Feb. 2015, ISSN: 0013-936X, 1520-5851. DOI: 10.1021/es5043707.

[40] A. Mellouki, G. Le Bras, and H. Sidebottom, "Kinetics and Mechanisms of the Oxidation of Oxygenated Organic Compounds in the Gas Phase," en, *Chemical Reviews*, vol. 103, no. 12, pp. 5077–5096, Dec. 2003, ISSN: 0009-2665, 1520-6890. DOI: 10.1021/cr020526x.

[41] R Atkinson, "Atmospheric chemistry of VOCs and NO_x," *Atmospheric Environment*, vol. 34, no. 12-14, pp. 2063–2101, 2000, ISSN: 13522310. DOI: 10.1016/S1352-2310(99)00460-4.

[42] J. L. Jimenez *et al.*, "Evolution of Organic Aerosols in the Atmosphere," en, *Science*, vol. 326, no. 5959, pp. 1525–1529, Dec. 2009, ISSN: 0036-8075, 1095-9203. DOI: 10.1126/science.1180353.

[43] T. B. Nguyen *et al.*, "Rapid deposition of oxidized biogenic compounds to a temperate forest," en, *Proceedings of the National Academy of Sciences*, vol. 112, no. 5, Feb. 2015, ISSN: 0027-8424, 1091-6490. DOI: 10.1073/pnas.1418702112. [Online]. Available: https://pnas.org/doi/full/10.1073/pnas.1418702112 (visited on 01/29/2024).

[44] M. Hallquist *et al.*, "The formation, properties and impact of secondary organic aerosol: Current and emerging issues," en, *Atmospheric Chemistry and Physics*, vol. 9, no. 14, pp. 5155–5236, Jul. 2009, ISSN: 1680-7324. DOI: 10.5194/acp-9-5155-2009. (visited on 01/29/2024).

[45] P. J. Ziemann and R. Atkinson, "Kinetics, products, and mechanisms of secondary organic aerosol formation," en, *Chemical Society Reviews*, vol. 41, no. 19, p. 6582, 2012, ISSN: 0306-0012, 1460-4744. DOI: 10.1039/c2cs35122f.

[46] S. Hatakeyama, M. Ohno, J. Weng, H. Takagi, and H. Akimoto, "Mechanism for the formation of gaseous and particulate products from ozone-cycloalkene reactions in air," en, *Environmental Science & Technology*, vol. 21, no. 1, pp. 52–57, Jan. 1987, ISSN: 0013-936X, 1520-5851. DOI: 10.1021/es00155a005.

[47] I. J. George and J. P. D. Abbatt, "Heterogeneous oxidation of atmospheric aerosol particles by gas-phase radicals," en, *Nature Chemistry*, vol. 2, no. 9, pp. 713–722, Sep. 2010, ISSN: 1755-4330, 1755-4349. DOI: 10.1038/nchem.806.

[48] F. Li, S. Zhou, L. Du, J. Zhao, J. Hang, and X. Wang, "Aqueous-phase chemistry of atmospheric phenolic compounds: A critical review of laboratory studies," *Science of The Total Environment*, vol. 856, p. 158 895, 2023.

[49] A. D. Estillore *et al.*, "Water Uptake and Hygroscopic Growth of Organosulfate Aerosol," en, *Environmental Science & Technology*, vol. 50, no. 8, pp. 4259–4268, Apr. 2016, ISSN: 0013-936X, 1520-5851. DOI: 10.1021/acs.est.5b05014.

[50] S. R. Suda *et al.*, "Influence of Functional Groups on Organic Aerosol Cloud Condensation Nucleus Activity," en, *Environmental Science & Technology*, vol. 48, no. 17, pp. 10 182–10 190, Sep. 2014, ISSN: 0013-936X, 1520-5851. DOI: 10.1021/es502147y.

[51] J. H. Kroll and J. H. Seinfeld, "Chemistry of secondary organic aerosol: Formation and evolution of low-volatility organics in the atmosphere," en, *Atmospheric Environment*, vol. 42, no. 16, pp. 3593–3624, May 2008, ISSN: 13522310. DOI: 10.1016/j.atmosenv.2008.01.003. (visited on 01/29/2024).

[52] J. F. Pankow and W. E. Asher, "SIMPOL.1: A simple group contribution method for predicting vapor pressures and enthalpies of vaporization of multifunctional organic compounds," en, *Atmospheric Chemistry and Physics*, vol. 8, no. 10, pp. 2773–2796, May 2008, ISSN: 1680-7324. DOI: 10.5194/acp-8-2773-2008.

[53] W. M. Champion, N. E. Rothfuss, M. D. Petters, and A. P. Grieshop, "Volatility and Viscosity Are Correlated in Terpene Secondary Organic Aerosol Formed in a Flow Reactor," en, *Environmental Science & Technology Letters*, vol. 6, no. 9, pp. 513–519, Sep. 2019, ISSN: 2328-8930, 2328-8930. DOI: 10.1021/acs.estlett.9b00412.

[54] Y. Li, U. Poschl, and M. Shiraiwa, "Molecular corridors and parameterizations of volatility in the chemical evolution of organic aerosols," en, *Atmospheric Chemistry and Physics*, vol. 16, no. 5, pp. 3327–3344, Mar. 2016, ISSN: 1680-7324. DOI: 10.5194/acp-16-3327-2016.

[55] M. Ehn, T. Berndt, J. Wildt, and T. Mentel, "Highly Oxygenated Molecules from Atmospheric Autoxidation of Hydrocarbons: A Prominent Challenge for Chemical Kinetics Studies: HIGHLY OXYGENATED MOLECULES FROM ATMOSPHERIC AUTOXIDATION OF HYDROCARBONS," en, *International Journal of Chemical Kinetics*, vol. 49, no. 11, pp. 821–831, Nov. 2017, ISSN: 05388066. DOI: 10.1002/kin.21130.

[56] J. D. Surratt *et al.*, "Organosulfate Formation in Biogenic Secondary Organic Aerosol," en, *The Journal of Physical Chemistry A*, vol. 112, no. 36, pp. 8345–8378, Sep. 2008, ISSN: 1089-5639, 1520-5215. DOI: 10.1021/jp802310p.

[57] K. C. Barsanti, J. H. Kroll, and J. A. Thornton, "Formation of Low-Volatility Organic Compounds in the Atmosphere: Recent Advancements and Insights," en, *The Journal of Physical Chemistry Letters*, vol. 8, no. 7, pp. 1503–1511, Apr. 2017, ISSN: 1948-7185, 1948-7185. DOI: 10.1021/acs.jpclett.6b02969.

[58] N. L. Ng *et al.*, "Contribution of First- versus Second-Generation Products to Secondary Organic Aerosols Formed in the Oxidation of Biogenic Hydrocarbons," en, *Environmental Science & Technology*, vol. 40, no. 7, pp. 2283–2297, Apr. 2006, ISSN: 0013-936X, 1520-5851. DOI: 10.1021/es052269u.

[59] M. Ehn *et al.*, "A large source of low-volatility secondary organic aerosol," en, *Nature*, vol. 506, no. 7489, pp. 476–479, Feb. 2014, ISSN: 0028-0836, 1476-4687. DOI: 10.1038/nature13032.

[60] N. L. Ng *et al.*, "Nitrate radicals and biogenic volatile organic compounds: Oxidation, mechanisms, and organic aerosol," en, *Atmospheric Chemistry and Physics*, vol. 17, no. 3, pp. 2103–2162, Feb. 2017, ISSN: 1680-7324. DOI: 10.5194/acp-17-2103-2017. [Online]. Available: https://acp.copernicus.org/articles/17/2103/2017/.

[61] K. E. Altieri, B. J. Turpin, and S. P. Seitzinger, "Oligomers, organosulfates, and nitrooxy organosulfates in rainwater identified by ultra-high resolution electrospray ionization FT-ICR mass spectrometry," en, *Atmospheric Chemistry and Physics*, vol. 9, no. 7, pp. 2533–2542, Apr. 2009, ISSN: 1680-7324. DOI: 10.5194/acp-9-2533-2009. [Online]. Available: https://acp.copernicus.org/articles/9/2533/2009/.

[62] M. Riva *et al.*, "Multiphase reactivity of gaseous hydroperoxide oligomers produced from isoprene ozonolysis in the presence of acidified aerosols," en, *Atmospheric Environment*, vol. 152, pp. 314–322, Mar. 2017, ISSN: 13522310. DOI: 10.1016/j.atmosenv.2016.12.040.

[63] J. Schindelka, Y. Iinuma, D. Hoffmann, and H. Herrmann, "Sulfate radical-initiated formation of isoprene-derived organosulfates in atmospheric aerosols," en, *Faraday Discussions*, vol. 165, p. 237, 2013, ISSN: 1359-6640, 1364-5498. DOI: 10.1039/c3fd00042g.

[64] J. F. Hamilton *et al.*, "Key Role of NO_3 Radicals in the Production of Isoprene Nitrates and Nitrooxyorganosulfates in Beijing," en, *Environmental Science & Technology*, vol. 55, no. 2, pp. 842–853, Jan. 2021, ISSN: 0013-936X, 1520-5851. DOI: 10.1021/acs.est.0c05689.

[65] C. Ye, K. Lu, H. Song, Y. Mu, J. Chen, and Y. Zhang, "A critical review of sulfate aerosol formation mechanisms during winter polluted periods," en, *Journal of Environmental Sciences*, vol. 123, pp. 387–399, Jan. 2023, ISSN: 10010742. DOI: 10.1016/j.jes.2022.07.011.

[66] S. Wang, Y. Zhao, A. W. H. Chan, M. Yao, Z. Chen, and J. P. D. Abbatt, "Organic Peroxides in Aerosol: Key Reactive Intermediates for Multiphase Processes in the Atmosphere," en, *Chemical Reviews*, vol. 123, no. 4, pp. 1635–1679, Feb. 2023, ISSN: 0009-2665, 1520-6890. DOI: 10.1021/acs.chemrev.2c00430.

[67] Y. Wang *et al.*, "Abundance of organosulfates derived from biogenic volatile organic compounds: Seasonal and spatial contrasts at four sites in China," en, *Science of The Total Environment*, vol. 806, p. 151 275, Feb. 2022, ISSN: 00489697. DOI: 10.1016/j.scitotenv.2021.151275.

[68] N Bukowiecki, J Dommen, A. Prevot, R Richter, E Weingartner, and U Baltensperger, "A mobile pollutant measurement laboratory measuring gas phase and aerosol ambient concentrations with high spatial and temporal resolution," *Atmospheric Environment*, vol. 36, no. 36-37, pp. 5569–5579, 2002.

[69] A. Zare, P. S. Romer, T. Nguyen, F. N. Keutsch, K. Skog, and R. C. Cohen, "A comprehensive organic nitrate chemistry: Insights into the lifetime of atmospheric organic nitrates," en, *Atmospheric Chemistry and Physics*, vol. 18, no. 20, pp. 15 419–15 436, Oct. 2018, ISSN: 1680-7324. DOI: 10.5194/acp-18-15419-2018. [Online]. Available: https://acp.copernicus.org/articles/18/15419/2018/.

[70] P. Lightfoot *et al.*, "Organic peroxy radicals: Kinetics, spectroscopy and tropospheric chemistry," en, *Atmospheric Environment. Part A. General Topics*, vol. 26, no. 10, pp. 1805–1961, Jul. 1992, ISSN: 09601686. DOI: 10.1016/0960-1686(92)90423-I.

[71] M. Krapf *et al.*, "Labile Peroxides in Secondary Organic Aerosol," en, *Chem*, vol. 1, no. 4, pp. 603–616, Oct. 2016, ISSN: 24519294. DOI: 10.1016/j.chempr.2016.09.007.

[72] S. A. Epstein, S. L. Blair, and S. A. Nizkorodov, "Direct Photolysis of α-Pinene Ozonolysis Secondary Organic Aerosol: Effect on Particle Mass and Peroxide Content," en, *Environmental Science & Technology*, vol. 48, no. 19, pp. 11 251–11 258, Oct. 2014, ISSN: 0013-936X, 1520-5851. DOI: 10.1021/es502350u.

[73] S. Wang *et al.*, "Organic Peroxides and Sulfur Dioxide in Aerosol: Source of Particulate Sulfate," en, *Environmental Science & Technology*, vol. 53, no. 18, pp. 10 695–10 704, Sep. 2019, ISSN: 0013-936X, 1520-5851. DOI: 10.1021/acs.est.9b02591.

[74] L. Du, X. Lv, M. Lily, K. Li, and N. Tsona Tchinda, "pH regulates the formation of organosulfates and inorganic sulfate from organic peroxide reaction with dissolved SO_2 in aquatic media," en, *Atmospheric Chemistry and Physics*, vol. 24, no. 3, pp. 1841–1853, Feb. 2024, ISSN: 1680-7324. DOI: 10.5194/acp-24-1841-2024.

[75] A. Foulds, M. A. H. Khan, T. J. Bannan, C. J. Percival, M. H. Lowenberg, and D. E. Shallcross, "Abundance of NO_3 Derived Organo-Nitrates and Their Importance in the Atmosphere," en, *Atmosphere*, vol. 12, no. 11, p. 1381, Oct. 2021, ISSN: 2073-4433. DOI: 10.3390/atmos12111381. [Online]. Available: https://www.mdpi.com/2073-4433/12/11/1381.

[76] C. Peng *et al.*, "Interactions of organosulfates with water vapor under sub- and supersaturated conditions," en, *Atmospheric Chemistry and Physics*, vol. 21, no. 9, pp. 7135–7148, May 2021, ISSN: 1680-7324. DOI: 10.5194/acp-21-7135-2021.

[77] H. Zhang *et al.*, "Organosulfates as Tracers for Secondary Organic Aerosol (SOA) Formation from 2-Methyl-3-Buten-2-ol (MBO) in the Atmosphere," en, *Environmental Science & Technology*, vol. 46, no. 17, pp. 9437–9446, Sep. 2012, ISSN: 0013-936X, 1520-5851. DOI: 10.1021/es301648z. [Online]. Available: https://pubs.acs.org/doi/10.1021/es301648z.

[78] A. M. K. Hansen *et al.*, "Hygroscopic properties and cloud condensation nuclei activation of limonene-derived organosulfates and their mixtures with ammonium sulfate," en, *Atmospheric Chemistry and Physics*, vol. 15, no. 24, pp. 14 071–14 089, Dec. 2015, ISSN: 1680-7324. DOI: 10.5194/acp-15-14071-2015.

[79] V. F. McNeill *et al.*, "Aqueous-Phase Secondary Organic Aerosol and Organosulfate Formation in Atmospheric Aerosols: A Modeling Study," en, *Environmental Science & Technology*, vol. 46, no. 15, pp. 8075–8081, Aug. 2012, ISSN: 0013-936X, 1520-5851. DOI: 10.1021/es3002986.

[80] D. H. Ehhalt, "Free Radicals in the Atmosphere," en, *Free Radical Research Communications*, vol. 3, no. 1-5, pp. 153–164, Jan. 1987, ISSN: 8755-0199. DOI: 10.3109/10715768709069780.

[81] D. Stone, L. K. Whalley, and D. E. Heard, "Tropospheric OH and HO_2 radicals: Field measurements and model comparisons," en, *Chemical Society Reviews*, vol. 41, no. 19, p. 6348, 2012, ISSN: 0306-0012, 1460-4744. DOI: 10.1039/c2cs35140d.

[82] J. J. Orlando and G. S. Tyndall, "Laboratory studies of organic peroxy radical chemistry: An overview with emphasis on recent issues of atmospheric significance," en, *Chemical Society Reviews*, vol. 41, no. 19, p. 6294, 2012, ISSN: 0306-0012, 1460-4744. DOI: 10.1039/c2cs35166h. (visited on 01/29/2024).

[83] S. Vaughan, C. E. Canosa-Mas, C. Pfrang, D. E. Shallcross, L. Watson, and R. P. Wayne, "Kinetic studies of reactions of the nitrate radical (NO_3) with peroxy radicals (RO_2): An indirect source of OH at night?" en, *Physical Chemistry Chemical Physics*, vol. 8, no. 32, p. 3749, 2006, ISSN: 1463-9076, 1463-9084. DOI: 10.1039/b605569a.

[84] D Jacob, "Heterogeneous chemistry and tropospheric ozone," *Atmospheric Environment*, vol. 34, no. 12-14, pp. 2131–2159, 2000, ISSN: 13522310.

[85] J. Abbatt and A. Ravishankara, "Opinion: Atmospheric Multiphase Chemistry: Past, Present, and Future," Aerosols/Laboratory Studies/Troposphere/-Chemistry (chemical composition and reactions), preprint, Mar. 2023. DOI: 10.5194/egusphere-2023-334. [Online]. Available: https://egusphere.copernicus.org/preprints/2023/egusphere-2023-334/.

[86] P. S. Monks, "Gas-phase radical chemistry in the troposphere," en, *Chemical Society Reviews*, vol. 34, no. 5, p. 376, 2005, ISSN: 0306-0012, 1460-4744. DOI: 10.1039/b307982c.

[87] K. H. Becker and D. Haaks, "Measurement of the Natural Lifetimes and Quenching Rate Constants of OH and OD Radicals," en, *Zeitschrift fur Naturforschung A*, vol. 28, no. 2, pp. 249–256, Feb. 1973, ISSN: 1865-7109, 0932-0784. DOI: 10.1515/zna-1973-0216.

[88] S. Gligorovski, R. Strekowski, S. Barbati, and D. Vione, "Environmental implications of hydroxyl radicals (oh)," *Chemical reviews*, vol. 115, no. 24, pp. 13 051–13 092, 2015.

[89] G. S. Tyndall *et al.*, "Atmospheric chemistry of small organic peroxy radicals," en, *Journal of Geophysical Research: Atmospheres*, vol. 106, no. D11, pp. 12 157–12 182, Jun. 2001, ISSN: 0148-0227. DOI: 10.1029/2000JD900746. [Online]. Available: https://agupubs.onlinelibrary.wiley.com/doi/10.1029/2000JD900746.

[90] D Shallcross, M Teresaraventosduran, M Bardwell, A Bacak, Z Solman, and C Percival, "A semi-empirical correlation for the rate coefficients for cross- and self-reactions of peroxy radicals in the gas-phase," en, *Atmospheric Environment*, vol. 39, no. 4, pp. 763–771, Feb. 2005, ISSN: 13522310. DOI: 10.1016/j.atmosenv.2004.09.072.

[91] G. Hasan, V. Salo, R. R. Valiev, J. Kubecka, and T. Kurten, "Comparing Reaction Routes for roor Intermediates Formed in Peroxy Radical Self- and Cross-Reactions," en, *The Journal of Physical Chemistry A*, vol. 124, no. 40, pp. 8305–8320, Oct. 2020, ISSN: 1089-5639, 1520-5215. DOI: 10.1021/acs.jpca.0c05960.

[92] T. Berndt *et al.*, "Accretion Product Formation from Self and CrossReactions of RO_2Radicals in the Atmosphere," en, *Angewandte Chemie International Edition*, vol. 57, no. 14, pp. 3820–3824, Mar. 2018, ISSN: 1433-7851, 1521-3773. DOI: 10.1002/anie.201710989.

[93] A. Marinoni *et al.*, "Hydrogen peroxide in natural cloud water: Sources and photoreactivity," en, *Atmospheric Research*, vol. 101, no. 1-2, pp. 256–263, Jul. 2011, ISSN: 01698095. DOI: 10.1016/j.atmosres.2011.02.013.

[94] T. K. V. Nguyen, Q. Zhang, J. L. Jimenez, M. Pike, and A. G. Carlton, "Liquid Water Ubiquitous Contributor to Aerosol Mass," en, *Environmental Science & Technology Letters*, vol. 3, no. 7, pp. 257–263, Jul. 2016, ISSN: 2328-8930, 2328-8930. DOI: 10.1021/acs.estlett.6b00167.

[95] Y. B. Lim, Y. Tan, M. J. Perri, S. P. Seitzinger, and B. J. Turpin, "Aqueous chemistry and its role in secondary organic aerosol (SOA) formation," en, *Atmospheric Chemistry and Physics*, vol. 10, no. 21, pp. 10 521–10 539, Nov. 2010, ISSN: 1680-7324. DOI: 10.5194/acp-10-10521-2010.

[96] D. Vione *et al.*, "Photochemical reactions in the tropospheric aqueous phase and on particulate matter," en, *Chemical Society Reviews*, 10.1039.b510796m, 2006, ISSN: 0306-0012, 1460-4744. DOI: 10.1039/b510796m.

[97] F. Bernard, R. Ciuraru, A. Boreave, and C. George, "Photosensitized Formation of Secondary Organic Aerosols above the Air/Water Interface," en, *Environmental Science & Technology*, vol. 50, no. 16, pp. 8678–8686, Aug. 2016, ISSN: 0013-936X, 1520-5851. DOI: 10.1021/acs.est.6b03520.

[98] I. Riipinen *et al.*, "The contribution of organics to atmospheric nanoparticle growth," en, *Nature Geoscience*, vol. 5, no. 7, pp. 453–458, Jul. 2012, ISSN: 1752-0894, 1752-0908. DOI: 10.1038/ngeo1499. [Online]. Available: https://www.nature.com/articles/ngeo1499.

[99] H. Herrmann, D. Hoffmann, T. Schaefer, P. Brauer, and A. Tilgner, "Tropospheric Aqueous Phase Free Radical Chemistry Radical Sources, Spectra, Reaction Kinetics and Prediction Tools," en, *ChemPhysChem*, vol. 11, no. 18, pp. 3796–3822, Dec. 2010, ISSN: 1439-4235, 1439-7641. DOI: 10.1002/cphc.201000533.

[100] L. Wen *et al.*, "T and pH Dependent Kinetics of the Reactions of oh with Glutaric and Adipic Acid for Atmospheric AqueousPhase Chemistry," en, *ACS Earth and Space Chemistry*, vol. 5, no. 8, pp. 1854–1864, Aug. 2021, ISSN: 2472-3452, 2472-3452. DOI: 10.1021/acsearthspacechem.1c00163.

[101] A. Bianco, M. Passananti, M. Brigante, and G. Mailhot, "Photochemistry of the Cloud Aqueous Phase: A Review," en, *Molecules*, vol. 25, no. 2, p. 423, Jan. 2020, ISSN: 1420-3049. DOI: 10.3390/molecules25020423.

[102] J. Kurz and K. Ballschmiter, "Vapour pressures, aqueous solubilities, Henry's law constants, partition coefficients between gas/water (Kgw), N-octanol/water (Kow) and gas/N-octanol (Kgo) of 106 polychlorinated diphenyl ethers (PCDE)," en, *Chemosphere*, vol. 38, no. 3, pp. 573–586, Feb. 1999, ISSN: 00456535. DOI: 10.1016/S0045-6535(98)00212-4.

[103] J. L. Cheung *et al.*, "Heterogeneous Interactions of NO_2 with Aqueous Surfaces," en, *The Journal of Physical Chemistry A*, vol. 104, no. 12, pp. 2655–2662, Mar. 2000, ISSN: 1089-5639, 1520-5215. DOI: 10.1021/jp992929f.

[104] T. Liu and J. P. Abbatt, "Oxidation of sulfur dioxide by nitrogen dioxide accelerated at the interface of deliquesced aerosol particles," *Nature Chemistry*, vol. 13, no. 12, pp. 1173–1177, 2021.

[105] B. C. Faust and J. M. Allen, "Aqueous-phase photochemical sources of peroxyl radicals and singlet molecular oxygen in clouds and fog," *Journal of Geophysical Research: Atmospheres*, vol. 97, no. D12, pp. 12 913–12 926, 1992, Publisher: Wiley Online Library.

[106] M. Hayyan, M. A. Hashim, and I. M. AlNashef, "Superoxide Ion: Generation and Chemical Implications," en, *Chemical Reviews*, vol. 116, no. 5, pp. 3029–3085, Mar. 2016, ISSN: 0009-2665, 1520-6890. DOI: 10.1021/acs.chemrev.5b00407.

[107] H. Herrmann, D. Hoffmann, T. Schaefer, P. Brauer, and A. Tilgner, "Tropospheric aqueous-phase free radical chemistry: Radical sources, spectra, reaction kinetics and prediction tools," *ChemPhysChem*, vol. 11, no. 18, pp. 3796–3822, 2010.

[108] L. Ma, C. Guzman, C. Niedek, T. Tran, Q. Zhang, and C. Anastasio, "Kinetics and Mass Yields of Aqueous Secondary Organic Aerosol from Highly Substituted Phenols Reacting with a Triplet Excited State," en, *Environmental Science & Technology*, vol. 55, no. 9, pp. 5772–5781, May 2021, ISSN: 0013-936X, 1520-5851. DOI: 10.1021/acs.est.1c00575.

[109] R. Kaur and C. Anastasio, "First Measurements of Organic Triplet Excited States in Atmospheric Waters," en, *Environmental Science & Technology*, vol. 52, no. 9, pp. 5218–5226, May 2018, ISSN: 0013-936X, 1520-5851. DOI: 10.1021/acs.est.7b06699.

[110] R. L. Siefert, A. M. Johansen, M. R. Hoffmann, and S. O. Pehkonen, "Measurements of trace metal (fe, cu, mn, cr) oxidation states in fog and stratus clouds," *Journal of the Air & Waste Management Association*, vol. 48, no. 2, pp. 128–143, 1998.

[111] G. Khaikin, Z. Alfassi, R. Huie, and P Neta, "Oxidation of ferrous and ferrocyanide ions by peroxyl radicals," *The Journal of Physical Chemistry*, vol. 100, no. 17, pp. 7072–7077, 1996.

[112] L. Deguillaume, M. Leriche, A. Monod, and N. Chaumerliac, "The role of transition metal ions on HO_x radicals in clouds a numerical evaluation of its impact on multiphase chemistry," en, *Atmospheric Chemistry and Physics*, vol. 4, no. 1, pp. 95–110, Jan. 2004, ISSN: 1680-7324. DOI: 10.5194/acp-4-95-2004.

[113] A. Ansari, J. Peral, X. Domenech, R. Clemente, and J. Casado, "Oxidation of S(IV) to S(VI) under Fenton, photo Fenton and γ FeOOH photocatalized conditions," en, *Journal of Molecular Catalysis A: Chemical*, vol. 112, no. 2, pp. 269–276, Oct. 1996, ISSN: 13811169. DOI: 10.1016/1381-1169(96)00043-X. (visited on 03/03/2024).

[114] L. Huang, R. E. Cochran, E. M. Coddens, and V. H. Grassian, "Formation of Organosulfur Compounds through Transition Metal Ion-Catalyzed Aqueous Phase Reactions," en, *Environmental Science & Technology Letters*, vol. 5, no. 6, pp. 315–321, Jun. 2018, ISSN: 2328-8930, 2328-8930. DOI: 10.1021/acs.estlett.8b00225. (visited on 03/03/2024).

[115] M. Bruggemann *et al.*, "Organosulfates in Ambient Aerosol State of Knowledge and Future Research Directions on Formation, Abundance, Fate, and Importance," en, *Environmental Science & Technology*, vol. 54, no. 7, pp. 3767–3782, Apr. 2020, ISSN: 0013-936X, 1520-5851. DOI: 10.1021/acs.est.9b06751.

[116] M. Gen, R. Zhang, D. D. Huang, Y. Li, and C. K. Chan, "Heterogeneous Oxidation of SO_2 in Sulfate Production during Nitrate Photolysis at 300 nm: Effect of pH, Relative Humidity, Irradiation Intensity, and the Presence of Organic Compounds," en, *Environmental Science & Technology*, vol. 53, no. 15, pp. 8757–8766, Aug. 2019, ISSN: 0013-936X, 1520-5851. DOI: 10.1021/acs.est.9b01623. [Online]. Available: https://pubs.acs.org/doi/10.1021/acs.est.9b01623 (visited on 03/03/2024).

[117] C. Von Sonntag and H. Schuchmann, "The Elucidation of Peroxyl Radical Reactions in Aqueous Solution with the Help of Radiation Chemical Methods," en, *Angewandte Chemie International Edition in English*, vol. 30, no. 10, pp. 1229–1253, Oct. 1991, ISSN: 0570-0833. DOI: 10.1002/anie.199112291.

[118] V. Pratap *et al.*, "Investigating the evolution of water-soluble organic carbon in evaporating cloud water," en, *Environmental Science: Atmospheres*, vol. 1, no. 1, pp. 21–30, 2021, ISSN: 2634-3606. DOI: 10.1039/D0EA00005A.

[119] D. J. Donaldson and K. T. Valsaraj, "Adsorption and Reaction of Trace Gas-Phase Organic Compounds on Atmospheric Water Film Surfaces: A Critical Review," en, *Environmental Science & Technology*, vol. 44, no. 3, pp. 865–873, Feb. 2010, ISSN: 0013-936X, 1520-5851. DOI: 10.1021/es902720s.

[120] J. He *et al.*, "Probing autoxidation of oleic acid at air-water interface: A neglected and significant pathway for secondary organic aerosols formation," en, *Environmental Research*, vol. 212, p. 113 232, Sep. 2022, ISSN: 00139351. DOI: 10.1016/j.envres.2022.113232. [Online]. Available: https://linkinghub.elsevier.com/retrieve/pii/S001393512200559X (visited on 01/29/2024).

[121] N. Zhang *et al.*, "Analytical methods for determining the peroxide value of edible oils: A mini-review," *Food Chemistry*, vol. 358, p. 129 834, 2021, Publisher: Elsevier.

[122] K. Li *et al.*, "Spontaneous dark formation of OH radicals at the interface of aqueous atmospheric droplets," en, *Proceedings of the National Academy of Sciences*, vol. 120, no. 15, e2220228120, Apr. 2023, ISSN: 0027-8424, 1091-6490. DOI: 10.1073/pnas.2220228120.

[123] G. H. Wang *et al.*, "Observation of atmospheric aerosols at Mt Hua and Mt Tai in central and east China during spring 2009 Part 2 Impact of dust storm on organic aerosol composition and size distribution," en, *Atmospheric Chemistry and Physics*, vol. 12, no. 9, pp. 4065–4080, May 2012, ISSN: 1680-7324. DOI: 10.5194/acp-12-4065-2012.

[124] A. Tilgner, P. Brauer, R. Wolke, and H. Herrmann, "Modelling multiphase chemistry in deliquescent aerosols and clouds using CAPRAM3 0i," en, *Journal of Atmospheric Chemistry*, vol. 70, no. 3, pp. 221–256, Sep. 2013, ISSN: 0167-7764, 1573-0662. DOI: 10.1007/s10874-013-9267-4.

[125] S. Enami, M. R. Hoffmann, and A. J. Colussi, "Stepwise Oxidation of Aqueous Dicarboxylic Acids by Gas Phase OH Radicals," en, *The Journal of Physical Chemistry Letters*, vol. 6, no. 3, pp. 527–534, Feb. 2015, ISSN: 1948-7185, 1948-7185. DOI: 10.1021/jz502432j.

[126] N. Hayeck, I. Mussa, S. Perrier, and C. George, "Production of Peroxy Radicals from the Photochemical Reaction of Fatty Acids at the Air Water Interface," en, *ACS Earth and Space Chemistry*, vol. 4, no. 8, pp. 1247–1253, Aug. 2020, ISSN: 2472-3452, 2472-3452. DOI: 10.1021/acsearthspacechem.0c00048.

[127] S. Enami and Y. Sakamoto, "OH Radical Oxidation of Surface Active *cis* Pinonic Acid at the Air Water Interface," en, *The Journal of Physical Chemistry A*, vol. 120, no. 20, pp. 3578–3587, May 2016, ISSN: 1089-5639, 1520-5215. DOI: 10.1021/acs.jpca.6b01261. [Online]. Available: https://pubs.acs.org/doi/10.1021/acs.jpca.6b01261 (visited on 01/29/2024).

[128] J. M. Anglada, M. T. C. Martins Costa, J. S. Francisco, and M. F. Ruiz-Lopez, "Photoinduced Oxidation Reactions at the Air Water Interface," en, *Journal of the American Chemical Society*, vol. 142, no. 38, pp. 16 140–16 155, Sep. 2020, ISSN: 0002-7863, 1520-5126. DOI: 10.1021/jacs.0c06858.

[129] J. G. Calvert *et al.*, "Chemical mechanisms of acid generation in the troposphere," en, *Nature*, vol. 317, no. 6032, pp. 27–35, Sep. 1985, ISSN: 0028-0836, 1476-4687. DOI: 10.1038/317027a0. [Online]. Available: https://www.nature.com/articles/317027a0 (visited on 01/29/2024).

[130] D. W. Gunz and M. R. Hoffmann, "Atmospheric chemistry of peroxides: A review," en, *Atmospheric Environment. Part A. General Topics*, vol. 24, no. 7, pp. 1601–1633, Jan. 1990, ISSN: 09601686. DOI: 10.1016/0960-1686(90)90496-A. [Online]. Available: https://linkinghub.elsevier.com/retrieve/pii/096016869090496A (visited on 01/29/2024).

[131] S. Mertes *et al.*, "Evolution of particle concentration and size distribution observed upwind, inside and downwind hill cap clouds at connected flow conditions during FEBUKO," en, *Atmospheric Environment*, vol. 39, no. 23-24, pp. 4233–4245, Jul. 2005, ISSN: 13522310. DOI: 10.1016/j.atmosenv.2005.02.009. (visited on 01/29/2024).

[132] G. P. Gervat *et al.*, "Field evidence for the oxidation of SO_2 by H_2O_2 in cap clouds," en, *Nature*, vol. 333, no. 6170, pp. 241–243, May 1988, ISSN: 0028-0836, 1476-4687. DOI: 10.1038/333241a0. [Online]. Available: https://www.nature.com/articles/333241a0 (visited on 01/29/2024).

[133] E. Harris *et al.*, "Enhanced Role of Transition Metal Ion Catalysis During In-Cloud Oxidation of SO_2, volume = 340," en, *Science*, no. 6133, pp. 727–730, May 2013, ISSN: 0036-8075, 1095-9203. DOI: 10.1126/science.1230911. (visited on 01/29/2024).

[134] D. A. Hegg, R. Majeed, P. F. Yuen, M. B. Baker, and T. V. Larson, "The impacts of SO_2 oxidation in cloud drops and in haze particles on aerosol light scattering and CCN activity," en, *Geophysical Research Letters*, vol. 23, no. 19, pp. 2613–2616, Sep. 1996, ISSN: 0094-8276, 1944-8007. DOI: 10.1029/96GL02419. [Online]. Available: https://agupubs.onlinelibrary.wiley.com/doi/10.1029/96GL02419 (visited on 01/29/2024).

[135] A. S. Chandler *et al.*, "Measurements of H_2O_2 and SO_2 in clouds and estimates of their reaction rate," en, *Nature*, vol. 336, no. 6199, pp. 562–565, Dec. 1988, ISSN: 0028-0836, 1476-4687. DOI: 10.1038/336562a0. [Online]. Available: https://www.nature.com/articles/336562a0 (visited on 03/03/2024).

[136] H. Li *et al.*, "Mechanistic Study of the Aqueous Reaction of Organic Peroxides with HSO_3^- on the Surface of a Water Droplet," en, *Angewandte Chemie*, vol. 133, no. 37, pp. 20 362–20 365, Sep. 2021, ISSN: 0044-8249, 1521-3757. DOI: 10.1002/ange.202105416. (visited on 01/29/2024).

[137] J. Ye, J. P. D. Abbatt, and A. W. H. Chan, "Novel pathway of SO_2 oxidation in the atmosphere: Reactions with monoterpene ozonolysis intermediates and secondary organic aerosol," en, *Atmospheric Chemistry and Physics*, vol. 18, no. 8, pp. 5549–5565, Apr. 2018, ISSN: 1680-7324. DOI: 10.5194/acp-18-5549-2018.

[138] S. Ding, Y. Chen, S. R. Devineni, C. M. Pavuluri, and X.-D. Li, "Distribution characteristics of organosulfates (OSs) in PM2.5 in Tianjin, Northern China: Quantitative analysis of total and three OS species," en, *Science of The Total Environment*, vol. 834, p. 155 314, Aug. 2022, ISSN: 00489697. DOI: 10.1016/j.scitotenv.2022.155314. [Online]. Available: https://linkinghub.elsevier.com/retrieve/pii/S004896972202407X (visited on 01/29/2024).

[139] M. C. Jacobson, H. â. Hansson, K. J. Noone, and R. J. Charlson, "Organic atmospheric aerosols: Review and state of the science," en, *Reviews of Geophysics*, vol. 38, no. 2, pp. 267–294, May 2000, ISSN: 8755-1209, 1944-9208. DOI:

10.1029/1998RG000045. [Online]. Available: https://agupubs.onlinelibrary.wiley.com/doi/10.1029/1998RG000045 (visited on 01/29/2024).

[140] B. J. Turpin, P. Saxena, and E. Andrews, "Measuring and simulating particulate organics in the atmosphere: Problems and prospects," en, *Atmospheric Environment*, vol. 34, no. 18, pp. 2983–3013, Jan. 2000, ISSN: 13522310. DOI: 10.1016/S1352-2310(99)00501-4. [Online]. Available: https://linkinghub.elsevier.com/retrieve/pii/S1352231099005014 (visited on 01/29/2024).

[141] T. Krawczyk and S. Baj, "Review: Advances in the Determination of Peroxides by Optical and Spectroscopic Methods," en, *Analytical Letters*, vol. 47, no. 13, pp. 2129–2147, Sep. 2014, ISSN: 0003-2719, 1532-236X. DOI: 10.1080/00032719.2014.900781. [Online]. Available: http://www.tandfonline.com/doi/abs/10.1080/00032719.2014.900781 (visited on 01/29/2024).

[142] M. Glasius and A. H. Goldstein, "Recent Discoveries and Future Challenges in Atmospheric Organic Chemistry," en, *Environmental Science & Technology*, vol. 50, no. 6, pp. 2754–2764, Mar. 2016, ISSN: 0013-936X, 1520-5851. DOI: 10.1021/acs.est.5b05105. [Online]. Available: https://pubs.acs.org/doi/10.1021/acs.est.5b05105 (visited on 01/29/2024).

[143] D. K. Farmer *et al.*, "Response of an aerosol mass spectrometer to organonitrates and organosulfates and implications for atmospheric chemistry," en, *Proceedings of the National Academy of Sciences*, vol. 107, no. 15, pp. 6670–6675, Apr. 2010, ISSN: 0027-8424, 1091-6490. DOI: 10.1073/pnas.0912340107. [Online]. Available: https://pnas.org/doi/full/10.1073/pnas.0912340107 (visited on 09/17/2023).

[144] K. Gao and T. Zhu, "Analytical methods for organosulfate detection in aerosol particles: Current status and future perspectives," en, *Science of The Total Environment*, vol. 784, p. 147 244, Aug. 2021, ISSN: 00489697. DOI: 10.1016/j.scitotenv.2021.147244. [Online]. Available: https://linkinghub.elsevier.com/retrieve/pii/S0048969721023159 (visited on 01/29/2024).

[145] Y. Qin, V. Perraud, B. J. Finlayson-Pitts, and L. M. Wingen, "Peroxides on the surface of organic aerosol particles using matrix-assisted ionization in vacuum (maiv) mass spectrometry," *Environmental Science & Technology*, vol. 57, no. 38, pp. 14 260–14 268, 2023.

[146] M. S. Claflin, J. Liu, L. M. Russell, and P. J. Ziemann, "Comparison of methods of functional group analysis using results from laboratory and field aerosol measurements," *Aerosol Science and Technology*, vol. 55, no. 9, pp. 1042–1058, 2021.

[147] K. R. Daellenbach *et al.*, "Characterization and source apportionment of organic aerosol using offline aerosol mass spectrometry," en, *Atmospheric Measurement Techniques*, vol. 9, no. 1, pp. 23–39, Jan. 2016, ISSN: 1867-8548. DOI: 10.5194/amt-9-23-2016. [Online]. Available: https://amt.copernicus.org/articles/9/23/2016/ (visited on 01/29/2024).

[148] M. Weloe and T. Hoffmann, "Application of time of flight aerosol mass spectrometry for the real time measurement of particle phase organic peroxides an online redox derivatization aerosol mass spectrometer (ORDAMS)," en, *Atmospheric Measurement Techniques*, vol. 13, no. 10, pp. 5725–5738, Oct. 2020, ISSN: 1867-8548. DOI: 10.5194/amt-13-5725-2020.

[149] Q. Zhang *et al.*, "Understanding atmospheric organic aerosols via factor analysis of aerosol mass spectrometry: A review," en, *Analytical and Bioanalytical Chemistry*, vol. 401, no. 10, pp. 3045–3067, Dec. 2011, ISSN: 1618-2642, 1618-2650. DOI: 10.1007/s00216-011-5355-y. (visited on 01/29/2024).

[150] L. G. Huey, "Measurement of trace atmospheric species by chemical ionization mass spectrometry: Speciation of reactive nitrogen and future directions," *Mass spectrometry reviews*, vol. 26, no. 2, pp. 166–184, 2007.

[151] Y. Zhang, R. Liu, D. Yang, Y. Guo, M. Li, and K. Hou, "Chemical ionization mass spectrometry: Developments and applications for on-line characterization of atmospheric aerosols and trace gases," *TrAC Trends in Analytical Chemistry*, vol. 168, p. 117 353, 2023.

[152] M. F. Sipin, S. A. Guazzotti, and K. A. Prather, "Recent Advances and Some Remaining Challenges in Analytical Chemistry of the Atmosphere," en, *Analytical Chemistry*, vol. 75, no. 12, pp. 2929–2940, Jun. 2003, ISSN: 0003-2700, 1520-6882. DOI: 10.1021/ac030143e. (visited on 01/29/2024).

[153] D. W. OSullivan, I. K. Silwal, A. S. McNeill, V. Treadaway, and B. G. Heikes, "Quantification of gas phase hydrogen peroxide and methyl peroxide in ambient air: Using atmospheric pressure chemical ionization mass spectrometry with O_2^-, and O_2^- (CO_2) reagent ions," *International Journal of Mass Spectrometry*, vol. 424, pp. 16–26, 2018.

[154] M. S. B. Munson and F. H. Field, "Chemical Ionization Mass Spectrometry. I. General Introduction," en, *Journal of the American Chemical Society*, vol. 88, no. 12, pp. 2621–2630, Jun. 1966, ISSN: 0002-7863, 1520-5126. DOI: 10.1021/ja00964a001. (visited on 01/29/2024).

[155] A. G. Harrison, *Chemical Ionization Mass Spectrometry*, en, 0th ed. Routledge, May 2018, ISBN: 978-1-351-46154-2. DOI: 10.1201/9781315139128. (visited on 01/30/2024).

[156] X. Cheng, Q. Chen, Y. Jie Li, Y. Zheng, K. Liao, and G. Huang, "Highly oxygenated organic molecules produced by the oxidation of benzene and toluene in a wide range of OH exposure and NO_x conditions," en, *Atmospheric Chemistry and Physics*, vol. 21, no. 15, pp. 12 005–12 019, Aug. 2021, ISSN: 1680-7324. DOI: 10.5194/acp-21-12005-2021.

[157] M. Riva *et al.*, "Evaluating the performance of five different chemical ionization techniques for detecting gaseous oxygenated organic species," en, *Atmospheric Measurement Techniques*, vol. 12, no. 4, pp. 2403–2421, Apr. 2019, ISSN: 1867-8548. DOI: 10.5194/amt-12-2403-2019.

[158] S. H. Budisulistiorini *et al.*, "Examining the effects of anthropogenic emissions on isoprene-derived secondary organic aerosol formation during the 2013 Southern Oxidant and Aerosol Study (SOAS) at the Look Rock, Tennessee ground site," en, *Atmospheric Chemistry and Physics*, vol. 15, no. 15, pp. 8871–8888, Aug. 2015, ISSN: 1680-7324. DOI: 10.5194/acp-15-8871-2015.

[159] A. Tiusanen, J. Ruiz-Jimenez, K. Hartonen, and S. K. Wiedmer, "Analytical methodologies for oxidized organic compounds in the atmosphere," *Environmental Science: Processes & Impacts*, vol. 25, no. 8, pp. 1263–1287, 2023.

[160] H. O. Pye *et al.*, "Anthropogenic enhancements to production of highly oxygenated molecules from autoxidation," *Proceedings of the National Academy of Sciences*, vol. 116, no. 14, pp. 6641–6646, 2019.

[161] T. B. Nguyen *et al.*, "Atmospheric fates of criegee intermediates in the ozonolysis of isoprene," *Physical Chemistry Chemical Physics*, vol. 18, no. 15, pp. 10 241–10 254, 2016.

[162] R. Cathcart, E. Schwiers, and B. N. Ames, "Detection of picomole levels of hydroperoxides using a fluorescent dichlorofluorescein assay," en, *Analytical Biochemistry*, vol. 134, no. 1, pp. 111–116, Oct. 1983, ISSN: 00032697. DOI: 10.1016/0003-2697(83)90270-1. (visited on 02/01/2024).

[163] M. Lee, B. G. Heikes, and D. W. O'Sullivan, "Hydrogen peroxide and organic hydroperoxide in the troposphere: A review," en, *Atmospheric Environment*, vol. 34, no. 21, pp. 3475–3494, Jan. 2000, ISSN: 13522310. DOI: 10.1016/S1352-2310(99)00432-X. (visited on 02/01/2024).

[164] P. Mertes, L. Pfaffenberger, J. Dommen, M. Kalberer, and U. Baltensperger, "Development of a sensitive long path absorption photometer to quantify peroxides in aerosol particles (Peroxide-LOPAP)," en, *Atmospheric Measurement Techniques*, vol. 5, no. 10, pp. 2339–2348, Oct. 2012, ISSN: 1867-8548. DOI: 10.5194/amt-5-2339-2012. [Online]. Available: https://amt.copernicus.org/articles/5/2339/2012/.

[165] S. Rankin-Turner, P. Sears, and L. M. Heaney, "Applications of ambient ionization mass spectrometry in 2022: An annual review," *Analytical Science Advances*, vol. 4, no. 5-6, pp. 133–153, 2023.

[166] B. Challen and R. Cramer, "Advances in ionisation techniques for mass spectrometry-based omics research," *Proteomics*, vol. 22, no. 15-16, p. 2 100 394, 2022.

[167] P. J. Roach, J. Laskin, and A. Laskin, "Molecular Characterization of Organic Aerosols Using Nanospray-Desorption/Electrospray Ionization-Mass Spectrometry," en, *Analytical Chemistry*, vol. 82, no. 19, pp. 7979–7986, Oct. 2010, ISSN: 0003-2700, 1520-6882. DOI: 10.1021/ac101449p. [Online]. Available: https://pubs.acs.org/doi/10.1021/ac101449p.

[168] J. Laskin *et al.*, "Molecular selectivity of brown carbon chromophores," *Environmental science & technology*, vol. 48, no. 20, pp. 12 047–12 055, 2014.

[169] S. Zhou, J. C. Rivera-Rios, F. N. Keutsch, and J. P. D. Abbatt, "Identification of organic hydroperoxides and peroxy acids using atmospheric pressure chemical ionization tandem mass spectrometry (APCI/MS/MS) application to secondary organic aerosol," English, *Atmospheric Measurement Techniques*, vol. 11, no. 5, pp. 3081–3089, May 2018, ISSN: 1867-1381. DOI: https://doi.org/10.5194/amt-11-3081-2018. (visited on 08/13/2019).

[170] K. S. Docherty, W. Wu, Y. B. Lim, and P. J. Ziemann, "Contributions of Organic Peroxides to Secondary Aerosol Formed from Reactions of Monoterpenes with O_3, volume = 39," en, *Environmental Science & Technology*, no. 11, pp. 4049–4059, Jun. 2005, ISSN: 0013-936X, 1520-5851. DOI: 10.1021/es050228s. (visited on 02/11/2024).

[171] K. Moore and L. J. Roberts, "Measurement of Lipid Peroxidation," en, *Free Radical Research*, vol. 28, no. 6, pp. 659–671, Jan. 1998, ISSN: 1071-5762, 1029-2470. DOI: 10.3109/10715769809065821. [Online]. Available: http://www.tandfonline.com/doi/full/10.3109/10715769809065821 (visited on 02/03/2024).

[172] J. I. Gray, "Measurement of lipid oxidation: A review," en, *Journal of the American Oil Chemists' Society*, vol. 55, no. 6, pp. 539–546, Jun. 1978, ISSN: 0003-021X, 1558-9331. DOI: 10.1007/BF02668066. [Online]. Available: https://aocs.onlinelibrary.wiley.com/doi/10.1007/BF02668066 (visited on 02/03/2024).

[173] J. M. Gebicki, J. Collins, A. Baoutina, and P. Phair, "The limitations of an iodometric aerobic assay for peroxides," *Analytical biochemistry*, vol. 240, no. 2, pp. 235–241, 1996.

[174] W. C. Bray and H. A. Liebhafsky, "REACTIONS INVOLVING HYDROGEN PEROXIDE, IODINE AND IODATE ION. I. INTRODUCTION," en, *Journal of the American Chemical Society*, vol. 53, no. 1, pp. 38–44, Jan. 1931, ISSN: 0002-7863, 1520-5126. DOI: 10.1021/ja01352a006. [Online]. Available: https://pubs.acs.org/doi/abs/10.1021/ja01352a006 (visited on 02/03/2024).

[175] W. A. Pryor and L. Castle, "[34] Chemical methods for the detection of lipid hydroperoxides," en, in *Methods in Enzymology*, vol. 105, Elsevier, 1984, pp. 293–299, ISBN: 978-0-12-182005-3. DOI: 10.1016/S0076-6879(84)05037-0. [Online]. Available: https://linkinghub.elsevier.com/retrieve/pii/S0076687984050370 (visited on 02/03/2024).

[176] T. D. Crowe and P. J. White, "Adaptation of the AOCS official method for measuring hydroperoxides from small scale oil samples," en, *Journal of the American Oil Chemists' Society*, vol. 78, no. 12, pp. 1267–1269, Dec. 2001, ISSN: 0003-021X, 1558-9331. DOI: 10.1007/s11745-001-0424-7.

[177] G. Yildiz, R. L. Wehling, and S. L. Cuppett, "Comparison of four analytical methods for the determination of peroxide value in oxidized soybean oils," en, *Journal of the American Oil Chemists' Society*, vol. 80, no. 2, pp. 103–107, Feb. 2003, ISSN: 0003-021X, 1558-9331. DOI: 10.1007/s11746-003-0659-3.

[Online]. Available: https://aocs.onlinelibrary.wiley.com/doi/10.1007/s11746-003-0659-3 (visited on 02/03/2024).

[178] G. L. Kok, K. Thompson, A. L. Lazrus, and S. E. McLaren, "Derivatization technique for the determination of peroxides in precipitation," en, *Analytical Chemistry*, vol. 58, no. 6, pp. 1192–1194, May 1986, ISSN: 0003-2700, 1520-6882. DOI: 10.1021/ac00297a047. (visited on 02/03/2024).

[179] S. G. Rhee, T.-S. Chang, W. Jeong, and D. Kang, "Methods for detection and measurement of hydrogen peroxide inside and outside of cells," en, *Molecules and Cells*, vol. 29, no. 6, pp. 539–549, Jun. 2010, ISSN: 1016-8478, 0219-1032. DOI: 10.1007/s10059-010-0082-3. [Online]. Available: http://link.springer.com/10.1007/s10059-010-0082-3 (visited on 02/03/2024).

[180] R. Zhao, C. M. Kenseth, Y. Huang, N. F. Dalleska, and J. H. Seinfeld, "Iodometry-Assisted Liquid Chromatography Electrospray Ionization Mass Spectrometry for Analysis of Organic Peroxides: An Application to Atmospheric Secondary Organic Aerosol," *Environmental Science & Technology*, vol. 52, no. 4, pp. 2108–2117, Feb. 2018, ISSN: 0013-936X. DOI: 10.1021/acs.est.7b04863. (visited on 08/08/2019).

[181] H. A. Liebhafsky and A. Mohammad, "The Kinetics of the Reduction, in Acid Solution, of Hydrogen Peroxide by Iodide Ion," en, *Journal of the American Chemical Society*, vol. 55, no. 10, pp. 3977–3986, Oct. 1933, ISSN: 0002-7863, 1520-5126. DOI: 10.1021/ja01337a010. [Online]. Available: https://pubs.acs.org/doi/abs/10.1021/ja01337a010 (visited on 04/02/2021).

[182] C. J. Michejda, R. L. Ayres, and E. P. Rack, "Reactions of iodine with olefins. I. Kinetics and mechanism of iodine addition to pentene isomers," en, *Journal of the American Chemical Society*, vol. 93, no. 6, pp. 1389–1394, Mar. 1971, ISSN: 0002-7863. DOI: 10.1021/ja00735a012. [Online]. Available: https://pubs.acs.org/doi/abs/10.1021/ja00735a012 (visited on 03/20/2021).

[183] T. Gautam, S. Wu, J. Ma, and R. Zhao, "Potential Matrix Effects in Iodometry Determination of Peroxides Induced by Olefins," en, *The Journal of Physical Chemistry A*, vol. 126, no. 17, pp. 2632–2644, May 2022, ISSN: 1089-5639, 1520-5215. DOI: 10.1021/acs.jpca.1c10717. [Online]. Available: https://pubs.acs.org/doi/10.1021/acs.jpca.1c10717 (visited on 10/15/2022).

[184] W. Zhang, L. Xu, and H. Zhang, "Recent advances in mass spectrometry techniques for atmospheric chemistry research on molecular-level," *Mass Spectrometry Reviews*, 2023.

[185] A. P. S. Hettiyadura *et al.*, "Determination of atmospheric organosulfates using HILIC chromatography with MS detection," en, *Atmospheric Measurement Techniques*, vol. 8, no. 6, pp. 2347–2358, Jun. 2015, ISSN: 1867-8548. DOI: 10.5194/amt-8-2347-2015. [Online]. Available: https://amt.copernicus.org/articles/8/2347/2015/.

[186] C. M. Kenseth *et al.*, "Synergistic o_3+ oh oxidation pathway to extremely low-volatility dimers revealed in β-pinene secondary organic aerosol," *Proceedings of the National Academy of Sciences*, vol. 115, no. 33, pp. 8301–8306, 2018.

[187] W. Fan, T. Chen, Z. Zhu, H. Zhang, Y. Qiu, and D. Yin, "A review of secondary organic aerosols formation focusing on organosulfates and organic nitrates," en, *Journal of Hazardous Materials*, vol. 430, p. 128 406, May 2022, ISSN: 03043894. DOI: 10.1016/j.jhazmat.2022.128406. (visited on 01/29/2024).

[188] P. S. J. Lakey *et al.*, "Chemical exposure-response relationship between air pollutants and reactive oxygen species in the human respiratory tract," en, *Scientific Reports*, vol. 6, no. 1, p. 32 916, Sep. 2016, ISSN: 2045-2322. DOI: 10.1038/srep32916. [Online]. Available: https://www.nature.com/articles/srep32916.

[189] Y. Han *et al.*, "Enhanced Production of Organosulfur Species during a Severe Winter Haze Episode in the Guanzhong Basin of Northwest China," en, *Environmental Science & Technology*, vol. 57, no. 23, pp. 8708–8718, Jun. 2023, ISSN: 0013-936X, 1520-5851. DOI: 10.1021/acs.est.3c02914. [Online]. Available: https://pubs.acs.org/doi/10.1021/acs.est.3c02914 (visited on 02/06/2024).

[190] H. Li *et al.*, "Nitrate-driven urban haze pollution during summertime over the North China Plain," en, *Atmospheric Chemistry and Physics*, vol. 18, no. 8, pp. 5293–5306, Apr. 2018, ISSN: 1680-7324. DOI: 10.5194/acp-18-5293-2018. [Online]. Available: https://acp.copernicus.org/articles/18/5293/2018/.

Chapter 2

Photooxidation initiated aqueous-phase formation of organic peroxides: delving into formation mechanisms

2.1 Introduction

Organic peroxides (ROOR, ROOH, H_2O_2) are key intermediates in promoting oxidative aging of hydrocarbons found in varying matrices such as atmosphere, petroleum/aviation fuels and food.[70, 191–193] Peroxides are known to facilitate the formation of highly oxygenated molecules (HOMs) with multiple hydroperoxy (-OOH) functional groups and[194–196] low volatilities,[92, 197, 198] which can further lead to the formation of secondary organic aerosol (SOA).[198] There have been many studies investigating the reaction pathways pertaining to the formation of HOMs including autoxidation, self-/cross-reactions of RO_2 radicals, RO_2/OH radical chemistry and RO_2+HO_2 reactions in low and high NO_x conditions.[91, 92, 191, 194–196, 199–202] Conventionally, gas-phase autoxidation is known to occur in pristine (low NO_x) [203] and urban environments (high NO_x),[204] but since the implementation of regulatory cap on NO_x emissions,[205, 206] unimolecular isomerization has gained traction in urban environments,[207] in addition to bimolecular RO_2 chemistry.[208] Currently, gas-phase autoxidation has been extensively studied,[209, 210] but the reaction pathways and conditions that inhibit/promote aqueous-phase autoxidation need to be evaluated.

Cloud droplets are photochemically active because they receive a considerable amount of sunlight, in particular, UV radiation that serves as the driver of tropospheric photochemistry.[101] Photochemical oxidation of WSOCs can be induced by oxidants such as OH radicals,[101, 211] superoxide ion ($O_2^{-\cdot}$),[212, 213] singlet oxygen ($^1O_2$) and[214] photosensitizers (excited triplet state or $^3C^*$).[108, 109] While many studies have reported multiphase detection of organic peroxides,[66, 215, 216] the conditions regarding their formation needs to be further investigated. Peroxides are reservoirs of HO_x and RO_x radicals and a class of reactive oxygen species (ROS), which can induce respiratory illnesses.[20, 217] Aqueous-phase photochemistry may give rise to ROOH intermediates that contribute to the burden of atmospheric ROS.[218] Despite numerous investigations in aqueous-phase OH radical initiated oxidation of varying water-soluble organic precursors,[95, 219–222] there is a lack of laboratory evidence which can assist in deconvoluting varying reaction pathways and the conditions favorable to the formation of peroxides. Detection of organic peroxides

and its radical intermediates can be challenging due to: (i) lack of selective analytical technique to allow targeted analysis,[169] (ii) lability due to weak O-O bond,[71, 218] (iii) inaccessibility of sensitive radical measurement techniques (e.g., EPR) to capture crucial RO_2 intermediates formed during autoxidation,[223] making it difficult to determine the underlying mechanism pertaining to their formation, and (iv) incorporation of unrealistic experimental conditions including UV light and oxidant/precursor concentrations during fundamental laboratory investigations.[224–227] In particular, unambiguous identification of organic peroxides using direct mass spectrometric (MS) measurements can be difficult due to the inability of MS to provide functional group information and successive fragmentations of molecules in the ion molecular region.[148, 228] As such, chemically derivatized methods can be useful for the successful characterization of select functional groups.[148, 229, 230] Based on the work of Zhao et al, a combination of MS with the chemical assay of iodometry has proven to be advantageous for the selective identification of organic peroxides in a complex matrix.[180]

The overall goal of this study is to further our understanding of the mechanisms and conditions under which ROOH species form during aqueous-phase photooxidation. Specific aims are: (i) examine the dependency of aqueous ROOHs under experimental conditions such as varying oxidant and precursor concentrations, (ii) demonstrate the effects of interaction between ROOHs and the wavelength of irradiated light, and (iii) explore the possibility of aqueous-phase autoxidation attributing to the formation of ROOHs. We hypothesize that the use of short-wavelength UV light(i.e., UVC centered around 254 nm), as well as exceeding levels of oxidant and precursor used in laboratory experiments, can suppress the formation of aqueous ROOHs.

2.2 Experimental

2.2.1 Materials

The following chemicals were purchased from Sigma Aldrich: 7-octenoic acid (7-OE, 99%), 1-octanoic acid (1-OA, 99%), acetic acid (AA, 99%), formic acid (FA, 99%), molecular iodine (I_2, crystallized, 99%), hydrogen peroxide (H_2O_2, 30 % w/w), cis-pinonic acid (CPA, 99%), pimelic acid (PMA, 99%) and azelaic acid (AZA, 99 %).

Potassium iodide (KI, 99%) was bought from Fisher Scientific to carry out iodometry experiments. All chemicals were used without purification. H_2O_2 stock solutions were prepared fresh on a weekly basis. Other chemicals included: ultra pure water (18.0 MΩ cm, Millipore) and acetonitrile (ACN, HPLC grade). A previously synthesized sample of pinic acid (PNA) was used as is in this study. Details on the synthesis procedure are outlined elsewhere.[231] Limononic acid (LMA) synthesis details are provided in Section A.1 (Appendix A).

2.2.2 Target Compounds

To demonstrate the prevalence of aqueous-phase formation of ROOH from a variety of precursor WSOC compunds, we experimented with four organic acids (OAcs) (structures shown in Figure 2.1). OAcs are ubiquitous in the atmosphere and cloud water.[232, 233] Practically, OAcs can be readily detected with the negative mode of electrospray ionization mass spectrometry ((-)ESI-MS) and soft ionization (ESI) made detection of labile oxygenated compounds feasible.[180, 231, 234, 235] 7-OE was further chosen as the model compounds for two reasons: (i) the carbon chain length of 7-OE enables its separation from ROOH products on a C18 column, and (ii) the terminal C=C serves as the predominant reaction site with the OH radical, making the reaction mechanism predictable.[236] For these reasons, 7-OE is used in this work to gauge the yield of ROOHs under various reaction conditions. 1-OA was chosen as a comparison to 7-OE, given the absence of the terminal C=C bond. PNA and LMA were chosen to illustrate the atmospheric relevance of autoxidation because they are major oxidation products from the ozonolysis of α-pinene and limonene, respectively.[220, 221]

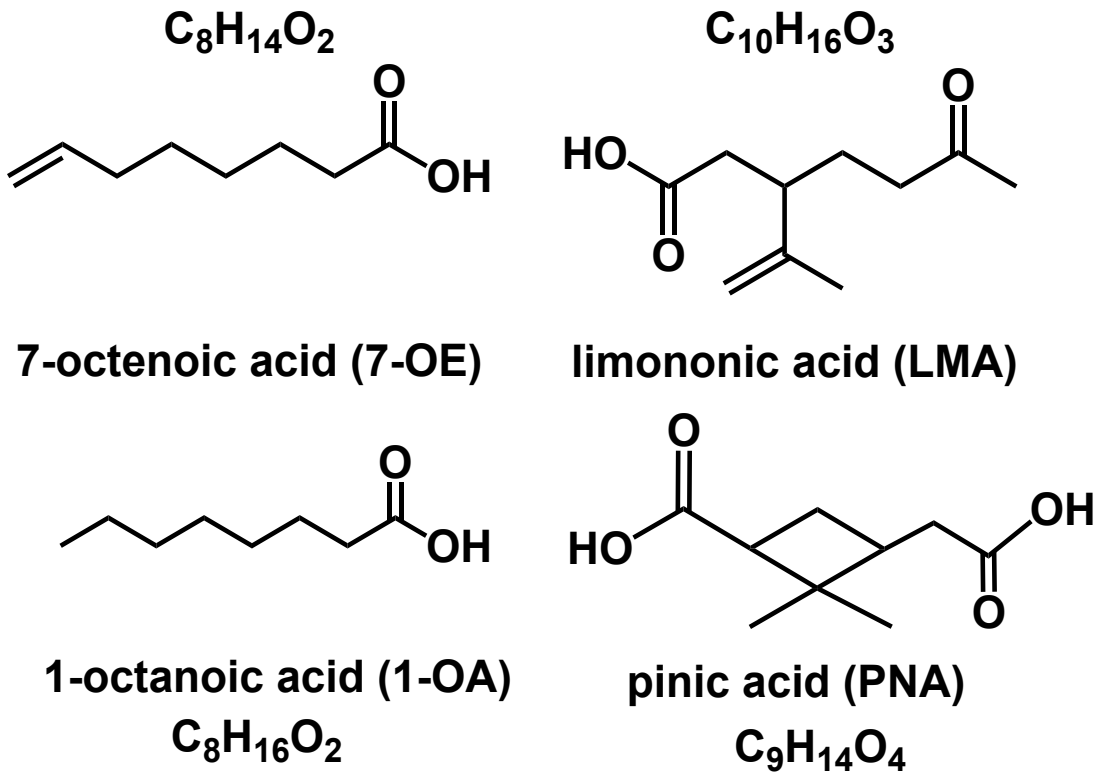

Figure 2.1: Structures of model organic acids (OAcs) employed to study photooxidation products.

2.2.3 Photochemical Reaction

The experimental apparatus consisted of a Rayonet photoreactor (PR2P200) with 16 Hg lamps (five of which were exposed to the sample) and a 10 mL quartz vessel with a magnetic stirrer to allow constant mixing. A fan was used to minimize temperature rising during photooxidation. The quartz vial was used for the efficient generation of OH radicals from H_2O_2.[231] The irradiation was performed with three different UV lights: UVC (254 nm), UVB (303 nm), and UVA (354 nm).[237]

For aqueous-phase photooxidation, an aqueous solution containing one of the OA species and H_2O_2 was oxidized in the quartz vial for specific time periods. The experimental variables adopted during the photooxidation of OAcs are listed in Table A.1 (Section A.2). The reaction progress was monitored by periodically sampling 840 μL

of the solution from the photoreactor using polytetrafluoroethylene (PTFE) tubing. These aliquots were immediately treated by an iodometry protocol and analyzed by the sampling method described below. Quality control was maintained by performing each reaction condition in triplicate.

2.2.4 Sample Analysis

2.2.4.1 Iodometry Protocol

To allow selective identification of ROOHs, the photooxidized samples were treated via the iodometry method outlined in Zhao et al.[180] Briefly, in the reaction vial, the concentration of I^- was maintained in excess (60 mM) to allow reduction of peroxides into their corresponding alcohols within 1 hr.[238] PMA and AZA were added as internal standards after photooxidation to account for instrumental variation and normalize the signal response of newly formed ROOHs. Photooxidized aliquots were processed as iodometry-control (ID-C) (without KI) and iodometry-treated (ID-T) (with KI). Specific reagent conditions for ID-C and ID-T are provided in Table A.2. To allow comparative analysis, we made sure that the matrix in ID-C and ID-T was identical to solely reflect changes induced by iodometry and not by differences due to dilution or acidification.[239] It is to be noted that there is hitherto rarely any evidence of the corresponding alcohol formed via the iodometric reduction of ROOH in the literature.[240] In this work, alcohols formed following iodometry were monitored (Section 2.3.1), thereby providing an additional parameter in the detection of peroxide products.

Due to possible interferences, such as ionization suppression by iodide (I^-)[180] and non-OH losses (e.g., decomposition, direct photolysis under irradiated wavelengths),[231] we performed additional control experiments. Our previous study showed that I_2 reacts with olefins,[183] which indicates that the disappearance of a peak during iodometry which is likely to recycle the formation of I_2 may give a false positive regarding identification of peroxy functional groups. As such an I_2 test is needed to confirm that the projected ROOHs do not react with I_2. The conditions for these experiments are outlined in Table A.2 and Table A.3 (Section A.3.1). From these experiments, we confirmed that ROOH products did not undergo side reactions

with I_2, internal standards showed no interference, and no product formation occurred between H_2O_2 and OA unless the light was shone on the mixture.

2.2.4.2 LC-MS Analysis

Sample analysis was performed using the Agilent 1200 SL HPLC system with a Phenomenex Luna column (1.6 μm particle size, 100 Å, 50 × 2.1 mm, polar C18), equipped with Agilent 6220 accurate-mass TOF and (-)ESI mode. Due to limited column availability, Phenomenex Kinetex (2.6 μm particle size, 100 Å, 50 × 2.1 mm, polar C18) with a security guard cartridge was also employed to analyze photooxidized samples. Specific instrument parameters are described in Section A.3.1. The ToF-MS used in this work could provide elemental compositions of detected compounds, which served as an additional method of identification. Elemental composition matches of potential product masses were acquired using the Agilent Mass Hunter software package (v.B04.00).

2.2.5 Investigation into Factors Affecting Aqueous-Phase Photooxidation

We probed into variables such as concentration, irradiation wavelength, and measurement time to understand the variability in photooxidized formation of ROOHs. We chose 7-OE as our model compound to allow molecular specificity with respect to the addition of successive OOH groups, as OH radicals can predominantly attach themselves to the C=C.[236] An overview of the conditions used in these experiments can be found in Table A.1 (Appendix A).

2.2.5.1 Wavelength

Given the fragility of the O-O bond,[71, 241] we examined the effects of wavelength of UV light used in irradiation. An aqueous solution of 7-OE and H_2O_2 was oxidized under three wavelengths: UVC, UVB and UVA.[237] The wavelength distribution spectrum and photon flux corresponding to each UV light are shown in Figure A.3 (Appendix A, Section A.4). Given that each UV type photolyzed H_2O_2 with different efficiency, specific adjustments were made for the experimental protocols. For UVC, a switch experiment was conducted, in which we initially irradiated an aqueous solution

of 7-OE at UVB to form peroxide products after which the solution was exposed to UVC. The concept was to acquire the degradation of ROOHs upon exposure to UVC. For UVA, we ramped the concentration of H_2O_2 to 150 mM such that the consumption rate of 7-OE would be equivalent to that under UVB. To observe the differences solely induced by the light exposed to the aqueous solution, comparisons were drawn between the yield of ROOHs. Since we do not have standard chemicals for ROOHs, we used the peak areas of ROOHs as proxies for their concentrations in this work. The calculations pertaining to the estimation of yield are described in Section A.6.1.

2.2.5.2 Concentration

We investigated the dependency of aqueous ROOHs on the concentration of precursor and oxidant by performing two sets of photooxidation experiments. In the first set, we maintained a constant concentration of 7-OE, while H_2O_2 was varied to achieve three different steady-state OH concentrations ($[OH]_{SS}$). Table A.1 (Section A.2) outlines the concentrations used for photooxidation experiment. $[OH]_{SS}$ was experimentally determined by observing the pseudo-first-order decay of 7-OE. Given that the second-order rate coefficient of 7-OE has never been reported in the literature, a relative rate kinetic investigation using pimelic acid as a reference compound was first conducted to determine it. Details on the kinetic investigation are described in Section A.6.2. For the second set of experiments, H_2O_2 was kept constant while the concentration of 7-OE was varied. Photooxidation exposure time was changed such that the consumption of 7-OE was relatively similar across varying H_2O_2 and 7-OE concentrations. The yield of ROOHs is estimated under these varying conditions. These observations are discussed in detail in Section 2.3.3.

2.3 Results & Discussion

2.3.1 Aqueous-Phase Photooxidation

To understand the mechanisms related to photooxidation initiated ROOHs, compounds with mono- and di-peroxy functionalities are identified. For this purpose, we performed detailed analyses on the peroxide functional group arising from the

photooxidation of each target compound. Figure 2.2 shows LC/(-)ESI-MS extracted ion chromatograms (EIC) corresponding to certain mass-to-charge (m/z) ratios of ROOHs originating from 7-OE, 1-OA, and PNA. The assessed ROOHs are represented in their deprotonated form ($[M\text{-}H]^-$) due to the carboxylic acid functional group on each OA.[180, 242] Figures 2.2 (A) and 2 (B) represent first- and second-generation ROOHs of 7-OE observed at m/z 191 (III, Figure A.4) and m/z 223 (IV, Figure A.4) respectively. Note, m/z 223 is found to be consistent with both autoxidation-initiated ROOH and second-generation product from OH initiated oxidation of ROOH, followed by the RO_2+HO_2 reaction.[243] The key to differentiate between these mechanisms is rapid (autoxidation) or staggered (second-generation) formation. Our experimental results indicate that instead of undergoing rapid formation, m/z 223 showed a staggered formation with a 5 min delay in comparison to m/z 191. However, our observations are gleaned from offline measurements and as such, online measurements for further confirmation would be needed.[244] We utilized m/z 191 (identified as ROOH) to further demonstrate the effects of wavelength and concentration in the following sections (2.3.2 & 2.3.3). Figure 2.2 (C) highlights the EIC of second-generation peroxide from 1-OA at m/z 207 ($[(C_8H_{16}O_6)\text{-}H]^-$). Figure 2.2 (D) is demonstrating the EIC of newly found ROOH from PNA, constituting 2-OOH groups at m/z 249 ($[(C_9H_{14}O_8)\text{-}H]^-$). Many of these products have a very small signal intensity and identifying them as ROOH is challenging. However, performing each reaction condition in triplicates offers confidence. Each EIC in Figure 2.2 is a comparison between ID-C and ID-T chromatograms obtained by averaging triplicate measurements. We have normalized the ion signal intensity with our internal standard (AZA). Currently, we have only shown one of the triplicate measurements for PNA and 1-OA to represent optimum chromatographic separation. An average chromatogram is shown in Figure A.7 (Appendix A, Section A.7.1). As an exception, we decreased I^- concentration by 10 times for the current investigation into PNA due to the overloading of salt concentration.

Similar to other studies, ion signals that dropped by more than 90% in triplicated experiments were categorized as ROOHs.[180, 245] Figure 2.2 (B) further demonstrates the selectivity of iodometry. Here, we observe multiple chromatographically separated peaks in the ID-C sample, amongst which only the peak at retention time

(Rt) of 1.6 min was reduced to >90%. The peaks in ID-T samples are noise after smoothing and do not represent EIC at specific m/z. In contrast, the peak at Rt of 3 min in Figure 2.2 (B) for the ID-C sample remained unchanged in comparison to the ID-T sample.

Apart from the reduction of signal response, alcohol formation is another indication of peroxy functionality on a compound.[170, 246] Although I^- is known to reduce ROOH to corresponding alcohols,[180, 245] previous studies have not demonstrated the formation of such alcohols.[180, 239, 245] In the current study, we have observed that m/z corresponding to alcohols from peroxide precursor showed an enhanced signal response when comparisons were drawn between ID-C and ID-T samples. For instance, the reduction of the first-generation peroxide of 7-OE (m/z 191) would yield an alcohol at m/z 175 due to the loss of one O atom. Thus, the overlayed normalized signal response of m/z 175 in the inset window of Figure 2.2 (A) showed an increased signal response when compared with the ID-C sample. This observation was unanimously observed for each ROOH product in experimented OAcs, as monitored in the insets of Figure 2.2 (B), 2.2 (C), and 2.2 (D). The formation of alcohols and other side products (e.g., Figure A.4, Russell mechanism) such as m/z 205 ($[(C_8H_{14}O_6)\text{-}H]^-$), m/z 173 ($[(C_8H_{14}O_4)\text{-}H]^-$) were observed during the photooxidation of select OAcs.[247, 248] Therefore, it is understandable that the peaks corresponding to alcohols were present before the iodometry treatment.

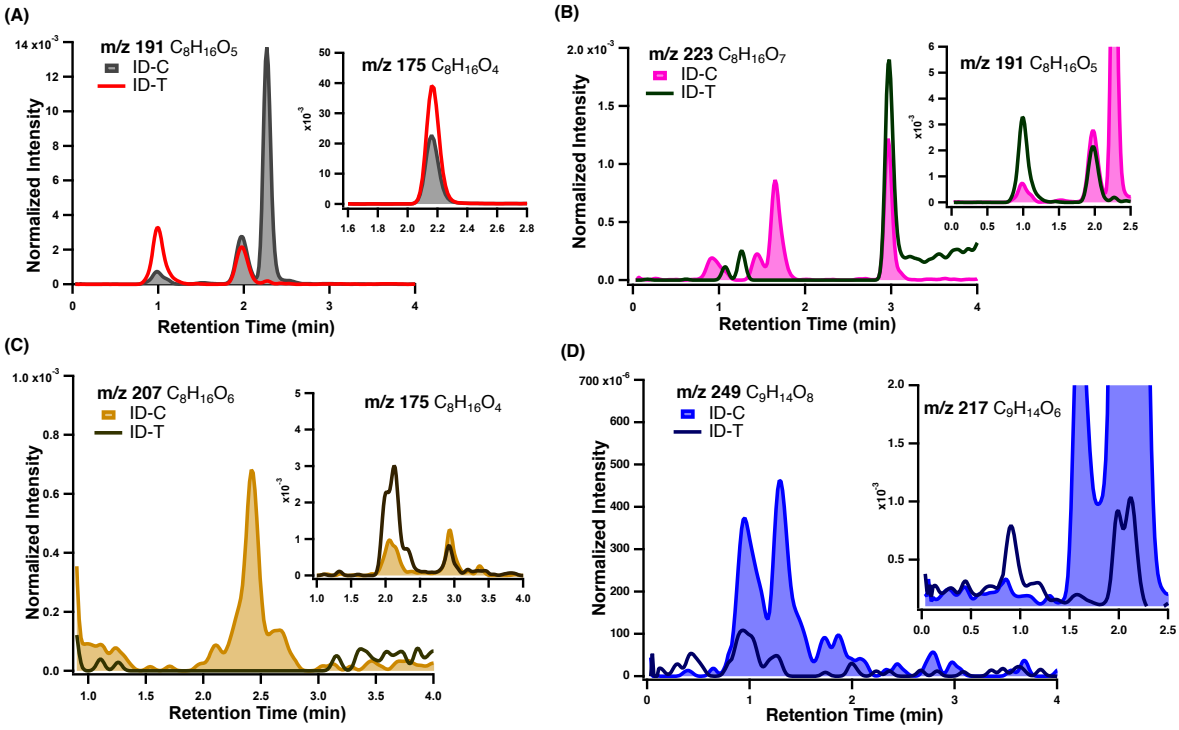

Figure 2.2: Extracted Ion Chromatogram (EIC) of key ROOHs from different OA precursors. Signals, in the format of $[M\text{-}H]^-$, for each sample have been normalized with respect to the internal standard. The inset represents the formation of corresponding alcohol after iodometry treatment. (A) First-generation ROOH of 7-OE at m/z 191 ($[(C_8H_{16}O_5)\text{-}H]^-$); (B) Second-generation ROOH of 7-OE at m/z 223 ($[(C_8H_{16}O_7)\text{-}H]^-$); (C) ROOH from 1-OA at m/z 207 ($[(C_8H_{16}O_6)\text{-}H]^-$); (D) ROOH from PNA is found at m/z 249 ($[(C_9H_{14}O_8)\text{-}H]^-$).

We assessed the environmental relevance of aqueous-phase photooxidation by studying peroxide formation in PNA and LMA, which are major oxidation products from the ozonolysis of terpenes.[220, 221, 244, 249–253] A recent study by Amorim et al,[244] explored aqueous-phase oxidation of PNA and highlighted the formation of first-generation peroxide products, but there was no evidence of the formation of second-generation oxygenated species. However, this could be due to different chemical conditions.[244] Based on the detailed oxidation mechanism of PNA[244] and general dependency of RO_2 radical-driven H-shifts on precursor structures,[254, 255] we found that the oxygenated products from PNA were similar to that of 1-OA (Appendix A, Figure A.5). In contrast, LMA only exhibited the formation of a first-generation peroxide at m/z 233 ($[(C_{10}H_{18}O_6)\text{-}H]^-$) as shown in Figure A.8

(Appendix A, Section A.7.2). The lack of second-generation ROOH product in LMA is likely not observed due to its signal being below the detection limit. Our current observations on LMA are consistent with the work of Witkowski et al.[222] A more detailed discussion on the mechanism for expected product formation is provided in Section A.5 (Appendix A). While aqueous-phase photochemical production of peroxides is known,[256] it is unclear whether autoxidation or RO_2+HO_2 radical chemistry can be related with this process. We have provided evidence on the aqueous-phase generation of products with multiple OOH groups in both synthetic (i.e., 7-OE) and atmospherically representative compounds. In the next section, we investigated the factors affecting the formation of these oxygenated compounds.

2.3.2 Wavelength Exposure

The fate of numerous water-soluble organic compounds in tropospheric cloud water can be photochemically controlled by oxidants such as HO_x radicals.[101] However, the production of such oxidants can be dependent on both the intensity and the type of incoming UV radiation.[101, 257] To quantify the impact of wavelength, we made a relative comparison in the amount of ROOHs formed by acquiring an empirical yield (γ) (eq-A2). Due to a lack of appropriate standards, we are currently unable to quantify the ROOHs and thus, assume that the peak area is proportional to the concentration of ROOHs as a preliminary way to estimate the γ of ROOHs. A more detailed discussion on the estimation of γ is provided in Section A.6.1 (Appendix A). Figure 2.3 displays experimentally determined γ of m/z 223 as a function of varying wavelengths. The inset window shows the absorption spectra corresponding to the lamps used in our photo reactor. The intensity of each lamp was kept constant as demonstrated by photon flux in Figure A.3 (Appendix A, Section A.4). The peroxide product at m/z 223 was non-quantifiable after exposure to UVC due to complete degradation during photooxidation. This degradation was corroborated via a switch experiment from UVB to UVC as shown in Figure A.9 (Appendix A, Section A.8.1). These observations highlight that UVC can compromise the stability of ROOHs, despite its efficient production of OH radicals.[257, 258] Photolysis of ROOH species by UVC gives rise to another OH radical and alkoxy radicals (RO),[72] which will subsequently decompose to form small OAcs (C_2-C_4). The method used in the cur-

rent study could not retain these small and polar compounds. In contrast to UVC, the peroxide production under UVB was relatively easier to estimate as noticed by an increase in the γ for m/z 223. Additionally, we also explored the effects of longer wavelengths on the formation of expected ROOHs. Due to the lower efficiency of OH radical generation at UVA,[130, 218, 219, 259] we scaled photooxidation time and the concentration of H_2O_2 to match the consumption of 7-OE across UVB and UVA (Table A.4). As such, the exposure time for UVA was carefully considered (Figure A.10) such that 56% of 7-OE was observed to be consumed amongst all wavelength exposures. Exposure to UVA showed a greater increase in the γ of m/z 223. This trend was similarly observed for the first-generation peroxide product at m/z 191 as shown in Figure A.9 (S7.2) (Appendix A, Section A.8.1). There have been several studies which have explored aqueous-phase photooxidation of OAcs,[219, 259, 260] a few of which have focused on the formation of organic peroxides.[243, 260, 261] UVC is often employed in laboratory-conducted aqueous-phase investigations on photochemical oxidation of OAcs,[258, 261, 262] but some studies have utilized UVA and UVB to achieve the same purpose.[219, 263] Our observations highlight that despite achieving steady-state concentration of OH radicals under varying irradiated wavelengths, photolytic degradation of RO_2 radicals is exacerbated under exposure to UVC rather than UVB and UVA.[264, 265] Additionally, while UVC may induce efficient generation of RO_2,[266, 267] this could impede ROOH formation in a similar manner as described in Section 2.3.3. Our findings demonstrate that the transformation of water-soluble organics could be crucially dependent on illuminated light utilized in cloud water simulators, especially for fundamental laboratory investigations.

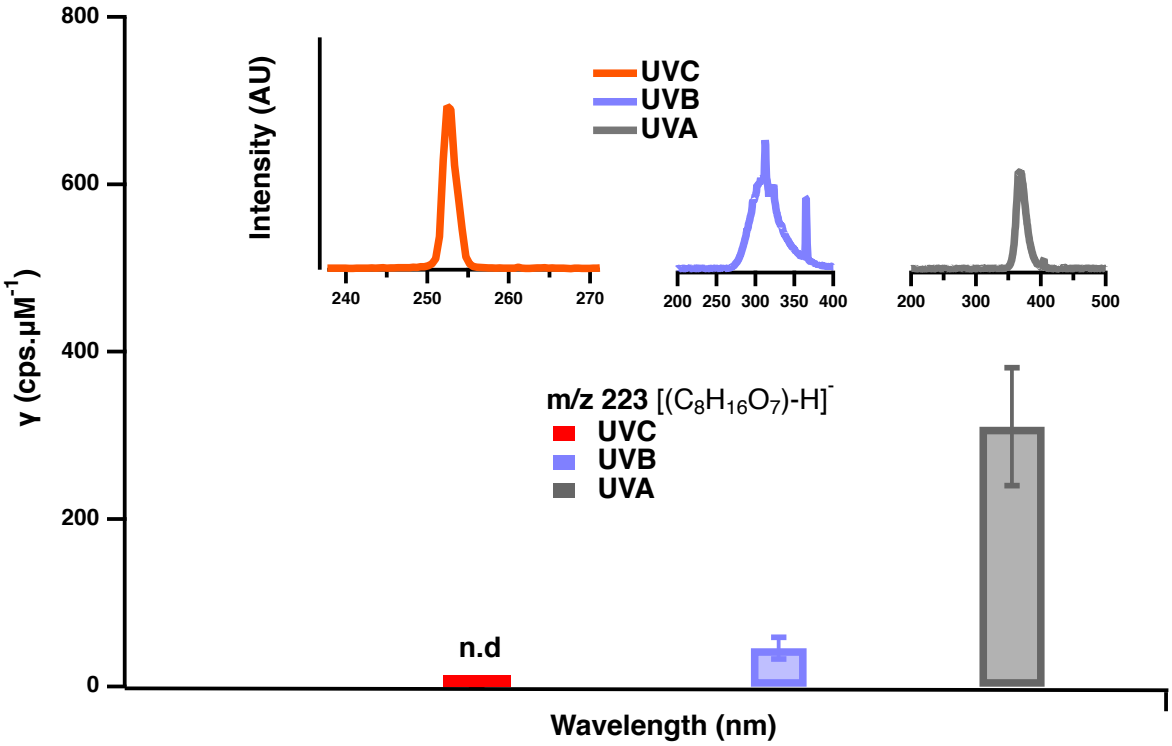

Figure 2.3: Estimated yield (γ) of second-generation product of 7-OE at m/z 223 as a function of varying wavelengths: UVC, UVB and UVA. Lack of product formation under UVC is represented as "Not detected". The inset represents the absorption spectra acquired using spectroradiometer for each wavelength. Error bars represent 1σ for triplicate measurements.

2.3.3 Effects of precursor and oxidant concentrations

Studies on gas-phase autoxidation have demonstrated that the lifetime of RO_2 radicals is a determinant factor for autoxidation.[209] RO_2 has multiple reaction pathways,[268] and the lifetime of RO_2 radicals is intricately affected by the concentration of reacting partners.[269] Thus, in this section, we have investigated the impact of reactant and oxidant concentrations on the γ of ROOHs. Figure 2.4 illustrates the intercomparison between γ of first- and second-generation ROOHs found at m/z 191 and m/z 223 respectively under varying oxidant and precursor concentrations. $[OH]_{SS}$ is estimated using the relative rate method as explained in Section A.6.2. Our current investigations were conducted with relevant steady-state cloud water OH concentrations to observe product formation.[99, 270] Figures 2.4 (A) and 2.4 (B) are representative of estimated yields for m/z 191 and m/z 223 as a function of in-

creasing $[OH]_{SS}$ while 7-OE is kept constant. The estimated $[OH]_{SS}$ corresponding to each H_2O_2 concentration is reported in Table S5. The γ of m/z 191 was estimated at ∼50-65% consumption of 7-OE while that of m/z 223 was estimated at >90% consumption. The reasoning behind this difference was based on the fact that γ is time-dependent, as shown in Figure A.10 (Appendix A, Section A.8.2). Therefore, in order to demonstrate the observations for the effects of RO_2 chemistry, we chose the period of OE consumption which would give a relatively consistent yield for each peroxide. Note that despite our careful attempts, it was difficult to acquire yield for m/z 223 under a lower 7-OE consumption range (20-50%). This is because there is not enough first-generation RO_2 radical (P1-Figure A.4) to successfully form the expected second-generation product. We observed a declining trend in the γ of m/z 191 and m/z 223 with increasing $[OH]_{SS}$. This trend can be understood on the basis of reaction pathways demonstrated in Figure 2.5. Under relatively lower $[OH]_{SS}$, we observed higher yields of m/z 191 and m/z 223. Such a trend could be due to the favoured formation of expected products under pathway 1c. However, as $[OH]_{SS}$ increases, termination by pathway 1c becomes less favourable due to the potentially interfering chemistry of HO_2 radicals as evident by pathways 1a and 1b.[235, 243]

Figures 2.4 (C) and 2.4 (D) illustrate the γ corresponding to m/z 191 and m/z 223 as a function of 7-OE concentration while H_2O_2 was maintained at a constant concentration. Similar to the measurements for increasing $[OH]_{SS}$, the γ of m/z 191 was estimated when 7-OE was partially consumed while that of m/z 223 was estimated under excessive consumption. The intercomparison between m/z 191 and m/z 223 showed a non-linear increase for γ of m/z 191, while γ of m/z 223 continuously declined with increasing 7-OE concentrations. Note, we also observed a steady decline in $[OH]_{SS}$ as 7-OE concentration was increased from 179 μM to 1000 μM. These values are reported in Table A.5 (Appendix A, Section A.6.1). The lifetime of RO_2 radicals can be very difficult to gauge due to undergoing multiple reaction pathways.[247, 271] Despite the complexity associated with RO_2 radicals,[269, 271, 272] we believe that the decreasing trend in the γ of m/z 223 (Figure 2.4 (D) can be attributed to pathway 1d in Figure 2.5. It is our understanding that at enhanced precursor concentrations, the RO_2 radicals can form unstable oxygenated intermediates (e.g., tetroxides),[247, 271] which are highly likely to decompose to alcohols and carbonyls. While additional

decomposition products such as ROOR can be expected,[272] it would be possible at even higher precursor concentrations (>10 mM), which are irrelevant to cloud water conditions. The potential products forming due to RO_2 + RO_2 radical chemistry (pathway 1D) such as ketone at m/z 173 ([($C_8H_{14}O_4$)-H]$^-$) and alcohol at m/z 175 ([($C_8H_{16}O_4$)-H]$^-$) have been observed in the current work as mentioned in the Section 2.3.1.

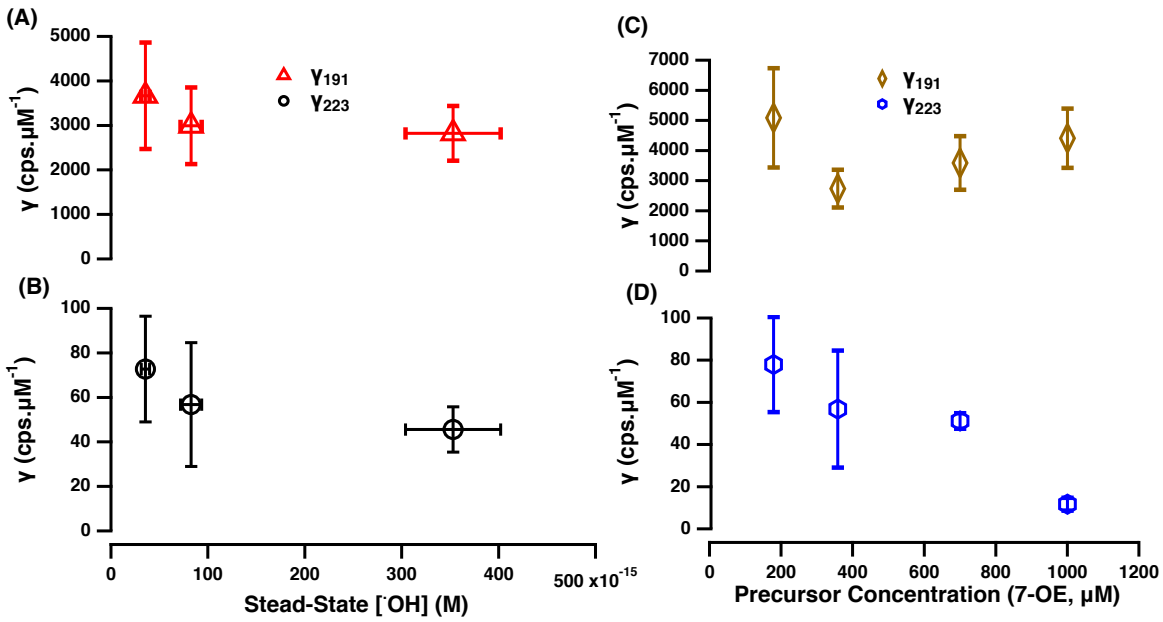

Figure 2.4: Estimated γ for first- and second-generation ROOHs, presented as a function of varying $[OH]_{SS}$ and precursor (7-OE) concentration. γ is shown as a function of increasing $[OH]_{SS}$ for (A) m/z 191 and (B) m/z 223. γ of m/z 191 and m/z 223 is demonstrated as a function of increasing 7-OE concentration in (C) and (D) respectively. Error bars represent 1σ from triplicate measurements.

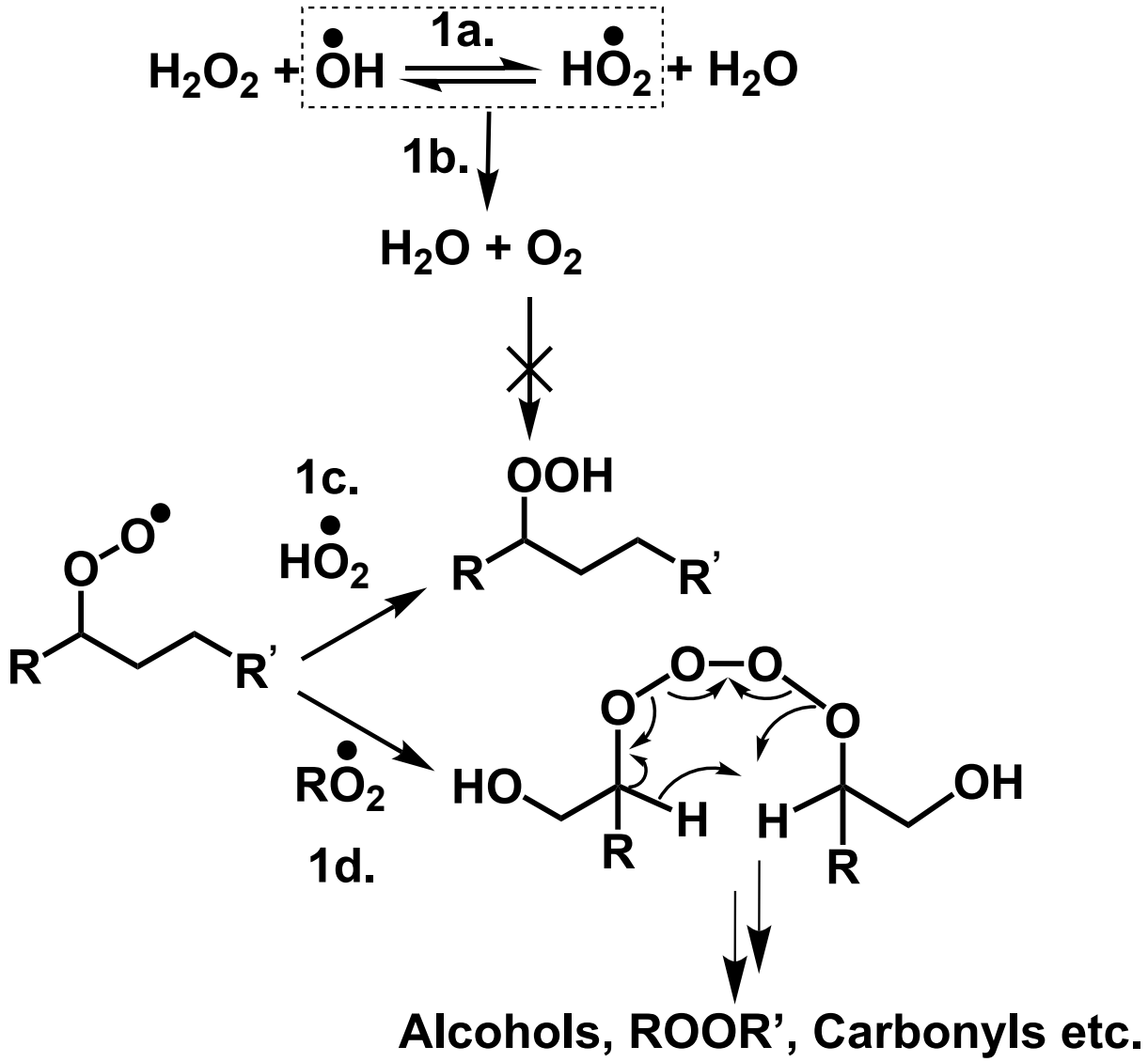

Figure 2.5: Major peroxy radical chemistry occurring during photooxidation experiments.

Based on the above observations, we hypothesize that the γ of aqueous ROOHs can be suppressed by increasing oxidant and precursor concentrations. Previous studies have shown that the total concentration of water-soluble organics in the ambient cloud water can vary between 67-500 μM (assuming a 3-5 C number range).[273] While our experimented concentration falls within this range, many of the laboratory-led aqueous-phase investigations have typically experimented with high concentrations of organic precursors and oxidants.[99, 225, 227, 243, 261, 263] These conditions can inadvertently suppress the formation of key aqueous intermediates (e.g, ROOH).

In addition to the total reported concentration of water-soluble organics in the literature, it is our understanding that RO_2 radical chemistry is likely to be governed by both the concentration and composition of WSOCs to facilitate aqueous ROOHs. For instance, in the recent work of Piletic et al,[274] modelled simulations using CMAQv5.2[275] on VOC oxidation highlighted the importance of factors such as stereoselectivity, alkyl substituents, ring conformations and steric hindrance, which can ultimately affect the formation of peroxy intermediates. This is further supported by our observations on the lack of second-generation ROOH product from sterically hindered precursor i.e. limononic acid (Section A.7.2).[222, 276] Thus, it is important to incorporate the structural limitations to carefully investigate the modelled representations of RO_2 radicals in both remote biogenic and urban environments. It is important to note that aside from the detailed approach adopted in our study, there is a lack of literature to evidence autoxidation-initiated ROOHs. Future work should incorporate sensitive radical measurements to pursue substantial evidence on the occurrence of aqueous-phase autoxidation.

2.4 Atmospheric Implications

In the current study, we have systematically investigated the aqueous formation of ROOHs, which can affect environment in varying degree (e.g., altering oxidative capacity, initiating atmospheric acidification etc.).[277, 278] Our findings demonstrate that ROOHs are observed in the aqueous-phase photooxidation of four OAcs employed in our study. Using a unique LC-MS technique assisted by iodometry, we confirmed that the observed ROOH species are consistent with those arising from OH/HO_2 rad-

ical chemistry or aqueous-phase autoxidation. Structural suitability, concentration, and irradiation wavelength play an important role in propagating the formation of observed ROOHs. While our study focused on a specific class of organic compounds, i.e., OA, we believe that the formation of ROOH studied here is applicable to a wide spectrum of water-soluble organic compounds present in cloud water. Generation of low-volatility HOMs such as peroxides,[160] add to the climate (SOA formation)[170, 245, 279] and health (ROS)[280] burden of atmospheric particulate matter. Further, ROOH species serve as reservoirs of radicals;[71] as such, their formation via radical chemistry has significant implications for the HO_x cycle and atmospheric oxidative capacity.[261, 281]

Based on our observations, we postulate that many of the previous laboratory studies may have overlooked the importance of aqueous-phase formation of HOMs with multiple OOH groups due to commonly used experimental conditions which in turn may have impeded the formation of key ROOH intermediates.[99, 225, 227] Ambient sunlight reaching the ground level contains no UVC,[282] while the photon flux increases exponentially from 290 nm (UVB) to 400 nm (UVA) and visible light.[282] Our observations show that the yield of ROOHs also followed an exponential increase as UV light with longer wavelengths (UVB and UVA) was used. UVC, which is irrelevant to the ambient sunlight yet has been used in laboratory studies,[258, 261, 262] has completely photolyzed ROOHs. Our observation also suggests that increasing concentrations of reactants, including both the OH radical and the precursor organic compound, favours the HO_2/RO_2 reaction pathway (Figure 2.5). However, the underlying chemistry is nonlinear and could not be explicitly explained with our approach. The OH radical concentration in ambient cloud water is in the range of 10^{-12}-10^{-14} M.[99, 101] On the other hand, the concentration of water-soluble organics in ambient cloud water can range between 67-500 μM (or 200-2230 μmol C L^{-1})[273]. In polluted environments, the concentration of water-soluble organic compounds in fog waters can be up to 800 μM (equivalent to 4000 μmol C L^{-1}).[273] The concentrations experimented in our study falls within this range (179-1000 μM). On the other hand, laboratory experiments have typically employed OH radical and organic precursors at much greater concentrations, which may have impeded RO_2/HO_2 radical chemistry.[95, 99, 225, 227, 261, 263]

While the aforementioned experimental observations highlight the occurrence of ROOHs in the aqueous-phase, the underlying mechanism (either OH/HO_2 chemistry or autoxidation) depends on an array of factors which could not be fully addressed in the current work. The observed ROOH products could not be quantified due to a lack of suitable ROOH standards or surrogates.[180, 283]Additionally, the ionization efficiencies of structurally varying molecules can be drastically different in ESI-MS.[242, 284] Future studies should utilize synthesized compounds or reasonable surrogates to achieve successful quantification of ROOH species. Lastly, without in-situ radical measurements,[285] it is difficult to determine the underlying mechanism pertaining to the formation of aqueous ROOHs. Currently, the key to differentiating between OH/HO_2 pathway or autoxidation relies on identifying staggered or immediate formation of ROOHs. While our offline measurements indicate a delay between first-and second-generation OOH products, future studies should incorporate online measurements for better time resolution to determine aqueous-phase oxidation products.[244] Overall, our study highlights the importance of reaction mechanisms favoring aqueous-phase formation of HOMs.

2.5 Acknowledgement

We thank the University of Alberta Department of Chemistry and MS facility to allow instrumental operation during the course of this project. We thank Dr. Julie Gibbs' laboratory for allowing the usage of LC instrumentation and acknowledge Anantha and Nahida for assisting with the purification of organic compounds. The research project was funded by NSERC Discovery Grant (RGPIN2018-03814) and Canada Foundation for Innovation (Project: 38334). PNA synthesis, purification, and characterization were conducted by Dr. Florence Williams (University of Iowa).

2.6 Appendix A

Additional experimental details, including product synthesis, mechanism, kinetic investigation, yield calculations and product characterization.

References

[20] P. H. Chowdhury, Q. He, R. Carmieli, C. Li, Y. Rudich, and M. Pardo, "Connecting the Oxidative Potential of Secondary Organic Aerosols with Reactive Oxygen Species in Exposed Lung Cells," en, *Environmental Science & Technology*, vol. 53, no. 23, pp. 13 949–13 958, Dec. 2019, ISSN: 0013-936X, 1520-5851. DOI: 10.1021/acs.est.9b04449.

[66] S. Wang, Y. Zhao, A. W. H. Chan, M. Yao, Z. Chen, and J. P. D. Abbatt, "Organic Peroxides in Aerosol: Key Reactive Intermediates for Multiphase Processes in the Atmosphere," en, *Chemical Reviews*, vol. 123, no. 4, pp. 1635–1679, Feb. 2023, ISSN: 0009-2665, 1520-6890. DOI: 10.1021/acs.chemrev.2c00430.

[70] P. Lightfoot *et al.*, "Organic peroxy radicals: Kinetics, spectroscopy and tropospheric chemistry," en, *Atmospheric Environment. Part A. General Topics*, vol. 26, no. 10, pp. 1805–1961, Jul. 1992, ISSN: 09601686. DOI: 10.1016/0960-1686(92)90423-I.

[71] M. Krapf *et al.*, "Labile Peroxides in Secondary Organic Aerosol," en, *Chem*, vol. 1, no. 4, pp. 603–616, Oct. 2016, ISSN: 24519294. DOI: 10.1016/j.chempr.2016.09.007.

[72] S. A. Epstein, S. L. Blair, and S. A. Nizkorodov, "Direct Photolysis of α-Pinene Ozonolysis Secondary Organic Aerosol: Effect on Particle Mass and Peroxide Content," en, *Environmental Science & Technology*, vol. 48, no. 19, pp. 11 251–11 258, Oct. 2014, ISSN: 0013-936X, 1520-5851. DOI: 10.1021/es502350u.

[91] G. Hasan, V. Salo, R. R. Valiev, J. Kubecka, and T. Kurten, "Comparing Reaction Routes for roor Intermediates Formed in Peroxy Radical Self- and Cross-Reactions," en, *The Journal of Physical Chemistry A*, vol. 124, no. 40, pp. 8305–8320, Oct. 2020, ISSN: 1089-5639, 1520-5215. DOI: 10.1021/acs.jpca.0c05960.

[92] T. Berndt *et al.*, "Accretion Product Formation from Self and CrossReactions of RO_2Radicals in the Atmosphere," en, *Angewandte Chemie International Edition*, vol. 57, no. 14, pp. 3820–3824, Mar. 2018, ISSN: 1433-7851, 1521-3773. DOI: 10.1002/anie.201710989.

[95] Y. B. Lim, Y. Tan, M. J. Perri, S. P. Seitzinger, and B. J. Turpin, "Aqueous chemistry and its role in secondary organic aerosol (SOA) formation," en, *Atmospheric Chemistry and Physics*, vol. 10, no. 21, pp. 10 521–10 539, Nov. 2010, ISSN: 1680-7324. DOI: 10.5194/acp-10-10521-2010.

[99] H. Herrmann, D. Hoffmann, T. Schaefer, P. Brauer, and A. Tilgner, "Tropospheric Aqueous Phase Free Radical Chemistry Radical Sources, Spectra, Reaction Kinetics and Prediction Tools," en, *ChemPhysChem*, vol. 11, no. 18, pp. 3796–3822, Dec. 2010, ISSN: 1439-4235, 1439-7641. DOI: 10.1002/cphc.201000533.

[101] A. Bianco, M. Passananti, M. Brigante, and G. Mailhot, "Photochemistry of the Cloud Aqueous Phase: A Review," en, *Molecules*, vol. 25, no. 2, p. 423, Jan. 2020, ISSN: 1420-3049. DOI: 10.3390/molecules25020423.

[108] L. Ma, C. Guzman, C. Niedek, T. Tran, Q. Zhang, and C. Anastasio, "Kinetics and Mass Yields of Aqueous Secondary Organic Aerosol from Highly Substituted Phenols Reacting with a Triplet Excited State," en, *Environmental Science & Technology*, vol. 55, no. 9, pp. 5772–5781, May 2021, ISSN: 0013-936X, 1520-5851. DOI: 10.1021/acs.est.1c00575.

[109] R. Kaur and C. Anastasio, "First Measurements of Organic Triplet Excited States in Atmospheric Waters," en, *Environmental Science & Technology*, vol. 52, no. 9, pp. 5218–5226, May 2018, ISSN: 0013-936X, 1520-5851. DOI: 10.1021/acs.est.7b06699.

[130] D. W. Gunz and M. R. Hoffmann, "Atmospheric chemistry of peroxides: A review," en, *Atmospheric Environment. Part A. General Topics*, vol. 24, no. 7, pp. 1601–1633, Jan. 1990, ISSN: 09601686. DOI: 10.1016/0960-1686(90)90496-A. [Online]. Available: https://linkinghub.elsevier.com/retrieve/pii/096016869090496A (visited on 01/29/2024).

[148] M. Weloe and T. Hoffmann, "Application of time of flight aerosol mass spectrometry for the real time measurement of particle phase organic peroxides an online redox derivatization aerosol mass spectrometer (ORDAMS)," en, *Atmospheric Measurement Techniques*, vol. 13, no. 10, pp. 5725–5738, Oct. 2020, ISSN: 1867-8548. DOI: 10.5194/amt-13-5725-2020.

[160] H. O. Pye *et al.*, "Anthropogenic enhancements to production of highly oxygenated molecules from autoxidation," *Proceedings of the National Academy of Sciences*, vol. 116, no. 14, pp. 6641–6646, 2019.

[169] S. Zhou, J. C. Rivera-Rios, F. N. Keutsch, and J. P. D. Abbatt, "Identification of organic hydroperoxides and peroxy acids using atmospheric pressure chemical ionization tandem mass spectrometry (APCI/MS/MS) application to secondary organic aerosol," English, *Atmospheric Measurement Techniques*, vol. 11, no. 5, pp. 3081–3089, May 2018, ISSN: 1867-1381. DOI: https://doi.org/10.5194/amt-11-3081-2018. (visited on 08/13/2019).

[170] K. S. Docherty, W. Wu, Y. B. Lim, and P. J. Ziemann, "Contributions of Organic Peroxides to Secondary Aerosol Formed from Reactions of Monoterpenes with O_3, volume = 39," en, *Environmental Science & Technology*, no. 11, pp. 4049–4059, Jun. 2005, ISSN: 0013-936X, 1520-5851. DOI: 10.1021/es050228s. (visited on 02/11/2024).

[180] R. Zhao, C. M. Kenseth, Y. Huang, N. F. Dalleska, and J. H. Seinfeld, "Iodometry-Assisted Liquid Chromatography Electrospray Ionization Mass Spectrometry for Analysis of Organic Peroxides: An Application to Atmospheric Secondary Organic Aerosol," *Environmental Science & Technology*, vol. 52, no. 4, pp. 2108–2117, Feb. 2018, ISSN: 0013-936X. DOI: 10.1021/acs.est.7b04863. (visited on 08/08/2019).

[183] T. Gautam, S. Wu, J. Ma, and R. Zhao, "Potential Matrix Effects in Iodometry Determination of Peroxides Induced by Olefins," en, *The Journal of Physical Chemistry A*, vol. 126, no. 17, pp. 2632–2644, May 2022, ISSN: 1089-5639, 1520-5215. DOI: 10.1021/acs.jpca.1c10717. [Online]. Available: https://pubs.acs.org/doi/10.1021/acs.jpca.1c10717 (visited on 10/15/2022).

[191] C. Fittschen, "The reaction of peroxy radicals with oh radicals," *Chemical Physics Letters*, vol. 725, pp. 102–108, 2019.

[192] N. A. Porter, "Mechanisms for the autoxidation of polyunsaturated lipids," en, *Accounts of Chemical Research*, vol. 19, no. 9, pp. 262–268, Sep. 1986, ISSN: 0001-4842, 1520-4898. DOI: 10.1021/ar00129a001. [Online]. Available: https://pubs.acs.org/doi/abs/10.1021/ar00129a001 (visited on 08/12/2022).

[193] R. A. Cox and J. A. Cole, "Chemical aspects of the autoignition of hydrocarbon air mixtures," en, *Combustion and Flame*, vol. 60, no. 2, pp. 109–123, May 1985, ISSN: 0010-2180. DOI: 10.1016/0010-2180(85)90001-X. (visited on 02/27/2022).

[194] A. A. Boyd, P.-M. Flaud, N. Daugey, and R. Lesclaux, "Rate constants for RO_2+ HO_2 reactions measured under a large excess of HO_2," *The Journal of Physical Chemistry A*, vol. 107, no. 6, pp. 818–821, 2003, Publisher: ACS Publications.

[195] P. Stevens *et al.*, "HO_2/OH and RO_2/HO_2 ratios during the Tropospheric OH Photochemistry Experiment Measurement and theory," *Journal of Geophysical Research: Atmospheres*, vol. 102, no. D5, pp. 6379–6391, 1997.

[196] U. Molteni *et al.*, "Formation of highly oxygenated organic molecules from aromatic compounds," *Atmospheric Chemistry and Physics*, vol. 18, no. 3, pp. 1909–1921, 2018, Publisher: Copernicus GmbH.

[197] T. Berndt *et al.*, "Hydroxyl radical-induced formation of highly oxidized organic compounds," *Nature communications*, vol. 7, no. 1, p. 13 677, 2016, Publisher: Nature Publishing Group UK London.

[198] O. Perakyla, M. Riva, L. Heikkinen, L. Quelever, P. Roldin, and M. Ehn, "Experimental investigation into the volatilities of highly oxygenated organic molecules (HOMs)," *Atmospheric Chemistry and Physics*, vol. 20, no. 2, pp. 649–669, 2020, Publisher: Copernicus GmbH.

[199] J. D. Crounse, L. B. Nielsen, S. Jorgensen, H. G. Kjaergaard, and P. O. Wennberg, "Autoxidation of Organic Compounds in the Atmosphere," *The Journal of Physical Chemistry Letters*, vol. 4, no. 20, pp. 3513–3520, Oct. 2013. DOI: 10.1021/jz4019207.

[200] E. Assaf, C. Schoemaecker, L. Vereecken, and C. Fittschen, "Experimental and theoretical investigation of the reaction of RO_2 radicals with OH radicals: Dependence of the HO_2 yield on the size of the alkyl group," *International journal of chemical kinetics*, vol. 50, no. 9, pp. 670–680, 2018, Publisher: Wiley Online Library.

[201] S. Wang, Q. Zhang, G. Wang, Y. Wei, W. Wang, and Q. Wang, "The neglected autoxidation pathways for the formation of highly oxygenated organic molecules (HOMs) and the nucleation of the HOMs generated by limonene," *Atmospheric Environment*, vol. 304, p. 119 727, 2023.

[202] R. Xu *et al.*, "Global simulations of monoterpene-derived peroxy radical fates and the distributions of highly oxygenated organic molecules (HOMs) and accretion products," *Atmospheric Chemistry and Physics*, vol. 22, no. 8, pp. 5477–5494, 2022, Publisher: Copernicus GmbH.

[203] J. P. Nascimento *et al.*, "Major Regional-Scale Production of O_3 and Secondary Organic Aerosol in Remote Amazon Regions from the Dynamics and Photochemistry of Urban and Forest Emissions," *Environmental Science & Technology*, vol. 56, no. 14, pp. 9924–9935, 2022, Publisher: ACS Publications.

[204] X. Fu *et al.*, "High-resolution simulation of local traffic-related no_x dispersion and distribution in a complex urban terrain," *Environmental Pollution*, vol. 263, p. 114 390, 2020.

[205] P. Ni, X. Wang, and H. Li, "A review on regulations, current status, effects and reduction strategies of emissions for marine diesel engines," *Fuel*, vol. 279, p. 118 477, 2020, Publisher: Elsevier.

[206] M. D. LaCount, R. A. Haeuber, T. R. Macy, and B. A. Murray, "Reducing power sector emissions under the 1990 Clean Air Act Amendments: A retrospective on 30 years of program development and implementation," *Atmospheric Environment*, vol. 245, p. 118 012, 2021, Publisher: Elsevier.

[207] E. Tsiligiannis, J. Hammes, C. M. Salvador, T. F. Mentel, and M. Hallquist, "Effect of NO_x on 1,3,5-trimethylbenzene (TMB) oxidation product distribution and particle formation," en, *Atmospheric Chemistry and Physics*, vol. 19, no. 23, pp. 15 073–15 086, Dec. 2019, ISSN: 1680-7324. DOI: 10.5194/acp-19-15073-2019. [Online]. Available: https://acp.copernicus.org/articles/19/15073/2019/.

[208] W. Zhang, Z. Zhao, C. Shen, and H. Zhang, "Unexpectedly Efficient Aging of Organic Aerosols Mediated by Autoxidation," *Environmental Science & Technology*, vol. 57, no. 17, pp. 6965–6974, 2023, Publisher: ACS Publications.

[209] E. Praske *et al.*, "Atmospheric autoxidation is increasingly important in urban and suburban North America," *Proceedings of the National Academy of Sciences*, vol. 115, no. 1, pp. 64–69, Jan. 2018. DOI: 10.1073/pnas.1715540115. [Online]. Available: http://www.pnas.org/doi/10.1073/pnas.1715540115 (visited on 06/11/2022).

[210] J. D. Crounse *et al.*, "Atmospheric Fate of Methacrolein. 1. Peroxy Radical Isomerization Following Addition of OH and O_2," en, *The Journal of Physical Chemistry A*, vol. 116, no. 24, pp. 5756–5762, Jun. 2012, ISSN: 1089-5639, 1520-5215. DOI: 10.1021/jp211560u.

[211] K. Stemmler and U. Von Gunten, "OH radical-initiated oxidation of organic compounds in atmospheric water phases: Part 2. Reactions of peroxyl radicals with transition metals," en, *Atmospheric Environment*, vol. 34, no. 25, pp. 4253–4264, Jul. 2000, ISSN: 13522310. DOI: 10.1016/S1352-2310(00)00219-3. [Online]. Available: https://linkinghub.elsevier.com/retrieve/pii/S1352231000002193 (visited on 01/29/2024).

[212] Y. Zuo and J. Hoigne, "Formation of hydrogen peroxide and depletion of oxalic acid in atmospheric water by photolysis of iron(III)-oxalato complexes," en, *Environmental Science & Technology*, vol. 26, no. 5, pp. 1014–1022, May 1992, ISSN: 0013-936X, 1520-5851. DOI: 10.1021/es00029a022. (visited on 01/29/2024).

[213] J. Wei, T. Fang, C. Wong, P. S. Lakey, S. A. Nizkorodov, and M. Shiraiwa, "Superoxide formation from aqueous reactions of biogenic secondary organic aerosols," *Environmental Science & Technology*, vol. 55, no. 1, pp. 260–270, 2020, Publisher: ACS Publications.

[214] R Kaur and C Anastasio, "Light absorption and the photoformation of hydroxyl radical and singlet oxygen in fog waters," *Atmospheric Environment*, vol. 164, pp. 387–397, 2017, Publisher: Elsevier.

[215] M. Yao *et al.*, "Multiphase reactions between secondary organic aerosol and sulfur dioxide: Kinetics and contributions to sulfate formation and aerosol aging," *Environmental Science & Technology Letters*, vol. 6, no. 12, pp. 768–774, 2019, Publisher: ACS Publications.

[216] M. Hu, K. Chen, J. Qiu, Y.-H. Lin, K. Tonokura, and S. Enami, "Decomposition mechanism of α-alkoxyalkyl-hydroperoxides in the liquid phase: Temperature dependent kinetics and theoretical calculations," *Environmental Science: Atmospheres*, vol. 2, no. 2, pp. 241–251, 2022, Publisher: Royal Society of Chemistry.

[217] S. Toyokuni, "Reactive oxygen species-induced molecular damage and its application in pathology," *Pathology international*, vol. 49, no. 2, pp. 91–102, 1999, Publisher: Wiley Online Library.

[218] K. M. Badali *et al.*, "Formation of hydroxyl radicals from photolysis of secondary organic aerosol material," English, *Atmospheric Chemistry and Physics*, vol. 15, no. 14, pp. 7831–7840, Jul. 2015, ISSN: 1680-7316. DOI: https://doi.org/10.5194/acp-15-7831-2015.

[219] T. Charbouillot *et al.*, "Mechanism of carboxylic acid photooxidation in atmospheric aqueous phase: Formation, fate and reactivity," en, *Atmospheric Environment*, vol. 56, pp. 1–8, Sep. 2012, ISSN: 1352-2310. DOI: 10.1016/j.atmosenv.2012.03.079. (visited on 11/11/2022).

[220] Y. Gong, Z. Chen, and H. Li, "The oxidation regime and SOA composition in limonene ozonolysis: Roles of different double bonds, radicals, and water," *Atmospheric Chemistry and Physics*, vol. 18, no. 20, pp. 15 105–15 123, 2018, ISSN: 1680-7316. DOI: 10.5194/acp-18-15105-2018.

[221] T. S Christoffersen *et al.*, "Cis-pinic acid, a possible precursor for organic aerosol formation from ozonolysis of α-pinene," en, *Atmospheric Environment*, vol. 32, no. 10, pp. 1657–1661, May 1998, ISSN: 1352-2310. DOI: 10.1016/S1352-2310(97)00448-2. (visited on 07/26/2022).

[222] B. Witkowski, S. Jurdana, and T. Gierczak, "Limononic Acid Oxidation by Hydroxyl Radicals and Ozone in the Aqueous Phase," en, *Environmental Science & Technology*, vol. 52, no. 6, pp. 3402–3411, Mar. 2018, ISSN: 0013-936X, 1520-5851. DOI: 10.1021/acs.est.7b04867. [Online]. Available: https://pubs.acs.org/doi/10.1021/acs.est.7b04867 (visited on 12/13/2020).

[223] H Fuchs *et al.*, "Intercomparison of peroxy radical measurements obtained at atmospheric conditions by laser-induced fluorescence and electron spin resonance spectroscopy," *Atmospheric Measurement Techniques*, vol. 2, no. 1, pp. 55–64, 2009, Publisher: Copernicus GmbH.

[224] J. Vejdani Amorim *et al.*, "Photo-oxidation of pinic acid in the aqueous phase: A mechanistic investigation under acidic and basic pH conditions," *Environmental Science: Atmospheres*, vol. 1, no. 5, pp. 276–287, 2021. DOI: 10.1039/D1EA00031D. (visited on 08/06/2021).

[225] R. Zhao, E. L. Mungall, A. K. Y. Lee, D. Aljawhary, and J. P. D. Abbatt, "Aqueous-phase photooxidation of levoglucosan – a mechanistic study using aerosol time-of-flight chemical ionization mass spectrometry (Aerosol ToF-CIMS)," English, *Atmospheric Chemistry and Physics*, vol. 14, no. 18, pp. 9695–9706, Sep. 2014, Publisher: Copernicus GmbH, ISSN: 1680-7316. DOI: 10.5194/acp-14-9695-2014. (visited on 12/23/2022).

[226] H. Herrmann *et al.*, "Tropospheric Aqueous Phase Chemistry Kinetics, Mechanisms, and Its Coupling to a Changing Gas Phase," en, *Chemical Reviews*, vol. 115, no. 10, pp. 4259–4334, May 2015, ISSN: 0009-2665, 1520-6890. DOI: 10.1021/cr500447k.

[227] P. Renard *et al.*, "Aqueous Phase Oligomerization of Methyl Vinyl Ketone by Atmospheric Radical Reactions," *The Journal of Physical Chemistry C*, vol. 118, no. 50, pp. 29 421–29 430, Dec. 2014, ISSN: 1932-7447. DOI: 10.1021/jp5065598. [Online]. Available: https://doi.org/10.1021/jp5065598 (visited on 11/11/2022).

[228] M.-C. Reinnig, J. Warnke, and T. Hoffmann, "Identification of organic hydroperoxides and hydroperoxy acids in secondary organic aerosol formed during the ozonolysis of different monoterpenes and sesquiterpenes by on-line analysis using atmospheric pressure chemical ionization ion trap mass spectrometry," en, *Rapid Communications in Mass Spectrometry*, vol. 23, no. 11, pp. 1735–1741, 2009, ISSN: 1097-0231. DOI: 10.1002/rcm.4065. [Online]. Available: https://onlinelibrary.wiley.com/doi/abs/10.1002/rcm.4065 (visited on 08/21/2019).

[229] W. L. Miller and D. R. Kester, "Hydrogen peroxide measurement in seawater by (p-hydroxyphenyl)acetic acid dimerization," *Analytical Chemistry*, vol. 60, no. 24, pp. 2711–2715, Dec. 1988, ISSN: 0003-2700. DOI: 10.1021/ac00175a014. [Online]. Available: https://doi.org/10.1021/ac00175a014 (visited on 10/01/2019).

[230] C. Deyrieux *et al.*, "Measurement of Peroxide Values in Oils by Triphenylphosphine/Triphenylphosphine Oxide (TPP/TPPO) Assay Coupled with FTIR-ATR Spectroscopy: Comparison with Iodometric Titration," *European Journal of Lipid Science and Technology*, vol. 120, no. 8, p. 1 800 109, 2018, Publisher: Wiley Online Library.

[231] J. V. Amorim *et al.*, "pH Dependence of the OH Reactivity of Organic Acids in the Aqueous Phase," en, *Environmental Science & Technology*, vol. 54, no. 19, pp. 12 484–12 492, Oct. 2020, ISSN: 0013-936X, 1520-5851. DOI: 10.1021/acs.est.0c03331. [Online]. Available: https://pubs.acs.org/doi/10.1021/acs.est.0c03331 (visited on 06/22/2021).

[232] A. Sorooshian, N. L. Ng, A. W. Chan, G. Feingold, R. C. Flagan, and J. H. Seinfeld, "Particulate organic acids and overall water-soluble aerosol composition measurements from the 2006 Gulf of Mexico Atmospheric Composition and Climate Study (GoMACCS)," *Journal of Geophysical Research: Atmospheres*, vol. 112, no. D13, 2007, Publisher: Wiley Online Library.

[233] X. Sun *et al.*, "Organic acids in cloud water and rainwater at a mountain site in acid rain areas of South China," en, *Environmental Science and Pollution Research*, vol. 23, no. 10, pp. 9529–9539, May 2016, ISSN: 1614-7499. DOI: 10.1007/s11356-016-6038-1. (visited on 11/24/2022).

[234] T. B. Nguyen, A. P. Bateman, D. L. Bones, S. A. Nizkorodov, J. Laskin, and A. Laskin, "High-resolution mass spectrometry analysis of secondary organic aerosol generated by ozonolysis of isoprene," en, *Atmospheric Environment*, vol. 44, no. 8, Mar. 2010, ISSN: 1352-2310. DOI: 10.1016/j.atmosenv.2009.12.019.

[235] Y. Tan, M. J. Perri, S. P. Seitzinger, and B. J. Turpin, "Effects of Precursor Concentration and Acidic Sulfate in Aqueous Glyoxal OH Radical Oxidation and Implications for Secondary Organic Aerosol," en, *Environmental Science & Technology*, vol. 43, no. 21, pp. 8105–8112, Nov. 2009, ISSN: 0013-936X, 1520-5851. DOI: 10.1021/es901742f. (visited on 08/29/2022).

[236] M. Zeng, N. Heine, and K. R. Wilson, "Evidence that Criegee intermediates drive autoxidation in unsaturated lipids," en, *Proceedings of the National Academy of Sciences*, vol. 117, no. 9, pp. 4486–4490, Mar. 2020, ISSN: 0027-8424, 1091-6490. DOI: 10.1073/pnas.1920765117. [Online]. Available: https://pnas.org/doi/full/10.1073/pnas.1920765117 (visited on 10/09/2022).

[237] S. S. Yashar and H. W. Lim, "Classification and evaluation of photodermatoses," en, *Dermatologic Therapy*, vol. 16, no. 1, pp. 1–7, Mar. 2003, ISSN: 1396-0296, 1529-8019. DOI: 10.1046/j.1529-8019.2003.01601.x. [Online]. Available: http://doi.wiley.com/10.1046/j.1529-8019.2003.01601.x (visited on 08/29/2022).

[238] G. Schmitz, "Iodine oxidation by hydrogen peroxide in acidic solutions, Bray-Liebhafsky reaction and other related reactions," en, *Physical Chemistry Chemical Physics*, vol. 12, no. 25, pp. 6605–6615, 2010. DOI: 10.1039/B927432D. [Online]. Available: http://pubs.rsc.org/en/content/articlelanding/2010/cp/b927432d (visited on 08/24/2021).

[239] C. M. Kenseth *et al.*, "Synergistic O_3 + OH oxidation pathway to extremely low-volatility dimers revealed in β-pinene secondary organic aerosol," en, *Proceedings of the National Academy of Sciences*, vol. 115, no. 33, pp. 8301–8306, Aug. 2018, ISSN: 0027-8424, 1091-6490. DOI: 10.1073/pnas.1804671115. (visited on 10/31/2022).

[240] H. A. Liebhafsky, "The catalytic decompostion of Hydrogen Peroxides by iodine-iodide couple at 25C," en, *Journal of the American Chemical Society*, vol. 54, no. 5, pp. 1792–1806, May 1932, ISSN: 0002-7863, 1520-5126. DOI: 10.1021/ja01344a011.

[241] A. Gabet, H. Metivier, C. de Brauer, G. Mailhot, and M. Brigante, "Hydrogen peroxide and persulfate activation using UVA-UVB radiation: Degradation of estrogenic compounds and application in sewage treatment plant waters," en, *Journal of Hazardous Materials*, vol. 405, p. 124 693, Mar. 2021, ISSN: 0304-3894. DOI: 10.1016/j.jhazmat.2020.124693. (visited on 11/12/2022).

[242] M. Oss, A. Kruve, K. Herodes, and I. Leito, "Electrospray Ionization Efficiency Scale of Organic Compounds," *Analytical Chemistry*, vol. 82, no. 7, pp. 2865–2872, Apr. 2010, ISSN: 0003-2700. DOI: 10.1021/ac902856t.

[243] Y. B. Lim, Y. Tan, and B. J. Turpin, "Chemical insights, explicit chemistry, and yields of secondary organic aerosol from OH radical oxidation of methylglyoxal and glyoxal in the aqueous phase," en, *Atmospheric Chemistry and Physics*, vol. 13, no. 17, pp. 8651–8667, Sep. 2013, ISSN: 1680-7324. DOI: 10.5194/acp-13-8651-2013. (visited on 08/14/2022).

[244] J. V. Amorim *et al.*, "Photo-oxidation of pinic acid in the aqueous phase: A mechanistic investigation under acidic and basic ph conditions," *Environmental Science: Atmospheres*, vol. 1, no. 5, pp. 276–287, 2021.

[245] M. Yao *et al.*, "Isomer-Resolved Reactivity of Organic Peroxides in Monoterpene-Derived Secondary Organic Aerosol," *Environmental Science & Technology*, vol. 56, no. 8, pp. 4882–4893, Apr. 2022, ISSN: 0013-936X. DOI: 10.1021/acs.est.2c01297. [Online]. Available: https://doi.org/10.1021/acs.est.2c01297 (visited on 07/24/2022).

[246] A. Mutzel, M. Rodigast, Y. Iinuma, O. Boge, and H. Herrmann, "An improved method for the quantification of SOA bound peroxides," en, *Atmospheric Environment*, vol. 67, pp. 365–369, Mar. 2013, ISSN: 13522310. DOI: 10.1016/j.atmosenv.2012.11.012.

[247] D. Lindsay *et al.*, "The Bimolecular Self-reactions of Secondary Peroxy Radicals. Product Studies," en, *Canadian Journal of Chemistry*, vol. 51, no. 6, pp. 870–880, Mar. 1973, ISSN: 0008-4042, 1480-3291. DOI: 10.1139/v73-131. (visited on 11/06/2022).

[248] V.-T. Salo, R. Valiev, S. Lehtola, and T. Kurten, "Gas-Phase Peroxyl Radical Recombination Reactions: A Computational Study of Formation and Decomposition of Tetroxides," en, *The Journal of Physical Chemistry A*, vol. 126, no. 25, pp. 4046–4056, Jun. 2022, ISSN: 1089-5639, 1520-5215. DOI: 10.1021/acs.jpca.2c01321. [Online]. Available: https://pubs.acs.org/doi/10.1021/acs.jpca.2c01321 (visited on 12/30/2022).

[249] J. Elm, T. Kurten, M. Bilde, and K. V. Mikkelsen, "Molecular Interaction of Pinic Acid with Sulfuric Acid: Exploring the Thermodynamic Landscape of Cluster Growth," *The Journal of Physical Chemistry A*, vol. 118, no. 36, pp. 7892–7900, Sep. 2014, ISSN: 1089-5639. DOI: 10.1021/jp503736s. [Online]. Available: https://doi.org/10.1021/jp503736s (visited on 07/18/2022).

[250] M. E. Jenkin, D. E. Shallcross, and J. N. Harvey, "Development and application of a possible mechanism for the generation of cis-pinic acid from the ozonolysis of α- and β-pinene," en, *Atmospheric Environment*, vol. 34, no. 18, pp. 2837–2850, Jan. 2000, ISSN: 1352-2310. DOI: 10.1016/S1352-2310(00)00087-X.

[251] L. Vereecken, J.-F. Muller, and J. Peeters, "Low-volatility poly-oxygenates in the OH-initiated atmospheric oxidation of α-pinene: Impact of non-traditional peroxyl radical chemistry," en, *Physical Chemistry Chemical Physics*, vol. 9, no. 38, p. 5241, 2007, ISSN: 1463-9076, 1463-9084. DOI: 10.1039/b708023a. [Online]. Available: http://xlink.rsc.org/?DOI=b708023a (visited on 08/28/2022).

[252] B. Witkowski, M. Al-sharafi, and T. Gierczak, "Ozonolysis of β-Caryophyllonic and Limononic Acids in the Aqueous Phase: Kinetics, Product Yield, and Mechanism," *Environmental Science & Technology*, vol. 53, no. 15, pp. 8823–8832, Aug. 2019, ISSN: 0013-936X. DOI: 10.1021/acs.est.9b02471.

[253] B. Witkowski and T. Gierczak, "Characterization of the limonene oxidation products with liquid chromatography coupled to the tandem mass spectrometry," en, *Atmospheric Environment*, vol. 154, pp. 297–307, Apr. 2017, ISSN: 1352-2310. DOI: 10.1016/j.atmosenv.2017.02.005. (visited on 06/19/2021).

[254] F. Bianchi *et al.*, "Highly oxygenated organic molecules (hom) from gas-phase autoxidation involving peroxy radicals: A key contributor to atmospheric aerosol," *Chemical reviews*, vol. 119, no. 6, pp. 3472–3509, 2019.

[255] M. P. Rissanen *et al.*, "Effects of chemical complexity on the autoxidation mechanisms of endocyclic alkene ozonolysis products: From methylcyclohexenes toward understanding α-pinene," *The Journal of Physical Chemistry A*, vol. 119, no. 19, pp. 4633–4650, 2015, Publisher: ACS Publications.

[256] B. C. Faust, C. Anastasio, J. M. Allen, and T. Arakaki, "Aqueous-Phase Photochemical Formation of Peroxides in Authentic Cloud and Fog Waters," en, *Science*, vol. 260, no. 5104, pp. 73–75, Apr. 1993, ISSN: 0036-8075, 1095-9203. DOI: 10.1126/science.8465202. [Online]. Available: https://www.science.org/doi/10.1126/science.8465202 (visited on 01/29/2024).

[257] T. Toki *et al.*, "Synergistic interaction between wavelength of light and concentration of H_2O_2 in bactericidal activity of photolysis of H_2O_2," en, *Journal of Bioscience and Bioengineering*, vol. 119, no. 3, pp. 358–362, Mar. 2015, ISSN: 1389-1723. DOI: 10.1016/j.jbiosc.2014.08.015. (visited on 11/13/2022).

[258] M. C. V. M. Starling, P. P. Souza, A. Le Person, C. C. Amorim, and J. Criquet, "Intensification of UV-C treatment to remove emerging contaminants by UV-C/H_2O_2 and UV-C/$S_2O_8{}^{2-}$: Susceptibility to photolysis and investigation of acute toxicity," en, *Chemical Engineering Journal*, Emerging advanced oxidation technologies and developing perspectives for water and wastewater treatment. Vol. 376, p. 120 856, Nov. 2019, ISSN: 1385-8947. DOI: 10.1016/j.cej.2019.01.135. (visited on 11/12/2022).

[259] A. Monod, E. Chevallier, R. Durand Jolibois, J. F. Doussin, B. Picquet-Varrault, and P. Carlier, "Photooxidation of methylhydroperoxide and ethylhydroperoxide in the aqueous phase under simulated cloud droplet conditions," en, *Atmospheric Environment*, vol. 41, no. 11, pp. 2412–2426, Apr. 2007, ISSN: 1352-2310. DOI: 10.1016/j.atmosenv.2006.10.006. (visited on 09/29/2022).

[260] Y. Tan, Y. B. Lim, K. E. Altieri, S. P. Seitzinger, and B. J. Turpin, "Mechanisms leading to oligomers and SOA through aqueous photooxidation: Insights from OH radical oxidation of acetic acid and methylglyoxal," en, *Atmospheric Chemistry and Physics*, vol. 12, no. 2, pp. 801–813, Jan. 2012, ISSN: 1680-7324. DOI: 10.5194/acp-12-801-2012. (visited on 08/14/2022).

[261] Y. Lim and B. Turpin, "Laboratory evidence of organic peroxide and peroxyhemiacetal formation in the aqueous phase and implications for aqueous oh," *Atmospheric Chemistry and Physics*, vol. 15, no. 22, pp. 12 867–12 877, 2015.

[262] R. Zhao *et al.*, "Rapid Aqueous-Phase Hydrolysis of Ester Hydroperoxides Arising from Criegee Intermediates and Organic Acids," *The Journal of Physical Chemistry A*, vol. 122, no. 23, pp. 5190–5201, Jun. 2018, ISSN: 1089-5639. DOI: 10.1021/acs.jpca.8b02195. [Online]. Available: https://doi.org/10.1021/acs.jpca.8b02195 (visited on 11/12/2021).

[263] Y. Liu *et al.*, "Aqueous phase processing of secondary organic aerosol from isoprene photooxidation," en, *Atmospheric Chemistry and Physics*, vol. 12, no. 13, pp. 5879–5895, Jul. 2012, ISSN: 1680-7324. DOI: 10.5194/acp-12-5879-2012. (visited on 11/12/2022).

[264] C. Roehl, Z Marka, J. Fry, and P. Wennberg, "Near-uv photolysis cross sections of CH_3OOH and $HOCH_2OOH$ determined via action spectroscopy," *Atmospheric Chemistry and Physics*, vol. 7, no. 3, pp. 713–720, 2007.

[265] T. Wallington, P Dagaut, and M. Kurylo, "Uv absorption cross sections and reaction kinetics and mechanisms for peroxy radicals in the gas phase," *Chemical reviews*, vol. 92, no. 4, pp. 667–710, 1992.

[266] O. Legrini, E. Oliveros, and A. M. Braun, "Photochemical processes for water treatment," *Chemical Reviews*, vol. 93, no. 2, pp. 671–698, Mar. 1993. DOI: 10.1021/cr00018a003. [Online]. Available: https://doi.org/10.1021/cr00018a003.

[267] Z. Peng and J. L. Jimenez, "Radical chemistry in oxidation flow reactors for atmospheric chemistry research," *Chemical Society Reviews*, vol. 49, no. 9, pp. 2570–2616, 2020. DOI: 10.1039/c9cs00766k. [Online]. Available: https://doi.org/10.1039/c9cs00766k.

[268] B. Noziere and L. Vereecken, "Direct Observation of Aliphatic Peroxy Radical Autoxidation and Water Effects: An Experimental and Theoretical Study," *Angewandte Chemie International Edition*, vol. 58, no. 39, pp. 13 976–13 982, 2019, ISSN: 1521-3773. DOI: 10.1002/anie.201907981.

[269] Y. Zhao, J. A. Thornton, and H. O. Pye, "Quantitative constraints on autoxidation and dimer formation from direct probing of monoterpene-derived peroxy radical chemistry," *Proceedings of the National Academy of Sciences*, vol. 115, no. 48, pp. 12 142–12 147, 2018.

[270] B. Witkowski and T. Gierczak, "*cis*- Pinonic Acid Oxidation by Hydroxyl Radicals in the Aqueous Phase under Acidic and Basic Conditions: Kinetics and Mechanism," en, *Environmental Science & Technology*, vol. 51, no. 17, pp. 9765–9773, Sep. 2017, ISSN: 0013-936X, 1520-5851. DOI: 10.1021/acs.est.7b02427. [Online]. Available: https://pubs.acs.org/doi/10.1021/acs.est.7b02427 (visited on 06/07/2020).

[271] A. L. Perkel and S. G. Voronina, "The specific features of the liquid-phase oxidation of saturated esters. Kinetics, reactivity and mechanisms of formation of destruction products," en, *Russian Chemical Bulletin*, vol. 69, no. 11, pp. 2031–2058, Nov. 2020, ISSN: 1066-5285, 1573-9171. DOI: 10.1007/s11172-020-2999-9. (visited on 12/25/2022).

[272] C. Fittschen, "The reaction of peroxy radicals with OH radicals," *Chemical Physics Letters*, vol. 725, pp. 102–108, 2019, Publisher: Elsevier.

[273] T. Arakaki *et al.*, "A General Scavenging Rate Constant for Reaction of Hydroxyl Radical with Organic Carbon in Atmospheric Waters," en, *Environmental Science & Technology*, vol. 47, no. 15, pp. 8196–8203, Aug. 2013, ISSN: 0013-936X, 1520-5851. DOI: 10.1021/es401927b. [Online]. Available: https://pubs.acs.org/doi/10.1021/es401927b (visited on 01/29/2024).

[274] I. R. Piletic and T. E. Kleindienst, "Rates and yields of unimolecular reactions producing highly oxidized peroxy radicals in the oh-induced autoxidation of α-pinene, β-pinene, and limonene," *The Journal of Physical Chemistry A*, vol. 126, no. 1, pp. 88–100, 2022.

[275] H. O. Pye *et al.*, "Anthropogenic enhancements to production of highly oxygenated molecules from autoxidation," *Proceedings of the National Academy of Sciences*, vol. 116, no. 14, pp. 6641–6646, 2019, Publisher: National Acad Sciences.

[276] Y. Chen *et al.*, "The oxidation mechanism and kinetics of limononic acid by hydroxyl radical in atmospheric aqueous phase," *Atmospheric Environment*, vol. 294, p. 119 527, 2023.

[277] B. C. Faust and J. M. Allen, "Aqueous-phase photochemical sources of peroxyl radicals and singlet molecular oxygen in clouds and fog," *Journal of Geophysical Research: Atmospheres*, vol. 97, no. D12, pp. 12 913–12 926, 1992.

[278] D. W. Gunz and M. R. Hoffmann, "Atmospheric chemistry of peroxides: A review," *Atmospheric Environment. Part A. General Topics*, vol. 24, no. 7, pp. 1601–1633, 1990.

[279] H. Li, Z. Chen, L. Huang, and D. Huang, "Organic peroxides' gas-particle partitioning and rapid heterogeneous decomposition on secondary organic aerosol," English, *Atmospheric Chemistry and Physics*, vol. 16, no. 3, pp. 1837–1848, 2016, ISSN: 16807316. DOI: http://dx.doi.org/10.5194/acp-16-1837-2016.

[280] H. Tong *et al.*, "Reactive oxygen species formed in aqueous mixtures of secondary organic aerosols and mineral dust influencing cloud chemistry and public health in the Anthropocene," en, *Faraday Discussions*, vol. 200, no. 0, pp. 251–270, Aug. 2017, ISSN: 1364-5498. DOI: 10.1039/C7FD00023E.

[281] S. Toyokuni, "Reactive oxygen species-induced molecular damage and its application in pathology," *Pathology international*, vol. 49, no. 2, pp. 91–102, 1999.

[282] A. Stapleton, "Ultraviolet Radiation and Plants: Burning Questions.," *The Plant Cell*, vol. 4, no. 11, pp. 1353–1358, Nov. 1992, ISSN: 1040-4651. (visited on 08/25/2022).

[283] C. M. Kenseth, N. J. Hafeman, Y. Huang, N. F. Dalleska, B. M. Stoltz, and J. H. Seinfeld, "Synthesis of carboxylic acid and dimer ester surrogates to constrain the abundance and distribution of molecular products in α-pinene and β-pinene secondary organic aerosol," *Environmental Science & Technology*, vol. 54, no. 20, pp. 12 829–12 839, 2020.

[284] A. Kruve, K. Kaupmees, J. Liigand, and I. Leito, "Negative electrospray ionization via deprotonation: Predicting the ionization efficiency," *Analytical chemistry*, vol. 86, no. 10, pp. 4822–4830, 2014.

[285] J Yanez, C. Sevilla, D Becker, and M. Sevilla, "Low-temperature autoxidation in unsaturated lipids: An electron spin resonance study," *Journal of Physical Chemistry*, vol. 91, no. 2, pp. 487–491, 1987.

Chapter 3

Potential matrix effects in iodometry determination of peroxides induced by olefins

Reprinted with permission and minor formatting changes from its original publication as:

Gautam:2022.

3.1 Introduction

Peroxides (H_2O_2, ROOH and ROOR) play pivotal roles in many research fields, including biochemistry, food preservation, and environmental chemistry.[170, 286–288] Lipids (polyunsaturated fatty acids, PUFAs) are naturally found in cells and edible oils.[289–292] Oxidation of lipids can form lipid peroxides, which can contribute to cellular damage,[293] cell aging,[294] cardiovascular diseases,[295, 296] and rancidity in food products.[293, 297, 298] Peroxides such as H_2O_2 are also released in bloom forming algae and upon oxidation of phenolic compounds in wines, which can induce cellular and environmental toxicity.[299–301] In the past few decades, organic peroxides have gained tremendous attention in the field of atmospheric chemistry. They have been found to be a dominant contributor to the formation of secondary organic aerosol (SOA) and can act as reservoirs of HO_x and RO_x radicals.[59, 170, 279]

Quantitative determination of peroxide species in complex matrices is often achieved via spectroscopic,[169, 302] chromatographic,[303] and electrochemcial approaches.[304] Conventionally adopted spectroscopic methods usually involve some version of iodometry,[305] which currently remains one of the most pursued methods for its unique selectivity towards total peroxides,[164, 180, 246, 287, 306] and its ability to quantify total peroxide content in any given matrix.[279, 307] This is achieved via reduction of a given peroxide by an iodide ion (I^-), generating a molecular iodine (I_2), which further complexes with I^- to form a triiodide ion (I_3^-).[174, 181] This process is illustrated by reactions (1) and (2) in Figure 3.1. Given the 1:1 stoichiometric relationship between I^- and peroxides, the absorbance of I_3^- can provide quantitative information for total peroxide concentration.[176]

A similar analytical approach to quantifying peroxides in lipids is known as "peroxide value" (PV), which proceeds via titration of liberated I_2 with a starch indicator and sodium thiosulfate titrant.[308] This is a standard method employed for measuring rancidity in oil and toxicity in lipids.[309, 310] Despite the experimental variations between PV method employed for lipid peroxides[311] and iodometry for aerosol bound peroxides,[246] the principal chemistry is the same as outlined by reactions (1) and (2) in Figure 3.1. Today, iodometry is still widely employed in a number of research fields,[73, 312–314] with its recent applications including peroxide

determination in vegetable oils,[315, 316] lipid extracts from meat,[317–319] outdoor and indoor environments.[180, 320–323]

Despite the selective and quantitative nature of iodometry, matrix interferences are known to cause bias against accurate estimation of total peroxide content.[324, 325] Currently, molecular oxygen (O_2) is the only known interference, causing an overestimation in peroxide content by reducing I^-- just as peroxides do.[176, 326] Halogens such as I_2 can potentially react with certain classes of organic compounds.[327] One such case is olefins (OEs), as illustrated by reaction (3) in Figure 3.1. In fact, reaction (3) is more prominently known for the quantification of the degree of unsaturation in fatty acids commonly found in vegetable oils.[328] This chemistry, known as "iodine value (IV)", is expressed as the amount of I_2 taken up by double bonds per 100 g of targeted oil.[329–333] Knowing that I_2 is an important intermediate for the formation of I_3^- (reaction (2)), the loss of I_2 through reaction (3) can potentially affect the accuracy of iodometry. While there is some knowledge about adsorption of I_2 molecules on OEs[334, 335] there has not been a systematic investigation conducted to determine the extent of the bias originating from OE interference.

Edible oils and biodiesel fuels are known to constitute >50% unsaturated fatty acids within their matrices.[336–340] PUFAs in marine algae and lipid extracts of meat products can constitute up to 20% of the total fat content. [341–343] Although OEs in outdoor air pollutants are generally depleted due to their reactivity towards oxidants,[344] air pollutants in the indoor environments can contain high OE content.[323] For instance, cooking aerosol is found to be abundant in OE content with some studies reporting ∼27% of OE in total organic compound fraction.[345–347] A recent study by Deming and Ziemann[323] found high OE content in indoor organic films with an average of ∼20% C=C. These OE enriched matrices highlight the potential interference that can occur during iodometric analyses.[292, 295, 348, 349]

The objective of this work is to explore whether the proposed OE-I_2 chemistry can compromise the accuracy of iodometry. Specifically, we aimed to investigate the effects of OE concentration, reaction time, and different OE species. Detailed analyses were also performed to provide fundamental aspects on kinetics, mechanisms and the products of OE-I_2 reaction. A simple kinetic model was built to reproduce the magnitude of interference from a given OE. Our observations demonstrate the importance

of understanding the impact of matrix effects on the accuracy of iodometry.

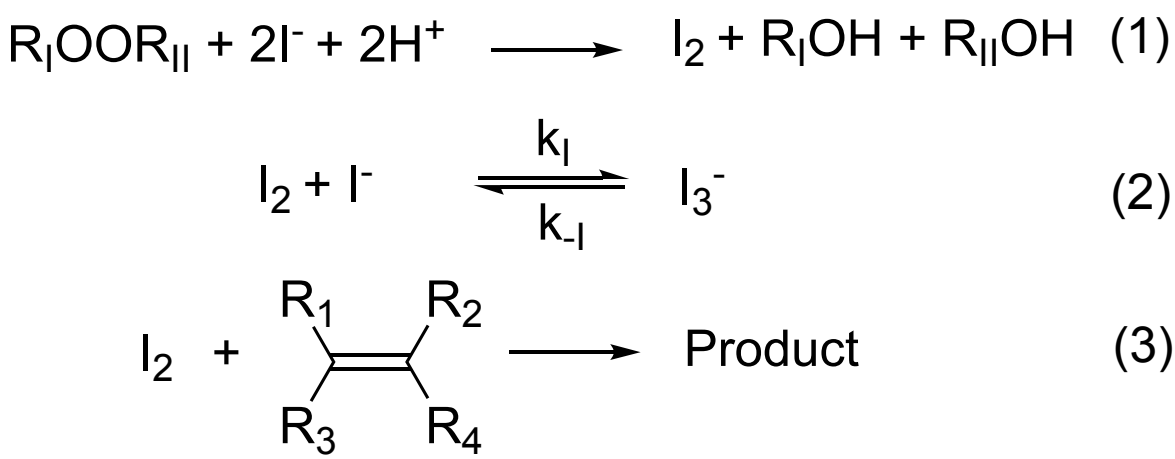

Figure 3.1: Reactions for iodometry and olefins.

3.2 Materials and Methods

3.2.1 Materials

The chemicals purchased from Sigma Aldrich were as following: octanoic acid (99%), 3-octenoic acid (trans, 99%), 7-octenoic acid (97%), 2-furoic acid (99%), benzoic acid (99%), hydrogen peroxide (H_2O_2, 30% w/w), tert-butyl hydroperoxide (t-BP, 70% w/w), α-pinene (99%), molecular iodine (I_2, 99%, crystallized), deuterated water (D_2O) (99.9% D), dimethyl sulfoxide (DMSO) (99.9%). These chemicals were bought from Fisher Scientific: potassium iodide (99%, ACS), acetic acid (99%), formic acid (99.9%). All chemicals were used without further purification. Some other chemicals used in our study were: ultra pure water (18.0 MΩ cm, Millipore), acetonitrile (HPLC grade), N_2 (from liquid N_2 boil-off), and O_2 (99.9%, Praxair).

3.2.2 Choice of Model Compounds

To establish our understanding of the OE-I_2 reactivity, we investigated the chemistry of I_2 with model olefin species: 3-octenoic acid (3-OE), 7-octenoic acids (7-OE) and methacrylic acid (MCA) (Figure 3.2). The choice of these OEs was based on a number of reasons. First, octenoic acids are medium chain acids which are simple and representative of larger unsaturated fatty acids (>C_{10}) naturally found in edible oils and animal fats.[350] Apart from fatty acids, we also experimented with methacrylic acid (MCA), which is a representation of small polar organic acids that are ubiquitous in the atmosphere.[351] Second, 3-OE and 7-OE differ in their positions of double bond, which offers an opportunity to investigate the impact of molecular structure. Third, organic acids can be detected by negative mode of electrospray ionization (ESI(-)), making chemical analyses easy. In addition to these OEs, we also tested a few other classes of compounds to examine the selectivity of I_2. These species include: (i) 1-octanoic acid (1-OA), representative of aliphatic organic acid, (ii) 2-furoic acid (2-FA), (iii) benzoic acid (BNA) and (iv) 4-nitroguaiacol (4-NG), which represents furans and aromatic compounds, respectively.

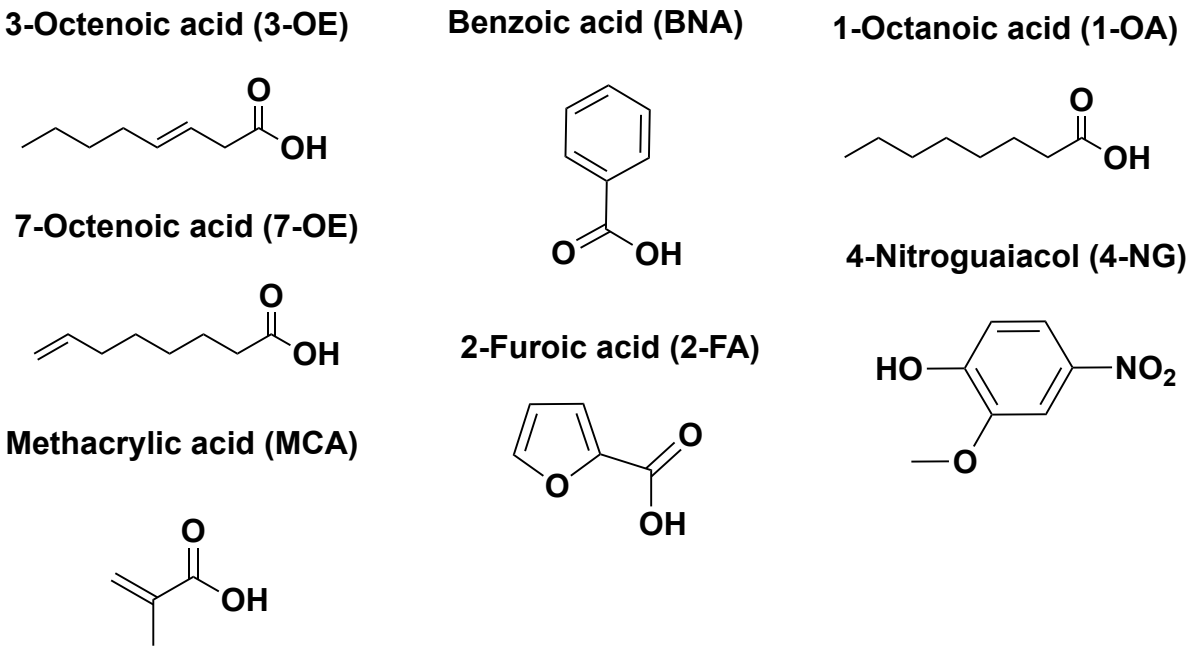

Figure 3.2: Compounds experimented for potential interfering chemistry.

3.2.3 Quantification of Olefin Interference

To probe the interference of OEs, UV-Vis spectroscopy is used for monitoring conventional iodometry and an experimental version of iodometry dosed with OEs (OE-dosed iodometry). Details on the conditions of these iodometry methods are listed in Table 3.1. All of the listed conditions, including both method blanks and experiments, were conducted in triplicates to ensure data quality and perform error analysis.

For conventional iodometry, we adapted and modified the method optimized previously.[246] Quantification of two hydroperoxides -H_2O_2 and t-BP- is achieved by monitoring the formation of I_3^-.[352] Briefly, a peroxide sample containing 47 μM of either H_2O_2 or t-BP was mixed with KI and acetic acid such that the final concentrations of KI and acetic acid were 60 mM and 12 mM, respectively. The acidic conditions employed in our experiments and in other versions of iodometry are necessary to facilitate redox chemistry.[246, 353, 354] The mixing of all reagents was done under exposure of air and the vial was immediately capped thereafter. The experimented peroxides were prepared fresh from stock solution stored in the refrigerator. The H_2O_2 concentration in the stock solution was confirmed every few months by collecting UV-Vis absorption spectra of the solution at λ_{240} nm, and calculating the concentration based on the molar absorptivity of H_2O_2 at this wavelength.[355, 356] While a typical reaction time for iodometry is 1 h,[164, 246, 262, 357] previous studies have reported incomplete reaction between I^- and peroxides within 1 h.[72, 358, 359] Thus, longer reaction times have also been employed in the literature.[72, 279, 360–362] Due to slower chemistry of t-BP,[363] the duration of studied iodometric reaction time was increased up to 24 h. For OE-dosed iodometry experiments, all the conditions were kept constant, but the solutions were spiked with a range of OE concentrations to simulate those in the sample matrix as discussed later. To reduce complexity of our procedure, we did not keep the solution under anoxic conditions. Thus, method blanks for both conventional and OE-dosed iodometry had to be carefully evaluated to account for interference caused by O_2. The method blanks for both systems were performed under the same conditions, except that the peroxide concentration was 0 μM. Particularly, for OE-dosed procedure, the same concentrations of OE were added to the blank solution, and the response was measured up to either 6

h or 24 h based on the peroxide employed for iodometry (Table 3.1).

In continuity of experimenting with commercial peroxides, we also performed experiments with SOA generated in our laboratory, as SOA is known to contain a wide spectrum of organic peroxides.[59, 228] Briefly, sampling for SOA occurred in a pyrex flow tube reactor via ozonolysis of α-pinene under room temperature and in the absence of nitrogen oxides. The collection of SOA occurred for 6 h on a pre-weighed filter (475 μm, Whatman quartz, 47 mm diameter) and immediately stored at (−16°C). Details on the collection procedure are explained elsewhere.[231] The SOA collected filter (m = 9.5 mg) was thawed before extraction in 25 mL MilliQ (18.0 MΩ cm) water via magnetic stirring for 5 min. The resulting extract was filtered using 0.22 μm polytrifluoroethylene (PTFE) syringe filter. The SOA extract showed no absorbance at the scanned wavelength during experiments indicating no prior background before iodometry. All of the experiments were monitored by a UV-Vis spectrophotometer. Specifically, Thermo Scientific 10S Genesys was employed, and spectrum was scanned from 325 to 700 nm. VISIONLITETM (v 850) was used for data recording. To monitor I_3^-, its absorbance at 351 nm and the corresponding molar absorptivity (ϵ = 26,400 L^{-1} mol^{-1} cm^{-1}) were used.[246, 352] The measurements for each sample were contained in a standard 1 cm quartz cuvette, with an identical cuvette containing MilliQ water as our reference cell. Another instrument (Agilent 8453) was also used in certain experiments to scan to a shorter wavelength (190-1100 nm).

Table 3.1: Experimental conditions for conventional and interfering iodometry system.

	Experimental conditions			
Reagents	Conventional iodometry	Conventional method blank	OE-dosed iodometry	OE-dosed method blank
Hydroperoxides[a] (μM)	47	0	47	0
KI (mM)	60	60	60	60
Acetic acid (mM)	12	12	12	12
OEs[b] (μ M)	0	0	100, 303 521, 711,1020	100, 303 521, 711,1020

[a] H_2O_2 or t-BP
[b] 3-OE, 7-OE or MCA

3.2.4 Investigations on the OE-I_2 Reaction

3.2.4.1 Monitoring the OE-I_2 Reaction

Experiments were carried out to examine four fundamental aspects of the OE-I_2 reaction: selectivity, reaction order, rate coefficient, and reaction mechanism. These experiments were performed by mixing a known concentration of I_2 with either OE or other compounds (Figure 3.2) in an aqueous solution and monitoring the decrease in the signal response. To do this, we first prepared a stock solution of 934 μM I_2 in 10 mL MilliQ water. This solution was stirred overnight, and the initial concentration of this solution was determined by UV-Vis spectrophotometer (Agilent 8453). Details on the quantitative assessment of I_2 are provided in Supporting Information (Appendix B, Section B.1). The decrease in the response of OE or other compounds was measured as a function of reaction time using reverse phase liquid chromatography mass spectrometry (LC-MS). Specifically, reaction samples were analyzed using an Agilent 1100 LC MSD (Model G1946D) equipped with an Agilent 1200 autosampler. A C18 (Kinetex 2.6 μm particle size, 100 Å, 50 x 2.1 mm) column was used with a gradient method of 0.1% formic acid in water (A) and 0.1% formic acid in acetonitrile (B) respectively. The gradient method was as follows: initial 1% B for 1 min, increase to 35% B at 6 min, 50% B at 7 min, 95% B at 8.50 min, and decrease to 1% B at 10 min. Aliquots of reaction mixture were injected at intervals of 15 min to monitor the reaction rate. ESI^- polarity was used as per following conditions: capillary voltage, 3500 V; Fragmentor voltage, 100 V; drying gas temperature, 350 °C; drying gas flow, 10.0 L min^{-1}; and nebulizer pressure, 30 PSI

A UV-Vis (Agilent 8453) spectrophotometer was used to monitor the decrease in the absorbance of I_2 in the OE-I_2 reaction mixture. This reaction was monitored at a wavelength of 460 nm, which corresponds to the maximum molar absorptivity for I_2 (ϵ = 746 L^{-1} mol^{-1} cm^{-1}) in an aqueous solution.[352]

3.2.4.2 Selectivity of OE-I_2 Reaction

The selectivity of the OE-I_2 reaction was examined with a variety of compounds shown in Figure 3.2. For this purpose, an aliquot of either OE or other compounds was added to the reaction vial containing an aliquot of I_2 (from stock solution) followed

by addition of acetic acid to maintain pH similar to that in iodometry. Additionally, control samples were also prepared following the same procedure, except that no I_2 was added. Aliquots of this reaction mixture were analyzed via the aforementioned LC-MS method.

3.2.4.3 Kinetics: Rate Order and Coefficient

For a systematic investigation into the rate order and rate coefficient of the OE-I_2 reaction, we chose 3-OE as our model compound. Our purpose of investigating reaction kinetics of the OE-I_2 reaction was to obtain a rate coefficient, which would be then incorporated into building a simple box model. A strategic approach was adopted such that either OE or I_2 were maintained under excess concentrations to allow the limiting reactant to follow a pseudo order. By deducing the pseudo order, the overall order of OE-I_2 can be determined. Briefly, an aliquot of 3-OE (52 μM) was added with an excess amount of I_2 in an acidified solution. The experiments were performed under two concentrations of I_2 (620 μM and 702 μM). Due to the solubility limit of I_2 in aqueous solutions,[364] the experimentally determined concentrations of I_2 were found to be comparable.

Similar conditions were also opted to monitor the reaction kinetics. To do this, an aliquot of I_2 ($\sim$100 μM) was added to 3-OE at a concentration in excess (1.87 mM). The decrease in [I_2] was observed by monitoring absorbance of I_2 using a UV-Vis spectrophotometer (Agilent 8453). From the pseudo kinetics, were able to deduce the rate coefficient of the OE-I_2 reaction.

3.2.4.4 Products and Mechanism

In this section, a series of experiments were performed to elucidate the formation of product(s) and the corresponding mechanism. To evaluate the formation of product(s) in 3-OE and 7-OE, we opted for high resolution LC-MS (HR-LC-MS) in ESI(-) mode. For identification with HR-LC-MS, the reaction samples were prepared in a similar manner as that of the kinetic experiments with an excess concentration of I_2 (620 μM) in comparison to OE. Specifically for this set of experiments, the concentration of OE was increased from 52 μM to 100 μM to enhance signal response. The reaction mixture was analyzed by LC-MS with the same separation method but with

a high resolution MS: an Agilent 6220 Accurate-Mass TOF HPLC/MS system.

To further confirm the reaction mechanism, we identified the product(s) using proton nuclear magnetic resonance (^{1}H NMR) spectroscopy. An aliquot of OE and DMSO (1.2 mM) was mixed with an aliquot of I_2 solution in D_2O such that the final concentrations for OE and DMSO were estimated to be 75 μM and 100 μM, respectively. DMSO serves as an internal standard for both qualitative and quantitative analyses, however for our case, only qualitative distinction is made between reactant and product spectra. Agilent VNRMS 700 MHz spectrometer equipped with Agilent 7620 automatic sampling system was used for data acquisition. Sample presaturation mode was applied for 2.0 s to suppress water signal. A relaxation delay of 0.1 s is used to allow recovery of magnetization following pulsed sequences with acquisition time of 3.0 s. Data processing was done with 0.25 Hz of line broadening for enhancement in signal to noise ratio. To assist with product characterization, an online tool (NMRdb) was used. The spectrum response is referenced to that of DMSO at 2.7 ppm. Details on the assignment of specific functional groups are discussed in Appendix B Section B.4.

3.2.5 Kinetic Modeling

To test whether we can employ the mechanistic and kinetic information from this work to predict effects of OEs on iodometry, we built a simple box model to simulate the conventional and OE-dosed iodometry system. For this purpose, two hydroperoxide (H_2O_2 and t-BP) based iodometry systems were reproduced using modeled simulations. The model is based on Matlab, and it is originally built for chamber experiments, but we have applied it to simpler aqueous phase chemistry.[231] Kinetic simulations for concentration of I_3^- were developed with a known value of rate constant for H_2O_2, while an experimentally determined value based on exponential fit was used for t-BP.[181, 238] The model assisted in examining a few scenarios to reproduce experimentally observed OE-I_2 interference, and this will be discussed in Section 3.3.5.

3.3 Results and Discussion

3.3.1 Detection of Peroxides with Conventional Iodometry

We first validated the reliability of the conventional iodometry method, and the results acquired are shown in Figure 3.3. Specifically, Figure 3.3 (A) shows the absorption spectra of the H_2O_2 (47 μM) sample and the conventional method blank recorded after 1 h of reaction. The spectrum for H_2O_2 sample exhibits a broad absorption peak at 351 nm, which is indicative of I_3^- absorption. On the other hand, the method blank shows absorption at a negligible level in comparison to the sample. Although dissolved O_2 is known to give rise to a growth of signals in samples and blanks,[176] its impact seems to be minor under our experimental conditions. Figure 3.3 (B) presents the time-dependent results obtained from conventional iodometry method. Herein, both H_2O_2 and t-BP are shown on the same graph. The y-axis indicates the concentration of I_3^- calculated from molar absorptivity at $\lambda = 351$ nm.[246, 352] The dashed line represents a theoretically expected concentration value (47 μM) for both peroxides. For the H_2O_2 case, $[I_3^-]$ recorded after 1 h of reaction is in a reasonable agreement with 1:1 stoichiometry expected in iodometry and demonstrates the reliability of the conventional iodometry method performed in this work.[176, 349] However, the corresponding growth profile cannot be observed in the case of t-BP. This is clearly noticed in Figure 3.3 (B), where the stoichiometric concentration relationship is not coherent over the course of 6 h of reaction time. Our results are in agreement with a few previous work,[164, 363, 365, 366] in which authors observed slower chemistry for complex peroxides other than H_2O_2. These results are indicative of the reason that a few previous studies have employed longer reaction time, up to six hours.[164, 180, 215]

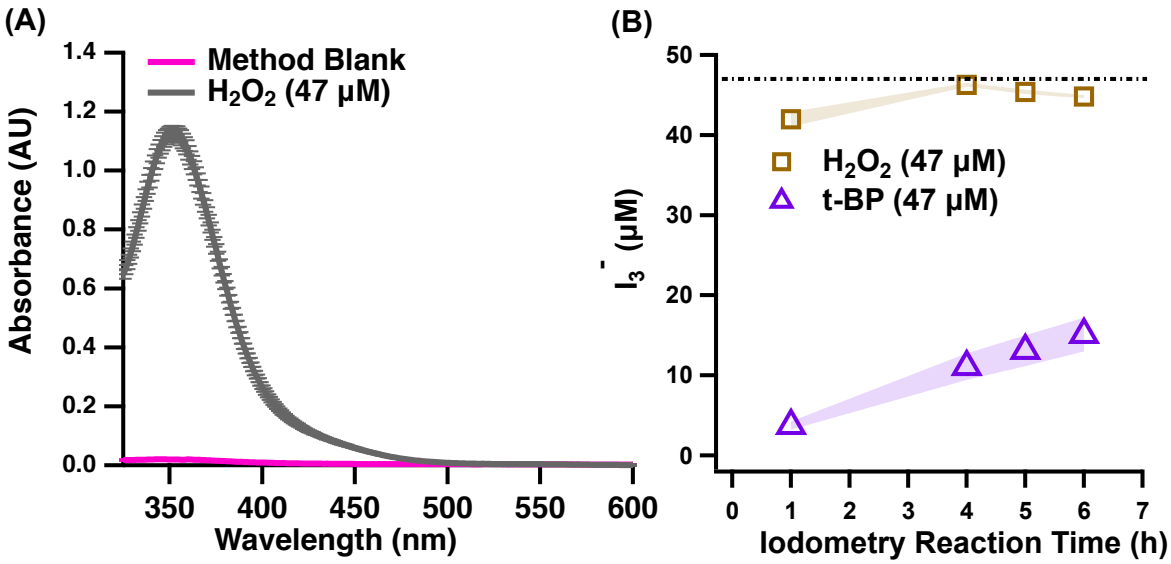

Figure 3.3: Conventional iodometry results. Errors represent 1σ standard deviations obtained from triplicate experiments. (A) Absorption spectra of H_2O_2 sample (47 μM) and method blank. (B) Time-dependent I_3^- concentration obtained from H_2O_2 and t-BP samples. The I_3^- concentration was found by converting absorbance at λ= 351 nm using molar absorption coefficient. Dashed line aids visual representation for expected concentration for both peroxides.

3.3.2 Observed Interference from Olefin

Having confirmed the reliability of our iodometry method in Section 3.3.1, we then dosed our reaction system with other compounds shown in Figure 3.2 as per described methodology in Table 3.1 (Section 3.2.3). To substantiate the interfering chemistry, Figure 3.4 (A) highlights the absorption spectra for a sample of H_2O_2 dosed with 3-OE (711 μM) along with the OE-dosed method blank recorded after 4 h of reaction time. For comparison, the spectra for H_2O_2 sample and conventional method blank are also added to the same graph. A clear decrease ($\sim$15%) in the absorption spectra is observed when the H_2O_2 sample is dosed with 3-OE. The given result is indicative that the interfering chemistry between OE and I_2 could downplay the accurate measurement of a peroxide.

A peculiar observation was noted in regards to 3-OE measurements. We observed noticeable growth in the 3-OE method blank. Figure B.2 (S2.1) (Appendix B, Section B.2) shows an increasing I_3^- absorption along with increasing 3-OE concentration. Although this response of 3-OE method blank is marginal in comparison to H_2O_2 sample, it is still higher than the conventional method blank. The response in 3-OE method blank was not due to dissolved O_2 interference. This is exemplified by an additional experiment, in which we constantly sparged the iodometry solution with N_2 gas to remove dissolved O_2. As shown in Figure B.2 (S2.2) (Appendix B, Section B.2), this sample showed no distinct differences in comparison to without N_2 sparging. The method blank for other OEs (7-OE, MCA) showed a response similar to that of conventional method blank and was hence evaluated at one representative concentration. We are currently unsure why only the 3-OE blank exhibited such growth, and this blank certainly affected our experiment, especially at lower (100 μM, 303 μM and 521 μM) dosed concentrations and short reaction time. To accurately account for this background issue, method blanks of 3-OE were evaluated at each concentration.

3.3.3 Factors Impinging on the Interference

To critically examine the interference due to reactions of OEs with I_2, certain factors were taken into consideration for evaluating the fundamentals behind this chemistry. These factors include: (i) concentration and reaction time; (ii) species of interfering compounds; (iii) species of peroxide. Details for each of these variables are described in following sections.

3.3.3.1 Concentration of Olefin and Reaction Time

The dosed concentration of OE was varied from 100 μM to 1020 μM. Figure 3.4 (B) shows the % difference between 3-OE-dosed and conventional iodometry observed at two 3-OE concentrations (100 and 711 μM). The observed % difference is calculated as per eq-3.1:

$$\%\text{Difference} = \frac{A_{OE} - A_p}{A_P} * 100, \qquad \text{(eq-3.1)}$$

where A_{OE} represents absorbance of I_3^- at 351 nm for iodometry method dosed with an OE, while A_P is the absorbance of I_3^- at 351 nm for conventional iodometry method. When 100 μM of 3-OE-dosed H_2O_2 sample is observed, the deviation from the conventional iodometry system (represented by dashed line) is less than 5%. But at 711 μM concentration of 3-OE almost 20% underestimation in H_2O_2 quantification is observed after 6 h of reaction time.

The % difference as a function of 3-OE concentrations at 1 h and 6 h iodometry times is presented in Figure B.3 (Appendix B, Section B.3). The trend is complicated, with a pronounced decrease observed at 711 μM and 1020 μM concentrations of 3-OE and 6 h of reaction time, but the trend with shorter reaction time and lower 3-OE concentrations (100 μM, 303 μM and 521 μM) were rather inconsistent. We believe that this inconsistency arises from the rising background when samples are dosed with 3-OE, and this has already been discussed in Section 3.3.2.

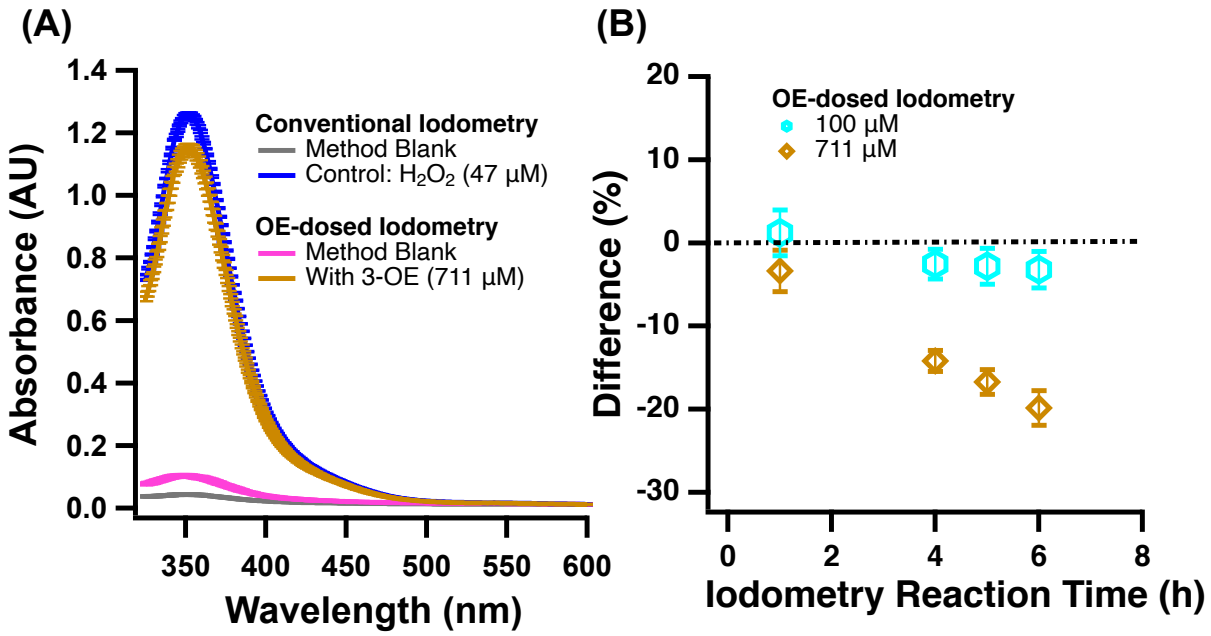

Figure 3.4: Conversion of absorption decrease into percentage difference. (A) Absorption spectra of conventional and OE-dosed iodometry after 4 h of reaction. The error bars represent 1 σ standard deviation from triplicates. (B) Percentage deviation between the conventional and OE-dosed iodometry, caused by 100 μM and 711 μM concentrations of 3-OE. The dashed line represents an ideal case of no deviation from conventional iodometry.

3.3.3.2 Species of Interfering Compounds

Figure 3.5 shows the comparison between % difference induced by three different OEs and 1-OA. Each of these represented organic acids was dosed with the same concentration (711 μM) in the iodometry system. While 1-OA shows negligible % difference, the other three species portray observable decreasing profiles. This observation exemplifies the selectivity of I_2 towards OEs but not to compounds without a double bond. Among the three OEs investigated, 3-OE exhibits a larger magnitude of interference compared to MCA and 7-OE, whose interferences are of similar magnitude. Thus, our observation indicates that an underestimation in peroxide content would be universal for OEs but can be dependent on each specific OE species. In future studies, a wider range of OEs, especially those representative of each target sample matrix, - indoor surfaces, lipids, and cellular membranes - should be investigated.

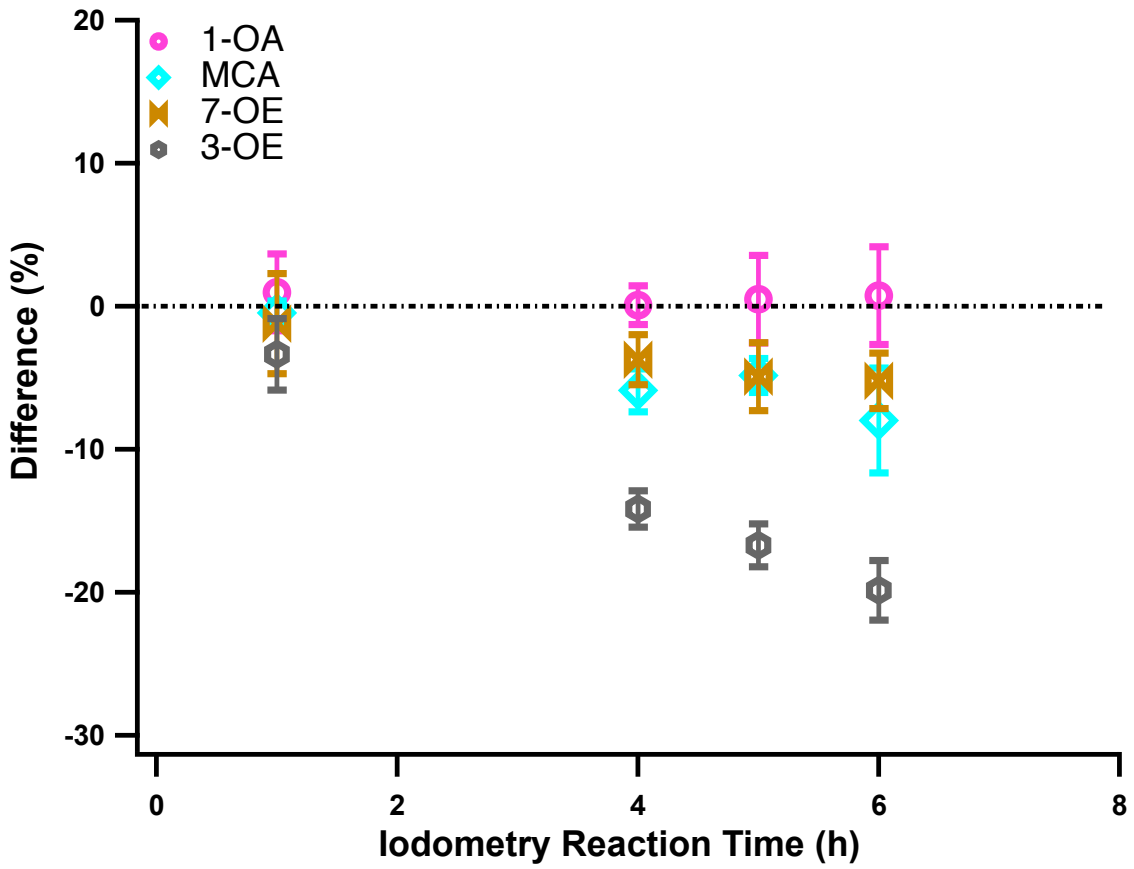

Figure 3.5: Percentage decrease in absorption of I_3^- caused by three different OEs and 1-OA. All the species were added at the same concentration (711 μM). The dashed line indicates conventional iodometry with no deviation.

3.3.3.3 Class of Peroxides

To demonstrate the effects of olefinic interference, we provide a direct comparison between three different peroxide samples (H_2O_2, t-BP and α-pinene SOA aqueous extract). In particular, the SOA extract represents a mixture of atmospherically relevant peroxide species, as α-pinene SOA is known to contain a wide variety of organic peroxides.[71, 170, 279, 367] Illustrated in Figure 3.6 is the comparison made among these three types of peroxides, each dosed with 3-OE at 711 μM concentration. The given reaction for each OE-dosed iodometry is measured at 1 h, 6 h and 24 h. The observed % difference due to OE interference is found to be relatively similar and consistent across different peroxide species. The larger uncertainty observed for t-BP in comparison to other peroxide species (H_2O_2, SOA extract) could be due to

its slower reactivity leading to a lower response during the initial time of reaction (1 h).[164] The interference should be dependent on the rate of the reaction between I_2 and OE. Thus, it is understandable that different peroxides do not show much variation at the measured reaction times. Furthermore, SOA encompasses a multitude of peroxide species,[368] and the fact that such peroxides also exhibit a similar degree of interference means that we can expect this interference across all peroxides to be the same, at least with respect to the same OE.

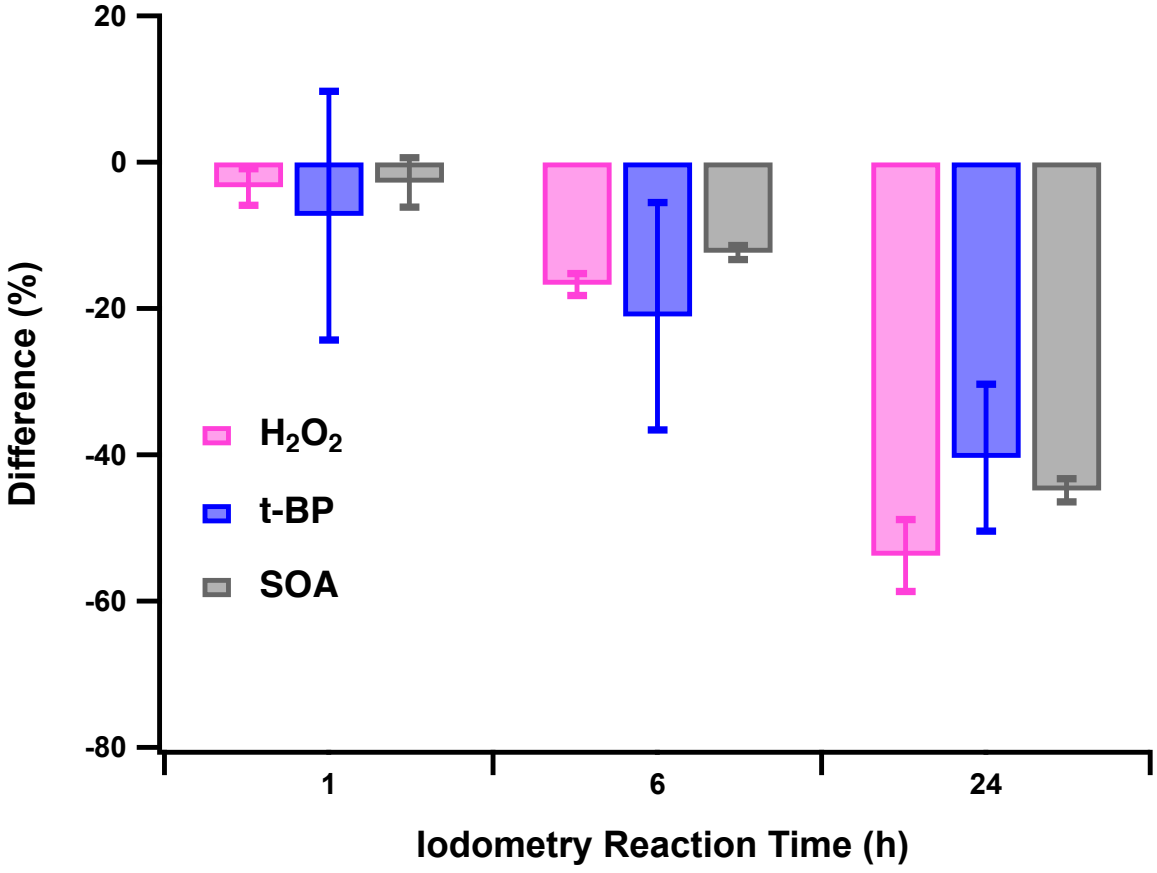

Figure 3.6: Percentage difference observed for H_2O_2, t-BP and SOA iodometry samples dosed with 3-OE at 711 μM and monitored at chosen reaction times.

3.3.4 Reaction Mechanism and Kinetics

Having proven the interference of OE in iodometry, we explore the feasibility of building a simple kinetic model to predict the interference. For this purpose, we set out to probe fundamental aspects of this interaction using analysis of 3-OE with direct addition of I_2 in aqueous solution.

3.3.4.1 Selectivity

In this section we explore the selectivity of I_2 towards OEs under typical conditions of iodometry. Specifically, we added I_2 to compounds shown in Figure 3.2 and monitored the reaction samples with and without the addition of I_2 over 120 min. Figure 3.7 shows ESI(-) signals for each of the experimented compounds monitored with the selective ion monitoring (SIM) mode. Similar to the observations from iodometry results (Figure 3.5), we noticed that 1-OA (A), which has no double bond, did not exhibit any change in its response. Meanwhile, 3-OE (B) and 7-OE (C) exhibited a continuous decrease in their signal responses as a function of reaction time. Although MCA is not tested in this experiment due to the inability of our C18 column to retain such a small and polar molecule, it is expected to react with I_2 based on the results presented in Figure 3.5. On the contrary, signal responses of BNA (D), 4-NG (E) and 2-FA (F) did not exhibit any observable decrease over a course of 2 h of reaction time. In these molecules, the π-electrons belong to an aromatic ring or a furan instead of an aliphatic structure. This observation highlights the selectivity of I_2 to the aliphatic compounds. While it is possible for furan and aromatic compounds to react with I_2, the conditions under which these reactions occur are not applicable to the goals of our study.[327, 369–371]

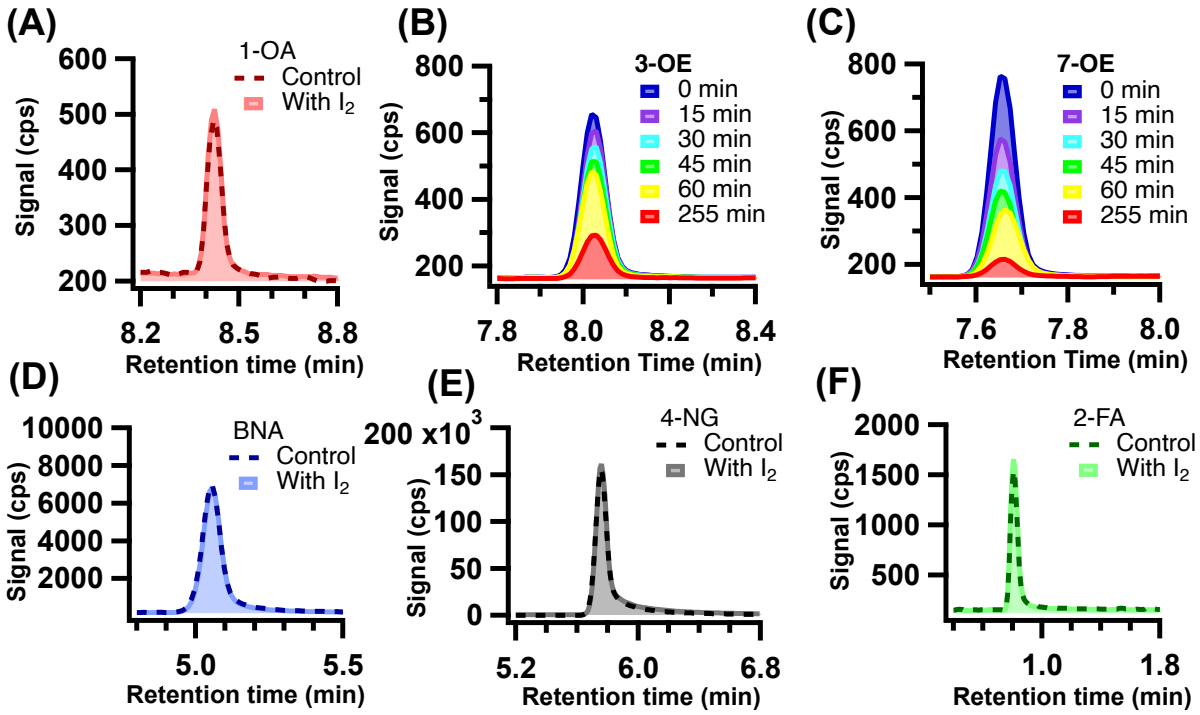

Figure 3.7: Selective reactivity of I_2 is portrayed with respect to different interfering compounds. (A) 1-OA (41 μM), (B) 3-OE (52 μM), (C) 7-OE (52 μM), (D) BNA (82 μM), (E) 4-NG (82 μM), (F) 2-FA (50 μM). Dashed lines indicate samples without any I_2 while color coded regions represent addition of I_2 in OEs and other compounds. For compounds that did not show any reaction, the signal is recorded 2 h after the I_2 addition.

3.3.4.2 Product Characterization

As mentioned in Section 3.2.4.4, HR-LC-MS and ^{1}H NMR were employed to determine reaction products. While we performed experiments with both 3-OE and 7-OE, we found that 7-OE provides more insightful information for the product identification and mechanism elucidation. For this reason, we focus on the case of 7-OE below. Figure 3.8 (A) shows ESI(-) extracted ion chromatogram (EIC) of a product of 7-OE from its reaction with I_2. This product is detected with an exact mass of 285.001 (as $[M\text{-}H]^-$) which corresponds with an addition of OH (m/z 17.003) and I (m/z 126.904) on 7-OE (m/z 141.092), with a mass difference of -3.89 ppm. Furthermore, Figure 3.8 (B) and (C) present a comparison for the ^{1}H NMR spectrum of the reactant and products. The reaction with I_2 resulted in a reduction of allylic H and formation of product peaks at $\delta = 3.2$ ppm. The results from both ^{1}H NMR and HR-LC-MS

highlight a mono iodo substituted product for 7-OE, but for 3-OE there is a possibility of two mono iodo substituted products due to the fact that the π-electrons are located in the middle position of the carbon chain. Details on the specific assignment of functional groups in 3-OE and 7-OE can be found in Appendix B Section B.4.1, while a discussion for the mechanisms behind this reaction is provided in Section B.4.2.

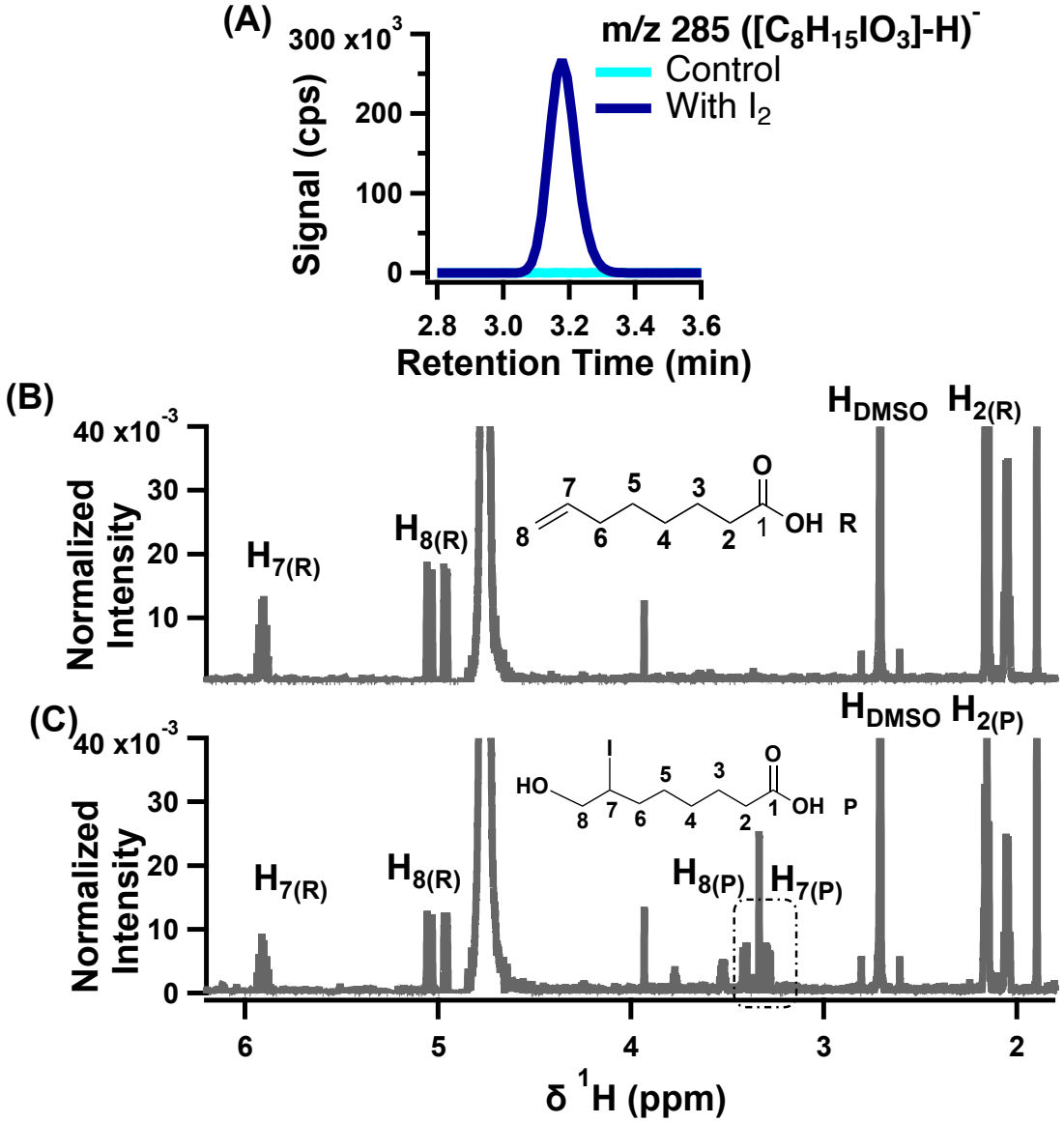

Figure 3.8: Extracted Ion Chromatogram (EIC) and ^{1}H NMR for 7-OE-I_2 reaction. Subscript (R) and (P) in ^{1}H NMR spectra represent reactant and product protons, respectively. (A) EIC for 7-OE (100 μM) reaction with I_2 resulting in product m/z 285.001 (B) ^{1}H NMR for 7-OE in D_2O. (C) ^{1}H NMR for 7-OE with I_2 in D_2O. The dashed-line box highlights peaks attributed to the products.

3.3.4.3 Reaction Order and Kinetics

To acquire the kinetics data to be input in our model, we determined the second order rate coefficient (k^{II}) for the 3-OE-I_2 reaction. This experiment was performed by reacting 3-OE (52 μM) with I_2 at a 10 times higher (620 μM) concentration. Given that I_2 is in excess and remains relatively constant during reaction, the decrease in [OE] can be explained by a pseudo rate coefficient. Figure 3.9 shows the decay profile of 3-OE during this experiment, presented as natural logarithmic of peak area. The plot is linear with an R^2 exceeding 0.99, confirming that the reaction is indeed pseudo first order with respect to 3-OE. The slope of this linear plot is equivalent to the pseudo first order rate coefficient (k^I), while k^{II} was calculated as 0.84 ± 0.02 $M^{-1}s^{-1}$ from k^I and [I_2]. To confirm this rate coefficient, we performed an experiment at another I_2 concentration (702 μM) and obtained a similar number. More details can be found in Appendix B Section B.5. Considering that we have confirmed the rate order associated with respect to 3-OE, a similar strategy was adopted for estimating rate order with respect to I_2. For this purpose, I_2 (∼100 μM) was reacted with 3-OE in excess. The plot (Appendix B, Figure B.6 (S5.2)) showed linearity with $R^2 = 0.99$, indicating that the reaction is also first order with respect to I_2.

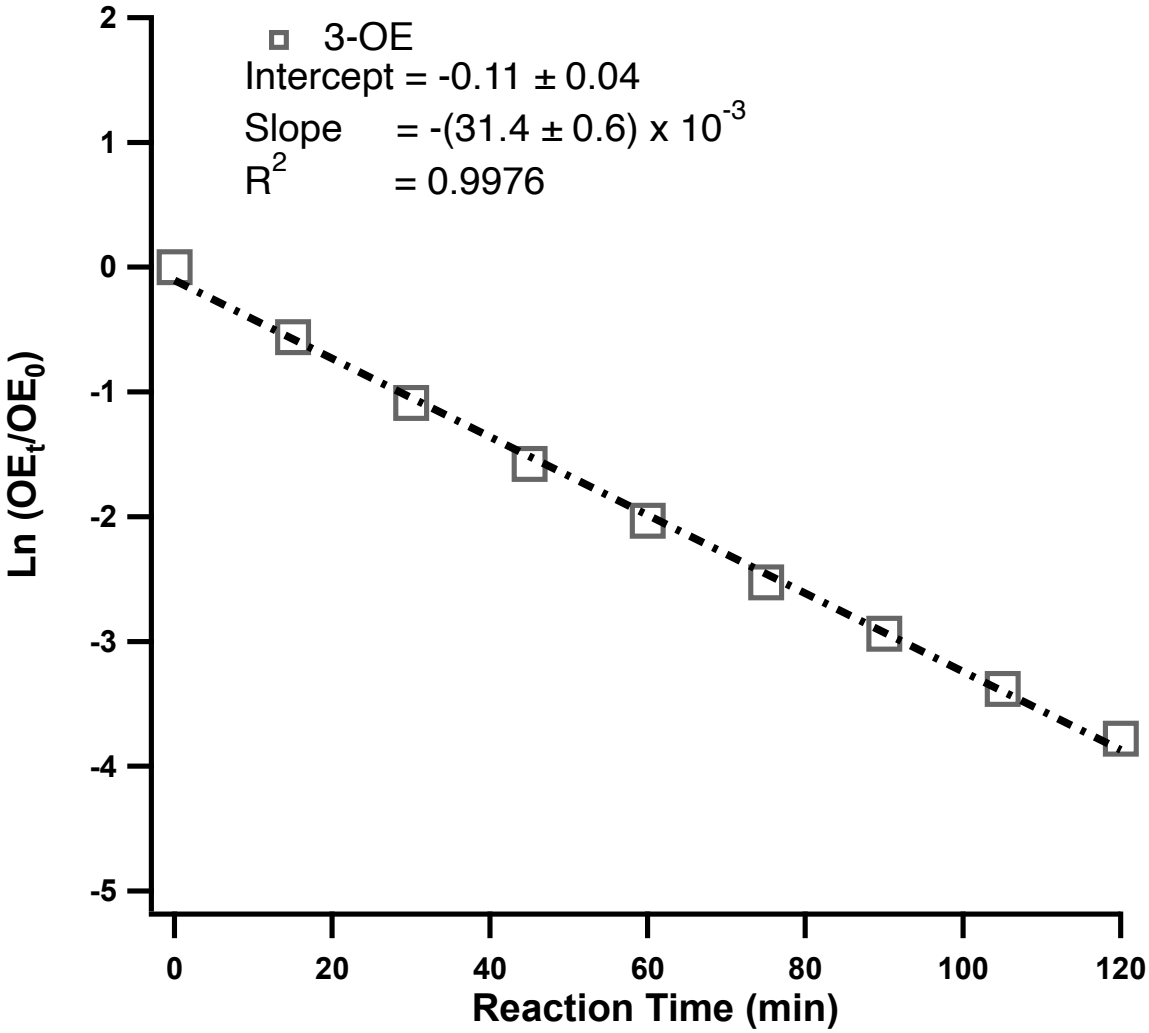

Figure 3.9: Pseudo first order decay in 3-OE with excess I_2. The decrease in natural logarithmic ratio of peak area is shown with respect to reaction time.

3.3.5 Kinetic Box Model

A box model is utilized to reproduce the observed OE interference based on the parameters obtained from kinetic experiments. The growth of I_3^- for the quantification of H_2O_2 and t-BP with iodometry was simulated and compared with experimentally determined concentration profiles. Our current model data is based on pH 3.1. This is the most commonly used acid concentration for iodometry.[180, 246] Given that acid is an important reagent used across different adaptations of iodometry,[170, 171] our model is able to predict this chemistry under relevant pH ranges.[180, 246].

Figure 3.10 compares the model and experimental results of I_3^- concentration in the H_2O_2 (A) and t-BP (B) iodometry reactions. The model scenarios, reactions, and rate coefficients used for the simulations are summarized in Section B.7 (Appendix B). The conventional iodometry was simulated based on rate constants suggested by Liebhfasky and Mohammad.[181, 238] The OE-dosed experiment considered a dose of 3-OE (711 μM) and was simulated using the k^{II} we determined in Section 3.3.4.3. As observed from Figure 3.10 (A), our model successfully simulated the deviation of I_3^- between 3-OE dosed and conventional iodometry, indicating that our model was successful in modeling the effects of OE on the detection using iodometry.

Figure 3.10 (B) shows a similar consensus between modeled and experimental projections for t-BP based iodometry system. Unlike H_2O_2, due to the lack of available literature on kinetics of t-BP with I^- in the aqueous phase, the modeled projections were developed using experimentally determined second order rate constant (Appendix B, Section B.6). While for the conventional iodometry case, a slight disparity was observed between the model and experimental results, an excellent agreement was obtained for the case dosed with 711 μM of 3-OE. Other than 711 μM concentration of 3-OE, we also compared the agreement between simulated and experimentally observed profiles of I_3^- at 100 μM and 1020 μM concentrations of 3-OE. Our simple model is generally successful in reproducing the magnitude of OE interference. However, we observe deviations at longer reaction times. That is likely due to more complex chemistry occurring at longer times, which is no longer captured in our simple box model. Details on the results and discussion at these concentrations are provided in Appendix B Section B.7.1.

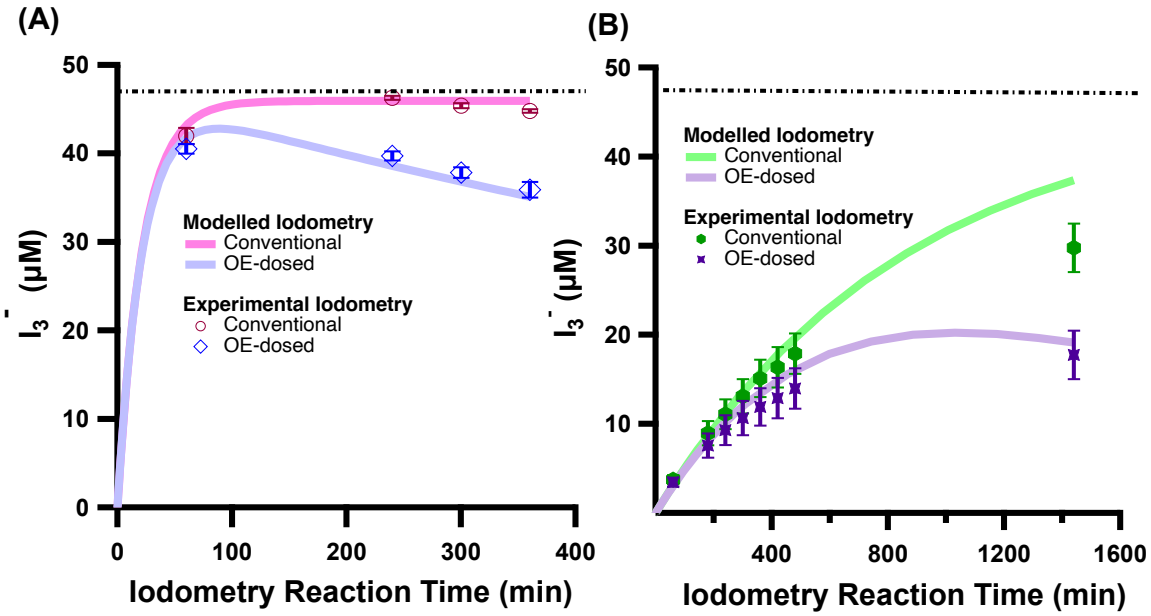

Figure 3.10: Comparison of modeled and experimentally observed concentration of I_3^- in iodometry reactions of H_2O_2 (A) and t-BP (B) over the course of respective reaction times.

Our choice of peroxides-H_2O_2 and t-BP- in these simulations, represent two extreme cases because H_2O_2 reacts rapidly with I^-, while t-BP much more slowly.[164, 181] Whereas many other organic peroxides, such as those present in SOA, fall in between.[279] The fact that our model was successful in simulating both H_2O_2 and t-BP, we are confident that it can be applied to other peroxide species. The complications here are that the reaction kinetics of peroxides with I^-, as well as OE with I_2 are both species dependent. This makes it difficult to apply one set of kinetics data to all of peroxide and OE species. However, as we demonstrated throughout this work, an empirical fit with the conventional iodometry, as well as a simple kinetic determination of OE-I_2 are sufficient to build a model that can reasonably predict the magnitude of deviation due to OE.

3.4 Implications

With the data obtained in this work, we have estimated the potential bias of OEs in common applications of iodometry, including outdoor and indoor air pollutants, edible oils, and fats from animals. We have outlined the estimated range of OE concentrations observed in these matrices in Table 3.2. The respective biases originating from these concentrations are also discussed below. Note that this serves as a first-cut estimate using data obtained with 3OE. The actual OEs present in the types of samples discussed below constitute a variety of species.[328, 337] A detailed explanation for these estimations are summarized in Appendix B Section B.8.

Table 3.2: Concentrations and deviations from OEs.

OE matrix	OE content (mM)[a]	Deviation (%)	Citation
Outdoor[b]	8.27 x 10^{-5}	Negligible	[372, 373]
Indoor[c]	0.19-2	3-20	[323]
Edible oils[d]	10.7-12-9	14-40	[374]
Lipids in meat[e]	10.2	14-40	[375]

[a] OE content in each sample matrix has been converted to OE concentrations in iodometry solutions.
[b] e.g., Maleic acid
[c] e.g., C=C content in dinning commons and student offices
[d] e.g., Linoleic acid in soybean oil
[e] e.g., PUFAs in brain tissue of Atlantic Herring

Firstly, the potential impact on the quantification of peroxides in air pollutants is evaluated. The concentration of OEs has been shown to be low in outdoor aerosols due to the reactivity of OEs with oxidants produced by photochemistry.[344, 376] For instance, OEs such as oleic acid and maleic acid are observed at 12 ng m^{-3} and 1.2 ng m^{-3} in particulate matter from Vienna and South East Asian coast, respectively.[372, 377]. These values, after considering extraction, concentration, and dilution in iodometry test, would result in a very low concentration (nmol range), as shown in Table 3.2. We do not expect that such amount of OE would lead to any noticeable degree of deviation. Over the last decade, indoor environments have gained insurmountable attention due to their strong link to human health.[378] As

such, a number of studies have been conducted on chemical analyses of indoor surface materials, which have been found to constitute a significant concentration of OEs.[379] In the recent work of Deming et al, ∼10 μmol m^{-2} surface alkene concentration was found, which is equivalent to 4 mM of C=C in a sample matrix. Considering the range of C=C concentrations observed in this study, these values would be further diluted during iodometry procedures as shown in Table 3.2. Based on these figures, we can expect that ∼3-20% bias against I_3^- measurements can occur. In fact, the wide range of alkene concentrations displayed in indoor surfaces are very well encapsulated in our study (100-1020 μM) and their potential contribution against determination of peroxide content cannot be ignored. In addition to indoor surfaces, cooking emissions are also a dominant source of OEs.[380] Katragadda *et al.*[381] have shown that emissions from cooking methods such as deep frying at temperatures above smoking point of an oil, can contain exceeding levels of OE. In the recent work of Wang *et al.*[322], iodometry was applied to quantify total peroxide content in primary organic aerosols emitted from heating of different edible oils. In this case, it is possible that the demonstrated OE interference can lead to inaccurate estimations of total peroxide content. However, the extent to which the bias can occur would be dependent on the iodometry reaction time.

Secondly, estimation of PV in edible oils is necessary to ensure oil quality for its consumption.[305] Generally, PV test applicable to oil matrices is based on the same principle as shown in Figure 3.1. Raw edible oils can contain PUFAs such as linoleic acid and linolenic acid.[382] This can be observed via the work of Guarrasi *et al.*[374] wherein the upper limit of linoleic acid (65 mM) in soybean oil after dilution as per the PV test (Table 3.2) would be equivalent to 12 mM.[315] The reaction time used in the PV test varies significantly across the literature,[324, 358, 360, 383, 384] with the majority employing a reaction time of <1 h. The bias induced by OE in the PV test was simulated with our kinetic model with peroxide and OE concentrations relevant to oil matrix. Details on this model are provided in Appendix B Section B.8. Our model predicted a deviation between 14-40%. Furthermore, given that our model is based on monounsaturated acid, real matrices with varying degree of unsaturation might exacerbate this bias. These factors should be considered in future studies to represent true bias.

Lastly, dietary intake of poly- and mono-unsaturated fatty acids in lipids could be associated with inflammatory bowel diseases and osteoprotic fractures.[385, 386] Some studies have reported ∼50 mM of PUFA content.[375] These values are obtained with considerations of the total fat content in a given meat and the percentage of PUFA. Such high concentrations of unsaturated acids could remain as potential interfering agents during PV tests. A recent study by Cropotova and Rustad[287] has investigated the amount of lipid hydroperoxides using the PV method in fish extracts. Considering the experimental dilution used during PV analysis, the concentration of PUFAs is ultimately similar to edible oils (∼10.7 mM), which could potentially induce 14-40% bias against quantitative measurements as shown in Table 3.2. Overall, the results from this study demonstrate that the OE-induced bias for iodometry may not affect applications to outdoor air pollutants but is not negligible for indoor environmental samples, food oils, and lipids from animal tissues.

3.5 Conclusions

Iodometry remains a popular technique to quantify total peroxide content in a variety of environmental and food samples due to its selectivity and quantitativeness. Thus, it is imperative to understand potential matrix effects on the accuracy of iodometry, and the current work represents the first of such practices. The observations obtained in our work support our hypothesis that olefinic species cause a negative bias against the quantification of organic peroxides. We found that the interference becomes more significant at higher concentrations and longer reaction times. The interference was observed from all investigated OEs but not from furan, aliphatic and aromatic compounds. The magnitude of interference is variable amongst OE species but consistent across different organic peroxides. This includes SOA extracts, which encompasses a multitude of peroxide species.[71, 180, 246]

The impact of this interference is noticeable OE concentrations over ∼1 mM in the iodometry solutions. Such levels of OE are irrelevant to most outdoor atmospheric aerosol samples. However, through a careful evaluation, we conclude that certain indoor environmental samples, as well as PV tests performed on oils and fats can suffer substantial bias due to OE, ranging from 3% to 40%. Furthermore, we have demonstrated that a simple box model can successfully reproduce the magnitude of inaccuracy induced by OEs. Despite the complexity of reaction kinetics being dependent on both the peroxides and the OE in a matrix, an empirical fitting using iodometry and a simple kinetic investigation were successful in collecting input data for our box model. This approach should be helpful for future investigations using iodometry, where OEs present in the sample matrix can potentially compromise its accuracy.

3.6 Acknowledgments

The authors thank the U of Alberta MS Facility for LC-MS support, Department of Chemistry for loaning undergraduate lab equipment, Dr. Sheref Mansy for UV-Vis instrument, NMR facility for data analysis, and Dr. Yuanglong Huang for assisting in the kinetic model. TG thanks Dr. Jean Cooley Award in Analytical Chemistry for

financial support. SW thanks Alberta Graduate Excellence Scholarship for financial support. This project is supported by NSERC (awards no: RGPIN2018-03814) and U of Alberta.

3.7 Appendix B

Additional experimental details, including quantification of I_2 and OE deviation, product characterization and mechanism, kinetics, model scenarios and calculations.

References

[59] M. Ehn *et al.*, "A large source of low-volatility secondary organic aerosol," en, *Nature*, vol. 506, no. 7489, pp. 476–479, Feb. 2014, ISSN: 0028-0836, 1476-4687. DOI: 10.1038/nature13032.

[71] M. Krapf *et al.*, "Labile Peroxides in Secondary Organic Aerosol," en, *Chem*, vol. 1, no. 4, pp. 603–616, Oct. 2016, ISSN: 24519294. DOI: 10.1016/j.chempr.2016.09.007.

[72] S. A. Epstein, S. L. Blair, and S. A. Nizkorodov, "Direct Photolysis of α-Pinene Ozonolysis Secondary Organic Aerosol: Effect on Particle Mass and Peroxide Content," en, *Environmental Science & Technology*, vol. 48, no. 19, pp. 11 251–11 258, Oct. 2014, ISSN: 0013-936X, 1520-5851. DOI: 10.1021/es502350u.

[73] S. Wang *et al.*, "Organic Peroxides and Sulfur Dioxide in Aerosol: Source of Particulate Sulfate," en, *Environmental Science & Technology*, vol. 53, no. 18, pp. 10 695–10 704, Sep. 2019, ISSN: 0013-936X, 1520-5851. DOI: 10.1021/acs.est.9b02591.

[164] P. Mertes, L. Pfaffenberger, J. Dommen, M. Kalberer, and U. Baltensperger, "Development of a sensitive long path absorption photometer to quantify peroxides in aerosol particles (Peroxide-LOPAP)," en, *Atmospheric Measurement Techniques*, vol. 5, no. 10, pp. 2339–2348, Oct. 2012, ISSN: 1867-8548. DOI: 10.5194/amt-5-2339-2012. [Online]. Available: https://amt.copernicus.org/articles/5/2339/2012/.

[169] S. Zhou, J. C. Rivera-Rios, F. N. Keutsch, and J. P. D. Abbatt, "Identification of organic hydroperoxides and peroxy acids using atmospheric pressure chemical ionization tandem mass spectrometry (APCI/MS/MS) application to secondary organic aerosol," English, *Atmospheric Measurement Techniques*, vol. 11, no. 5, pp. 3081–3089, May 2018, ISSN: 1867-1381. DOI: https://doi.org/10.5194/amt-11-3081-2018. (visited on 08/13/2019).

[170] K. S. Docherty, W. Wu, Y. B. Lim, and P. J. Ziemann, "Contributions of Organic Peroxides to Secondary Aerosol Formed from Reactions of Monoterpenes with O_3, volume = 39," en, *Environmental Science & Technology*, no. 11, pp. 4049–4059, Jun. 2005, ISSN: 0013-936X, 1520-5851. DOI: 10.1021/es050228s. (visited on 02/11/2024).

[171] K. Moore and L. J. Roberts, "Measurement of Lipid Peroxidation," en, *Free Radical Research*, vol. 28, no. 6, pp. 659–671, Jan. 1998, ISSN: 1071-5762, 1029-2470. DOI: 10.3109/10715769809065821. [Online]. Available: http://www.tandfonline.com/doi/full/10.3109/10715769809065821 (visited on 02/03/2024).

[174] W. C. Bray and H. A. Liebhafsky, "REACTIONS INVOLVING HYDROGEN PEROXIDE, IODINE AND IODATE ION. I. INTRODUCTION," en, *Journal of the American Chemical Society*, vol. 53, no. 1, pp. 38–44, Jan. 1931, ISSN: 0002-7863, 1520-5126. DOI: 10.1021/ja01352a006. [Online]. Available: https://pubs.acs.org/doi/abs/10.1021/ja01352a006 (visited on 02/03/2024).

[176] T. D. Crowe and P. J. White, "Adaptation of the AOCS official method for measuring hydroperoxides from small scale oil samples," en, *Journal of the American Oil Chemists' Society*, vol. 78, no. 12, pp. 1267–1269, Dec. 2001, ISSN: 0003-021X, 1558-9331. DOI: 10.1007/s11745-001-0424-7.

[180] R. Zhao, C. M. Kenseth, Y. Huang, N. F. Dalleska, and J. H. Seinfeld, "Iodometry-Assisted Liquid Chromatography Electrospray Ionization Mass Spectrometry for Analysis of Organic Peroxides: An Application to Atmospheric Secondary Organic Aerosol," *Environmental Science & Technology*, vol. 52, no. 4, pp. 2108–2117, Feb. 2018, ISSN: 0013-936X. DOI: 10.1021/acs.est.7b04863. (visited on 08/08/2019).

[181] H. A. Liebhafsky and A. Mohammad, "The Kinetics of the Reduction, in Acid Solution, of Hydrogen Peroxide by Iodide Ion," en, *Journal of the American Chemical Society*, vol. 55, no. 10, pp. 3977–3986, Oct. 1933, ISSN: 0002-7863, 1520-5126. DOI: 10.1021/ja01337a010. [Online]. Available: https://pubs.acs.org/doi/abs/10.1021/ja01337a010 (visited on 04/02/2021).

[215] M. Yao *et al.*, "Multiphase reactions between secondary organic aerosol and sulfur dioxide: Kinetics and contributions to sulfate formation and aerosol aging," *Environmental Science & Technology Letters*, vol. 6, no. 12, pp. 768–774, 2019, Publisher: ACS Publications.

[228] M.-C. Reinnig, J. Warnke, and T. Hoffmann, "Identification of organic hydroperoxides and hydroperoxy acids in secondary organic aerosol formed during the ozonolysis of different monoterpenes and sesquiterpenes by on-line analysis using atmospheric pressure chemical ionization ion trap mass spectrometry," en, *Rapid Communications in Mass Spectrometry*, vol. 23, no. 11, pp. 1735–1741, 2009, ISSN: 1097-0231. DOI: 10.1002/rcm.4065. [Online]. Available: https://onlinelibrary.wiley.com/doi/abs/10.1002/rcm.4065 (visited on 08/21/2019).

[231] J. V. Amorim *et al.*, "pH Dependence of the OH Reactivity of Organic Acids in the Aqueous Phase," en, *Environmental Science & Technology*, vol. 54, no. 19, pp. 12 484–12 492, Oct. 2020, ISSN: 0013-936X, 1520-5851. DOI: 10.1021/acs.est.0c03331. [Online]. Available: https://pubs.acs.org/doi/10.1021/acs.est.0c03331 (visited on 06/22/2021).

[238] G. Schmitz, "Iodine oxidation by hydrogen peroxide in acidic solutions, Bray-Liebhafsky reaction and other related reactions," en, *Physical Chemistry Chemical Physics*, vol. 12, no. 25, pp. 6605–6615, 2010. DOI: 10.1039/B927432D. [Online]. Available: http://pubs.rsc.org/en/content/articlelanding/2010/cp/b927432d (visited on 08/24/2021).

[246] A. Mutzel, M. Rodigast, Y. Iinuma, O. Boge, and H. Herrmann, "An improved method for the quantification of SOA bound peroxides," en, *Atmospheric Environment*, vol. 67, pp. 365–369, Mar. 2013, ISSN: 13522310. DOI: 10.1016/j.atmosenv.2012.11.012.

[262] R. Zhao *et al.*, "Rapid Aqueous-Phase Hydrolysis of Ester Hydroperoxides Arising from Criegee Intermediates and Organic Acids," *The Journal of Physical Chemistry A*, vol. 122, no. 23, pp. 5190–5201, Jun. 2018, ISSN: 1089-5639. DOI: 10.1021/acs.jpca.8b02195. [Online]. Available: https://doi.org/10.1021/acs.jpca.8b02195 (visited on 11/12/2021).

[279] H. Li, Z. Chen, L. Huang, and D. Huang, "Organic peroxides' gas-particle partitioning and rapid heterogeneous decomposition on secondary organic aerosol," English, *Atmospheric Chemistry and Physics*, vol. 16, no. 3, pp. 1837–1848, 2016, ISSN: 16807316. DOI: http://dx.doi.org/10.5194/acp-16-1837-2016.

[286] S. Mueller, H.-D. Riedel, and W. Stremmel, "Determination of Catalase Activity at Physiological Hydrogen Peroxide Concentrations," en, *Analytical Biochemistry*, vol. 245, no. 1, pp. 55–60, Feb. 1997, ISSN: 00032697. DOI: 10.1006/abio.1996.9939. [Online]. Available: https://linkinghub.elsevier.com/retrieve/pii/S000326979699939X (visited on 11/20/2020).

[287] J. Cropotova and T. Rustad, "A new fluorimetric method for simultaneous determination of lipid and protein hydroperoxides in muscle foods with the use of diphenyl-1-pyrenylphosphine (DPPP)," en, *LWT*, vol. 128, p. 109 467, Jun. 2020, ISSN: 0023-6438. DOI: 10.1016/j.lwt.2020.109467. (visited on 11/30/2021).

[288] S Brul and P Coote, "Preservative agents in foods: Mode of action and microbial resistance mechanisms," en, *International Journal of Food Microbiology*, vol. 50, no. 1, pp. 1–17, Sep. 1999, ISSN: 0168-1605. DOI: 10.1016/S0168-1605(99)00072-0. (visited on 12/06/2021).

[289] J. D. Grujic-Milanovic *et al.*, "Excesive consumption of unsaturated fatty acids leads to oxidative and inflammatory instability in Wistar rats," en, *Biomedicine & Pharmacotherapy*, vol. 139, p. 111 691, Jul. 2021, ISSN: 0753-3322. DOI: 10.1016/j.biopha.2021.111691.

[290] G. Thangavelu, M. G. Colazo, D. J. Ambrose, M. Oba, E. K. Okine, and M. K. Dyck, "Diets enriched in unsaturated fatty acids enhance early embryonic development in lactating Holstein cows," en, *Theriogenology*, vol. 68, no. 7, pp. 949–957, Oct. 2007, ISSN: 0093-691X. DOI: 10.1016/j.theriogenology.2007.07.002. (visited on 12/07/2021).

[291] E. Muro, G. E. Atilla-Gokcumen, and U. S. Eggert, "Lipids in cell biology: How can we understand them better?" *Molecular Biology of the Cell*, vol. 25, no. 12, pp. 1819–1823, Jun. 2014, ISSN: 1059-1524. DOI: 10.1091/mbc.e13-09-0516. (visited on 12/02/2021).

[292] E. Niki, Y. Yoshida, Y. Saito, and N. Noguchi, "Lipid peroxidation: Mechanisms, inhibition, and biological effects," *Biochemical and Biophysical Research Communications*, Celebrating 50 Years of Oxygenases, vol. 338, no. 1, pp. 668–676, Dec. 2005, ISSN: 0006-291X. DOI: 10.1016/j.bbrc.2005.08.072. (visited on 07/31/2019).

[293] P. Haberzettl and B. G. Hill, "Oxidized lipids activate autophagy in a JNK-dependent manner by stimulating the endoplasmic reticulum stress response," en, *Redox Biology*, vol. 1, no. 1, pp. 56–64, Jan. 2013, ISSN: 2213-2317. DOI: 10.1016/j.redox.2012.10.003. (visited on 12/07/2021).

[294] D. Pratico, "Lipid Peroxidation and the Aging Process," *Science of Aging Knowledge Environment*, vol. 2002, no. 50, re5–re5, Dec. 2002. DOI: 10.1126/sageke.2002.50.re5. [Online]. Available: https://www.science.org/doi/full/10.1126/sageke.2002.50.re5 (visited on 12/07/2021).

[295] M. M. Gaschler and B. R. Stockwell, "Lipid peroxidation in cell death," *Biochemical and biophysical research communications*, vol. 482, no. 3, pp. 419–425, Jan. 2017, ISSN: 0006-291X. DOI: 10.1016/j.bbrc.2016.10.086. (visited on 12/03/2021).

[296] M. Valko, C. J. Rhodes, J. Moncol, M. Izakovic, and M. Mazur, "Free radicals, metals and antioxidants in oxidative stress-induced cancer," en, *Chemico-Biological Interactions*, vol. 160, no. 1, pp. 1–40, Mar. 2006, ISSN: 0009-2797. DOI: 10.1016/j.cbi.2005.12.009. (visited on 12/06/2021).

[297] Y.-E. Sun, W.-D. Wang, H.-W. Chen, and C. Li, "Autoxidation of Unsaturated Lipids in Food Emulsion," en, *Critical Reviews in Food Science and Nutrition*, vol. 51, no. 5, pp. 453–466, Apr. 2011, ISSN: 1040-8398, 1549-7852. (visited on 05/11/2021).

[298] M. M. Campo, G. R. Nute, S. I. Hughes, M. Enser, J. D. Wood, and R. I. Richardson, "Flavour perception of oxidation in beef," en, *Meat Science*, vol. 72, no. 2, pp. 303–311, Feb. 2006, ISSN: 0309-1740. DOI: 10.1016/j.meatsci.2005.07.015. (visited on 12/06/2021).

[299] J. M. Diaz, S. Plummer, C. Tomas, and C. Alves-de Souza, "Production of extracellular superoxide and hydrogen peroxide by five marine species of harmful bloom-forming algae," *Journal of plankton research*, vol. 40, no. 6, pp. 667–677, 2018.

[300] C. M. Oliveira, A. C. S. Ferreira, V. De Freitas, and A. M. Silva, "Oxidation mechanisms occurring in wines," en, *Food Research International*, vol. 44, no. 5, pp. 1115–1126, Jun. 2011, ISSN: 09639969. DOI: 10.1016/j.foodres.2011.03.050. [Online]. Available: https://linkinghub.elsevier.com/retrieve/pii/S0963996911002092 (visited on 12/05/2021).

[301] P. C. Chai, L. H. Long, and B. Halliwell, "Contribution of hydrogen peroxide to the cytotoxicity of green tea and red wines," en, *Biochemical and Biophysical Research Communications*, vol. 304, no. 4, pp. 650–654, May 2003, ISSN: 0006-291X. DOI: 10.1016/S0006-291X(03)00655-7. (visited on 12/07/2021).

[302] S. Dermiş, S. Can, and B. Doğru, "Determination of peroxide values of some fixed oils by using the mfox method," *Spectroscopy Letters*, vol. 45, no. 5, pp. 359–363, 2012.

[303] M. J. Lagarda, J. G. Mañez, P. Manglano, and R. Farre, "Lipid hydroperoxides determination in milk-based infant formulae by gas chromatography," *European journal of lipid science and technology*, vol. 105, no. 7, pp. 339–345, 2003.

[304] H. Karami, M. Rasekh, and E. Mirzaee-Ghaleh, "Qualitative analysis of edible oil oxidation using an olfactory machine," *Journal of Food Measurement and Characterization*, vol. 14, no. 5, pp. 2600–2610, 2020.

[305] N. Zhang *et al.*, "Analytical methods for determining the peroxide value of edible oils: A mini-review," *Food Chemistry*, vol. 358, p. 129 834, 2021.

[306] C. Liang and B. He, "A titration method for determining individual oxidant concentration in the dual sodium persulfate and hydrogen peroxide oxidation system," *Chemosphere*, vol. 198, pp. 297–302, 2018.

[307] C. Deyrieux *et al.*, "Measurement of peroxide values in oils by triphenylphosphine/triphenylphosphine oxide (tpp/tppo) assay coupled with ftir-atr spectroscopy: Comparison with iodometric titration," *European Journal of Lipid Science and Technology*, vol. 120, no. 8, p. 1 800 109, 2018.

[308] W. W. Christie, "Lipid analysis," *Trends in Food Science & Technology*, vol. 11, no. 7, p. 145, 1996.

[309] A. O. M. Cd 8b 90, "Peroxide value Acetic Acid-Isooctane Method," *Official methods and recommended practices of the Am. Oil Chem. Soc.*, 1989, Publisher: AOCS Champaign, IL, USA.

[310] K. Yagi, "Lipid peroxides and human diseases," *Chemistry and physics of lipids*, vol. 45, no. 2-4, pp. 337–351, 1987.

[311] L. Gheysen, C. Dejonghe, T. Bernaerts, A. Van Loey, L. De Cooman, and I. Foubert, "Measuring primary lipid oxidation in food products enriched with colored microalgae," *Food Analytical Methods*, vol. 12, no. 10, pp. 2150–2160, 2019.

[312] S. Alfei, P. Oliveri, and C. Malegori, "Assessment of the efficiency of a nanospherical gallic acid dendrimer for long-term preservation of essential oils: An integrated chemometric-assisted ftir study," *ChemistrySelect*, vol. 4, no. 30, pp. 8891–8901, 2019.

[313] M. Cullere *et al.*, "Effect of the incorporation of a fermented rooibos (aspalathus linearis) extract in the manufacturing of rabbit meat patties on their physical, chemical, and sensory quality during refrigerated storage," *LWT*, vol. 108, pp. 31–38, 2019.

[314] S. Devaramani, K. S. Kumar, B. Suma, and M Pandurangappa, "Rhodamine b phenylhydrazide as a new chemosensor for sulfite quantification: Application to food samples," *Materials Today: Proceedings*, vol. 49, pp. 748–755, 2022.

[315] F. Longobardi, F. Contillo, L. Catucci, L. Tommasi, F. Caponio, and V. M. Paradiso, "Analysis of peroxide value in olive oils with an easy and green method," *Food Control*, vol. 130, p. 108 295, 2021.

[316] W. E. Gilbraith, J. C. Carter, K. L. Adams, K. S. Booksh, and J. M. Ottaway, "Improving prediction of peroxide value of edible oils using regularized regression models," *Molecules*, vol. 26, no. 23, p. 7281, 2021.

[317] M. Tareq, S. Rahman, and M. Hashem, "Effect of clove powder and garlic paste on quality and safety of raw chicken meat at refrigerated storage," *World J Nutr Food Sci*, vol. 1, no. 1, p. 1002, 2018.

[318] E. Rasinska, J. Rutkowska, E. Czarniecka-Skubina, and K. Tambor, "Effects of cooking methods on changes in fatty acids contents, lipid oxidation and volatile compounds of rabbit meat," *Lwt*, vol. 110, pp. 64–70, 2019.

[319] A. Bilska, "Effect of morus alba leaf extract dose on lipid oxidation, microbiological stability, and sensory evaluation of functional liver pâtes during refrigerated storage," *Plos one*, vol. 16, no. 12, e0260030, 2021.

[320] M. Yao *et al.*, "Multiphase reactions between secondary organic aerosol and sulfur dioxide: Kinetics and contributions to sulfate formation and aerosol aging," *Environmental Science & Technology Letters*, vol. 6, no. 12, pp. 768–774, 2019.

[321] Z. Zhao *et al.*, "Diverse reactions in highly functionalized organic aerosols during thermal desorption," *ACS Earth and Space Chemistry*, vol. 4, no. 2, pp. 283–296, 2019.

[322] S. Wang, M. Takhar, Y. Zhao, L. N. S. Al Rashdi, and A. W. H. Chan, "Dynamic Oxidative Potential of Organic Aerosol from Heated Cooking Oil," *ACS Earth and Space Chemistry*, vol. 5, no. 5, pp. 1150–1162, May 2021, Publisher: American Chemical Society. DOI: 10.1021/acsearthspacechem.1c00038. [Online]. Available: https://doi.org/10.1021/acsearthspacechem.1c00038 (visited on 11/19/2021).

[323] B. L. Deming and P. J. Ziemann, "Quantification of alkenes on indoor surfaces and implications for chemical sources and sinks," en, *Indoor Air*, vol. 30, no. 5, pp. 914–924, Sep. 2020, ISSN: 0905-6947, 1600-0668. DOI: 10.1111/ina.12662. [Online]. Available: https://onlinelibrary.wiley.com/doi/abs/10.1111/ina.12662 (visited on 12/13/2020).

[324] C. Lea, "Methods for determining peroxide in lipids," *Journal of the Science of Food and Agriculture*, vol. 3, no. 12, pp. 586–594, 1952.

[325] J. M. Gebicki, J. Collins, A. Baoutina, and P. Phair, "The Limitations of an Iodometric Aerobic Assay for Peroxides," en, *Analytical Biochemistry*, vol. 240, no. 2, pp. 235–241, Sep. 1996, ISSN: 00032697. DOI: 10.1006/abio.1996.0353. [Online]. Available: https://linkinghub.elsevier.com/retrieve/pii/S000326979690353X (visited on 02/03/2024).

[326] D. K. Banerjee and C. C. Budke, "Spectrophotometric Determination of Traces of Peroxides in Organic Solvents.," en, *Analytical Chemistry*, vol. 36, no. 4, pp. 792–796, Apr. 1964, ISSN: 0003-2700, 1520-6882. DOI: 10.1021/ac60210a027. [Online]. Available: https://pubs.acs.org/doi/abs/10.1021/ac60210a027 (visited on 06/24/2021).

[327] S. Stavber, M. Jereb, and M. Zupan, "Electrophilic Iodination of Organic Compounds Using Elemental Iodine or Iodides," en, *Synthesis*, vol. 2008, no. 10, pp. 1487–1513, May 2008, ISSN: 0039-7881, 1437-210X. DOI: 10.1055/s-2008-1067037. [Online]. Available: http://www.thieme-connect.de/DOI/DOI?10.1055/s-2008-1067037 (visited on 08/26/2021).

[328] J. E. Hunter, "N-3 fatty acids from vegetable oils," en, *The American Journal of Clinical Nutrition*, vol. 51, no. 5, pp. 809–814, May 1990, ISSN: 0002-9165, 1938-3207. DOI: 10.1093/ajcn/51.5.809. (visited on 12/08/2021).

[329] J. Chebet, T. Kinyanjui, and P. K. Cheplogoi, "Impact of frying on iodine value of vegetable oils before and after deep frying in different types of food in kenya," *Journal of Scientific and Innovative Research*, vol. 5, no. 5, pp. 193–196, 2016.

[330] E. E. Gooch, "Determination of the Iodine Value of Selected Oils: An Experiment Combining FTIR Spectroscopy with Iodometric Titrations," en, *The Chemical Educator*, vol. 6, no. 1, pp. 7–9, Feb. 2001, ISSN: 1430-4171. DOI: 10.1007/s00897000438a. [Online]. Available: http://link.springer.com/10.1007/s00897000438a (visited on 12/13/2020).

[331] Y. B. C. Man, G. Setiowaty, and F. R. v. d. Voort, "Determination of iodine value of palm oil by fourier transform infrared spectroscopy," en, *Journal of the American Oil Chemists' Society*, vol. 76, no. 6, pp. 693–699, 1999, ISSN: 1558-9331. DOI: https://doi.org/10.1007/s11746-999-0161-9. [Online]. Available: http://aocs.onlinelibrary.wiley.com/doi/abs/10.1007/s11746-999-0161-9 (visited on 12/13/2020).

[332] C.-c. Lee and B. D. Pollard, "Determination of iodine value fatty acids by a flow-injection method," en, *Analytica Chimica Acta*, vol. 158, pp. 157–167, Jan. 1984, ISSN: 0003-2670. DOI: 10.1016/S0003-2670(00)84824-2. [Online]. Available: http://www.sciencedirect.com/science/article/pii/S0003267000848242 (visited on 11/22/2020).

[333] T. Haryati, Y. B. Che Man, H. M. Ghazali, B. A. Asbi, and L. Buana, "Determination of iodine value of palm oil based on triglyceride composition," en, *Journal of the American Oil Chemists' Society*, vol. 75, no. 7, pp. 789–792, Jul. 1998, ISSN: 0003-021X, 1558-9331. DOI: 10.1007/s11746-998-0227-0. [Online]. Available: https://aocs.onlinelibrary.wiley.com/doi/10.1007/s11746-998-0227-0 (visited on 02/03/2024).

[334] M. Barsukova, I. Veselova, and T. Shekhovtsova, "Main methods and approaches to the determination of markers of oxidative stress organic peroxide compounds and hydrogen peroxide," *Journal of Analytical Chemistry*, vol. 74, no. 5, pp. 425–436, 2019.

[335] E. D. N. S. Abeyrathne, K. Nam, and D. U. Ahn, "Analytical methods for lipid oxidation and antioxidant capacity in food systems," *Antioxidants*, vol. 10, no. 10, p. 1587, 2021.

[336] R. G. Bernett, J. T. Doi, and W. K. Musker, "Iodocyclization of alkene thioethers. Kinetic evidence against an iodonium ion intermediate," en, *The Journal of Organic Chemistry*, vol. 50, no. 12, pp. 2048–2050, Jun. 1985, ISSN: 0022-3263, 1520-6904. DOI: 10.1021/jo00212a008. [Online]. Available: https://pubs.acs.org/doi/abs/10.1021/jo00212a008 (visited on 06/27/2021).

[337] S. Xu *et al.*, "Localisation of c= c bond and absolute quantification of unsaturated fatty acids in vegetable oils based on photochemical derivatisation reaction coupled with mass spectrometry," *International Journal of Food Science & Technology*, vol. 55, no. 7, pp. 2883–2892, 2020.

[338] R. Domínguez, M. Pateiro, M. Gagaoua, F. J. Barba, W. Zhang, and J. M. Lorenzo, "A comprehensive review on lipid oxidation in meat and meat products," *Antioxidants*, vol. 8, no. 10, p. 429, 2019.

[339] L. Das, D. K. Bora, S. Pradhan, M. K. Naik, and S. Naik, "Long-term storage stability of biodiesel produced from karanja oil," *Fuel*, vol. 88, no. 11, pp. 2315–2318, 2009.

[340] Ş. Altun, "Effect of the degree of unsaturation of biodiesel fuels on the exhaust emissions of a diesel power generator," *Fuel*, vol. 117, pp. 450–457, 2014.

[341] L Chuecas and J. Riley, "The component fatty acids of some sea-weed fats," *Journal of the Marine Biological Association of the United Kingdom*, vol. 46, no. 1, pp. 153–159, 1966.

[342] Z. Nitsan, Y Carasso, Z. Zoref, and I Nir, "Effect of diet on the fatty acid profile of adipose tissues and muscle fat of kids," in *Annales de zootechnie*, vol. 36, 1987, pp. 339–341.

[343] V Banskalieva, T Sahlu, and A. Goetsch, "Fatty acid composition of goat muscles and fat depots: A review," *Small Ruminant Research*, vol. 37, no. 3, pp. 255–268, 2000.

[344] D. Ray and D. Waddington, "Gas phase oxidation of alkenes Part II. The oxidation of 2-methylbutene-2 and 2,3-dimethylbutene-2," en, *Combustion and Flame*, vol. 20, no. 3, pp. 327–334, Jun. 1973, ISSN: 00102180. (visited on 12/06/2021).

[345] L.-Y. He *et al.*, "Characterization of high-resolution aerosol mass spectra of primary organic aerosol emissions from Chinese cooking and biomass burning," en, *Atmospheric Chemistry and Physics*, vol. 10, no. 23, pp. 11 535–11 543, Dec. 2010, ISSN: 1680-7324. DOI: 10.5194/acp-10-11535-2010. [Online]. Available: https://acp.copernicus.org/articles/10/11535/2010/ (visited on 08/26/2021).

[346] X. Zhao *et al.*, "Composition profiles of organic aerosols from Chinese residential cooking: Case study in urban Guangzhou, south China," en, *Journal of Atmospheric Chemistry*, vol. 72, no. 1, pp. 1–18, Mar. 2015, ISSN: 0167-7764, 1573-0662. DOI: 10.1007/s10874-015-9298-0. (visited on 08/26/2021).

[347] Y. Zhao, M. Hu, S. Slanina, and Y. Zhang, "Chemical Compositions of Fine Particulate Organic Matter Emitted from Chinese Cooking," *Environmental Science & Technology*, vol. 41, no. 1, pp. 99–105, Jan. 2007, ISSN: 0013-936X. DOI: 10.1021/es0614518. [Online]. Available: https://doi.org/10.1021/es0614518 (visited on 08/26/2021).

[348] B. Bhowmik, G. L. Jendrasiak, and B. Rosenberg, "Charge Transfer Complexes of Lipids with Iodine," en, *Nature*, vol. 215, no. 5103, pp. 842–843, Aug. 1967, ISSN: 0028-0836, 1476-4687. DOI: 10.1038/215842a0. (visited on 12/03/2021).

[349] W. Jessup, R. T. Dean, and J. M. Gebicki, "[29] Iodometric determination of hydroperoxides in lipids and proteins," en, in *Methods in Enzymology*, vol. 233, Elsevier, 1994, pp. 289–303, ISBN: 978-0-12-182134-0. DOI: 10.1016/S0076-6879(94)33032-8. [Online]. Available: https://linkinghub.elsevier.com/retrieve/pii/S0076687994330328 (visited on 11/22/2020).

[350] Y. Endo, "Analytical methods to evaluate the quality of edible fats and oils: The jocs standard methods for analysis of fats, oils and related materials (2013) and advanced methods," *Journal of oleo science*, vol. 67, no. 1, pp. 1–10, 2018.

[351] S. Yu, "Role of organic acids (formic, acetic, pyruvic and oxalic) in the formation of cloud condensation nuclei (CCN): A review," en, *Atmospheric Research*, vol. 53, no. 4, pp. 185–217, May 2000, ISSN: 0169-8095. DOI: 10.1016/S0169-8095(00)00037-5. (visited on 12/12/2021).

[352] A. D. Awtrey and R. E. Connick, "The Absorption Spectra of I_2 , I_3^- , I^- , IO_3^-," en, *Journal of the American Chemical Society*, vol. 73, no. 4, pp. 1842–1843, Apr. 1951, ISSN: 0002-7863, 1520-5126. DOI: 10.1021/ja01148a504.

[353] L. Hartman and M. D. White, "Reagents for iodometric determination of peroxides in fats," *Analytical Chemistry*, vol. 24, no. 3, pp. 527–529, 1952.

[354] P. Ratrinia, U. Komala, *et al.*, "The effect of addition mangrove leaves powder to lipid oxidation of chocolate bar during the shelf life," in *IOP Conference Series: Earth and Environmental Science*, IOP Publishing, vol. 967, 2022, p. 012 023.

[355] B. Lei, N. Adachi, and T. Arai, "Measurement of the extracellular H_2O_2 in the brain by microdialysis," en, *Brain Research Protocols*, vol. 3, no. 1, pp. 33–36, Sep. 1998, ISSN: 1385-299X. DOI: 10.1016/S1385-299X(98)00018-X. (visited on 11/28/2021).

[356] H. Yu, L. Jin, Y. Dai, H. Li, and Y. Xiao, "From a BODIPY rhodamine scaffold to a ratiometric fluorescent probe for nitric oxide," en, *New Journal of Chemistry*, vol. 37, no. 6, p. 1688, 2013, ISSN: 1144-0546, 1369-9261. DOI: 10.1039/c3nj41127c.

[357] K. Sato, S. Hatakeyama, and T. Imamura, "Secondary Organic Aerosol Formation during the Photooxidation of Toluene, NO_x Dependence of Chemical Composition," *The Journal of Physical Chemistry A*, vol. 111, no. 39, pp. 9796–9808, Oct. 2007, ISSN: 1089-5639. DOI: 10.1021/jp071419f.

[358] M. J. Calandra, Y. Wang, and C. Beckett, "Iodide reaction times of peroxyhemiacetals (phas) in the peroxide value titration; implications for the testing of citrus oils," *Flavour and Fragrance Journal*, vol. 35, no. 2, pp. 131–138, 2020.

[359] A. Lezerovich, "Determination of peroxide value by conventional difference and difference-derivative spectrophotometry," *Journal of the American Oil Chemists Society*, vol. 62, no. 10, pp. 1495–1500, 1985.

[360] G. Martinez Tellez, O. Ledea Lozano, and M. F. Díaz Gómez, "Measurement of peroxidic species in ozonized sunflower oil," *Ozone: Science and Engineering*, vol. 28, no. 3, pp. 181–185, 2006.

[361] M. Cirlini, A Caligiani, G Palla, A De Ascentiis, and P Tortini, "Stability studies of ozonized sunflower oil and enriched cosmetics with a dedicated peroxide value determination," *Ozone: Science & Engineering*, vol. 34, no. 4, pp. 293–299, 2012.

[362] S. A. Epstein, D. Shemesh, V. T. Tran, S. A. Nizkorodov, and R. B. Gerber, "Absorption Spectra and Photolysis of Methyl Peroxide in Liquid and Frozen Water," en, *The Journal of Physical Chemistry A*, vol. 116, no. 24, pp. 6068–6077, Jun. 2012, ISSN: 1089-5639, 1520-5215. DOI: 10.1021/jp211304v. [Online]. Available: https://pubs.acs.org/doi/10.1021/jp211304v (visited on 07/05/2021).

[363] C. J. Battaglia, "Kinetics and Mechanism of the Spontaneous Decompositions of Some Peroxoacids, Hydrogen Peroxide and tert-Butyl Hydroperoxide," en, vol. 85, p. 6, 1963.

[364] H. Hartley and N. P. Campbell, "LXIX The solubility of iodine in water," en, *J. Chem. Soc., Trans.*, vol. 93, no. 0, pp. 741–745, 1908, ISSN: 0368-1645. DOI: 10.1039/CT9089300741. (visited on 04/23/2021).

[365] T. A. Foglia, L. S. Silbert, and P. D. Vail, "XII.* Gas-liquid and high-performance liquid chromatographic analysis of aliphatic hydroperoxides and dialkyl peroxides," en, p. 9, 1993.

[366] J. Sanchez and T. N. Myers, "Peroxides and Peroxide Compounds, Organic Peroxides," en, in *Kirk-Othmer Encyclopedia of Chemical Technology*, 2000, ISBN: 978-0-471-23896-6. DOI: 10.1002/0471238961.1518070119011403.a01.

[367] M. Shiraiwa *et al.*, "Aerosol Health Effects from Molecular to Global Scales," *Environmental Science & Technology*, vol. 51, no. 23, pp. 13 545–13 567, Dec. 2017, ISSN: 0013-936X. DOI: 10.1021/acs.est.7b04417. [Online]. Available: https://doi.org/10.1021/acs.est.7b04417 (visited on 09/27/2019).

[368] X. Zhang *et al.*, "Highly Oxygenated Multifunctional Compounds in α-Pinene Secondary Organic Aerosol," *Environmental Science & Technology*, vol. 51, no. 11, pp. 5932–5940, Jun. 2017, ISSN: 0013-936X. DOI: 10.1021/acs.est.6b06588. (visited on 08/15/2019).

[369] I. V. Bodrikov, Y. A. Kurskii, A. A. Chiyanov, N. V. Borisova, and A. Y. Subbotin, "Sterically driven allyl substitution in alkenes with electrophilic iodine," en, *Doklady Chemistry*, vol. 450, no. 2, pp. 162–164, Jun. 2013, ISSN: 0012-5008, 1608-3113. DOI: 10.1134/S0012500813060049. [Online]. Available: http://link.springer.com/10.1134/S0012500813060049 (visited on 07/26/2021).

[370] A. N. French, S. Bissmire, and T. Wirth, "Iodine electrophiles in stereoselective reactions: Recent developments and synthetic applications," en, *Chemical Society Reviews*, vol. 33, no. 6, pp. 354–362, 2004. DOI: 10.1039/B310389G. [Online]. Available: http://pubs.rsc.org/en/content/articlelanding/2004/cs/b310389g (visited on 03/19/2021).

[371] Z. Z. Song and H. N. C. Wong, "4-disubstituted furans, 5. Regiospecific mono-ipso-iodination of 3,4-bis(trimethylsilyl)furan and regiospecific ipso-iodination of tris[(4-alkyl- or -aryl)furan-3-yl]boroxines to 4-substituted 3-(trimethylsilyl)furans and unsymmetrical, 3,4-disubstituted furans," en, *Liebigs Annalen der Chemie*, vol. 1994, no. 1, pp. 29–34, 1994, ISSN: 1099-0690. DOI: 10.1002/jlac.199419940107. (visited on 12/09/2021).

[372] M. Mochida, N. Umemoto, K. Kawamura, H.-J. Lim, and B. J. Turpin, "Bimodal size distributions of various organic acids and fatty acids in the marine atmosphere: Influence of anthropogenic aerosols, asian dusts, and sea spray off the coast of east asia," *Journal of Geophysical Research: Atmospheres*, vol. 112, no. D15, 2007.

[373] M. Mochida *et al.*, "Spatial distributions of oxygenated organic compounds (dicarboxylic acids, fatty acids, and levoglucosan) in marine aerosols over the western pacific and off the coast of east asia: Continental outflow of organic aerosols during the ace-asia campaign," *Journal of Geophysical Research: Atmospheres*, vol. 108, no. D23, 2003.

[374] V Guarrasi, M. Mangione, V Sanfratello, V Martorana, and D Bulone, "Quantification of underivatized fatty acids from vegetable oils by hplc with uv detection," *Journal of chromatographic science*, vol. 48, no. 8, pp. 663–668, 2010.

[375] G Mourente and D. Tocher, "Lipid class and fatty acid composition of brain lipids from atlantic herring (clupea harengus) at different stages of development," *Marine Biology*, vol. 112, no. 4, pp. 553–558, 1992.

[376] G. D. Smith, E. Woods, C. L. DeForest, T. Baer, and R. E. Miller, "Reactive Uptake of Ozone by Oleic Acid Aerosol Particles: Application of Single-Particle Mass Spectrometry to Heterogeneous Reaction Kinetics," en, *The Journal of Physical Chemistry A*, vol. 106, no. 35, pp. 8085–8095, Sep. 2002, ISSN: 1089-5639, 1520-5215. DOI: 10.1021/jp020527t. [Online]. Available: https://pubs.acs.org/doi/10.1021/jp020527t (visited on 06/30/2021).

[377] A. Limbeck and H. Puxbaum, "Organic acids in continental background aerosols," *Atmospheric Environment*, vol. 33, no. 12, pp. 1847–1852, 1999.

[378] C. Weschler, "Chemistry in indoor environments: 20 years of research," *Indoor Air*, vol. 21, no. 3, pp. 205–218, 2011.

[379] J. Kang, J. Liu, and J. Pei, "The indoor volatile organic compound (voc) characteristics and source identification in a new university campus in tianjin, china," *Journal of the Air Waste Management Association*, vol. 67, no. 6, pp. 725–737, 2017.

[380] S. Z. He *et al.*, "Measurement of atmospheric hydrogen peroxide and organic peroxides in Beijing before and during the 2008 Olympic Games: Chemical and physical factors influencing their concentrations," en, *Journal of Geophysical Research: Atmospheres*, vol. 115, no. D17, 2010, ISSN: 2156-2202. DOI: 10.1029/2009JD013544. [Online]. Available: https://agupubs.onlinelibrary.wiley.com/doi/abs/10.1029/2009JD013544 (visited on 05/23/2019).

[381] H. R. Katragadda, A. Fullana, S. Sidhu, and Á. A. Carbonell-Barrachina, "Emissions of volatile aldehydes from heated cooking oils," *Food Chemistry*, vol. 120, no. 1, pp. 59–65, 2010.

[382] A. Kamal-Eldin and R. Andersson, "A multivariate study of the correlation between tocopherol content and fatty acid composition in vegetable oils," *Journal of the American Oil Chemists' Society*, vol. 74, no. 4, pp. 375–380, 1997.

[383] V. Mureşan *et al.*, "Determination of peroxide value in sunflower halva using a spectrophotometric method," *Bulletin UASVM Agriculture*, vol. 67, no. 2, pp. 334–339, 2010.

[384] T. Gutfinger, M. Peled, and A. Letan, "Iodometric determination of the peroxide value of edible oils," *Journal of the Association of Official Analytical Chemists*, vol. 59, no. 1, pp. 148–152, 1976.

[385] H. Mozaffari, E. Daneshzad, B. Larijani, N. Bellissimo, and L. Azadbakht, "Dietary intake of fish, n-3 polyunsaturated fatty acids, and risk of inflammatory bowel disease: A systematic review and meta-analysis of observational studies," *European Journal of Nutrition*, vol. 59, no. 1, pp. 1–17, 2020.

[386] H Mozaffari, K Djafarian, M. Mofrad, and S Shab-Bidar, "Dietary fat, saturated fatty acid, and monounsaturated fatty acid intakes and risk of bone fracture: A systematic review and meta-analysis of observational studies," *Osteoporosis International*, vol. 29, no. 9, pp. 1949–1961, 2018.

Chapter 4

Chemical insights into molecular composition of organic aerosols in the urban region of Houston, Texas

4.1 Introduction

Atmospheric fine particulate matter ($PM_{2.5}$) imposes a tremendous burden on human health by inducing oxidative stress,[387] deteriorates air quality via haze formation[388] and alter Earth's radiation budget by influencing light absorption, scattering, and cloud formation properties.[389–391] Organic matter within atmospheric particles (20-90% by particle mass)[392] can influence secondary organic aerosol (SOA) formation[393, 394] and affect the hygroscopicity of suspended particles, [395, 396] thereby acting as the cloud condensation nuclei (CCN).[397] SOA, originating from atmospheric oxidative processing of biogenic and anthropogenic volatile organic compounds (VOCs), has garnered worldwide attention due to contributions towards heavy haze formation episodes in urban regions.[44, 398, 399] Many field studies have revealed that isoprene, monoterpenes, sesquiterpenes and aromatic hydrocarbons (PAHs) are major SOA precursors, thereby contributing significantly towards abundance of biogenic and anthropogenic SOA.[44, 400]

SOA constitutes a wide range of compounds, including oxidized hydrocarbons, nitrates, imines, amines, and others [401–403]. Generally, these organic constituents can be classified into four major categories: compounds containing only C, H and O (CHO), compounds containing C, H, N and O (CHNO), compounds containing C, H, O and S (CHOS), and compounds containing C, H, N, O and S (CHNOS) [404, 405]. Organosulfates (CHOS), CHNOS, and organonitrates (CHNO) are known important SOA tracers and assist in understanding the anthropogenic sulfur/NO_x budget [406, 407]. CHOS and CHNOS play an important role in defining the composition of suburban SOA [408], with CHOS accounting for 10-30% of organic mass [115, 187]. Furthermore, CHOS/CHNOS and CHNO may indicate aqueous-phase processing of biogenic/anthropogenic VOCs [187, 409, 410]. As such, their molecular characterization and formation mechanisms have been a focal point in many chamber and field studies [56, 411–415]. Field sampling data has shown that CHOS can contribute up to 12% of the total sulfur [416] (or 30% of total organic mass) [56, 187, 417], while CHNO contribute > 60% of the total nitrate mass [418, 419]. Numerous studies have shown that CHOS tend to exhibit seasonal variation [420–422], thereby demonstrating strong correlation towards regional formation sources (i.e., biogenic vs

anthropogenic VOC sources) [422–424]. The formation of CHOS is possible through multiple pathways including substitution of CHNOs by sulfate [425], organic peroxide catalyzed conversion of SO_2 (g) [73, 426], sulfate radical initiated oxidation [63], and reactions of unsaturated organic compounds with SO_2 [427–430]. CHNOS may be either formed via reaction of CHNOs with sulfate or during photooxidation of VOCs through peroxy radical dominated pathways [431]. Formation mechanisms of CHNOs can involve nitrate (NO_3) radical initiated oxidation of VOCs, which often determines the nighttime NO_3 budget [431]. Recent work by Ning et al. [432] has demonstrated that the persistence of monoterpene derived CHOS can significantly depreciate air quality by accelerating haze formation. Additionally, the CHOS formation is an indicator for heterogeneous uptake reactions of anthropogenic SO_2 (g), likely impacting aerosol acidity [433].

Liquid water content in aerosols is known to facilitate the formation of CHOS/CHNO.[187, 434, 435] This indicates a potential link between occurrence of cloud events (e.g., convective) and CHOS/CHNO,[49, 409] especially since convective clouds vertically transport chemical compounds (gases, particles etc.), thereby affecting how vertical profiles of such species interact with radiation.[436] Additionally, laboratory studies have shown that meteorological factors such as relative humidity (RH) can inhibit and/or promote CHOS formation,[76, 437–439] whereas their elevated structure-dependent hygroscopicity (0.6)[30, 76, 78, 440, 441] can facilitate condensed phase partitioning, thereby accelerating particle growth and CCN forming potential of aerosols.[115, 442]

SOA composition widely varies across forested,[443, 444] urban[445] and remote regions.[446] While biogenic VOCs such as isoprene remain a consistent precursor for SOA in different environments,[447, 448] the Atmospheric Radiation Measurement (ARM) TRacking Aerosol Convention interactions ExpeRiment (TRACER) campaign location in southwestern Houston, Texas (TX) represents a unique geographical location for which further investigation of SOA molecular composition is warranted.[447, 449, 450] Houston, TX has remained a significant focus in the scientific community due to its high PM concentrations attributable to dense urbanization and industrial emissions,[451–453] with southeast and northeast locations (e.g., La Porte) investigated elsewhere.[454–457] Some of these studies have found high concen-

trations of CHNOs contributing up to 66% of the OA mass and[456] predominantly influenced by biogenic precursors such as sesquiterpenes.[458]

The field sampling site is composed of agricultural land, which is also in proximity to both the urban Houston and coastal locations (Appendix C Figure C.1). This indicates that the aerosol composition can be widely influenced by biogenic, anthropogenic and inorganic (i.e., marine) constituents. The objective of this study is to understand daily and day-and night-time variation in the aerosol composition across the ancillary site (S3, Figure C.1) located in southwestern Houston. Specifically, we aim to: (i) study molecular composition of SOA, particularly sulfate/nitrate enriched species, (ii) understand the influence of meteorological factors on aerosol constituents, and (iii) provide a possible association between sulfate/nitrate enriched species and cloud formation events (e.g., convective).

4.2 Materials and Methods

4.2.1 Sample Collection

The filter samples were collected during TRACER field campaign at the ancillary site (-29.328000, -95.741000) on the southwest of downtown Houston (Appendix C, Figure C.1). The ground samples were collected using an aerosol collector on 47 mm polytetrafluoroethylene (PTFE) filters by pulling air at 30 L/min for ∼12 h. Two samples were collected each day (day and night respectively) over the period of June 2 to June 14, 2022 (Table C.1). Samples were stored at -20 °C until analysis. Co-located particle samples for micro-spectroscopy analysis were collected via a sioutas cascade impactor (sioutasSKC) at 9 L/min (Model B1B-090V12AN-00, Parker Hannifin).[459] Particles were collected on four different stages: A, B, C & D. All the micro-spectroscopy analyses were performed on stage D particles, which has a 50% cut-off particle diameter 0.15 μm. Stage D is chosen for its good sample loading in comparison to stages A, B and C.[459]

4.2.2 Nanospray Desorption ElectroSpray Ionization High-Resolution Mass Spectrometry (Nano-DESI-HRMS)

The design and implementation of nano-DESI is based on previous work described elsewhere.[167, 445, 460–462] All nano-DESI experiments were coupled to a high resolution LTQ Velos Orbitrap mass spectrometer (Thermo Scientific, Waltham) in a negative ion mode. Samples were analyzed by MS1 (m/z 100-650) with a mass resolution of 100,000 (unitless) at m/z 400 and organic solvent mixture of 7:3 ACN:Water (HPLC-grade, Fischer Scientific $\geq$ 99.9 %) at a flow rate of 0.75 μL/min. The maximum ion injection time was 500 ms to reach an automatic gain control (AGC) target of 300,000. The MS inlet capillary was maintained at 275 °C for all analyses. While nano-DESI-HRMS is a non-exhaustive method for particle-bound characterization of OAs, additional attempts to pursue extraction based methods (e.g., solid-phase extraction with heated electrospray ionization coupled to HRMS)[463] were found to be unsuccessful. As such, nano-DESI-HRMS was primarily utilized for sample analysis.

4.2.3 HRMS Analysis

The nano-DESI assembly (Appendix C, Figure C.2) was scanned along the XY plane of the substrate at 50 μm/s within a 1 cm radius of the filter center.[402] Briefly, 100 MS1 scans were collected for each sample, which were then averaged in Xcalibur (Thermo Scientific). Centroid peak lists were subsequently processed via MFAssignR,[464] an open source molecular formula assignment software package. All samples were analyzed in triplicates to ensure data quality and offer confidence in measurements. Final MF assignments were limited in the form of $C_xH_yO_zN_{0-3}S_{0-1}$ with restrictions: $0.3 \leq$ H:C ≤ 3.0; $0.3 \leq$ O:C ≤ 3.0; $-20 \leq$ DBE-O ≤ 20 (Double bond equivalents minus oxygen count). Using the volatility parameters, MFs may be classified as: volatile organic carbon (VOC), intermediate VOC (IVOC), semi VOC (SVOC), low VOC (LVOC), or extremely low VOC (ELVOC).[54] Further details on data processing and molecular parametrization based on aromaticity index (AI), DBE are outlined in Appendix C, Figure C.3 and Section C.3.1.

4.2.4 Chemical Imaging and Single-Particle Analysis

We investigated the elemental composition, morphology and size of the particles using computer controlled scanning electron microscope (CCSEM, FEI Quanta Environmental) coupled with the energy-dispersive X-ray (EDX) spectrometer.[459, 465] CCSEM-EDX was operated at 20 kV and 480 pA current at 293 K and under vacuum conditions (2×10^{-6} Torr), resulting in the caveats of the loss of volatile compounds. The particles detected by the X-ray were subsequently categorized into eight distinct groups which are illustrated in Figure C.4 (Appendix C, Section C.4.1). The carbon (C) feature of the particles was analyzed employing scanning transmission X-ray microscopy with near-edge X-ray absorption fine structure spectroscopy (STXM/NEXAFS) at C-K-edge at Advanced Light Source beamline 5.3.2.2., located at the Lawrence Berkeley National Laboratory.[466–468] STXM data can be employed to examine particles that include inorganic substances (IN), organic carbon (OC), elemental carbon mixed with organic carbon (OCEC), inorganic substances infused with organic carbon (OCIn), and mixtures of organic carbon, elemental carbon, and inorganic inclusions (OCInEC). Additional details on particle and organic feature classification are provided in Appendix C, Section C.4.1.

4.2.5 Remote sensing Measurements

The Department of Energy (DOE) ARM Micropulse Lidar is a ground-based active remote-sensing system designed to capture detailed vertical profiles of atmospheric aerosols and clouds [469]. Lidar backscattered signal intensity measurements were acquired at the La Porte, TX campaign site (76 km away from the ancillary site). Operating at a short wavelength of 532 nm, lidar can provide accurate detections of clouds including shallow clouds and thin cirrus.[470] The Ka-band ARM Zenith Radar (KAZR) is a zenith-pointing doppler radar system that operates at a millimeter wavelength.[471] Therefore, KAZR is more sensitive to larger particles such as cloud drops and ice crystals. Due to different sensitivities, combined doppler-lidar data provide complementary detections of cloud vertical structures.

4.3 Results and Discussion

4.3.1 Chemical Imaging of Individual Particles

CCSEM-EDX based size-resolved chemical composition (Figure C.5) shows that particles ranging from 0.1-2 μm in early June (i.e., June 3 and June 4) days (Figures C.5 (A) and (B)) were dominated by sulfate and carbonaceous particles (29-41%), (Table C.2) whereas particles in June 11 and June 12 (Figures C.5 (C) and (D)) were enriched with dust (39-64%). Figures C.5 (E)-(H) demonstrate organic volume fraction in each day, wherein June 3 and June 4 were found to constitute 23-41% of organics in contrast to 0.5-0.9% in June 11 and June 12 (Table C.3). Given the organic enrichment found in June 3 to June 4, HYSPLIT air mass trajectories (Figure C.6, Section C.5.1) were examined. From these, June 3 and June 4 exhibited northern wind influence with an elevated organic fraction, while southern winds dominated later June (i.e., June 11 to June 14) sampling periods demonstrating an increased inorganic fraction. Figure 4.1 illustrates the carbon speciation map and STXM/NEXFAS comparison for the organic fractions observed during June 3, June 4, June 11 and June 12. From the carbon speciation map (Figures 4.1 (A)-(D)), it is observed that particles in each sampling day were internally mixed but those in June 4 (Figure 4.1 (B)) showed elevated organic coating in contrast to particles in June 3 (Figure 4.1 (A)), June 11 (Figure 4.1 (C)) and June 12 (Figure 4.1 (D)). Additionally, particles in June 3 and June 4 exhibited higher OCEC fraction (1-5%) (Table C.3) than those in June 11 and June 12 (0-0.9%), which could be indicative of anthropogenic influence.[472] Thus from these observations, it is understood that particles in June 11 and June 12 were under the influence of inorganics and as such, subsequent analysis in Sections 4.3.2, 4.3.3 & 4.3.4 will focus on organic enriched sampling periods of June 3 and June 4.

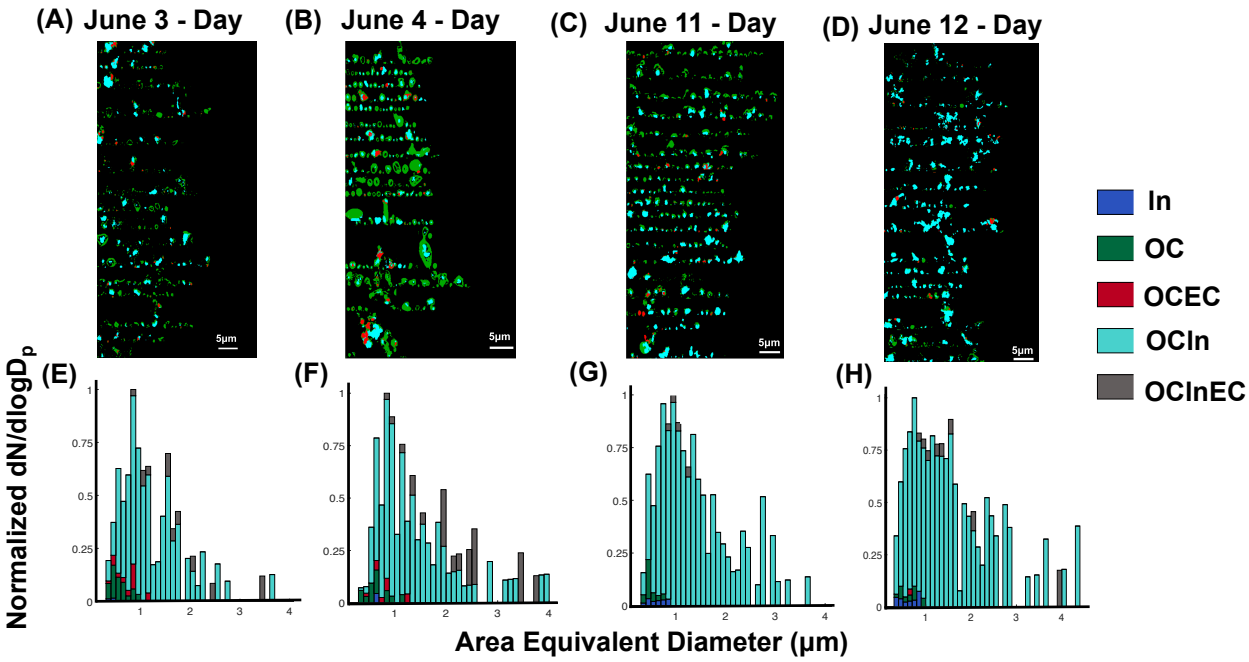

Figure 4.1: Carbon-speciation maps corresponding to June 3 (A), June 4 (B), June 11 (C) and June 12 (D). Color spectrum: green, cyan and red indicate: OC-rich, EC-rich, and In-rich areas, respectively.[459] Histograms (E)-(H) show mixing state of particles across June 3, June 4, June 11 and June 12 respectively.[473–475] Color spectrum: blue, green, red, cyan and grey are indicative of: In, OC, OCEC, OCIn and OCInEC respectively.

4.3.2 Composition of Atmospheric Particles Across Sampling Periods

Figure 4.2 (A) shows a Van Krevelen (VK) diagram and Figure 4.2 (B) displays a plot of average carbon oxidation state (OS_C) as a function of logarithmic saturation mass concentration ($\log_{10}C_0$) for all molecular features (MFs) in organic aerosols that were observed across all daytime sampling periods (i.e., June 2 to June 14, Table C.1). MFs that were found in every day across June 2 to June 14 are colored according to their group (e.g., CHO) while MFs found in different combinations of days (e.g., unique to June 11, June 2 to June 11) are shaded grey. Overall, 291 MFs were found to be common across all daytime samples accounting for 13% of total MFs, while the rest of MFs accounted for 87% of the population, indicating high variability of MFs within sampling days.

Within these 291 MFs commonly observed across all days, 216 were identified as

CHO, 16 as CHNO and 59 as CHOS. This classification is represented in the pie plots, which are scaled according to their weighted abundance (ion signal intensity) as well as the number distribution within the total set of MFs. CHO and CHOS were most abundant in all daytime sampling periods. The characterized common CHOS exhibit O:C ratio > 1.0 (1.2 ± 0.4). The average mass for these common MFs is less than 300 (CHO: 271 ± 62, CHNO: 181 ± 20, CHOS: 239 ± 40) indicating lack of oligomers which are usually found during ozonolysis of VOCs.[413, 476, 477]

Figure 4.2 (B) shows the molecular corridor classification based on volatility for the assigned MFs.[31, 54] $\log_{10}C_0$ is represented against OS_C to identify the degree of oxidation for species and is estimated as per the work of Kroll et al.[478] A positive OS_C is indicative of increase in oxidation of carbon which also reflects an increase in O atoms.[478] The OS_C values for molecular groups in common MFs are less than 0 (CHO: -0.14 ± 0.65, CHNO: -0.63 ± 0.26, CHOS: -0.48 ± 0.55) which demonstrates that the characterized species are likely to be saturated.[479] Interestingly from the volatility distribution, only 2% (or 6 MFs) of the common MFs were classified as ELVOC, while 44% (or 128 MFs) were found in LVOC, 11% (or 32 MFs) in IVOC and 43% (or 125 MFs) in the SVOC bin. A similar description of MFs across nighttime sampling set is provided in Section C.6.1 (Figure C.9). Briefly, similar to the daytime, within the 223 common MFs observed across all nighttime samples, 4% of these MFs were categorized as ELVOCs while 41-48% of MFs were considered S-LVOCs. Furthermore, within the common MFs subset, 28% (or 62 MFs) were CHOS MFs while 5% (or 12 MFs) and 67% (or 149 MFs) were CHNO and CHO MFs, respectively. Thus, it is worth noting that across different sampling periods (daytime and nighttime), the classification of MFs as ELVOC may be more episodic as discussed in Section 4.3.3.

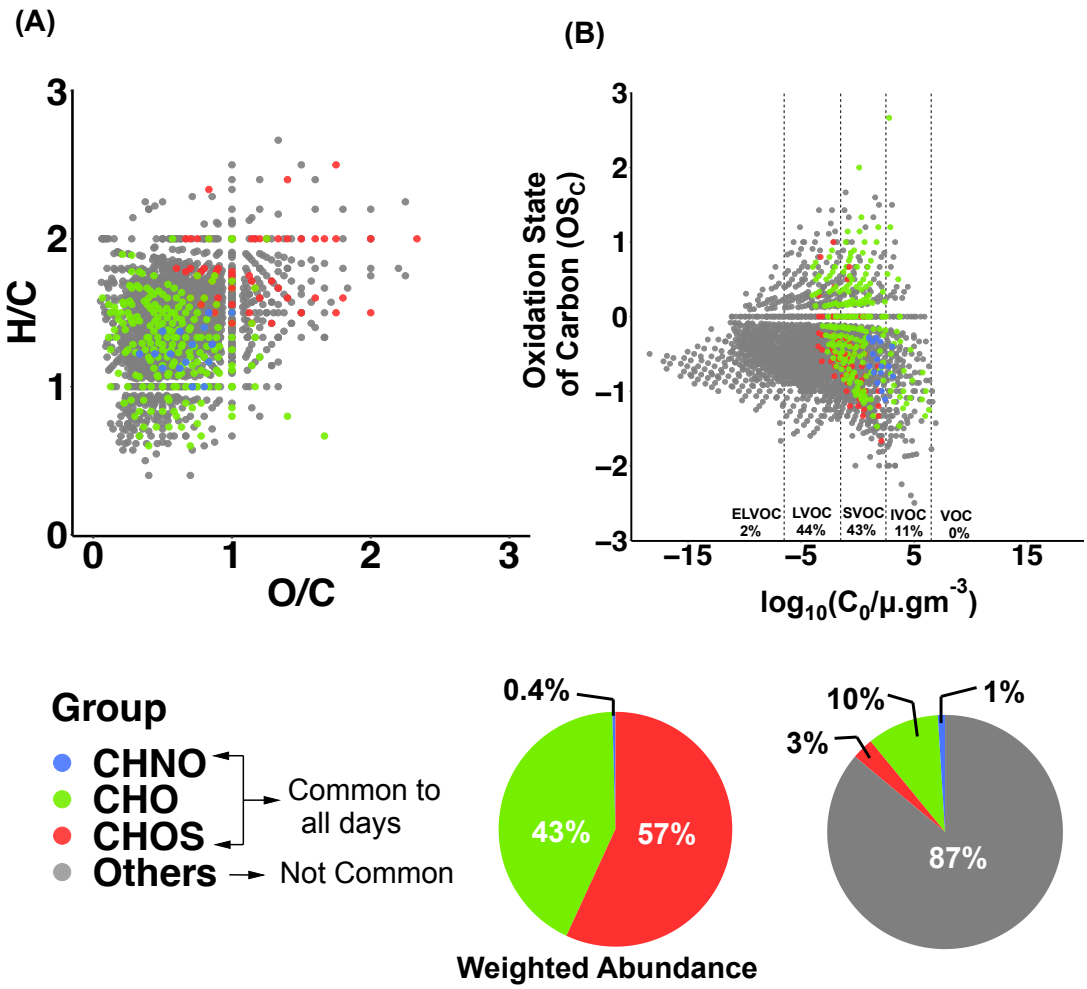

Figure 4.2: General molecular feature representation in OA found across all daytime sampling periods. (A) Van Krevelen diagram for MFs found across all daytime samples is differentiated on the basis of group. MFs found to be common or unique amongst other combinations of sampling periods are shaded grey. (B) Volatility classification of uniquely common MFs to demonstrate distribution of each group of MFs based on their group. The pie charts represent the common MFs which are either scaled according to their percent weighted abundance or number based distribution amongst the total number of MFs (shaded grey).

The common MFs classified as SVOC can influence particle-phase chemistry by diffusing on to existing particles, thereby increasing viscosity and forming oligomers through accretion reactions.[480, 481] Chamber studies have revealed that SVOCs can contribute up to 10% of SOA mass under low NO_x regimes[482] and as such, within the urban environment it is possible with relatively higher NO_x concentrations, MFs in S-LVOC can contribute > 30% of SOA mass.[403, 420, 447, 482, 483] Overall, it is possible that the episodic transport of biogenic VOC can influence the formation of S-IVOCs in the urban atmosphere.[401]

Urban regions can be influenced by biogenic precursors and contribute to the formation of particle-bound CHOS as demonstrated by the work of Bryant et al[431] and Tao et al.[402] Similarly, in the current study, amongst the common MFs, CHOS such as $C_5H_{10}O_6S$, $C_5H_{10}O_5S$, and $C_5H_8O_6S$ are traceable to biogenic precursors (e.g., isoprene).[402] Another case of biogenic influence is exemplified by the observation of $C_{14}H_{22}O_3$ at m/z 237.1496 which is likely an aldehyde product from NO_x/β-caryophyllene reaction.[484, 485] The postulated precursor sources of additional CHOS found commonly in June 2 to June 14 are listed in Table C.5 (Section C.7). With respect to the precursor classification of CHO compounds, anthropogenic influence was observed. For instance, compounds such as $C_7H_{10}O_8$ (m/z 221.0303), $C_9H_{12}O_7$ (m/z 231.0510), $C_9H_{14}O_8$ (m/z 249.0615) and $C_{18}H_{26}O_8$ (m/z 369.1555) are reported in chamber studies from oxidation of 1,3,5-trimethylbenzene (1,3,5-TMB),[486] which is emitted in the urban atmosphere from automobile exhausts.[487] In general, the common features in OAs found across different sampling periods are influenced by both biogenic and anthropogenic precursors.

To further understand the distribution of MFs, Figure 4.3 displays UpSet plot, which shows unique features found in each sampling event and its intersection from a daytime sampling pool. Briefly, from a total of 2192 MFs in the daytime sample pool, MFs that were unique to June 3, unique to June 4 and common to all days account for 65% of the total population. Thus, MFs found only in June 3, June 4 are shown in Figure 4.3 (B), while rest of the MFs found across all other intersections (e.g., June 3 to June 4, June 2 to June 14 etc.) are labelled as "others" and shaded grey. Similarly, Figures C.10 (A) and (B) demonstrate UpSet plot and VK diagram constructed from nighttime sample pool. Herein, from a total of 2592 MFs, those unique to June 2 to

June 4, unique to June 3, unique to June 4 and common to all nights account for 69% of the total population. Thus, samples with most unique MFs are represented in VK diagram in Figure C.9 (A) (Appendix C, Section C.6.1).

Aside from observing the distribution of MFs, organic concentration across each sampling period of June 2022 was probed via Aerosol Chemical Speciation Monitor (ACSM) characterization (Appendix C, Section C.6.3).[488] Figures C.12 (A) and (B) illustrate the distribution of organics and CHNOs from June 1 to June 14 which revealed that organic enrichment was centered mostly in June 1 to June 9 periods with a consistent decline in concentration of organics in later June sampling periods.

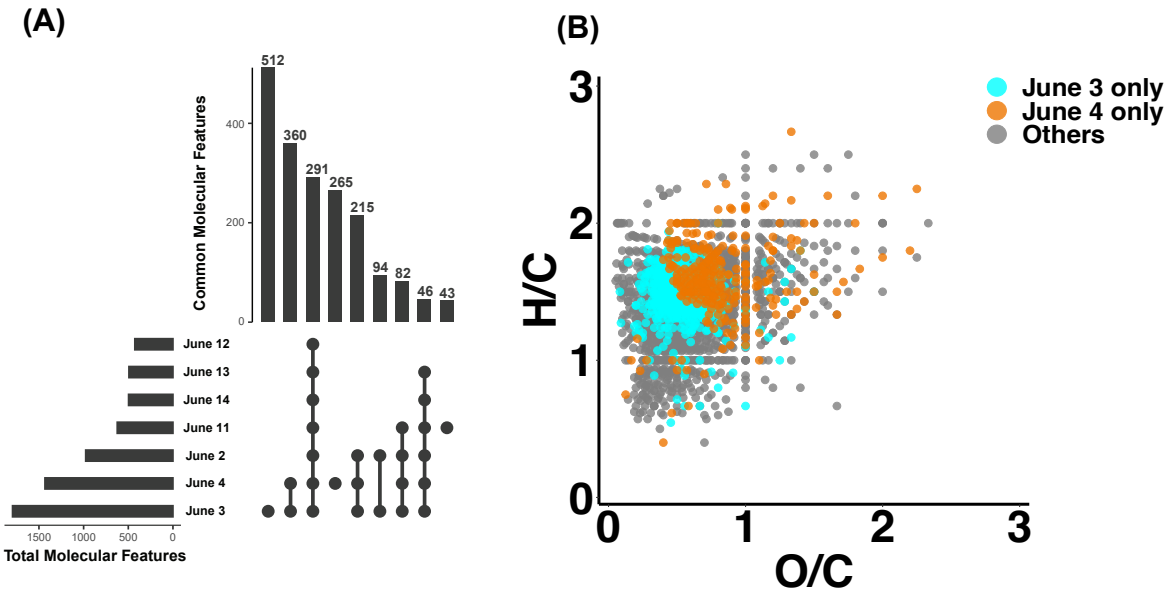

Figure 4.3: Distribution of MFs across all daytime samples for June. (A) Upset plot demonstrates the number of MFs observed in each daytime sampling period. The bars are representative of the number of MFs that are unique to that particular event or its combination. Herein, the UpSet plot only shows intersection with unique MFs > 43 , while the entire distribution is shown in Figure C.11 (Section C.6.2). (B) VK diagram for MFs observed across daytime sampling periods from June 3 to June 4. Colored MFs represent events with most populated features while MFs across all other intersections are shaded grey.

While Figure 4.3 and Figure C.9 represent unique MFs across different intersections of sampling periods, it is worth noting that even without interday comparisons, June 3 and June 4 were the only sampling periods which exhibited > 1000 MFs (Table C.4, Appendix C, Section C.6.4). In contrast, later June sampling periods had < 700 MFs which is further reflected by the VK diagrams and mass spectra shown in Figures C.13, C.14 and C.15 (Appendix C, Section C.6.5). Moreover, the mass spectra corresponding to the daytime sampling periods of June 3 and June 4 shown in Figure C.16 indicate significant distribution of MFs up to m/z 550, which is contrasting to the spectral observations made for later June periods in Figure C.15. This low abundance of organic fraction in later June sampling periods could be due to shifting wind distributions, bringing significant sea-spray aerosol influence (i.e., inorganics dominance) as indicated by HYSPLIT trajectory plots (Figure C.6, Section C.5.1) and micro-spectroscopic analysis.[489] Herein, aside from land-based influence in June 3 and June 4, later sampling periods experienced consistent sea-breeze and minimal organic concentration. Despite the lower organic features in later June periods, m/z 215.02 ($C_5H_{12}O_7S$; suspected to be 2-methyltetrol organosulfate) showed consistent dominance (highest peak) across all samples as exemplified by the mass spectra in Figures C.15 and C.16. This isoprene derived CHOS has been previously reported for similar sampling locations.[56, 411, 412, 420, 490–493]

It is noteworthy that aside from June 3 to June 4, no CHNOS were found in later June periods, which could be either due to the lack of oxidative processing of CHNOs during the sampling periods or their signal intensity being below the detection limit. Thus, based on the organics dominance observed for June 3 and June 4 (Figures 4.2 and 4.3), these dates were chosen as a case study to further investigate the impact of meteorological factors (e.g., wind direction, RH) on the formation of sulfate/nitrate enriched species.

4.3.3 Sample Comparison: Atmospheric Drivers to Molecular Variations

Figure 4.4 demonstrates early June sample comparison from the daytime sample pool. MFs that are unique to June 3 and June 4 are colored according to their molecular group while the rest of MFs found in different intersections of each sampling period (e.g., June 2 to June 3, June 11 to June 12) are labelled as "common" and shaded grey. Figures 4.4 (A) and (B) illustrate the comparison of VK diagram for 512 unique MFs in June 3 from total of 2192 MFs. Herein, 223 were CHNO MF (23% by weighted abundance) and 278 were CHO MF (76% by weighted abundance). Very few CHOS and CHNOS (<1% by weighted abundance) were observed. Contrasting to June 3, June 4 exhibited some distinct CHOS/CHNOS compounds. Figure 4.4 (B) shows a similar VK comparison for unique MFs observed in June 4 from a total of 2192 MFs. Within the 265 unique MFs in June 4, 144 MFs were CHOS (74% by weighted abundance), 91 MFs were CHNOS (22% by weighted abundance), with very few CHO/CHNO MFs ($< 3\%$ by weighted abundance). Based on the subset comparison of unique MFs, the O:C ratios of CHNOs in June 3 (0.6 ± 0.2) and June 4 (0.7 ± 0.2) were > 0.5, O:N ratios (June 3: 10.8 ± 2.7, June 4: 8.7 ± 1.6) > 3 with average mass > 300 (June 3: 433 ± 89, June 4: 318 ± 29) and DBE values (June 3: 6.2 ± 1.5, June 4: 7.2 ± 2.1) > 5 which likely indicates that these species are oxygenated and saturated.[494–496] Additionally, elevated O:C/O:N ratios is indicative of high NO_x oxidative environment for June 3 and June 4 sampling days which is further demonstrated by our observations of increased CHNO concentrations in Figure C.12 (B) (Appendix C, Section C.6.3). A similar comparison for CHNOS revealed O:C ratios > 0.5 (June 3: 0.7 ± 0.1, June 4: 1.0 ± 0.4), O:N ratios > 3 (June 3: 14.1 ± 1.5, June 4: 10.3 ± 2.1), average mass > 350 (June 3: 529 ± 32, June 4: 378 ± 79) and < 5 DBE values, (June 3: 5.3 ± 0.7, June 4: 3.3 ± 1.5) indicating higher oxygenation but also more saturation in contrast to ≤ 0.5 O:C ratios for CHOs observed in June 3 and June 4.[497] The saturation degree is also reflected by average AIs, which are considerably lower for CHNOs in June 3 (0) and CHNOS in June 4 (0.4 ± 1.4) in comparison to the CHNO/CHNOS classification observed in urban regions such as Shanghai, Guangzhou etc.,[498] indicating the lack of aromaticity in observed aerosol

constituents.

Aside from using nano-DESI-HRMS to understand molecular variations, meteorological parameters (Table C.1) were probed to investigate their influence on observed variation in CHOS/CHNOS and CHNOs. Wind rose plots were utilized to elucidate formation sources of CHOS, CHNOS and CHNO that were unique to June 3 and June 4. Agreeing with our findings from HYSPLIT trajectory plots (Figure C.6, Section C.5.1), wind rose plots show dominance of marine influenced southern winds in June 2, as well as for June 11 to June 14 (Figure C.7, Section C.5.2). Contrasting wind direction was observed for early June in Figures 4.4 (C) and (D). Herein, we observed that northwestern winds in June 4 could be a carryover for terrestrial carbon source which is essential for the formation of CHOS unique to June 4.[499] The impact of RH may not be explicit towards formation of CHOS, CHNOS and CHNO as literature reported works have shown that RH can both inhibit and/or promote the formation of these species.[411, 438, 500] This is further illustrated by Figure C.8 (Section C.5.3) demonstrating temporal variation in RH and temperature across June (June 1 to June 14) sampling periods. Some studies have shown that the concentration of CHOS/CHNO can decrease with increasing RH via hydrolysis, but this can be structure dependent.[115, 406, 500] However, this decomposition can be also impacted by other compounding factors (e.g., wind direction, NO_x and wet aerosol chemistry).[411] Despite minimal variation in RH across both daytimes (June 3 = 54.3%, June 4 = 60.8%), the observed CHOS unique to the daytime period of June 4 have been previously reported in cloud water samples.[501] This indicates that there may be a potential association between CHOS (unique to June 4) and cloud formation. Clouds formed with hygroscopic species such as CHOS ($\kappa = 0.6$)[30, 76, 78, 440, 441] may produce strong backscattered radiation signals in contrast to dust. Based on the doppler-lidar signal measurements acquired from La Porte campaign site (Figure C.17, Section C.8), we observed scattered clouds for June 3 and a convective cloud event for June 4. Specifically, we noticed strong signal reflectivity (-20 to 40 dBZ) for June 4 (Figures C.17 (A)) but weak (< -20 dBZ) for June 3 (Figures C.17 (B)).[436] These measurements serve as an evidence on potential positive link between RH influenced formation of observed CHOS and convective cloud structure.

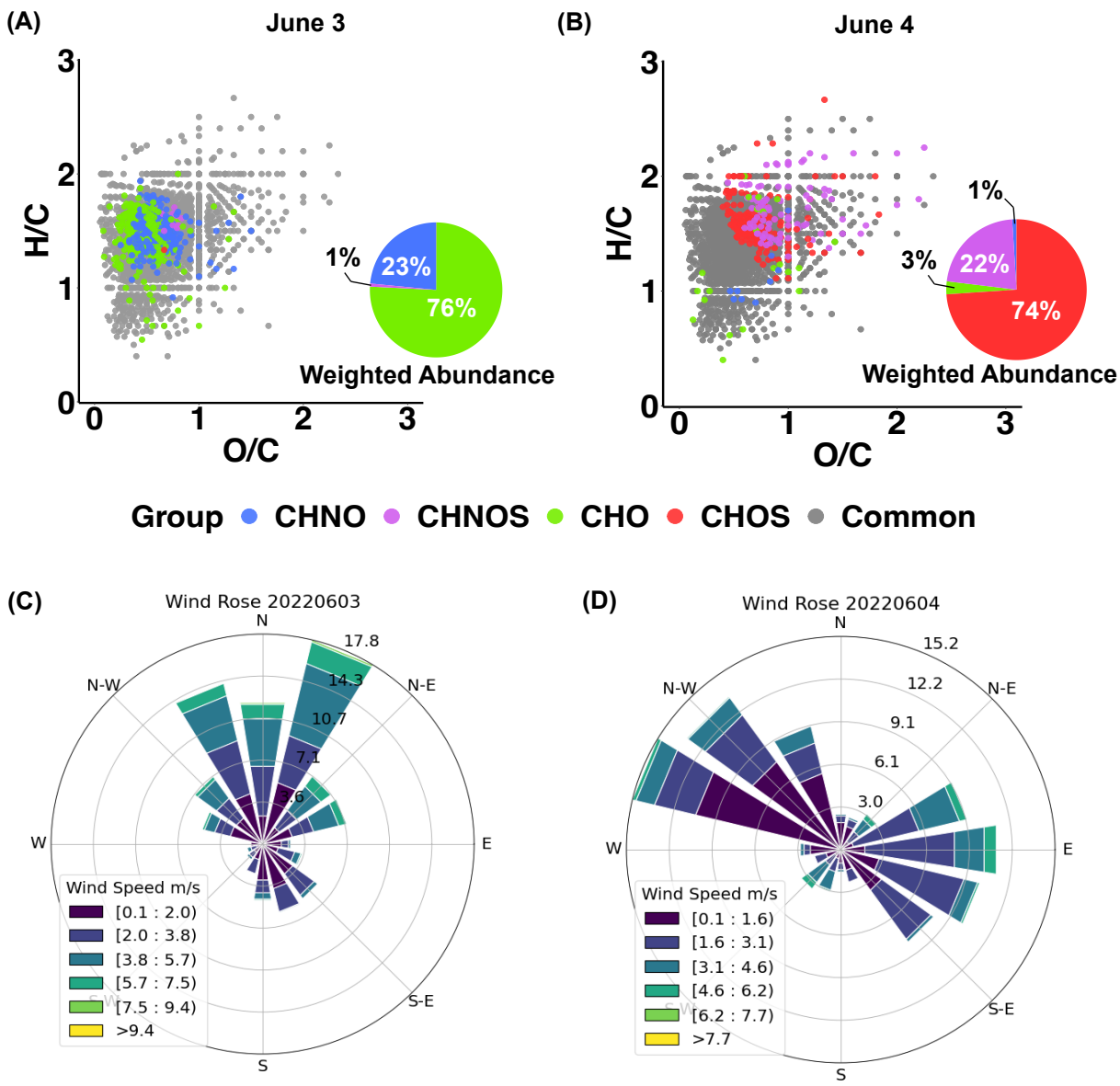

Figure 4.4: Comparison of VK diagrams in the negative ionization mode across daytime sampling periods of June 3 (A) and June 4 (B) during TRACER-ARM campaign. The features found common in both sampling periods and all other intersections (e.g., June 2 to June 3, June 3 to June 11, June 2 to June 14 etc.) are shaded grey while the features found unique in June 3 and 4 are colored according to the molecular groups. The inset pie chart shows weighted abundance distribution (%) of different functional groups which is unique to each sampling period. (C) and (D) represent the wind rose plots for June 3 and June 4 respectively. The circular format indicates the direction the wind blew from towards the epicenter and the length of each spoke shows how often wind blew from that direction. The colors of each spoke indicate the wind speed in m.s^{-1}.

The prevalence of CHOS/CHNOS observed only in June 4 is further probed via volatility set comparison. Figure 4.5 demonstrates the OS_C variation for unique MFs found across early June as a function of $\log_{10}C_0$. Note, the MFs plotted in Figures 4.5 (A) and (B) are a subset of all daytime MFs such that only unique features corresponding to that respective sampling period (i.e., June 3 and June 4) are colored according to their molecular group while the rest of MFs are shaded grey. Figure 4.5 (A) shows the volatility bin distribution for unique CHO/CHNO MFs found in the daytime June 3 sample. From a total of 512 MFs in June 3, 75% (or 382 MFs) were classified as ELVOC, 13% (or 65 MFs) as LVOC, 5% (or 28 MFs) as IVOC and 7% (or 35 MFs) as SVOC. The average O:C ratios for compounds in CHO (278 MFs), CHNO (223 MFs), CHOS (1 MF) and CHNO (10 MFs) groups were > 0.6 while H:C ratios were ≤ 1.5 (Table C.4) and DBE values between 5-7 indicating less oxidation and less saturation, respectively.[54, 404] Figure 4.5 (B) exhibits the volatility distribution of unique CHOS/CHNOS in daytime June 4. Here, similar to June 3, 74% (or 195 MFs) were ELVOCs, 18% (or 47 MFs) were LVOCs, 2% (or 6 MFs) were IVOCs, and 6% (or 17 MFs) were SVOCs from a total of 265 MFs. Within the unique MFs in June 4, 109 CHOS and 78 CHNOS were found with O:C ratio > 0.7 in the ELVOC bin. The pie charts in Figures 4.5 (A) and (B) reflect the number based percent distribution of MFs, with colored regions of pie plot representing unique MFs found in June 3 and June 4, while the grey shaded region indicates rest of the MFs found across the entire pool of daytime samples. The OS_C values corresponding to each of the daytime periods are outlined in Table C.4 (Section C.6.4). We noticed that most of the functional groups unique to early June sample periods exhibited < 0 OS_C and < 0.5 AI values (Table C.4), which is indicative that these compounds are reduced. In fact, Wang et al have shown that CHOS and CHNOS characterized in urban aerosols from Shanghai, Gunagzhou were also found to have lower OSc values in comparison to the CHO and CHNO species.[498] This lower degree of oxidation ($OS_C < 0$, Table C.4) and C atoms > 7 could be characteristic of biomass burning aerosol.[502]

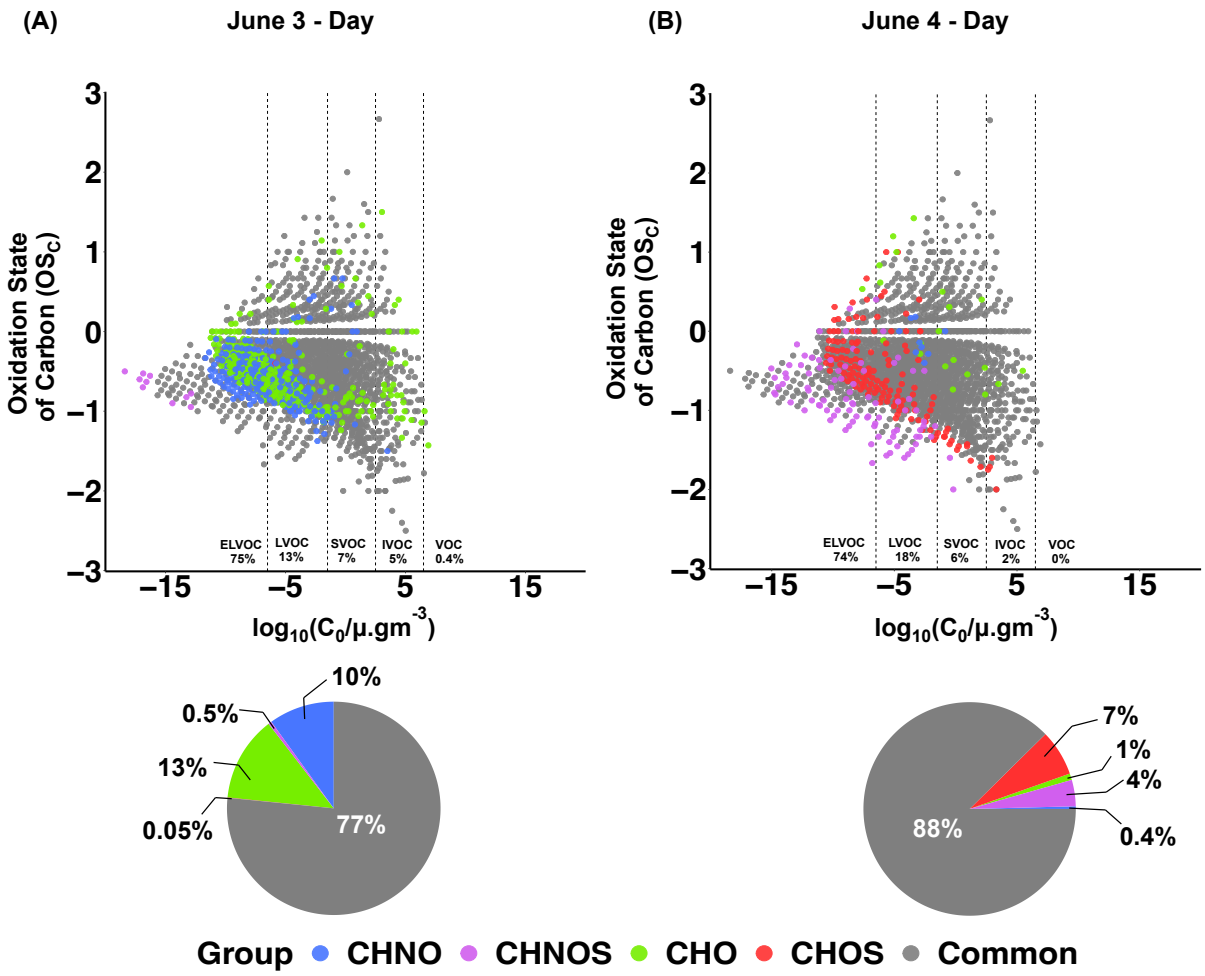

Figure 4.5: Molecular corridors for classified organic species in sampling periods of June 3 and June 4. The daytime comparison in June 3 (A) and June 4 (B) demonstrates volatility based classification of MFs unique to each sampling period. The features which are found either common to both days or across other intersections in daytime sample pool (e.g., June 2 to June 4, June 11 to June 12 etc.) are shaded grey while features unique to each day are colored according to the molecular groups. The bottom pie plots corresponding to each volatility classification represent number based percent distribution of features unique to June 3 (512 MFs) and June 4 (265 MFs) from a total of 2192 MFs.

Table C.5 (Section C.7) outlines the list of CHOS, CHNOS and CHNO which were found to be common amongst all daytime samples (June 2 to June 14), unique to June 3 and/or unique to June 4. Based on the list in Table C.5, it is perceived that the CHOS, CHNOS and CHNO are of biogenic carbon sources, primarily VOC precursors such as isoprene, α-pinene/terpinene and d-limonene, while a few are anthropogenic (e.g., $C_{10}H_{16}O_9S$).[501] Given, the geographical location of the sampling site (Figure C.1), it is likely that urban emission ($\sim$66 km) from northern wind carryover could be resulting in potential increase of CHOS via reactive uptake of SO_2(g) during the daytime.[9] Aside from potential sources of CHOS/CHNOS, the photochemically induced losses and/or gains of CHOS and CHNO were further elucidated by drawing comparisons between characterized molecular formulae across daytime and nighttime periods. The results from this comparison are discussed in the section below.

4.3.4 Daytime and Nighttime Chemistry

Figure 4.6 illustrates the variation in OS_C as a function of $\log_{10}C_0$ for MFs found unique across daytime-nighttime sample pool of June 3 and June 4. Figures 4.6 (A) and (B) demonstrate the day to night variations in MFs for June 3. Herein, from a total of 2193 MFs, the day to night contrast of MFs from the pool of 277 unique MFs in daytime and 397 unique MFs in nighttime is highlighted by > 90% gain in CHNOs, 73% increase in CHOS, 84% increase in CHNOS but 35% loss of CHOs. Moreover, there was a noticeable increase in low volatile fraction specifically for June 3 (Figures 4.6 (A) and (B)), such that 69% increase in ELVOCs was observed from 32% (or 89 MFs) in daytime to 71% (or 283 MFs) in nighttime. Figures 4.6 (C) and (D) demonstrate a similar OS_C variation for MFs unique to daytime and nighttime periods in June 4. Herein from a total of 2145 MFs, day to night transformation from 181 unique MFs in daytime and 712 unique MFs in nighttime is observed via 97% increase in CHNOs, 90% increase in CHOs but 65% decrease in CHOS and 36% decrease in CHNOS was observed. In contrast to June 3, there was a noticeable 67% decrease in ELVOC fraction in June 4 from 64% (or 116 MFs) in daytime to 50% (or 356 MFs) in nighttime.

When comparing AI, the unique subset of CHNO found in June 3 and June 4 showed increase from day (June 3: 0.1 ± 0.1, June 4: 0) to night (June 3: 0.3 ± 0.2, June 4: 0.3 ± 0.3) (Table C.4). However, the overall AI and DBE values for CHNO across day and night periods for both June 3 and June 4 were below 0.5 and 7.5 respectively. The observed CHNOs across nighttime periods of June 3 and June 4 predominantly occupy the ELVOC region with O:C ratio > 0.5 and O:N ratio > 9.0 (Table C.4). The prevalence of CHNOs across nighttime periods for both June 3 and June 4 is strongly indicative of NO_3 radical chemistry as demonstrated by Xie at al[502] and Foulds et al.[75]

Overall, while the day-night trends for CHNOs were distinct in favoring nocturnal formation for both June 3 and June 4,[431] no such trend was observed for CHOS/CHNOS. This could be due to varying monoterpene emissions, which are positively dependent on solar radiation and temperature. However, based on the similar trends in wind speed, temperature and RH parameters outlined in Table C.1, it is unlikely that

these meteorological factors would illicit the observed variations in CHOS/CHNOS. As such, it is possible that aerosol acidity, oxidant concentrations (e.g., NO_x) and gaseous uptake of SO_2 might explain the likely increase and decrease of CHOS/CHNOS from day to night in June 3 and June 4 respectively.[411, 503, 504]

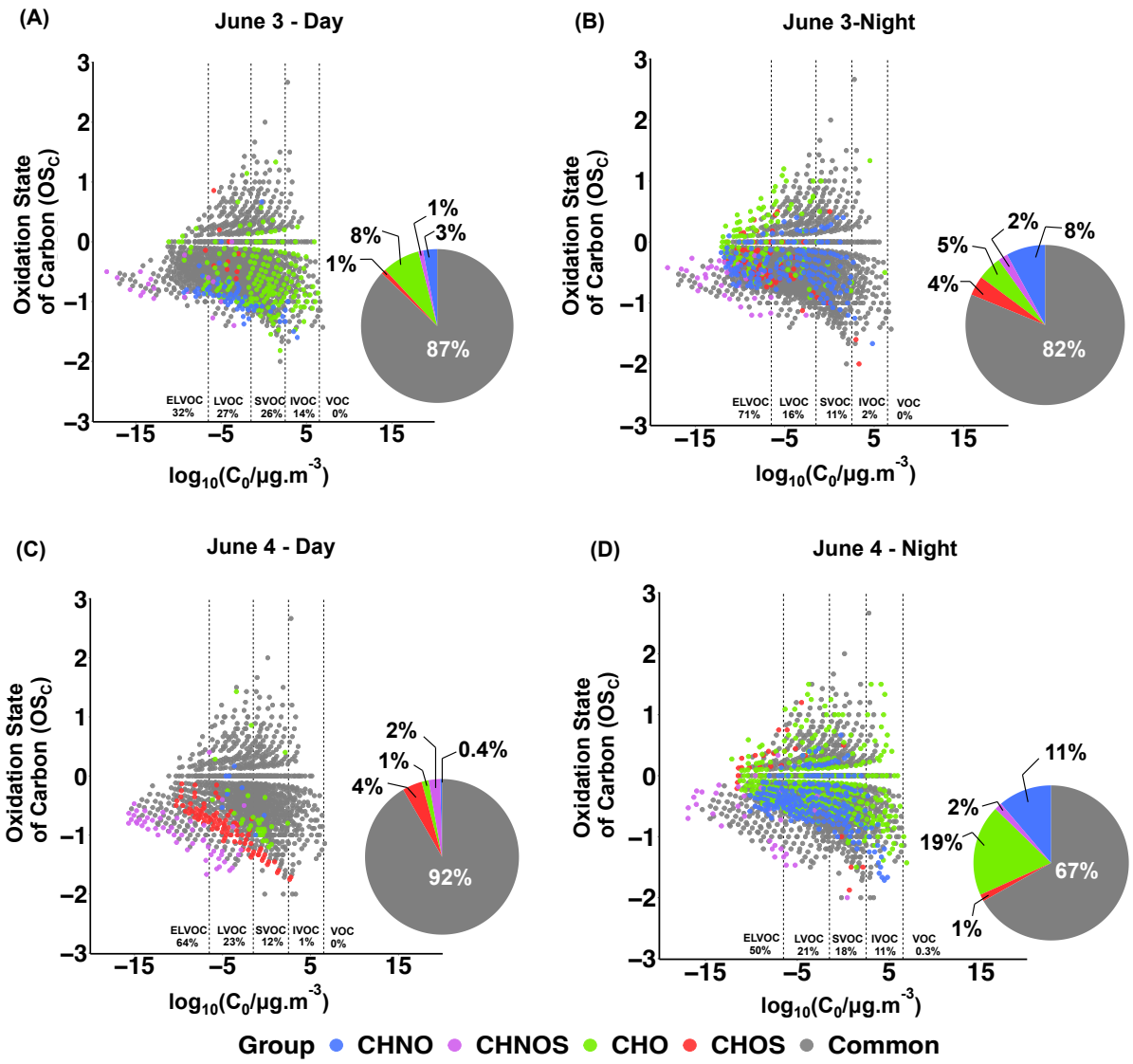

Figure 4.6: Photochemical and oxidative processing of organic features observed across June 3 and June 4. The daytime and nighttime chemistry is shown for June 3 in (A) and (B) respectively while for June 4 in (C) and (D) respectively. Note, MFs that are unique within the day-night sample sets of June 3 and June 4, are colored according to their molecular groups while the features which are common in day and night sample sets are shaded grey. The current comparison of MFs is drawn from set of features which are not only exclusive to the June 3 and June 4 but could be found across other sampling periods.

Within the subset of MFs observed between day and night comparisons of June 3 and June 4, CHNO and CHOS were found to be of biogenic carbon source (Table C.5). For instance, amongst the unique CHNO compounds observed in June 4, $C_9H_{15}NO_7$ (m/z = 248.0776, daytime), $C_{20}H_{29}NO_{13}$ (m/z = 490.1562, nighttime) and $C_{15}H_{25}NO_8$ (m/z = 346.1505, day and night) were reportedly originating from biogenic precursors such as β-caryophyllene, d-limonene and anthropogenic precursors such as 1,3,5-trimethylbenzene (TMB).[485, 486, 505] This also included CHNOS such as $C_{10}H_{17}NO_7S$ (m/z 294.0653) which is common amongst both daytimes. This CHNOS compound has been previously reported in the chamber studies of Surratt et al,[56] Huang et al[506] and various sampling locations including metropolitan central region of Delhi[507] and Belgian forests which are heavily influenced by urban pollution.[413] In terms of CHO classification, we have observed MF consistent with terpenoic acids such as $C_9H_{14}O_4$ (cis-pinic acid, m/z 185.0819), $C_7H_{10}O_4$ (terebic acid, m/z 157.0508),$C_8H_{12}O_4$ (terpenylic acid, m/z 171.0664)[413] across both daytimes. However, there were noticeable CHO compounds found common across the nighttime periods of June 3 and June 4 such as $C_{18}H_{28}O_11$ (m/z 419.1557), $C_{18}H_{26}O_{11}$ (m/z 417.1402),$C_{18}H_{28}O_{10}$ (m/z 403.1609) that were also reported in the work of Wang et al and originate from the ozonolysis of 1,3,5-TMB.[486]

4.4 Atmospheric Implications

This study provides molecular level daily and day-and night-time variation on the occurrence of CHOS, CHNOS and CHNO. Interestingly, the emergence of CHOS, CHNOS and CHNO is observed to be episodic in consecutive day and night sampling periods (i.e., June 3 to June 4). Meteorological conditions such as wind direction revealed that the formation of these particle-bound species in early June sampling periods is under the influence of land based sources. In contrast, later June sampling periods consistently lacked organic MFs (< 700 MFs) due to marine influenced airmass and dominance of inorganic fraction (i.e. salts). Nocturnal formation was observed for CHNOs across June 3 and June 4, but S-containing compounds deviated from nighttime favored trend. Remote sensing measurements revealed potential association between cloud formation events and the emergence of CHOS/CHNOS and CHNOs.

CHOS/CHNOS and CHNO classified under ELVOC region are often highly viscous (10^{12} Pa s)[508–510] influencing hygroscopic growth, altering physicochemical properties[187, 409, 440, 511]and initiating particle ice-nucleation.[512] In the recent work of Wolf et al, isoprene derived CHOS (e.g., $C_5H_{12}O_7S$) was found to influence cirrus type of cloud formation.[513] To further understand if there is a potential link between CHOS/CHNOS/CHNO and cloud formation events, we probed doppler-lidar signal measurements. It is understood that doppler-lidar signal attenuation can occur as hygroscopic particles grow.[514, 515] In the recent work of Maloney et al,[516] cloud formation is probed via CAM5/CRMA. Therein, the authors found that high ice clouds in the middle troposphere can be influenced by CHOS and CHNO.[78, 516] In current study, June 4 represented an interesting event which coincided with a convective cloud structure. All the other sampling periods were observed to have shallow or scattered clouds. These observations suggest that acidic sulfate particles such as CHOS may play an important role in influencing cloud formation events such as convective clouds. Future studies could probe how meteorological conditions and boundary layer structure would influence vertical profile of aerosols by understanding variations in molecular composition of aerosols before and after convective cloud events to determine the association between CHOS, CHNOS/CHNO and cloud

formation.

4.5 Acknowledgement

A portion of this research was performed on a project award (FICS.2022) and used resources at the Environmental Molecular Sciences Laboratory (EMSL) and the Atmospheric Radiation Measurement facility (ARM), which are Department of Energy (DOE) Office of Science User Facilities. Both facilities are sponsored by the Biological and Environmental Research (BER) program and operated under Contract No. DE-AC05-76RL01830 (EMSL) and DE-FG03-00ER62913 and DE-FG03-97ER62338 (ARM). The ARM Program was sponsored by the U.S. DOE's BER program. Additional funding is provided by the Office of BER in the DOE under contract no. DE-SC0012704 to Brookhaven National Laboratory. We also acknowledge support from the DOE BER Atmospheric System Research Program. The authors gratefully acknowledge ARM support stuff for the field sampling. STXM-NEXAFS analysis at beamline 5.3.2.2 of the Advanced Light Source (ALS) at Lawrence Berkeley National Laboratory (LBNL) is supported by the Director, Office of Science, Office of Basic Energy Sciences of the U.S. DOE under Contract No. DE-AC02- 05CH11231.

4.6 Appendix C

Additional experimental details, including topographical map, meterelogical parameters, predicted parameters, mass spectra, van krevelen diagrams and remote sensing measurements.

References

[9] H. Deng *et al.*, "Daytime SO_2 chemistry on ubiquitous urban surfaces as a source of organic sulfur compounds in ambient air," en, *Science Advances*, vol. 8, no. 39, eabq6830, Sep. 2022, ISSN: 2375-2548. DOI: 10.1126/sciadv.abq6830.

[30] M. D. Petters and S. M. Kreidenweis, "A single parameter representation of hygroscopic growth and cloud condensation nucleus activity," en, *Atmospheric Chemistry and Physics*, vol. 7, no. 8, pp. 1961–1971, Apr. 2007, ISSN: 1680-7324. DOI: 10.5194/acp-7-1961-2007.

[31] N. M. Donahue, S. A. Epstein, S. N. Pandis, and A. L. Robinson, "A two-dimensional volatility basis set: 1. organic-aerosol mixing thermodynamics," en, *Atmospheric Chemistry and Physics*, vol. 11, no. 7, pp. 3303–3318, Apr. 2011, ISSN: 1680-7324. DOI: 10.5194/acp-11-3303-2011. [Online]. Available: https://acp.copernicus.org/articles/11/3303/2011/.

[44] M. Hallquist *et al.*, "The formation, properties and impact of secondary organic aerosol: Current and emerging issues," en, *Atmospheric Chemistry and Physics*, vol. 9, no. 14, pp. 5155–5236, Jul. 2009, ISSN: 1680-7324. DOI: 10.5194/acp-9-5155-2009. (visited on 01/29/2024).

[49] A. D. Estillore *et al.*, "Water Uptake and Hygroscopic Growth of Organosulfate Aerosol," en, *Environmental Science & Technology*, vol. 50, no. 8, pp. 4259–4268, Apr. 2016, ISSN: 0013-936X, 1520-5851. DOI: 10.1021/acs.est.5b05014.

[54] Y. Li, U. Poschl, and M. Shiraiwa, "Molecular corridors and parameterizations of volatility in the chemical evolution of organic aerosols," en, *Atmospheric Chemistry and Physics*, vol. 16, no. 5, pp. 3327–3344, Mar. 2016, ISSN: 1680-7324. DOI: 10.5194/acp-16-3327-2016.

[56] J. D. Surratt *et al.*, "Organosulfate Formation in Biogenic Secondary Organic Aerosol," en, *The Journal of Physical Chemistry A*, vol. 112, no. 36, pp. 8345–8378, Sep. 2008, ISSN: 1089-5639, 1520-5215. DOI: 10.1021/jp802310p.

[63] J. Schindelka, Y. Iinuma, D. Hoffmann, and H. Herrmann, "Sulfate radical-initiated formation of isoprene-derived organosulfates in atmospheric aerosols," en, *Faraday Discussions*, vol. 165, p. 237, 2013, ISSN: 1359-6640, 1364-5498. DOI: 10.1039/c3fd00042g.

[73] S. Wang *et al.*, "Organic Peroxides and Sulfur Dioxide in Aerosol: Source of Particulate Sulfate," en, *Environmental Science & Technology*, vol. 53, no. 18, pp. 10 695–10 704, Sep. 2019, ISSN: 0013-936X, 1520-5851. DOI: 10.1021/acs.est.9b02591.

[75] A. Foulds, M. A. H. Khan, T. J. Bannan, C. J. Percival, M. H. Lowenberg, and D. E. Shallcross, "Abundance of NO_3 Derived Organo-Nitrates and Their Importance in the Atmosphere," en, *Atmosphere*, vol. 12, no. 11, p. 1381, Oct. 2021, ISSN: 2073-4433. DOI: 10.3390/atmos12111381. [Online]. Available: https://www.mdpi.com/2073-4433/12/11/1381.

[76] C. Peng *et al.*, "Interactions of organosulfates with water vapor under sub- and supersaturated conditions," en, *Atmospheric Chemistry and Physics*, vol. 21, no. 9, pp. 7135–7148, May 2021, ISSN: 1680-7324. DOI: 10.5194/acp-21-7135-2021.

[78] A. M. K. Hansen *et al.*, "Hygroscopic properties and cloud condensation nuclei activation of limonene-derived organosulfates and their mixtures with ammonium sulfate," en, *Atmospheric Chemistry and Physics*, vol. 15, no. 24, pp. 14 071–14 089, Dec. 2015, ISSN: 1680-7324. DOI: 10.5194/acp-15-14071-2015.

[115] M. Bruggemann *et al.*, "Organosulfates in Ambient Aerosol State of Knowledge and Future Research Directions on Formation, Abundance, Fate, and Importance," en, *Environmental Science & Technology*, vol. 54, no. 7, pp. 3767–3782, Apr. 2020, ISSN: 0013-936X, 1520-5851. DOI: 10.1021/acs.est.9b06751.

[167] P. J. Roach, J. Laskin, and A. Laskin, "Molecular Characterization of Organic Aerosols Using Nanospray-Desorption/Electrospray Ionization-Mass Spectrometry," en, *Analytical Chemistry*, vol. 82, no. 19, pp. 7979–7986, Oct. 2010, ISSN: 0003-2700, 1520-6882. DOI: 10.1021/ac101449p. [Online]. Available: https://pubs.acs.org/doi/10.1021/ac101449p.

[187] W. Fan, T. Chen, Z. Zhu, H. Zhang, Y. Qiu, and D. Yin, "A review of secondary organic aerosols formation focusing on organosulfates and organic nitrates," en, *Journal of Hazardous Materials*, vol. 430, p. 128 406, May 2022, ISSN: 03043894. DOI: 10.1016/j.jhazmat.2022.128406. (visited on 01/29/2024).

[387] K.-H. Kim, E. Kabir, and S. Kabir, "A review on the human health impact of airborne particulate matter," *Environment international*, vol. 74, pp. 136–143, 2015.

[388] J. Wu *et al.*, "Aerosol–photolysis interaction reduces particulate matter during wintertime haze events," *Proceedings of the National Academy of Sciences*, vol. 117, no. 18, pp. 9755–9761, 2020.

[389] U. Poschl, "Atmospheric Aerosols: Composition, Transformation, Climate and Health Effects," *Angewandte Chemie International Edition*, vol. 44, no. 46, pp. 7520–7540, Nov. 2005, ISSN: 1433-7851. DOI: 10.1002/anie.200501122.

[390] E. J. Boone *et al.*, "Aqueous Processing of Atmospheric Organic Particles in Cloud Water Collected via Aircraft Sampling," en, *Environmental Science & Technology*, vol. 49, no. 14, pp. 8523–8530, Jul. 2015, ISSN: 0013-936X, 1520-5851. DOI: 10.1021/acs.est.5b01639. [Online]. Available: https://pubs.acs.org/doi/10.1021/acs.est.5b01639 (visited on 09/17/2023).

[391] Y. Huang *et al.*, "Quantification of global primary emissions of pm2. 5, pm10, and tsp from combustion and industrial process sources," *Environmental science & technology*, vol. 48, no. 23, pp. 13 834–13 843, 2014.

[392] J. L. Jimenez *et al.*, "Evolution of organic aerosols in the atmosphere," *science*, vol. 326, no. 5959, pp. 1525–1529, 2009.

[393] M. Bilde *et al.*, "Saturation Vapor Pressures and Transition Enthalpies of Low-Volatility Organic Molecules of Atmospheric Relevance: From Dicarboxylic Acids to Complex Mixtures," en, *Chemical Reviews*, vol. 115, no. 10, pp. 4115–4156, May 2015, ISSN: 0009-2665, 1520-6890. DOI: 10.1021/cr5005502. [Online]. Available: https://pubs.acs.org/doi/10.1021/cr5005502.

[394] M Kanakidou *et al.*, "Organic aerosol and global climate modelling: A review," en, *Atmos. Chem. Phys.*, p. 71, 2005.

[395] J. Duplissy *et al.*, "Relating hygroscopicity and composition of organic aerosol particulate matter," en, *Atmospheric Chemistry and Physics*, vol. 11, no. 3, pp. 1155–1165, Feb. 2011, ISSN: 1680-7324. DOI: 10.5194/acp-11-1155-2011. [Online]. Available: https://acp.copernicus.org/articles/11/1155/2011/.

[396] X. Liu and J. Wang, "How important is organic aerosol hygroscopicity to aerosol indirect forcing?" *Environmental Research Letters*, vol. 5, no. 4, p. 044 010, 2010.

[397] A Asa-Awuku, G. Engelhart, B. Lee, S. N. Pandis, and A. Nenes, "Relating ccn activity, volatility, and droplet growth kinetics of β-caryophyllene secondary organic aerosol," *Atmospheric Chemistry and Physics*, vol. 9, no. 3, pp. 795–812, 2009.

[398] T. Han *et al.*, "Role of secondary aerosols in haze formation in summer in the megacity beijing," *Journal of environmental sciences*, vol. 31, pp. 51–60, 2015.

[399] M. Camredon, B. Aumont, J. Lee-Taylor, and S. Madronich, "The soa/voc/no_x system: An explicit model of secondary organic aerosol formation," en, *Atmospheric Chemistry and Physics*, vol. 7, no. 21, pp. 5599–5610, Nov. 2007, ISSN: 1680-7324. DOI: 10.5194/acp-7-5599-2007.

[400] E. U. Emanuelsson *et al.*, "Formation of anthropogenic secondary organic aerosol (SOA) and its influence on biogenic SOA properties," en, *Atmospheric Chemistry and Physics*, vol. 13, no. 5, pp. 2837–2855, Mar. 2013, ISSN: 1680-7324. DOI: 10.5194/acp-13-2837-2013.

[401] L. Wu, X. Wang, S. Lu, M. Shao, and Z. Ling, "Emission inventory of semi-volatile and intermediate-volatility organic compounds and their effects on secondary organic aerosol over the Pearl River Delta region," en, *Atmospheric Chemistry and Physics*, vol. 19, no. 12, pp. 8141–8161, Jun. 2019, ISSN: 1680-7324. DOI: 10.5194/acp-19-8141-2019. [Online]. Available: https://acp.copernicus.org/articles/19/8141/2019/ (visited on 09/17/2023).

[402] S. Tao *et al.*, "Molecular Characterization of Organosulfates in Organic Aerosols from Shanghai and Los Angeles Urban Areas by Nanospray-Desorption Electrospray Ionization High-Resolution Mass Spectrometry," en, *Environmental Science & Technology*, vol. 48, no. 18, pp. 10 993–11 001, Sep. 2014, ISSN: 0013-936X, 1520-5851. DOI: 10.1021/es5024674. (visited on 09/17/2023).

[403] Y. Wang, R. Tong, and J. Z. Yu, "Chemical Synthesis of Multifunctional Air Pollutants: Terpene-Derived Nitrooxy Organosulfates," en, *Environmental Science & Technology*, vol. 55, no. 13, pp. 8573–8582, Jul. 2021, ISSN: 0013-936X, 1520-5851. DOI: 10.1021/acs.est.1c00348. [Online]. Available: https://pubs.acs.org/doi/10.1021/acs.est.1c00348 (visited on 09/17/2023).

[404] Y. Zhao, A. G. Hallar, and L. R. Mazzoleni, "Atmospheric organic matter in clouds: Exact masses and molecular formula identification using ultrahigh-resolution FT-ICR mass spectrometry," en, *Atmospheric Chemistry and Physics*, vol. 13, no. 24, pp. 12 343–12 362, Dec. 2013, ISSN: 1680-7324. DOI: 10.5194/acp-13-12343-2013. [Online]. Available: https://acp.copernicus.org/articles/13/12343/2013/.

[405] C. Ning *et al.*, "Molecular characterization of dissolved organic matters in winter atmospheric fine particulate matters (PM2.5) from a coastal city of northeast China," en, *Science of The Total Environment*, vol. 689, pp. 312–321, Nov. 2019, ISSN: 00489697. DOI: 10.1016/j.scitotenv.2019.06.418.

[406] K. S. Hu, A. I. Darer, and M. J. Elrod, "Thermodynamics and kinetics of the hydrolysis of atmospherically relevant organonitrates and organosulfates," en, *Atmospheric Chemistry and Physics*, vol. 11, no. 16, pp. 8307–8320, Aug. 2011, ISSN: 1680-7324. DOI: 10.5194/acp-11-8307-2011. [Online]. Available: https://acp.copernicus.org/articles/11/8307/2011/ (visited on 09/17/2023).

[407] B. H. Lee *et al.*, "Highly functionalized organic nitrates in the southeast united states: Contribution to secondary organic aerosol and reactive nitrogen budgets," *Proceedings of the National Academy of Sciences*, vol. 113, no. 6, pp. 1516–1521, 2016.

[408] M. Thoma, F. Bachmeier, F. L. Gottwald, M. Simon, and A. L. Vogel, "Mass spectrometry-based aerosolomics: A new approach to resolve sources, composition, and partitioning of secondary organic aerosol," *Atmospheric Measurement Techniques*, vol. 15, no. 23, pp. 7137–7154, 2022.

[409] K. A. Pratt, M. N. Fiddler, P. B. Shepson, A. G. Carlton, and J. D. Surratt, "Organosulfates in cloud water above the Ozarks' isoprene source region," en, *Atmospheric Environment*, vol. 77, pp. 231–238, Oct. 2013, ISSN: 13522310. DOI: 10.1016/j.atmosenv.2013.05.011. (visited on 10/01/2023).

[410] D. A. Day, S. Liu, L. M. Russell, and P. J. Ziemann, "Organonitrate group concentrations in submicron particles with high nitrate and organic fractions in coastal southern California," en, *Atmospheric Environment*, vol. 44, no. 16, pp. 1970–1979, May 2010, ISSN: 13522310. DOI: 10.1016/j.atmosenv.2010.02.045. (visited on 10/01/2023).

[411] Q. T. Nguyen *et al.*, "Understanding the anthropogenic influence on formation of biogenic secondary organic aerosols in Denmark via analysis of organosulfates and related oxidation products," en, *Atmospheric Chemistry and Physics*, vol. 14, no. 17, pp. 8961–8981, Sep. 2014, ISSN: 1680-7324. DOI: 10.5194/acp-14-8961-2014.

[412] J. D. Surratt *et al.*, "Evidence for Organosulfates in Secondary Organic Aerosol," en, *Environmental Science & Technology*, vol. 41, no. 2, pp. 517–527, Jan. 2007, ISSN: 0013-936X, 1520-5851. DOI: 10.1021/es062081q. [Online]. Available: https://pubs.acs.org/doi/10.1021/es062081q (visited on 09/17/2023).

[413] Y. Gomez-Gonzalez *et al.*, "Chemical characterisation of atmospheric aerosols during a 2007 summer field campaign at Brasschaat, Belgium: Sources and source processes of biogenic secondary organic aerosol," en, *Atmospheric Chemistry and Physics*, vol. 12, no. 1, pp. 125–138, Jan. 2012, ISSN: 1680-7324. DOI: 10.5194/acp-12-125-2012. (visited on 10/01/2023).

[414] K. Kristensen and M. Glasius, "Organosulfates and oxidation products from biogenic hydrocarbons in fine aerosols from a forest in North West Europe during spring," en, *Atmospheric Environment*, vol. 45, no. 27, pp. 4546–4556, Sep. 2011, ISSN: 13522310. DOI: 10.1016/j.atmosenv.2011.05.063. [Online]. Available: https://linkinghub.elsevier.com/retrieve/pii/S1352231011005802.

[415] D. R. Worton *et al.*, "Origins and composition of fine atmospheric carbonaceous aerosol in the Sierra Nevada Mountains, California," en, *Atmospheric Chemistry and Physics*, vol. 11, no. 19, pp. 10 219–10 241, Oct. 2011, ISSN: 1680-7324. DOI: 10.5194/acp-11-10219-2011. (visited on 11/26/2023).

[416] H. Lukacs, A. Gelencser, A. Hoffer, G. Kiss, K. Horvath, and Z. Hartyani, "Quantitative assessment of organosulfates in size-segregated rural fine aerosol," en, *Atmospheric Chemistry and Physics*, vol. 9, no. 1, pp. 231–238, Jan. 2009, ISSN: 1680-7324. DOI: 10.5194/acp-9-231-2009.

[417] M. P. Tolocka and B. Turpin, "Contribution of Organosulfur Compounds to Organic Aerosol Mass," en, *Environmental Science & Technology*, vol. 46, no. 15, pp. 7978–7983, Aug. 2012, ISSN: 0013-936X, 1520-5851. DOI: 10.1021/es300651v. [Online]. Available: https://pubs.acs.org/doi/10.1021/es300651v.

[418] B. R. Ayres *et al.*, "Organic nitrate aerosol formation via NO_3 + biogenic volatile organic compounds in the southeastern United States," en, *Atmospheric Chemistry and Physics*, vol. 15, no. 23, pp. 13 377–13 392, Dec. 2015, ISSN: 1680-7324. DOI: 10.5194/acp-15-13377-2015.

[419] L. Xu, S. Suresh, H. Guo, R. J. Weber, and N. L. Ng, "Aerosol characterization over the southeastern United States using high-resolution aerosol mass spectrometry: Spatial and seasonal variation of aerosol composition and sources with a focus on organic nitrates," en, *Atmospheric Chemistry and Physics*, vol. 15, no. 13, pp. 7307–7336, Jul. 2015, ISSN: 1680-7324. DOI: 10.5194/acp-15-7307-2015.

[420] Y. Wang *et al.*, "Organosulfates in atmospheric aerosols in Shanghai, China: Seasonal and interannual variability, origin, and formation mechanisms," en, *Atmospheric Chemistry and Physics*, vol. 21, no. 4, pp. 2959–2980, Feb. 2021, ISSN: 1680-7324. DOI: 10.5194/acp-21-2959-2021. [Online]. Available: https://acp.copernicus.org/articles/21/2959/2021/.

[421] J. C. Ditto, T. Joo, J. H. Slade, P. B. Shepson, N. L. Ng, and D. R. Gentner, "Nontargeted Tandem Mass Spectrometry Analysis Reveals Diversity and Variability in Aerosol Functional Groups across Multiple Sites, Seasons, and Times of Day," en, *Environmental Science & Technology Letters*, vol. 7, no. 2, pp. 60–69, Feb. 2020, ISSN: 2328-8930, 2328-8930. DOI: 10.1021/acs.estlett.9b00702. [Online]. Available: https://pubs.acs.org/doi/10.1021/acs.estlett.9b00702 (visited on 11/26/2023).

[422] Y. Ma, X. Xu, W. Song, F. Geng, and L. Wang, "Seasonal and diurnal variations of particulate organosulfates in urban Shanghai, China," en, *Atmospheric Environment*, vol. 85, pp. 152–160, Mar. 2014, ISSN: 13522310. DOI: 10.1016/j.atmosenv.2013.12.017.

[423] S. Kundu, T. A. Quraishi, G. Yu, C. Suarez, F. N. Keutsch, and E. A. Stone, "Evidence and quantitation of aromatic organosulfates in ambient aerosols in Lahore, Pakistan," en, *Atmospheric Chemistry and Physics*, vol. 13, no. 9, pp. 4865–4875, May 2013, ISSN: 1680-7324. DOI: 10.5194/acp-13-4865-2013. [Online]. Available: https://acp.copernicus.org/articles/13/4865/2013/ (visited on 09/17/2023).

[424] E. A. Stone, L. Yang, L. E. Yu, and M. Rupakheti, "Characterization of organosulfates in atmospheric aerosols at Four Asian locations," en, *Atmospheric Environment*, vol. 47, pp. 323–329, Feb. 2012, ISSN: 13522310. DOI: 10.1016/j.atmosenv.2011.10.058. [Online]. Available: https://linkinghub.elsevier.com/retrieve/pii/S1352231011011514 (visited on 09/17/2023).

[425] A. I. Darer, N. C. Cole-Filipiak, A. E. O Connor, and M. J. Elrod, "Formation and Stability of Atmospherically Relevant Isoprene Derived Organosulfates and Organonitrates," en, *Environmental Science & Technology*, vol. 45, no. 5, pp. 1895–1902, Mar. 2011, ISSN: 0013-936X, 1520-5851. DOI: 10.1021/es103797z.

[426] M. Riva, T. Da Silva Barbosa, Y.-H. Lin, E. A. Stone, A. Gold, and J. D. Surratt, "Chemical characterization of organosulfates in secondary organic aerosol-derived from the photooxidation of alkanes," en, *Atmospheric Chemistry and Physics*, vol. 16, no. 17, pp. 11 001–11 018, Sep. 2016, ISSN: 1680-7324. DOI: 10.5194/acp-16-11001-2016. (visited on 11/26/2023).

[427] M. Le Breton *et al.*, "Online gas- and particle-phase measurements of organosulfates, organosulfonates and nitrooxy organosulfates in Beijing utilizing a FIGAERO ToF-CIMS," en, *Atmospheric Chemistry and Physics*, vol. 18, no. 14, pp. 10 355–10 371, Jul. 2018, ISSN: 1680-7324. DOI: 10.5194/acp-18-10355-2018. [Online]. Available: https://acp.copernicus.org/articles/18/10355/2018/.

[428] J. Shang *et al.*, "SO_2 Uptake on Oleic Acid: A New Formation Pathway of Organosulfur Compounds in the Atmosphere," en, *Environmental Science & Technology Letters*, vol. 3, no. 2, pp. 67–72, Feb. 2016, ISSN: 2328-8930, 2328-8930. DOI: 10.1021/acs.estlett.6b00006. [Online]. Available: https://pubs.acs.org/doi/10.1021/acs.estlett.6b00006.

[429] M. Passananti *et al.*, "Organosulfate Formation through the Heterogeneous Reaction of SO_2 with Unsaturated Fatty Acids and Long Chain Alkenes," en, *Angewandte Chemie International Edition*, vol. 55, no. 35, pp. 10 336–10 339, Aug. 2016, ISSN: 1433-7851, 1521-3773. DOI: 10.1002/anie.201605266.

[430] M. Zhu *et al.*, "Organosulfur Compounds Formed from Heterogeneous Reaction between SO_2 and Particulate Bound Unsaturated Fatty Acids in Ambient Air," en, *Environmental Science & Technology Letters*, vol. 6, no. 6, pp. 318–322, Jun. 2019, ISSN: 2328-8930, 2328-8930. DOI: 10.1021/acs.estlett.9b00218.

[431] D. J. Bryant *et al.*, "Importance of Oxidants and Temperature in the Formation of Biogenic Organosulfates and Nitrooxy Organosulfates," en, *ACS Earth and Space Chemistry*, vol. 5, no. 9, pp. 2291–2306, Sep. 2021, ISSN: 2472-3452, 2472-3452. DOI: 10.1021/acsearthspacechem.1c00204. [Online]. Available: https://pubs.acs.org/doi/10.1021/acsearthspacechem.1c00204.

[432] C. Ning, Y. Gao, H. Zhang, H. Yu, R. Cao, and J. Chen, "Urban particulate water-soluble organic matter in winter: Size-resolved molecular characterization, role of the S-containing compounds on haze formation," en, *Science of The Total Environment*, vol. 875, p. 162 657, Jun. 2023, ISSN: 00489697. DOI: 10.1016/j.scitotenv.2023.162657.

[433] B. Friedman, P. Brophy, W. H. Brune, and D. K. Farmer, "Anthropogenic Sulfur Perturbations on Biogenic Oxidation: SO_2 Additions Impact Gas Phase OH Oxidation Products of α- and β-Pinene," en, *Environmental Science & Technology*, vol. 50, no. 3, pp. 1269–1279, Feb. 2016, ISSN: 0013-936X, 1520-5851. DOI: 10.1021/acs.est.5b05010.

[434] W. Huang *et al.*, "Exploring the inorganic and organic nitrate aerosol formation regimes at a suburban site on the North China Plain," en, *Science of The Total Environment*, vol. 768, p. 144 538, May 2021, ISSN: 00489697. DOI: 10.1016/j.scitotenv.2020.144538.

[435] W. Huang *et al.*, "Size Dependent Nighttime Formation of Particulate Secondary Organic Nitrates in Urban Air," en, *Journal of Geophysical Research: Atmospheres*, vol. 128, no. 18, e2022JD038189, Sep. 2023, ISSN: 2169-897X, 2169-8996. DOI: 10.1029/2022JD038189.

[436] B. Ervens, "Modeling the processing of aerosol and trace gases in clouds and fogs," *Chemical reviews*, vol. 115, no. 10, pp. 4157–4198, 2015.

[437] J. Liao *et al.*, "Airborne measurements of organosulfates over the continental U.S.," en, *Journal of Geophysical Research: Atmospheres*, vol. 120, no. 7, pp. 2990–3005, Apr. 2015, ISSN: 2169-897X, 2169-8996. DOI: 10.1002/2014JD022378. [Online]. Available: https://agupubs.onlinelibrary.wiley.com/doi/10.1002/2014JD022378 (visited on 09/17/2023).

[438] G. Duporte *et al.*, "Experimental Study of the Formation of Organosulfates from α-Pinene Oxidation. Part I: Product Identification, Formation Mechanisms and Effect of Relative Humidity," en, *The Journal of Physical Chemistry A*, vol. 120, no. 40, pp. 7909–7923, Oct. 2016, ISSN: 1089-5639, 1520-5215. DOI: 10.1021/acs.jpca.6b08504.

[439] L. Xu, N. T. Tsona, and L. Du, "Relative Humidity Changes the Role of SO_2 in Biogenic Secondary Organic Aerosol Formation," en, *The Journal of Physical Chemistry Letters*, vol. 12, no. 30, pp. 7365–7372, Aug. 2021, ISSN: 1948-7185, 1948-7185. DOI: 10.1021/acs.jpclett.1c01550. [Online]. Available: https://pubs.acs.org/doi/10.1021/acs.jpclett.1c01550.

[440] A. L. Vogel *et al.*, "Aerosol Chemistry Resolved by Mass Spectrometry: Linking Field Measurements of Cloud Condensation Nuclei Activity to Organic Aerosol Composition," en, *Environmental Science & Technology*, vol. 50, no. 20, pp. 10 823–10 832, Oct. 2016, ISSN: 0013-936X, 1520-5851. DOI: 10.1021/acs.est.6b01675. [Online]. Available: https://pubs.acs.org/doi/10.1021/acs.est.6b01675.

[441] L. Guo *et al.*, "Comprehensive characterization of hygroscopic properties of methanesulfonates," *Atmospheric Environment*, vol. 224, p. 117 349, 2020.

[442] B. H. Lee *et al.*, "Highly functionalized organic nitrates in the southeast United States: Contribution to secondary organic aerosol and reactive nitrogen budgets," *Proceedings of the National Academy of Sciences*, vol. 113, no. 6, pp. 1516–1521, 2016, Publisher: National Acad Sciences.

[443] J. G. Slowik *et al.*, "Characterization of a large biogenic secondary organic aerosol event from eastern Canadian forests," en, *Atmospheric Chemistry and Physics*, vol. 10, no. 6, pp. 2825–2845, Mar. 2010, ISSN: 1680-7324. DOI: 10.5194/acp-10-2825-2010. [Online]. Available: https://acp.copernicus.org/articles/10/2825/2010/.

[444] E. Freney *et al.*, "Aerosol composition and the contribution of SOA formation over Mediterranean forests," en, *Atmospheric Chemistry and Physics*, vol. 18, no. 10, pp. 7041–7056, May 2018, ISSN: 1680-7324. DOI: 10.5194/acp-18-7041-2018. [Online]. Available: https://acp.copernicus.org/articles/18/7041/2018/.

[445] G. W. Vandergrift, A. S. M. Shawon, D. N. Dexheimer, M. A. Zawadowicz, F. Mei, and S. China, "Molecular Characterization of Organosulfate-Dominated Aerosols over Agricultural Fields from the Southern Great Plains by High-Resolution Mass Spectrometry," en, *ACS Earth and Space Chemistry*, vol. 6, no. 7, pp. 1733–1741, Jul. 2022, ISSN: 2472-3452, 2472-3452. DOI: 10.1021/acsearthspacechem.2c00043. [Online]. Available: https://pubs.acs.org/doi/10.1021/acsearthspacechem.2c00043.

[446] N. H. Robinson *et al.*, "Evidence for a significant proportion of Secondary Organic Aerosol from isoprene above a maritime tropical forest," en, *Atmospheric Chemistry and Physics*, vol. 11, no. 3, pp. 1039–1050, Feb. 2011, ISSN:

1680-7324. doi: 10.5194/acp-11-1039-2011. [Online]. Available: https://acp.copernicus.org/articles/11/1039/2011/.

[447] R. Bahreini *et al.*, "Organic aerosol formation in urban and industrial plumes near Houston and Dallas, Texas," en, *Journal of Geophysical Research*, vol. 114, D00F16, Aug. 2009, issn: 0148-0227. doi: 10.1029/2008JD011493. [Online]. Available: http://doi.wiley.com/10.1029/2008JD011493 (visited on 09/17/2023).

[448] M. Leuchner and B. Rappengluck, "VOC source receptor relationships in Houston during Texas II," en, *Atmospheric Environment*, vol. 44, no. 33, pp. 4056–4067, Oct. 2010, issn: 13522310. doi: 10.1016/j.atmosenv.2009.02.029. (visited on 11/26/2023).

[449] T. Bates *et al.*, "Boundary layer aerosol chemistry during texas/gomaccs 2006: Insights into aerosol sources and transformation processes," *Journal of Geophysical Research: Atmospheres*, vol. 113, no. D7, 2008.

[450] M. P. Jensen *et al.*, "A succession of cloud, precipitation, aerosol, and air quality field experiments in the coastal urban environment," *Bulletin of the American Meteorological Society*, vol. 103, no. 2, pp. 103–105, 2022.

[451] S. McKeen *et al.*, "An evaluation of real time air quality forecasts and their urban emissions over eastern Texas during the summer of 2006 Second Texas Air Quality Study field study," en, *Journal of Geophysical Research: Atmospheres*, vol. 114, no. D7, 2008JD011697, Apr. 2009, issn: 0148-0227. doi: 10.1029/2008JD011697. [Online]. Available: https://agupubs.onlinelibrary.wiley.com/doi/10.1029/2008JD011697.

[452] D. D. Parrish *et al.*, "Overview of the Second Texas Air Quality Study (Texas II) and the Gulf of Mexico Atmospheric Composition and Climate Study (GoMACCS)," en, *Journal of Geophysical Research: Atmospheres*, vol. 114, no. D7, 2009JD011842, Apr. 2009, issn: 0148-0227. doi: 10.1029/2009JD011842. [Online]. Available: https://agupubs.onlinelibrary.wiley.com/doi/10.1029/2009JD011842.

[453] M. Webster, J. Nam, Y. Kimura, H. Jeffries, W. Vizuete, and D. T. Allen, "The effect of variability in industrial emissions on ozone formation in Houston, Texas," en, *Atmospheric Environment*, vol. 41, no. 40, pp. 9580–9593, Dec. 2007, issn: 13522310. doi: 10.1016/j.atmosenv.2007.08.052. [Online]. Available: https://linkinghub.elsevier.com/retrieve/pii/S1352231007007546.

[454] M. Russell and D. T. Allen, "Seasonal and spatial trends in primary and secondary organic carbon concentrations in southeast Texas," en, *Atmospheric Environment*, vol. 38, no. 20, pp. 3225–3239, Jun. 2004, issn: 13522310. doi: 10.1016/j.atmosenv.2004.03.013. [Online]. Available: https://linkinghub.elsevier.com/retrieve/pii/S1352231004002018.

[455] L. A. Garnes and D. T. Allen, "Size Distributions of Organonitrates in Ambient Aerosol Collected in Houston, Texas," en, *Aerosol Science and Technology*, vol. 36, no. 10, pp. 983–992, Oct. 2002, ISSN: 0278-6826, 1521-7388. DOI: 10.1080/02786820290092186. [Online]. Available: http://www.tandfonline.com/doi/abs/10.1080/02786820290092186 (visited on 10/01/2023).

[456] Q. Dai *et al.*, "Seasonal differences in formation processes of oxidized organic aerosol near Houston, TX," en, *Atmospheric Chemistry and Physics*, vol. 19, no. 14, pp. 9641–9661, Jul. 2019, ISSN: 1680-7324. DOI: 10.5194/acp-19-9641-2019. [Online]. Available: https://acp.copernicus.org/articles/19/9641/2019/ (visited on 10/01/2023).

[457] I. M. Al-Naiema *et al.*, "Source apportionment of fine particulate matter in Houston, Texas: Insights to secondary organic aerosols," en, *Atmospheric Chemistry and Physics*, vol. 18, no. 21, pp. 15 601–15 622, Oct. 2018, ISSN: 1680-7324. DOI: 10.5194/acp-18-15601-2018. [Online]. Available: https://acp.copernicus.org/articles/18/15601/2018/.

[458] H. Zhang and Q. Ying, "Secondary organic aerosol formation and source apportionment in Southeast Texas," en, *Atmospheric Environment*, vol. 45, no. 19, pp. 3217–3227, Jun. 2011, ISSN: 13522310. DOI: 10.1016/j.atmosenv.2011.03.046. [Online]. Available: https://linkinghub.elsevier.com/retrieve/pii/S1352231011003177 (visited on 10/01/2023).

[459] N. N. Lata, Z. Cheng, D. Dexheimer, D. Zhang, F. Mei, and S. China, "Vertical Gradient of Size-Resolved Aerosol Compositions over the Arctic Reveals Cloud Processed Aerosol in-Cloud and above Cloud," en, *Environmental Science & Technology*, vol. 57, no. 14, pp. 5821–5830, Apr. 2023, ISSN: 0013-936X, 1520-5851. DOI: 10.1021/acs.est.2c09498. [Online]. Available: https://pubs.acs.org/doi/10.1021/acs.est.2c09498.

[460] J. Laskin *et al.*, "High-Resolution Desorption Electrospray Ionization Mass Spectrometry for Chemical Characterization of Organic Aerosols," en, *Analytical Chemistry*, vol. 82, no. 5, pp. 2048–2058, Mar. 2010, ISSN: 0003-2700, 1520-6882. DOI: 10.1021/ac902801f.

[461] P. J. Roach, J. Laskin, and A. Laskin, "Nanospray desorption electrospray ionization: An ambient method for liquid-extraction surface sampling in mass spectrometry," en, *The Analyst*, vol. 135, no. 9, p. 2233, 2010, ISSN: 0003-2654, 1364-5528. DOI: 10.1039/c0an00312c.

[462] A. Laskin, J. Laskin, and S. A. Nizkorodov, "Mass spectrometric approaches for chemical characterisation of atmospheric aerosols: Critical review of the most recent advances," en, *Environmental Chemistry*, vol. 9, no. 3, p. 163, 2012, ISSN: 1448-2517. DOI: 10.1071/EN12052.

[463] A. Ijaz, W. Kew, S. China, S. K. Schum, and L. R. Mazzoleni, "Molecular Characterization of Organophosphorus Compounds in Wildfire Smoke Using 21-T Fourier Transform-Ion Cyclotron Resonance Mass Spectrometry," en,

Analytical Chemistry, vol. 94, no. 42, pp. 14 537–14 545, Oct. 2022, ISSN: 0003-2700, 1520-6882. DOI: 10.1021/acs.analchem.2c00916. [Online]. Available: https://pubs.acs.org/doi/10.1021/acs.analchem.2c00916.

[464] S. K. Schum, L. E. Brown, and L. R. Mazzoleni, "MFAssignR: Molecular formula assignment software for ultrahigh resolution mass spectrometry analysis of environmental complex mixtures," en, *Environmental Research*, vol. 191, p. 110 114, Dec. 2020, ISSN: 00139351. DOI: 10.1016/j.envres.2020.110114. [Online]. Available: https://linkinghub.elsevier.com/retrieve/pii/S0013935120310112.

[465] Z. Cheng *et al.*, "Cloud condensation nuclei activity of internally mixed particle populations at a remote marine free troposphere site in the North Atlantic Ocean," en, *Science of The Total Environment*, vol. 904, p. 166 865, Dec. 2023, ISSN: 00489697. DOI: 10.1016/j.scitotenv.2023.166865. [Online]. Available: https://linkinghub.elsevier.com/retrieve/pii/S0048969723054906.

[466] R. C. Moffet, T. Henn, A. Laskin, and M. K. Gilles, "Automated Chemical Analysis of Internally Mixed Aerosol Particles Using X-ray Spectromicroscopy at the Carbon K-Edge," en, *Analytical Chemistry*, vol. 82, no. 19, pp. 7906–7914, Oct. 2010, ISSN: 0003-2700, 1520-6882. DOI: 10.1021/ac1012909. [Online]. Available: https://pubs.acs.org/doi/10.1021/ac1012909.

[467] M. Fraund, T. Park, L. Yao, D. Bonanno, D. Q. Pham, and R. C. Moffet, "Quantitative capabilities of STXM to measure spatially resolved organic volume fractions of mixed organic inorganic particles," en, *Atmospheric Measurement Techniques*, vol. 12, no. 3, pp. 1619–1633, Mar. 2019, ISSN: 1867-8548. DOI: 10.5194/amt-12-1619-2019.

[468] D. A. Knopf *et al.*, "Microspectroscopic imaging and characterization of individually identified ice nucleating particles from a case field study," en, *Journal of Geophysical Research: Atmospheres*, vol. 119, no. 17, Sep. 2014, ISSN: 2169-897X, 2169-8996. DOI: 10.1002/2014JD021866. [Online]. Available: https://agupubs.onlinelibrary.wiley.com/doi/10.1002/2014JD021866.

[469] C. J. Flynn, A. Mendoza, Y. Zheng, and S. Mathur, "Novel polarization-sensitive micropulse lidar measurement technique," en, *Optics Express*, vol. 15, no. 6, p. 2785, 2007, ISSN: 1094-4087. DOI: 10.1364/OE.15.002785. [Online]. Available: https://opg.optica.org/oe/abstract.cfm?uri=oe-15-6-2785.

[470] Z. Wang and K. Sassen, "Cloud Type and Macrophysical Property Retrieval Using Multiple Remote Sensors," en, *Journal of Applied Meteorology*, vol. 40, no. 10, pp. 1665–1682, Oct. 2001, ISSN: 0894-8763, 1520-0450. DOI: 10.1175/1520-0450(2001)040<1665:CTAMPR>2.0.CO;2. [Online]. Available: http://journals.ametsoc.org/doi/10.1175/1520-0450(2001)040<1665:CTAMPR>2.0.CO;2.

[471] "The ARM Radar Network: At the Leading Edge of Cloud and Precipitation Observations," vol. 101, ISSN: 0003-0007, 1520-0477. DOI: 10.1175/BAMS-D-18-0288.1. [Online]. Available: https://journals.ametsoc.org/view/journals/bams/101/5/bams-d-18-0288.1.xml.

[472] N. N. Lata *et al.*, "Aerosol Composition, Mixing State, and Phase State of Free Tropospheric Particles and Their Role in Ice Cloud Formation," en, *ACS Earth and Space Chemistry*, vol. 5, no. 12, pp. 3499–3510, Dec. 2021, ISSN: 2472-3452, 2472-3452. DOI: 10.1021/acsearthspacechem.1c00315. [Online]. Available: https://pubs.acs.org/doi/10.1021/acsearthspacechem.1c00315 (visited on 09/17/2023).

[473] J. M. Tomlin *et al.*, "Chemical imaging of fine mode atmospheric particles collected from a research aircraft over agricultural fields," *ACS Earth and Space Chemistry*, vol. 4, no. 11, pp. 2171–2184, 2020.

[474] J. M. Tomlin *et al.*, "Impact of dry intrusion events on the composition and mixing state of particles during the winter aerosol and cloud experiment in the eastern north atlantic (ace-ena)," *Atmospheric Chemistry and Physics*, vol. 21, no. 24, pp. 18 123–18 146, 2021.

[475] D. Knopf *et al.*, "Aerosol–ice formation closure: A southern great plains field campaign," *Bulletin of the American Meteorological Society*, vol. 102, no. 10, E1952–E1971, 2021.

[476] A. Wisthaler and C. J. Weschler, "Reactions of ozone with human skin lipids: Sources of carbonyls, dicarbonyls, and hydroxycarbonyls in indoor air," en, *Proceedings of the National Academy of Sciences*, vol. 107, no. 15, pp. 6568–6575, Apr. 2010, ISSN: 0027-8424, 1091-6490. DOI: 10.1073/pnas.0904498106.

[477] K. Dzepina *et al.*, "Molecular characterization of free tropospheric aerosol collected at the Pico Mountain Observatory: A case study with a long-range transported biomass burning plume," en, *Atmospheric Chemistry and Physics*, vol. 15, no. 9, pp. 5047–5068, May 2015, ISSN: 1680-7324. DOI: 10.5194/acp-15-5047-2015. [Online]. Available: https://acp.copernicus.org/articles/15/5047/2015/.

[478] "Carbon oxidation state as a metric for describing the chemistry of atmospheric organic aerosol," vol. 3, pp. 133–139, Feb. 2011, ISSN: 1755-4349. DOI: 10.1038/nchem.948. [Online]. Available: http://www.nature.com/articles/nchem.948.

[479] J. H. Kroll, C. Y. Lim, S. H. Kessler, and K. R. Wilson, "Heterogeneous Oxidation of Atmospheric Organic Aerosol: Kinetics of Changes to the Amount and Oxidation State of Particle-Phase Organic Carbon," en, *The Journal of Physical Chemistry A*, vol. 119, no. 44, pp. 10 767–10 783, Nov. 2015, ISSN: 1089-5639, 1520-5215. DOI: 10.1021/acs.jpca.5b06946. [Online]. Available: https://pubs.acs.org/doi/10.1021/acs.jpca.5b06946.

[480] M. J. Apsokardu and M. V. Johnston, "Nanoparticle growth by particle-phase chemistry," en, *Atmospheric Chemistry and Physics*, vol. 18, no. 3, pp. 1895–1907, Feb. 2018, ISSN: 1680-7324. DOI: 10.5194/acp-18-1895-2018. [Online]. Available: https://acp.copernicus.org/articles/18/1895/2018/.

[481] R. A. Zaveri *et al.*, "Particle-Phase Diffusion Modulates Partitioning of Semivolatile Organic Compounds to Aged Secondary Organic Aerosol," en, *Environmental Science & Technology*, vol. 54, no. 5, pp. 2595–2605, Mar. 2020, ISSN: 0013-936X, 1520-5851. DOI: 10.1021/acs.est.9b05514. [Online]. Available: https://pubs.acs.org/doi/10.1021/acs.est.9b05514.

[482] W. Hu *et al.*, "Oxidation Flow Reactor Results in a Chinese Megacity Emphasize the Important Contribution of S/IVOCs to Ambient SOA Formation," en, *Environmental Science & Technology*, vol. 56, no. 11, pp. 6880–6893, Jun. 2022, ISSN: 0013-936X, 1520-5851. DOI: 10.1021/acs.est.1c03155. [Online]. Available: https://pubs.acs.org/doi/10.1021/acs.est.1c03155.

[483] Y. Chen *et al.*, "Nonequilibrium Behavior in Isoprene Secondary Organic Aerosol," en, *Environmental Science & Technology*, vol. 57, no. 38, pp. 14 182–14 193, Sep. 2023, ISSN: 0013-936X, 1520-5851. DOI: 10.1021/acs.est.3c03532. [Online]. Available: https://pubs.acs.org/doi/10.1021/acs.est.3c03532.

[484] A. Goldstein, L. Yee, and N. Kreisberg, "Investigating secondary aerosol processes in the amazon through molecular-level characterization of semi-volatile organics," Tech. Rep., 2020. DOI: 10.2172/1673764.

[485] M. N. Chan *et al.*, "Influence of aerosol acidity on the chemical composition of secondary organic aerosol from β-caryophyllene," en, *Atmospheric Chemistry and Physics*, vol. 11, no. 4, pp. 1735–1751, Feb. 2011, ISSN: 1680-7324. DOI: 10.5194/acp-11-1735-2011.

[486] Y. Wang *et al.*, "Secondary reactions of aromatics-derived oxygenated organic molecules lead to plentiful highly oxygenated organic molecules within an intraday OH exposure," Gases/Laboratory Studies/Troposphere/Chemistry (chemical composition and reactions), preprint, Aug. 2023. DOI: 10.5194/egusphere-2023-1702. [Online]. Available: https://egusphere.copernicus.org/preprints/2023/egusphere-2023-1702/ (visited on 09/17/2023).

[487] S. Ponnusamy, L. Sandhiya, and K. Senthilkumar, "The atmospheric oxidation mechanism and kinetics of 1,3,5 trimethylbenzene initiated by OH radicals a theoretical study," en, *New Journal of Chemistry*, vol. 41, no. 18, pp. 10 259–10 271, 2017, ISSN: 1144-0546, 1369-9261. DOI: 10.1039/C7NJ01285C.

[488] C. Parworth *et al.*, "Long-term measurements of submicrometer aerosol chemistry at the Southern Great Plains (SGP) using an Aerosol Chemical Speciation Monitor (ACSM)," en, *Atmospheric Environment*, vol. 106, pp. 43–55, Apr. 2015, ISSN: 13522310. DOI: 10.1016/j.atmosenv.2015.01.060. (visited on 10/01/2023).

[489] M. C. Facchini *et al.*, "Important Source of Marine Secondary Organic Aerosol from Biogenic Amines," en, *Environmental Science & Technology*, vol. 42, no. 24, pp. 9116–9121, Dec. 2008, ISSN: 0013-936X, 1520-5851. DOI: 10.1021/es8018385. [Online]. Available: https://pubs.acs.org/doi/10.1021/es8018385.

[490] S. S. Petters *et al.*, "Organosulfates from Dark Aqueous Reactions of Isoprene-Derived Epoxydiols Under Cloud and Fog Conditions: Kinetics, Mechanism, and Effect of Reaction Environment on Regioselectivity of Sulfate Addition," en, *ACS Earth and Space Chemistry*, vol. 5, no. 3, pp. 474–486, Mar. 2021, ISSN: 2472-3452, 2472-3452. DOI: 10.1021/acsearthspacechem.0c00293. [Online]. Available: https://pubs.acs.org/doi/10.1021/acsearthspacechem.0c00293.

[491] H. Zhang, J. D. Surratt, Y. H. Lin, J. Bapat, and R. M. Kamens, "Effect of relative humidity on SOA formation from isoprene/NO photooxidation: Enhancement of 2-methylglyceric acid and its corresponding oligoesters under dry conditions," en, *Atmospheric Chemistry and Physics*, vol. 11, no. 13, pp. 6411–6424, Jul. 2011, ISSN: 1680-7324. DOI: 10.5194/acp-11-6411-2011. [Online]. Available: https://acp.copernicus.org/articles/11/6411/2011/.

[492] Y. Gomez Gonzalez *et al.*, "Characterization of organosulfates from the photooxidation of isoprene and unsaturated fatty acids in ambient aerosol using liquid chromatography/ electrospray ionization mass spectrometry," en, *Journal of Mass Spectrometry*, vol. 43, no. 3, pp. 371–382, Mar. 2008, ISSN: 1076-5174, 1096-9888. DOI: 10.1002/jms.1329.

[493] Y. Chen *et al.*, "Seasonal contribution of isoprene-derived organosulfates to total water-soluble fine particulate organic sulfur in the united states," *ACS Earth and Space Chemistry*, vol. 5, no. 9, pp. 2419–2432, 2021.

[494] T. B. Nguyen, J. Laskin, A. Laskin, and S. A. Nizkorodov, "Nitrogen-Containing Organic Compounds and Oligomers in Secondary Organic Aerosol Formed by Photooxidation of Isoprene," en, *Environmental Science & Technology*, vol. 45, no. 16, pp. 6908–6918, Aug. 2011, ISSN: 0013-936X, 1520-5851. DOI: 10.1021/es201611n.

[495] S. Su *et al.*, "High Molecular Diversity of Organic Nitrogen in Urban Snow in North China," en, *Environmental Science & Technology*, vol. 55, no. 8, pp. 4344–4356, Apr. 2021, ISSN: 0013-936X, 1520-5851. DOI: 10.1021/acs.est.0c06851. [Online]. Available: https://pubs.acs.org/doi/10.1021/acs.est.0c06851.

[496] T. Reemtsma *et al.*, "Identification of Fulvic Acids and Sulfated and Nitrated Analogues in Atmospheric Aerosol by Electrospray Ionization Fourier Transform Ion Cyclotron Resonance Mass Spectrometry," en, *Analytical Chemistry*, vol. 78, no. 24, pp. 8299–8304, Dec. 2006, ISSN: 0003-2700, 1520-6882. DOI: 10.1021/ac061320p. [Online]. Available: https://pubs.acs.org/doi/10.1021/ac061320p.

[497] Y. Ye, H. Zhan, X. Yu, J. Li, X. Wang, and Z. Xie, "Detection of organosulfates and nitrooxy-organosulfates in Arctic and Antarctic atmospheric aerosols, using ultra-high resolution FT-ICR mass spectrometry," en, *Science of The Total Environment*, vol. 767, p. 144 339, May 2021, ISSN: 00489697. DOI: 10.1016/j.scitotenv.2020.144339. [Online]. Available: https://linkinghub.elsevier.com/retrieve/pii/S0048969720378700.

[498] K. Wang *et al.*, "Urban organic aerosol composition in eastern China differs from north to south: Molecular insight from a liquid chromatography mass spectrometry orbitrap study," en, *Atmospheric Chemistry and Physics*, vol. 21, no. 11, pp. 9089–9104, Jun. 2021, ISSN: 1680-7324. DOI: 10.5194/acp-21-9089-2021. [Online]. Available: https://acp.copernicus.org/articles/21/9089/2021/.

[499] S. L. Lewis, G. Saliba, L. M. Russell, P. K. Quinn, T. S. Bates, and M. J. Behrenfeld, "Seasonal Differences in Submicron Marine Aerosol Particle Organic Composition in the North Atlantic," *Frontiers in Marine Science*, vol. 8, p. 720 208, Sep. 2021, ISSN: 2296-7745. DOI: 10.3389/fmars.2021.720208.

[500] S. Liu, J. E. Shilling, C. Song, N. Hiranuma, R. A. Zaveri, and L. M. Russell, "Hydrolysis of Organonitrate Functional Groups in Aerosol Particles," en, *Aerosol Science and Technology*, vol. 46, no. 12, pp. 1359–1369, Dec. 2012, ISSN: 0278-6826, 1521-7388. DOI: 10.1080/02786826.2012.716175. [Online]. Available: http://www.tandfonline.com/doi/abs/10.1080/02786826.2012.716175.

[501] R. D. Cook *et al.*, "Biogenic, urban, and wildfire influences on the molecular composition of dissolved organic compounds in cloud water," en, *Atmospheric Chemistry and Physics*, vol. 17, no. 24, pp. 15 167–15 180, Dec. 2017, ISSN: 1680-7324. DOI: 10.5194/acp-17-15167-2017. [Online]. Available: https://acp.copernicus.org/articles/17/15167/2017/.

[502] Q. Xie *et al.*, "Molecular characterization of firework-related urban aerosols using Fourier transform ion cyclotron resonance mass spectrometry," en, *Atmospheric Chemistry and Physics*, vol. 20, no. 11, pp. 6803–6820, Jun. 2020, ISSN: 1680-7324. DOI: 10.5194/acp-20-6803-2020. [Online]. Available: https://acp.copernicus.org/articles/20/6803/2020/ (visited on 10/01/2023).

[503] Q.-F. He *et al.*, "Organosulfates from Pinene and Isoprene over the Pearl River Delta, South China: Seasonal Variation and Implication in Formation Mechanisms," en, *Environmental Science & Technology*, vol. 48, no. 16, pp. 9236–9245, Aug. 2014, ISSN: 0013-936X, 1520-5851. DOI: 10.1021/es501299v. [Online]. Available: https://pubs.acs.org/doi/10.1021/es501299v (visited on 09/17/2023).

[504] Y. Wang *et al.*, "Comparative Study of Particulate Organosulfates in Contrasting Atmospheric Environments: Field Evidence for the Significant Influence of Anthropogenic Sulfate and NO_x," en, *Environmental Science & Technology Letters*, vol. 7, no. 11, pp. 787–794, Nov. 2020, ISSN: 2328-8930, 2328-8930. DOI: 10.1021/acs.estlett.0c00550.

[505] C. Faxon, J. Hammes, M. Le Breton, R. K. Pathak, and M. Hallquist, "Characterization of organic nitrate constituents of secondary organic aerosol (SOA) from nitrate-radical-initiated oxidation of limonene using high-resolution chemical ionization mass spectrometry," en, *Atmospheric Chemistry and Physics*, vol. 18, no. 8, pp. 5467–5481, Apr. 2018, ISSN: 1680-7324. DOI: 10.5194/acp-18-5467-2018. [Online]. Available: https://acp.copernicus.org/articles/18/5467/2018/ (visited on 09/17/2023).

[506] L. Huang *et al.*, "Biogenic and Anthropogenic Contributions to Atmospheric Organosulfates in a Typical Megacity in Eastern China," en, *Journal of Geophysical Research: Atmospheres*, vol. 128, no. 17, e2023JD038848, Sep. 2023, ISSN: 2169-897X, 2169-8996. DOI: 10.1029/2023JD038848. [Online]. Available: https://agupubs.onlinelibrary.wiley.com/doi/10.1029/2023JD038848 (visited on 09/17/2023).

[507] D. J. Bryant *et al.*, "Biogenic and anthropogenic sources of isoprene and monoterpenes and their secondary organic aerosol in Delhi, India," en, *Atmospheric Chemistry and Physics*, vol. 23, no. 1, pp. 61–83, Jan. 2023, ISSN: 1680-7324. DOI: 10.5194/acp-23-61-2023. [Online]. Available: https://acp.copernicus.org/articles/23/61/2023/.

[508] R. Schmedding *et al.*, "Predicting secondary organic aerosol phase state and viscosity and its effect on multiphase chemistry in a regional-scale air quality model," *Atmospheric chemistry and physics*, vol. 20, no. 13, pp. 8201–8225, 2020.

[509] M. Riva *et al.*, "Increasing isoprene epoxydiol-to-inorganic sulfate aerosol ratio results in extensive conversion of inorganic sulfate to organosulfur forms: Implications for aerosol physicochemical properties," *Environmental science & technology*, vol. 53, no. 15, pp. 8682–8694, 2019.

[510] N. E. Rothfuss and M. D. Petters, "Influence of functional groups on the viscosity of organic aerosol," *Environmental science & technology*, vol. 51, no. 1, pp. 271–279, 2017.

[511] P. E. Ohno *et al.*, "Gas-Particle Uptake and Hygroscopic Growth by Organosulfate Particles," en, *ACS Earth and Space Chemistry*, vol. 6, no. 10, pp. 2481–2490, Oct. 2022, ISSN: 2472-3452, 2472-3452. DOI: 10.1021/acsearthspacechem.2c00195. [Online]. Available: https://pubs.acs.org/doi/10.1021/acsearthspacechem.2c00195.

[512] D. A. Knopf, P. A. Alpert, and B. Wang, "The Role of Organic Aerosol in Atmospheric Ice Nucleation: A Review," en, *ACS Earth and Space Chemistry*, vol. 2, no. 3, pp. 168–202, Mar. 2018, ISSN: 2472-3452, 2472-3452. DOI: 10.1021/acsearthspacechem.7b00120. [Online]. Available: https://pubs.acs.org/doi/10.1021/acsearthspacechem.7b00120.

[513] M. J. Wolf *et al.*, "A biogenic secondary organic aerosol source of cirrus ice nucleating particles," en, *Nature Communications*, vol. 11, no. 1, p. 4834, Oct. 2020, ISSN: 2041-1723. DOI: 10.1038/s41467-020-18424-6. [Online]. Available: https://www.nature.com/articles/s41467-020-18424-6.

[514] W. Schimmel *et al.*, "Identifying cloud droplets beyond lidar attenuation from vertically-pointing cloud radar observations using artificial neural networks," Clouds/Remote Sensing/Data Processing and Information Retrieval, preprint, May 2022. DOI: 10.5194/amt-2022-149. [Online]. Available: https://amt.copernicus.org/preprints/amt-2022-149/amt-2022-149.pdf.

[515] C. M. Fajardo-Zambrano *et al.*, "Lidar and radar signal simulation: Stability assessment of the aerosol–cloud interaction index," *Remote Sensing*, vol. 14, no. 6, p. 1333, 2022.

[516] C. Maloney *et al.*, "The Balance Between Heterogeneous and Homogeneous Nucleation of Ice Clouds Using CAM5/CARMA," en, *Journal of Geophysical Research: Atmospheres*, vol. 127, no. 6, e2021JD035540, Mar. 2022, ISSN: 2169-897X, 2169-8996. DOI: 10.1029/2021JD035540. [Online]. Available: https://agupubs.onlinelibrary.wiley.com/doi/10.1029/2021JD035540 (visited on 09/17/2023).

Chapter 5

Conclusion and Future Work

Contributions: The introduction was written by Tania Gautam with review and feedback by Dr. Ran Zhao.

5.1 Thesis Summary

The goals of this thesis are firstly to resolve molecular ambiguity of aqueous ROOHs and elucidate their novel formation processes by applying the reactive LC technique, secondly, to determine the extent to which the conventional approach to the chemical derivatization technique can be compromised under the deliberate introduction of artifacts during quantification of peroxides, and lastly, to apply a robust and versatile advanced HRMS technique to characterize a wide range of particle-bound organics (i.e., ROS, OS, ON) in ambient aerosol samples and elucidate the impact of meteorological parameters. Starting with Chapter 2, I investigated the emergence of bulk-phase aqueous ROOHs during photooxidation of a wide range of WSOCs. More specifically, a straight chain unsaturated OAc was photooxidized to allow structural prediction of newly formed HOMs with multiple OOH groups. This unique strategy combined with a reactive LC approach has assisted in the selective determination of ROOHs in an aqueous mixture of other compounds such as carbonyls, carboxylic acids etc. Through this study, we have attempted to raise the question if autoxidation can be an important reaction pathway to facilitate the formation of aqueous-phase ROOHs. However, despite our strategic experimental approach, it is evident that the lack of online measurements has made it difficult to conclusively rely on autoxidation as a major reaction pathway for aqueous-phase ROOHs. However, the experimental parameters (e.g., concentration, wavelength) studied may have broader implications regarding the conditions favourable to the formation of aqueous ROOHs in future laboratory investigations. Throughout Chapter 3, I have investigated the experimental limits of the conventional iodometry method, which is known to undergo interferences from reducing agents such as OEs. This halogen chemistry has been widely used in food chemistry to determine the degree of unsaturation.[517, 518] Up until the application of iodometry in atmospheric matrices,[170] there has never been any systematic investigation to determine if olefinic compounds can cause interference to underestimate total peroxide content. With this study, I have examined a wide variety of unsaturated organic compounds including aromatics, straight-chain unsaturated acids and aliphatics. Our results show that linear unsaturated compounds can react with halogen species such as I_2 - a key intermediate in iodometry. However, this

underestimation in peroxide content will occur during extended periods of bench reaction and relatively higher concentrations (>500 μM) of olefinic compounds. I have determined that in the case of atmospheric samples including complex mixtures of SOA, it is unlikely that olefinic concentrations will reach the level of causing interference with the conventional iodometry approach. Thus, this study showed that while atmospheric samples would largely be safe from the bias caused during iodometric reduction of peroxides, indoor surfaces, food and lipids need further careful evaluation when peroxide content is being determined with this method. In Chapter 4, I have adopted a broader approach to understanding the role of ROS and sulfate/nitrate enriched particle-bound species in ambient aerosol samples. Complementary, to separation-based techniques that have been utilized in Chapters 2 and 3, here I have adopted a far more robust analytical approach, i.e., nano-DESI-HRMS which bypasses any sample preparation steps and allows analysis of a wide range of organic compounds with ESI-a soft ionization source,[519] thereby minimizing potential losses of labile compounds. Through this study, I have determined that sulfate/nitrate enriched species are more episodic during day-to-day comparisons, with meteorological factors such as wind direction playing a determining role in the emergence of OSs. Furthermore, photochemical processing may be alluding to the dominance of ONs. There could likely be potential CHO compounds with peroxy functionality, however, the application of chemical derivatization techniques (e.g., iodometry) to resolve the molecular ambiguity is difficult in complex matrices with high salt concentrations.

5.2 Challenges Ahead

5.2.1 Research on ROS and OS/ON

Climate change exacerbates the adverse effects of air pollutants by influencing regional pollutant concentrations through various mechanisms such as increased wildfires,[520] changes in precipitation patterns,[521] and T induced photochemical reactions of VOCs.[522] Peroxides, which regulate atmospheric oxidative capacity, and OS/ON, which significantly contribute to secondary organic aerosol (SOA) formation, are key drivers of air pollution.[523, 524] While fundamental laboratory studies have advanced our understanding of the molecular complexity of particle-bound ROS like

peroxides,[170, 525] considerable ambiguity remains regarding their formation mechanisms in atmospheric aqueous media, such as cloud water. Specifically, challenges associated with sensitive determination of peroxides, OS/ON remain due to: (i) chemical diversity i.e., complex formation pathways with multiple precursors,[526] (ii) lack of quantitative analysis because of low concentrations,[527] (iii) chemical instability during sampling and analysis,[71, 425] and (iv) matrix interferences by inorganic constituents.[184, 185] In general, offline chemical derivatization techniques (utilized in Chapters 2 and 3) offer unparalleled insights into reactive constituents (e.g., peroxides, OS),[528, 529] while direct MS techniques such as nano-DESI-HRMS provide bulk analysis of most organic constituents with minimal degradation losses.[530]

5.2.2 Aqueous Formation Mechanisms

Atmospheric aqueous media (e.g., cloud water, fog droplets) is home to a diverse array of constituents including oxidants (OH, H_2O_2, $^1O_2$, $^3C^*$),[101] antioxidants ($O_2^{-\cdot}$, Fe^{2+}),[212, 531] and anthropogenic gaseous components (e.g., SO_2, NO_x)[532, 533] In general, these constituents can influence reaction pathways including autoxidation to yield HOMs such as peroxides.[534] Throughout our discussion in Chapter 2, we raised the question if the rapid formation of HOMs (e.g., ROOHs) could be attributed to a never-before elucidated autoxidation mechanism, which may be inhibited or promoted by these aqueous constituents, adding complex radical pathways (e.g., RO_2/OH).[535, 536] We considered specific roles that the majority of aqueous species can play in facilitating ROOH formation. For instance, TMIs, O_2^-. can inadvertently facilitate catalytic recycling of HO_x radicals, $^1O_2$ can selectively react with electron-rich compounds, suppressing OH oxidation pathways, $^3C^*$ - an important aqueous-phase oxidant with its relatively comparable concentration than OH radicals,[99, 109, 537, 538] is the most likely candidate to inhibit autoxidation through H-abstraction of target compounds. Gaseous components such as NO_x have low water solubility (K_H = 1.2 x 10^{-2} M atm^{-1}) and are less likely to interfere with autoxidation, however SO_2 with high water solubility (K_H = 2.3 x10^2 M^{-1} atm)[532, 539, 540] can be a sink for autoxidation-initiated peroxides which can facilitate oxidation of inorganic sulfur leading to aqueous OSs.[66, 73, 541, 542] In all scenarios, it is clear that while autoxidation can be a dominant reaction pathway to initiate per-

oxide formation in bulk aqueous media, this cannot be determined indiscriminately from offline derivatization assisted LC-MS techniques adopted in our study. In particular, radical intermediates such as RO_2 formed via intramolecular H-abstraction[536, 543] are the key to examine the reaction pathways yielding peroxides. To exclusively measure these intermediates, electron paramagnetic resonance (EPR) spectroscopy can be used to allow direct detection of free radicals such as OH, RO_2 in complex systems. We have shared some preliminary results on applying EPR to detect free radicals in Section 5.3.2.

5.3 Proposed Research Venues

5.3.1 HOMs Formation in Photochemical Oxidation of Fires Emission

Fires occurring at the urban-wildland interface (UWI) can be fueled by both anthropogenic (e.g., plastic) and biogenic (e.g., biomass) materials, further depreciating air quality and imposing a burden on public health.[544, 545] OAs emitted during these fires are known to be composed of a wide range of organic compounds including aromatics (e.g., benzene, toluene), polyaromatics, alkanes, plasticizers, sugars and many more.[546, 547] Despite extensive research into the characterization of organic compounds emerging from biomass-burning fires, UWI fires are highly complex and challenging when discerning the formation pathways and physico-chemical properties of HOMs. In particular, determining reaction mechanisms and kinetics regarding the formation of HOMs is challenging due to: (i) the chemical complexity of the matrix, making it difficult to isolate and characterize specific formation pathways,[548](ii) the transient nature of combustion, leading to rapid transformation in composition and concentration of emitted species,[549] (iii) limited experimental data for control combustion analysis of HOMs,[550] (iv) low concentrations and shorter lifetimes of crucial intermediates (e.g., 5-or 6-membered RO_2 cyclic state),[551] and (v) ambient conditions such as T, RH and solar radiation, influencing the formation of oxygenated derivative during oxidation of aromatics.[552] Thus, the atmospheric burden of HOMs emerging from photochemical oxidation during UWI fires can be better understood. Currently, the magnitude and mechanism of HOM formation from fire emissions re-

main unclear. In particular, the formation of peroxides from aqueous-phase autoxidation of aromatic precursors is lacking. From our work in Chapter 2, the aqueous-phase formation of ROOHs from various OAcs inspired us to investigate their formation from complex precursors such as aromatic compounds. Recent evidence on gas-phase oxidation of aromatic hydrocarbons indicate the formation ROOHs,[156] with some pointing towards RO_2/HO_2 radical chemistry as major facilitator for generation of HOMs.[553, 554] A future study can be conducted with an aim to systematically study the evolution of oxygenated derivatives by using simpler aromatics as model compounds by pursuing their oxidation in the aqueous-phase. In the past decade there has been a perception that the formation of HOMs from aromatic precursors would not undergo autoxidation,[555] however recently we have seen a shift in this perception evidencing autoxidation as facilitator for the formation of HOMs.[555, 556] While there are numerous studies evidencing gas-phase autoxidation-initiated formation of HOMs from aromatic precursors,[529, 553, 554, 557, 558] there is no such evidence in aqueous-phase. We hypothesize that photochemical oxidation of aromatics may yield aqueous ROOHs whose formation mechanisms will be vastly contrasting to simpler OAcs. Moreover, the iodometry-assisted LC-MS method applied in Chapter 2 may be advantageous to selectively identify the aqueous ROOHs emerging from aromatic precursors.

Benzoic acid (BNA, C_6H_5COOH) is a simple aromatic acid found in vehicle exhausts with its aqueous concentration reaching 0.3 $ng.m^{-3}$ in the Indo-Gangetic Plain.[559, 560] BNA is a known catalyst enhancing nucleation of sulfuric acid contributing to new particle formation.[559, 561] Given that aromatic compounds tend to undergo different H-abstraction mechanisms during autoxidation,[562] we explored the formation of aqueous ROOHs emerging during photooxidation of BNA via application of iodometry-assisted LC-MS method. Figure 5.1 shows the preliminary data for a first-generation ROOH (m/z 153, $C_7H_6O_4$). This data opens new avenues for exploring autoxidation in water-soluble aromatic compounds. Future studies should further incorporate field campaigns with targeted analysis of HOMs in atmospheric aqueous media via the application of advanced analytical techniques.

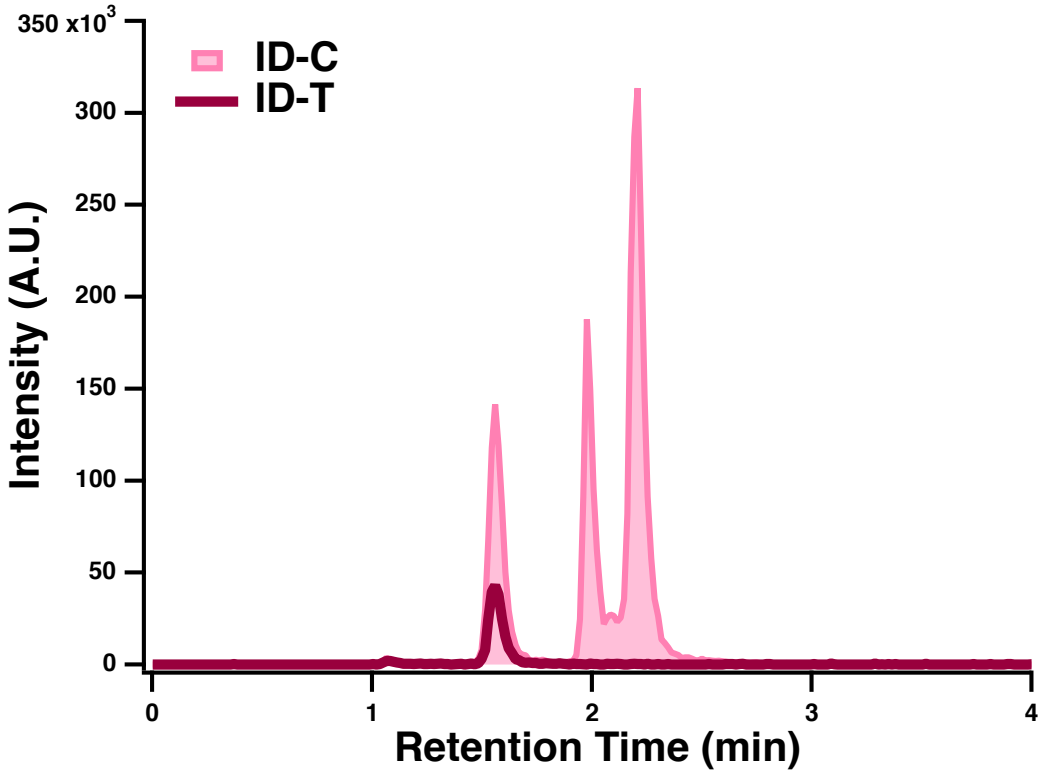

Figure 5.1: Extracted Ion Chromatogram (EIC) of ROOH from aromatic precursor (i.e., benzoic acid). First-generation ROOH observed at m/z 153 ($[C_7H_6O_4)\text{-}H]^-$). Iodometry control (ID-C) indicated oxidized sample aliquot without addition of KI while iodometry treatment (ID-T) indicated a sample with KI.

5.3.2 Crucial Radical Intermediates

Electron paramagnetic resonance (EPR) spectroscopy is a powerful technique used to study paramagnetic species including free radicals in various systems.[563] In atmospheric chemistry, understanding the fate, transformation and formation of RO_2 radicals is critical in determining their role in atmospheric oxidation processes.[210] RO_2 radicals propagate the formation of crucial oxidative derivatives during the autoxidation of VOCs, thus playing a significant role in the creation of SOA and influencing both climate and health outcomes.[367] Conventional MS-based approaches provide valuable information in assessing products of RO_2 chemistry but are often limited in allowing direct detection and quantification of free radicals.[564] In Chapter 2, we observed the formation of aqueous ROOHs, but the lack of radical measurements hindered our assertion on differentiating between autoxidation and RO_2/OH radical chemistry. The application of EPR spectroscopy offers a unique opportunity to over-

come these limitations and pursue sensitive determination of RO_2 radicals, especially in real-time atmospheric conditions. We propose a future study based on an EPR approach to sensitively determine oxy-radical species and their reaction mechanisms during the photochemical oxidation of water-soluble species. Specific objectives of this research are: (i) development of an EPR technique to detect and quantify RO_2 radicals in the aqueous-phase, (ii) determine the lifetime of RO_2 radicals under varying oxidant and precursor concentrations, (iii) qualitatively determine RO_2 radicals originating from simple organic acids and complex aromatics, i.e., comparative analysis of biogenic and anthropogenic sources, and (iv) translate experimental results to field campaigns. Currently, two EPR approaches are adopted for free radical determination in particulate matter, i.e., direct determination and solvent extraction method.[565] As a case study, we have applied EPR for determination of varying radicals emerging from combustion of polymeric precursor such as plastic. Figure 5.2 demonstrates OH and RO_2/RO radical profiles acquired via 5-diethoxyphosphoryl-5-methyl-1-pyrroline N-oxide (DEPMPO) as a spin trap. This technique opens new avenues for in-situ radical determination to understand the formation mechanisms behind HOMs. Future studies should assess the applicability of EPR-based methodologies for sensitive radical determination and acquire kinetics/reaction mechanisms pertaining to the aqueous formation of oxygenated derivatives such as peroxides.

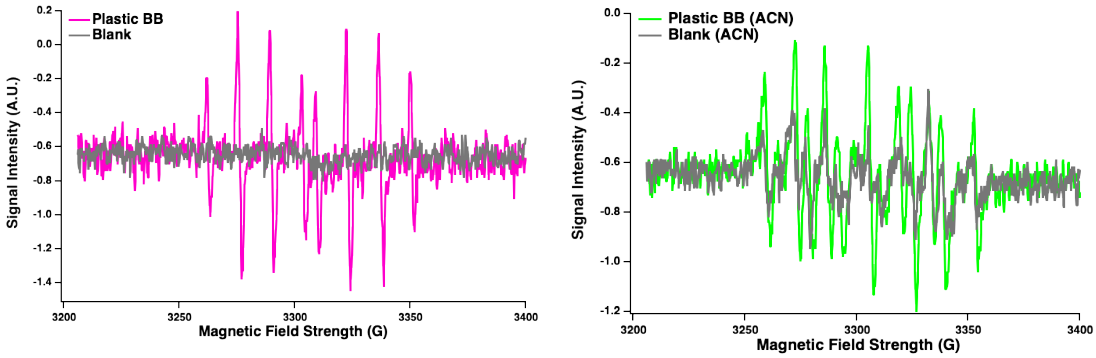

Figure 5.2: EPR profile for radicals found in the combustion of the anthropogenic source. (A) OH radical profile is compared with a blank air sample. (B) RO_2/RO radical mixture from plastic emission PM is characterized by ACN as a trapping solvent.

5.3.3 Halogen Chemistry

OEs or alkenes are a class of unsaturated hydrocarbons which are widely used in industrial processes including polymer production and fuel synthesis.[566, 567] Indoor environments serve as reservoirs for VOCs including OEs, originating from sources such as cooking, heating, and cleaning products.[568] Indoor surfaces such as carpets, and hard floors represent interesting matrices with >20% olefinic content by mass.[569] Indoor OEs can undergo oxidation by oxidants such as O_3, ROS, thereby propagating the formation of indoor ROOHs.[570] As such, understanding the prevalence and distribution of indoor OEs is crucial for assessing indoor air quality and its impact on human health.[571] Currently, there is a scarcity of data on the long-term fate and transport of OEs within indoor environments.[572] Additionally, there is limited knowledge of the mechanisms governing their adsorption, desorption and reactions on indoor surfaces, which impedes accurate modelling and prediction of indoor air pollutants.[573] Therefore, developing a sensitive analytical method for the determination of indoor OEs can aid in mitigating indoor air pollution and public health management.[574] Through our detailed observations in Chapter 3, we affirmed that halogens such as I_2 can selectively react with aliphatic unsaturated organic compounds while aromatic compounds exhibit slow decay over 24 hours of reaction time.[575] Interestingly, this reaction can be utilized as a possible method to determine the olefinic content in indoor matrices, especially since these olefinic precursors can be a source for ROOHs.[576] Furthermore, halogen specificity can be probed with molecular bromine (Br_2), but due to its environmental toxicity, I_2 may prove to be a safe agent. Thus, a research project designed for targeted analysis of indoor OEs can assist in understanding the dynamic transformation of these pollutants. Moreover, exploring halogenating agents or derivatization reactions can offer enhanced sensitivity and specificity for OE detection methods, thereby opening new avenues for analytical chemistry.

5.3.4 Role of Viscosity and Altitude

Ambient aerosols are complex mixtures of solid or liquid suspended particles, with a diverse array of organic and inorganic compounds.[577] Amongst the organic com-

pounds, peroxides, OSs and ONs play crucial roles in altering aerosol properties such as viscosity, hygroscopicity.[49, 578–580] Chemical derivatization assisted LC-MS techniques have provided molecular specificity with regards to speciation of peroxides, however for characterization of OS/ON, these methods are often time-consuming, prone to artifacts/matrix effects and physico-chemical analyte losses.[187] In Chapter 4, to maintain sample integrity, nano-DESI-HRMS was utilized to deconvolute molecular speciation of particle-bound organics in ambient aerosol samples. Details on molecular composition indicated a mixture of organic acids, OS, ON and perhaps peroxides. While molecular characterization assists in determining the volatility of identified species, the information acquired in Chapter 4 can be further disseminated to predict viscosity trends. In particular, diurnal trends in OA composition can influence phase state.[508] The Viscosity of OA is essential to determining and predicting their atmospheric impact.[581] Glass transition temperature (Tg) is a known parameter that can be used to determine the viscosity of OAs. Specifically, if the ambient temperature is less than Tg, particles are more likely to exhibit a solid glass-like phase state and liquid if Tg is below ambient temperature.[582] From the data provided in Chapter 4, we can further determine the viscosity of OAs in each day and night. Lastly, we can further characterize OA composition as a function of altitude. In particular, the TRACER-ARM campaign utilizes a tethered balloon system 1.5 km above ground level and below clouds in clear air. Determining OA composition above and below the boundary layer can be important to consider the development of the convective boundary layer[583] and understand the contribution of hygroscopic species such as OS/ON in leading to convective cloud formation.

References

[49] A. D. Estillore *et al.*, "Water Uptake and Hygroscopic Growth of Organosulfate Aerosol," en, *Environmental Science & Technology*, vol. 50, no. 8, pp. 4259–4268, Apr. 2016, ISSN: 0013-936X, 1520-5851. DOI: 10.1021/acs.est.5b05014.

[66] S. Wang, Y. Zhao, A. W. H. Chan, M. Yao, Z. Chen, and J. P. D. Abbatt, "Organic Peroxides in Aerosol: Key Reactive Intermediates for Multiphase Processes in the Atmosphere," en, *Chemical Reviews*, vol. 123, no. 4, pp. 1635–1679, Feb. 2023, ISSN: 0009-2665, 1520-6890. DOI: 10.1021/acs.chemrev.2c00430.

[71] M. Krapf *et al.*, "Labile Peroxides in Secondary Organic Aerosol," en, *Chem*, vol. 1, no. 4, pp. 603–616, Oct. 2016, ISSN: 24519294. DOI: 10.1016/j.chempr.2016.09.007.

[73] S. Wang *et al.*, "Organic Peroxides and Sulfur Dioxide in Aerosol: Source of Particulate Sulfate," en, *Environmental Science & Technology*, vol. 53, no. 18, pp. 10 695–10 704, Sep. 2019, ISSN: 0013-936X, 1520-5851. DOI: 10.1021/acs.est.9b02591.

[99] H. Herrmann, D. Hoffmann, T. Schaefer, P. Brauer, and A. Tilgner, "Tropospheric Aqueous Phase Free Radical Chemistry Radical Sources, Spectra, Reaction Kinetics and Prediction Tools," en, *ChemPhysChem*, vol. 11, no. 18, pp. 3796–3822, Dec. 2010, ISSN: 1439-4235, 1439-7641. DOI: 10.1002/cphc.201000533.

[101] A. Bianco, M. Passananti, M. Brigante, and G. Mailhot, "Photochemistry of the Cloud Aqueous Phase: A Review," en, *Molecules*, vol. 25, no. 2, p. 423, Jan. 2020, ISSN: 1420-3049. DOI: 10.3390/molecules25020423.

[109] R. Kaur and C. Anastasio, "First Measurements of Organic Triplet Excited States in Atmospheric Waters," en, *Environmental Science & Technology*, vol. 52, no. 9, pp. 5218–5226, May 2018, ISSN: 0013-936X, 1520-5851. DOI: 10.1021/acs.est.7b06699.

[156] X. Cheng, Q. Chen, Y. Jie Li, Y. Zheng, K. Liao, and G. Huang, "Highly oxygenated organic molecules produced by the oxidation of benzene and toluene in a wide range of OH exposure and NO_x conditions," en, *Atmospheric Chemistry and Physics*, vol. 21, no. 15, pp. 12 005–12 019, Aug. 2021, ISSN: 1680-7324. DOI: 10.5194/acp-21-12005-2021.

[170] K. S. Docherty, W. Wu, Y. B. Lim, and P. J. Ziemann, "Contributions of Organic Peroxides to Secondary Aerosol Formed from Reactions of Monoterpenes with O_3, volume = 39," en, *Environmental Science & Technology*, no. 11, pp. 4049–4059, Jun. 2005, ISSN: 0013-936X, 1520-5851. DOI: 10.1021/es050228s. (visited on 02/11/2024).

[184] W. Zhang, L. Xu, and H. Zhang, "Recent advances in mass spectrometry techniques for atmospheric chemistry research on molecular-level," *Mass Spectrometry Reviews*, 2023.

[185] A. P. S. Hettiyadura *et al.*, "Determination of atmospheric organosulfates using HILIC chromatography with MS detection," en, *Atmospheric Measurement Techniques*, vol. 8, no. 6, pp. 2347–2358, Jun. 2015, ISSN: 1867-8548. DOI: 10.5194/amt-8-2347-2015. [Online]. Available: https://amt.copernicus.org/articles/8/2347/2015/.

[187] W. Fan, T. Chen, Z. Zhu, H. Zhang, Y. Qiu, and D. Yin, "A review of secondary organic aerosols formation focusing on organosulfates and organic nitrates," en, *Journal of Hazardous Materials*, vol. 430, p. 128 406, May 2022, ISSN: 03043894. DOI: 10.1016/j.jhazmat.2022.128406. (visited on 01/29/2024).

[210] J. D. Crounse *et al.*, "Atmospheric Fate of Methacrolein. 1. Peroxy Radical Isomerization Following Addition of OH and O_2," en, *The Journal of Physical Chemistry A*, vol. 116, no. 24, pp. 5756–5762, Jun. 2012, ISSN: 1089-5639, 1520-5215. DOI: 10.1021/jp211560u.

[212] Y. Zuo and J. Hoigne, "Formation of hydrogen peroxide and depletion of oxalic acid in atmospheric water by photolysis of iron(III)-oxalato complexes," en, *Environmental Science & Technology*, vol. 26, no. 5, pp. 1014–1022, May 1992, ISSN: 0013-936X, 1520-5851. DOI: 10.1021/es00029a022. (visited on 01/29/2024).

[367] M. Shiraiwa *et al.*, "Aerosol Health Effects from Molecular to Global Scales," *Environmental Science & Technology*, vol. 51, no. 23, pp. 13 545–13 567, Dec. 2017, ISSN: 0013-936X. DOI: 10.1021/acs.est.7b04417. [Online]. Available: https://doi.org/10.1021/acs.est.7b04417 (visited on 09/27/2019).

[425] A. I. Darer, N. C. Cole-Filipiak, A. E. O Connor, and M. J. Elrod, "Formation and Stability of Atmospherically Relevant Isoprene Derived Organosulfates and Organonitrates," en, *Environmental Science & Technology*, vol. 45, no. 5, pp. 1895–1902, Mar. 2011, ISSN: 0013-936X, 1520-5851. DOI: 10.1021/es103797z.

[508] R. Schmedding *et al.*, "Predicting secondary organic aerosol phase state and viscosity and its effect on multiphase chemistry in a regional-scale air quality model," *Atmospheric chemistry and physics*, vol. 20, no. 13, pp. 8201–8225, 2020.

[517] P. de la Mare and P. Robertson, "550. the kinetics of halogen addition to unsaturated compounds. part xxi. the mechanisms of addition reactions," *Journal of the Chemical Society (Resumed)*, pp. 2838–2842, 1950.

[518] J. S. Fritz and G. E. Wood, "Determination of olefinic unsaturation by bromination," *Analytical Chemistry*, vol. 40, no. 1, pp. 134–139, 1968.

[519] R. Chen *et al.*, "Recent applications of ambient ionization mass spectrometry in environmental analysis," en, *Trends in Environmental Analytical Chemistry*, vol. 15, pp. 1–11, Jul. 2017, ISSN: 22141588. DOI: 10.1016/j.teac.2017.07.001. [Online]. Available: https://linkinghub.elsevier.com/retrieve/pii/S2214158817300338 (visited on 02/12/2024).

[520] G. Di Virgilio *et al.*, "Climate change increases the potential for extreme wildfires," *Geophysical Research Letters*, vol. 46, no. 14, pp. 8517–8526, 2019.

[521] M. H. Dore, "Climate change and changes in global precipitation patterns: What do we know?" *Environment international*, vol. 31, no. 8, pp. 1167–1181, 2005.

[522] D. Narumi, A. Kondo, and Y. Shimoda, "The effect of the increase in urban temperature on the concentration of photochemical oxidants," *Atmospheric Environment*, vol. 43, no. 14, pp. 2348–2359, 2009.

[523] G. Cao, X. Zhao, D. Hu, R. Zhu, and F. Ouyang, "Development and application of a quantification method for water soluble organosulfates in atmospheric aerosols," *Environmental pollution*, vol. 225, pp. 316–322, 2017.

[524] S. Wang *et al.*, "Relationship between chemical composition and oxidative potential of secondary organic aerosol from polycyclic aromatic hydrocarbons," en, *Atmospheric Chemistry and Physics*, vol. 18, no. 6, pp. 3987–4003, Mar. 2018, ISSN: 1680-7324. DOI: 10.5194/acp-18-3987-2018. [Online]. Available: https://acp.copernicus.org/articles/18/3987/2018/.

[525] Y. Lim and B. Turpin, "Laboratory evidence of organic peroxide and peroxyhemiacetal formation in the aqueous phase and implications for aqueous OH," *Atmospheric Chemistry and Physics*, vol. 15, no. 22, pp. 12 867–12 877, 2015, Publisher: Copernicus GmbH.

[526] N. Ng, J. Kroll, A. Chan, P. Chhabra, R. Flagan, and J. Seinfeld, "Secondary organic aerosol formation from m-xylene, toluene, and benzene," *Atmospheric Chemistry and Physics*, vol. 7, no. 14, pp. 3909–3922, 2007.

[527] R. M. Duarte, J. T. Matos, and A. C. Duarte, "Multidimensional analytical characterization of water-soluble organic aerosols: Challenges and new perspectives," *Applied Sciences*, vol. 11, no. 6, p. 2539, 2021.

[528] G. Spolnik, P. Wach, K. J. Rudzinski, K. Skotak, W. Danikiewicz, and R. Szmigielski, "Improved uhplc-ms/ms methods for analysis of isoprene-derived organosulfates," *Analytical chemistry*, vol. 90, no. 5, pp. 3416–3423, 2018.

[529] S. Wang, R. Wu, T. Berndt, M. Ehn, and L. Wang, "Formation of highly oxidized radicals and multifunctional products from the atmospheric oxidation of alkylbenzenes," *Environmental science & technology*, vol. 51, no. 15, pp. 8442–8449, 2017.

[530] F. Bianchi *et al.*, "Ms-based analytical techniques: Advances in spray-based methods and ei-lc-ms applications," *Journal of analytical methods in chemistry*, vol. 2018, 2018.

[531] L. Deguillaume, M. Leriche, K. Desboeufs, G. Mailhot, C. George, and N. Chaumerliac, "Transition Metals in Atmospheric Liquid Phases: Sources, Reactivity, and Sensitive Parameters," en, *Chemical Reviews*, vol. 105, no. 9, pp. 3388–3431, Sep. 2005, ISSN: 0009-2665, 1520-6890. DOI: 10.1021/cr040649c. [Online]. Available: https://pubs.acs.org/doi/10.1021/cr040649c.

[532] P. H. Daum, S. E. Schwartz, and L. Newman, "Acidic and related constituents in liquid water stratiform clouds," en, *Journal of Geophysical Research: Atmospheres*, vol. 89, no. D1, pp. 1447–1458, Feb. 1984, ISSN: 0148-0227. DOI: 10.1029/JD089iD01p01447.

[533] J. J. Schwab *et al.*, "Atmospheric chemistry measurements at whiteface mountain, ny: Cloud water chemistry, precipitation chemistry, and particulate matter," *Aerosol and Air Quality Research*, vol. 16, no. 3, pp. 841–854, 2016.

[534] C. Anastasio, B. C. Faust, and J. M. Allen, "Aqueous phase photochemical formation of hydrogen peroxide in authentic cloud waters," *Journal of Geophysical Research: Atmospheres*, vol. 99, no. D4, pp. 8231–8248, 1994.

[535] A. T. Archibald, A. S. Petit, C. J. Percival, J. N. Harvey, and D. E. Shallcross, "On the importance of the reaction between OH and RO_2 radicals," en, *Atmospheric Science Letters*, vol. 10, no. 2, pp. 102–108, Apr. 2009, ISSN: 1530-261X, 1530-261X. DOI: 10.1002/asl.216.

[536] M. Lucarini and G. F. Pedulli, "Free radical intermediates in the inhibition of the autoxidation reaction," en, *Chemical Society Reviews*, vol. 39, no. 6, p. 2106, 2010, ISSN: 0306-0012, 1460-4744. DOI: 10.1039/b901838g. [Online]. Available: http://xlink.rsc.org/?DOI=b901838g (visited on 02/10/2024).

[537] R. Kaur, B. M. Hudson, J. Draper, D. J. Tantillo, and C. Anastasio, "Aqueous reactions of organic triplet excited states with atmospheric alkenes," *Atmospheric Chemistry and Physics*, vol. 19, no. 7, pp. 5021–5032, 2019, Publisher: Copernicus Publications Gottingen, Germany.

[538] L. He, T. Schaefer, T. Otto, A. Kroflic, and H. Herrmann, "Kinetic and theoretical study of the atmospheric aqueous-phase reactions of oh radicals with methoxyphenolic compounds," *The Journal of Physical Chemistry A*, vol. 123, no. 36, pp. 7828–7838, 2019.

[539] S. E. Schwartz, "Mass-transport considerations pertinent to aqueous phase reactions of gases in liquid-water clouds," in *Chemistry of multiphase atmospheric systems*, Springer, 1986, pp. 415–471.

[540] Q. Zhang *et al.*, "Variability of so_2 in an intensive fog in north china plain: Evidence of high solubility of so_2," *Particuology*, vol. 11, no. 1, pp. 41–47, 2013.

[541] J. A. Lind, A. L. Lazrus, and G. L. Kok, "Aqueous phase oxidation of sulfur (iv) by hydrogen peroxide, methylhydroperoxide, and peroxyacetic acid," *Journal of Geophysical Research: Atmospheres*, vol. 92, no. D4, pp. 4171–4177, 1987.

[542] E. Dovrou, J. C. Rivera-Rios, K. H. Bates, and F. N. Keutsch, "Sulfate formation via cloud processing from isoprene hydroxyl hydroperoxides (ISOPOOH)," *Environmental science & technology*, vol. 53, no. 21, pp. 12 476–12 484, 2019, Publisher: ACS Publications.

[543] T. Jokinen *et al.*, "Rapid Autoxidation Forms Highly Oxidized RO_2 Radicals in the Atmosphere," en, *Angewandte Chemie International Edition*, vol. 53, no. 52, pp. 14 596–14 600, Dec. 2014, ISSN: 1433-7851, 1521-3773. DOI: 10.1002/anie.201408566.

[544] S. Modugno, H. Balzter, B. Cole, and P. Borrelli, "Mapping regional patterns of large forest fires in wildland–urban interface areas in europe," *Journal of environmental management*, vol. 172, pp. 112–126, 2016.

[545] C. M. Villarruel, L. A. Figueroa, and J. F. Ranville, "Quantification of bioaccessible and environmentally relevant trace metals in structure ash from a wildland–urban interface fire," *Environmental Science & Technology*, 2024.

[546] B. R. Simoneit, P. M. Medeiros, and B. M. Didyk, "Combustion products of plastics as indicators for refuse burning in the atmosphere," *Environmental science & technology*, vol. 39, no. 18, pp. 6961–6970, 2005.

[547] J. Reid, R Koppmann, T. Eck, and D. Eleuterio, "A review of biomass burning emissions part ii: Intensive physical properties of biomass burning particles," *Atmospheric chemistry and physics*, vol. 5, no. 3, pp. 799–825, 2005.

[548] J. Gilman *et al.*, "Biomass burning emissions and potential air quality impacts of volatile organic compounds and other trace gases from fuels common in the us," *Atmospheric Chemistry and Physics*, vol. 15, no. 24, pp. 13 915–13 938, 2015.

[549] S. Akagi *et al.*, "Emission factors for open and domestic biomass burning for use in atmospheric models," *Atmospheric Chemistry and Physics*, vol. 11, no. 9, pp. 4039–4072, 2011.

[550] C. D. Cappa and J. L. Jimenez, "Quantitative estimates of the volatility of ambient organic aerosol," en, *Atmospheric Chemistry and Physics*, vol. 10, no. 12, pp. 5409–5424, Jun. 2010, ISSN: 1680-7324. DOI: 10.5194/acp-10-5409-2010. [Online]. Available: https://acp.copernicus.org/articles/10/5409/2010/.

[551] L. Yee *et al.*, "Secondary organic aerosol formation from biomass burning intermediates: Phenol and methoxyphenols," *Atmospheric Chemistry and Physics*, vol. 13, no. 16, pp. 8019–8043, 2013.

[552] S. Li *et al.*, "Evolution of organic aerosol from wood smoke influenced by burning phase and solar radiation," *Journal of Geophysical Research: Atmospheres*, vol. 126, no. 8, e2021JD034534, 2021.

[553] T. Chen *et al.*, "Smog chamber study on the role of no x in soa and o_3 formation from aromatic hydrocarbons," *Environmental Science & Technology*, vol. 56, no. 19, pp. 13 654–13 663, 2022.

[554] M. Wang *et al.*, "Photo-oxidation of aromatic hydrocarbons produces low-volatility organic compounds," *Environmental science & technology*, vol. 54, no. 13, pp. 7911–7921, 2020.

[555] D. Minakata, K. Li, P. Westerhoff, and J. Crittenden, "Development of a group contribution method to predict aqueous phase hydroxyl radical (ho) reaction rate constants," *Environmental science & technology*, vol. 43, no. 16, pp. 6220–6227, 2009.

[556] R. Volkamer *et al.*, "Oh-initiated oxidation of benzene part i. phenol formation under atmospheric conditions," *Physical Chemistry Chemical Physics*, vol. 4, no. 9, pp. 1598–1610, 2002.

[557] X. Cheng *et al.*, "Oxygenated organic molecules produced by low-no x photooxidation of aromatic compounds: Contributions to secondary organic aerosol and steric hindrance," *Atmospheric Chemistry and Physics*, vol. 24, no. 4, pp. 2099–2112, 2024.

[558] M. Zhu, S. Wang, Y. Zhang, Z. Yu, Y. Yu, and X. Wang, "Particle-bound highly oxidized organic molecules derived from aromatic hydrocarbons in an urban atmosphere," *Environmental Science & Technology Letters*, vol. 9, no. 12, pp. 1030–1036, 2022.

[559] X. Zhang, C. Zhang, X. Sun, J. Yang, and C. Zhu, "Mechanism and kinetic study of the reaction of benzoic acid with oh, no 3 and so 4- radicals in the atmosphere," *RSC advances*, vol. 9, no. 33, pp. 18 971–18 977, 2019.

[560] S. K. Boreddy, T. Mochizuki, K. Kawamura, S. Bikkina, and M. Sarin, "Homologous series of low molecular weight (c1-c10) monocarboxylic acids, benzoic acid and hydroxyacids in fine-mode (pm2. 5) aerosols over the bay of bengal: Influence of heterogeneity in air masses and formation pathways," *Atmospheric environment*, vol. 167, pp. 170–180, 2017.

[561] H. Wang *et al.*, "The effect of water molecules and air humidity on the cluster formation from benzoic acid with sulfuric acid/ammonia/dimethylamine: A molecular-scale investigation," *Journal of Molecular Liquids*, vol. 390, p. 123 001, 2023.

[562] J. Helberg and D. A. Pratt, "Autoxidation vs. antioxidants–the fight for forever," *Chemical Society Reviews*, vol. 50, no. 13, pp. 7343–7358, 2021.

[563] I. Spasojević, "Free radicals and antioxidants at a glance using epr spectroscopy," *Critical reviews in clinical laboratory sciences*, vol. 48, no. 3, pp. 114–142, 2011.

[564] H. Iwahashi, C. E. Parker, R. P. Mason, and K. B. Tomer, "Combined liquid chromatography/electron paramagnetic resonance spectrometry/electrospray ionization mass spectrometry for radical identification," *Analytical chemistry*, vol. 64, no. 19, pp. 2244–2252, 1992.

[565] Q. Chen *et al.*, "Rapid determination of environmentally persistent free radicals (epfrs) in atmospheric particles with a quartz sheet-based approach using electron paramagnetic resonance (epr) spectroscopy," *Atmospheric Environment*, vol. 184, pp. 140–145, 2018.

[566] C. P. Nicholas, "Applications of light olefin oligomerization to the production of fuels and chemicals," *Applied Catalysis A: General*, vol. 543, pp. 82–97, 2017.

[567] M. Klapper, D. Joe, S. Nietzel, J. W. Krumpfer, and K. Mullen, "Olefin polymerization with supported catalysts as an exercise in nanotechnology," *Chemistry of Materials*, vol. 26, no. 1, pp. 802–819, 2014.

[568] C. J. Weschler and W. W. Nazaroff, "Semivolatile organic compounds in indoor environments," *Atmospheric environment*, vol. 42, no. 40, pp. 9018–9040, 2008.

[569] C. J. Weschler, A. T. Hodgson, and J. D. Wooley, "Indoor chemistry: Ozone, volatile organic compounds, and carpets," en, *Environmental Science & Technology*, vol. 26, no. 12, pp. 2371–2377, Dec. 1992, ISSN: 0013-936X, 1520-5851. DOI: 10.1021/es00036a006.

[570] M. Shiraiwa *et al.*, "Modelling consortium for chemistry of indoor environments (moccie): Integrating chemical processes from molecular to room scales," *Environmental Science: Processes & Impacts*, vol. 21, no. 8, pp. 1240–1254, 2019.

[571] W. W. Nazaroff and C. J. Weschler, "Cleaning products and air fresheners: Exposure to primary and secondary air pollutants," *Atmospheric environment*, vol. 38, no. 18, pp. 2841–2865, 2004.

[572] W. Nazaroff and A. Goldstein, "Indoor chemistry: Research opportunities and challenges," *Indoor air*, vol. 25, no. 4, pp. 357–361, 2015.

[573] G. Sarwar, D. A. Olson, R. L. Corsi, and C. J. Weschler, "Indoor fine particles: The role of terpene emissions from consumer products," *Journal of the Air & Waste Management Association*, vol. 54, no. 3, pp. 367–377, 2004.

[574] T. Vera, F Villanueva, L Wimmerová, and E. Tolis, "An overview of methodologies for the determination of volatile organic compounds in indoor air," *Applied Spectroscopy Reviews*, vol. 57, no. 8, pp. 625–674, 2022.

[575] R. M. Pagni *et al.*, "Reactions of unsaturated compounds with iodine and bromine on. gamma. alumina," *The Journal of Organic Chemistry*, vol. 53, no. 19, pp. 4477–4482, 1988.

[576] Z. Zhou, L. R. Crilley, J. C. Ditto, T. C. VandenBoer, and J. P. D. Abbatt, "Chemical Fate of Oils on Indoor Surfaces: Ozonolysis and Peroxidation," en, *Environmental Science & Technology*, vol. 57, no. 41, pp. 15 546–15 557, Oct. 2023, ISSN: 0013-936X, 1520-5851. DOI: 10.1021/acs.est.3c04009. [Online]. Available: https://pubs.acs.org/doi/10.1021/acs.est.3c04009 (visited on 02/12/2024).

[577] A. W. H. Chan *et al.*, "Detailed chemical characterization of unresolved complex mixtures in atmospheric organics: Insights into emission sources, atmospheric processing, and secondary organic aerosol formation," en, *Journal of Geophysical Research: Atmospheres*, vol. 118, no. 12, pp. 6783–6796, Jun. 2013, ISSN: 2169-897X, 2169-8996. DOI: 10.1002/jgrd.50533. [Online]. Available:

https://agupubs.onlinelibrary.wiley.com/doi/10.1002/jgrd.50533 (visited on 02/09/2024).

[578] N. E. Rothfuss and M. D. Petters, "Influence of Functional Groups on the Viscosity of Organic Aerosol," en, *Environmental Science & Technology*, vol. 51, no. 1, pp. 271–279, Jan. 2017, ISSN: 0013-936X, 1520-5851. DOI: 10.1021/acs.est.6b04478. [Online]. Available: https://pubs.acs.org/doi/10.1021/acs.est.6b04478 (visited on 02/09/2024).

[579] F. D. Pope, P. J. Gallimore, S. J. Fuller, R. A. Cox, and M. Kalberer, "Ozonolysis of Maleic Acid Aerosols: Effect upon Aerosol Hygroscopicity, Phase and Mass," en, *Environmental Science & Technology*, vol. 44, no. 17, pp. 6656–6660, Sep. 2010, ISSN: 0013-936X, 1520-5851. DOI: 10.1021/es1008278. (visited on 02/09/2024).

[580] M. L. Pohlker *et al.*, "Global organic and inorganic aerosol hygroscopicity and its effect on radiative forcing," en, *Nature Communications*, vol. 14, no. 1, p. 6139, Oct. 2023, ISSN: 2041-1723. DOI: 10.1038/s41467-023-41695-8. [Online]. Available: https://www.nature.com/articles/s41467-023-41695-8.

[581] J. P. Reid *et al.*, "The viscosity of atmospherically relevant organic particles," *Nature communications*, vol. 9, no. 1, p. 956, 2018.

[582] W.-S. W. DeRieux *et al.*, "Predicting the glass transition temperature and viscosity of secondary organic material using molecular composition," en, *Atmospheric Chemistry and Physics*, vol. 18, no. 9, pp. 6331–6351, May 2018, ISSN: 1680-7324. DOI: 10.5194/acp-18-6331-2018. [Online]. Available: https://acp.copernicus.org/articles/18/6331/2018/ (visited on 02/09/2024).

[583] M. Collaud Coen *et al.*, "Identification of topographic features influencing aerosol observations at high altitude stations," *Atmospheric Chemistry and Physics*, vol. 18, no. 16, pp. 12 289–12 313, 2018.

Bibliography

[1] A. A. Almetwally, M. Bin-Jumah, and A. A. Allam, "Ambient air pollution and its influence on human health and welfare: An overview," en, *Environmental Science and Pollution Research*, vol. 27, no. 20, pp. 24 815–24 830, Jul. 2020, ISSN: 0944-1344, 1614-7499. DOI: 10.1007/s11356-020-09042-2.

[2] S. Mosley, "Environmental History of Air Pollution and Protection," en, in *The Basic Environmental History*, M. Agnoletti and S. Neri Serneri, Eds., vol. 4, Cham: Springer International Publishing, 2014, pp. 143–169, ISBN: 978-3-319-09179-2 978-3-319-09180-8. DOI: 10.1007/978-3-319-09180-8_5.

[3] J. H. Seinfeld, "Air pollution A half century of progress," en, *AIChE Journal*, vol. 50, no. 6, pp. 1096–1108, Jun. 2004, ISSN: 0001-1541, 1547-5905. DOI: 10.1002/aic.10102.

[4] J. Fenger, "Air pollution in the last 50 years From local to global," en, *Atmospheric Environment*, vol. 43, no. 1, pp. 13–22, Jan. 2009, ISSN: 13522310. DOI: 10.1016/j.atmosenv.2008.09.061.

[5] D. Vallero, "The State of the Atmosphere," en, in *Fundamentals of Air Pollution*, Elsevier, 2014, pp. 3–22, ISBN: 978-0-12-401733-7. DOI: 10.1016/B978-0-12-401733-7.00001-3.

[6] B. Brunekreef and S. T. Holgate, "Air pollution and health," en, *The Lancet*, vol. 360, no. 9341, pp. 1233–1242, Oct. 2002, ISSN: 01406736. DOI: 10.1016/S0140-6736(02)11274-8.

[7] I. Colbeck and M. Lazaridis, "Aerosols and environmental pollution," *Naturwissenschaften*, vol. 97, pp. 117–131, 2010.

[8] M. S. Hammer *et al.*, "Global Estimates and Long-Term Trends of Fine Particulate Matter Concentrations (1998 to 2018)," en, *Environmental Science & Technology*, vol. 54, no. 13, pp. 7879–7890, Jul. 2020, ISSN: 0013-936X, 1520-5851. DOI: 10.1021/acs.est.0c01764.

[9] H. Deng *et al.*, "Daytime SO_2 chemistry on ubiquitous urban surfaces as a source of organic sulfur compounds in ambient air," en, *Science Advances*, vol. 8, no. 39, eabq6830, Sep. 2022, ISSN: 2375-2548. DOI: 10.1126/sciadv.abq6830.

[10] M. Zhang, Y. Wang, Y. Ma, L. Wang, W. Gong, and B. Liu, "Spatial distribution and temporal variation of aerosol optical depth and radiative effect in south china and its adjacent area," *Atmospheric Environment*, vol. 188, pp. 120–128, 2018.

[11] R Timmermans *et al.*, "Source apportionment of pm2. 5 across china using lotos-euros," *Atmospheric Environment*, vol. 164, pp. 370–386, 2017.

[12] M. Pandolfi *et al.*, "Long-range and local air pollution: What can we learn from chemical speciation of particulate matter at paired sites?" en, *Atmospheric Chemistry and Physics*, vol. 20, no. 1, pp. 409–429, Jan. 2020, ISSN: 1680-7324. DOI: 10.5194/acp-20-409-2020.

[13] X. Shan, L. Liu, G. Li, K. Xu, B. Liu, and W. Jiang, "$PM_{2.5}$ and the typical components cause organelle damage, apoptosis and necrosis: Role of reactive oxygen species," en, *Science of The Total Environment*, vol. 782, p. 146 785, Aug. 2021, ISSN: 00489697. DOI: 10.1016/j.scitotenv.2021.146785. (visited on 01/29/2024).

[14] H. Hong *et al.*, "Cytotoxicity induced by iodinated haloacetamides via ROS accumulation and apoptosis in HepG-2 cells," en, *Environmental Pollution*, vol. 242, pp. 191–197, Nov. 2018, ISSN: 02697491. DOI: 10.1016/j.envpol.2018.06.090.

[15] T. Fang, P. S. J. Lakey, R. J. Weber, and M. Shiraiwa, "Oxidative Potential of Particulate Matter and Generation of Reactive Oxygen Species in Epithelial Lining Fluid," en, *Environmental Science & Technology*, vol. 53, no. 21, pp. 12 784–12 792, Nov. 2019, ISSN: 0013-936X, 1520-5851. DOI: 10.1021/acs.est.9b03823.

[16] A. Valavanidis, T. Vlachogianni, K. Fiotakis, and S. Loridas, "Pulmonary Oxidative Stress, Inflammation and Cancer Respirable Particulate Matter, Fibrous Dusts and Ozone as Major Causes of Lung Carcinogenesis through Reactive Oxygen Species Mechanisms," en, *International Journal of Environmental Research and Public Health*, vol. 10, no. 9, pp. 3886–3907, Aug. 2013, ISSN: 1660-4601. DOI: 10.3390/ijerph10093886.

[17] J. T. Bates *et al.*, "Reactive Oxygen Species Generation Linked to Sources of Atmospheric Particulate Matter and Cardiorespiratory Effects," en, *Environmental Science & Technology*, vol. 49, no. 22, pp. 13 605–13 612, Nov. 2015, ISSN: 0013-936X, 1520-5851. DOI: 10.1021/acs.est.5b02967.

[18] L. Guo *et al.*, "Comprehensive characterization of hygroscopic properties of methanesulfonates," *Atmospheric Environment*, vol. 224, p. 117 349, 2020, Publisher: Elsevier.

[19] W. Wang *et al.*, "Influence of covid-19 lockdown on the variation of organic aerosols: Insight into its molecular composition and oxidative potential," *Environmental Research*, vol. 206, p. 112 597, 2022.

[20] P. H. Chowdhury, Q. He, R. Carmieli, C. Li, Y. Rudich, and M. Pardo, "Connecting the Oxidative Potential of Secondary Organic Aerosols with Reactive Oxygen Species in Exposed Lung Cells," en, *Environmental Science & Technology*, vol. 53, no. 23, pp. 13 949–13 958, Dec. 2019, ISSN: 0013-936X, 1520-5851. DOI: 10.1021/acs.est.9b04449.

[21] P. Liu *et al.*, "Lability of secondary organic particulate matter," en, *Proceedings of the National Academy of Sciences*, vol. 113, no. 45, pp. 12 643–12 648, Nov. 2016, ISSN: 0027-8424, 1091-6490. DOI: 10.1073/pnas.1603138113.

[22] P. J. Ziemann and R. Atkinson, "Kinetics, products, and mechanisms of secondary organic aerosol formation," *Chemical Society Reviews*, vol. 41, no. 19, pp. 6582–6605, 2012.

[23] Y. Kuang, W. Xu, J. Tao, N. Ma, C. Zhao, and M. Shao, "A Review on Laboratory Studies and Field Measurements of Atmospheric Organic Aerosol Hygroscopicity and Its Parameterization Based on Oxidation Levels," en, *Current Pollution Reports*, vol. 6, no. 4, pp. 410–424, Dec. 2020, ISSN: 2198-6592. DOI: 10.1007/s40726-020-00164-2.

[24] C. Zhao, X. Tie, and Y. Lin, "A possible positive feedback of reduction of precipitation and increase in aerosols over eastern central china," *Geophysical Research Letters*, vol. 33, no. 11, 2006.

[25] M Song, P. Liu, S. Hanna, Y. Li, S. Martin, and A. Bertram, "Relative humidity-dependent viscosities of isoprene-derived secondary organic material and atmospheric implications for isoprene-dominant forests," *Atmospheric Chemistry and Physics*, vol. 15, no. 9, pp. 5145–5159, 2015.

[26] A. P. Bateman, A. K. Bertram, and S. T. Martin, "Hygroscopic influence on the semisolid-to-liquid transition of secondary organic materials," *The Journal of Physical Chemistry A*, vol. 119, no. 19, pp. 4386–4395, 2015.

[27] T. Koop, J. Bookhold, M. Shiraiwa, and U. Poschl, "Glass transition and phase state of organic compounds: Dependency on molecular properties and implications for secondary organic aerosols in the atmosphere," *Physical Chemistry Chemical Physics*, vol. 13, no. 43, pp. 19 238–19 255, 2011.

[28] J. H. Slade and D. A. Knopf, "Multiphase oh oxidation kinetics of organic aerosol: The role of particle phase state and relative humidity," *Geophysical Research Letters*, vol. 41, no. 14, pp. 5297–5306, 2014.

[29] S. Han *et al.*, "Hygroscopicity of organic compounds as a function of organic functionality, water solubility, molecular weight, and oxidation level," en, *Atmospheric Chemistry and Physics*, vol. 22, no. 6, pp. 3985–4004, Mar. 2022, ISSN: 1680-7324. DOI: 10.5194/acp-22-3985-2022. [Online]. Available: https://acp.copernicus.org/articles/22/3985/2022/.

[30] M. D. Petters and S. M. Kreidenweis, "A single parameter representation of hygroscopic growth and cloud condensation nucleus activity," en, *Atmospheric Chemistry and Physics*, vol. 7, no. 8, pp. 1961–1971, Apr. 2007, ISSN: 1680-7324. DOI: 10.5194/acp-7-1961-2007.

[31] N. M. Donahue, S. A. Epstein, S. N. Pandis, and A. L. Robinson, "A two-dimensional volatility basis set: 1. organic-aerosol mixing thermodynamics," en, *Atmospheric Chemistry and Physics*, vol. 11, no. 7, pp. 3303–3318, Apr. 2011, ISSN: 1680-7324. DOI: 10.5194/acp-11-3303-2011. [Online]. Available: https://acp.copernicus.org/articles/11/3303/2011/.

[32] Q. Zhang *et al.*, "Ubiquity and dominance of oxygenated species in organic aerosols in anthropogenically influenced Northern Hemisphere midlatitudes," en, *Geophysical Research Letters*, vol. 34, no. 13, 2007GL029979, Jul. 2007, ISSN: 0094-8276, 1944-8007. DOI: 10.1029/2007GL029979.

[33] A. Clarke *et al.*, "Indoex aerosol: A comparison and summary of chemical, microphysical, and optical properties observed from land, ship, and aircraft," *Journal of Geophysical Research: Atmospheres*, vol. 107, no. D19, INX2–32, 2002.

[34] T. M. VanReken *et al.*, "Toward aerosol/cloud condensation nuclei (ccn) closure during crystal-face," *Journal of Geophysical Research: Atmospheres*, vol. 108, no. D20, 2003.

[35] C. Ronneau, "Atmospheric Chemistry: Fundamentals and Experimental Techniques," en, *Eos, Transactions American Geophysical Union*, vol. 68, no. 49, pp. 1643–1643, Dec. 1987, ISSN: 0096-3941, 2324-9250. DOI: 10.1029/EO068i049p01643-01.

[36] G. Isaacman-VanWertz *et al.*, "Chemical evolution of atmospheric organic carbon over multiple generations of oxidation," en, *Nature Chemistry*, vol. 10, no. 4, pp. 462–468, Apr. 2018, ISSN: 1755-4330, 1755-4349. DOI: 10.1038/s41557-018-0002-2.

[37] H. Akimoto, *Atmospheric Reaction Chemistry* (Springer Atmospheric Sciences). Tokyo: Springer Japan, 2016, ISBN: 978-4-431-55868-2 978-4-431-55870-5. DOI: 10.1007/978-4-431-55870-5.

[38] V. P. Barber, W. H. Green, and J. H. Kroll, "Screening for New Pathways in Atmospheric Oxidation Chemistry with Automated Mechanism Generation," en, *The Journal of Physical Chemistry A*, vol. 125, no. 31, pp. 6772–6788, Aug. 2021, ISSN: 1089-5639, 1520-5215. DOI: 10.1021/acs.jpca.1c04297.

[39] V. F. McNeill, "Aqueous Organic Chemistry in the Atmosphere: Sources and Chemical Processing of Organic Aerosols," en, *Environmental Science & Technology*, vol. 49, no. 3, pp. 1237–1244, Feb. 2015, ISSN: 0013-936X, 1520-5851. DOI: 10.1021/es5043707.

[40] A. Mellouki, G. Le Bras, and H. Sidebottom, "Kinetics and Mechanisms of the Oxidation of Oxygenated Organic Compounds in the Gas Phase," en, *Chemical Reviews*, vol. 103, no. 12, pp. 5077–5096, Dec. 2003, ISSN: 0009-2665, 1520-6890. DOI: 10.1021/cr020526x.

[41] R Atkinson, "Atmospheric chemistry of VOCs and NO_x," *Atmospheric Environment*, vol. 34, no. 12-14, pp. 2063–2101, 2000, ISSN: 13522310. DOI: 10.1016/S1352-2310(99)00460-4.

[42] J. L. Jimenez *et al.*, "Evolution of Organic Aerosols in the Atmosphere," en, *Science*, vol. 326, no. 5959, pp. 1525–1529, Dec. 2009, ISSN: 0036-8075, 1095-9203. DOI: 10.1126/science.1180353.

[43] T. B. Nguyen *et al.*, "Rapid deposition of oxidized biogenic compounds to a temperate forest," en, *Proceedings of the National Academy of Sciences*, vol. 112, no. 5, Feb. 2015, ISSN: 0027-8424, 1091-6490. DOI: 10.1073/pnas.1418702112. [Online]. Available: https://pnas.org/doi/full/10.1073/pnas.1418702112 (visited on 01/29/2024).

[44] M. Hallquist *et al.*, "The formation, properties and impact of secondary organic aerosol: Current and emerging issues," en, *Atmospheric Chemistry and Physics*, vol. 9, no. 14, pp. 5155–5236, Jul. 2009, ISSN: 1680-7324. DOI: 10.5194/acp-9-5155-2009. (visited on 01/29/2024).

[45] P. J. Ziemann and R. Atkinson, "Kinetics, products, and mechanisms of secondary organic aerosol formation," en, *Chemical Society Reviews*, vol. 41, no. 19, p. 6582, 2012, ISSN: 0306-0012, 1460-4744. DOI: 10.1039/c2cs35122f.

[46] S. Hatakeyama, M. Ohno, J. Weng, H. Takagi, and H. Akimoto, "Mechanism for the formation of gaseous and particulate products from ozone-cycloalkene reactions in air," en, *Environmental Science & Technology*, vol. 21, no. 1, pp. 52–57, Jan. 1987, ISSN: 0013-936X, 1520-5851. DOI: 10.1021/es00155a005.

[47] I. J. George and J. P. D. Abbatt, "Heterogeneous oxidation of atmospheric aerosol particles by gas-phase radicals," en, *Nature Chemistry*, vol. 2, no. 9, pp. 713–722, Sep. 2010, ISSN: 1755-4330, 1755-4349. DOI: 10.1038/nchem.806.

[48] F. Li, S. Zhou, L. Du, J. Zhao, J. Hang, and X. Wang, "Aqueous-phase chemistry of atmospheric phenolic compounds: A critical review of laboratory studies," *Science of The Total Environment*, vol. 856, p. 158 895, 2023.

[49] A. D. Estillore *et al.*, "Water Uptake and Hygroscopic Growth of Organosulfate Aerosol," en, *Environmental Science & Technology*, vol. 50, no. 8, pp. 4259–4268, Apr. 2016, ISSN: 0013-936X, 1520-5851. DOI: 10.1021/acs.est.5b05014.

[50] S. R. Suda *et al.*, "Influence of Functional Groups on Organic Aerosol Cloud Condensation Nucleus Activity," en, *Environmental Science & Technology*, vol. 48, no. 17, pp. 10 182–10 190, Sep. 2014, ISSN: 0013-936X, 1520-5851. DOI: 10.1021/es502147y.

[51] J. H. Kroll and J. H. Seinfeld, "Chemistry of secondary organic aerosol: Formation and evolution of low-volatility organics in the atmosphere," en, *Atmospheric Environment*, vol. 42, no. 16, pp. 3593–3624, May 2008, ISSN: 13522310. DOI: 10.1016/j.atmosenv.2008.01.003. (visited on 01/29/2024).

[52] J. F. Pankow and W. E. Asher, "SIMPOL.1: A simple group contribution method for predicting vapor pressures and enthalpies of vaporization of multifunctional organic compounds," en, *Atmospheric Chemistry and Physics*, vol. 8, no. 10, pp. 2773–2796, May 2008, ISSN: 1680-7324. DOI: 10.5194/acp-8-2773-2008.

[53] W. M. Champion, N. E. Rothfuss, M. D. Petters, and A. P. Grieshop, "Volatility and Viscosity Are Correlated in Terpene Secondary Organic Aerosol Formed in a Flow Reactor," en, *Environmental Science & Technology Letters*, vol. 6, no. 9, pp. 513–519, Sep. 2019, ISSN: 2328-8930, 2328-8930. DOI: 10.1021/acs.estlett.9b00412.

[54] Y. Li, U. Poschl, and M. Shiraiwa, "Molecular corridors and parameterizations of volatility in the chemical evolution of organic aerosols," en, *Atmospheric Chemistry and Physics*, vol. 16, no. 5, pp. 3327–3344, Mar. 2016, ISSN: 1680-7324. DOI: 10.5194/acp-16-3327-2016.

[55] M. Ehn, T. Berndt, J. Wildt, and T. Mentel, "Highly Oxygenated Molecules from Atmospheric Autoxidation of Hydrocarbons: A Prominent Challenge for Chemical Kinetics Studies: HIGHLY OXYGENATED MOLECULES FROM ATMOSPHERIC AUTOXIDATION OF HYDROCARBONS," en, *International Journal of Chemical Kinetics*, vol. 49, no. 11, pp. 821–831, Nov. 2017, ISSN: 05388066. DOI: 10.1002/kin.21130.

[56] J. D. Surratt *et al.*, "Organosulfate Formation in Biogenic Secondary Organic Aerosol," en, *The Journal of Physical Chemistry A*, vol. 112, no. 36, pp. 8345–8378, Sep. 2008, ISSN: 1089-5639, 1520-5215. DOI: 10.1021/jp802310p.

[57] K. C. Barsanti, J. H. Kroll, and J. A. Thornton, "Formation of Low-Volatility Organic Compounds in the Atmosphere: Recent Advancements and Insights," en, *The Journal of Physical Chemistry Letters*, vol. 8, no. 7, pp. 1503–1511, Apr. 2017, ISSN: 1948-7185, 1948-7185. DOI: 10.1021/acs.jpclett.6b02969.

[58] N. L. Ng *et al.*, "Contribution of First- versus Second-Generation Products to Secondary Organic Aerosols Formed in the Oxidation of Biogenic Hydrocarbons," en, *Environmental Science & Technology*, vol. 40, no. 7, pp. 2283–2297, Apr. 2006, ISSN: 0013-936X, 1520-5851. DOI: 10.1021/es052269u.

[59] M. Ehn *et al.*, "A large source of low-volatility secondary organic aerosol," en, *Nature*, vol. 506, no. 7489, pp. 476–479, Feb. 2014, ISSN: 0028-0836, 1476-4687. DOI: 10.1038/nature13032.

[60] N. L. Ng *et al.*, "Nitrate radicals and biogenic volatile organic compounds: Oxidation, mechanisms, and organic aerosol," en, *Atmospheric Chemistry and Physics*, vol. 17, no. 3, pp. 2103–2162, Feb. 2017, ISSN: 1680-7324. DOI: 10.5194/acp-17-2103-2017. [Online]. Available: https://acp.copernicus.org/articles/17/2103/2017/.

[61] K. E. Altieri, B. J. Turpin, and S. P. Seitzinger, "Oligomers, organosulfates, and nitrooxy organosulfates in rainwater identified by ultra-high resolution electrospray ionization FT-ICR mass spectrometry," en, *Atmospheric Chemistry and Physics*, vol. 9, no. 7, pp. 2533–2542, Apr. 2009, ISSN: 1680-7324. DOI: 10.5194/acp-9-2533-2009. [Online]. Available: https://acp.copernicus.org/articles/9/2533/2009/.

[62] M. Riva *et al.*, "Multiphase reactivity of gaseous hydroperoxide oligomers produced from isoprene ozonolysis in the presence of acidified aerosols," en, *Atmospheric Environment*, vol. 152, pp. 314–322, Mar. 2017, ISSN: 13522310. DOI: 10.1016/j.atmosenv.2016.12.040.

[63] J. Schindelka, Y. Iinuma, D. Hoffmann, and H. Herrmann, "Sulfate radical-initiated formation of isoprene-derived organosulfates in atmospheric aerosols," en, *Faraday Discussions*, vol. 165, p. 237, 2013, ISSN: 1359-6640, 1364-5498. DOI: 10.1039/c3fd00042g.

[64] J. F. Hamilton *et al.*, "Key Role of NO_3 Radicals in the Production of Isoprene Nitrates and Nitrooxyorganosulfates in Beijing," en, *Environmental Science & Technology*, vol. 55, no. 2, pp. 842–853, Jan. 2021, ISSN: 0013-936X, 1520-5851. DOI: 10.1021/acs.est.0c05689.

[65] C. Ye, K. Lu, H. Song, Y. Mu, J. Chen, and Y. Zhang, "A critical review of sulfate aerosol formation mechanisms during winter polluted periods," en, *Journal of Environmental Sciences*, vol. 123, pp. 387–399, Jan. 2023, ISSN: 10010742. DOI: 10.1016/j.jes.2022.07.011.

[66] S. Wang, Y. Zhao, A. W. H. Chan, M. Yao, Z. Chen, and J. P. D. Abbatt, "Organic Peroxides in Aerosol: Key Reactive Intermediates for Multiphase Processes in the Atmosphere," en, *Chemical Reviews*, vol. 123, no. 4, pp. 1635–1679, Feb. 2023, ISSN: 0009-2665, 1520-6890. DOI: 10.1021/acs.chemrev.2c00430.

[67] Y. Wang *et al.*, "Abundance of organosulfates derived from biogenic volatile organic compounds: Seasonal and spatial contrasts at four sites in China," en, *Science of The Total Environment*, vol. 806, p. 151 275, Feb. 2022, ISSN: 00489697. DOI: 10.1016/j.scitotenv.2021.151275.

[68] N Bukowiecki, J Dommen, A. Prevot, R Richter, E Weingartner, and U Baltensperger, "A mobile pollutant measurement laboratory measuring gas phase and aerosol ambient concentrations with high spatial and temporal resolution," *Atmospheric Environment*, vol. 36, no. 36-37, pp. 5569–5579, 2002.

[69] A. Zare, P. S. Romer, T. Nguyen, F. N. Keutsch, K. Skog, and R. C. Cohen, "A comprehensive organic nitrate chemistry: Insights into the lifetime of atmospheric organic nitrates," en, *Atmospheric Chemistry and Physics*, vol. 18, no. 20, pp. 15 419–15 436, Oct. 2018, ISSN: 1680-7324. DOI: 10.5194/acp-18-15419-2018. [Online]. Available: https://acp.copernicus.org/articles/18/15419/2018/.

[70] P. Lightfoot *et al.*, "Organic peroxy radicals: Kinetics, spectroscopy and tropospheric chemistry," en, *Atmospheric Environment. Part A. General Topics*, vol. 26, no. 10, pp. 1805–1961, Jul. 1992, ISSN: 09601686. DOI: 10.1016/0960-1686(92)90423-I.

[71] M. Krapf *et al.*, "Labile Peroxides in Secondary Organic Aerosol," en, *Chem*, vol. 1, no. 4, pp. 603–616, Oct. 2016, ISSN: 24519294. DOI: 10.1016/j.chempr.2016.09.007.

[72] S. A. Epstein, S. L. Blair, and S. A. Nizkorodov, "Direct Photolysis of α-Pinene Ozonolysis Secondary Organic Aerosol: Effect on Particle Mass and Peroxide Content," en, *Environmental Science & Technology*, vol. 48, no. 19, pp. 11 251–11 258, Oct. 2014, ISSN: 0013-936X, 1520-5851. DOI: 10.1021/es502350u.

[73] S. Wang *et al.*, "Organic Peroxides and Sulfur Dioxide in Aerosol: Source of Particulate Sulfate," en, *Environmental Science & Technology*, vol. 53, no. 18, pp. 10 695–10 704, Sep. 2019, ISSN: 0013-936X, 1520-5851. DOI: 10.1021/acs.est.9b02591.

[74] L. Du, X. Lv, M. Lily, K. Li, and N. Tsona Tchinda, "pH regulates the formation of organosulfates and inorganic sulfate from organic peroxide reaction with dissolved SO_2 in aquatic media," en, *Atmospheric Chemistry and Physics*, vol. 24, no. 3, pp. 1841–1853, Feb. 2024, ISSN: 1680-7324. DOI: 10.5194/acp-24-1841-2024.

[75] A. Foulds, M. A. H. Khan, T. J. Bannan, C. J. Percival, M. H. Lowenberg, and D. E. Shallcross, "Abundance of NO_3 Derived Organo-Nitrates and Their Importance in the Atmosphere," en, *Atmosphere*, vol. 12, no. 11, p. 1381, Oct. 2021, ISSN: 2073-4433. DOI: 10.3390/atmos12111381. [Online]. Available: https://www.mdpi.com/2073-4433/12/11/1381.

[76] C. Peng *et al.*, "Interactions of organosulfates with water vapor under sub- and supersaturated conditions," en, *Atmospheric Chemistry and Physics*, vol. 21, no. 9, pp. 7135–7148, May 2021, ISSN: 1680-7324. DOI: 10.5194/acp-21-7135-2021.

[77] H. Zhang *et al.*, "Organosulfates as Tracers for Secondary Organic Aerosol (SOA) Formation from 2-Methyl-3-Buten-2-ol (MBO) in the Atmosphere," en, *Environmental Science & Technology*, vol. 46, no. 17, pp. 9437–9446, Sep. 2012, ISSN: 0013-936X, 1520-5851. DOI: 10.1021/es301648z. [Online]. Available: https://pubs.acs.org/doi/10.1021/es301648z.

[78] A. M. K. Hansen *et al.*, "Hygroscopic properties and cloud condensation nuclei activation of limonene-derived organosulfates and their mixtures with ammonium sulfate," en, *Atmospheric Chemistry and Physics*, vol. 15, no. 24, pp. 14 071–14 089, Dec. 2015, ISSN: 1680-7324. DOI: 10.5194/acp-15-14071-2015.

[79] V. F. McNeill *et al.*, "Aqueous-Phase Secondary Organic Aerosol and Organosulfate Formation in Atmospheric Aerosols: A Modeling Study," en, *Environmental Science & Technology*, vol. 46, no. 15, pp. 8075–8081, Aug. 2012, ISSN: 0013-936X, 1520-5851. DOI: 10.1021/es3002986.

[80] D. H. Ehhalt, "Free Radicals in the Atmosphere," en, *Free Radical Research Communications*, vol. 3, no. 1-5, pp. 153–164, Jan. 1987, ISSN: 8755-0199. DOI: 10.3109/10715768709069780.

[81] D. Stone, L. K. Whalley, and D. E. Heard, "Tropospheric OH and HO_2 radicals: Field measurements and model comparisons," en, *Chemical Society Reviews*, vol. 41, no. 19, p. 6348, 2012, ISSN: 0306-0012, 1460-4744. DOI: 10.1039/c2cs35140d.

[82] J. J. Orlando and G. S. Tyndall, "Laboratory studies of organic peroxy radical chemistry: An overview with emphasis on recent issues of atmospheric significance," en, *Chemical Society Reviews*, vol. 41, no. 19, p. 6294, 2012, ISSN: 0306-0012, 1460-4744. DOI: 10.1039/c2cs35166h. (visited on 01/29/2024).

[83] S. Vaughan, C. E. Canosa-Mas, C. Pfrang, D. E. Shallcross, L. Watson, and R. P. Wayne, "Kinetic studies of reactions of the nitrate radical (NO_3) with peroxy radicals (RO_2): An indirect source of OH at night?" en, *Physical Chemistry Chemical Physics*, vol. 8, no. 32, p. 3749, 2006, ISSN: 1463-9076, 1463-9084. DOI: 10.1039/b605569a.

[84] D Jacob, "Heterogeneous chemistry and tropospheric ozone," *Atmospheric Environment*, vol. 34, no. 12-14, pp. 2131–2159, 2000, ISSN: 13522310.

[85] J. Abbatt and A. Ravishankara, "Opinion: Atmospheric Multiphase Chemistry: Past, Present, and Future," Aerosols/Laboratory Studies/Troposphere/-Chemistry (chemical composition and reactions), preprint, Mar. 2023. DOI: 10.5194/egusphere-2023-334. [Online]. Available: https://egusphere.copernicus.org/preprints/2023/egusphere-2023-334/.

[86] P. S. Monks, "Gas-phase radical chemistry in the troposphere," en, *Chemical Society Reviews*, vol. 34, no. 5, p. 376, 2005, ISSN: 0306-0012, 1460-4744. DOI: 10.1039/b307982c.

[87] K. H. Becker and D. Haaks, "Measurement of the Natural Lifetimes and Quenching Rate Constants of OH and OD Radicals," en, *Zeitschrift fur Naturforschung A*, vol. 28, no. 2, pp. 249–256, Feb. 1973, ISSN: 1865-7109, 0932-0784. DOI: 10.1515/zna-1973-0216.

[88] S. Gligorovski, R. Strekowski, S. Barbati, and D. Vione, "Environmental implications of hydroxyl radicals (oh)," *Chemical reviews*, vol. 115, no. 24, pp. 13 051–13 092, 2015.

[89] G. S. Tyndall *et al.*, "Atmospheric chemistry of small organic peroxy radicals," en, *Journal of Geophysical Research: Atmospheres*, vol. 106, no. D11, pp. 12 157–12 182, Jun. 2001, ISSN: 0148-0227. DOI: 10.1029/2000JD900746. [Online]. Available: https://agupubs.onlinelibrary.wiley.com/doi/10.1029/2000JD900746.

[90] D Shallcross, M Teresaraventosduran, M Bardwell, A Bacak, Z Solman, and C Percival, "A semi-empirical correlation for the rate coefficients for cross- and self-reactions of peroxy radicals in the gas-phase," en, *Atmospheric Environment*, vol. 39, no. 4, pp. 763–771, Feb. 2005, ISSN: 13522310. DOI: 10.1016/j.atmosenv.2004.09.072.

[91] G. Hasan, V. Salo, R. R. Valiev, J. Kubecka, and T. Kurten, "Comparing Reaction Routes for roor Intermediates Formed in Peroxy Radical Self- and Cross-Reactions," en, *The Journal of Physical Chemistry A*, vol. 124, no. 40, pp. 8305–8320, Oct. 2020, ISSN: 1089-5639, 1520-5215. DOI: 10.1021/acs.jpca.0c05960.

[92] T. Berndt *et al.*, "Accretion Product Formation from Self and CrossReactions of RO_2Radicals in the Atmosphere," en, *Angewandte Chemie International Edition*, vol. 57, no. 14, pp. 3820–3824, Mar. 2018, ISSN: 1433-7851, 1521-3773. DOI: 10.1002/anie.201710989.

[93] A. Marinoni *et al.*, "Hydrogen peroxide in natural cloud water: Sources and photoreactivity," en, *Atmospheric Research*, vol. 101, no. 1-2, pp. 256–263, Jul. 2011, ISSN: 01698095. DOI: 10.1016/j.atmosres.2011.02.013.

[94] T. K. V. Nguyen, Q. Zhang, J. L. Jimenez, M. Pike, and A. G. Carlton, "Liquid Water Ubiquitous Contributor to Aerosol Mass," en, *Environmental Science & Technology Letters*, vol. 3, no. 7, pp. 257–263, Jul. 2016, ISSN: 2328-8930, 2328-8930. DOI: 10.1021/acs.estlett.6b00167.

[95] Y. B. Lim, Y. Tan, M. J. Perri, S. P. Seitzinger, and B. J. Turpin, "Aqueous chemistry and its role in secondary organic aerosol (SOA) formation," en, *Atmospheric Chemistry and Physics*, vol. 10, no. 21, pp. 10 521–10 539, Nov. 2010, ISSN: 1680-7324. DOI: 10.5194/acp-10-10521-2010.

[96] D. Vione *et al.*, "Photochemical reactions in the tropospheric aqueous phase and on particulate matter," en, *Chemical Society Reviews*, 10.1039.b510796m, 2006, ISSN: 0306-0012, 1460-4744. DOI: 10.1039/b510796m.

[97] F. Bernard, R. Ciuraru, A. Boreave, and C. George, "Photosensitized Formation of Secondary Organic Aerosols above the Air/Water Interface," en, *Environmental Science & Technology*, vol. 50, no. 16, pp. 8678–8686, Aug. 2016, ISSN: 0013-936X, 1520-5851. DOI: 10.1021/acs.est.6b03520.

[98] I. Riipinen *et al.*, "The contribution of organics to atmospheric nanoparticle growth," en, *Nature Geoscience*, vol. 5, no. 7, pp. 453–458, Jul. 2012, ISSN: 1752-0894, 1752-0908. DOI: 10.1038/ngeo1499. [Online]. Available: https://www.nature.com/articles/ngeo1499.

[99] H. Herrmann, D. Hoffmann, T. Schaefer, P. Brauer, and A. Tilgner, "Tropospheric Aqueous Phase Free Radical Chemistry Radical Sources, Spectra, Reaction Kinetics and Prediction Tools," en, *ChemPhysChem*, vol. 11, no. 18, pp. 3796–3822, Dec. 2010, ISSN: 1439-4235, 1439-7641. DOI: 10.1002/cphc.201000533.

[100] L. Wen *et al.*, "T and pH Dependent Kinetics of the Reactions of oh with Glutaric and Adipic Acid for Atmospheric AqueousPhase Chemistry," en, *ACS Earth and Space Chemistry*, vol. 5, no. 8, pp. 1854–1864, Aug. 2021, ISSN: 2472-3452, 2472-3452. DOI: 10.1021/acsearthspacechem.1c00163.

[101] A. Bianco, M. Passananti, M. Brigante, and G. Mailhot, "Photochemistry of the Cloud Aqueous Phase: A Review," en, *Molecules*, vol. 25, no. 2, p. 423, Jan. 2020, ISSN: 1420-3049. DOI: 10.3390/molecules25020423.

[102] J. Kurz and K. Ballschmiter, "Vapour pressures, aqueous solubilities, Henry's law constants, partition coefficients between gas/water (Kgw), N-octanol/water (Kow) and gas/N-octanol (Kgo) of 106 polychlorinated diphenyl ethers (PCDE)," en, *Chemosphere*, vol. 38, no. 3, pp. 573–586, Feb. 1999, ISSN: 00456535. DOI: 10.1016/S0045-6535(98)00212-4.

[103] J. L. Cheung *et al.*, "Heterogeneous Interactions of NO_2 with Aqueous Surfaces," en, *The Journal of Physical Chemistry A*, vol. 104, no. 12, pp. 2655–2662, Mar. 2000, ISSN: 1089-5639, 1520-5215. DOI: 10.1021/jp992929f.

[104] T. Liu and J. P. Abbatt, "Oxidation of sulfur dioxide by nitrogen dioxide accelerated at the interface of deliquesced aerosol particles," *Nature Chemistry*, vol. 13, no. 12, pp. 1173–1177, 2021.

[105] B. C. Faust and J. M. Allen, "Aqueous-phase photochemical sources of peroxyl radicals and singlet molecular oxygen in clouds and fog," *Journal of Geophysical Research: Atmospheres*, vol. 97, no. D12, pp. 12 913–12 926, 1992, Publisher: Wiley Online Library.

[106] M. Hayyan, M. A. Hashim, and I. M. AlNashef, "Superoxide Ion: Generation and Chemical Implications," en, *Chemical Reviews*, vol. 116, no. 5, pp. 3029–3085, Mar. 2016, ISSN: 0009-2665, 1520-6890. DOI: 10.1021/acs.chemrev.5b00407.

[107] H. Herrmann, D. Hoffmann, T. Schaefer, P. Brauer, and A. Tilgner, "Tropospheric aqueous-phase free radical chemistry: Radical sources, spectra, reaction kinetics and prediction tools," *ChemPhysChem*, vol. 11, no. 18, pp. 3796–3822, 2010.

[108] L. Ma, C. Guzman, C. Niedek, T. Tran, Q. Zhang, and C. Anastasio, "Kinetics and Mass Yields of Aqueous Secondary Organic Aerosol from Highly Substituted Phenols Reacting with a Triplet Excited State," en, *Environmental Science & Technology*, vol. 55, no. 9, pp. 5772–5781, May 2021, ISSN: 0013-936X, 1520-5851. DOI: 10.1021/acs.est.1c00575.

[109] R. Kaur and C. Anastasio, "First Measurements of Organic Triplet Excited States in Atmospheric Waters," en, *Environmental Science & Technology*, vol. 52, no. 9, pp. 5218–5226, May 2018, ISSN: 0013-936X, 1520-5851. DOI: 10.1021/acs.est.7b06699.

[110] R. L. Siefert, A. M. Johansen, M. R. Hoffmann, and S. O. Pehkonen, "Measurements of trace metal (fe, cu, mn, cr) oxidation states in fog and stratus clouds," *Journal of the Air & Waste Management Association*, vol. 48, no. 2, pp. 128–143, 1998.

[111] G. Khaikin, Z. Alfassi, R. Huie, and P Neta, "Oxidation of ferrous and ferrocyanide ions by peroxyl radicals," *The Journal of Physical Chemistry*, vol. 100, no. 17, pp. 7072–7077, 1996.

[112] L. Deguillaume, M. Leriche, A. Monod, and N. Chaumerliac, "The role of transition metal ions on HO_x radicals in clouds a numerical evaluation of its impact on multiphase chemistry," en, *Atmospheric Chemistry and Physics*, vol. 4, no. 1, pp. 95–110, Jan. 2004, ISSN: 1680-7324. DOI: 10.5194/acp-4-95-2004.

[113] A. Ansari, J. Peral, X. Domenech, R. Clemente, and J. Casado, "Oxidation of S(IV) to S(VI) under Fenton, photo Fenton and γ FeOOH photocatalized conditions," en, *Journal of Molecular Catalysis A: Chemical*, vol. 112, no. 2, pp. 269–276, Oct. 1996, ISSN: 13811169. DOI: 10.1016/1381-1169(96)00043-X. (visited on 03/03/2024).

[114] L. Huang, R. E. Cochran, E. M. Coddens, and V. H. Grassian, "Formation of Organosulfur Compounds through Transition Metal Ion-Catalyzed Aqueous Phase Reactions," en, *Environmental Science & Technology Letters*, vol. 5, no. 6, pp. 315–321, Jun. 2018, ISSN: 2328-8930, 2328-8930. DOI: 10.1021/acs.estlett.8b00225. (visited on 03/03/2024).

[115] M. Bruggemann *et al.*, "Organosulfates in Ambient Aerosol State of Knowledge and Future Research Directions on Formation, Abundance, Fate, and Importance," en, *Environmental Science & Technology*, vol. 54, no. 7, pp. 3767–3782, Apr. 2020, ISSN: 0013-936X, 1520-5851. DOI: 10.1021/acs.est.9b06751.

[116] M. Gen, R. Zhang, D. D. Huang, Y. Li, and C. K. Chan, "Heterogeneous Oxidation of SO_2 in Sulfate Production during Nitrate Photolysis at 300 nm: Effect of pH, Relative Humidity, Irradiation Intensity, and the Presence of Organic Compounds," en, *Environmental Science & Technology*, vol. 53, no. 15, pp. 8757–8766, Aug. 2019, ISSN: 0013-936X, 1520-5851. DOI: 10.1021/acs.est.9b01623. [Online]. Available: https://pubs.acs.org/doi/10.1021/acs.est.9b01623 (visited on 03/03/2024).

[117] C. Von Sonntag and H. Schuchmann, "The Elucidation of Peroxyl Radical Reactions in Aqueous Solution with the Help of Radiation Chemical Methods," en, *Angewandte Chemie International Edition in English*, vol. 30, no. 10, pp. 1229–1253, Oct. 1991, ISSN: 0570-0833. DOI: 10.1002/anie.199112291.

[118] V. Pratap *et al.*, "Investigating the evolution of water-soluble organic carbon in evaporating cloud water," en, *Environmental Science: Atmospheres*, vol. 1, no. 1, pp. 21–30, 2021, ISSN: 2634-3606. DOI: 10.1039/D0EA00005A.

[119] D. J. Donaldson and K. T. Valsaraj, "Adsorption and Reaction of Trace Gas-Phase Organic Compounds on Atmospheric Water Film Surfaces: A Critical Review," en, *Environmental Science & Technology*, vol. 44, no. 3, pp. 865–873, Feb. 2010, ISSN: 0013-936X, 1520-5851. DOI: 10.1021/es902720s.

[120] J. He *et al.*, "Probing autoxidation of oleic acid at air-water interface: A neglected and significant pathway for secondary organic aerosols formation," en, *Environmental Research*, vol. 212, p. 113 232, Sep. 2022, ISSN: 00139351. DOI: 10.1016/j.envres.2022.113232. [Online]. Available: https://linkinghub.elsevier.com/retrieve/pii/S001393512200559X (visited on 01/29/2024).

[121] N. Zhang *et al.*, "Analytical methods for determining the peroxide value of edible oils: A mini-review," *Food Chemistry*, vol. 358, p. 129 834, 2021, Publisher: Elsevier.

[122] K. Li *et al.*, "Spontaneous dark formation of OH radicals at the interface of aqueous atmospheric droplets," en, *Proceedings of the National Academy of Sciences*, vol. 120, no. 15, e2220228120, Apr. 2023, ISSN: 0027-8424, 1091-6490. DOI: 10.1073/pnas.2220228120.

[123] G. H. Wang *et al.*, "Observation of atmospheric aerosols at Mt Hua and Mt Tai in central and east China during spring 2009 Part 2 Impact of dust storm on organic aerosol composition and size distribution," en, *Atmospheric Chemistry and Physics*, vol. 12, no. 9, pp. 4065–4080, May 2012, ISSN: 1680-7324. DOI: 10.5194/acp-12-4065-2012.

[124] A. Tilgner, P. Brauer, R. Wolke, and H. Herrmann, "Modelling multiphase chemistry in deliquescent aerosols and clouds using CAPRAM3 0i," en, *Journal of Atmospheric Chemistry*, vol. 70, no. 3, pp. 221–256, Sep. 2013, ISSN: 0167-7764, 1573-0662. DOI: 10.1007/s10874-013-9267-4.

[125] S. Enami, M. R. Hoffmann, and A. J. Colussi, "Stepwise Oxidation of Aqueous Dicarboxylic Acids by Gas Phase OH Radicals," en, *The Journal of Physical Chemistry Letters*, vol. 6, no. 3, pp. 527–534, Feb. 2015, ISSN: 1948-7185, 1948-7185. DOI: 10.1021/jz502432j.

[126] N. Hayeck, I. Mussa, S. Perrier, and C. George, "Production of Peroxy Radicals from the Photochemical Reaction of Fatty Acids at the Air Water Interface," en, *ACS Earth and Space Chemistry*, vol. 4, no. 8, pp. 1247–1253, Aug. 2020, ISSN: 2472-3452, 2472-3452. DOI: 10.1021/acsearthspacechem.0c00048.

[127] S. Enami and Y. Sakamoto, "OH Radical Oxidation of Surface Active *cis* Pinonic Acid at the Air Water Interface," en, *The Journal of Physical Chemistry A*, vol. 120, no. 20, pp. 3578–3587, May 2016, ISSN: 1089-5639, 1520-5215. DOI: 10.1021/acs.jpca.6b01261. [Online]. Available: https://pubs.acs.org/doi/10.1021/acs.jpca.6b01261 (visited on 01/29/2024).

[128] J. M. Anglada, M. T. C. Martins Costa, J. S. Francisco, and M. F. Ruiz-Lopez, "Photoinduced Oxidation Reactions at the Air Water Interface," en, *Journal of the American Chemical Society*, vol. 142, no. 38, pp. 16 140–16 155, Sep. 2020, ISSN: 0002-7863, 1520-5126. DOI: 10.1021/jacs.0c06858.

[129] J. G. Calvert *et al.*, "Chemical mechanisms of acid generation in the troposphere," en, *Nature*, vol. 317, no. 6032, pp. 27–35, Sep. 1985, ISSN: 0028-0836, 1476-4687. DOI: 10.1038/317027a0. [Online]. Available: https://www.nature.com/articles/317027a0 (visited on 01/29/2024).

[130] D. W. Gunz and M. R. Hoffmann, "Atmospheric chemistry of peroxides: A review," en, *Atmospheric Environment. Part A. General Topics*, vol. 24, no. 7, pp. 1601–1633, Jan. 1990, ISSN: 09601686. DOI: 10.1016/0960-1686(90)90496-A. [Online]. Available: https://linkinghub.elsevier.com/retrieve/pii/096016869090496A (visited on 01/29/2024).

[131] S. Mertes *et al.*, "Evolution of particle concentration and size distribution observed upwind, inside and downwind hill cap clouds at connected flow conditions during FEBUKO," en, *Atmospheric Environment*, vol. 39, no. 23-24, pp. 4233–4245, Jul. 2005, ISSN: 13522310. DOI: 10.1016/j.atmosenv.2005.02.009. (visited on 01/29/2024).

[132] G. P. Gervat *et al.*, "Field evidence for the oxidation of SO_2 by H_2O_2 in cap clouds," en, *Nature*, vol. 333, no. 6170, pp. 241–243, May 1988, ISSN: 0028-0836, 1476-4687. DOI: 10.1038/333241a0. [Online]. Available: https://www.nature.com/articles/333241a0 (visited on 01/29/2024).

[133] E. Harris *et al.*, "Enhanced Role of Transition Metal Ion Catalysis During In-Cloud Oxidation of SO_2, volume = 340," en, *Science*, no. 6133, pp. 727–730, May 2013, ISSN: 0036-8075, 1095-9203. DOI: 10.1126/science.1230911. (visited on 01/29/2024).

[134] D. A. Hegg, R. Majeed, P. F. Yuen, M. B. Baker, and T. V. Larson, "The impacts of SO_2 oxidation in cloud drops and in haze particles on aerosol light scattering and CCN activity," en, *Geophysical Research Letters*, vol. 23, no. 19, pp. 2613–2616, Sep. 1996, ISSN: 0094-8276, 1944-8007. DOI: 10.1029/96GL02419. [Online]. Available: https://agupubs.onlinelibrary.wiley.com/doi/10.1029/96GL02419 (visited on 01/29/2024).

[135] A. S. Chandler *et al.*, "Measurements of H_2O_2 and SO_2 in clouds and estimates of their reaction rate," en, *Nature*, vol. 336, no. 6199, pp. 562–565, Dec. 1988, ISSN: 0028-0836, 1476-4687. DOI: 10.1038/336562a0. [Online]. Available: https://www.nature.com/articles/336562a0 (visited on 03/03/2024).

[136] H. Li *et al.*, "Mechanistic Study of the Aqueous Reaction of Organic Peroxides with HSO_3^- on the Surface of a Water Droplet," en, *Angewandte Chemie*, vol. 133, no. 37, pp. 20 362–20 365, Sep. 2021, ISSN: 0044-8249, 1521-3757. DOI: 10.1002/ange.202105416. (visited on 01/29/2024).

[137] J. Ye, J. P. D. Abbatt, and A. W. H. Chan, "Novel pathway of SO_2 oxidation in the atmosphere: Reactions with monoterpene ozonolysis intermediates and secondary organic aerosol," en, *Atmospheric Chemistry and Physics*, vol. 18, no. 8, pp. 5549–5565, Apr. 2018, ISSN: 1680-7324. DOI: 10.5194/acp-18-5549-2018.

[138] S. Ding, Y. Chen, S. R. Devineni, C. M. Pavuluri, and X.-D. Li, "Distribution characteristics of organosulfates (OSs) in PM2.5 in Tianjin, Northern China: Quantitative analysis of total and three OS species," en, *Science of The Total Environment*, vol. 834, p. 155 314, Aug. 2022, ISSN: 00489697. DOI: 10.1016/j.scitotenv.2022.155314. [Online]. Available: https://linkinghub.elsevier.com/retrieve/pii/S004896972202407X (visited on 01/29/2024).

[139] M. C. Jacobson, H. â. Hansson, K. J. Noone, and R. J. Charlson, "Organic atmospheric aerosols: Review and state of the science," en, *Reviews of Geophysics*, vol. 38, no. 2, pp. 267–294, May 2000, ISSN: 8755-1209, 1944-9208. DOI:

10.1029/1998RG000045. [Online]. Available: https://agupubs.onlinelibrary.wiley.com/doi/10.1029/1998RG000045 (visited on 01/29/2024).

[140] B. J. Turpin, P. Saxena, and E. Andrews, "Measuring and simulating particulate organics in the atmosphere: Problems and prospects," en, *Atmospheric Environment*, vol. 34, no. 18, pp. 2983–3013, Jan. 2000, ISSN: 13522310. DOI: 10.1016/S1352-2310(99)00501-4. [Online]. Available: https://linkinghub.elsevier.com/retrieve/pii/S1352231099005014 (visited on 01/29/2024).

[141] T. Krawczyk and S. Baj, "Review: Advances in the Determination of Peroxides by Optical and Spectroscopic Methods," en, *Analytical Letters*, vol. 47, no. 13, pp. 2129–2147, Sep. 2014, ISSN: 0003-2719, 1532-236X. DOI: 10.1080/00032719.2014.900781. [Online]. Available: http://www.tandfonline.com/doi/abs/10.1080/00032719.2014.900781 (visited on 01/29/2024).

[142] M. Glasius and A. H. Goldstein, "Recent Discoveries and Future Challenges in Atmospheric Organic Chemistry," en, *Environmental Science & Technology*, vol. 50, no. 6, pp. 2754–2764, Mar. 2016, ISSN: 0013-936X, 1520-5851. DOI: 10.1021/acs.est.5b05105. [Online]. Available: https://pubs.acs.org/doi/10.1021/acs.est.5b05105 (visited on 01/29/2024).

[143] D. K. Farmer *et al.*, "Response of an aerosol mass spectrometer to organonitrates and organosulfates and implications for atmospheric chemistry," en, *Proceedings of the National Academy of Sciences*, vol. 107, no. 15, pp. 6670–6675, Apr. 2010, ISSN: 0027-8424, 1091-6490. DOI: 10.1073/pnas.0912340107. [Online]. Available: https://pnas.org/doi/full/10.1073/pnas.0912340107 (visited on 09/17/2023).

[144] K. Gao and T. Zhu, "Analytical methods for organosulfate detection in aerosol particles: Current status and future perspectives," en, *Science of The Total Environment*, vol. 784, p. 147 244, Aug. 2021, ISSN: 00489697. DOI: 10.1016/j.scitotenv.2021.147244. [Online]. Available: https://linkinghub.elsevier.com/retrieve/pii/S0048969721023159 (visited on 01/29/2024).

[145] Y. Qin, V. Perraud, B. J. Finlayson-Pitts, and L. M. Wingen, "Peroxides on the surface of organic aerosol particles using matrix-assisted ionization in vacuum (maiv) mass spectrometry," *Environmental Science & Technology*, vol. 57, no. 38, pp. 14 260–14 268, 2023.

[146] M. S. Claflin, J. Liu, L. M. Russell, and P. J. Ziemann, "Comparison of methods of functional group analysis using results from laboratory and field aerosol measurements," *Aerosol Science and Technology*, vol. 55, no. 9, pp. 1042–1058, 2021.

[147] K. R. Daellenbach *et al.*, "Characterization and source apportionment of organic aerosol using offline aerosol mass spectrometry," en, *Atmospheric Measurement Techniques*, vol. 9, no. 1, pp. 23–39, Jan. 2016, ISSN: 1867-8548. DOI: 10.5194/amt-9-23-2016. [Online]. Available: https://amt.copernicus.org/articles/9/23/2016/ (visited on 01/29/2024).

[148] M. Weloe and T. Hoffmann, "Application of time of flight aerosol mass spectrometry for the real time measurement of particle phase organic peroxides an online redox derivatization aerosol mass spectrometer (ORDAMS)," en, *Atmospheric Measurement Techniques*, vol. 13, no. 10, pp. 5725–5738, Oct. 2020, ISSN: 1867-8548. DOI: 10.5194/amt-13-5725-2020.

[149] Q. Zhang *et al.*, "Understanding atmospheric organic aerosols via factor analysis of aerosol mass spectrometry: A review," en, *Analytical and Bioanalytical Chemistry*, vol. 401, no. 10, pp. 3045–3067, Dec. 2011, ISSN: 1618-2642, 1618-2650. DOI: 10.1007/s00216-011-5355-y. (visited on 01/29/2024).

[150] L. G. Huey, "Measurement of trace atmospheric species by chemical ionization mass spectrometry: Speciation of reactive nitrogen and future directions," *Mass spectrometry reviews*, vol. 26, no. 2, pp. 166–184, 2007.

[151] Y. Zhang, R. Liu, D. Yang, Y. Guo, M. Li, and K. Hou, "Chemical ionization mass spectrometry: Developments and applications for on-line characterization of atmospheric aerosols and trace gases," *TrAC Trends in Analytical Chemistry*, vol. 168, p. 117 353, 2023.

[152] M. F. Sipin, S. A. Guazzotti, and K. A. Prather, "Recent Advances and Some Remaining Challenges in Analytical Chemistry of the Atmosphere," en, *Analytical Chemistry*, vol. 75, no. 12, pp. 2929–2940, Jun. 2003, ISSN: 0003-2700, 1520-6882. DOI: 10.1021/ac030143e. (visited on 01/29/2024).

[153] D. W. OSullivan, I. K. Silwal, A. S. McNeill, V. Treadaway, and B. G. Heikes, "Quantification of gas phase hydrogen peroxide and methyl peroxide in ambient air: Using atmospheric pressure chemical ionization mass spectrometry with O_2^-, and O_2^- (CO_2) reagent ions," *International Journal of Mass Spectrometry*, vol. 424, pp. 16–26, 2018.

[154] M. S. B. Munson and F. H. Field, "Chemical Ionization Mass Spectrometry. I. General Introduction," en, *Journal of the American Chemical Society*, vol. 88, no. 12, pp. 2621–2630, Jun. 1966, ISSN: 0002-7863, 1520-5126. DOI: 10.1021/ja00964a001. (visited on 01/29/2024).

[155] A. G. Harrison, *Chemical Ionization Mass Spectrometry*, en, 0th ed. Routledge, May 2018, ISBN: 978-1-351-46154-2. DOI: 10.1201/9781315139128. (visited on 01/30/2024).

[156] X. Cheng, Q. Chen, Y. Jie Li, Y. Zheng, K. Liao, and G. Huang, "Highly oxygenated organic molecules produced by the oxidation of benzene and toluene in a wide range of OH exposure and NO_x conditions," en, *Atmospheric Chemistry and Physics*, vol. 21, no. 15, pp. 12 005–12 019, Aug. 2021, ISSN: 1680-7324. DOI: 10.5194/acp-21-12005-2021.

[157] M. Riva *et al.*, "Evaluating the performance of five different chemical ionization techniques for detecting gaseous oxygenated organic species," en, *Atmospheric Measurement Techniques*, vol. 12, no. 4, pp. 2403–2421, Apr. 2019, ISSN: 1867-8548. DOI: 10.5194/amt-12-2403-2019.

[158] S. H. Budisulistiorini *et al.*, "Examining the effects of anthropogenic emissions on isoprene-derived secondary organic aerosol formation during the 2013 Southern Oxidant and Aerosol Study (SOAS) at the Look Rock, Tennessee ground site," en, *Atmospheric Chemistry and Physics*, vol. 15, no. 15, pp. 8871–8888, Aug. 2015, ISSN: 1680-7324. DOI: 10.5194/acp-15-8871-2015.

[159] A. Tiusanen, J. Ruiz-Jimenez, K. Hartonen, and S. K. Wiedmer, "Analytical methodologies for oxidized organic compounds in the atmosphere," *Environmental Science: Processes & Impacts*, vol. 25, no. 8, pp. 1263–1287, 2023.

[160] H. O. Pye *et al.*, "Anthropogenic enhancements to production of highly oxygenated molecules from autoxidation," *Proceedings of the National Academy of Sciences*, vol. 116, no. 14, pp. 6641–6646, 2019.

[161] T. B. Nguyen *et al.*, "Atmospheric fates of criegee intermediates in the ozonolysis of isoprene," *Physical Chemistry Chemical Physics*, vol. 18, no. 15, pp. 10 241–10 254, 2016.

[162] R. Cathcart, E. Schwiers, and B. N. Ames, "Detection of picomole levels of hydroperoxides using a fluorescent dichlorofluorescein assay," en, *Analytical Biochemistry*, vol. 134, no. 1, pp. 111–116, Oct. 1983, ISSN: 00032697. DOI: 10.1016/0003-2697(83)90270-1. (visited on 02/01/2024).

[163] M. Lee, B. G. Heikes, and D. W. O'Sullivan, "Hydrogen peroxide and organic hydroperoxide in the troposphere: A review," en, *Atmospheric Environment*, vol. 34, no. 21, pp. 3475–3494, Jan. 2000, ISSN: 13522310. DOI: 10.1016/S1352-2310(99)00432-X. (visited on 02/01/2024).

[164] P. Mertes, L. Pfaffenberger, J. Dommen, M. Kalberer, and U. Baltensperger, "Development of a sensitive long path absorption photometer to quantify peroxides in aerosol particles (Peroxide-LOPAP)," en, *Atmospheric Measurement Techniques*, vol. 5, no. 10, pp. 2339–2348, Oct. 2012, ISSN: 1867-8548. DOI: 10.5194/amt-5-2339-2012. [Online]. Available: https://amt.copernicus.org/articles/5/2339/2012/.

[165] S. Rankin-Turner, P. Sears, and L. M. Heaney, "Applications of ambient ionization mass spectrometry in 2022: An annual review," *Analytical Science Advances*, vol. 4, no. 5-6, pp. 133–153, 2023.

[166] B. Challen and R. Cramer, "Advances in ionisation techniques for mass spectrometry-based omics research," *Proteomics*, vol. 22, no. 15-16, p. 2 100 394, 2022.

[167] P. J. Roach, J. Laskin, and A. Laskin, "Molecular Characterization of Organic Aerosols Using Nanospray-Desorption/Electrospray Ionization-Mass Spectrometry," en, *Analytical Chemistry*, vol. 82, no. 19, pp. 7979–7986, Oct. 2010, ISSN: 0003-2700, 1520-6882. DOI: 10.1021/ac101449p. [Online]. Available: https://pubs.acs.org/doi/10.1021/ac101449p.

[168] J. Laskin *et al.*, "Molecular selectivity of brown carbon chromophores," *Environmental science & technology*, vol. 48, no. 20, pp. 12 047–12 055, 2014.

[169] S. Zhou, J. C. Rivera-Rios, F. N. Keutsch, and J. P. D. Abbatt, "Identification of organic hydroperoxides and peroxy acids using atmospheric pressure chemical ionization tandem mass spectrometry (APCI/MS/MS) application to secondary organic aerosol," English, *Atmospheric Measurement Techniques*, vol. 11, no. 5, pp. 3081–3089, May 2018, ISSN: 1867-1381. DOI: https://doi.org/10.5194/amt-11-3081-2018. (visited on 08/13/2019).

[170] K. S. Docherty, W. Wu, Y. B. Lim, and P. J. Ziemann, "Contributions of Organic Peroxides to Secondary Aerosol Formed from Reactions of Monoterpenes with O_3, volume = 39," en, *Environmental Science & Technology*, no. 11, pp. 4049–4059, Jun. 2005, ISSN: 0013-936X, 1520-5851. DOI: 10.1021/es050228s. (visited on 02/11/2024).

[171] K. Moore and L. J. Roberts, "Measurement of Lipid Peroxidation," en, *Free Radical Research*, vol. 28, no. 6, pp. 659–671, Jan. 1998, ISSN: 1071-5762, 1029-2470. DOI: 10.3109/10715769809065821. [Online]. Available: http://www.tandfonline.com/doi/full/10.3109/10715769809065821 (visited on 02/03/2024).

[172] J. I. Gray, "Measurement of lipid oxidation: A review," en, *Journal of the American Oil Chemists' Society*, vol. 55, no. 6, pp. 539–546, Jun. 1978, ISSN: 0003-021X, 1558-9331. DOI: 10.1007/BF02668066. [Online]. Available: https://aocs.onlinelibrary.wiley.com/doi/10.1007/BF02668066 (visited on 02/03/2024).

[173] J. M. Gebicki, J. Collins, A. Baoutina, and P. Phair, "The limitations of an iodometric aerobic assay for peroxides," *Analytical biochemistry*, vol. 240, no. 2, pp. 235–241, 1996.

[174] W. C. Bray and H. A. Liebhafsky, "REACTIONS INVOLVING HYDROGEN PEROXIDE, IODINE AND IODATE ION. I. INTRODUCTION," en, *Journal of the American Chemical Society*, vol. 53, no. 1, pp. 38–44, Jan. 1931, ISSN: 0002-7863, 1520-5126. DOI: 10.1021/ja01352a006. [Online]. Available: https://pubs.acs.org/doi/abs/10.1021/ja01352a006 (visited on 02/03/2024).

[175] W. A. Pryor and L. Castle, "[34] Chemical methods for the detection of lipid hydroperoxides," en, in *Methods in Enzymology*, vol. 105, Elsevier, 1984, pp. 293–299, ISBN: 978-0-12-182005-3. DOI: 10.1016/S0076-6879(84)05037-0. [Online]. Available: https://linkinghub.elsevier.com/retrieve/pii/S0076687984050370 (visited on 02/03/2024).

[176] T. D. Crowe and P. J. White, "Adaptation of the AOCS official method for measuring hydroperoxides from small scale oil samples," en, *Journal of the American Oil Chemists' Society*, vol. 78, no. 12, pp. 1267–1269, Dec. 2001, ISSN: 0003-021X, 1558-9331. DOI: 10.1007/s11745-001-0424-7.

[177] G. Yildiz, R. L. Wehling, and S. L. Cuppett, "Comparison of four analytical methods for the determination of peroxide value in oxidized soybean oils," en, *Journal of the American Oil Chemists' Society*, vol. 80, no. 2, pp. 103–107, Feb. 2003, ISSN: 0003-021X, 1558-9331. DOI: 10.1007/s11746-003-0659-3.

[Online]. Available: https://aocs.onlinelibrary.wiley.com/doi/10.1007/s11746-003-0659-3 (visited on 02/03/2024).

[178] G. L. Kok, K. Thompson, A. L. Lazrus, and S. E. McLaren, "Derivatization technique for the determination of peroxides in precipitation," en, *Analytical Chemistry*, vol. 58, no. 6, pp. 1192–1194, May 1986, ISSN: 0003-2700, 1520-6882. DOI: 10.1021/ac00297a047. (visited on 02/03/2024).

[179] S. G. Rhee, T.-S. Chang, W. Jeong, and D. Kang, "Methods for detection and measurement of hydrogen peroxide inside and outside of cells," en, *Molecules and Cells*, vol. 29, no. 6, pp. 539–549, Jun. 2010, ISSN: 1016-8478, 0219-1032. DOI: 10.1007/s10059-010-0082-3. [Online]. Available: http://link.springer.com/10.1007/s10059-010-0082-3 (visited on 02/03/2024).

[180] R. Zhao, C. M. Kenseth, Y. Huang, N. F. Dalleska, and J. H. Seinfeld, "Iodometry-Assisted Liquid Chromatography Electrospray Ionization Mass Spectrometry for Analysis of Organic Peroxides: An Application to Atmospheric Secondary Organic Aerosol," *Environmental Science & Technology*, vol. 52, no. 4, pp. 2108–2117, Feb. 2018, ISSN: 0013-936X. DOI: 10.1021/acs.est.7b04863. (visited on 08/08/2019).

[181] H. A. Liebhafsky and A. Mohammad, "The Kinetics of the Reduction, in Acid Solution, of Hydrogen Peroxide by Iodide Ion," en, *Journal of the American Chemical Society*, vol. 55, no. 10, pp. 3977–3986, Oct. 1933, ISSN: 0002-7863, 1520-5126. DOI: 10.1021/ja01337a010. [Online]. Available: https://pubs.acs.org/doi/abs/10.1021/ja01337a010 (visited on 04/02/2021).

[182] C. J. Michejda, R. L. Ayres, and E. P. Rack, "Reactions of iodine with olefins. I. Kinetics and mechanism of iodine addition to pentene isomers," en, *Journal of the American Chemical Society*, vol. 93, no. 6, pp. 1389–1394, Mar. 1971, ISSN: 0002-7863. DOI: 10.1021/ja00735a012. [Online]. Available: https://pubs.acs.org/doi/abs/10.1021/ja00735a012 (visited on 03/20/2021).

[183] T. Gautam, S. Wu, J. Ma, and R. Zhao, "Potential Matrix Effects in Iodometry Determination of Peroxides Induced by Olefins," en, *The Journal of Physical Chemistry A*, vol. 126, no. 17, pp. 2632–2644, May 2022, ISSN: 1089-5639, 1520-5215. DOI: 10.1021/acs.jpca.1c10717. [Online]. Available: https://pubs.acs.org/doi/10.1021/acs.jpca.1c10717 (visited on 10/15/2022).

[184] W. Zhang, L. Xu, and H. Zhang, "Recent advances in mass spectrometry techniques for atmospheric chemistry research on molecular-level," *Mass Spectrometry Reviews*, 2023.

[185] A. P. S. Hettiyadura *et al.*, "Determination of atmospheric organosulfates using HILIC chromatography with MS detection," en, *Atmospheric Measurement Techniques*, vol. 8, no. 6, pp. 2347–2358, Jun. 2015, ISSN: 1867-8548. DOI: 10.5194/amt-8-2347-2015. [Online]. Available: https://amt.copernicus.org/articles/8/2347/2015/.

[186] C. M. Kenseth *et al.*, "Synergistic o_3+ oh oxidation pathway to extremely low-volatility dimers revealed in β-pinene secondary organic aerosol," *Proceedings of the National Academy of Sciences*, vol. 115, no. 33, pp. 8301–8306, 2018.

[187] W. Fan, T. Chen, Z. Zhu, H. Zhang, Y. Qiu, and D. Yin, "A review of secondary organic aerosols formation focusing on organosulfates and organic nitrates," en, *Journal of Hazardous Materials*, vol. 430, p. 128 406, May 2022, ISSN: 03043894. DOI: 10.1016/j.jhazmat.2022.128406. (visited on 01/29/2024).

[188] P. S. J. Lakey *et al.*, "Chemical exposure-response relationship between air pollutants and reactive oxygen species in the human respiratory tract," en, *Scientific Reports*, vol. 6, no. 1, p. 32 916, Sep. 2016, ISSN: 2045-2322. DOI: 10.1038/srep32916. [Online]. Available: https://www.nature.com/articles/srep32916.

[189] Y. Han *et al.*, "Enhanced Production of Organosulfur Species during a Severe Winter Haze Episode in the Guanzhong Basin of Northwest China," en, *Environmental Science & Technology*, vol. 57, no. 23, pp. 8708–8718, Jun. 2023, ISSN: 0013-936X, 1520-5851. DOI: 10.1021/acs.est.3c02914. [Online]. Available: https://pubs.acs.org/doi/10.1021/acs.est.3c02914 (visited on 02/06/2024).

[190] H. Li *et al.*, "Nitrate-driven urban haze pollution during summertime over the North China Plain," en, *Atmospheric Chemistry and Physics*, vol. 18, no. 8, pp. 5293–5306, Apr. 2018, ISSN: 1680-7324. DOI: 10.5194/acp-18-5293-2018. [Online]. Available: https://acp.copernicus.org/articles/18/5293/2018/.

[191] C. Fittschen, "The reaction of peroxy radicals with oh radicals," *Chemical Physics Letters*, vol. 725, pp. 102–108, 2019.

[192] N. A. Porter, "Mechanisms for the autoxidation of polyunsaturated lipids," en, *Accounts of Chemical Research*, vol. 19, no. 9, pp. 262–268, Sep. 1986, ISSN: 0001-4842, 1520-4898. DOI: 10.1021/ar00129a001. [Online]. Available: https://pubs.acs.org/doi/abs/10.1021/ar00129a001 (visited on 08/12/2022).

[193] R. A. Cox and J. A. Cole, "Chemical aspects of the autoignition of hydrocarbon air mixtures," en, *Combustion and Flame*, vol. 60, no. 2, pp. 109–123, May 1985, ISSN: 0010-2180. DOI: 10.1016/0010-2180(85)90001-X. (visited on 02/27/2022).

[194] A. A. Boyd, P.-M. Flaud, N. Daugey, and R. Lesclaux, "Rate constants for RO_2+ HO_2 reactions measured under a large excess of HO_2," *The Journal of Physical Chemistry A*, vol. 107, no. 6, pp. 818–821, 2003, Publisher: ACS Publications.

[195] P. Stevens *et al.*, "HO_2/OH and RO_2/HO_2 ratios during the Tropospheric OH Photochemistry Experiment Measurement and theory," *Journal of Geophysical Research: Atmospheres*, vol. 102, no. D5, pp. 6379–6391, 1997.

[196] U. Molteni *et al.*, "Formation of highly oxygenated organic molecules from aromatic compounds," *Atmospheric Chemistry and Physics*, vol. 18, no. 3, pp. 1909–1921, 2018, Publisher: Copernicus GmbH.

[197] T. Berndt *et al.*, "Hydroxyl radical-induced formation of highly oxidized organic compounds," *Nature communications*, vol. 7, no. 1, p. 13 677, 2016, Publisher: Nature Publishing Group UK London.

[198] O. Perakyla, M. Riva, L. Heikkinen, L. Quelever, P. Roldin, and M. Ehn, "Experimental investigation into the volatilities of highly oxygenated organic molecules (HOMs)," *Atmospheric Chemistry and Physics*, vol. 20, no. 2, pp. 649–669, 2020, Publisher: Copernicus GmbH.

[199] J. D. Crounse, L. B. Nielsen, S. Jorgensen, H. G. Kjaergaard, and P. O. Wennberg, "Autoxidation of Organic Compounds in the Atmosphere," *The Journal of Physical Chemistry Letters*, vol. 4, no. 20, pp. 3513–3520, Oct. 2013. DOI: 10.1021/jz4019207.

[200] E. Assaf, C. Schoemaecker, L. Vereecken, and C. Fittschen, "Experimental and theoretical investigation of the reaction of RO_2 radicals with OH radicals: Dependence of the HO_2 yield on the size of the alkyl group," *International journal of chemical kinetics*, vol. 50, no. 9, pp. 670–680, 2018, Publisher: Wiley Online Library.

[201] S. Wang, Q. Zhang, G. Wang, Y. Wei, W. Wang, and Q. Wang, "The neglected autoxidation pathways for the formation of highly oxygenated organic molecules (HOMs) and the nucleation of the HOMs generated by limonene," *Atmospheric Environment*, vol. 304, p. 119 727, 2023.

[202] R. Xu *et al.*, "Global simulations of monoterpene-derived peroxy radical fates and the distributions of highly oxygenated organic molecules (HOMs) and accretion products," *Atmospheric Chemistry and Physics*, vol. 22, no. 8, pp. 5477–5494, 2022, Publisher: Copernicus GmbH.

[203] J. P. Nascimento *et al.*, "Major Regional-Scale Production of O_3 and Secondary Organic Aerosol in Remote Amazon Regions from the Dynamics and Photochemistry of Urban and Forest Emissions," *Environmental Science & Technology*, vol. 56, no. 14, pp. 9924–9935, 2022, Publisher: ACS Publications.

[204] X. Fu *et al.*, "High-resolution simulation of local traffic-related no_x dispersion and distribution in a complex urban terrain," *Environmental Pollution*, vol. 263, p. 114 390, 2020.

[205] P. Ni, X. Wang, and H. Li, "A review on regulations, current status, effects and reduction strategies of emissions for marine diesel engines," *Fuel*, vol. 279, p. 118 477, 2020, Publisher: Elsevier.

[206] M. D. LaCount, R. A. Haeuber, T. R. Macy, and B. A. Murray, "Reducing power sector emissions under the 1990 Clean Air Act Amendments: A retrospective on 30 years of program development and implementation," *Atmospheric Environment*, vol. 245, p. 118 012, 2021, Publisher: Elsevier.

[207] E. Tsiligiannis, J. Hammes, C. M. Salvador, T. F. Mentel, and M. Hallquist, "Effect of NO_x on 1,3,5-trimethylbenzene (TMB) oxidation product distribution and particle formation," en, *Atmospheric Chemistry and Physics*, vol. 19, no. 23, pp. 15 073–15 086, Dec. 2019, ISSN: 1680-7324. DOI: 10.5194/acp-19-15073-2019. [Online]. Available: https://acp.copernicus.org/articles/19/15073/2019/.

[208] W. Zhang, Z. Zhao, C. Shen, and H. Zhang, "Unexpectedly Efficient Aging of Organic Aerosols Mediated by Autoxidation," *Environmental Science & Technology*, vol. 57, no. 17, pp. 6965–6974, 2023, Publisher: ACS Publications.

[209] E. Praske *et al.*, "Atmospheric autoxidation is increasingly important in urban and suburban North America," *Proceedings of the National Academy of Sciences*, vol. 115, no. 1, pp. 64–69, Jan. 2018. DOI: 10.1073/pnas.1715540115. [Online]. Available: http://www.pnas.org/doi/10.1073/pnas.1715540115 (visited on 06/11/2022).

[210] J. D. Crounse *et al.*, "Atmospheric Fate of Methacrolein. 1. Peroxy Radical Isomerization Following Addition of OH and O_2," en, *The Journal of Physical Chemistry A*, vol. 116, no. 24, pp. 5756–5762, Jun. 2012, ISSN: 1089-5639, 1520-5215. DOI: 10.1021/jp211560u.

[211] K. Stemmler and U. Von Gunten, "OH radical-initiated oxidation of organic compounds in atmospheric water phases: Part 2. Reactions of peroxyl radicals with transition metals," en, *Atmospheric Environment*, vol. 34, no. 25, pp. 4253–4264, Jul. 2000, ISSN: 13522310. DOI: 10.1016/S1352-2310(00)00219-3. [Online]. Available: https://linkinghub.elsevier.com/retrieve/pii/S1352231000002193 (visited on 01/29/2024).

[212] Y. Zuo and J. Hoigne, "Formation of hydrogen peroxide and depletion of oxalic acid in atmospheric water by photolysis of iron(III)-oxalato complexes," en, *Environmental Science & Technology*, vol. 26, no. 5, pp. 1014–1022, May 1992, ISSN: 0013-936X, 1520-5851. DOI: 10.1021/es00029a022. (visited on 01/29/2024).

[213] J. Wei, T. Fang, C. Wong, P. S. Lakey, S. A. Nizkorodov, and M. Shiraiwa, "Superoxide formation from aqueous reactions of biogenic secondary organic aerosols," *Environmental Science & Technology*, vol. 55, no. 1, pp. 260–270, 2020, Publisher: ACS Publications.

[214] R Kaur and C Anastasio, "Light absorption and the photoformation of hydroxyl radical and singlet oxygen in fog waters," *Atmospheric Environment*, vol. 164, pp. 387–397, 2017, Publisher: Elsevier.

[215] M. Yao *et al.*, "Multiphase reactions between secondary organic aerosol and sulfur dioxide: Kinetics and contributions to sulfate formation and aerosol aging," *Environmental Science & Technology Letters*, vol. 6, no. 12, pp. 768–774, 2019, Publisher: ACS Publications.

[216] M. Hu, K. Chen, J. Qiu, Y.-H. Lin, K. Tonokura, and S. Enami, "Decomposition mechanism of α-alkoxyalkyl-hydroperoxides in the liquid phase: Temperature dependent kinetics and theoretical calculations," *Environmental Science: Atmospheres*, vol. 2, no. 2, pp. 241–251, 2022, Publisher: Royal Society of Chemistry.

[217] S. Toyokuni, "Reactive oxygen species-induced molecular damage and its application in pathology," *Pathology international*, vol. 49, no. 2, pp. 91–102, 1999, Publisher: Wiley Online Library.

[218] K. M. Badali *et al.*, "Formation of hydroxyl radicals from photolysis of secondary organic aerosol material," English, *Atmospheric Chemistry and Physics*, vol. 15, no. 14, pp. 7831–7840, Jul. 2015, ISSN: 1680-7316. DOI: https://doi.org/10.5194/acp-15-7831-2015.

[219] T. Charbouillot *et al.*, "Mechanism of carboxylic acid photooxidation in atmospheric aqueous phase: Formation, fate and reactivity," en, *Atmospheric Environment*, vol. 56, pp. 1–8, Sep. 2012, ISSN: 1352-2310. DOI: 10.1016/j.atmosenv.2012.03.079. (visited on 11/11/2022).

[220] Y. Gong, Z. Chen, and H. Li, "The oxidation regime and SOA composition in limonene ozonolysis: Roles of different double bonds, radicals, and water," *Atmospheric Chemistry and Physics*, vol. 18, no. 20, pp. 15 105–15 123, 2018, ISSN: 1680-7316. DOI: 10.5194/acp-18-15105-2018.

[221] T. S Christoffersen *et al.*, "Cis-pinic acid, a possible precursor for organic aerosol formation from ozonolysis of α-pinene," en, *Atmospheric Environment*, vol. 32, no. 10, pp. 1657–1661, May 1998, ISSN: 1352-2310. DOI: 10.1016/S1352-2310(97)00448-2. (visited on 07/26/2022).

[222] B. Witkowski, S. Jurdana, and T. Gierczak, "Limononic Acid Oxidation by Hydroxyl Radicals and Ozone in the Aqueous Phase," en, *Environmental Science & Technology*, vol. 52, no. 6, pp. 3402–3411, Mar. 2018, ISSN: 0013-936X, 1520-5851. DOI: 10.1021/acs.est.7b04867. [Online]. Available: https://pubs.acs.org/doi/10.1021/acs.est.7b04867 (visited on 12/13/2020).

[223] H Fuchs *et al.*, "Intercomparison of peroxy radical measurements obtained at atmospheric conditions by laser-induced fluorescence and electron spin resonance spectroscopy," *Atmospheric Measurement Techniques*, vol. 2, no. 1, pp. 55–64, 2009, Publisher: Copernicus GmbH.

[224] J. Vejdani Amorim *et al.*, "Photo-oxidation of pinic acid in the aqueous phase: A mechanistic investigation under acidic and basic pH conditions," *Environmental Science: Atmospheres*, vol. 1, no. 5, pp. 276–287, 2021. DOI: 10.1039/D1EA00031D. (visited on 08/06/2021).

[225] R. Zhao, E. L. Mungall, A. K. Y. Lee, D. Aljawhary, and J. P. D. Abbatt, "Aqueous-phase photooxidation of levoglucosan – a mechanistic study using aerosol time-of-flight chemical ionization mass spectrometry (Aerosol ToF-CIMS)," English, *Atmospheric Chemistry and Physics*, vol. 14, no. 18,

pp. 9695–9706, Sep. 2014, Publisher: Copernicus GmbH, ISSN: 1680-7316. DOI: 10.5194/acp-14-9695-2014. (visited on 12/23/2022).

[226] H. Herrmann *et al.*, "Tropospheric Aqueous Phase Chemistry Kinetics, Mechanisms, and Its Coupling to a Changing Gas Phase," en, *Chemical Reviews*, vol. 115, no. 10, pp. 4259–4334, May 2015, ISSN: 0009-2665, 1520-6890. DOI: 10.1021/cr500447k.

[227] P. Renard *et al.*, "Aqueous Phase Oligomerization of Methyl Vinyl Ketone by Atmospheric Radical Reactions," *The Journal of Physical Chemistry C*, vol. 118, no. 50, pp. 29 421–29 430, Dec. 2014, ISSN: 1932-7447. DOI: 10.1021/jp5065598. [Online]. Available: https://doi.org/10.1021/jp5065598 (visited on 11/11/2022).

[228] M.-C. Reinnig, J. Warnke, and T. Hoffmann, "Identification of organic hydroperoxides and hydroperoxy acids in secondary organic aerosol formed during the ozonolysis of different monoterpenes and sesquiterpenes by on-line analysis using atmospheric pressure chemical ionization ion trap mass spectrometry," en, *Rapid Communications in Mass Spectrometry*, vol. 23, no. 11, pp. 1735–1741, 2009, ISSN: 1097-0231. DOI: 10.1002/rcm.4065. [Online]. Available: https://onlinelibrary.wiley.com/doi/abs/10.1002/rcm.4065 (visited on 08/21/2019).

[229] W. L. Miller and D. R. Kester, "Hydrogen peroxide measurement in seawater by (p-hydroxyphenyl)acetic acid dimerization," *Analytical Chemistry*, vol. 60, no. 24, pp. 2711–2715, Dec. 1988, ISSN: 0003-2700. DOI: 10.1021/ac00175a014. [Online]. Available: https://doi.org/10.1021/ac00175a014 (visited on 10/01/2019).

[230] C. Deyrieux *et al.*, "Measurement of Peroxide Values in Oils by Triphenylphosphine/Triphenylphosphine Oxide (TPP/TPPO) Assay Coupled with FTIR-ATR Spectroscopy: Comparison with Iodometric Titration," *European Journal of Lipid Science and Technology*, vol. 120, no. 8, p. 1 800 109, 2018, Publisher: Wiley Online Library.

[231] J. V. Amorim *et al.*, "pH Dependence of the OH Reactivity of Organic Acids in the Aqueous Phase," en, *Environmental Science & Technology*, vol. 54, no. 19, pp. 12 484–12 492, Oct. 2020, ISSN: 0013-936X, 1520-5851. DOI: 10.1021/acs.est.0c03331. [Online]. Available: https://pubs.acs.org/doi/10.1021/acs.est.0c03331 (visited on 06/22/2021).

[232] A. Sorooshian, N. L. Ng, A. W. Chan, G. Feingold, R. C. Flagan, and J. H. Seinfeld, "Particulate organic acids and overall water-soluble aerosol composition measurements from the 2006 Gulf of Mexico Atmospheric Composition and Climate Study (GoMACCS)," *Journal of Geophysical Research: Atmospheres*, vol. 112, no. D13, 2007, Publisher: Wiley Online Library.

[233] X. Sun *et al.*, "Organic acids in cloud water and rainwater at a mountain site in acid rain areas of South China," en, *Environmental Science and Pollution Research*, vol. 23, no. 10, pp. 9529–9539, May 2016, ISSN: 1614-7499. DOI: 10.1007/s11356-016-6038-1. (visited on 11/24/2022).

[234] T. B. Nguyen, A. P. Bateman, D. L. Bones, S. A. Nizkorodov, J. Laskin, and A. Laskin, "High-resolution mass spectrometry analysis of secondary organic aerosol generated by ozonolysis of isoprene," en, *Atmospheric Environment*, vol. 44, no. 8, Mar. 2010, ISSN: 1352-2310. DOI: 10.1016/j.atmosenv.2009.12.019.

[235] Y. Tan, M. J. Perri, S. P. Seitzinger, and B. J. Turpin, "Effects of Precursor Concentration and Acidic Sulfate in Aqueous Glyoxal OH Radical Oxidation and Implications for Secondary Organic Aerosol," en, *Environmental Science & Technology*, vol. 43, no. 21, pp. 8105–8112, Nov. 2009, ISSN: 0013-936X, 1520-5851. DOI: 10.1021/es901742f. (visited on 08/29/2022).

[236] M. Zeng, N. Heine, and K. R. Wilson, "Evidence that Criegee intermediates drive autoxidation in unsaturated lipids," en, *Proceedings of the National Academy of Sciences*, vol. 117, no. 9, pp. 4486–4490, Mar. 2020, ISSN: 0027-8424, 1091-6490. DOI: 10.1073/pnas.1920765117. [Online]. Available: https://pnas.org/doi/full/10.1073/pnas.1920765117 (visited on 10/09/2022).

[237] S. S. Yashar and H. W. Lim, "Classification and evaluation of photodermatoses," en, *Dermatologic Therapy*, vol. 16, no. 1, pp. 1–7, Mar. 2003, ISSN: 1396-0296, 1529-8019. DOI: 10.1046/j.1529-8019.2003.01601.x. [Online]. Available: http://doi.wiley.com/10.1046/j.1529-8019.2003.01601.x (visited on 08/29/2022).

[238] G. Schmitz, "Iodine oxidation by hydrogen peroxide in acidic solutions, Bray-Liebhafsky reaction and other related reactions," en, *Physical Chemistry Chemical Physics*, vol. 12, no. 25, pp. 6605–6615, 2010. DOI: 10.1039/B927432D. [Online]. Available: http://pubs.rsc.org/en/content/articlelanding/2010/cp/b927432d (visited on 08/24/2021).

[239] C. M. Kenseth *et al.*, "Synergistic O_3 + OH oxidation pathway to extremely low-volatility dimers revealed in β-pinene secondary organic aerosol," en, *Proceedings of the National Academy of Sciences*, vol. 115, no. 33, pp. 8301–8306, Aug. 2018, ISSN: 0027-8424, 1091-6490. DOI: 10.1073/pnas.1804671115. (visited on 10/31/2022).

[240] H. A. Liebhafsky, "The catalytic decompostion of Hydrogen Peroxides by iodine-iodide couple at 25C," en, *Journal of the American Chemical Society*, vol. 54, no. 5, pp. 1792–1806, May 1932, ISSN: 0002-7863, 1520-5126. DOI: 10.1021/ja01344a011.

[241] A. Gabet, H. Metivier, C. de Brauer, G. Mailhot, and M. Brigante, "Hydrogen peroxide and persulfate activation using UVA-UVB radiation: Degradation of estrogenic compounds and application in sewage treatment plant waters," en,

Journal of Hazardous Materials, vol. 405, p. 124 693, Mar. 2021, ISSN: 0304-3894. DOI: 10.1016/j.jhazmat.2020.124693. (visited on 11/12/2022).

[242] M. Oss, A. Kruve, K. Herodes, and I. Leito, "Electrospray Ionization Efficiency Scale of Organic Compounds," *Analytical Chemistry*, vol. 82, no. 7, pp. 2865–2872, Apr. 2010, ISSN: 0003-2700. DOI: 10.1021/ac902856t.

[243] Y. B. Lim, Y. Tan, and B. J. Turpin, "Chemical insights, explicit chemistry, and yields of secondary organic aerosol from OH radical oxidation of methylglyoxal and glyoxal in the aqueous phase," en, *Atmospheric Chemistry and Physics*, vol. 13, no. 17, pp. 8651–8667, Sep. 2013, ISSN: 1680-7324. DOI: 10.5194/acp-13-8651-2013. (visited on 08/14/2022).

[244] J. V. Amorim *et al.*, "Photo-oxidation of pinic acid in the aqueous phase: A mechanistic investigation under acidic and basic ph conditions," *Environmental Science: Atmospheres*, vol. 1, no. 5, pp. 276–287, 2021.

[245] M. Yao *et al.*, "Isomer-Resolved Reactivity of Organic Peroxides in Monoterpene-Derived Secondary Organic Aerosol," *Environmental Science & Technology*, vol. 56, no. 8, pp. 4882–4893, Apr. 2022, ISSN: 0013-936X. DOI: 10.1021/acs.est.2c01297. [Online]. Available: https://doi.org/10.1021/acs.est.2c01297 (visited on 07/24/2022).

[246] A. Mutzel, M. Rodigast, Y. Iinuma, O. Boge, and H. Herrmann, "An improved method for the quantification of SOA bound peroxides," en, *Atmospheric Environment*, vol. 67, pp. 365–369, Mar. 2013, ISSN: 13522310. DOI: 10.1016/j.atmosenv.2012.11.012.

[247] D. Lindsay *et al.*, "The Bimolecular Self-reactions of Secondary Peroxy Radicals. Product Studies," en, *Canadian Journal of Chemistry*, vol. 51, no. 6, pp. 870–880, Mar. 1973, ISSN: 0008-4042, 1480-3291. DOI: 10.1139/v73-131. (visited on 11/06/2022).

[248] V.-T. Salo, R. Valiev, S. Lehtola, and T. Kurten, "Gas-Phase Peroxyl Radical Recombination Reactions: A Computational Study of Formation and Decomposition of Tetroxides," en, *The Journal of Physical Chemistry A*, vol. 126, no. 25, pp. 4046–4056, Jun. 2022, ISSN: 1089-5639, 1520-5215. DOI: 10.1021/acs.jpca.2c01321. [Online]. Available: https://pubs.acs.org/doi/10.1021/acs.jpca.2c01321 (visited on 12/30/2022).

[249] J. Elm, T. Kurten, M. Bilde, and K. V. Mikkelsen, "Molecular Interaction of Pinic Acid with Sulfuric Acid: Exploring the Thermodynamic Landscape of Cluster Growth," *The Journal of Physical Chemistry A*, vol. 118, no. 36, pp. 7892–7900, Sep. 2014, ISSN: 1089-5639. DOI: 10.1021/jp503736s. [Online]. Available: https://doi.org/10.1021/jp503736s (visited on 07/18/2022).

[250] M. E. Jenkin, D. E. Shallcross, and J. N. Harvey, "Development and application of a possible mechanism for the generation of cis-pinic acid from the ozonolysis of α- and β-pinene," en, *Atmospheric Environment*, vol. 34, no. 18, pp. 2837–2850, Jan. 2000, ISSN: 1352-2310. DOI: 10.1016/S1352-2310(00)00087-X.

[251] L. Vereecken, J.-F. Muller, and J. Peeters, "Low-volatility poly-oxygenates in the OH-initiated atmospheric oxidation of α-pinene: Impact of non-traditional peroxyl radical chemistry," en, *Physical Chemistry Chemical Physics*, vol. 9, no. 38, p. 5241, 2007, ISSN: 1463-9076, 1463-9084. DOI: 10.1039/b708023a. [Online]. Available: http://xlink.rsc.org/?DOI=b708023a (visited on 08/28/2022).

[252] B. Witkowski, M. Al-sharafi, and T. Gierczak, "Ozonolysis of β-Caryophyllonic and Limononic Acids in the Aqueous Phase: Kinetics, Product Yield, and Mechanism," *Environmental Science & Technology*, vol. 53, no. 15, pp. 8823–8832, Aug. 2019, ISSN: 0013-936X. DOI: 10.1021/acs.est.9b02471.

[253] B. Witkowski and T. Gierczak, "Characterization of the limonene oxidation products with liquid chromatography coupled to the tandem mass spectrometry," en, *Atmospheric Environment*, vol. 154, pp. 297–307, Apr. 2017, ISSN: 1352-2310. DOI: 10.1016/j.atmosenv.2017.02.005. (visited on 06/19/2021).

[254] F. Bianchi *et al.*, "Highly oxygenated organic molecules (hom) from gas-phase autoxidation involving peroxy radicals: A key contributor to atmospheric aerosol," *Chemical reviews*, vol. 119, no. 6, pp. 3472–3509, 2019.

[255] M. P. Rissanen *et al.*, "Effects of chemical complexity on the autoxidation mechanisms of endocyclic alkene ozonolysis products: From methylcyclohexenes toward understanding α-pinene," *The Journal of Physical Chemistry A*, vol. 119, no. 19, pp. 4633–4650, 2015, Publisher: ACS Publications.

[256] B. C. Faust, C. Anastasio, J. M. Allen, and T. Arakaki, "Aqueous-Phase Photochemical Formation of Peroxides in Authentic Cloud and Fog Waters," en, *Science*, vol. 260, no. 5104, pp. 73–75, Apr. 1993, ISSN: 0036-8075, 1095-9203. DOI: 10.1126/science.8465202. [Online]. Available: https://www.science.org/doi/10.1126/science.8465202 (visited on 01/29/2024).

[257] T. Toki *et al.*, "Synergistic interaction between wavelength of light and concentration of H_2O_2 in bactericidal activity of photolysis of H_2O_2," en, *Journal of Bioscience and Bioengineering*, vol. 119, no. 3, pp. 358–362, Mar. 2015, ISSN: 1389-1723. DOI: 10.1016/j.jbiosc.2014.08.015. (visited on 11/13/2022).

[258] M. C. V. M. Starling, P. P. Souza, A. Le Person, C. C. Amorim, and J. Criquet, "Intensification of UV-C treatment to remove emerging contaminants by UV-C/H_2O_2 and UV-C/$S_2O_8{}^{2-}$: Susceptibility to photolysis and investigation of acute toxicity," en, *Chemical Engineering Journal*, Emerging advanced oxidation technologies and developing perspectives for water and wastewater treatment. Vol. 376, p. 120 856, Nov. 2019, ISSN: 1385-8947. DOI: 10.1016/j.cej.2019.01.135. (visited on 11/12/2022).

[259] A. Monod, E. Chevallier, R. Durand Jolibois, J. F. Doussin, B. Picquet-Varrault, and P. Carlier, "Photooxidation of methylhydroperoxide and ethylhydroperoxide in the aqueous phase under simulated cloud droplet conditions," en, *Atmospheric Environment*, vol. 41, no. 11, pp. 2412–2426, Apr. 2007, ISSN: 1352-2310. DOI: 10.1016/j.atmosenv.2006.10.006. (visited on 09/29/2022).

[260] Y. Tan, Y. B. Lim, K. E. Altieri, S. P. Seitzinger, and B. J. Turpin, "Mechanisms leading to oligomers and SOA through aqueous photooxidation: Insights from OH radical oxidation of acetic acid and methylglyoxal," en, *Atmospheric Chemistry and Physics*, vol. 12, no. 2, pp. 801–813, Jan. 2012, ISSN: 1680-7324. DOI: 10.5194/acp-12-801-2012. (visited on 08/14/2022).

[261] Y. Lim and B. Turpin, "Laboratory evidence of organic peroxide and peroxyhemiacetal formation in the aqueous phase and implications for aqueous oh," *Atmospheric Chemistry and Physics*, vol. 15, no. 22, pp. 12 867–12 877, 2015.

[262] R. Zhao *et al.*, "Rapid Aqueous-Phase Hydrolysis of Ester Hydroperoxides Arising from Criegee Intermediates and Organic Acids," *The Journal of Physical Chemistry A*, vol. 122, no. 23, pp. 5190–5201, Jun. 2018, ISSN: 1089-5639. DOI: 10.1021/acs.jpca.8b02195. [Online]. Available: https://doi.org/10.1021/acs.jpca.8b02195 (visited on 11/12/2021).

[263] Y. Liu *et al.*, "Aqueous phase processing of secondary organic aerosol from isoprene photooxidation," en, *Atmospheric Chemistry and Physics*, vol. 12, no. 13, pp. 5879–5895, Jul. 2012, ISSN: 1680-7324. DOI: 10.5194/acp-12-5879-2012. (visited on 11/12/2022).

[264] C. Roehl, Z Marka, J. Fry, and P. Wennberg, "Near-uv photolysis cross sections of CH_3OOH and $HOCH_2OOH$ determined via action spectroscopy," *Atmospheric Chemistry and Physics*, vol. 7, no. 3, pp. 713–720, 2007.

[265] T. Wallington, P Dagaut, and M. Kurylo, "Uv absorption cross sections and reaction kinetics and mechanisms for peroxy radicals in the gas phase," *Chemical reviews*, vol. 92, no. 4, pp. 667–710, 1992.

[266] O. Legrini, E. Oliveros, and A. M. Braun, "Photochemical processes for water treatment," *Chemical Reviews*, vol. 93, no. 2, pp. 671–698, Mar. 1993. DOI: 10.1021/cr00018a003. [Online]. Available: https://doi.org/10.1021/cr00018a003.

[267] Z. Peng and J. L. Jimenez, "Radical chemistry in oxidation flow reactors for atmospheric chemistry research," *Chemical Society Reviews*, vol. 49, no. 9, pp. 2570–2616, 2020. DOI: 10.1039/c9cs00766k. [Online]. Available: https://doi.org/10.1039/c9cs00766k.

[268] B. Noziere and L. Vereecken, "Direct Observation of Aliphatic Peroxy Radical Autoxidation and Water Effects: An Experimental and Theoretical Study," *Angewandte Chemie International Edition*, vol. 58, no. 39, pp. 13 976–13 982, 2019, ISSN: 1521-3773. DOI: 10.1002/anie.201907981.

[269] Y. Zhao, J. A. Thornton, and H. O. Pye, "Quantitative constraints on autoxidation and dimer formation from direct probing of monoterpene-derived peroxy radical chemistry," *Proceedings of the National Academy of Sciences*, vol. 115, no. 48, pp. 12 142–12 147, 2018.

[270] B. Witkowski and T. Gierczak, "*cis*- Pinonic Acid Oxidation by Hydroxyl Radicals in the Aqueous Phase under Acidic and Basic Conditions: Kinetics and Mechanism," en, *Environmental Science & Technology*, vol. 51, no. 17, pp. 9765–9773, Sep. 2017, ISSN: 0013-936X, 1520-5851. DOI: 10.1021/acs.est.7b02427. [Online]. Available: https://pubs.acs.org/doi/10.1021/acs.est.7b02427 (visited on 06/07/2020).

[271] A. L. Perkel and S. G. Voronina, "The specific features of the liquid-phase oxidation of saturated esters. Kinetics, reactivity and mechanisms of formation of destruction products," en, *Russian Chemical Bulletin*, vol. 69, no. 11, pp. 2031–2058, Nov. 2020, ISSN: 1066-5285, 1573-9171. DOI: 10.1007/s11172-020-2999-9. (visited on 12/25/2022).

[272] C. Fittschen, "The reaction of peroxy radicals with OH radicals," *Chemical Physics Letters*, vol. 725, pp. 102–108, 2019, Publisher: Elsevier.

[273] T. Arakaki *et al.*, "A General Scavenging Rate Constant for Reaction of Hydroxyl Radical with Organic Carbon in Atmospheric Waters," en, *Environmental Science & Technology*, vol. 47, no. 15, pp. 8196–8203, Aug. 2013, ISSN: 0013-936X, 1520-5851. DOI: 10.1021/es401927b. [Online]. Available: https://pubs.acs.org/doi/10.1021/es401927b (visited on 01/29/2024).

[274] I. R. Piletic and T. E. Kleindienst, "Rates and yields of unimolecular reactions producing highly oxidized peroxy radicals in the oh-induced autoxidation of α-pinene, β-pinene, and limonene," *The Journal of Physical Chemistry A*, vol. 126, no. 1, pp. 88–100, 2022.

[275] H. O. Pye *et al.*, "Anthropogenic enhancements to production of highly oxygenated molecules from autoxidation," *Proceedings of the National Academy of Sciences*, vol. 116, no. 14, pp. 6641–6646, 2019, Publisher: National Acad Sciences.

[276] Y. Chen *et al.*, "The oxidation mechanism and kinetics of limononic acid by hydroxyl radical in atmospheric aqueous phase," *Atmospheric Environment*, vol. 294, p. 119 527, 2023.

[277] B. C. Faust and J. M. Allen, "Aqueous-phase photochemical sources of peroxyl radicals and singlet molecular oxygen in clouds and fog," *Journal of Geophysical Research: Atmospheres*, vol. 97, no. D12, pp. 12 913–12 926, 1992.

[278] D. W. Gunz and M. R. Hoffmann, "Atmospheric chemistry of peroxides: A review," *Atmospheric Environment. Part A. General Topics*, vol. 24, no. 7, pp. 1601–1633, 1990.

[279] H. Li, Z. Chen, L. Huang, and D. Huang, "Organic peroxides' gas-particle partitioning and rapid heterogeneous decomposition on secondary organic aerosol," English, *Atmospheric Chemistry and Physics*, vol. 16, no. 3, pp. 1837–1848, 2016, ISSN: 16807316. DOI: http://dx.doi.org/10.5194/acp-16-1837-2016.

[280] H. Tong *et al.*, "Reactive oxygen species formed in aqueous mixtures of secondary organic aerosols and mineral dust influencing cloud chemistry and public health in the Anthropocene," en, *Faraday Discussions*, vol. 200, no. 0, pp. 251–270, Aug. 2017, ISSN: 1364-5498. DOI: 10.1039/C7FD00023E.

[281] S. Toyokuni, "Reactive oxygen species-induced molecular damage and its application in pathology," *Pathology international*, vol. 49, no. 2, pp. 91–102, 1999.

[282] A. Stapleton, "Ultraviolet Radiation and Plants: Burning Questions.," *The Plant Cell*, vol. 4, no. 11, pp. 1353–1358, Nov. 1992, ISSN: 1040-4651. (visited on 08/25/2022).

[283] C. M. Kenseth, N. J. Hafeman, Y. Huang, N. F. Dalleska, B. M. Stoltz, and J. H. Seinfeld, "Synthesis of carboxylic acid and dimer ester surrogates to constrain the abundance and distribution of molecular products in α-pinene and β-pinene secondary organic aerosol," *Environmental Science & Technology*, vol. 54, no. 20, pp. 12 829–12 839, 2020.

[284] A. Kruve, K. Kaupmees, J. Liigand, and I. Leito, "Negative electrospray ionization via deprotonation: Predicting the ionization efficiency," *Analytical chemistry*, vol. 86, no. 10, pp. 4822–4830, 2014.

[285] J Yanez, C. Sevilla, D Becker, and M. Sevilla, "Low-temperature autoxidation in unsaturated lipids: An electron spin resonance study," *Journal of Physical Chemistry*, vol. 91, no. 2, pp. 487–491, 1987.

[286] S. Mueller, H.-D. Riedel, and W. Stremmel, "Determination of Catalase Activity at Physiological Hydrogen Peroxide Concentrations," en, *Analytical Biochemistry*, vol. 245, no. 1, pp. 55–60, Feb. 1997, ISSN: 00032697. DOI: 10.1006/abio.1996.9939. [Online]. Available: https://linkinghub.elsevier.com/retrieve/pii/S000326979699939X (visited on 11/20/2020).

[287] J. Cropotova and T. Rustad, "A new fluorimetric method for simultaneous determination of lipid and protein hydroperoxides in muscle foods with the use of diphenyl-1-pyrenylphosphine (DPPP)," en, *LWT*, vol. 128, p. 109 467, Jun. 2020, ISSN: 0023-6438. DOI: 10.1016/j.lwt.2020.109467. (visited on 11/30/2021).

[288] S Brul and P Coote, "Preservative agents in foods: Mode of action and microbial resistance mechanisms," en, *International Journal of Food Microbiology*, vol. 50, no. 1, pp. 1–17, Sep. 1999, ISSN: 0168-1605. DOI: 10.1016/S0168-1605(99)00072-0. (visited on 12/06/2021).

[289] J. D. Grujic-Milanovic *et al.*, "Excesive consumption of unsaturated fatty acids leads to oxidative and inflammatory instability in Wistar rats," en, *Biomedicine & Pharmacotherapy*, vol. 139, p. 111 691, Jul. 2021, ISSN: 0753-3322. DOI: 10.1016/j.biopha.2021.111691.

[290] G. Thangavelu, M. G. Colazo, D. J. Ambrose, M. Oba, E. K. Okine, and M. K. Dyck, "Diets enriched in unsaturated fatty acids enhance early embryonic development in lactating Holstein cows," en, *Theriogenology*, vol. 68, no. 7, pp. 949–957, Oct. 2007, ISSN: 0093-691X. DOI: 10.1016/j.theriogenology.2007.07.002. (visited on 12/07/2021).

[291] E. Muro, G. E. Atilla-Gokcumen, and U. S. Eggert, "Lipids in cell biology: How can we understand them better?" *Molecular Biology of the Cell*, vol. 25, no. 12, pp. 1819–1823, Jun. 2014, ISSN: 1059-1524. DOI: 10.1091/mbc.e13-09-0516. (visited on 12/02/2021).

[292] E. Niki, Y. Yoshida, Y. Saito, and N. Noguchi, "Lipid peroxidation: Mechanisms, inhibition, and biological effects," *Biochemical and Biophysical Research Communications*, Celebrating 50 Years of Oxygenases, vol. 338, no. 1, pp. 668–676, Dec. 2005, ISSN: 0006-291X. DOI: 10.1016/j.bbrc.2005.08.072. (visited on 07/31/2019).

[293] P. Haberzettl and B. G. Hill, "Oxidized lipids activate autophagy in a JNK-dependent manner by stimulating the endoplasmic reticulum stress response," en, *Redox Biology*, vol. 1, no. 1, pp. 56–64, Jan. 2013, ISSN: 2213-2317. DOI: 10.1016/j.redox.2012.10.003. (visited on 12/07/2021).

[294] D. Pratico, "Lipid Peroxidation and the Aging Process," *Science of Aging Knowledge Environment*, vol. 2002, no. 50, re5–re5, Dec. 2002. DOI: 10.1126/sageke.2002.50.re5. [Online]. Available: https://www.science.org/doi/full/10.1126/sageke.2002.50.re5 (visited on 12/07/2021).

[295] M. M. Gaschler and B. R. Stockwell, "Lipid peroxidation in cell death," *Biochemical and biophysical research communications*, vol. 482, no. 3, pp. 419–425, Jan. 2017, ISSN: 0006-291X. DOI: 10.1016/j.bbrc.2016.10.086. (visited on 12/03/2021).

[296] M. Valko, C. J. Rhodes, J. Moncol, M. Izakovic, and M. Mazur, "Free radicals, metals and antioxidants in oxidative stress-induced cancer," en, *Chemico-Biological Interactions*, vol. 160, no. 1, pp. 1–40, Mar. 2006, ISSN: 0009-2797. DOI: 10.1016/j.cbi.2005.12.009. (visited on 12/06/2021).

[297] Y.-E. Sun, W.-D. Wang, H.-W. Chen, and C. Li, "Autoxidation of Unsaturated Lipids in Food Emulsion," en, *Critical Reviews in Food Science and Nutrition*, vol. 51, no. 5, pp. 453–466, Apr. 2011, ISSN: 1040-8398, 1549-7852. (visited on 05/11/2021).

[298] M. M. Campo, G. R. Nute, S. I. Hughes, M. Enser, J. D. Wood, and R. I. Richardson, "Flavour perception of oxidation in beef," en, *Meat Science*, vol. 72, no. 2, pp. 303–311, Feb. 2006, ISSN: 0309-1740. DOI: 10.1016/j.meatsci.2005.07.015. (visited on 12/06/2021).

[299] J. M. Diaz, S. Plummer, C. Tomas, and C. Alves-de Souza, "Production of extracellular superoxide and hydrogen peroxide by five marine species of harmful bloom-forming algae," *Journal of plankton research*, vol. 40, no. 6, pp. 667–677, 2018.

[300] C. M. Oliveira, A. C. S. Ferreira, V. De Freitas, and A. M. Silva, "Oxidation mechanisms occurring in wines," en, *Food Research International*, vol. 44, no. 5, pp. 1115–1126, Jun. 2011, ISSN: 09639969. DOI: 10.1016/j.foodres.2011.03.050. [Online]. Available: https://linkinghub.elsevier.com/retrieve/pii/S0963996911002092 (visited on 12/05/2021).

[301] P. C. Chai, L. H. Long, and B. Halliwell, "Contribution of hydrogen peroxide to the cytotoxicity of green tea and red wines," en, *Biochemical and Biophysical Research Communications*, vol. 304, no. 4, pp. 650–654, May 2003, ISSN: 0006-291X. DOI: 10.1016/S0006-291X(03)00655-7. (visited on 12/07/2021).

[302] S. Dermiş, S. Can, and B. Doğru, "Determination of peroxide values of some fixed oils by using the mfox method," *Spectroscopy Letters*, vol. 45, no. 5, pp. 359–363, 2012.

[303] M. J. Lagarda, J. G. Mañez, P. Manglano, and R. Farre, "Lipid hydroperoxides determination in milk-based infant formulae by gas chromatography," *European journal of lipid science and technology*, vol. 105, no. 7, pp. 339–345, 2003.

[304] H. Karami, M. Rasekh, and E. Mirzaee-Ghaleh, "Qualitative analysis of edible oil oxidation using an olfactory machine," *Journal of Food Measurement and Characterization*, vol. 14, no. 5, pp. 2600–2610, 2020.

[305] N. Zhang *et al.*, "Analytical methods for determining the peroxide value of edible oils: A mini-review," *Food Chemistry*, vol. 358, p. 129 834, 2021.

[306] C. Liang and B. He, "A titration method for determining individual oxidant concentration in the dual sodium persulfate and hydrogen peroxide oxidation system," *Chemosphere*, vol. 198, pp. 297–302, 2018.

[307] C. Deyrieux *et al.*, "Measurement of peroxide values in oils by triphenylphosphine/triphenylphosphine oxide (tpp/tppo) assay coupled with ftir-atr spectroscopy: Comparison with iodometric titration," *European Journal of Lipid Science and Technology*, vol. 120, no. 8, p. 1 800 109, 2018.

[308] W. W. Christie, "Lipid analysis," *Trends in Food Science & Technology*, vol. 11, no. 7, p. 145, 1996.

[309] A. O. M. Cd 8b 90, "Peroxide value Acetic Acid-Isooctane Method," *Official methods and recommended practices of the Am. Oil Chem. Soc.*, 1989, Publisher: AOCS Champaign, IL, USA.

[310] K. Yagi, "Lipid peroxides and human diseases," *Chemistry and physics of lipids*, vol. 45, no. 2-4, pp. 337–351, 1987.

[311] L. Gheysen, C. Dejonghe, T. Bernaerts, A. Van Loey, L. De Cooman, and I. Foubert, "Measuring primary lipid oxidation in food products enriched with colored microalgae," *Food Analytical Methods*, vol. 12, no. 10, pp. 2150–2160, 2019.

[312] S. Alfei, P. Oliveri, and C. Malegori, "Assessment of the efficiency of a nanospherical gallic acid dendrimer for long-term preservation of essential oils: An integrated chemometric-assisted ftir study," *ChemistrySelect*, vol. 4, no. 30, pp. 8891–8901, 2019.

[313] M. Cullere *et al.*, "Effect of the incorporation of a fermented rooibos (aspalathus linearis) extract in the manufacturing of rabbit meat patties on their physical, chemical, and sensory quality during refrigerated storage," *LWT*, vol. 108, pp. 31–38, 2019.

[314] S. Devaramani, K. S. Kumar, B. Suma, and M Pandurangappa, "Rhodamine b phenylhydrazide as a new chemosensor for sulfite quantification: Application to food samples," *Materials Today: Proceedings*, vol. 49, pp. 748–755, 2022.

[315] F. Longobardi, F. Contillo, L. Catucci, L. Tommasi, F. Caponio, and V. M. Paradiso, "Analysis of peroxide value in olive oils with an easy and green method," *Food Control*, vol. 130, p. 108 295, 2021.

[316] W. E. Gilbraith, J. C. Carter, K. L. Adams, K. S. Booksh, and J. M. Ottaway, "Improving prediction of peroxide value of edible oils using regularized regression models," *Molecules*, vol. 26, no. 23, p. 7281, 2021.

[317] M. Tareq, S. Rahman, and M. Hashem, "Effect of clove powder and garlic paste on quality and safety of raw chicken meat at refrigerated storage," *World J Nutr Food Sci*, vol. 1, no. 1, p. 1002, 2018.

[318] E. Rasinska, J. Rutkowska, E. Czarniecka-Skubina, and K. Tambor, "Effects of cooking methods on changes in fatty acids contents, lipid oxidation and volatile compounds of rabbit meat," *Lwt*, vol. 110, pp. 64–70, 2019.

[319] A. Bilska, "Effect of morus alba leaf extract dose on lipid oxidation, microbiological stability, and sensory evaluation of functional liver pâtes during refrigerated storage," *Plos one*, vol. 16, no. 12, e0260030, 2021.

[320] M. Yao *et al.*, "Multiphase reactions between secondary organic aerosol and sulfur dioxide: Kinetics and contributions to sulfate formation and aerosol aging," *Environmental Science & Technology Letters*, vol. 6, no. 12, pp. 768–774, 2019.

[321] Z. Zhao *et al.*, "Diverse reactions in highly functionalized organic aerosols during thermal desorption," *ACS Earth and Space Chemistry*, vol. 4, no. 2, pp. 283–296, 2019.

[322] S. Wang, M. Takhar, Y. Zhao, L. N. S. Al Rashdi, and A. W. H. Chan, "Dynamic Oxidative Potential of Organic Aerosol from Heated Cooking Oil," *ACS Earth and Space Chemistry*, vol. 5, no. 5, pp. 1150–1162, May 2021, Publisher: American Chemical Society. DOI: 10.1021/acsearthspacechem.1c00038. [Online]. Available: https://doi.org/10.1021/acsearthspacechem.1c00038 (visited on 11/19/2021).

[323] B. L. Deming and P. J. Ziemann, "Quantification of alkenes on indoor surfaces and implications for chemical sources and sinks," en, *Indoor Air*, vol. 30, no. 5, pp. 914–924, Sep. 2020, ISSN: 0905-6947, 1600-0668. DOI: 10.1111/ina.12662. [Online]. Available: https://onlinelibrary.wiley.com/doi/abs/10.1111/ina.12662 (visited on 12/13/2020).

[324] C. Lea, "Methods for determining peroxide in lipids," *Journal of the Science of Food and Agriculture*, vol. 3, no. 12, pp. 586–594, 1952.

[325] J. M. Gebicki, J. Collins, A. Baoutina, and P. Phair, "The Limitations of an Iodometric Aerobic Assay for Peroxides," en, *Analytical Biochemistry*, vol. 240, no. 2, pp. 235–241, Sep. 1996, ISSN: 00032697. DOI: 10.1006/abio.1996.0353. [Online]. Available: https://linkinghub.elsevier.com/retrieve/pii/S000326979690353X (visited on 02/03/2024).

[326] D. K. Banerjee and C. C. Budke, "Spectrophotometric Determination of Traces of Peroxides in Organic Solvents.," en, *Analytical Chemistry*, vol. 36, no. 4, pp. 792–796, Apr. 1964, ISSN: 0003-2700, 1520-6882. DOI: 10.1021/ac60210a027. [Online]. Available: https://pubs.acs.org/doi/abs/10.1021/ac60210a027 (visited on 06/24/2021).

[327] S. Stavber, M. Jereb, and M. Zupan, "Electrophilic Iodination of Organic Compounds Using Elemental Iodine or Iodides," en, *Synthesis*, vol. 2008, no. 10, pp. 1487–1513, May 2008, ISSN: 0039-7881, 1437-210X. DOI: 10.1055/s-2008-1067037. [Online]. Available: http://www.thieme-connect.de/DOI/DOI?10.1055/s-2008-1067037 (visited on 08/26/2021).

[328] J. E. Hunter, "N-3 fatty acids from vegetable oils," en, *The American Journal of Clinical Nutrition*, vol. 51, no. 5, pp. 809–814, May 1990, ISSN: 0002-9165, 1938-3207. DOI: 10.1093/ajcn/51.5.809. (visited on 12/08/2021).

[329] J. Chebet, T. Kinyanjui, and P. K. Cheplogoi, "Impact of frying on iodine value of vegetable oils before and after deep frying in different types of food in kenya," *Journal of Scientific and Innovative Research*, vol. 5, no. 5, pp. 193–196, 2016.

[330] E. E. Gooch, "Determination of the Iodine Value of Selected Oils: An Experiment Combining FTIR Spectroscopy with Iodometric Titrations," en, *The Chemical Educator*, vol. 6, no. 1, pp. 7–9, Feb. 2001, ISSN: 1430-4171. DOI: 10.1007/s00897000438a. [Online]. Available: http://link.springer.com/10.1007/s00897000438a (visited on 12/13/2020).

[331] Y. B. C. Man, G. Setiowaty, and F. R. v. d. Voort, "Determination of iodine value of palm oil by fourier transform infrared spectroscopy," en, *Journal of the American Oil Chemists' Society*, vol. 76, no. 6, pp. 693–699, 1999, ISSN: 1558-9331. DOI: https://doi.org/10.1007/s11746-999-0161-9. [Online]. Available: http://aocs.onlinelibrary.wiley.com/doi/abs/10.1007/s11746-999-0161-9 (visited on 12/13/2020).

[332] C.-c. Lee and B. D. Pollard, "Determination of iodine value fatty acids by a flow-injection method," en, *Analytica Chimica Acta*, vol. 158, pp. 157–167, Jan. 1984, ISSN: 0003-2670. DOI: 10.1016/S0003-2670(00)84824-2. [Online]. Available: http://www.sciencedirect.com/science/article/pii/S0003267000848242 (visited on 11/22/2020).

[333] T. Haryati, Y. B. Che Man, H. M. Ghazali, B. A. Asbi, and L. Buana, "Determination of iodine value of palm oil based on triglyceride composition," en, *Journal of the American Oil Chemists' Society*, vol. 75, no. 7, pp. 789–792, Jul. 1998, ISSN: 0003-021X, 1558-9331. DOI: 10.1007/s11746-998-0227-0. [Online]. Available: https://aocs.onlinelibrary.wiley.com/doi/10.1007/s11746-998-0227-0 (visited on 02/03/2024).

[334] M. Barsukova, I. Veselova, and T. Shekhovtsova, "Main methods and approaches to the determination of markers of oxidative stress organic peroxide compounds and hydrogen peroxide," *Journal of Analytical Chemistry*, vol. 74, no. 5, pp. 425–436, 2019.

[335] E. D. N. S. Abeyrathne, K. Nam, and D. U. Ahn, "Analytical methods for lipid oxidation and antioxidant capacity in food systems," *Antioxidants*, vol. 10, no. 10, p. 1587, 2021.

[336] R. G. Bernett, J. T. Doi, and W. K. Musker, "Iodocyclization of alkene thioethers. Kinetic evidence against an iodonium ion intermediate," en, *The Journal of Organic Chemistry*, vol. 50, no. 12, pp. 2048–2050, Jun. 1985, ISSN: 0022-3263, 1520-6904. DOI: 10.1021/jo00212a008. [Online]. Available: https://pubs.acs.org/doi/abs/10.1021/jo00212a008 (visited on 06/27/2021).

[337] S. Xu *et al.*, "Localisation of c= c bond and absolute quantification of unsaturated fatty acids in vegetable oils based on photochemical derivatisation reaction coupled with mass spectrometry," *International Journal of Food Science & Technology*, vol. 55, no. 7, pp. 2883–2892, 2020.

[338] R. Domínguez, M. Pateiro, M. Gagaoua, F. J. Barba, W. Zhang, and J. M. Lorenzo, "A comprehensive review on lipid oxidation in meat and meat products," *Antioxidants*, vol. 8, no. 10, p. 429, 2019.

[339] L. Das, D. K. Bora, S. Pradhan, M. K. Naik, and S. Naik, "Long-term storage stability of biodiesel produced from karanja oil," *Fuel*, vol. 88, no. 11, pp. 2315–2318, 2009.

[340] Ş. Altun, "Effect of the degree of unsaturation of biodiesel fuels on the exhaust emissions of a diesel power generator," *Fuel*, vol. 117, pp. 450–457, 2014.

[341] L Chuecas and J. Riley, "The component fatty acids of some sea-weed fats," *Journal of the Marine Biological Association of the United Kingdom*, vol. 46, no. 1, pp. 153–159, 1966.

[342] Z. Nitsan, Y Carasso, Z. Zoref, and I Nir, "Effect of diet on the fatty acid profile of adipose tissues and muscle fat of kids," in *Annales de zootechnie*, vol. 36, 1987, pp. 339–341.

[343] V Banskalieva, T Sahlu, and A. Goetsch, "Fatty acid composition of goat muscles and fat depots: A review," *Small Ruminant Research*, vol. 37, no. 3, pp. 255–268, 2000.

[344] D. Ray and D. Waddington, "Gas phase oxidation of alkenes Part II. The oxidation of 2-methylbutene-2 and 2,3-dimethylbutene-2," en, *Combustion and Flame*, vol. 20, no. 3, pp. 327–334, Jun. 1973, ISSN: 00102180. (visited on 12/06/2021).

[345] L.-Y. He *et al.*, "Characterization of high-resolution aerosol mass spectra of primary organic aerosol emissions from Chinese cooking and biomass burning," en, *Atmospheric Chemistry and Physics*, vol. 10, no. 23, pp. 11 535–11 543, Dec. 2010, ISSN: 1680-7324. DOI: 10.5194/acp-10-11535-2010. [Online]. Available: https://acp.copernicus.org/articles/10/11535/2010/ (visited on 08/26/2021).

[346] X. Zhao *et al.*, "Composition profiles of organic aerosols from Chinese residential cooking: Case study in urban Guangzhou, south China," en, *Journal of Atmospheric Chemistry*, vol. 72, no. 1, pp. 1–18, Mar. 2015, ISSN: 0167-7764, 1573-0662. DOI: 10.1007/s10874-015-9298-0. (visited on 08/26/2021).

[347] Y. Zhao, M. Hu, S. Slanina, and Y. Zhang, "Chemical Compositions of Fine Particulate Organic Matter Emitted from Chinese Cooking," *Environmental Science & Technology*, vol. 41, no. 1, pp. 99–105, Jan. 2007, ISSN: 0013-936X. DOI: 10.1021/es0614518. [Online]. Available: https://doi.org/10.1021/es0614518 (visited on 08/26/2021).

[348] B. Bhowmik, G. L. Jendrasiak, and B. Rosenberg, "Charge Transfer Complexes of Lipids with Iodine," en, *Nature*, vol. 215, no. 5103, pp. 842–843, Aug. 1967, ISSN: 0028-0836, 1476-4687. DOI: 10.1038/215842a0. (visited on 12/03/2021).

[349] W. Jessup, R. T. Dean, and J. M. Gebicki, "[29] Iodometric determination of hydroperoxides in lipids and proteins," en, in *Methods in Enzymology*, vol. 233, Elsevier, 1994, pp. 289–303, ISBN: 978-0-12-182134-0. DOI: 10.1016/S0076-6879(94)33032-8. [Online]. Available: https://linkinghub.elsevier.com/retrieve/pii/S0076687994330328 (visited on 11/22/2020).

[350] Y. Endo, "Analytical methods to evaluate the quality of edible fats and oils: The jocs standard methods for analysis of fats, oils and related materials (2013) and advanced methods," *Journal of oleo science*, vol. 67, no. 1, pp. 1–10, 2018.

[351] S. Yu, "Role of organic acids (formic, acetic, pyruvic and oxalic) in the formation of cloud condensation nuclei (CCN): A review," en, *Atmospheric Research*, vol. 53, no. 4, pp. 185–217, May 2000, ISSN: 0169-8095. DOI: 10.1016/S0169-8095(00)00037-5. (visited on 12/12/2021).

[352] A. D. Awtrey and R. E. Connick, "The Absorption Spectra of I_2 , I_3^- , I^- , IO_3^-," en, *Journal of the American Chemical Society*, vol. 73, no. 4, pp. 1842–1843, Apr. 1951, ISSN: 0002-7863, 1520-5126. DOI: 10.1021/ja01148a504.

[353] L. Hartman and M. D. White, "Reagents for iodometric determination of peroxides in fats," *Analytical Chemistry*, vol. 24, no. 3, pp. 527–529, 1952.

[354] P. Ratrinia, U. Komala, *et al.*, "The effect of addition mangrove leaves powder to lipid oxidation of chocolate bar during the shelf life," in *IOP Conference Series: Earth and Environmental Science*, IOP Publishing, vol. 967, 2022, p. 012 023.

[355] B. Lei, N. Adachi, and T. Arai, "Measurement of the extracellular H_2O_2 in the brain by microdialysis," en, *Brain Research Protocols*, vol. 3, no. 1, pp. 33–36, Sep. 1998, ISSN: 1385-299X. DOI: 10.1016/S1385-299X(98)00018-X. (visited on 11/28/2021).

[356] H. Yu, L. Jin, Y. Dai, H. Li, and Y. Xiao, "From a BODIPY rhodamine scaffold to a ratiometric fluorescent probe for nitric oxide," en, *New Journal of Chemistry*, vol. 37, no. 6, p. 1688, 2013, ISSN: 1144-0546, 1369-9261. DOI: 10.1039/c3nj41127c.

[357] K. Sato, S. Hatakeyama, and T. Imamura, "Secondary Organic Aerosol Formation during the Photooxidation of Toluene, NO_x Dependence of Chemical Composition," *The Journal of Physical Chemistry A*, vol. 111, no. 39, pp. 9796–9808, Oct. 2007, ISSN: 1089-5639. DOI: 10.1021/jp071419f.

[358] M. J. Calandra, Y. Wang, and C. Beckett, "Iodide reaction times of peroxyhemiacetals (phas) in the peroxide value titration; implications for the testing of citrus oils," *Flavour and Fragrance Journal*, vol. 35, no. 2, pp. 131–138, 2020.

[359] A. Lezerovich, "Determination of peroxide value by conventional difference and difference-derivative spectrophotometry," *Journal of the American Oil Chemists Society*, vol. 62, no. 10, pp. 1495–1500, 1985.

[360] G. Martinez Tellez, O. Ledea Lozano, and M. F. Díaz Gómez, "Measurement of peroxidic species in ozonized sunflower oil," *Ozone: Science and Engineering*, vol. 28, no. 3, pp. 181–185, 2006.

[361] M. Cirlini, A Caligiani, G Palla, A De Ascentiis, and P Tortini, "Stability studies of ozonized sunflower oil and enriched cosmetics with a dedicated peroxide value determination," *Ozone: Science & Engineering*, vol. 34, no. 4, pp. 293–299, 2012.

[362] S. A. Epstein, D. Shemesh, V. T. Tran, S. A. Nizkorodov, and R. B. Gerber, "Absorption Spectra and Photolysis of Methyl Peroxide in Liquid and Frozen Water," en, *The Journal of Physical Chemistry A*, vol. 116, no. 24, pp. 6068–6077, Jun. 2012, ISSN: 1089-5639, 1520-5215. DOI: 10.1021/jp211304v. [Online]. Available: https://pubs.acs.org/doi/10.1021/jp211304v (visited on 07/05/2021).

[363] C. J. Battaglia, "Kinetics and Mechanism of the Spontaneous Decompositions of Some Peroxoacids, Hydrogen Peroxide and tert-Butyl Hydroperoxide," en, vol. 85, p. 6, 1963.

[364] H. Hartley and N. P. Campbell, "LXIX The solubility of iodine in water," en, *J. Chem. Soc., Trans.*, vol. 93, no. 0, pp. 741–745, 1908, ISSN: 0368-1645. DOI: 10.1039/CT9089300741. (visited on 04/23/2021).

[365] T. A. Foglia, L. S. Silbert, and P. D. Vail, "XII.* Gas-liquid and high-performance liquid chromatographic analysis of aliphatic hydroperoxides and dialkyl peroxides," en, p. 9, 1993.

[366] J. Sanchez and T. N. Myers, "Peroxides and Peroxide Compounds, Organic Peroxides," en, in *Kirk-Othmer Encyclopedia of Chemical Technology*, 2000, ISBN: 978-0-471-23896-6. DOI: 10.1002/0471238961.1518070119011403.a01.

[367] M. Shiraiwa *et al.*, "Aerosol Health Effects from Molecular to Global Scales," *Environmental Science & Technology*, vol. 51, no. 23, pp. 13 545–13 567, Dec. 2017, ISSN: 0013-936X. DOI: 10.1021/acs.est.7b04417. [Online]. Available: https://doi.org/10.1021/acs.est.7b04417 (visited on 09/27/2019).

[368] X. Zhang *et al.*, "Highly Oxygenated Multifunctional Compounds in α-Pinene Secondary Organic Aerosol," *Environmental Science & Technology*, vol. 51, no. 11, pp. 5932–5940, Jun. 2017, ISSN: 0013-936X. DOI: 10.1021/acs.est.6b06588. (visited on 08/15/2019).

[369] I. V. Bodrikov, Y. A. Kurskii, A. A. Chiyanov, N. V. Borisova, and A. Y. Subbotin, "Sterically driven allyl substitution in alkenes with electrophilic iodine," en, *Doklady Chemistry*, vol. 450, no. 2, pp. 162–164, Jun. 2013, ISSN: 0012-5008, 1608-3113. DOI: 10.1134/S0012500813060049. [Online]. Available: http://link.springer.com/10.1134/S0012500813060049 (visited on 07/26/2021).

[370] A. N. French, S. Bissmire, and T. Wirth, "Iodine electrophiles in stereoselective reactions: Recent developments and synthetic applications," en, *Chemical Society Reviews*, vol. 33, no. 6, pp. 354–362, 2004. DOI: 10.1039/B310389G. [Online]. Available: http://pubs.rsc.org/en/content/articlelanding/2004/cs/b310389g (visited on 03/19/2021).

[371] Z. Z. Song and H. N. C. Wong, "4-disubstituted furans, 5. Regiospecific mono-ipso-iodination of 3,4-bis(trimethylsilyl)furan and regiospecific ipso-iodination of tris[(4-alkyl- or -aryl)furan-3-yl]boroxines to 4-substituted 3-(trimethylsilyl)furans and unsymmetrical, 3,4-disubstituted furans," en, *Liebigs Annalen der Chemie*, vol. 1994, no. 1, pp. 29–34, 1994, ISSN: 1099-0690. DOI: 10.1002/jlac.199419940107. (visited on 12/09/2021).

[372] M. Mochida, N. Umemoto, K. Kawamura, H.-J. Lim, and B. J. Turpin, "Bimodal size distributions of various organic acids and fatty acids in the marine atmosphere: Influence of anthropogenic aerosols, asian dusts, and sea spray off the coast of east asia," *Journal of Geophysical Research: Atmospheres*, vol. 112, no. D15, 2007.

[373] M. Mochida *et al.*, "Spatial distributions of oxygenated organic compounds (dicarboxylic acids, fatty acids, and levoglucosan) in marine aerosols over the western pacific and off the coast of east asia: Continental outflow of organic aerosols during the ace-asia campaign," *Journal of Geophysical Research: Atmospheres*, vol. 108, no. D23, 2003.

[374] V Guarrasi, M. Mangione, V Sanfratello, V Martorana, and D Bulone, "Quantification of underivatized fatty acids from vegetable oils by hplc with uv detection," *Journal of chromatographic science*, vol. 48, no. 8, pp. 663–668, 2010.

[375] G Mourente and D. Tocher, "Lipid class and fatty acid composition of brain lipids from atlantic herring (clupea harengus) at different stages of development," *Marine Biology*, vol. 112, no. 4, pp. 553–558, 1992.

[376] G. D. Smith, E. Woods, C. L. DeForest, T. Baer, and R. E. Miller, "Reactive Uptake of Ozone by Oleic Acid Aerosol Particles: Application of Single-Particle Mass Spectrometry to Heterogeneous Reaction Kinetics," en, *The Journal of Physical Chemistry A*, vol. 106, no. 35, pp. 8085–8095, Sep. 2002, ISSN: 1089-5639, 1520-5215. DOI: 10.1021/jp020527t. [Online]. Available: https://pubs.acs.org/doi/10.1021/jp020527t (visited on 06/30/2021).

[377] A. Limbeck and H. Puxbaum, "Organic acids in continental background aerosols," *Atmospheric Environment*, vol. 33, no. 12, pp. 1847–1852, 1999.

[378] C. Weschler, "Chemistry in indoor environments: 20 years of research," *Indoor Air*, vol. 21, no. 3, pp. 205–218, 2011.

[379] J. Kang, J. Liu, and J. Pei, "The indoor volatile organic compound (voc) characteristics and source identification in a new university campus in tianjin, china," *Journal of the Air Waste Management Association*, vol. 67, no. 6, pp. 725–737, 2017.

[380] S. Z. He *et al.*, "Measurement of atmospheric hydrogen peroxide and organic peroxides in Beijing before and during the 2008 Olympic Games: Chemical and physical factors influencing their concentrations," en, *Journal of Geophysical Research: Atmospheres*, vol. 115, no. D17, 2010, ISSN: 2156-2202. DOI: 10.1029/2009JD013544. [Online]. Available: https://agupubs.onlinelibrary.wiley.com/doi/abs/10.1029/2009JD013544 (visited on 05/23/2019).

[381] H. R. Katragadda, A. Fullana, S. Sidhu, and Á. A. Carbonell-Barrachina, "Emissions of volatile aldehydes from heated cooking oils," *Food Chemistry*, vol. 120, no. 1, pp. 59–65, 2010.

[382] A. Kamal-Eldin and R. Andersson, "A multivariate study of the correlation between tocopherol content and fatty acid composition in vegetable oils," *Journal of the American Oil Chemists' Society*, vol. 74, no. 4, pp. 375–380, 1997.

[383] V. Mureşan *et al.*, "Determination of peroxide value in sunflower halva using a spectrophotometric method," *Bulletin UASVM Agriculture*, vol. 67, no. 2, pp. 334–339, 2010.

[384] T. Gutfinger, M. Peled, and A. Letan, "Iodometric determination of the peroxide value of edible oils," *Journal of the Association of Official Analytical Chemists*, vol. 59, no. 1, pp. 148–152, 1976.

[385] H. Mozaffari, E. Daneshzad, B. Larijani, N. Bellissimo, and L. Azadbakht, "Dietary intake of fish, n-3 polyunsaturated fatty acids, and risk of inflammatory bowel disease: A systematic review and meta-analysis of observational studies," *European Journal of Nutrition*, vol. 59, no. 1, pp. 1–17, 2020.

[386] H Mozaffari, K Djafarian, M. Mofrad, and S Shab-Bidar, "Dietary fat, saturated fatty acid, and monounsaturated fatty acid intakes and risk of bone fracture: A systematic review and meta-analysis of observational studies," *Osteoporosis International*, vol. 29, no. 9, pp. 1949–1961, 2018.

[387] K.-H. Kim, E. Kabir, and S. Kabir, "A review on the human health impact of airborne particulate matter," *Environment international*, vol. 74, pp. 136–143, 2015.

[388] J. Wu *et al.*, "Aerosol–photolysis interaction reduces particulate matter during wintertime haze events," *Proceedings of the National Academy of Sciences*, vol. 117, no. 18, pp. 9755–9761, 2020.

[389] U. Poschl, "Atmospheric Aerosols: Composition, Transformation, Climate and Health Effects," *Angewandte Chemie International Edition*, vol. 44, no. 46, pp. 7520–7540, Nov. 2005, ISSN: 1433-7851. DOI: 10.1002/anie.200501122.

[390] E. J. Boone *et al.*, "Aqueous Processing of Atmospheric Organic Particles in Cloud Water Collected via Aircraft Sampling," en, *Environmental Science & Technology*, vol. 49, no. 14, pp. 8523–8530, Jul. 2015, ISSN: 0013-936X, 1520-5851. DOI: 10.1021/acs.est.5b01639. [Online]. Available: https://pubs.acs.org/doi/10.1021/acs.est.5b01639 (visited on 09/17/2023).

[391] Y. Huang *et al.*, "Quantification of global primary emissions of pm2. 5, pm10, and tsp from combustion and industrial process sources," *Environmental science & technology*, vol. 48, no. 23, pp. 13 834–13 843, 2014.

[392] J. L. Jimenez *et al.*, "Evolution of organic aerosols in the atmosphere," *science*, vol. 326, no. 5959, pp. 1525–1529, 2009.

[393] M. Bilde *et al.*, "Saturation Vapor Pressures and Transition Enthalpies of Low-Volatility Organic Molecules of Atmospheric Relevance: From Dicarboxylic Acids to Complex Mixtures," en, *Chemical Reviews*, vol. 115, no. 10, pp. 4115–4156, May 2015, ISSN: 0009-2665, 1520-6890. DOI: 10.1021/cr5005502. [Online]. Available: https://pubs.acs.org/doi/10.1021/cr5005502.

[394] M Kanakidou *et al.*, "Organic aerosol and global climate modelling: A review," en, *Atmos. Chem. Phys.*, p. 71, 2005.

[395] J. Duplissy *et al.*, "Relating hygroscopicity and composition of organic aerosol particulate matter," en, *Atmospheric Chemistry and Physics*, vol. 11, no. 3, pp. 1155–1165, Feb. 2011, ISSN: 1680-7324. DOI: 10.5194/acp-11-1155-2011. [Online]. Available: https://acp.copernicus.org/articles/11/1155/2011/.

[396] X. Liu and J. Wang, "How important is organic aerosol hygroscopicity to aerosol indirect forcing?" *Environmental Research Letters*, vol. 5, no. 4, p. 044 010, 2010.

[397] A Asa-Awuku, G. Engelhart, B. Lee, S. N. Pandis, and A. Nenes, "Relating ccn activity, volatility, and droplet growth kinetics of β-caryophyllene secondary organic aerosol," *Atmospheric Chemistry and Physics*, vol. 9, no. 3, pp. 795–812, 2009.

[398] T. Han *et al.*, "Role of secondary aerosols in haze formation in summer in the megacity beijing," *Journal of environmental sciences*, vol. 31, pp. 51–60, 2015.

[399] M. Camredon, B. Aumont, J. Lee-Taylor, and S. Madronich, "The soa/voc/no$_x$ system: An explicit model of secondary organic aerosol formation," en, *Atmospheric Chemistry and Physics*, vol. 7, no. 21, pp. 5599–5610, Nov. 2007, ISSN: 1680-7324. DOI: 10.5194/acp-7-5599-2007.

[400] E. U. Emanuelsson *et al.*, "Formation of anthropogenic secondary organic aerosol (SOA) and its influence on biogenic SOA properties," en, *Atmospheric Chemistry and Physics*, vol. 13, no. 5, pp. 2837–2855, Mar. 2013, ISSN: 1680-7324. DOI: 10.5194/acp-13-2837-2013.

[401] L. Wu, X. Wang, S. Lu, M. Shao, and Z. Ling, "Emission inventory of semi-volatile and intermediate-volatility organic compounds and their effects on secondary organic aerosol over the Pearl River Delta region," en, *Atmospheric Chemistry and Physics*, vol. 19, no. 12, pp. 8141–8161, Jun. 2019, ISSN: 1680-7324. DOI: 10.5194/acp-19-8141-2019. [Online]. Available: https://acp.copernicus.org/articles/19/8141/2019/ (visited on 09/17/2023).

[402] S. Tao *et al.*, "Molecular Characterization of Organosulfates in Organic Aerosols from Shanghai and Los Angeles Urban Areas by Nanospray-Desorption Electrospray Ionization High-Resolution Mass Spectrometry," en, *Environmental Science & Technology*, vol. 48, no. 18, pp. 10 993–11 001, Sep. 2014, ISSN: 0013-936X, 1520-5851. DOI: 10.1021/es5024674. (visited on 09/17/2023).

[403] Y. Wang, R. Tong, and J. Z. Yu, "Chemical Synthesis of Multifunctional Air Pollutants: Terpene-Derived Nitrooxy Organosulfates," en, *Environmental Science & Technology*, vol. 55, no. 13, pp. 8573–8582, Jul. 2021, ISSN: 0013-936X, 1520-5851. DOI: 10.1021/acs.est.1c00348. [Online]. Available: https://pubs.acs.org/doi/10.1021/acs.est.1c00348 (visited on 09/17/2023).

[404] Y. Zhao, A. G. Hallar, and L. R. Mazzoleni, "Atmospheric organic matter in clouds: Exact masses and molecular formula identification using ultrahigh-resolution FT-ICR mass spectrometry," en, *Atmospheric Chemistry and Physics*, vol. 13, no. 24, pp. 12 343–12 362, Dec. 2013, ISSN: 1680-7324. DOI: 10.5194/acp-13-12343-2013. [Online]. Available: https://acp.copernicus.org/articles/13/12343/2013/.

[405] C. Ning *et al.*, "Molecular characterization of dissolved organic matters in winter atmospheric fine particulate matters (PM2.5) from a coastal city of northeast China," en, *Science of The Total Environment*, vol. 689, pp. 312–321, Nov. 2019, ISSN: 00489697. DOI: 10.1016/j.scitotenv.2019.06.418.

[406] K. S. Hu, A. I. Darer, and M. J. Elrod, "Thermodynamics and kinetics of the hydrolysis of atmospherically relevant organonitrates and organosulfates," en, *Atmospheric Chemistry and Physics*, vol. 11, no. 16, pp. 8307–8320, Aug. 2011, ISSN: 1680-7324. DOI: 10.5194/acp-11-8307-2011. [Online]. Available: https://acp.copernicus.org/articles/11/8307/2011/ (visited on 09/17/2023).

[407] B. H. Lee *et al.*, "Highly functionalized organic nitrates in the southeast united states: Contribution to secondary organic aerosol and reactive nitrogen budgets," *Proceedings of the National Academy of Sciences*, vol. 113, no. 6, pp. 1516–1521, 2016.

[408] M. Thoma, F. Bachmeier, F. L. Gottwald, M. Simon, and A. L. Vogel, "Mass spectrometry-based aerosolomics: A new approach to resolve sources, composition, and partitioning of secondary organic aerosol," *Atmospheric Measurement Techniques*, vol. 15, no. 23, pp. 7137–7154, 2022.

[409] K. A. Pratt, M. N. Fiddler, P. B. Shepson, A. G. Carlton, and J. D. Surratt, "Organosulfates in cloud water above the Ozarks' isoprene source region," en, *Atmospheric Environment*, vol. 77, pp. 231–238, Oct. 2013, ISSN: 13522310. DOI: 10.1016/j.atmosenv.2013.05.011. (visited on 10/01/2023).

[410] D. A. Day, S. Liu, L. M. Russell, and P. J. Ziemann, "Organonitrate group concentrations in submicron particles with high nitrate and organic fractions in coastal southern California," en, *Atmospheric Environment*, vol. 44, no. 16, pp. 1970–1979, May 2010, ISSN: 13522310. DOI: 10.1016/j.atmosenv.2010.02.045. (visited on 10/01/2023).

[411] Q. T. Nguyen *et al.*, "Understanding the anthropogenic influence on formation of biogenic secondary organic aerosols in Denmark via analysis of organosulfates and related oxidation products," en, *Atmospheric Chemistry and Physics*, vol. 14, no. 17, pp. 8961–8981, Sep. 2014, ISSN: 1680-7324. DOI: 10.5194/acp-14-8961-2014.

[412] J. D. Surratt *et al.*, "Evidence for Organosulfates in Secondary Organic Aerosol," en, *Environmental Science & Technology*, vol. 41, no. 2, pp. 517–527, Jan. 2007, ISSN: 0013-936X, 1520-5851. DOI: 10.1021/es062081q. [Online]. Available: https://pubs.acs.org/doi/10.1021/es062081q (visited on 09/17/2023).

[413] Y. Gomez-Gonzalez *et al.*, "Chemical characterisation of atmospheric aerosols during a 2007 summer field campaign at Brasschaat, Belgium: Sources and source processes of biogenic secondary organic aerosol," en, *Atmospheric Chemistry and Physics*, vol. 12, no. 1, pp. 125–138, Jan. 2012, ISSN: 1680-7324. DOI: 10.5194/acp-12-125-2012. (visited on 10/01/2023).

[414] K. Kristensen and M. Glasius, "Organosulfates and oxidation products from biogenic hydrocarbons in fine aerosols from a forest in North West Europe during spring," en, *Atmospheric Environment*, vol. 45, no. 27, pp. 4546–4556, Sep. 2011, ISSN: 13522310. DOI: 10.1016/j.atmosenv.2011.05.063. [Online]. Available: https://linkinghub.elsevier.com/retrieve/pii/S1352231011005802.

[415] D. R. Worton *et al.*, "Origins and composition of fine atmospheric carbonaceous aerosol in the Sierra Nevada Mountains, California," en, *Atmospheric Chemistry and Physics*, vol. 11, no. 19, pp. 10 219–10 241, Oct. 2011, ISSN: 1680-7324. DOI: 10.5194/acp-11-10219-2011. (visited on 11/26/2023).

[416] H. Lukacs, A. Gelencser, A. Hoffer, G. Kiss, K. Horvath, and Z. Hartyani, "Quantitative assessment of organosulfates in size-segregated rural fine aerosol," en, *Atmospheric Chemistry and Physics*, vol. 9, no. 1, pp. 231–238, Jan. 2009, ISSN: 1680-7324. DOI: 10.5194/acp-9-231-2009.

[417] M. P. Tolocka and B. Turpin, "Contribution of Organosulfur Compounds to Organic Aerosol Mass," en, *Environmental Science & Technology*, vol. 46, no. 15, pp. 7978–7983, Aug. 2012, ISSN: 0013-936X, 1520-5851. DOI: 10.1021/es300651v. [Online]. Available: https://pubs.acs.org/doi/10.1021/es300651v.

[418] B. R. Ayres *et al.*, "Organic nitrate aerosol formation via NO_3 + biogenic volatile organic compounds in the southeastern United States," en, *Atmospheric Chemistry and Physics*, vol. 15, no. 23, pp. 13 377–13 392, Dec. 2015, ISSN: 1680-7324. DOI: 10.5194/acp-15-13377-2015.

[419] L. Xu, S. Suresh, H. Guo, R. J. Weber, and N. L. Ng, "Aerosol characterization over the southeastern United States using high-resolution aerosol mass spectrometry: Spatial and seasonal variation of aerosol composition and sources with a focus on organic nitrates," en, *Atmospheric Chemistry and Physics*, vol. 15, no. 13, pp. 7307–7336, Jul. 2015, ISSN: 1680-7324. DOI: 10.5194/acp-15-7307-2015.

[420] Y. Wang *et al.*, "Organosulfates in atmospheric aerosols in Shanghai, China: Seasonal and interannual variability, origin, and formation mechanisms," en, *Atmospheric Chemistry and Physics*, vol. 21, no. 4, pp. 2959–2980, Feb. 2021, ISSN: 1680-7324. DOI: 10.5194/acp-21-2959-2021. [Online]. Available: https://acp.copernicus.org/articles/21/2959/2021/.

[421] J. C. Ditto, T. Joo, J. H. Slade, P. B. Shepson, N. L. Ng, and D. R. Gentner, "Nontargeted Tandem Mass Spectrometry Analysis Reveals Diversity and Variability in Aerosol Functional Groups across Multiple Sites, Seasons, and Times of Day," en, *Environmental Science & Technology Letters*, vol. 7, no. 2, pp. 60–69, Feb. 2020, ISSN: 2328-8930, 2328-8930. DOI: 10.1021/acs.estlett.9b00702. [Online]. Available: https://pubs.acs.org/doi/10.1021/acs.estlett.9b00702 (visited on 11/26/2023).

[422] Y. Ma, X. Xu, W. Song, F. Geng, and L. Wang, "Seasonal and diurnal variations of particulate organosulfates in urban Shanghai, China," en, *Atmospheric Environment*, vol. 85, pp. 152–160, Mar. 2014, ISSN: 13522310. DOI: 10.1016/j.atmosenv.2013.12.017.

[423] S. Kundu, T. A. Quraishi, G. Yu, C. Suarez, F. N. Keutsch, and E. A. Stone, "Evidence and quantitation of aromatic organosulfates in ambient aerosols in Lahore, Pakistan," en, *Atmospheric Chemistry and Physics*, vol. 13, no. 9, pp. 4865–4875, May 2013, ISSN: 1680-7324. DOI: 10.5194/acp-13-4865-2013.

[Online]. Available: https://acp.copernicus.org/articles/13/4865/2013/ (visited on 09/17/2023).

[424] E. A. Stone, L. Yang, L. E. Yu, and M. Rupakheti, "Characterization of organosulfates in atmospheric aerosols at Four Asian locations," en, *Atmospheric Environment*, vol. 47, pp. 323–329, Feb. 2012, ISSN: 13522310. DOI: 10.1016/j.atmosenv.2011.10.058. [Online]. Available: https://linkinghub.elsevier.com/retrieve/pii/S1352231011011514 (visited on 09/17/2023).

[425] A. I. Darer, N. C. Cole-Filipiak, A. E. O Connor, and M. J. Elrod, "Formation and Stability of Atmospherically Relevant Isoprene Derived Organosulfates and Organonitrates," en, *Environmental Science & Technology*, vol. 45, no. 5, pp. 1895–1902, Mar. 2011, ISSN: 0013-936X, 1520-5851. DOI: 10.1021/es103797z.

[426] M. Riva, T. Da Silva Barbosa, Y.-H. Lin, E. A. Stone, A. Gold, and J. D. Surratt, "Chemical characterization of organosulfates in secondary organic aerosol-derived from the photooxidation of alkanes," en, *Atmospheric Chemistry and Physics*, vol. 16, no. 17, pp. 11 001–11 018, Sep. 2016, ISSN: 1680-7324. DOI: 10.5194/acp-16-11001-2016. (visited on 11/26/2023).

[427] M. Le Breton *et al.*, "Online gas- and particle-phase measurements of organosulfates, organosulfonates and nitrooxy organosulfates in Beijing utilizing a FIGAERO ToF-CIMS," en, *Atmospheric Chemistry and Physics*, vol. 18, no. 14, pp. 10 355–10 371, Jul. 2018, ISSN: 1680-7324. DOI: 10.5194/acp-18-10355-2018. [Online]. Available: https://acp.copernicus.org/articles/18/10355/2018/.

[428] J. Shang *et al.*, "SO_2 Uptake on Oleic Acid: A New Formation Pathway of Organosulfur Compounds in the Atmosphere," en, *Environmental Science & Technology Letters*, vol. 3, no. 2, pp. 67–72, Feb. 2016, ISSN: 2328-8930, 2328-8930. DOI: 10.1021/acs.estlett.6b00006. [Online]. Available: https://pubs.acs.org/doi/10.1021/acs.estlett.6b00006.

[429] M. Passananti *et al.*, "Organosulfate Formation through the Heterogeneous Reaction of SO_2 with Unsaturated Fatty Acids and Long Chain Alkenes," en, *Angewandte Chemie International Edition*, vol. 55, no. 35, pp. 10 336–10 339, Aug. 2016, ISSN: 1433-7851, 1521-3773. DOI: 10.1002/anie.201605266.

[430] M. Zhu *et al.*, "Organosulfur Compounds Formed from Heterogeneous Reaction between SO_2 and Particulate Bound Unsaturated Fatty Acids in Ambient Air," en, *Environmental Science & Technology Letters*, vol. 6, no. 6, pp. 318–322, Jun. 2019, ISSN: 2328-8930, 2328-8930. DOI: 10.1021/acs.estlett.9b00218.

[431] D. J. Bryant *et al.*, "Importance of Oxidants and Temperature in the Formation of Biogenic Organosulfates and Nitrooxy Organosulfates," en, *ACS Earth and Space Chemistry*, vol. 5, no. 9, pp. 2291–2306, Sep. 2021, ISSN: 2472-3452, 2472-3452. DOI: 10.1021/acsearthspacechem.1c00204. [Online]. Available: https://pubs.acs.org/doi/10.1021/acsearthspacechem.1c00204.

[432] C. Ning, Y. Gao, H. Zhang, H. Yu, R. Cao, and J. Chen, "Urban particulate water-soluble organic matter in winter: Size-resolved molecular characterization, role of the S-containing compounds on haze formation," en, *Science of The Total Environment*, vol. 875, p. 162 657, Jun. 2023, ISSN: 00489697. DOI: 10.1016/j.scitotenv.2023.162657.

[433] B. Friedman, P. Brophy, W. H. Brune, and D. K. Farmer, "Anthropogenic Sulfur Perturbations on Biogenic Oxidation: SO_2 Additions Impact Gas Phase OH Oxidation Products of α- and β-Pinene," en, *Environmental Science & Technology*, vol. 50, no. 3, pp. 1269–1279, Feb. 2016, ISSN: 0013-936X, 1520-5851. DOI: 10.1021/acs.est.5b05010.

[434] W. Huang *et al.*, "Exploring the inorganic and organic nitrate aerosol formation regimes at a suburban site on the North China Plain," en, *Science of The Total Environment*, vol. 768, p. 144 538, May 2021, ISSN: 00489697. DOI: 10.1016/j.scitotenv.2020.144538.

[435] W. Huang *et al.*, "Size Dependent Nighttime Formation of Particulate Secondary Organic Nitrates in Urban Air," en, *Journal of Geophysical Research: Atmospheres*, vol. 128, no. 18, e2022JD038189, Sep. 2023, ISSN: 2169-897X, 2169-8996. DOI: 10.1029/2022JD038189.

[436] B. Ervens, "Modeling the processing of aerosol and trace gases in clouds and fogs," *Chemical reviews*, vol. 115, no. 10, pp. 4157–4198, 2015.

[437] J. Liao *et al.*, "Airborne measurements of organosulfates over the continental U.S.," en, *Journal of Geophysical Research: Atmospheres*, vol. 120, no. 7, pp. 2990–3005, Apr. 2015, ISSN: 2169-897X, 2169-8996. DOI: 10.1002/2014JD022378. [Online]. Available: https://agupubs.onlinelibrary.wiley.com/doi/10.1002/2014JD022378 (visited on 09/17/2023).

[438] G. Duporte *et al.*, "Experimental Study of the Formation of Organosulfates from α-Pinene Oxidation. Part I: Product Identification, Formation Mechanisms and Effect of Relative Humidity," en, *The Journal of Physical Chemistry A*, vol. 120, no. 40, pp. 7909–7923, Oct. 2016, ISSN: 1089-5639, 1520-5215. DOI: 10.1021/acs.jpca.6b08504.

[439] L. Xu, N. T. Tsona, and L. Du, "Relative Humidity Changes the Role of SO_2 in Biogenic Secondary Organic Aerosol Formation," en, *The Journal of Physical Chemistry Letters*, vol. 12, no. 30, pp. 7365–7372, Aug. 2021, ISSN: 1948-7185, 1948-7185. DOI: 10.1021/acs.jpclett.1c01550. [Online]. Available: https://pubs.acs.org/doi/10.1021/acs.jpclett.1c01550.

[440] A. L. Vogel *et al.*, "Aerosol Chemistry Resolved by Mass Spectrometry: Linking Field Measurements of Cloud Condensation Nuclei Activity to Organic Aerosol Composition," en, *Environmental Science & Technology*, vol. 50, no. 20, pp. 10 823–10 832, Oct. 2016, ISSN: 0013-936X, 1520-5851. DOI: 10.1021/acs.est.6b01675. [Online]. Available: https://pubs.acs.org/doi/10.1021/acs.est.6b01675.

[441] L. Guo *et al.*, "Comprehensive characterization of hygroscopic properties of methanesulfonates," *Atmospheric Environment*, vol. 224, p. 117 349, 2020.

[442] B. H. Lee *et al.*, "Highly functionalized organic nitrates in the southeast United States: Contribution to secondary organic aerosol and reactive nitrogen budgets," *Proceedings of the National Academy of Sciences*, vol. 113, no. 6, pp. 1516–1521, 2016, Publisher: National Acad Sciences.

[443] J. G. Slowik *et al.*, "Characterization of a large biogenic secondary organic aerosol event from eastern Canadian forests," en, *Atmospheric Chemistry and Physics*, vol. 10, no. 6, pp. 2825–2845, Mar. 2010, ISSN: 1680-7324. DOI: 10.5194/acp-10-2825-2010. [Online]. Available: https://acp.copernicus.org/articles/10/2825/2010/.

[444] E. Freney *et al.*, "Aerosol composition and the contribution of SOA formation over Mediterranean forests," en, *Atmospheric Chemistry and Physics*, vol. 18, no. 10, pp. 7041–7056, May 2018, ISSN: 1680-7324. DOI: 10.5194/acp-18-7041-2018. [Online]. Available: https://acp.copernicus.org/articles/18/7041/2018/.

[445] G. W. Vandergrift, A. S. M. Shawon, D. N. Dexheimer, M. A. Zawadowicz, F. Mei, and S. China, "Molecular Characterization of Organosulfate-Dominated Aerosols over Agricultural Fields from the Southern Great Plains by High-Resolution Mass Spectrometry," en, *ACS Earth and Space Chemistry*, vol. 6, no. 7, pp. 1733–1741, Jul. 2022, ISSN: 2472-3452, 2472-3452. DOI: 10.1021/acsearthspacechem.2c00043. [Online]. Available: https://pubs.acs.org/doi/10.1021/acsearthspacechem.2c00043.

[446] N. H. Robinson *et al.*, "Evidence for a significant proportion of Secondary Organic Aerosol from isoprene above a maritime tropical forest," en, *Atmospheric Chemistry and Physics*, vol. 11, no. 3, pp. 1039–1050, Feb. 2011, ISSN: 1680-7324. DOI: 10.5194/acp-11-1039-2011. [Online]. Available: https://acp.copernicus.org/articles/11/1039/2011/.

[447] R. Bahreini *et al.*, "Organic aerosol formation in urban and industrial plumes near Houston and Dallas, Texas," en, *Journal of Geophysical Research*, vol. 114, D00F16, Aug. 2009, ISSN: 0148-0227. DOI: 10.1029/2008JD011493. [Online]. Available: http://doi.wiley.com/10.1029/2008JD011493 (visited on 09/17/2023).

[448] M. Leuchner and B. Rappengluck, "VOC source receptor relationships in Houston during Texas II," en, *Atmospheric Environment*, vol. 44, no. 33, pp. 4056–4067, Oct. 2010, ISSN: 13522310. DOI: 10.1016/j.atmosenv.2009.02.029. (visited on 11/26/2023).

[449] T. Bates *et al.*, "Boundary layer aerosol chemistry during texas/gomaccs 2006: Insights into aerosol sources and transformation processes," *Journal of Geophysical Research: Atmospheres*, vol. 113, no. D7, 2008.

[450] M. P. Jensen *et al.*, "A succession of cloud, precipitation, aerosol, and air quality field experiments in the coastal urban environment," *Bulletin of the American Meteorological Society*, vol. 103, no. 2, pp. 103–105, 2022.

[451] S. McKeen *et al.*, "An evaluation of real time air quality forecasts and their urban emissions over eastern Texas during the summer of 2006 Second Texas Air Quality Study field study," en, *Journal of Geophysical Research: Atmospheres*, vol. 114, no. D7, 2008JD011697, Apr. 2009, ISSN: 0148-0227. DOI: 10.1029/2008JD011697. [Online]. Available: https://agupubs.onlinelibrary.wiley.com/doi/10.1029/2008JD011697.

[452] D. D. Parrish *et al.*, "Overview of the Second Texas Air Quality Study (Texas II) and the Gulf of Mexico Atmospheric Composition and Climate Study (GoMACCS)," en, *Journal of Geophysical Research: Atmospheres*, vol. 114, no. D7, 2009JD011842, Apr. 2009, ISSN: 0148-0227. DOI: 10.1029/2009JD011842. [Online]. Available: https://agupubs.onlinelibrary.wiley.com/doi/10.1029/2009JD011842.

[453] M. Webster, J. Nam, Y. Kimura, H. Jeffries, W. Vizuete, and D. T. Allen, "The effect of variability in industrial emissions on ozone formation in Houston, Texas," en, *Atmospheric Environment*, vol. 41, no. 40, pp. 9580–9593, Dec. 2007, ISSN: 13522310. DOI: 10.1016/j.atmosenv.2007.08.052. [Online]. Available: https://linkinghub.elsevier.com/retrieve/pii/S1352231007007546.

[454] M. Russell and D. T. Allen, "Seasonal and spatial trends in primary and secondary organic carbon concentrations in southeast Texas," en, *Atmospheric Environment*, vol. 38, no. 20, pp. 3225–3239, Jun. 2004, ISSN: 13522310. DOI: 10.1016/j.atmosenv.2004.03.013. [Online]. Available: https://linkinghub.elsevier.com/retrieve/pii/S1352231004002018.

[455] L. A. Garnes and D. T. Allen, "Size Distributions of Organonitrates in Ambient Aerosol Collected in Houston, Texas," en, *Aerosol Science and Technology*, vol. 36, no. 10, pp. 983–992, Oct. 2002, ISSN: 0278-6826, 1521-7388. DOI: 10.1080/02786820290092186. [Online]. Available: http://www.tandfonline.com/doi/abs/10.1080/02786820290092186 (visited on 10/01/2023).

[456] Q. Dai *et al.*, "Seasonal differences in formation processes of oxidized organic aerosol near Houston, TX," en, *Atmospheric Chemistry and Physics*, vol. 19, no. 14, pp. 9641–9661, Jul. 2019, ISSN: 1680-7324. DOI: 10.5194/acp-19-9641-2019. [Online]. Available: https://acp.copernicus.org/articles/19/9641/2019/ (visited on 10/01/2023).

[457] I. M. Al-Naiema *et al.*, "Source apportionment of fine particulate matter in Houston, Texas: Insights to secondary organic aerosols," en, *Atmospheric Chemistry and Physics*, vol. 18, no. 21, pp. 15 601–15 622, Oct. 2018, ISSN: 1680-7324. DOI: 10.5194/acp-18-15601-2018. [Online]. Available: https://acp.copernicus.org/articles/18/15601/2018/.

[458] H. Zhang and Q. Ying, "Secondary organic aerosol formation and source apportionment in Southeast Texas," en, *Atmospheric Environment*, vol. 45, no. 19, pp. 3217–3227, Jun. 2011, ISSN: 13522310. DOI: 10.1016/j.atmosenv.2011.03.046. [Online]. Available: https://linkinghub.elsevier.com/retrieve/pii/S1352231011003177 (visited on 10/01/2023).

[459] N. N. Lata, Z. Cheng, D. Dexheimer, D. Zhang, F. Mei, and S. China, "Vertical Gradient of Size-Resolved Aerosol Compositions over the Arctic Reveals Cloud Processed Aerosol in-Cloud and above Cloud," en, *Environmental Science & Technology*, vol. 57, no. 14, pp. 5821–5830, Apr. 2023, ISSN: 0013-936X, 1520-5851. DOI: 10.1021/acs.est.2c09498. [Online]. Available: https://pubs.acs.org/doi/10.1021/acs.est.2c09498.

[460] J. Laskin *et al.*, "High-Resolution Desorption Electrospray Ionization Mass Spectrometry for Chemical Characterization of Organic Aerosols," en, *Analytical Chemistry*, vol. 82, no. 5, pp. 2048–2058, Mar. 2010, ISSN: 0003-2700, 1520-6882. DOI: 10.1021/ac902801f.

[461] P. J. Roach, J. Laskin, and A. Laskin, "Nanospray desorption electrospray ionization: An ambient method for liquid-extraction surface sampling in mass spectrometry," en, *The Analyst*, vol. 135, no. 9, p. 2233, 2010, ISSN: 0003-2654, 1364-5528. DOI: 10.1039/c0an00312c.

[462] A. Laskin, J. Laskin, and S. A. Nizkorodov, "Mass spectrometric approaches for chemical characterisation of atmospheric aerosols: Critical review of the most recent advances," en, *Environmental Chemistry*, vol. 9, no. 3, p. 163, 2012, ISSN: 1448-2517. DOI: 10.1071/EN12052.

[463] A. Ijaz, W. Kew, S. China, S. K. Schum, and L. R. Mazzoleni, "Molecular Characterization of Organophosphorus Compounds in Wildfire Smoke Using 21-T Fourier Transform-Ion Cyclotron Resonance Mass Spectrometry," en, *Analytical Chemistry*, vol. 94, no. 42, pp. 14 537–14 545, Oct. 2022, ISSN: 0003-2700, 1520-6882. DOI: 10.1021/acs.analchem.2c00916. [Online]. Available: https://pubs.acs.org/doi/10.1021/acs.analchem.2c00916.

[464] S. K. Schum, L. E. Brown, and L. R. Mazzoleni, "MFAssignR: Molecular formula assignment software for ultrahigh resolution mass spectrometry analysis of environmental complex mixtures," en, *Environmental Research*, vol. 191, p. 110 114, Dec. 2020, ISSN: 00139351. DOI: 10.1016/j.envres.2020.110114. [Online]. Available: https://linkinghub.elsevier.com/retrieve/pii/S0013935120310112.

[465] Z. Cheng *et al.*, "Cloud condensation nuclei activity of internally mixed particle populations at a remote marine free troposphere site in the North Atlantic Ocean," en, *Science of The Total Environment*, vol. 904, p. 166 865, Dec. 2023, ISSN: 00489697. DOI: 10.1016/j.scitotenv.2023.166865. [Online]. Available: https://linkinghub.elsevier.com/retrieve/pii/S0048969723054906.

[466] R. C. Moffet, T. Henn, A. Laskin, and M. K. Gilles, "Automated Chemical Analysis of Internally Mixed Aerosol Particles Using X-ray Spectromicroscopy at the Carbon K-Edge," en, *Analytical Chemistry*, vol. 82, no. 19, pp. 7906–7914, Oct. 2010, ISSN: 0003-2700, 1520-6882. DOI: 10.1021/ac1012909. [Online]. Available: https://pubs.acs.org/doi/10.1021/ac1012909.

[467] M. Fraund, T. Park, L. Yao, D. Bonanno, D. Q. Pham, and R. C. Moffet, "Quantitative capabilities of STXM to measure spatially resolved organic volume fractions of mixed organic inorganic particles," en, *Atmospheric Measurement Techniques*, vol. 12, no. 3, pp. 1619–1633, Mar. 2019, ISSN: 1867-8548. DOI: 10.5194/amt-12-1619-2019.

[468] D. A. Knopf *et al.*, "Microspectroscopic imaging and characterization of individually identified ice nucleating particles from a case field study," en, *Journal of Geophysical Research: Atmospheres*, vol. 119, no. 17, Sep. 2014, ISSN: 2169-897X, 2169-8996. DOI: 10.1002/2014JD021866. [Online]. Available: https://agupubs.onlinelibrary.wiley.com/doi/10.1002/2014JD021866.

[469] C. J. Flynn, A. Mendoza, Y. Zheng, and S. Mathur, "Novel polarization-sensitive micropulse lidar measurement technique," en, *Optics Express*, vol. 15, no. 6, p. 2785, 2007, ISSN: 1094-4087. DOI: 10.1364/OE.15.002785. [Online]. Available: https://opg.optica.org/oe/abstract.cfm?uri=oe-15-6-2785.

[470] Z. Wang and K. Sassen, "Cloud Type and Macrophysical Property Retrieval Using Multiple Remote Sensors," en, *Journal of Applied Meteorology*, vol. 40, no. 10, pp. 1665–1682, Oct. 2001, ISSN: 0894-8763, 1520-0450. DOI: 10.1175/1520-0450(2001)040<1665:CTAMPR>2.0.CO;2. [Online]. Available: http://journals.ametsoc.org/doi/10.1175/1520-0450(2001)040<1665:CTAMPR>2.0.CO;2.

[471] "The ARM Radar Network: At the Leading Edge of Cloud and Precipitation Observations," vol. 101, ISSN: 0003-0007, 1520-0477. DOI: 10.1175/BAMS-D-18-0288.1. [Online]. Available: https://journals.ametsoc.org/view/journals/bams/101/5/bams-d-18-0288.1.xml.

[472] N. N. Lata *et al.*, "Aerosol Composition, Mixing State, and Phase State of Free Tropospheric Particles and Their Role in Ice Cloud Formation," en, *ACS Earth and Space Chemistry*, vol. 5, no. 12, pp. 3499–3510, Dec. 2021, ISSN: 2472-3452, 2472-3452. DOI: 10.1021/acsearthspacechem.1c00315. [Online]. Available: https://pubs.acs.org/doi/10.1021/acsearthspacechem.1c00315 (visited on 09/17/2023).

[473] J. M. Tomlin *et al.*, "Chemical imaging of fine mode atmospheric particles collected from a research aircraft over agricultural fields," *ACS Earth and Space Chemistry*, vol. 4, no. 11, pp. 2171–2184, 2020.

[474] J. M. Tomlin *et al.*, "Impact of dry intrusion events on the composition and mixing state of particles during the winter aerosol and cloud experiment in the eastern north atlantic (ace-ena)," *Atmospheric Chemistry and Physics*, vol. 21, no. 24, pp. 18 123–18 146, 2021.

[475] D. Knopf *et al.*, "Aerosol–ice formation closure: A southern great plains field campaign," *Bulletin of the American Meteorological Society*, vol. 102, no. 10, E1952–E1971, 2021.

[476] A. Wisthaler and C. J. Weschler, "Reactions of ozone with human skin lipids: Sources of carbonyls, dicarbonyls, and hydroxycarbonyls in indoor air," en, *Proceedings of the National Academy of Sciences*, vol. 107, no. 15, pp. 6568–6575, Apr. 2010, ISSN: 0027-8424, 1091-6490. DOI: 10.1073/pnas.0904498106.

[477] K. Dzepina *et al.*, "Molecular characterization of free tropospheric aerosol collected at the Pico Mountain Observatory: A case study with a long-range transported biomass burning plume," en, *Atmospheric Chemistry and Physics*, vol. 15, no. 9, pp. 5047–5068, May 2015, ISSN: 1680-7324. DOI: 10.5194/acp-15-5047-2015. [Online]. Available: https://acp.copernicus.org/articles/15/5047/2015/.

[478] "Carbon oxidation state as a metric for describing the chemistry of atmospheric organic aerosol," vol. 3, pp. 133–139, Feb. 2011, ISSN: 1755-4349. DOI: 10.1038/nchem.948. [Online]. Available: http://www.nature.com/articles/nchem.948.

[479] J. H. Kroll, C. Y. Lim, S. H. Kessler, and K. R. Wilson, "Heterogeneous Oxidation of Atmospheric Organic Aerosol: Kinetics of Changes to the Amount and Oxidation State of Particle-Phase Organic Carbon," en, *The Journal of Physical Chemistry A*, vol. 119, no. 44, pp. 10 767–10 783, Nov. 2015, ISSN: 1089-5639, 1520-5215. DOI: 10.1021/acs.jpca.5b06946. [Online]. Available: https://pubs.acs.org/doi/10.1021/acs.jpca.5b06946.

[480] M. J. Apsokardu and M. V. Johnston, "Nanoparticle growth by particle-phase chemistry," en, *Atmospheric Chemistry and Physics*, vol. 18, no. 3, pp. 1895–1907, Feb. 2018, ISSN: 1680-7324. DOI: 10.5194/acp-18-1895-2018. [Online]. Available: https://acp.copernicus.org/articles/18/1895/2018/.

[481] R. A. Zaveri *et al.*, "Particle-Phase Diffusion Modulates Partitioning of Semivolatile Organic Compounds to Aged Secondary Organic Aerosol," en, *Environmental Science & Technology*, vol. 54, no. 5, pp. 2595–2605, Mar. 2020, ISSN: 0013-936X, 1520-5851. DOI: 10.1021/acs.est.9b05514. [Online]. Available: https://pubs.acs.org/doi/10.1021/acs.est.9b05514.

[482] W. Hu *et al.*, "Oxidation Flow Reactor Results in a Chinese Megacity Emphasize the Important Contribution of S/IVOCs to Ambient SOA Formation," en, *Environmental Science & Technology*, vol. 56, no. 11, pp. 6880–6893, Jun. 2022, ISSN: 0013-936X, 1520-5851. DOI: 10.1021/acs.est.1c03155. [Online]. Available: https://pubs.acs.org/doi/10.1021/acs.est.1c03155.

[483] Y. Chen *et al.*, "Nonequilibrium Behavior in Isoprene Secondary Organic Aerosol," en, *Environmental Science & Technology*, vol. 57, no. 38, pp. 14 182–14 193, Sep. 2023, ISSN: 0013-936X, 1520-5851. DOI: 10.1021/acs.est.3c03532. [Online]. Available: https://pubs.acs.org/doi/10.1021/acs.est.3c03532.

[484] A. Goldstein, L. Yee, and N. Kreisberg, "Investigating secondary aerosol processes in the amazon through molecular-level characterization of semi-volatile organics," Tech. Rep., 2020. DOI: 10.2172/1673764.

[485] M. N. Chan *et al.*, "Influence of aerosol acidity on the chemical composition of secondary organic aerosol from β-caryophyllene," en, *Atmospheric Chemistry and Physics*, vol. 11, no. 4, pp. 1735–1751, Feb. 2011, ISSN: 1680-7324. DOI: 10.5194/acp-11-1735-2011.

[486] Y. Wang *et al.*, "Secondary reactions of aromatics-derived oxygenated organic molecules lead to plentiful highly oxygenated organic molecules within an intraday OH exposure," Gases/Laboratory Studies/Troposphere/Chemistry (chemical composition and reactions), preprint, Aug. 2023. DOI: 10.5194/egusphere-2023-1702. [Online]. Available: https://egusphere.copernicus.org/preprints/2023/egusphere-2023-1702/ (visited on 09/17/2023).

[487] S. Ponnusamy, L. Sandhiya, and K. Senthilkumar, "The atmospheric oxidation mechanism and kinetics of 1,3,5 trimethylbenzene initiated by OH radicals a theoretical study," en, *New Journal of Chemistry*, vol. 41, no. 18, pp. 10 259–10 271, 2017, ISSN: 1144-0546, 1369-9261. DOI: 10.1039/C7NJ01285C.

[488] C. Parworth *et al.*, "Long-term measurements of submicrometer aerosol chemistry at the Southern Great Plains (SGP) using an Aerosol Chemical Speciation Monitor (ACSM)," en, *Atmospheric Environment*, vol. 106, pp. 43–55, Apr. 2015, ISSN: 13522310. DOI: 10.1016/j.atmosenv.2015.01.060. (visited on 10/01/2023).

[489] M. C. Facchini *et al.*, "Important Source of Marine Secondary Organic Aerosol from Biogenic Amines," en, *Environmental Science & Technology*, vol. 42, no. 24, pp. 9116–9121, Dec. 2008, ISSN: 0013-936X, 1520-5851. DOI: 10.1021/es8018385. [Online]. Available: https://pubs.acs.org/doi/10.1021/es8018385.

[490] S. S. Petters *et al.*, "Organosulfates from Dark Aqueous Reactions of Isoprene-Derived Epoxydiols Under Cloud and Fog Conditions: Kinetics, Mechanism, and Effect of Reaction Environment on Regioselectivity of Sulfate Addition," en, *ACS Earth and Space Chemistry*, vol. 5, no. 3, pp. 474–486, Mar. 2021, ISSN: 2472-3452, 2472-3452. DOI: 10.1021/acsearthspacechem.0c00293. [Online]. Available: https://pubs.acs.org/doi/10.1021/acsearthspacechem.0c00293.

[491] H. Zhang, J. D. Surratt, Y. H. Lin, J. Bapat, and R. M. Kamens, "Effect of relative humidity on SOA formation from isoprene/NO photooxidation: Enhancement of 2-methylglyceric acid and its corresponding oligoesters under dry conditions," en, *Atmospheric Chemistry and Physics*, vol. 11, no. 13, pp. 6411–6424, Jul. 2011, ISSN: 1680-7324. DOI: 10.5194/acp-11-6411-2011. [Online]. Available: https://acp.copernicus.org/articles/11/6411/2011/.

[492] Y. Gomez Gonzalez *et al.*, "Characterization of organosulfates from the photooxidation of isoprene and unsaturated fatty acids in ambient aerosol using liquid chromatography/ electrospray ionization mass spectrometry," en, *Journal of Mass Spectrometry*, vol. 43, no. 3, pp. 371–382, Mar. 2008, ISSN: 1076-5174, 1096-9888. DOI: 10.1002/jms.1329.

[493] Y. Chen *et al.*, "Seasonal contribution of isoprene-derived organosulfates to total water-soluble fine particulate organic sulfur in the united states," *ACS Earth and Space Chemistry*, vol. 5, no. 9, pp. 2419–2432, 2021.

[494] T. B. Nguyen, J. Laskin, A. Laskin, and S. A. Nizkorodov, "Nitrogen-Containing Organic Compounds and Oligomers in Secondary Organic Aerosol Formed by Photooxidation of Isoprene," en, *Environmental Science & Technology*, vol. 45, no. 16, pp. 6908–6918, Aug. 2011, ISSN: 0013-936X, 1520-5851. DOI: 10.1021/es201611n.

[495] S. Su *et al.*, "High Molecular Diversity of Organic Nitrogen in Urban Snow in North China," en, *Environmental Science & Technology*, vol. 55, no. 8, pp. 4344–4356, Apr. 2021, ISSN: 0013-936X, 1520-5851. DOI: 10.1021/acs.est.0c06851. [Online]. Available: https://pubs.acs.org/doi/10.1021/acs.est.0c06851.

[496] T. Reemtsma *et al.*, "Identification of Fulvic Acids and Sulfated and Nitrated Analogues in Atmospheric Aerosol by Electrospray Ionization Fourier Transform Ion Cyclotron Resonance Mass Spectrometry," en, *Analytical Chemistry*, vol. 78, no. 24, pp. 8299–8304, Dec. 2006, ISSN: 0003-2700, 1520-6882. DOI: 10.1021/ac061320p. [Online]. Available: https://pubs.acs.org/doi/10.1021/ac061320p.

[497] Y. Ye, H. Zhan, X. Yu, J. Li, X. Wang, and Z. Xie, "Detection of organosulfates and nitrooxy-organosulfates in Arctic and Antarctic atmospheric aerosols, using ultra-high resolution FT-ICR mass spectrometry," en, *Science of The Total Environment*, vol. 767, p. 144 339, May 2021, ISSN: 00489697. DOI: 10.1016/j.scitotenv.2020.144339. [Online]. Available: https://linkinghub.elsevier.com/retrieve/pii/S0048969720378700.

[498] K. Wang *et al.*, "Urban organic aerosol composition in eastern China differs from north to south: Molecular insight from a liquid chromatography mass spectrometry orbitrap study," en, *Atmospheric Chemistry and Physics*, vol. 21, no. 11, pp. 9089–9104, Jun. 2021, ISSN: 1680-7324. DOI: 10.5194/acp-21-9089-2021. [Online]. Available: https://acp.copernicus.org/articles/21/9089/2021/.

[499] S. L. Lewis, G. Saliba, L. M. Russell, P. K. Quinn, T. S. Bates, and M. J. Behrenfeld, "Seasonal Differences in Submicron Marine Aerosol Particle Organic Composition in the North Atlantic," *Frontiers in Marine Science*, vol. 8, p. 720 208, Sep. 2021, ISSN: 2296-7745. DOI: 10.3389/fmars.2021.720208.

[500] S. Liu, J. E. Shilling, C. Song, N. Hiranuma, R. A. Zaveri, and L. M. Russell, "Hydrolysis of Organonitrate Functional Groups in Aerosol Particles," en, *Aerosol Science and Technology*, vol. 46, no. 12, pp. 1359–1369, Dec. 2012, ISSN: 0278-6826, 1521-7388. DOI: 10.1080/02786826.2012.716175. [Online]. Available: http://www.tandfonline.com/doi/abs/10.1080/02786826.2012.716175.

[501] R. D. Cook *et al.*, "Biogenic, urban, and wildfire influences on the molecular composition of dissolved organic compounds in cloud water," en, *Atmospheric Chemistry and Physics*, vol. 17, no. 24, pp. 15 167–15 180, Dec. 2017, ISSN: 1680-7324. DOI: 10.5194/acp-17-15167-2017. [Online]. Available: https://acp.copernicus.org/articles/17/15167/2017/.

[502] Q. Xie *et al.*, "Molecular characterization of firework-related urban aerosols using Fourier transform ion cyclotron resonance mass spectrometry," en, *Atmospheric Chemistry and Physics*, vol. 20, no. 11, pp. 6803–6820, Jun. 2020, ISSN: 1680-7324. DOI: 10.5194/acp-20-6803-2020. [Online]. Available: https://acp.copernicus.org/articles/20/6803/2020/ (visited on 10/01/2023).

[503] Q.-F. He *et al.*, "Organosulfates from Pinene and Isoprene over the Pearl River Delta, South China: Seasonal Variation and Implication in Formation Mechanisms," en, *Environmental Science & Technology*, vol. 48, no. 16, pp. 9236–9245, Aug. 2014, ISSN: 0013-936X, 1520-5851. DOI: 10.1021/es501299v. [Online]. Available: https://pubs.acs.org/doi/10.1021/es501299v (visited on 09/17/2023).

[504] Y. Wang *et al.*, "Comparative Study of Particulate Organosulfates in Contrasting Atmospheric Environments: Field Evidence for the Significant Influence of Anthropogenic Sulfate and NO_x," en, *Environmental Science & Technology Letters*, vol. 7, no. 11, pp. 787–794, Nov. 2020, ISSN: 2328-8930, 2328-8930. DOI: 10.1021/acs.estlett.0c00550.

[505] C. Faxon, J. Hammes, M. Le Breton, R. K. Pathak, and M. Hallquist, "Characterization of organic nitrate constituents of secondary organic aerosol (SOA) from nitrate-radical-initiated oxidation of limonene using high-resolution chemical ionization mass spectrometry," en, *Atmospheric Chemistry and Physics*, vol. 18, no. 8, pp. 5467–5481, Apr. 2018, ISSN: 1680-7324. DOI: 10.5194/acp-18-5467-2018. [Online]. Available: https://acp.copernicus.org/articles/18/5467/2018/ (visited on 09/17/2023).

[506] L. Huang *et al.*, "Biogenic and Anthropogenic Contributions to Atmospheric Organosulfates in a Typical Megacity in Eastern China," en, *Journal of Geophysical Research: Atmospheres*, vol. 128, no. 17, e2023JD038848, Sep. 2023, ISSN: 2169-897X, 2169-8996. DOI: 10.1029/2023JD038848. [Online]. Available: https://agupubs.onlinelibrary.wiley.com/doi/10.1029/2023JD038848 (visited on 09/17/2023).

[507] D. J. Bryant *et al.*, "Biogenic and anthropogenic sources of isoprene and monoterpenes and their secondary organic aerosol in Delhi, India," en, *Atmospheric Chemistry and Physics*, vol. 23, no. 1, pp. 61–83, Jan. 2023, ISSN: 1680-7324. DOI: 10.5194/acp-23-61-2023. [Online]. Available: https://acp.copernicus.org/articles/23/61/2023/.

[508] R. Schmedding *et al.*, "Predicting secondary organic aerosol phase state and viscosity and its effect on multiphase chemistry in a regional-scale air quality model," *Atmospheric chemistry and physics*, vol. 20, no. 13, pp. 8201–8225, 2020.

[509] M. Riva *et al.*, "Increasing isoprene epoxydiol-to-inorganic sulfate aerosol ratio results in extensive conversion of inorganic sulfate to organosulfur forms: Implications for aerosol physicochemical properties," *Environmental science & technology*, vol. 53, no. 15, pp. 8682–8694, 2019.

[510] N. E. Rothfuss and M. D. Petters, "Influence of functional groups on the viscosity of organic aerosol," *Environmental science & technology*, vol. 51, no. 1, pp. 271–279, 2017.

[511] P. E. Ohno *et al.*, "Gas-Particle Uptake and Hygroscopic Growth by Organosulfate Particles," en, *ACS Earth and Space Chemistry*, vol. 6, no. 10, pp. 2481–2490, Oct. 2022, ISSN: 2472-3452, 2472-3452. DOI: 10.1021/acsearthspacechem.2c00195. [Online]. Available: https://pubs.acs.org/doi/10.1021/acsearthspacechem.2c00195.

[512] D. A. Knopf, P. A. Alpert, and B. Wang, "The Role of Organic Aerosol in Atmospheric Ice Nucleation: A Review," en, *ACS Earth and Space Chemistry*, vol. 2, no. 3, pp. 168–202, Mar. 2018, ISSN: 2472-3452, 2472-3452. DOI: 10.1021/acsearthspacechem.7b00120. [Online]. Available: https://pubs.acs.org/doi/10.1021/acsearthspacechem.7b00120.

[513] M. J. Wolf *et al.*, "A biogenic secondary organic aerosol source of cirrus ice nucleating particles," en, *Nature Communications*, vol. 11, no. 1, p. 4834, Oct. 2020, ISSN: 2041-1723. DOI: 10.1038/s41467-020-18424-6. [Online]. Available: https://www.nature.com/articles/s41467-020-18424-6.

[514] W. Schimmel *et al.*, "Identifying cloud droplets beyond lidar attenuation from vertically-pointing cloud radar observations using artificial neural networks," Clouds/Remote Sensing/Data Processing and Information Retrieval, preprint, May 2022. DOI: 10.5194/amt-2022-149. [Online]. Available: https://amt.copernicus.org/preprints/amt-2022-149/amt-2022-149.pdf.

[515] C. M. Fajardo-Zambrano *et al.*, "Lidar and radar signal simulation: Stability assessment of the aerosol–cloud interaction index," *Remote Sensing*, vol. 14, no. 6, p. 1333, 2022.

[516] C. Maloney *et al.*, "The Balance Between Heterogeneous and Homogeneous Nucleation of Ice Clouds Using CAM5/CARMA," en, *Journal of Geophysical Research: Atmospheres*, vol. 127, no. 6, e2021JD035540, Mar. 2022, ISSN: 2169-897X, 2169-8996. DOI: 10.1029/2021JD035540. [Online]. Available: https://agupubs.onlinelibrary.wiley.com/doi/10.1029/2021JD035540 (visited on 09/17/2023).

[517] P. de la Mare and P. Robertson, "550. the kinetics of halogen addition to unsaturated compounds. part xxi. the mechanisms of addition reactions," *Journal of the Chemical Society (Resumed)*, pp. 2838–2842, 1950.

[518] J. S. Fritz and G. E. Wood, "Determination of olefinic unsaturation by bromination," *Analytical Chemistry*, vol. 40, no. 1, pp. 134–139, 1968.

[519] R. Chen *et al.*, "Recent applications of ambient ionization mass spectrometry in environmental analysis," en, *Trends in Environmental Analytical Chemistry*, vol. 15, pp. 1–11, Jul. 2017, ISSN: 22141588. DOI: 10.1016/j.teac.2017.07.001. [Online]. Available: https://linkinghub.elsevier.com/retrieve/pii/S2214158817300338 (visited on 02/12/2024).

[520] G. Di Virgilio *et al.*, "Climate change increases the potential for extreme wildfires," *Geophysical Research Letters*, vol. 46, no. 14, pp. 8517–8526, 2019.

[521] M. H. Dore, "Climate change and changes in global precipitation patterns: What do we know?" *Environment international*, vol. 31, no. 8, pp. 1167–1181, 2005.

[522] D. Narumi, A. Kondo, and Y. Shimoda, "The effect of the increase in urban temperature on the concentration of photochemical oxidants," *Atmospheric Environment*, vol. 43, no. 14, pp. 2348–2359, 2009.

[523] G. Cao, X. Zhao, D. Hu, R. Zhu, and F. Ouyang, "Development and application of a quantification method for water soluble organosulfates in atmospheric aerosols," *Environmental pollution*, vol. 225, pp. 316–322, 2017.

[524] S. Wang *et al.*, "Relationship between chemical composition and oxidative potential of secondary organic aerosol from polycyclic aromatic hydrocarbons," en, *Atmospheric Chemistry and Physics*, vol. 18, no. 6, pp. 3987–4003, Mar. 2018, ISSN: 1680-7324. DOI: 10.5194/acp-18-3987-2018. [Online]. Available: https://acp.copernicus.org/articles/18/3987/2018/.

[525] Y. Lim and B. Turpin, "Laboratory evidence of organic peroxide and peroxyhemiacetal formation in the aqueous phase and implications for aqueous OH," *Atmospheric Chemistry and Physics*, vol. 15, no. 22, pp. 12 867–12 877, 2015, Publisher: Copernicus GmbH.

[526] N. Ng, J. Kroll, A. Chan, P. Chhabra, R. Flagan, and J. Seinfeld, "Secondary organic aerosol formation from m-xylene, toluene, and benzene," *Atmospheric Chemistry and Physics*, vol. 7, no. 14, pp. 3909–3922, 2007.

[527] R. M. Duarte, J. T. Matos, and A. C. Duarte, "Multidimensional analytical characterization of water-soluble organic aerosols: Challenges and new perspectives," *Applied Sciences*, vol. 11, no. 6, p. 2539, 2021.

[528] G. Spolnik, P. Wach, K. J. Rudzinski, K. Skotak, W. Danikiewicz, and R. Szmigielski, "Improved uhplc-ms/ms methods for analysis of isoprene-derived organosulfates," *Analytical chemistry*, vol. 90, no. 5, pp. 3416–3423, 2018.

[529] S. Wang, R. Wu, T. Berndt, M. Ehn, and L. Wang, "Formation of highly oxidized radicals and multifunctional products from the atmospheric oxidation of alkylbenzenes," *Environmental science & technology*, vol. 51, no. 15, pp. 8442–8449, 2017.

[530] F. Bianchi *et al.*, "Ms-based analytical techniques: Advances in spray-based methods and ei-lc-ms applications," *Journal of analytical methods in chemistry*, vol. 2018, 2018.

[531] L. Deguillaume, M. Leriche, K. Desboeufs, G. Mailhot, C. George, and N. Chaumerliac, "Transition Metals in Atmospheric Liquid Phases: Sources, Reactivity, and Sensitive Parameters," en, *Chemical Reviews*, vol. 105, no. 9, pp. 3388–3431, Sep. 2005, ISSN: 0009-2665, 1520-6890. DOI: 10.1021/cr040649c. [Online]. Available: https://pubs.acs.org/doi/10.1021/cr040649c.

[532] P. H. Daum, S. E. Schwartz, and L. Newman, "Acidic and related constituents in liquid water stratiform clouds," en, *Journal of Geophysical Research: Atmospheres*, vol. 89, no. D1, pp. 1447–1458, Feb. 1984, ISSN: 0148-0227. DOI: 10.1029/JD089iD01p01447.

[533] J. J. Schwab *et al.*, "Atmospheric chemistry measurements at whiteface mountain, ny: Cloud water chemistry, precipitation chemistry, and particulate matter," *Aerosol and Air Quality Research*, vol. 16, no. 3, pp. 841–854, 2016.

[534] C. Anastasio, B. C. Faust, and J. M. Allen, "Aqueous phase photochemical formation of hydrogen peroxide in authentic cloud waters," *Journal of Geophysical Research: Atmospheres*, vol. 99, no. D4, pp. 8231–8248, 1994.

[535] A. T. Archibald, A. S. Petit, C. J. Percival, J. N. Harvey, and D. E. Shallcross, "On the importance of the reaction between OH and RO_2 radicals," en, *Atmospheric Science Letters*, vol. 10, no. 2, pp. 102–108, Apr. 2009, ISSN: 1530-261X, 1530-261X. DOI: 10.1002/asl.216.

[536] M. Lucarini and G. F. Pedulli, "Free radical intermediates in the inhibition of the autoxidation reaction," en, *Chemical Society Reviews*, vol. 39, no. 6, p. 2106, 2010, ISSN: 0306-0012, 1460-4744. DOI: 10.1039/b901838g. [Online]. Available: http://xlink.rsc.org/?DOI=b901838g (visited on 02/10/2024).

[537] R. Kaur, B. M. Hudson, J. Draper, D. J. Tantillo, and C. Anastasio, "Aqueous reactions of organic triplet excited states with atmospheric alkenes," *Atmospheric Chemistry and Physics*, vol. 19, no. 7, pp. 5021–5032, 2019, Publisher: Copernicus Publications Gottingen, Germany.

[538] L. He, T. Schaefer, T. Otto, A. Kroflic, and H. Herrmann, "Kinetic and theoretical study of the atmospheric aqueous-phase reactions of oh radicals with methoxyphenolic compounds," *The Journal of Physical Chemistry A*, vol. 123, no. 36, pp. 7828–7838, 2019.

[539] S. E. Schwartz, "Mass-transport considerations pertinent to aqueous phase reactions of gases in liquid-water clouds," in *Chemistry of multiphase atmospheric systems*, Springer, 1986, pp. 415–471.

[540] Q. Zhang *et al.*, "Variability of so_2 in an intensive fog in north china plain: Evidence of high solubility of so_2," *Particuology*, vol. 11, no. 1, pp. 41–47, 2013.

[541] J. A. Lind, A. L. Lazrus, and G. L. Kok, "Aqueous phase oxidation of sulfur (iv) by hydrogen peroxide, methylhydroperoxide, and peroxyacetic acid," *Journal of Geophysical Research: Atmospheres*, vol. 92, no. D4, pp. 4171–4177, 1987.

[542] E. Dovrou, J. C. Rivera-Rios, K. H. Bates, and F. N. Keutsch, "Sulfate formation via cloud processing from isoprene hydroxyl hydroperoxides (ISOPOOH)," *Environmental science & technology*, vol. 53, no. 21, pp. 12 476–12 484, 2019, Publisher: ACS Publications.

[543] T. Jokinen *et al.*, "Rapid Autoxidation Forms Highly Oxidized RO_2 Radicals in the Atmosphere," en, *Angewandte Chemie International Edition*, vol. 53, no. 52, pp. 14 596–14 600, Dec. 2014, ISSN: 1433-7851, 1521-3773. DOI: 10.1002/anie.201408566.

[544] S. Modugno, H. Balzter, B. Cole, and P. Borrelli, "Mapping regional patterns of large forest fires in wildland–urban interface areas in europe," *Journal of environmental management*, vol. 172, pp. 112–126, 2016.

[545] C. M. Villarruel, L. A. Figueroa, and J. F. Ranville, "Quantification of bioaccessible and environmentally relevant trace metals in structure ash from a wildland–urban interface fire," *Environmental Science & Technology*, 2024.

[546] B. R. Simoneit, P. M. Medeiros, and B. M. Didyk, "Combustion products of plastics as indicators for refuse burning in the atmosphere," *Environmental science & technology*, vol. 39, no. 18, pp. 6961–6970, 2005.

[547] J. Reid, R Koppmann, T. Eck, and D. Eleuterio, "A review of biomass burning emissions part ii: Intensive physical properties of biomass burning particles," *Atmospheric chemistry and physics*, vol. 5, no. 3, pp. 799–825, 2005.

[548] J. Gilman *et al.*, "Biomass burning emissions and potential air quality impacts of volatile organic compounds and other trace gases from fuels common in the us," *Atmospheric Chemistry and Physics*, vol. 15, no. 24, pp. 13 915–13 938, 2015.

[549] S. Akagi *et al.*, "Emission factors for open and domestic biomass burning for use in atmospheric models," *Atmospheric Chemistry and Physics*, vol. 11, no. 9, pp. 4039–4072, 2011.

[550] C. D. Cappa and J. L. Jimenez, "Quantitative estimates of the volatility of ambient organic aerosol," en, *Atmospheric Chemistry and Physics*, vol. 10, no. 12, pp. 5409–5424, Jun. 2010, ISSN: 1680-7324. DOI: 10.5194/acp-10-5409-2010. [Online]. Available: https://acp.copernicus.org/articles/10/5409/2010/.

[551] L. Yee *et al.*, "Secondary organic aerosol formation from biomass burning intermediates: Phenol and methoxyphenols," *Atmospheric Chemistry and Physics*, vol. 13, no. 16, pp. 8019–8043, 2013.

[552] S. Li *et al.*, "Evolution of organic aerosol from wood smoke influenced by burning phase and solar radiation," *Journal of Geophysical Research: Atmospheres*, vol. 126, no. 8, e2021JD034534, 2021.

[553] T. Chen *et al.*, "Smog chamber study on the role of no x in soa and o_3 formation from aromatic hydrocarbons," *Environmental Science & Technology*, vol. 56, no. 19, pp. 13 654–13 663, 2022.

[554] M. Wang *et al.*, "Photo-oxidation of aromatic hydrocarbons produces low-volatility organic compounds," *Environmental science & technology*, vol. 54, no. 13, pp. 7911–7921, 2020.

[555] D. Minakata, K. Li, P. Westerhoff, and J. Crittenden, "Development of a group contribution method to predict aqueous phase hydroxyl radical (ho) reaction rate constants," *Environmental science & technology*, vol. 43, no. 16, pp. 6220–6227, 2009.

[556] R. Volkamer *et al.*, "Oh-initiated oxidation of benzene part i. phenol formation under atmospheric conditions," *Physical Chemistry Chemical Physics*, vol. 4, no. 9, pp. 1598–1610, 2002.

[557] X. Cheng *et al.*, "Oxygenated organic molecules produced by low-no x photooxidation of aromatic compounds: Contributions to secondary organic aerosol and steric hindrance," *Atmospheric Chemistry and Physics*, vol. 24, no. 4, pp. 2099–2112, 2024.

[558] M. Zhu, S. Wang, Y. Zhang, Z. Yu, Y. Yu, and X. Wang, "Particle-bound highly oxidized organic molecules derived from aromatic hydrocarbons in an urban atmosphere," *Environmental Science & Technology Letters*, vol. 9, no. 12, pp. 1030–1036, 2022.

[559] X. Zhang, C. Zhang, X. Sun, J. Yang, and C. Zhu, "Mechanism and kinetic study of the reaction of benzoic acid with oh, no 3 and so 4- radicals in the atmosphere," *RSC advances*, vol. 9, no. 33, pp. 18 971–18 977, 2019.

[560] S. K. Boreddy, T. Mochizuki, K. Kawamura, S. Bikkina, and M. Sarin, "Homologous series of low molecular weight (c1-c10) monocarboxylic acids, benzoic acid and hydroxyacids in fine-mode (pm2. 5) aerosols over the bay of bengal: Influence of heterogeneity in air masses and formation pathways," *Atmospheric environment*, vol. 167, pp. 170–180, 2017.

[561] H. Wang *et al.*, "The effect of water molecules and air humidity on the cluster formation from benzoic acid with sulfuric acid/ammonia/dimethylamine: A molecular-scale investigation," *Journal of Molecular Liquids*, vol. 390, p. 123 001, 2023.

[562] J. Helberg and D. A. Pratt, "Autoxidation vs. antioxidants–the fight for forever," *Chemical Society Reviews*, vol. 50, no. 13, pp. 7343–7358, 2021.

[563] I. Spasojević, "Free radicals and antioxidants at a glance using epr spectroscopy," *Critical reviews in clinical laboratory sciences*, vol. 48, no. 3, pp. 114–142, 2011.

[564] H. Iwahashi, C. E. Parker, R. P. Mason, and K. B. Tomer, "Combined liquid chromatography/electron paramagnetic resonance spectrometry/electrospray ionization mass spectrometry for radical identification," *Analytical chemistry*, vol. 64, no. 19, pp. 2244–2252, 1992.

[565] Q. Chen *et al.*, "Rapid determination of environmentally persistent free radicals (epfrs) in atmospheric particles with a quartz sheet-based approach using electron paramagnetic resonance (epr) spectroscopy," *Atmospheric Environment*, vol. 184, pp. 140–145, 2018.

[566] C. P. Nicholas, "Applications of light olefin oligomerization to the production of fuels and chemicals," *Applied Catalysis A: General*, vol. 543, pp. 82–97, 2017.

[567] M. Klapper, D. Joe, S. Nietzel, J. W. Krumpfer, and K. Mullen, "Olefin polymerization with supported catalysts as an exercise in nanotechnology," *Chemistry of Materials*, vol. 26, no. 1, pp. 802–819, 2014.

[568] C. J. Weschler and W. W. Nazaroff, "Semivolatile organic compounds in indoor environments," *Atmospheric environment*, vol. 42, no. 40, pp. 9018–9040, 2008.

[569] C. J. Weschler, A. T. Hodgson, and J. D. Wooley, "Indoor chemistry: Ozone, volatile organic compounds, and carpets," en, *Environmental Science & Technology*, vol. 26, no. 12, pp. 2371–2377, Dec. 1992, ISSN: 0013-936X, 1520-5851. DOI: 10.1021/es00036a006.

[570] M. Shiraiwa *et al.*, "Modelling consortium for chemistry of indoor environments (moccie): Integrating chemical processes from molecular to room scales," *Environmental Science: Processes & Impacts*, vol. 21, no. 8, pp. 1240–1254, 2019.

[571] W. W. Nazaroff and C. J. Weschler, "Cleaning products and air fresheners: Exposure to primary and secondary air pollutants," *Atmospheric environment*, vol. 38, no. 18, pp. 2841–2865, 2004.

[572] W. Nazaroff and A. Goldstein, "Indoor chemistry: Research opportunities and challenges," *Indoor air*, vol. 25, no. 4, pp. 357–361, 2015.

[573] G. Sarwar, D. A. Olson, R. L. Corsi, and C. J. Weschler, "Indoor fine particles: The role of terpene emissions from consumer products," *Journal of the Air & Waste Management Association*, vol. 54, no. 3, pp. 367–377, 2004.

[574] T. Vera, F Villanueva, L Wimmerová, and E. Tolis, "An overview of methodologies for the determination of volatile organic compounds in indoor air," *Applied Spectroscopy Reviews*, vol. 57, no. 8, pp. 625–674, 2022.

[575] R. M. Pagni *et al.*, "Reactions of unsaturated compounds with iodine and bromine on. gamma. alumina," *The Journal of Organic Chemistry*, vol. 53, no. 19, pp. 4477–4482, 1988.

[576] Z. Zhou, L. R. Crilley, J. C. Ditto, T. C. VandenBoer, and J. P. D. Abbatt, "Chemical Fate of Oils on Indoor Surfaces: Ozonolysis and Peroxidation," en, *Environmental Science & Technology*, vol. 57, no. 41, pp. 15 546–15 557, Oct. 2023, ISSN: 0013-936X, 1520-5851. DOI: 10.1021/acs.est.3c04009. [Online]. Available: https://pubs.acs.org/doi/10.1021/acs.est.3c04009 (visited on 02/12/2024).

[577] A. W. H. Chan *et al.*, "Detailed chemical characterization of unresolved complex mixtures in atmospheric organics: Insights into emission sources, atmospheric processing, and secondary organic aerosol formation," en, *Journal of Geophysical Research: Atmospheres*, vol. 118, no. 12, pp. 6783–6796, Jun. 2013, ISSN: 2169-897X, 2169-8996. DOI: 10.1002/jgrd.50533. [Online]. Available: https://agupubs.onlinelibrary.wiley.com/doi/10.1002/jgrd.50533 (visited on 02/09/2024).

[578] N. E. Rothfuss and M. D. Petters, "Influence of Functional Groups on the Viscosity of Organic Aerosol," en, *Environmental Science & Technology*, vol. 51, no. 1, pp. 271–279, Jan. 2017, ISSN: 0013-936X, 1520-5851. DOI: 10.1021/acs.est.6b04478. [Online]. Available: https://pubs.acs.org/doi/10.1021/acs.est.6b04478 (visited on 02/09/2024).

[579] F. D. Pope, P. J. Gallimore, S. J. Fuller, R. A. Cox, and M. Kalberer, "Ozonolysis of Maleic Acid Aerosols: Effect upon Aerosol Hygroscopicity, Phase and Mass," en, *Environmental Science & Technology*, vol. 44, no. 17, pp. 6656–6660, Sep. 2010, ISSN: 0013-936X, 1520-5851. DOI: 10.1021/es1008278. (visited on 02/09/2024).

[580] M. L. Pohlker *et al.*, "Global organic and inorganic aerosol hygroscopicity and its effect on radiative forcing," en, *Nature Communications*, vol. 14, no. 1, p. 6139, Oct. 2023, ISSN: 2041-1723. DOI: 10.1038/s41467-023-41695-8. [Online]. Available: https://www.nature.com/articles/s41467-023-41695-8.

[581] J. P. Reid *et al.*, "The viscosity of atmospherically relevant organic particles," *Nature communications*, vol. 9, no. 1, p. 956, 2018.

[582] W.-S. W. DeRieux *et al.*, "Predicting the glass transition temperature and viscosity of secondary organic material using molecular composition," en, *Atmospheric Chemistry and Physics*, vol. 18, no. 9, pp. 6331–6351, May 2018, ISSN: 1680-7324. DOI: 10.5194/acp-18-6331-2018. [Online]. Available: https://acp.copernicus.org/articles/18/6331/2018/ (visited on 02/09/2024).

[583] M. Collaud Coen *et al.*, "Identification of topographic features influencing aerosol observations at high altitude stations," *Atmospheric Chemistry and Physics*, vol. 18, no. 16, pp. 12 289–12 313, 2018.

[584] H. Lignell, S. A. Epstein, M. R. Marvin, D. Shemesh, B. Gerber, and S. Nizkorodov, "Experimental and Theoretical Study of Aqueous *cis* -Pinonic Acid Photolysis," en, *The Journal of Physical Chemistry A*, vol. 117, no. 48, pp. 12 930–12 945, Dec. 2013, ISSN: 1089-5639, 1520-5215. DOI: 10.1021/jp4093018. [Online]. Available: https://pubs.acs.org/doi/10.1021/jp4093018 (visited on 06/07/2020).

[585] Y. Huang *et al.*, "The Caltech Photooxidation Flow Tube reactor: Design, fluid dynamics and characterization," en, *Atmospheric Measurement Techniques*, vol. 10, no. 3, pp. 839–867, Mar. 2017, ISSN: 1867-8548. DOI: 10.5194/amt-10-839-2017. [Online]. Available: https://amt.copernicus.org/articles/10/839/2017/ (visited on 11/12/2022).

[586] E. S. Galbavy, K. Ram, and C. Anastasio, "2-Nitrobenzaldehyde as a chemical actinometer for solution and ice photochemistry," en, *Journal of Photochemistry and Photobiology A: Chemistry*, vol. 209, no. 2-3, pp. 186–192, Jan. 2010, ISSN: 10106030. DOI: 10.1016/j.jphotochem.2009.11.013. [Online]. Available: https://linkinghub.elsevier.com/retrieve/pii/S101060300900433X (visited on 08/29/2022).

[587] P. O. Wennberg *et al.*, "Gas-Phase Reactions of Isoprene and Its Major Oxidation Products," *Chemical Reviews*, vol. 118, no. 7, pp. 3337–3390, Apr. 2018, ISSN: 0009-2665. DOI: 10.1021/acs.chemrev.7b00439.

[588] K. H. Moller, T. Berndt, and H. G. Kjaergaard, "Atmospheric Autoxidation of Amines," *Environmental Science & Technology*, vol. 54, no. 18, pp. 11 087–11 099, Sep. 2020, Publisher: American Chemical Society, ISSN: 0013-936X. DOI: 10.1021/acs.est.0c03937. (visited on 06/09/2022).

[589] F. Bianchi *et al.*, "Highly oxygenated organic molecules (HOM) from gas-phase autoxidation involving peroxy radicals: A key contributor to atmospheric aerosol," *Chemical reviews*, vol. 119, no. 6, pp. 3472–3509, 2019, Publisher: ACS Publications.

[590] R. Harnisch, G. Lauterbach, and W. Pritzkow, "Kinetics of Peroxyradical Attack at Cyclic Hydrocarbons: Ring-strain effects on H-abstraction," de, *Journal fi£¡r Praktische Chemie/Chemiker-Zeitung*, vol. 337, no. 1, pp. 60–62, 1995, ISSN: 0941-1216, 1521-3897. DOI: 10.1002/prac.19953370113. (visited on 11/20/2022).

[591] L Vereecken and J Peeters, "H-atom abstraction by OH-radicals from (biogenic) (poly)alkenes: C-H bond strengths and abstraction rates," en, *Chemical Physics Letters*, vol. 333, no. 1-2, pp. 162–168, Jan. 2001, ISSN: 00092614. DOI: 10.1016/S0009-2614(00)01347-6.

[592] T. Kurten *et al.*, "Computational Study of Hydrogen Shifts and Ring-Opening Mechanisms in α-Pinene Ozonolysis Products," en, *The Journal of Physical Chemistry A*, vol. 119, no. 46, pp. 11 366–11 375, Nov. 2015, ISSN: 1089-5639, 1520-5215. DOI: 10.1021/acs.jpca.5b08948. (visited on 11/20/2022).

[593] E. Assaf, C. Schoemaecker, L. Vereecken, and C. Fittschen, "Experimental and theoretical investigation of the reaction of ro_2 radicals with oh radicals: Dependence of the ho_2 yield on the size of the alkyl group," *International journal of chemical kinetics*, vol. 50, no. 9, pp. 670–680, 2018.

[594] H. Johnson and R. Clark, "Determination of bromine number of olefinic hydrocarbons," *Analytical Chemistry*, vol. 19, no. 11, pp. 869–872, 1947.

[595] G. Bellucci, C. Chiappe, R. Bianchini, D. Lenoir, and R. Herges, "Nature of the Interaction of Olefin-Bromine Complexes. Inference from (E)-2,2,5,5-Tetramethyl-3,4-diphenylhex-3-ene, the First Example of an Olefin Whose Reaction with Bromine Stops at the Stage of .pi. Complex Formation," en, *Journal of the American Chemical Society*, vol. 117, no. 48, pp. 12 001–12 002, Dec. 1995, ISSN: 0002-7863, 1520-5126. DOI: 10.1021/ja00153a025. [Online].

Available: https://pubs.acs.org/doi/abs/10.1021/ja00153a025 (visited on 06/27/2021).

[596] S. S. Hepperle, Q. Li, and A. L. L. East, "Mechanism of Cis/Trans Equilibration of Alkenes via Iodine Catalysis," en, *The Journal of Physical Chemistry A*, vol. 109, no. 48, pp. 10 975–10 981, Dec. 2005, ISSN: 1089-5639, 1520-5215. DOI: 10.1021/jp053727o. (visited on 06/25/2021).

[597] A. J. Cresswell, S. T.-C. Eey, and S. E. Denmark, "Catalytic, Stereoselective Dihalogenation of Alkenes: Challenges and Opportunities," en, *Angewandte Chemie International Edition*, vol. 54, no. 52, 2015, ISSN: 1521-3773. DOI: 10.1002/anie.201507152. [Online]. Available: https://onlinelibrary.wiley.com/doi/abs/10.1002/anie.201507152 (visited on 07/18/2021).

[598] M. Jereb, M. Zupan, and S. Stavber, "Hydrogen peroxide induced iodine transfer into alkenes," en, *Green Chemistry*, vol. 7, no. 2, p. 100, 2005, ISSN: 1463-9262, 1463-9270. DOI: 10.1039/b407592g. [Online]. Available: http://xlink.rsc.org/?DOI=b407592g (visited on 08/17/2021).

[599] I. Lengyel, I. R. Epstein, and K. Kustin, "Kinetics of iodine hydrolysis," en, *Inorganic Chemistry*, vol. 32, no. 25, pp. 5880–5882, Dec. 1993, ISSN: 0020-1669, 1520-510X. DOI: 10.1021/ic00077a036. [Online]. Available: https://pubs.acs.org/doi/abs/10.1021/ic00077a036 (visited on 04/21/2021).

[600] G. V. Buxton and R. M. Sellers, "Radiation-induced redox reactions of iodine species in aqueous solution. Formation and characterisation of III, IIV, IVI and IVIII, the stability of hypoiodous acid and the chemistry of the interconversion of iodide and iodate," en, *Journal of the Chemical Society, Faraday Transactions 1: Physical Chemistry in Condensed Phases*, vol. 81, no. 2, p. 449, 1985, ISSN: 0300-9599. DOI: 10.1039/f19858100449. [Online]. Available: http://xlink.rsc.org/?DOI=f19858100449.

[601] E. G. Bligh and W. J. Dyer, "A rapid method of total lipid extraction and purification," *Canadian journal of biochemistry and physiology*, vol. 37, no. 8, pp. 911–917, 1959.

[602] T Perez-Palacios, J Ruiz, D Martín, E Muriel, and T Antequera, "Comparison of different methods for total lipid quantification in meat and meat products," *Food chemistry*, vol. 110, no. 4, pp. 1025–1029, 2008.

[603] J. Folch, M. Lees, G. H. Sloane Stanley, *et al.*, "A simple method for the isolation and purification of total lipids from animal tissues," *J biol Chem*, vol. 226, no. 1, pp. 497–509, 1957.

[604] A. J. Sheppard, *Lipid manual: methodology suitable for fatty acid-cholesterol analysis*. Wm. C. Brown Publishers, 1992.

[605] D. B. Konuskan, M. Arslan, and A. Oksuz, "Physicochemical properties of cold pressed sunflower, peanut, rapeseed, mustard and olive oils grown in the eastern mediterranean region," *Saudi Journal of Biological Sciences*, vol. 26, no. 2, pp. 340–344, 2019.

[606] O. J. Houshia, O. Zaid, H. Shqair, M. Zaid, N. Fashafsheh, and R. Bzoor, "Effect of olive oil adulteration on peroxide value, delta-k and on the acidity nabali-baladi olive oil quality," *Delta*, vol. 266, k274, 2014.

[607] B. P. Koch and T. Dittmar, "From mass to structure: An aromaticity index for high resolution mass data of natural organic matter," en, *Rapid Communications in Mass Spectrometry*, vol. 20, no. 5, pp. 926–932, Mar. 2006, ISSN: 0951-4198, 1097-0231. DOI: 10.1002/rcm.2386.

[608] H. O. T. Pye *et al.*, "On the implications of aerosol liquid water and phase separation for organic aerosol mass," en, *Atmospheric Chemistry and Physics*, vol. 17, no. 1, pp. 343–369, Jan. 2017, ISSN: 1680-7324. DOI: 10.5194/acp-17-343-2017. [Online]. Available: https://acp.copernicus.org/articles/17/343/2017/.

[609] D. Q. Pham *et al.*, "Biological Impacts on Carbon Speciation and Morphology of Sea Spray Aerosol," en, *ACS Earth and Space Chemistry*, vol. 1, no. 9, pp. 551–561, Nov. 2017, ISSN: 2472-3452, 2472-3452. DOI: 10.1021/acsearthspacechem.7b00069. [Online]. Available: https://pubs.acs.org/doi/10.1021/acsearthspacechem.7b00069.

[610] M. Fraund *et al.*, "Elemental Mixing State of Aerosol Particles Collected in Central Amazonia during GoAmazon2014/15," en, *Atmosphere*, vol. 8, no. 9, p. 173, Sep. 2017, ISSN: 2073-4433. DOI: 10.3390/atmos8090173. [Online]. Available: https://www.mdpi.com/2073-4433/8/9/173.

[611] R. C. Moffet *et al.*, "Morphology and mixing of black carbon particles collected in central california during the cares field study," *Atmospheric Chemistry and Physics*, vol. 16, no. 22, pp. 14 515–14 525, 2016.

[612] M Jaoui, S Leungsakul, and R. Kamens, "Gas and particle products distribution from the reaction of β-caryophyllene with ozone," *Journal of Atmospheric Chemistry*, vol. 45, pp. 261–287, 2003.

[613] D. Cai, X. Wang, J. Chen, and X. Li, "Molecular Characterization of Organosulfates in Highly Polluted Atmosphere Using Ultra High Resolution Mass Spectrometry," en, *Journal of Geophysical Research: Atmospheres*, vol. 125, no. 8, e2019JD032253, Apr. 2020, ISSN: 2169-897X, 2169-8996. DOI: 10.1029/2019JD032253.

[614] H. Sun *et al.*, "Molecular characterization of humic-like substances (HULIS) in atmospheric particles (PM2.5) in offshore Eastern China Sea (OECS) using solid-phase extraction coupled with ESI FT-ICR MS," en, *Atmospheric Environment*, vol. 294, p. 119 523, Feb. 2023, ISSN: 13522310. DOI: 10.1016/j.atmosenv.2022.119523. [Online]. Available: https://linkinghub.elsevier.com/retrieve/pii/S135223102200588X.

[615] J. D. Surratt *et al.*, "Effect of Acidity on Secondary Organic Aerosol Formation from Isoprene," en, *Environmental Science & Technology*, vol. 41, no. 15, pp. 5363–5369, Aug. 2007, ISSN: 0013-936X, 1520-5851. DOI: 10.1021/es0704176. [Online]. Available: https://pubs.acs.org/doi/10.1021/es0704176.

[616] X. Kong *et al.*, "Molecular characterization and optical properties of primary emissions from a residential wood burning boiler," en, *Science of The Total Environment*, vol. 754, p. 142 143, Feb. 2021, ISSN: 00489697. DOI: 10.1016/j.scitotenv.2020.142143. [Online]. Available: https://linkinghub.elsevier.com/retrieve/pii/S0048969720356722.

[617] M. Jensen, *ARM KAZR-ARSCL Value Added Product*, en, 2012. DOI: 10.5439/1052058.

[618] D. Flynn, C Sivaraman, J Comstock, and D. Zhang, "Micropulse Lidar Cloud Mask (MPLCMASK) Value-Added Product for the Fast-Switching Polarized Micropulse Lidar Technical Report," Tech. Rep. DOE/SC-ARM/TR-098, 1019283, PNNL-20561, Jul. 2020, DOE/SC–ARM/TR–098, 1019283, PNNL–20561. DOI: 10.2172/1019283. [Online]. Available: https://www.osti.gov/servlets/purl/1019283/.

Appendix A: Chapter 2

Supplementary information for Chapter 2

A.1 Synthesis of Limononic Acid (LMA)

Limononic acid was synthesized as per the procedure outlined by Witkowski et al.[222]. Briefly, 10 mM aqueous solution of CPA was irradiated with UVB light for 90 min using a photoreactor. The irradiated solution was analyzed using Agilent HPLC-UV (G1312A). A Kinetex column (2.6 μm particle size, 100Å, 150 x 4.1 mm) was utilized for optimum separation. The gradient elution constituting 0.1% formic acid (FA) in Acetonitrile (B) and 0.1% FA in water (A) with 500 μL injection volume was as follows: 0-0.5 min 15% B, 0.5-17 min linear gradient to 40% B, 17-18 min linear gradient to 90% B, 18-19 min isocratic 90%, 19.5 min 15% B, 19.5-25 min 15% B and 25.0-29.0 min 1% B. VWD detector was set at a wavelength of 283 nm and chromatographically separated aliquots were manually collected in a glass vial and freeze-dried overnight. The purified white powder was stored in the fridge before analysis. The structure of LMA was confirmed with ^{1}H NMR as presented in Figure A.1 (S1.1). Although we observed complexity in lower chemical shifts to assign methyl (-CH_2 and -CH_3) protons, the doublet at 4.8 ppm represented the allylic protons unique to LMA. An online predictor tool (NMRdb) was utilized to rank the proton shifts as shown in Figure A.1 (S1.2). Similar chemical shifts are also observed in the work of Witkowski and Lignell et al.[222, 584]

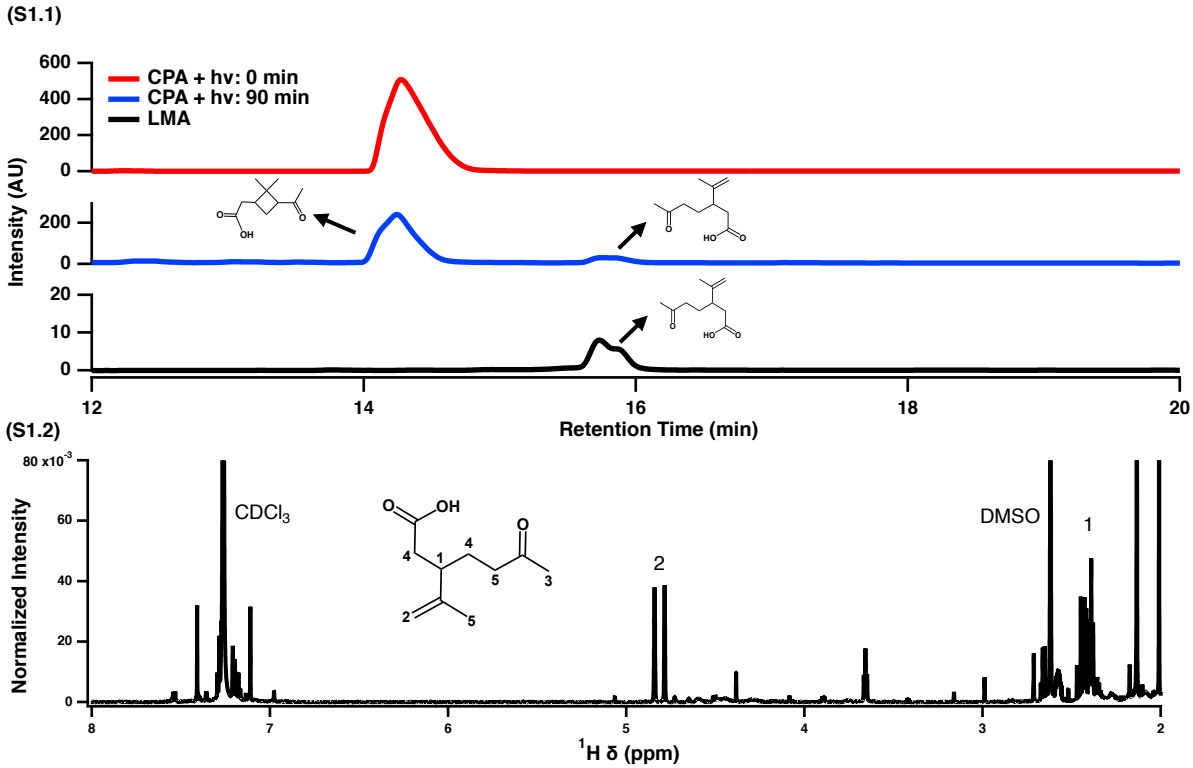

Figure A.1: Determination of the purity of LMA using HPLC-UV and ^{1}H NMR. (S1.1) Chromatogram of CPA, irradiated CPA solution and purified LMA at 283 nm. (S1.2) ^{1}H NMR of the synthesized and purified LMA in $CDCl_3$.

A.2 Experimental Conditions for Photooxidation of Organic Acids

Table A.1 is a brief summary of the conditions applied during the photooxidation of organic acids (OAcs).

Table A.1: Experimental conditions used for photooxidation of OAcs.

Compounds	[OAcs][a] (μM)	[H_2O_2][a] (mM)	UV (nm)	Irradiation time (min)
7-OE	179	5	UVB	0-15
	358	1	UVB	0-25
		5		0-15
		10		0-15
	358	5	UVC	0-5
		150	UVA	0-33
	700	5	UVB	0-15
	1000			0-25
1-OA	358	5	UVB	0-15
LMA	150			
PNA	100			

[a] refers to final concentrations in the quartz vial prior to irradiation;

A.3 Sample Analysis

A.3.1 Method Controls

The experimental conditions in the iodometry protocol and to examine possible interfering reactions are outlined in Table A.2. First, we examined the suppression caused by iodide ion (I^-) in the ion signal intensity of our internal standards. This was achieved by reducing the concentration of I^- from 60 mM to 6 mM in the ID-T treated sample while keeping all other conditions identical. The results from this experiment are discussed in Section A.3.2. Second, to eliminate the possibility that newly formed ROOHs would experience matrix effects due to side reactions between olefins and molecular iodine (I_2),[183] we investigated the reactivity of newly formed ROOHs with I_2. Briefly, the oxidized aqueous solution of OAc and H_2O_2 was treated under I_2-C and I_2-T conditions. The concentration estimation of aqueous I_2 is de-

scribed elsewhere.[183] The results on these investigations are provided in Section A.3.2.

Table A.2: Controls for iodometry protocols.

Reagent	**ID-C**[a]	**ID-T**[b]	**I_2-C**[c]	**I_2-T**[d]
Sample (mL)	0.840	0.840	0.500	0.500
KI (mM)	-	60	-	-
Acetic acid (mM)	30	30	30	30
I2 (μM)	-	-	-	620
Internal standard (μM)	15	15	30	30

[a] iodometry-control;
[b] iodometry-treated;
[c] iodine-control;
[d] iodine-treated;

To illustrate that the formation of expected ROOHs is solely due to OH reaction, we performed additional control experiments as outlined in Table A.3. The aliquots from each control condition were treated as per the iodometry protocol. From these control experiments, we inferred that the formation of products did not occur without OH radical initiation and respective precursor in the aqueous mixture.

Table A.3: Experimental controls for photooxidation.

Controls	**Precursors**		**UV lamp**
	H_2O_2	**OAc**	
H_2O_2 control	No	Yes	Yes
Method blank	Yes	No	Yes

Instrumental Parameters:

For optimum separation of products from varying OAcs, gradient elution was carried out using 0.1% FA in water (A) and 0.1% FA in ACN (B). The gradient applied was as follows: initial 1% B for 1 min, linear gradient from 1% to 95% B for 5 min, hold 1 min for 95% B and decrease to 1% B at 0.5 min. (-)ESI polarity was used based on

the following conditions: capillary voltage, 3200V; fragmentor voltage, 125 V; drying gas, 9.0 L min^{-1} at 325 °C; and nebulizer pressure, 20 psi. Experimental analysis for interference with molecular iodine (I_2) was performed on the waters QTOF HPLC-MS instrument. A C18 (Kinetex 2.6 μm particle size, 100Å, 50 x 2.1 mm) column was used. The gradient elution program with 0.1% formic acid in water (A) and 0.1% formic acid in acetonitrile (B) was as follows: 0.0-0.5 min 1% B, increase to 25% B for 2.0 min, 35% B for 4.0 min, increase to 55% B at 6.0 min, hold for 95% B at 7.0-7.5 min and decrease to 1% B at 8.0-12.0 min. 2 μL sample was injected using Agilent 1200 series autosampler (G1312B).

A.3.2 Potential Interferences

Figure A.2 compares the (-)ESI-EIC for specific mass-to-charge ratios (m/z) in the deprotonated forms. Figure A.2 (S2.1) shows a comparison of EIC for AZA at m/z 187 between ID-C and ID-T samples. These experiments were performed with 10 times reduced concentration of I^-. We observed a negligible change in the ion signal intensity, thereby confirming the non-reactivity of AZA. This result also shows that ion suppression induced by I^- is negligible. Figure A.2 (S2.2) compares EIC for the first-generation hydroperoxide from 7-OE at m/z 191 between I_2-C and I_2-T samples. Based on Figure A.2 (S2.2), we observed no change in the signal intensity, indicating that the newly formed hydroperoxides does not contain any C=C bonds and hence would not experience I_2 interference.[183]

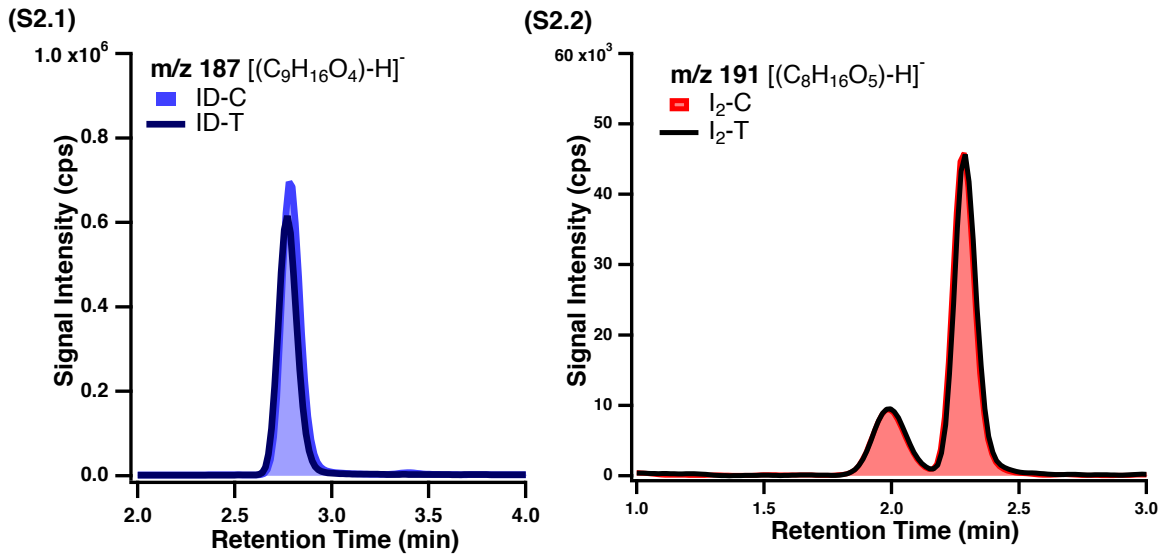

Figure A.2: Examination of Extracted Ion Chromatograms (EICs) for possible interferences due to ionization suppression and side reactions. The EICs are represented in $[M\text{-}H]^-$ format for specific m/z. (S2.1) EIC for AZA at m/z 187; (S2.2) EIC corresponds to m/z 191.

A.4 Photox Flux and Wavelength Distribution Spectrum

Quantification of photon flux is necessary for each type of lamp and an essential prerequisite for photooxidation experiments.[585] Photon flux measurements estimate the number of light molecules reaching the aqueous solution inside the photoreactor. Flux was estimated by calculating the parameters listed in eq-A1. To evaluate I(λ), we performed direct measurements using a spectroradiometer (Ocean, Optics USB2000+ER) and chemical actinometry with 2-nitrobenzaldehyde (2-NB). The spectroradiometer allowed for the recording of emission spectra of UVA-UVC lamps, while actinometry with 2-NB allowed for the quantification of the first-order photolysis rate of 2-NB ($J_N B$).[586] Briefly, the direct photolysis rate of 2-NB was monitored using the HPLC-UV system as described in the work of Galbavy et al.[586] To determine the photon flux (I(λ)), the recorded spectra were linearly scaled until it matched

the observed $J_N B$ value.

$$J_{2\mathrm{NB}}\,(\mathrm{s}^{-1}) = \frac{2.303 \times 10^3}{N_\mathrm{A}} \int_{\lambda_\mathrm{min}}^{\lambda_\mathrm{max}} \mathrm{I}(\lambda)\,\phi(\lambda)\,\sigma(\lambda)\,\mathrm{d}\lambda \qquad \text{(eq-A1)}$$

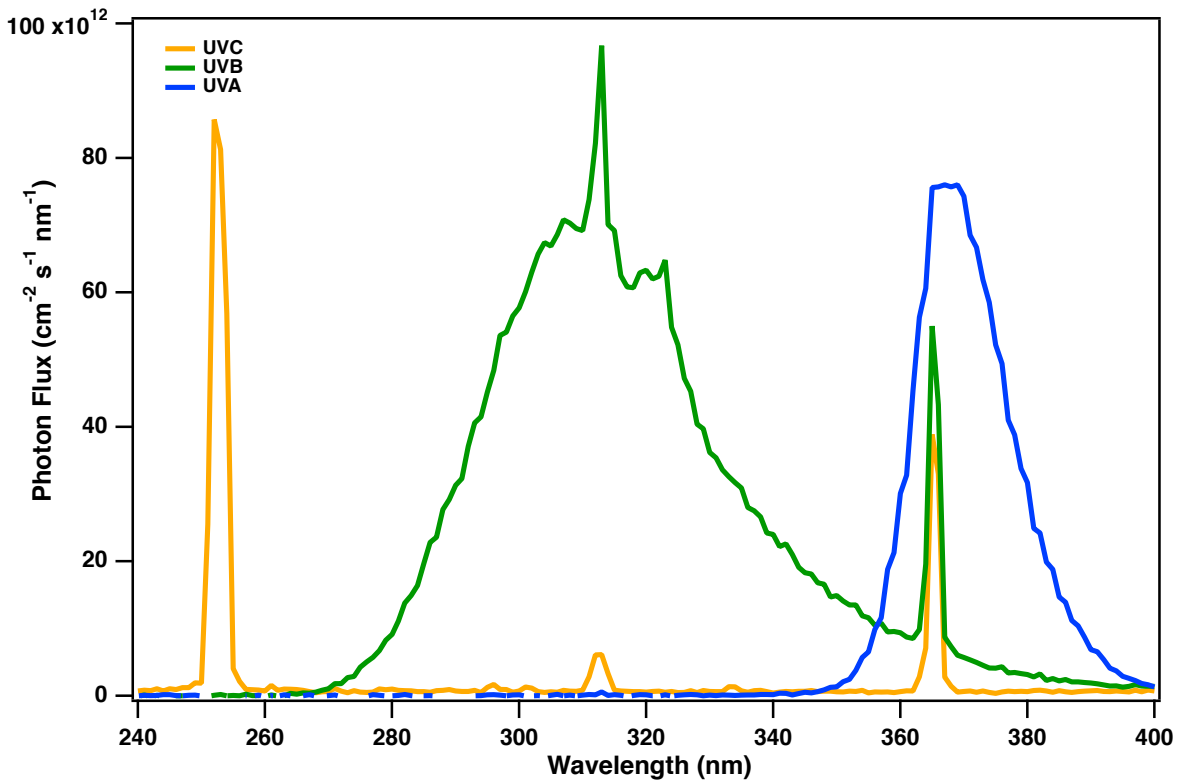

Figure A.3: Photon flux spectrum ranging from 240 nm to 400 nm is expressed as $\mathrm{cm}^{-2}\ \mathrm{s}^{-1}\ \mathrm{nm}^{-1}$, for distinct ultraviolet (UV) lamps used in photo reactor during photooxidation of OAcs.

A.5 Mechanism for Peroxide Formation

To understand the formation of ROOHs from different OAcs, 7-OE and PNA are utilized to exemplify the product formation as shown in Figure A.4 and A.5, respectively. 7-OE represents the formation of photooxidation initiated ROOHs for an unsaturated OAc. The first step of the process is the formation of peroxy radical (RO_2) (P-1) which typically proceeds via the attack of an OH radical on the allylic π-electrons.[55] The newly formed P-1 radical could either undergo intramolecular H-abstraction (A-1)[587, 588] or follow bimolecular termination reactions.[589] In our discussions here, we only focused on the termination reactions by hydroperoxy (HO_2) radicals, which led to the formation of first-generation ROOH (III) at m/z 191. Due to the lack of radical measurements, it is likely that the formation of second-generation RO_2 radical could be via HO_2 termination of P-2 radical or OH/RO radical facilitated HO_2 termination. In any case, the formation of second-generation ROOH (IV) would occur.

Following the autoxidation pathway, a 1,5 H-shift from $P-1$ radical would yield a short-lived carbon-centred radical ($A-1$), which is highly likely to react with a dissolved O_2 molecule to form another RO_2 radical ($P-2$), subsequently undergoing another intramolecular H-shift. Usually, such H-shifts could depend on the strength of the C-H bond at the potential H-abstraction site and the steric restraint for the RO_2 radical to reach that site.[590, 591] In our case, a successful 1,5 $H-$shift is followed by the formation of $P-2$,[592] such that two more oxygen atoms are now added to the precursor. The second-generation $P-2$ radical eventually undergoes termination by HO_2 radicals, thereby successfully generating a second-generation peroxide (IV) at m/z 223. It is important to note that for each of the peroxy radicals ($P-1$ and $P-2$) we also expect the formation of either a short-lived tetroxide intermediate (e.g., $I-1$),[247] or subsequent intramolecular $H-$shifts to form compounds with more ROOH functional groups. The tetroxide intermediate can decompose to a variety of

products including carbonyl, alcohol and ROOR species, which we did not focus on in this study.[247, 271] Products arising from subsequent oxidation steps will likely have too small of a signal intensity to be detected by our LC/ESI-MS technique. The product formation in a saturated OAc is demonstrated by showing the mechanism for PNA in Figure A.5.

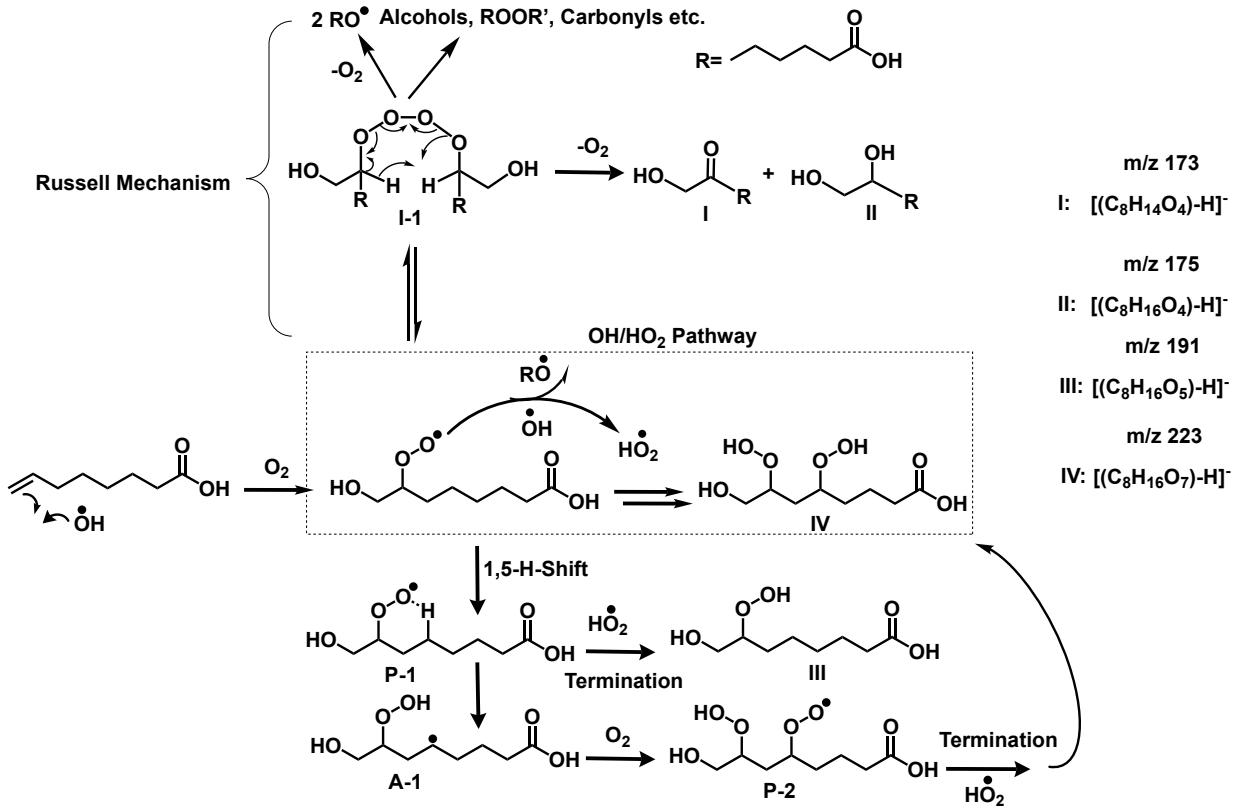

Figure A.4: A proposed photooxidation mechanism for the formation of products from 7-OE.[243, 247, 271, 535, 593]

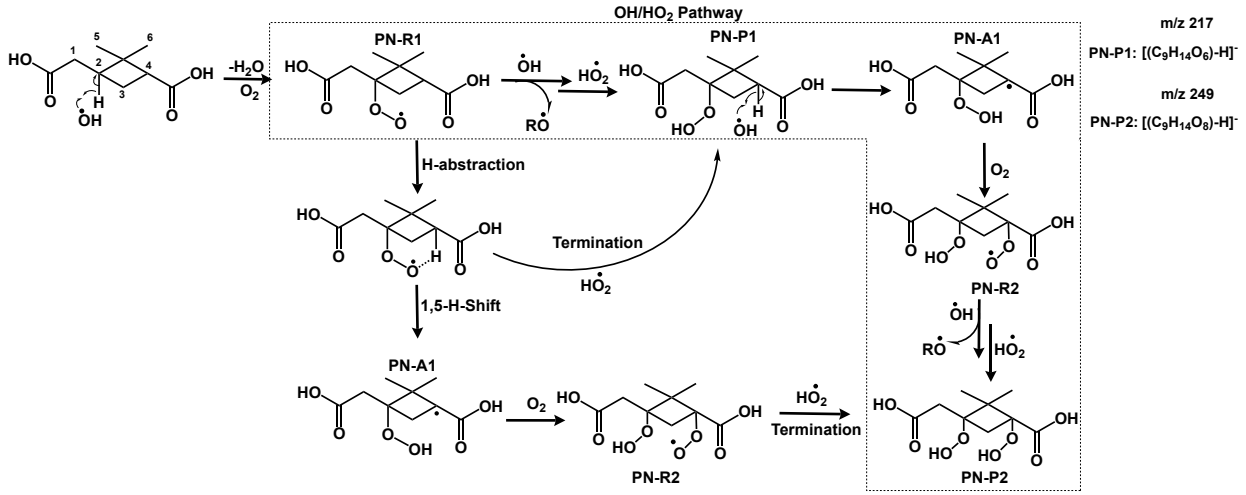

Figure A.5: Proposed mechanism for photooxidation of PNA.[224]

A.6 Estimation of Peroxide Yield

In this section, we provide a detailed discussion of kinetic investigations to acquire yields of newly formed ROOHs.

A.6.1 Yield

Experimental conditions for photooxidationproducts are outlined in Table A.1. The yield (γ) for the photooxidation product from 7-OE is calculated as per eq-A2. The calculations pertaining to steady-state OH concentrations ($[OH]_{SS}$) are outlined in A.6.2.

$$\gamma = \frac{PA_{prod,t}}{\Delta 7OE} = \frac{PA_{prod,t}}{C_i(\frac{PA_0 - PA_t}{PA_0})} \qquad \text{(eq-A2)}$$

where $PA_{prod,t}$ represents the peak area of the ROOH product at time t, while PA_0 and PA_t represent the peak areas of the precursor (7-OE) at time 0 and t, respectively. C_i is the initial concentration of 7-OE used in the experiment.

Table A.4: Comparison of γ (cps.μM^{-1}) across varying wavelengths.

[7-OE] (μM)	**[H_2O_2] (mM)**	**Wavelength Type**	**γ^a x 10 (m/z 223)**	**γ^a x 10^3 (m/z 191)**
358	5	UVC	NaN	NaN
358	5	UVB	4.59±1.29	3.00±0.862
358	150	UVA	31.0±7.03	15.7±3.47

[a] γ of m/z 223 and m/z 191 was obtained when 7-OE was almost 56% consumed;

Table A.5: Comparison of γ (cps.μM^{-1}) across oxidant and precursor concentrations.

[7-OE] (μM)	**[OH] x 10^{-14} (M)**	**γ^a (m/z 223)**	**γ^b x 10^3 (m/z 191)**
179	16.3±2.41	78.0±22.6	5.09±1.65
358	8.25±1.09	56.8±27.8	2.74±0.624
700	4.39±0.647	51.2±3.67	3.59±0.891
1000	4.00±0.581	11.8±3.02	4.41±0.984
358	3.54±0.433	72.8±23.8	3.67±1.20
358	8.25±1.09	56.8±27.8	3.00±0.862
358	35.3±4.90	45.6±10.2	2.82±0.613

[a] γ of m/z 223 was obtained when 7-OE was almost excessively consumed;
[b] γ of m/z 191 was obtained when 7-OE was almost ∼50-60% consumed;

A.6.2 Kinetic Investigation

A kinetic investigation was pursued to determine the rate coefficient of 7-OE with OH and estimate $[OH]_{SS}$. A relative rate kinetic method[231] was adopted with PMA as the reference compound and 7-OE as the target compound. For this, an aqueous solution of 4 mL 7-OE (716 μM) mixed with 4 mL H_2O_2 (10 mM) and 15 μL of PMA (60 μM) was irradiated for 13 min and aliquots were periodically taken at 1

min intervals.

$$ln(\frac{[S]_0}{[S]_t}) = \frac{k_S^{II}}{k_R^{II}} ln(\frac{[R]_0}{[R]_t}) \quad \text{(eq-A3)}$$

Here, [S] and [R] correspond to the concentrations of 7-OE and PMA, respectively, before turning on lamps (time = 0) and during the experiment (time = t).

Figure A.6 reflects the kinetic observations for 7-OE. Figure A.6.1 demonstrates the relative rate plot between the natural logarithmic ratio of the peak area of 7-OE with respect to the natural logarithmic ratio of PMA. The curve was found to be linear with a high R^2 (0.998). Using eq-A4, the rate coefficient for the loss of 7-OE with OH was acquired (Table A.6).[270] Figure A.6 (S4.2) shows the first-order rate of decay in 7-OE under three different H_2O_2 concentrations (Table A.7). This decay showed linearity with a high R^2 (>0.95) for all concentrations. Figure A.6 (S4.3) is evidence of the first-order decay rate for 7-OE under constant H_2O_2 concentration. We observed good linearity with high R^2 (>0.95) for varying 7-OE concentrations (Table A.7). Utilizing the rate coefficient obtained from eq-A3, $[OH]_{SS}$ was estimated using eq-A4. The estimated OH concentrations and observed first-order rate coefficients are listed in Table A.7.

$$k^{II} = k^{obs}.[^{\bullet}OH] \quad \text{(eq-A4)}$$

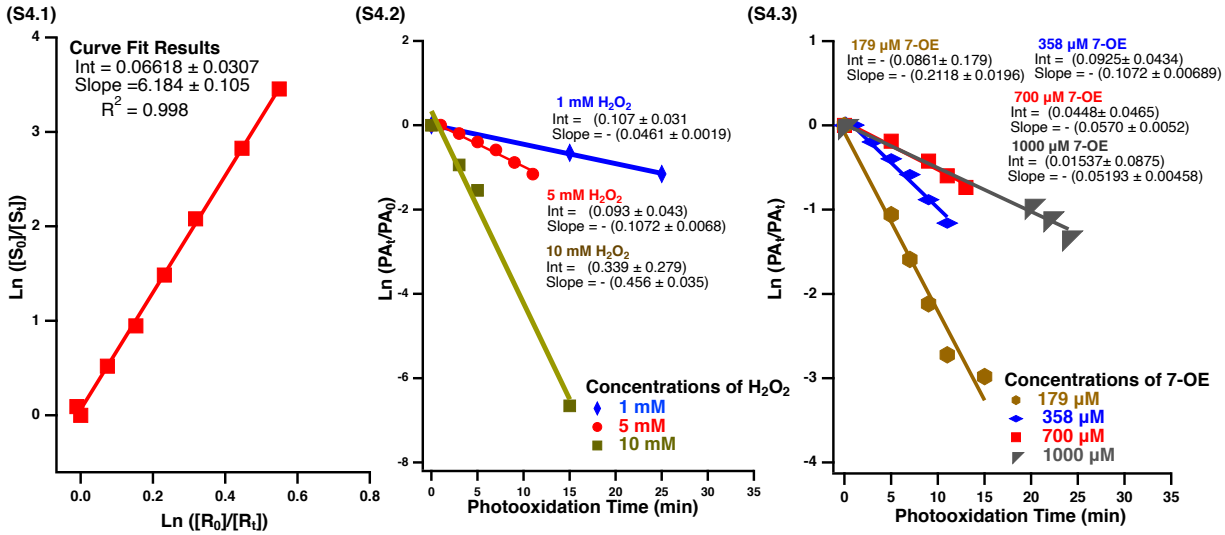

Figure A.6: Kinetic observations to acquire rate coefficient and estimate $[OH]_{SS}$. (S4.1) Relative rate method for second-order rate coefficient determination of 7-OE. PMA is chosen as a reference compound and 7-OE is the target compound. (S4.2) Estimation of observed first-order decay in 7-OE under varying concentrations of H_2O_2. (S4.3) First-order decay in different concentrations of 7-OE under constant H_2O_2 concentration.

Table A.6: Experimentally determined rate coefficients.

Precursors	$\mathbf{k^{obs}}$ **(s^{-1}) x 10^{-3}**	$\mathbf{k^{II}}$ **(M^{-1} s^{-1}) x 10^{9}**
7-OE + OH	1.79±0.01[a]	21.6±2.50[a]
PMA + OH	-	3.5±0.4[b]

[a] This study;
[b] Reference value from literature;[253]

Table A.7: Rate Coefficients under Varying oxidant and precursor concentrations.

Precursors			
[7-OE] (μ**M**)	**[H_2O_2]** (**mM**)	**k**^obs (**s**$^{-1}$) **x 10**$^{-3}$	**[OH]**$_{SS}$ **(M) x 10**$^{-14}$
358	1	0.767±0.0308	3.54±0.433
358	5	1.79±0.113	8.25±1.09
358	10	7.64±0.587	35.3±4.90
179	5	3.53±0.327	16.3±2.41
358	5	1.79±0.113	8.25±1.09
700	5	0.950±0.0870	4.39±0.647
1000	5	0.865±0.0763	4.00±0.581

A.7 Identification of Photooxidation Products

A.7.1 Photooxidation Products in 1-OA and PNA

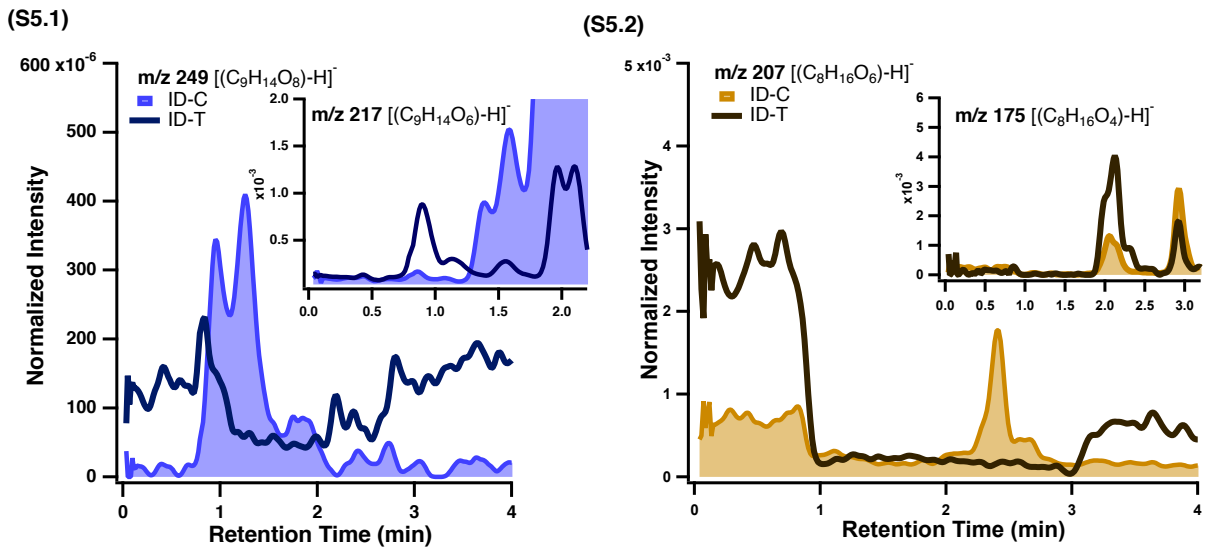

Figure A.7: EIC for second-generation ROOHs from 1-OA and PNA. Signal responses have been normalized with respect to AZA. Each EIC is shown in [M-H]$^-$ format for respective ions. The inset windows are EICs corresponding to the alcohols from the iodometry reduction of ROOHs. (S5.1) Average EIC for ROOH from PNA at m/z 249 ([($C_9H_{14}O_8$)-H]$^-$) and the alcohol from this ROOH at m/z 217 ([($C_9H_{14}O_6$)-H]$^-$). (S5.2) Average triplicate EIC for ROOH from 1-OA at m/z 207 ([($C_8H_{16}O_6$)-H]$^-$) and alcohol at m/z 175 ([($C_8H_{16}O_4$)-H]$^-$).

A.7.2 Hydroperoxide from LMA

LMA was photooxidized under similar conditions as that of other OAcs. Figure A.8 represents the EIC of first-generation hydroperoxide ion at m/z 233 from a purified extract of LMA. The signal response in the [M-H]- format has been normalized with respect to the internal standard (AZA). Here, the peroxide ion showed more than 90% signal reduction as evidenced by the comparison between the ID-C and ID-T samples. The inset window provides a comparison of m/z 217 between ID-C and ID-T samples. Unlike other OAcs, we did not observe an enhancement in the signal response of alcohol (m/z 217) from its corresponding peroxide precursor. However, upon examination of the mass spectra at m/z 217, the chemical formula matching the alcohol ([($C_{10}H_{18}O_5$)-H]$^-$) was only found in the ID-T sample and not in ID-C. This observation provides additional validation for the detection of first-generation

ROOH in LMA.

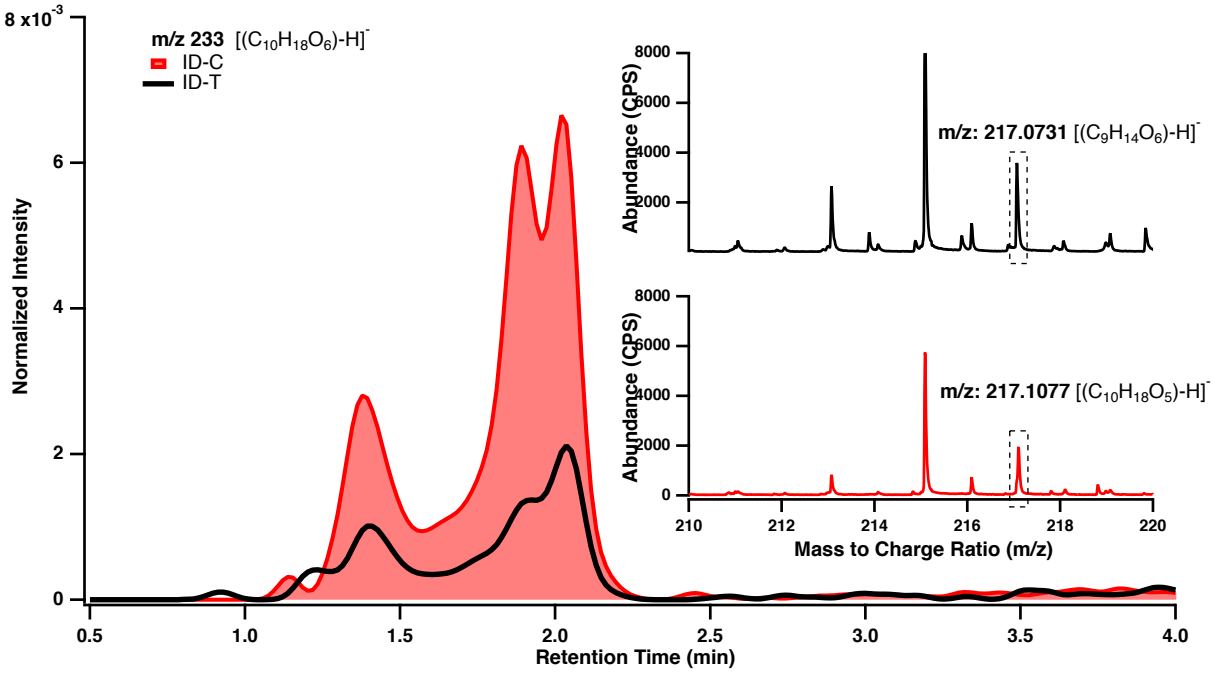

Figure A.8: EIC of first-generation peroxide ion at m/z 233. The inset window is the MS spectra for alcohol ion at m/z 217.

A.8 Factors Affecting Photooxidation

A.8.1 Impact of Wavelength

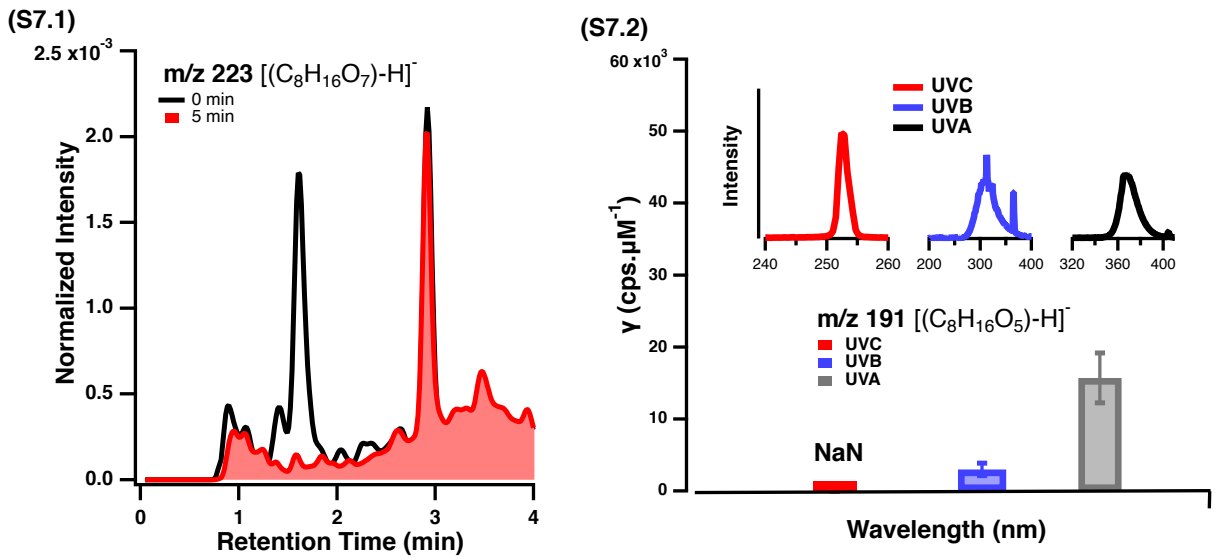

Figure A.9: Effects of wavelength on the formation of ROOHs from 7-OE. (S7.1) The switch experiment from UVB to UVC, demonstrated with the EIC of peroxide ion at m/z 223. Comparisons are drawn between 0 min and 5 min of photooxidation time under UVC exposure. Signal response is normalized with AZA. (S7.2) γ for peroxide ion at m/z 191 under exposure to UVC, UVB and UVA wavelengths. The inset window reflects the absorption spectra under each wavelength. Error bars represent 1σ of triplicate measurements.

A.8.2 Concentration:Periodic Monitoring

Figure A.10 illustrates the sequential monitoring of the photooxidized solution of 7-OE at 358 μM concentration. To demonstrate the evolution of second-generation peroxide on the same graph, we have scaled the γ of m/z 223 by a factor of 30. Note, m/z 191 shows a peaked response in its γ at 50-65 % consumption of 7-OE, whereas in this range the γ of m/z 223 has yet to peak. Hence, for equivalent comparison, we chose 50-65 % and >90 % consumption of 7-OE to estimate the yield of m/z 191 and m/z 223 respectively. These comparisons were used to understand the effects of concentration.

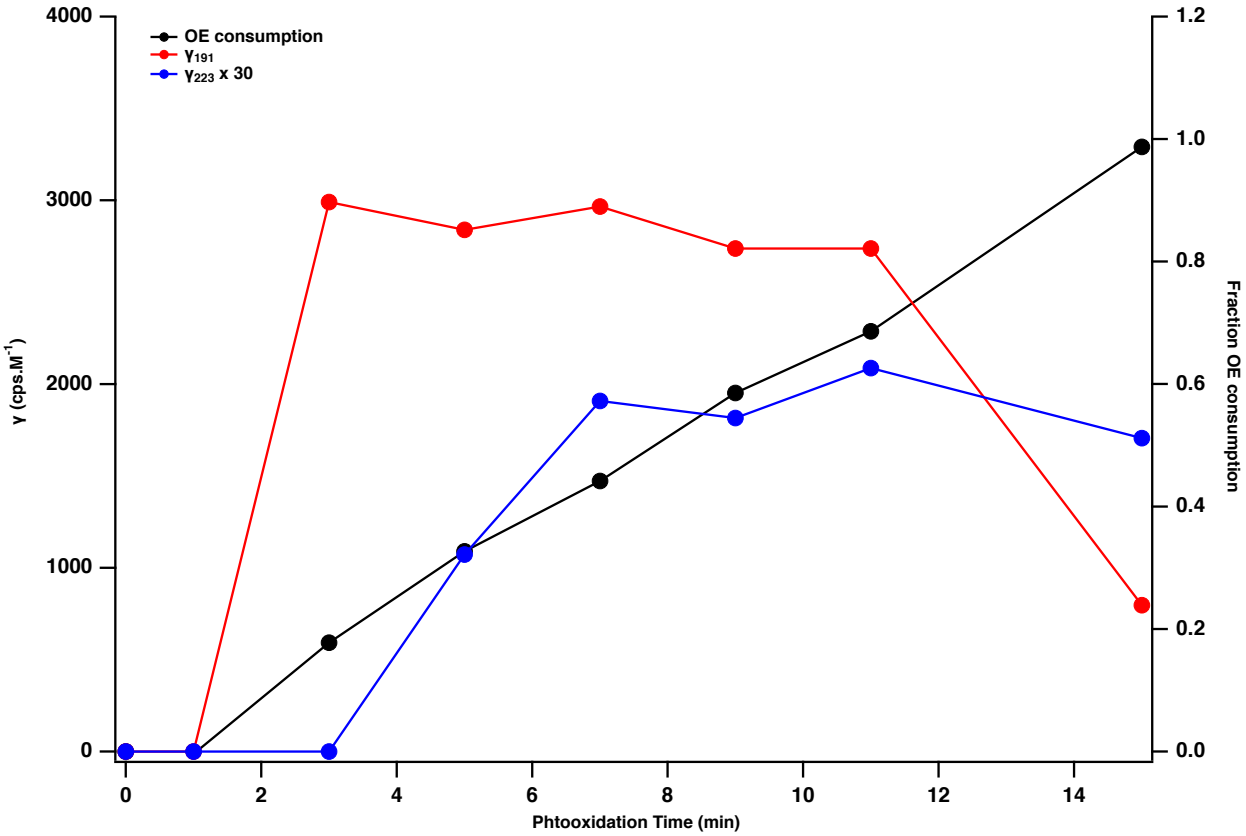

Figure A.10: Comparison of yields for first- and second-generated ROOHs from 7-OE. The left axis is representing the yield for m/z 191 and 223, while the right axis is showing the fractional 7-OE consumption over periodic monitoring during photooxidation.

Appendix B: Chapter 3

Supplementary information for Chapter 3

B.1 Quantitative estimation on dissolved I_2 in water

In this section, details in the assessment of I_2 quantification are provided. A UV-Vis spectrophotometer (Agilent 8453) is used to scan between 190 and 1100 nm. The concentration for I_2 in water was estimated at 460 nm (ϵ = 746 M^{-1} cm^{-1}). This wavelength is prone to interference from I_3^- (ϵ = 975 M^{-1} cm^{-1}),[352] and thus, to correct for absorption interference the equation eq-B1 was applied:

$$[I_2] = (\frac{A_{I_2}}{\epsilon_{I_2}} * 10^6) - (\frac{A_{I_3^-}}{\epsilon_{I_3^-}} * 10^6) \qquad \text{(eq-B1)}$$

where, A_{I_2} = absorbance at 460 nm; $A_{I_3^-}$ = absorbance at 351 nm; ϵ_{I_2} = (molar absorptivity of I_2 at 460 nm) 746 M^{-1} cm^{-1}; $\epsilon_{I_3^-}$ = (molar absorptivity of I_3^- at 351 nm) 26,400 M^{-1} cm^{-1};

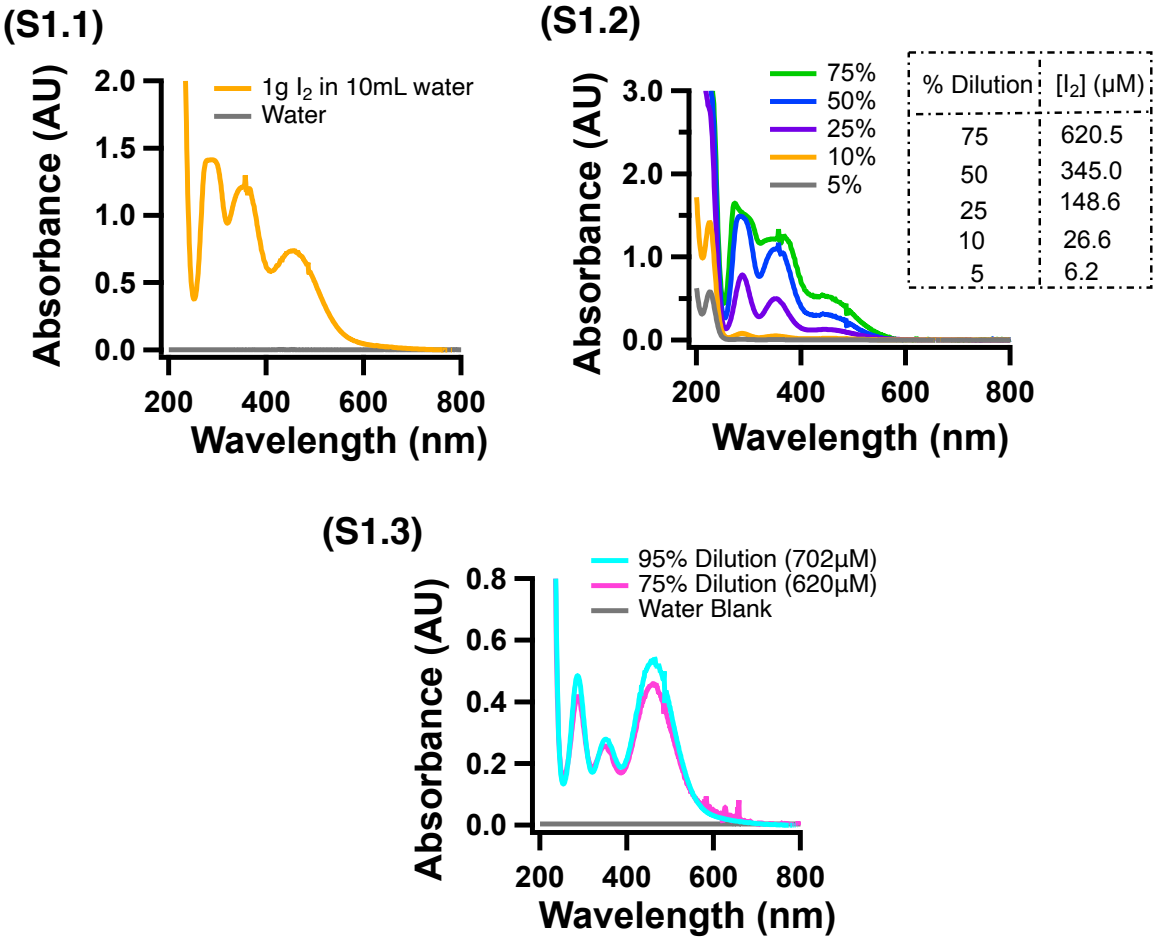

Figure B.1: Quantification of I_2 aqueous solution using UV-Vis measurements. (S1.1) Pure I_2 solution absorbance at 460 nm. (S1.2) Beer's Law agreement in I_2 solution for concentration estimation. (S1.3) Absorbance profile for excess I_2 aqueous solution for pseudo order experiments.

B.2 Analysis of method blanks for experimented organic acid in iodometry.

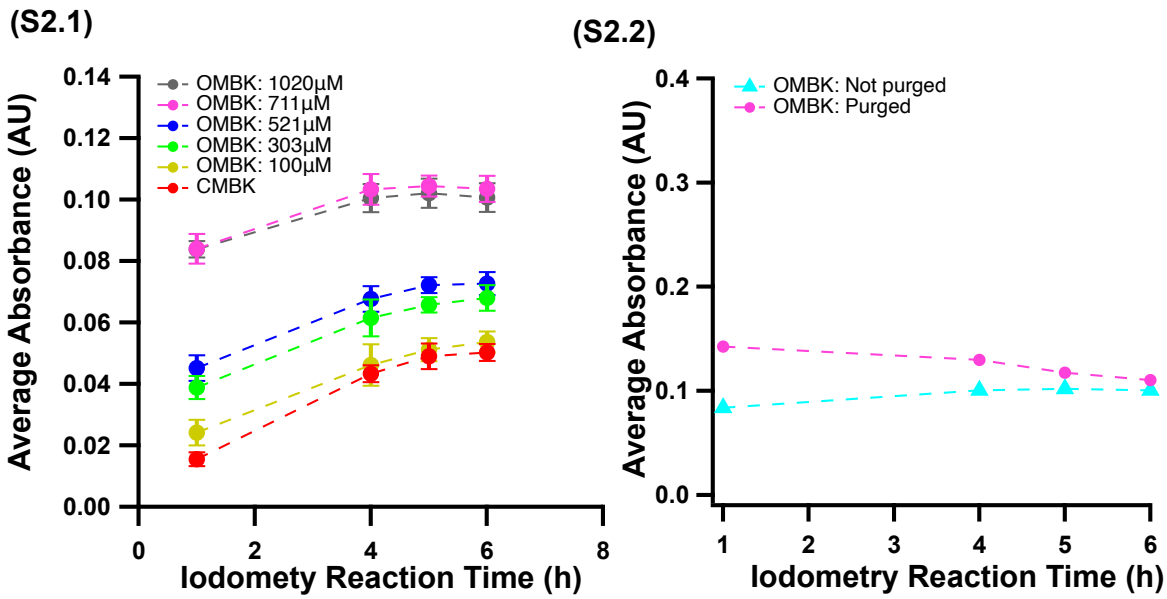

Figure B.2: Method blanks to account for background response of O_2. (S2.1) Average absorbance at $\lambda = 351$ nm for conventional iodometry method blank (CMBK) and 3-OE dosed iodometry method blank (OMBK) with a variety of 3-OE concentrations added. (S2.2) Comparison of OMBK between purged and non-purged samples with N_2. Absorbance response recorded for 3-OE method blank at maximum concentration (1020 μM).

B.3 Quantitative assessment on the observed interference of 3-OE-dosed iodometry.

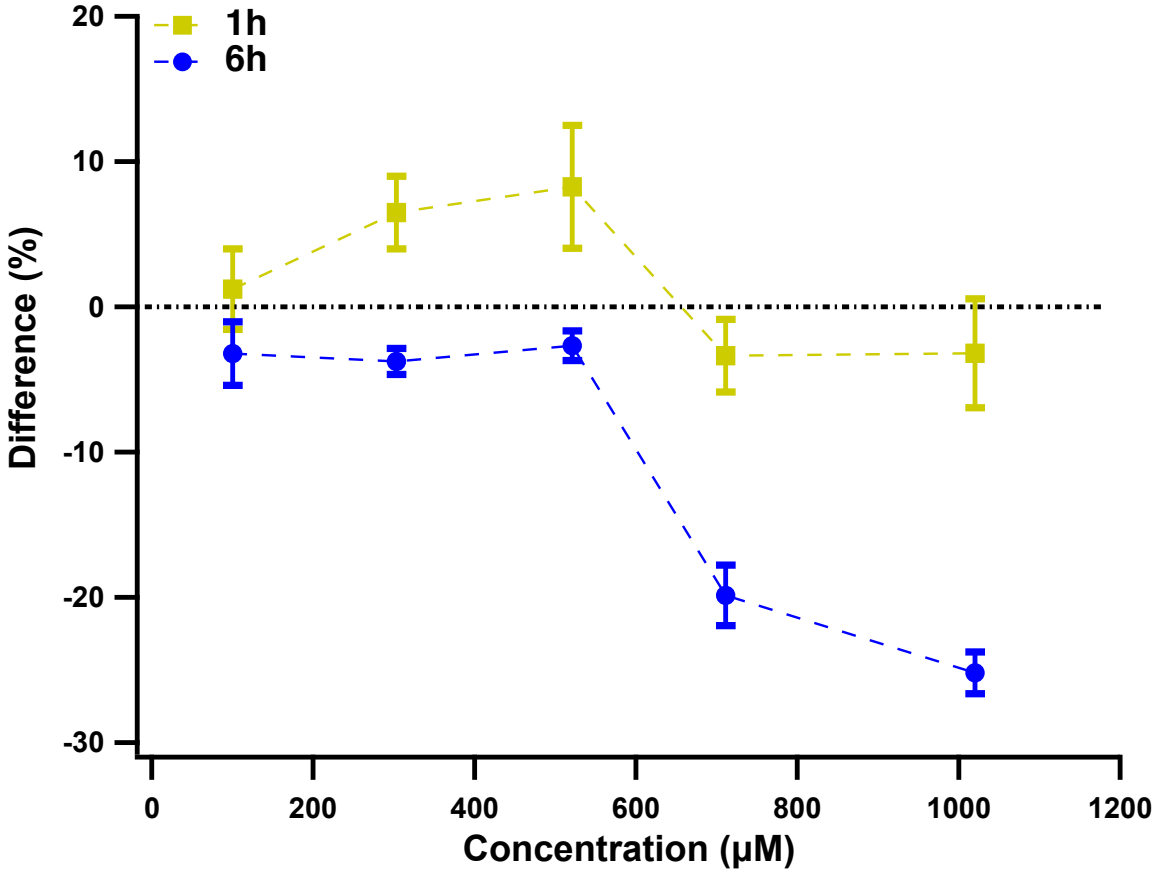

Figure B.3: Percentage difference observed for low (100 μM) to high (1020 μM) range of 3-OE concentrations in the OE-dosed iodometry at 1 h and 6 h of reaction times.

B.4 Mechanism and product characterization

B.4.1 Product characterization

We investigated the product(s) arising for I_2 reaction with 7-OE and 3-OE using ^{1}H NMR and HR-LC-MS analysis. To provide insights into the structure of the product, the acquired ^{1}H NMR spectra for 7-OE, with and without the addition of I_2 are shown in Figure 3.8 (B) and (C) in the main document respectively. The interpretation of NMR spectra below is based on general chemical shifts of organic compounds and an NMR simulation tool (NMRdb). Since DMSO is used as an internal standard, the responses in each spectra are normalized to the response of DMSO to allow direct comparison of signal intensities. The DMSO chemical shift is identified at 2.7 ppm for both samples. The singlet peak at 4.8 ppm is attributed to H_2O impurity present in D_2O. Observing (B) and (C), signature peaks of 7-OE i.e. the vinyl ($H_{7(R)}$) and $H_{8(R)}$ at 5.9 and 5.0 ppm) and methyl protons (H_2 at 2.2 ppm) were identified. Upon adding I_2 to the 7-OE solution, a few peaks appeared in the chemical shift (δ) region of 3.0-3.4 ppm, which are attributable to the product. A decrease in the reactant signal (e.g, $H_{7(R)}$ and $H_{8(R)}$) is also observed. Particularly, $\delta = 3.3$ ppm is attributed to $H_{7(P)}$ while $\delta = 3.4$ ppm is due to $H_{8(P)}$. The higher chemical shift is assigned for H_8 proton due to deshielding effects of the OH functional group. Another possible scenario to consider is, if OH were to be attached at C_7 position. As per the online simulator tool, we believe that the OH bond formation at C_7 position would cause an appearance of a new multiplet at $\delta = 4.0$ ppm. This deshielded chemical shift is absent in Figure 3.8 (C) (main document), which leads to a conclusion that the bonds for OH and I are indeed formed at C_8 and C_7 positions, respectively.

Figure B.4 (S4.1) shows the ESI(-)EIC comparison between control and addition of 3-OE-I_2 samples, where the emergence of the product is marked by a new peak at retention time (RT) = 3.4 min and detected as $[2M\text{-}H]^-$ at m/z 571.001 with a mass difference of 2.59 ppm. This mass is an expected dimer of m/z 285.001. The

product analysis for 3-OE is a little more complex than 7-OE. There is a possibility that two mono hydroxy iodo substituted compounds are formed for 3-OE in aqueous solution. Due to the location of π-electrons in the middle position, it is believed that the addition of halogen (I) can either occur at C_3 or C_4 position. The understanding on specific bond formation is provided by ^{1}H NMR analysis. Figure B.4 (S4.2) and B.4.3 show ^{1}H NMR spectra for 3-OE in case of with and without the addition of I_2 respectively. Both spectra have been normalised with respect to the DMSO response which is identified at $\delta = 2.7$ ppm. The singlet peak observed at 4.8 ppm is attributed to H_2O impurity. Comparing Figure B.4 (S4.2) and B.4 (S4.3), we first identified the double bond protons ($H_{3(R)}$) and $H_{4(R)}$) in 3-OE as a multiplet at $\delta = 5.6$ ppm. These reactant protons show a decrease in their signal response upon addition of I_2 to the 3-OE sample (Figure B.4 (S4.3)). The methyl protons (H_2) were found at $\delta = 2.9$ ppm as a doublet (d). As mentioned earlier, the product for 3-OE could be observed as a mixture of two products: P1 and P2. The distinction between P1 and P2 is made on the basis of deshielding effects observed by the protons: H_3 and H_4. In the case of P1, we consider the addition of OH and I at positions C_3 and C_4 respectively. Such an arrangement of the halogen (I) and nucleophile (OH) exhibits distinct chemical shifts for protons: $H_{3(P1)}$ and $H_{4(P1)}$ in $\delta = 3.0$-4.6 ppm. The evident proton shift at 3.0 ppm is characteristic of $H_{4(P1)}$ experiencing deshielding effects caused by C_4-I bond formation. On the other hand, $H_{3(P1)}$ appears more deshielded than $H_{4(P1)}$ at $\delta = 4.4$ ppm, as a result of C_3-OH bond formation and proximity of the carboxylic acid functional group. Arguably, if the reverse scenario is considered such that the addition of I occurs at C_3 but OH at C_4, we would then observe the formation of P2. The C_3-I bond formation causes a deshielded chemical shift for $H_{3(P2)}$ at 3.0 ppm. Meanwhile, $\delta = 3.4$ ppm is attributed to $H_{4(P2)}$ due to C_4-OH bond formation and proximity of alkyl groups. Thus, it is fair to conclude that the addition of I_2 to 3-OE could yield two mono iodo substituted products.

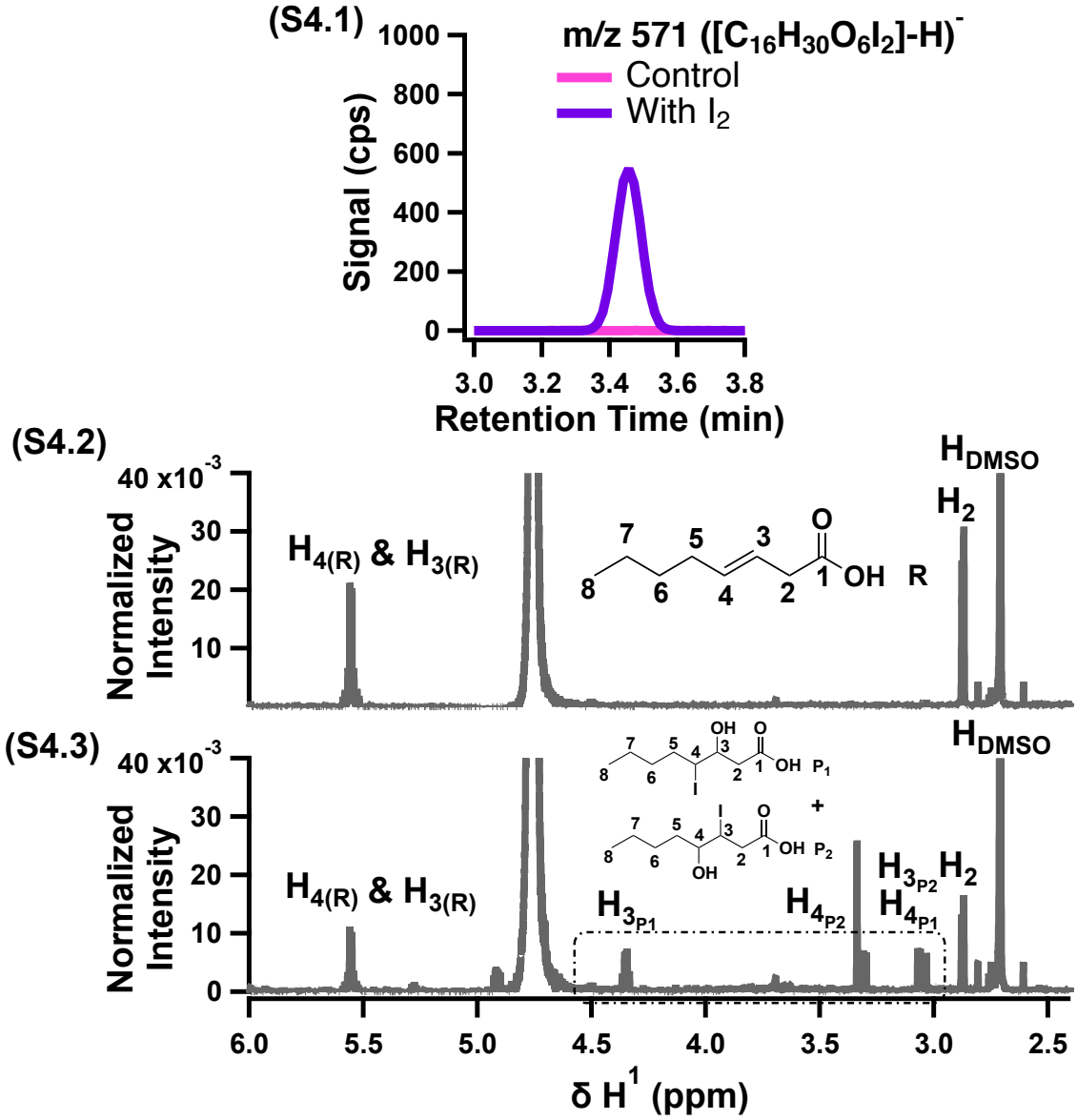

Figure B.4: ESI(-)Extracted Ion Chromatogram (EIC) and ^{1}H NMR spectra for 3-OE-I_2 reaction. Subscripts (R), (P1) and (P2) in ^{1}H NMR spectra represent reactant and product(s) protons respectively. (S4.1) EIC for 3-OE (100 μM) resulting in product mass at m/z 571.001- a dimer of m/z 285.001. (S4.2) ^{1}H NMR for 3-OE in D_2O. (S4.3) ^{1}H NMR for 3-OE with I_2 in D_2O.

B.4.2 Proposed Mechanism for OE-I_2

Substitution reactions of diatomic halogens e.g., Br_2 have been previously investigated on OEs with a varying degree of unsaturation.[323, 594, 595] The OE-I_2 reactivity in our study is expected to follow a similar reaction mechanism. Outlined in Figure B.5, the first interaction between diatomic iodine and π-electrons is known to occur through a π-complex formation.[182, 336, 596, 597] Recalling reaction (2) in Figure 1, it is noticed that an interfering reaction between OE and I_2 deters I_2 to form I_3^-. Considering the mildly acidic conditions employed in our study, we believe that the polarization of I_2 occurs, which allows the formation of cyclic intermediate or haliranium ion.[327, 597] This intermediate is the least stable and easily susceptible to an attack by nucleophiles, such as H_2O and I^-. The most abundant nucleophile, H_2O, is attracted to the haliranium ion by a shift in the electron density towards I^+, which renders the addition of H_2O on the least sterically hindered site.[598] This creates a final product with a hydroxy iodo substitution through the process of anti-Markovnikov addition, where the halogen (I) is attached on a sterically hindered site in comparison to OH.[598] Another likely candidate is the di-iodo hydroxy product, which is formed via the attack of I^-; however, no evidence of this product was found by the analysis of HR-LC-MS and ^{1}H NMR (Figure 3.8). We believe that only a mono iodo substituted product is being formed. However in case of 3-OE, there is a possibility of two mono iodo substituted products based on our discussion in Section B.4.1.

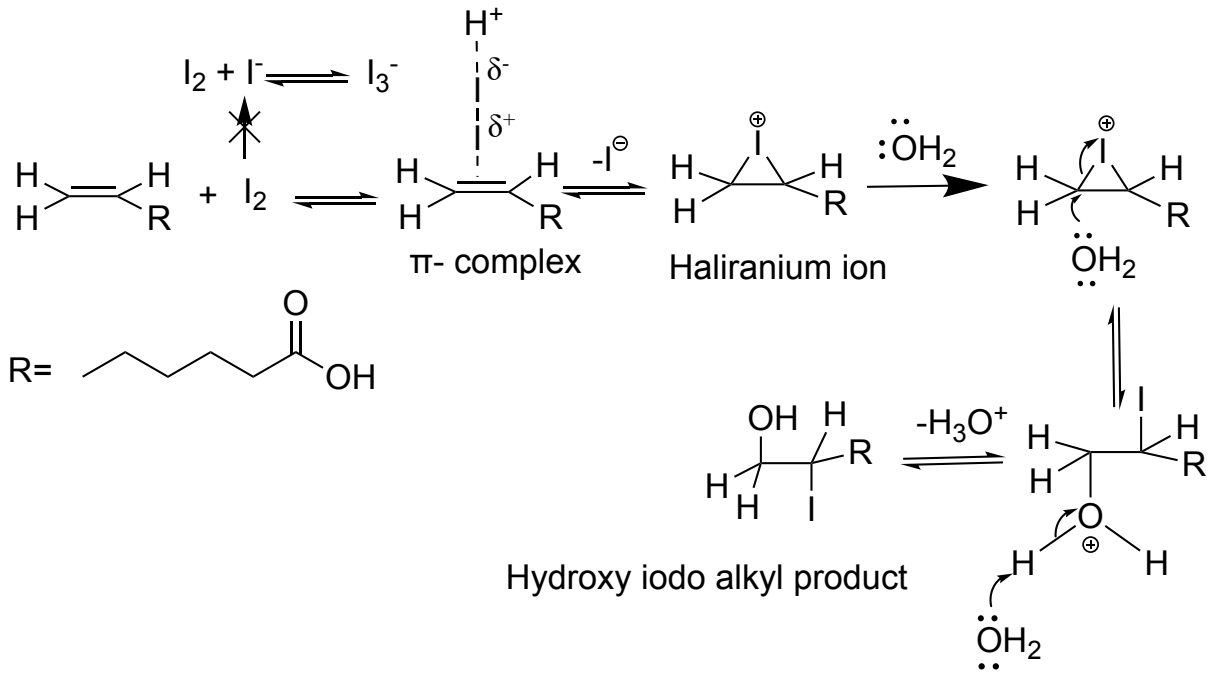

Figure B.5: Reaction mechanism of reaction between 7-OE and I_2.

B.5 Kinetics for OE-I_2 reaction under pseudo order conditions.

The investigation behind the kinetics of 3-OE was studied under two of the excess I_2 concentrations. Figure B.6 shows a linear decay profile in the monitored reactant (3-OE and I_2), when the other reactant is maintained under excess concentration. Figure B.6 (S5.1) is a plot of 3-OE under excess I_2 concentration (702 μM). This plot is linear as observed with high R^2 (0.99). From this plot, the acquired first order rate coefficient (k^I) is relatively agreeable with rate coefficient obtained from another concentration of I_2 as shown in the main document. Table B.1 shows a good agreement between the second order rate coefficient (k^{II}) for 3-OE under both conditions.

Figure B.6 (S5.2) is evident of I_2 following pseudo-first order kinetics when 3-OE is maintained in excess. The measurement of decrease in I_2 absorbance is marked at

460 nm, which is then converted into the concentration of I_2 via Beer's Law using equation eq-B1 (Section B.1). These results stipulate that the observed rate order is indeed 1 with respect to each reactant.

Table B.1: Rate coefficients for pseudo first order experiments.

[3-OE] (μM)	Excess [I_2] (μM)	$k^I \times 10^{-3}$ (s^{-1})	k^{II} (M^{-1} s^{-1})
52	620	0.52 ± 0.01	0.84 ± 0.02
52	702	0.61 ± 0.02	0.87 ± 0.03

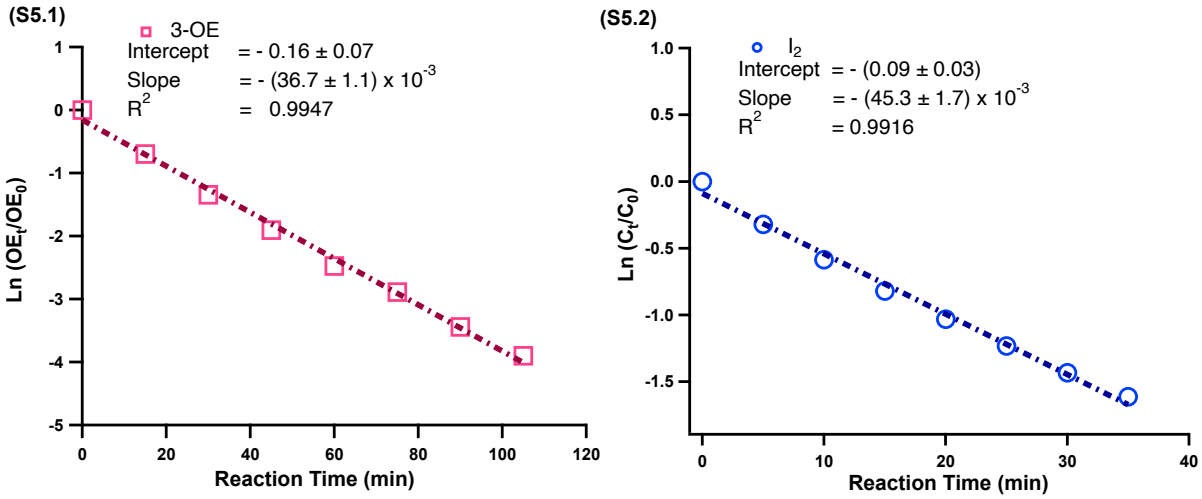

Figure B.6: Pseudo first order decay for 3-OE and I_2. (S5.1) Decreasing natural logarithmic profile for 3-OE (52 μM) measured as a function of reaction time with LC-MS. (S5.2) UV-Vis measured decrease in natural logarithmic ratio of I_2 concentration as a function of reaction time under excess 3-OE (1.87 mM).

B.6 Estimation on second order rate constant for tert-butyl hydroperoxide.

To acquire a second order rate constant (k^{II}) for modelling t-BP concentration profile, we used an exponential fit on our experimental data as described by equation eq-B2. The reaction is assumed to proceed under pseudo-first order conditions due to excess concentration of I^- (60 mM). As such, the first order rate constant (k^I) obtained from fitted data leads to the calculation of second order rate constant as per equations eq-B3 and eq-B4.

$$y = y_0 + A(e^{(-\frac{1}{\tau})*x}) \tag{eq-B2}$$

$$k^I = \frac{1}{\tau} \tag{eq-B3}$$

$$k^{II} = \frac{1}{[I^-]} \tag{eq-B4}$$

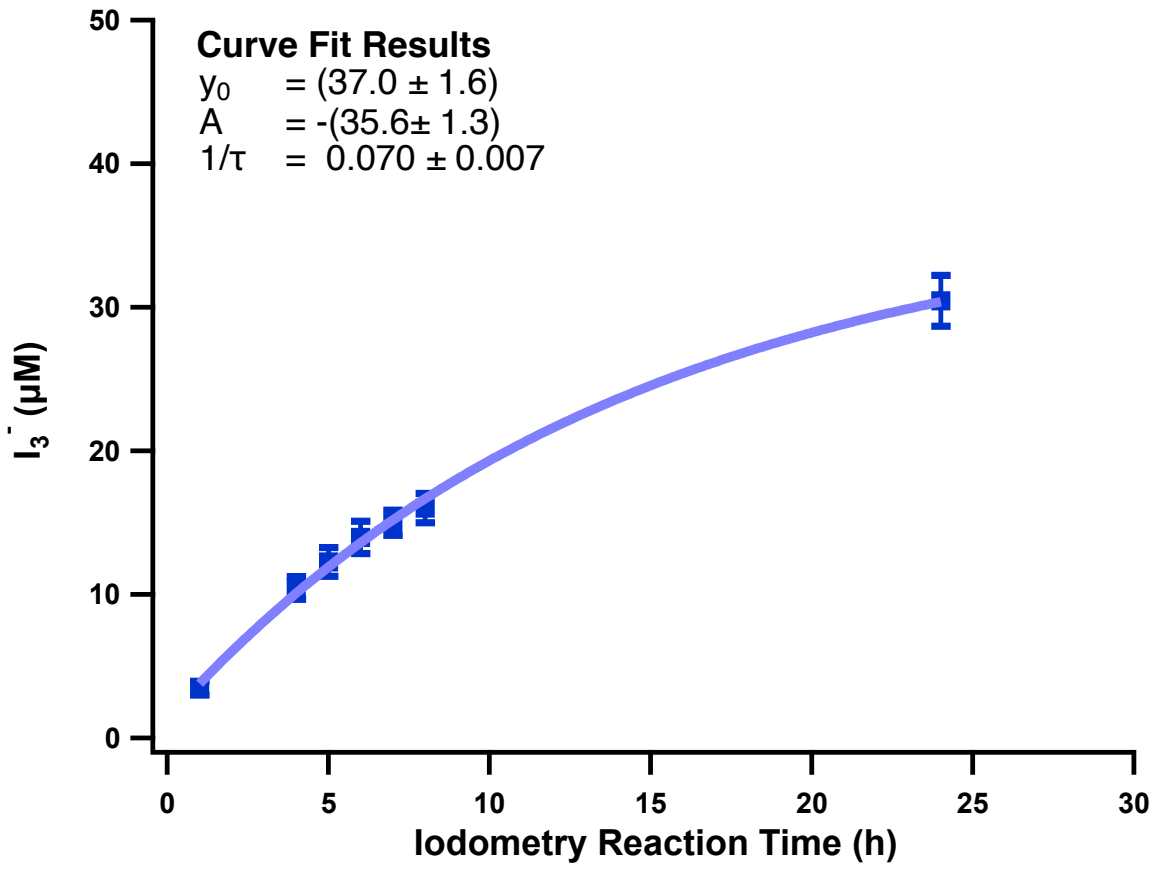

Figure B.7: Exponential fitting on experimentally determined concentration of I_3^-.

B.7 Scenarios considered for simple box model.

In the following section, details on the scenarios considered for the kinetic model are described. Table B.2 outlines the scenarios applied with initial conditions of compounds and Table B.3 describes reactions and rate coefficients used in each applicable scenario. We approached kinetics using two model scenarios. For our first scenario, the goal was to reproduce experimental observations in H_2O_2 and t-BP based conventional iodometry systems. While the second scenario takes into account the deviation observed during OE-dosed iodometry reaction for both peroxides. We are aware that I_2 can undergo complex equilibria in the aqueous phase, forming different species e.g., HOI, I_2OH^-.[599] However, the formation of such species is pH dependent and many of them are considered relatively unimportant in the current conditions employed for our model.

Table B.2: Initial concentrations of compounds for model scenarios.

Scenarios	**Initial concentrations**				
	H_2O_2 / t-BP (μM)	3-OE (μM)	I^- (mM)	I_2 (μM)	I_3^- (μM)
Conventional iodometry	47	0	60	0	0
OE-dosed iodometry	47	711	60	0	0

Acronyms: t-BP: tert-butyl hydroperoxide, 3-OE: 3-octenoic acid, P: product.

a: From this study

b: Reaction considered for conventional iodometry

c: Reaction considered for OE-dosed iodometry

Table B.3: Reactions and rate coefficients used in box model for aqueous phase chemistry.

Reaction	$\mathbf{k}^{II}$ (M^{-1} s^{-1} unless noted otherwise)	**Ref**	**Footnote**
$H_2O_2 + H^+ + I^- \rightarrow H_2O + I_2$	0.013	[181, 238]	b,c
t-BP $+ H^+ + I^- \rightarrow$ t-B-OH $+ I_2$	3.2×10^{-4}	-	a,b,c
$I^- + I_2 \rightarrow I_3^-$	6.2×10^{9}	[599]	b,c
$I_3^- \rightarrow I^- + I_2$	8.5×10^{6} (s^{-1})	[599]	b,c
I_2 + 3-OE $\rightarrow$ P	0.84	-	c

B.7.1 Simulated I_3^- concentration profile at varying concentrations of OE.

The scenarios listed in Table B.2 were re-examined under low (100 μM) and high (1020 μM) concentrations of 3-OE. Figure B.8 shows H_2O_2 and t-BP based iodometry systems for comparison between the simulated and experimentally observed concentration profiles of I_3^-. Figure B.8.1 is for H_2O_2, wherein the concentration profiles of I_3^- show good agreement between simulated and experimental results. Figure B.8.2 shows the generated profile of I_3^- for t-BP and herein, we also observe relatively good agreement between experimental and simulated profiles. Although for low concentration of 3-OE (100 μM), our model overestimates the deviation in concentration of I_3^- in t-BP, this difference is non-existent when we compare the concentration profiles for higher concentration 3-OE (1020 μM). We also notice that significant deviations appear at longer reaction times (6 h for H_2O_2 and 24 h for t-BP). In reality, I_2 and I^- establish multiple equilibria in the aqueous phase, which is also highly dependent on pH and other constituents in the solution.[599, 600] The simplified model built in this work likely won't be able to capture all of those detailed chemistry. Overall, these results attest to the functionality of our simple model to consider the impact of range of OE concentrations on the observed interference.

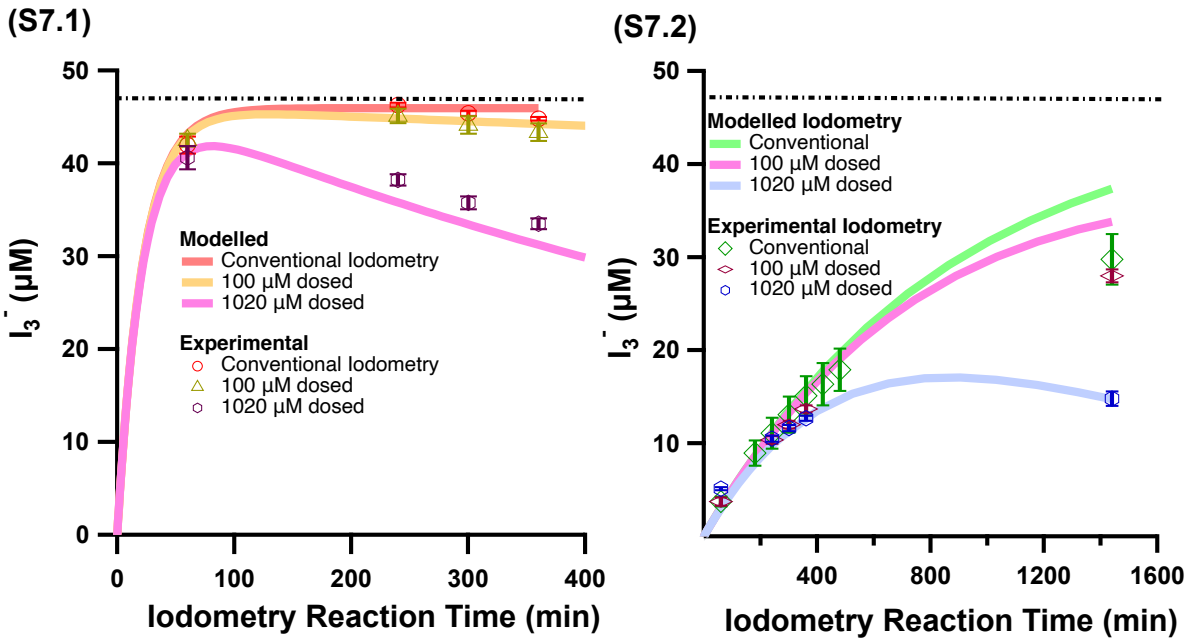

Figure B.8: Exponential fitting on experimentally determined concentration of I_3^-.

B.8 Summarized calculations for iodometry biases.

In this section, we have described calculations used to estimate the bias originating from OE concentrations in different matrices as discussed in Section 3.4 in the main document.

Firstly, based on the work of Deming and Ziemann[323], we examined C=C content in indoor surfaces and converted their reported values into respective mM equivalents. For instance, ∼10 μmol m^{-2} C=C content in films obtained from floors would be equivalent to 4 mM in a concentrated extract of 1 mL and 0.40 m^2 sampling surface area. Using a factor of 2 dilution during iodometry, the final C=C content in an iodometry sample would be then equivalent to 2 mM. On the other hand, C=C content in films obtained from vertical surfaces (3.9 μmol m^{-2} from a 0.16 m^2 sampling area) would be equivalent to ∼624 μM in a diluted extract of the film or 312 μM in an iodometry applied sample. Based on these figures, we can estimate that during longer iodometric reaction times (>4 h), ∼3% bias can originate from C=C concentration in vertical films, while floor samples would increase this bias to ∼20%.

Secondly, edible oils can contain a wide range of unsaturated fatty acids as demonstrated in the work of Guarrasi *et al.*[374] From this work, we first quantified linoleic acid in an oil extract and then in a PV diluted sample. Considering the matrix of soybean oil, using the relative w/w % of linoleic acid, following the 40 fold dilution on a 5 g oil sample and final extraction of sample in 4 mL solution as per the procedure in the work of Guarrasi *et al.*[374], we would observe linoleic acid between 53-64 mM. This sample of soybean oil would be further diluted by a factor of 5 as per the modified PV test,[315] which would then result in final linoleic acid concentration at 11-13 mM.

Thirdly, we examined milimolar equivalents of polyunsaturated fatty acids (PUFAs) in lipids from different animals. There are many methods applied for lipid extraction,[601, 602] however for the sake of our study, we would follow the extrac-

tion procedure as outlined by Folch *et al.*[603] Based on this method, 1 g of fat would be extracted and concentrated in a 1 mL solvent. Following this analogy, the relative w/w % of PUFAs (with respect to total fat content) in lipids from different animal parts e.g., brain, rump and leg were converted into their mM equivalent values. For instance, brain extracts of Atlantic Herring can contain ∼34% of PUFAs.[375] Similarly, lipid content in leg muscle of goat and rump of sheep have been found to contain ∼13% and ∼3.8% PUFAs respectively.[343] Based on an average PUFA molecular weight of 334.6 g/mol,[604] we could observe up to 51 mM of unsaturated content from lipids. A factor of 5 dilution associated with the PV test would then result in final PUFA content at 10 mM.[315] Similar dilutions of lipid extracts from sheep and goat would also yield 3.9 mM and 1.1 mM in sample diluted for PV test.

From our discussion above, we showed that both edible oils and lipid extracts from animal issue can contain up to 10 mM of OEs in the final solutions used for the PV test. Given that this concentration of OE is beyond the experiment conditions that we employed in this work, we have used our kinetic box model to roughly estimate the extent of deviation expected for such OE contents. It is our within our knowledge that conventional PV tests do not quantify peroxide content based on I_3^- measurements,[307] however recent PV tests also used spectroscopy.[315] The consumption of I_2 by OEs will result in the same magnitude of deviation for iodometry monitored by both spectroscopic and titration methods. In other words, the deviation of I_3^- in our model can be directly interpreted as deviation expected in the PV test.

Figure B.9 is demonstrating the simulated concentration of I_3^- at 1 mM H_2O_2, which is within the observed peroxide content range in non-oxidized edible oils.[605] Further, OE representation is based on 10 mM of 3-OE, which is equivalent to OE content in the matrix of oil and animal extracts as mentioned above. We observed that the deviation between the convential and OE-dosed iodometry test scaled with the increasing reaction time. The bias is within 14%-40% for <1 h of reaction time, applied in many studies.[307, 315, 606] Based on our model results, we would expect

that the deviation induced by OE contents in edible oil and animal lipids would fall within this range.

We understand that our model for PV test here is a rough estimate for a number of reasons. It must be noticed that real oil samples can constitute wide variety of unsaturated fatty acids with multiple C=C bonds and[337] as such, the potential deviation against PV measurements would be further accentuated. The OE concentration used in this case (10 mM) is much higher than we experimented (1.02 mM); thus, the model result is an extrapolation of our experimental observations. In the future, deviation induced in high OE concentration (10 mM) must be experimentally confirmed.

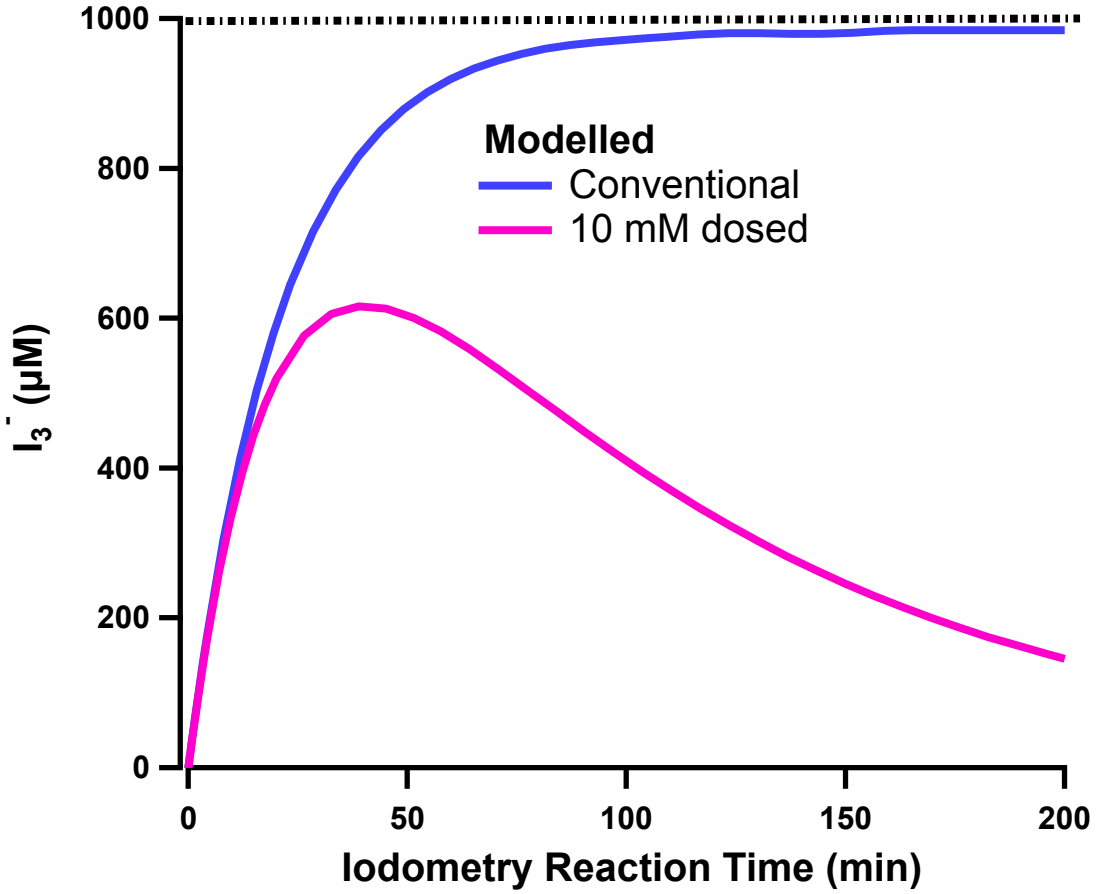

Figure B.9: Predicted bias against I_3^- at representative concentrations of OE and H_2O_2 in edible oils and animal fats.

Appendix C: Chapter 4

Supplementary information for Chapter 4

C.1 TRACER field campaign topological map

Sample collection map

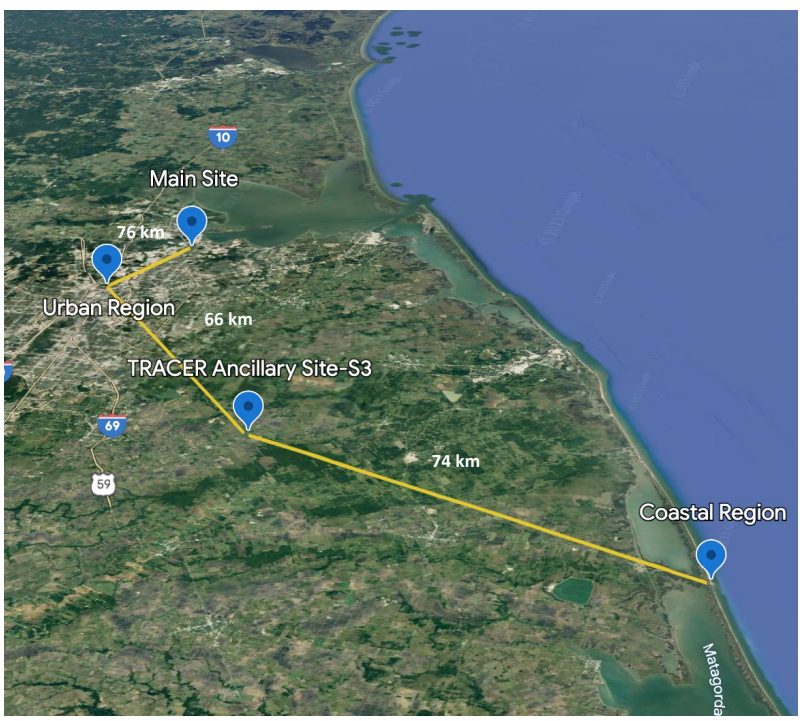

Figure C.1: Location of ancillary (S3) site (Arm user facility) for TRACER field campaign over rural southwestern Houston, TX. Distance to Houston urban region is 66 km, coastal distance is 74 km and distance between ancillary and main site is 76 km.

Table C.1: Meteorological conditions for day and night sampling periods during collection of samples in TRACER-ARM campaign.

Date mm/dd/2022 (CDT)	Time (UTC)		Temperature (T) (°C)	Relative Humidity (RH, %)	Wind Speed ($m.s^{-1}$)	Wind direction (°)
06/02-Day	15:35 06/02/2022	00:35 06/03/2022	31 ± 1	53.5 ± 8.1	3.8±1.3	183 ± 112
06/02-Night	00:55 06/03/2022	13:05 06/03/2022	24±2	85.6 ± 6.4	1.6±0.8	
06/03-Day	13:30 06/03/2022	21:46 06/03/2022	29±2	54.3 ±8.1	4.2± 1.3	159 ± 127
06/03-Night	22:09 06/03/2022	13:16 06/04/2022	25±4	74.8 ± 16.4	2.1±1.4	
06/04-Day	13:40 06/04/2022	00:02 06/05/2022	29±2	60.8 ± 8.9	2.6±1.3	197 ± 107
06/04-Night	01:10 06/05/2022	13:55 06/05/2022	23±1	91.5 ± 4.85	1.1±0.5	
06/11-Day	13:35 06/11/2022	22:19 06/011/2022	32.±2	55.6 ± 12.0	4.4±1.6	197 ± 34
06/11-Night	22:51 06/11/2022	13:53 06/12/2022	27±3	84.6±11.6	2.7±1.6	
06/12-Day	14:03 06/12/2022	22:09 06/12/2022	33± 2	53.6± 9.7	6.5±1.6	186 ± 23
06/12-Night	22:21 06/12/2022	11:58 06/13/2022	30±3	81.7±15.3	2.2±1.4	
06/13-Day	12:08 06/13/2022	20:10 06/13/2022	31±3	59.8±18.4	5.3±2.4	167 ± 29
06/13-Night	20:16 06/13/2022	11:50 06/14/2022	28±3	77.1±16.8	2.9±1.9	
06/14-Day	12:05 06/14/2022	20:09 06/14/2022	30±2	61.8±15.3	4.6±1.9	160 ± 23
06/14-Night	20:12 06/14/2022	12:51 06/15/2022	28±3	75.5±15.0	4.2±2.1	

C.2 nano-DESI Design

The nano-DESI/sample interface was mounted to the MS source. Two fused silica capillaries (150 μm O.D., 50 μm I.D.; Polymicro Technologies, Phoenix, USA) were aligned at $\sim$90° using micro- 5 positioners (Quater Research & Development, model XYZ 500 MIM (inline); Bend, USA), and the secondary capillary tip was positioned $\sim$1 mm from the MS inlet. A 7/3 acetonitrile:water v/v solvent mixture (Optima LC-MS grade; Fisher Chemical, Hampton USA) was flowed at 0.75 μL/min via a syringe pump through the primary capillary, such that a solvent junction between the primary and secondary capillaries and sample surface was established when the nano-DESI assembly was positioned sufficiently close to the sample surface (Figure C.2).[445]

Solvent compositions (i.e. polarities) are known to influence the extraction of organic compounds in complex atmospheric matrices (e.g., SOA). However, the solvent composition used in the current work has been previously shown to be effective for a broad range of SOA compounds.[167] -3.5 kV was applied to the solvent at the syringe needle. Once the liquid junction was established, the sample substrate was scanned along the XY plane at 50 μm/s within a 1 cm radius of the filter center. The position of the sample relative to the nano-DESI assembly was manually adjusted via an XYZ stage and custom LabVIEW software (National Instruments, Austin, USA).

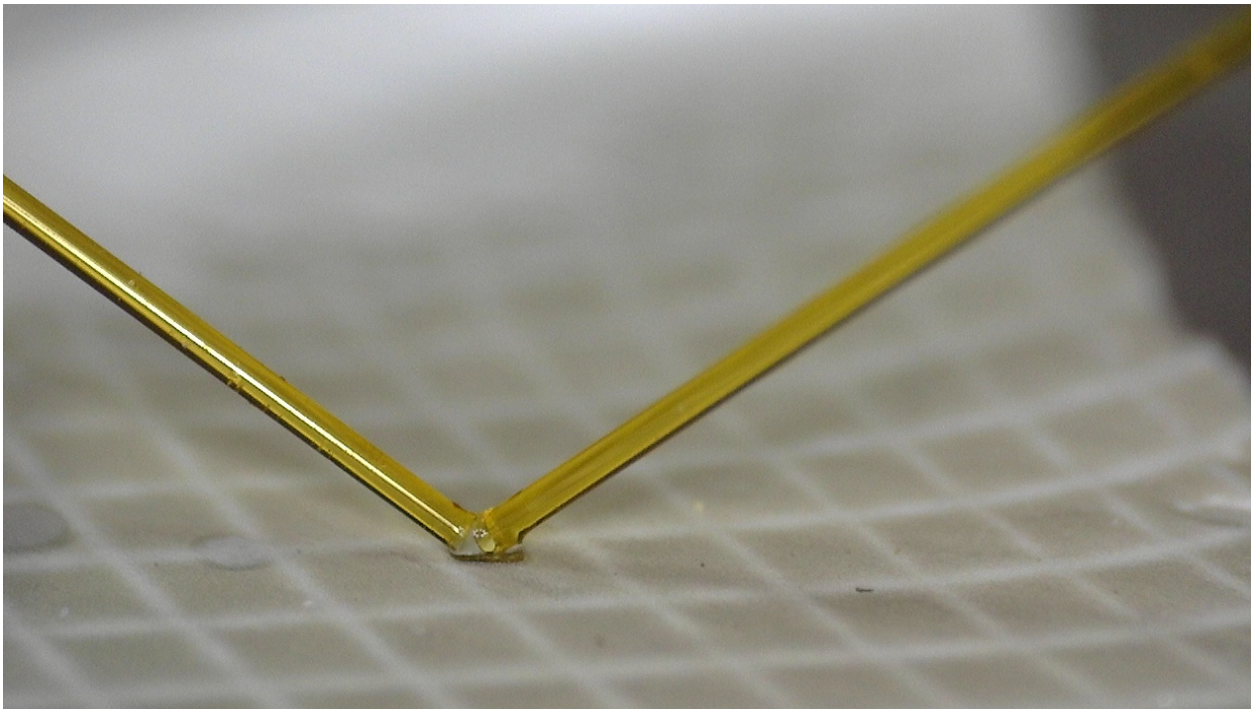

Figure C.2: nano-DESI analysis design of TRACER field samples from downtown rural region in Houston, TX (ancillary site).

C.3 MfAssignR Data Processing

A detailed protocol for MfAssignR data processing is outlined in Figure C.3.

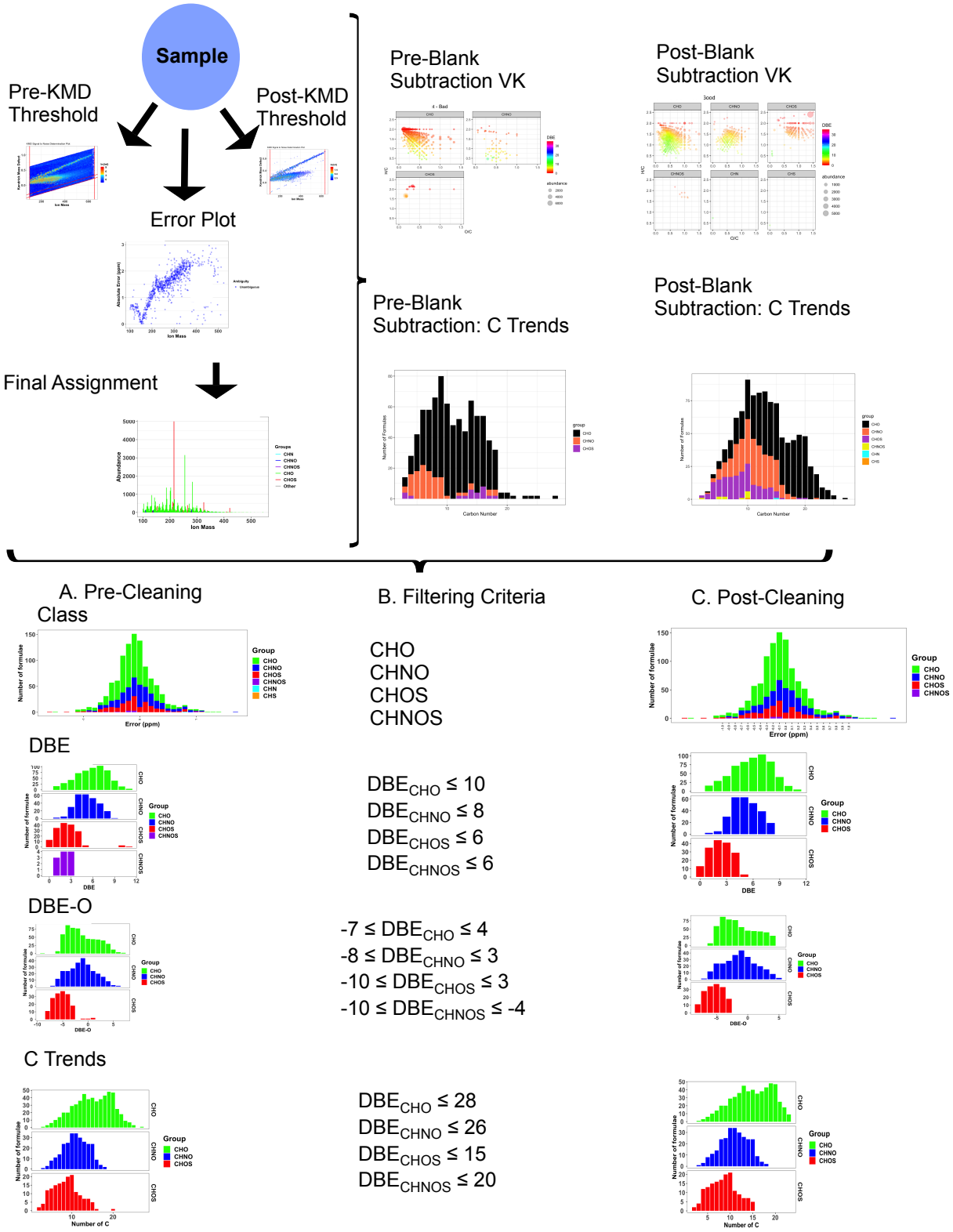

Figure C.3: Data processing methodology adopted for all of the sampling periods across June. To ensure data quality, samples were analyzed in triplicate measurements.

C.3.1 Parametrization of Molecular Assignments

The calculations of predicted parameters were performed as outlined in the work of Donahue et al.[31, 54, 445, 607] Average carbon oxidation states (OS_C) and volatilities ($\log_{10}C_0$; logarithmic saturation mass concentration (μg.m^{-3})) were calculated according to models developed by Kroll et al., respectively.[54, 478, 607] Based on the calculated parameters, we were able to classify individual formulae in five different volatility bins: volatile organic carbon (VOC: $\log_{10}C_0$)> 6.47 μg.m^{-3}), intermediate VOC (IVOC: 2.47 < $\log_{10}C_0$) $\leq$ μg.m^{-3}), semi VOC (SVOC: -0.52 < $\log_{10}C_0$) $\leq$ 2.47 μg.m^{-3}), low VOC (LVOC: -3.52 < $\log_{10}C_0$) $\leq$ -0.52 μg.m^{-3}) and extremely low VOC (ELVOC: $\log_{10}C_0$) $\leq$ -3.52 μg.m^{-3}).[31, 54, 550, 608] Using modified aromaticity index (AI) and carbon number, individual molecular formulae may be classified as "condensed aromatic", "aromatic", "high O unsaturated", "low O unsaturated" or "aliphatic". The Elemental ratios and predicted parameters corresponding to each sampling period are described in Table C.4 (Section C.6.4). Across all samples, 22-76% of mass spectral features were unambiguously assigned a molecular formula.

C.4 Micro-Spectroscopic Analysis: CCSEM-EDX and STXM

C.4.1 Chemical Imaging and Single Particle Analysis

The individual atmospheric particles were probed with a computer-controlled environmental scanning electron microscope (CCSEM FEI, Quanta 3D) coupled with an energy-dispersive X-ray (EDX) spectrometer with a Si (Li) detector having an active surface area of 10 mm^2. A 0.48 nA beam current and a 20 kV accelerating voltage were used to get the X-ray spectra. The EDAX software automatically detects particles' chemical composition and derives their morphological characteristics such as projected diameter, area, and aspect ratio. The spectrum obtained from each single particle was quantified to get the relative atomic fraction of the element of interest which includes C, N, O, Na, Mg, Al, Si, P, S, Cl, K, Ca, Mn, Fe, Zn and Cu. Cu signals in EDX spectra are mostly caused by copper TEM grids and the beryllium-copper alloy mounting plate that holds the sample. The atomic percentage data obtained from CCSEM-EDX were then classified following the particle classification shown in Figure C.4.[459] We classified the particles into ten categories based on their elemental compositions (atomic %): 1) Biological, 2) Na-rich, 3) Na-rich/sulfate, 4) sulfate, 5) carbonaceous, 6) dust, 7) carbonaceous coated dust and 8) others. At first, the particles were segregated into two categories based on the atomic percentage of K and P present in the particles. The particles abundant with [K] $\geq$ 0.2 and [P] $\geq$ 0.2 are categorized as 'biological' class. The rest of the particles were then divided into two sub-categories based on the percentage of Na they contained. The aerosol particles can be classified as either sodium-rich or sodium-deficient. The Na-rich particles were categorized into two categories based on the combined abundance of aluminum, silicon, iron, and calcium, which represents the overall abundance of mineral components. Particles with a high sodium content, referred to as "Na-rich" particles, were characterized by a greater abundance of sodium compared to other

mineral elements such as aluminum, silicon, iron, and calcium. The classification of the "Na-rich/Sulfates" class was based on the relative concentrations of sodium and sulfur elements. Specifically, if the concentration of sodium ([Na]) was greater than or equal to the concentration of sulfur ([S]), it fell into the "Na-rich/Sulfates" category. Conversely, if the concentration of sodium was less than the concentration of sulfur, it was classified as "Na-rich/Sulfates." Particles with a sodium deficiency ([Na] $<$ 1 atomic %) were categorized into four distinct classes. Particles mostly composed of carbon, nitrogen, and oxygen elements, accounting for about 99% of their atomic composition, were classified as "Carbonaceous particles." Particles with a sulfur concentration exceeding a threshold level of 0.5 atomic percent were categorized as "sulfate" when the principal constituent elements, namely carbon (C), nitrogen (N), oxygen (O), and sulfur (S), were determined to collectively account for more than 99 atomic percent. Particles containing [Al, Si, Fe, Ca] percent above 4% were classed as dust. Particles with [Al, Si, Fe, Ca] concentrations of less than 4% were divided into two categories. Particles with an atomic percentage of Al, Si, Fe, and Ca greater than 0.8% and [C, N, O] percentages greater than 85% were categorized as carbonaceous coated dust, while the remaining particles were classified as 'other' category.

The carbon characteristics shown by the aerosol population were examined by the utilization of STXM/NEXAFS technique.[466, 609, 610] The investigation of chemical bonding between elements can be conducted by utilizing synchrotron light beams emitted from a synchrotron light source. These beams are directed through raster-scanned samples, allowing for the analysis of chemical bonding at specific photon energies. X-ray absorption spectra of the carbon K-edge were obtained by scanning particles with energy levels ranging from 278 to 320 eV. To acquire an optical density (OD_E), the initial step involves applying the Beer-Lambert Law to convert the X-ray

generated by the particles at various energies and positions.

$$OD_E = -ln\frac{I(E)}{I_0(E)} = \mu(E)\rho t \qquad \text{(eq-C1)}$$

Here, I is the intensity at a given energy, I^0 is the background intensity, is the mass absorption coefficient at X-ray energy E, is the mass density and t is the particle thickness2. For this study both spectral "stacks" were acquired at 111 energy levels of the carbon K-edge and "maps" were taken at 11 distinct energies at the carbon K-edge.[466] Carbon compositions and mixing states of individual particles were measured using spatially resolved spectra. STXM imaging was performed using a 25 nm zone plate.

The utilization of scanning transmission X-ray microscopy (STXM) data enables the evaluation of various categories of internally mixed particles.[466, 609–611] For instance, it allows for the assessment of organic carbon (OC) particles, where the distribution of organic mass is uniform throughout the entire particle. Additionally, STXM data can be used to analyze particles that consist of a combination of elemental carbon and organic carbon (EC+OC), characterized by the presence of higher C=C, sp_2 hybridized bonds alongside organic functionalities. Furthermore, STXM data can be employed to examine particles that involve the infusion of inorganic substances with organic carbon (IN+OC). Lastly, STXM data can also be utilized to investigate particles that contain mixtures of organic carbon, elemental carbon, and inorganic inclusions (OC+EC+IN). The utilization of carbon K-edge images can help facilitate the determination of the organic volume fraction (OVF).[467] The optical density at energy levels of 278 eV (pre-edge) and 320 eV (post-edge) was utilized to determine the thickness of both organic and inorganic components. In this study, sodium chloride (NaCl) with a density of 2.16 g cm^{-3} and adipic acid with a density of 1.36 g cm^{-3} are employed as representative substances for inorganic and organic ingredients, respectively.

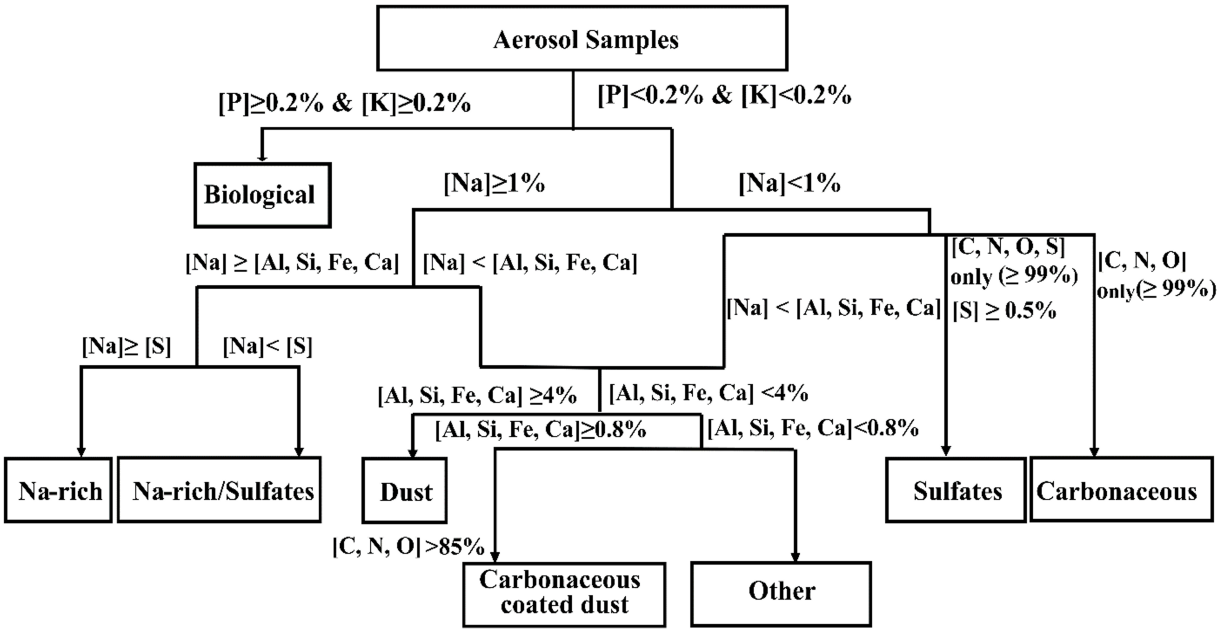

Figure C.4: Classification scheme used to identify the types of particles analyzed by CCSEM-EDX.[459]

C.4.2 CCSEM-STXM Analysis

We probed the size-resolved chemical composition and organic volume fraction (OVF) using CCSEM-EDX and STXM/NEXAFS respectively. These measurements assist in understanding characteristic organic fractions for respective sampling periods complimentary to the mass spectrometric analysis. Tables C.2 and C.3 outline the number of particles and classification of each particle. Figure C.5 demonstrates the size resolved chemical speciation and organic volume fraction of particles collected from daytime June sampling periods. The CCSEM-EDX results shown in Figures C.5 (A)-(D) demonstrate that early June (i.e., June 3 and June 4) sampling periods exhibited 29-41% of sulfate enriched particles whereas June 11 and June 12 samples were observed to constitute a large fraction of dust particles (39-64%) and very low (< 10%) sulfate/carbonaceous particles. Despite sample collection being 1 m above ground, it is possible that the occurrence of a dust storm could have likely implicated our observations with respect to June 11 and June 12 sampling periods shown in (C) and

(D).

Figures C.5 (E)-(H) demonstrate that smaller size particles (< 2 μm) are found to be organic rich across June 3, June 4, June 11 and June 12 respectively.[472] Estimated OVF demonstrated that a significant fraction (60-80%) of particles was enriched with organics. In contrast, particles on June 11 (Figure C.5 (G)) June 12 (Figure C.5 (H) devoid of organic matter. In fact, $< 20\%$ of particles are found to constitute organics. STXM/NEXFAS and carbon-speciation maps for June 3, June 4, June 11 and June 12 sampling periods are discussed in main document.

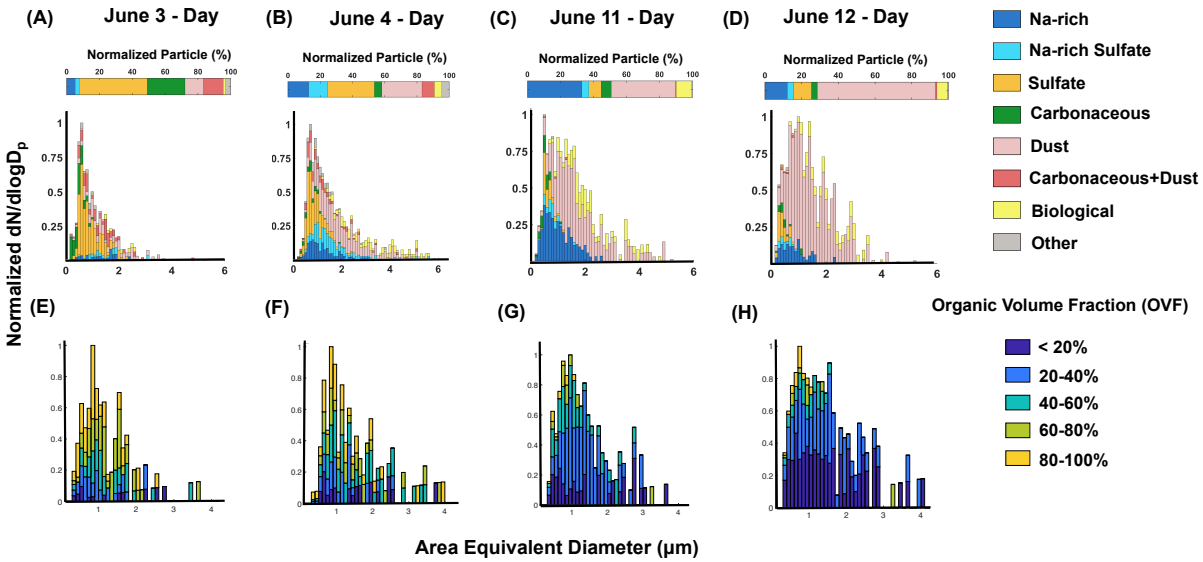

Figure C.5: Size-resolved elemental classification of particles using CCSEM-EDX is shown in (A)-(D). The bar plot represent size-resolved classification for particles on June 3, June 4, June 11 and June 12 daytime samples. The bar at the top of each panel shows the number fraction of particle classes. N.P. stands for number of particles analyzed. Histograms (E)-(H) show size-resolved organic fraction observed across June 3, June 4, June 11 and June 12 respectively. Darker shade indicates particles with lower organic volume fraction while lighter shade indicates higher organic fraction.

Table C.2: Microscopic classification of particles.

Sample	Total particle analyzed per sample	Na-rich (%)	Na-rich sulfate (%)	Sulfate (%)	Carbonaceous (%)	Dust (%)	Carbonaceous+Dust (%)	Biological (%)
06/02/22 Day	3367	29.6	10.8	15.9	1.4	22.5	8.9	6.8
06/02/22 Night	955	12.4	5.6	18.3	6.6	36.7	13.9	5.1
06/03/22 Day	850	5.2	2.6	41.3	23.1	11.2	12.1	1.4
06/04/22 Day	3011	12.8	11.9	28.8	4.7	24.8	7.7	4.6
06/04/22 Night	2134	0.5	0.3	16.2	41.1	27.8	12.7	0.9
06/11/22 Day	1099	33.0	4.2	7.5	6.1	38.8	0.5	9.3
06/11/22 Night	1365	14.1	7.3	15.7	3.2	48.3	0.6	10.2
06/12/22 Day	934	12.2	3.4	9.7	3.2	64.2	0.9	5.6
06/12/22 Night	1157	9.2	0.6	5.1	9.3	58.1	4.4	12.5

Table C.3: Particle classification according to STXM/NEXFAS.

Sample	**# of Particles**	**In**[a] (%)	**OC**[b] (%)	**OCEC**[c] (%)	**OCIn**[d] (%)	**OCInEC**[e] (%)
06/03/22 Day	264	0.76	11.36	4.55	79.17	4.17
06/04/22 Day	241	0.78	8.14	2.71	80.23	8.14
06/04/22 Night	285	1.05	5.26	1.05	81.05	11.58
06/11/22 Day	329	2.13	5.47	0.00	90.88	1.52
06/11/22 Night	182	1.82	6.69	0.30	85.71	5.47
06/12/22 Day	230	3.10	2.79	0.31	91.33	2.48
06/12/22 Night	207	3.67	3.06	0.92	80.12	12.23

[a] Inorganic carbon [b] organic carbon [c] combination of organic carbon and elemental carbon [d] infusion of inorganic substances with organic carbon [e] combination of organic carbon, elemental carbon and inorganic substances

C.5 Meterelogical Plots

C.5.1 Variation in HYSPLIT Tracjectories

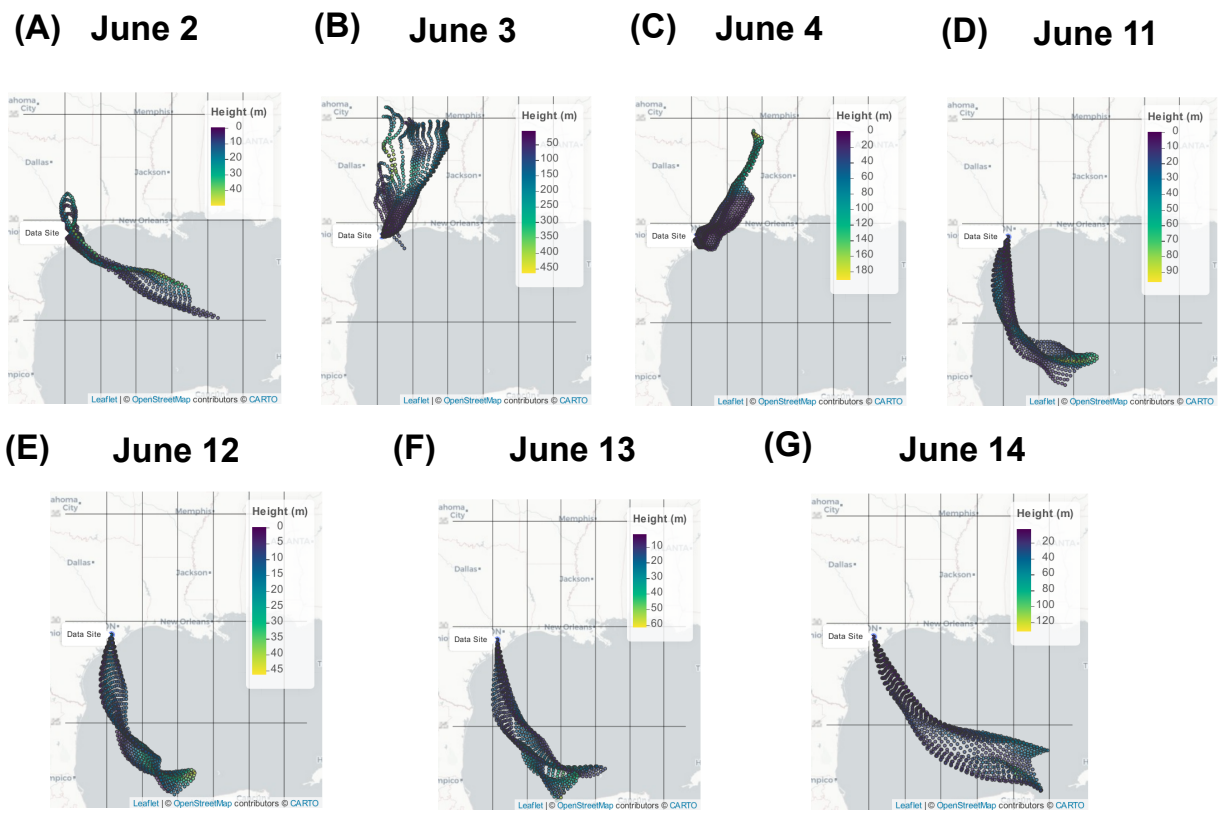

Figure C.6: 48 hour back trajectories associated with distinct air mass during TRACER-ARM campaign. The color bar represents height from above ground (10m).

C.5.2 Wind Rose Plots

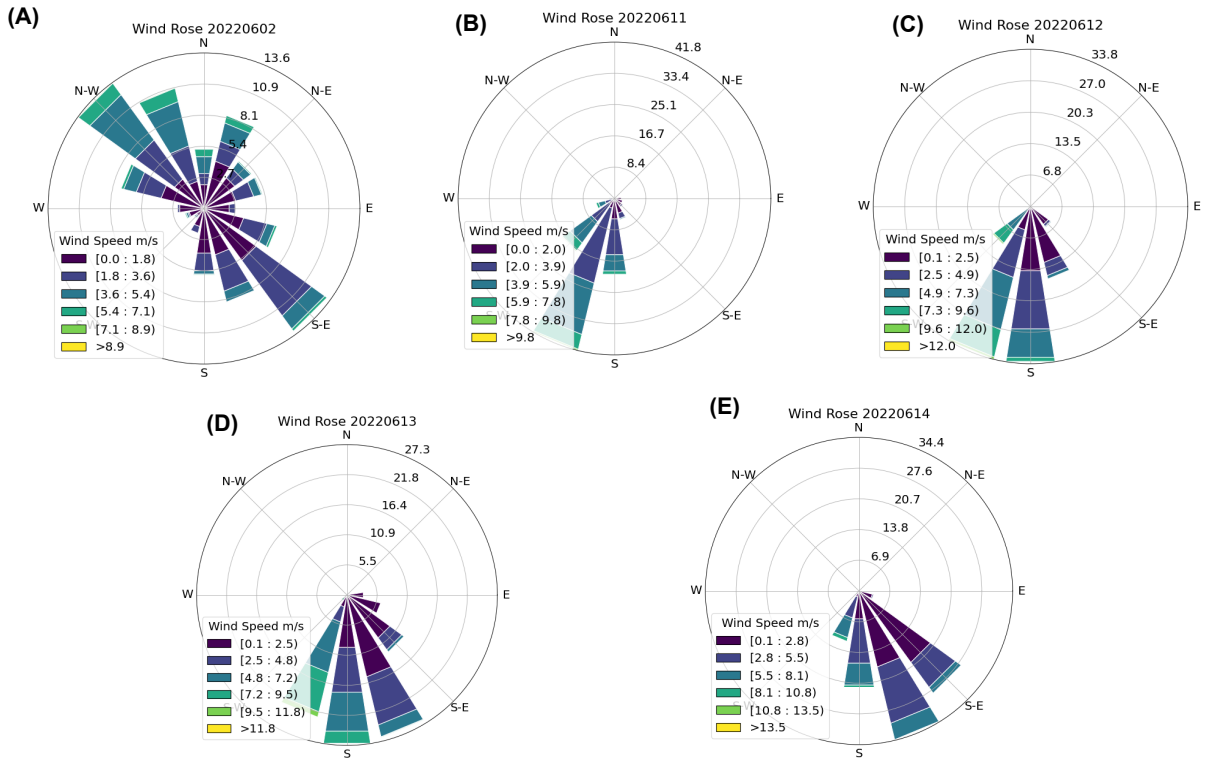

Figure C.7: Wind rose map for each sampling period shows the general wind direction and wind speed. The circular format indicates the direction the wind blew from towards the epicentre and the length of each spoke shows how often wind blew from that direction. The colors of each spoke indicate the wind speed in m.s^{-1}.

C.5.3 Relative Humidity and Temperature Plots

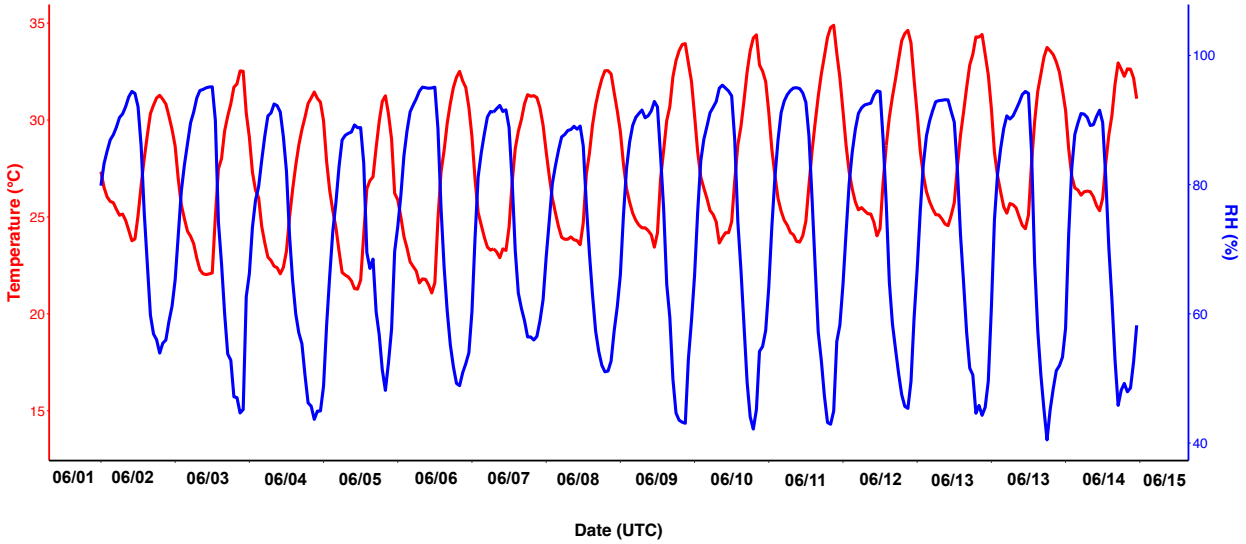

Figure C.8: Variation in relative humidity and temperature across sampling periods of June during TRACER-ARM campaign.

C.6 Intersections of Molecular Features Across Sampling Periods

C.6.1 Characterization of Molecular Groups

Figure C.9 shows Van Krevelen diagram and OS_C as a function of $\log_{10}C_0$. From a total of 2592 molecular features (MFs), 223 were found to be common in all nighttime periods accounting for ∼9% of the total population. The common MFs are colored according to their groups whereas the MFs found in varying combinations of the nighttime sample set (e.g., June 11, June 2 to June 4) are shaded grey. Within these common MFs, 149 were of CHO class, 12 of CHNO and 62 of CHOS. The average O:C ratio for CHOs (0.61 ± 0.24) and CHNOs (0.59 ± 0.19) was < 0.5 while those of CHOSs (1.16 ± 0.37) was > 1. This likely indicates higher degree of oxygenation for CHOS than CHO/CHNO but overall MFs are saturated due to low (2-5) DBE values.[404] The inset pie plots show the distribution of MFs which is either scaled according to their number within total population or weighted abundance (ion signal intensity) demonstrating the prevalence of CHOS. Figure C.9 (B) shows the variability in volatility classification of these common MFs as a function of oxidation state of carbon (OS_C). Given that the OS_C value for each molecular group in subset of common MFs is less than 0 (CHO: -0.08 ± 0.63, CHNO: -0.68 ± 0.31, CHOS: -0.36 ± 0.57), this indicates that the observed MFs are less likely to be oxidized.[478] From the volatility classification of common MFs, 4% (or 9 MFs) MFs were categorized in ELVOC bin, 48% (or 106 MFs) in LVOC bin, 7% (or 16 MFs) in IVOC bin, 41% (or 92 MFs) in SVOC bin.

The observed CHNO were not as abundant as other groups as demonstrated by the pie plots. Interestingly, no CHNOS were observed amongst the nighttime common features. Some of the CHNO e.g., $C_7H_9NO_5$ were reported to have biogenic VOC precursor i.e., d-limonene. [505] Some literature reported CHO compounds e.g., $C_{14}H_{20}O_4$ (m/z 251.1290) originate from biogenic sources (e.g., β-caryophyllene) [612] while a majority e.g., $C_7H_8O_7$ (m/z 203.0197), $C_7H_{12}O_7$ (m/z 205.0354), $C_8H_{10}O_7$ (m/z 217.0354), $C_7H_8O_8$ (m/z 219.0146), $C_9H_{12}O_7$ (m/z 231.0511) are of anthropogenic sources (i.e., 1,3,5,-trimethylbenzene).[486] Thus, the common MFs found in nighttime sample set are found to be influenced by both biogenic and anthropogenic precursors.

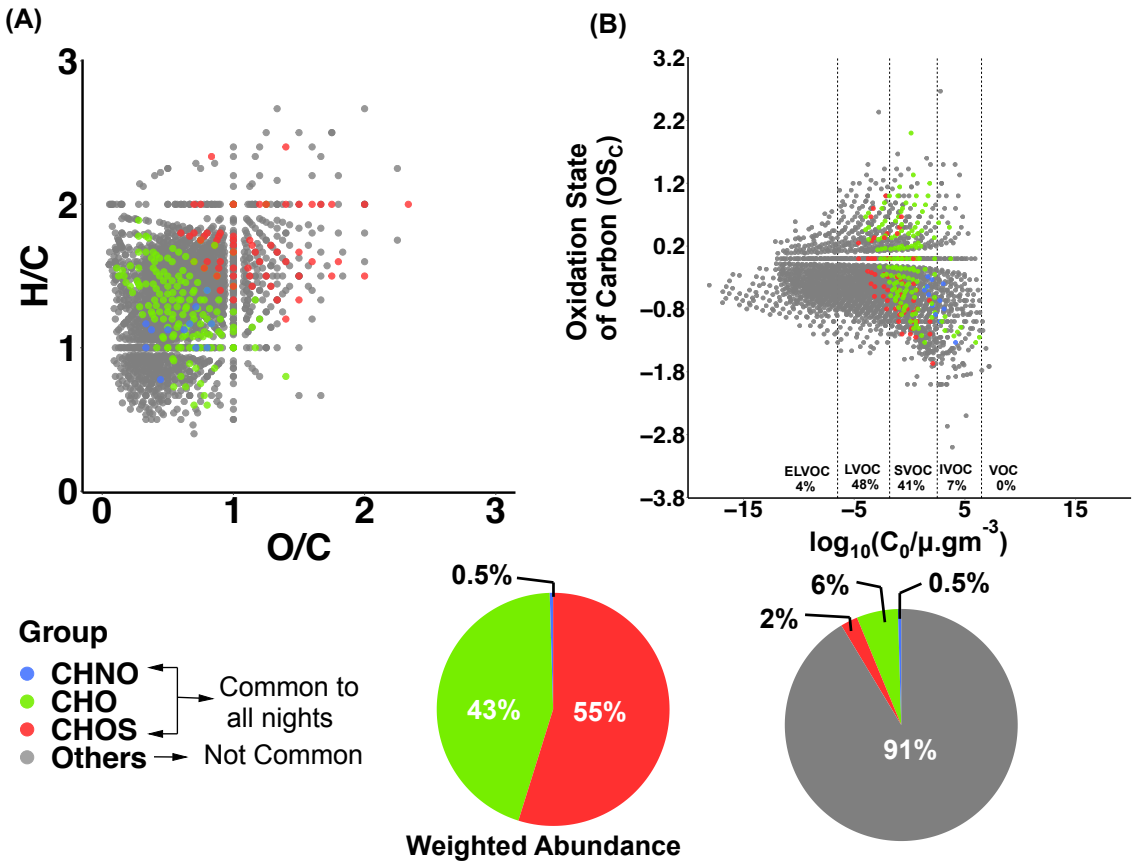

Figure C.9: Distribution of molecular features found common to all nighttime sampling periods. (A) Van Krevelen diagram for common MFs in nighttime samples colored according to functional groups. The MFs that are not common but found across different intersection of sampling period are shaded grey. (B) Oxidation State of carbon (OS_C) to represent volatility distribution of common MFs is shown as a function of logarithmic saturation mass concentration ($\log_{10}C_0$). The pie plots reflect the distribution of common MFs which are scaled according to ion signal intensity of a molecular group or number based percent distribution from the total MF population.

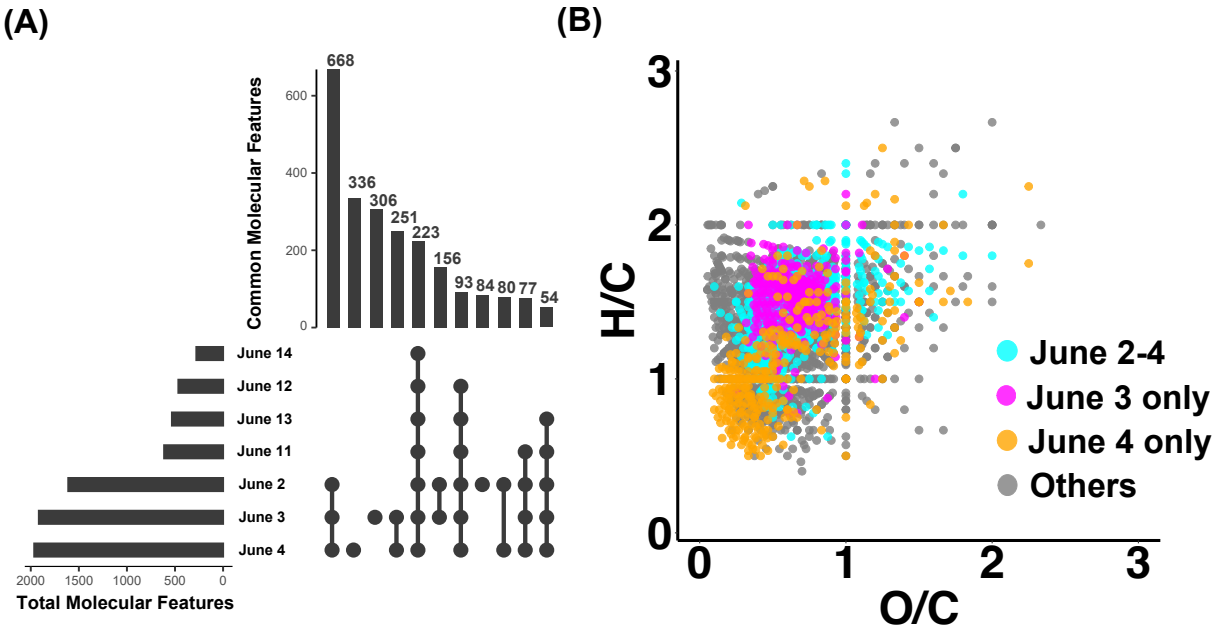

Figure C.10: Distribution of MFs across the experimentally analyzed nighttime sampling periods. (A) MFs found across each sampling period is shown in the upset plot. Bars indicate the number of MFs found unique to each intersection. (B) VK diagram shows most populated unique MFs across different intersections. Colored features represent the density of MFs unique to June 2 to June 4, June 3 and June 4, while MFs found in rest of the intersections (e.g., June 2-June 12, June 3 to June 14) are labelled as "others" and shaded grey.

C.6.2 Distribution of Molecular Features in Nighttime Sample Pool

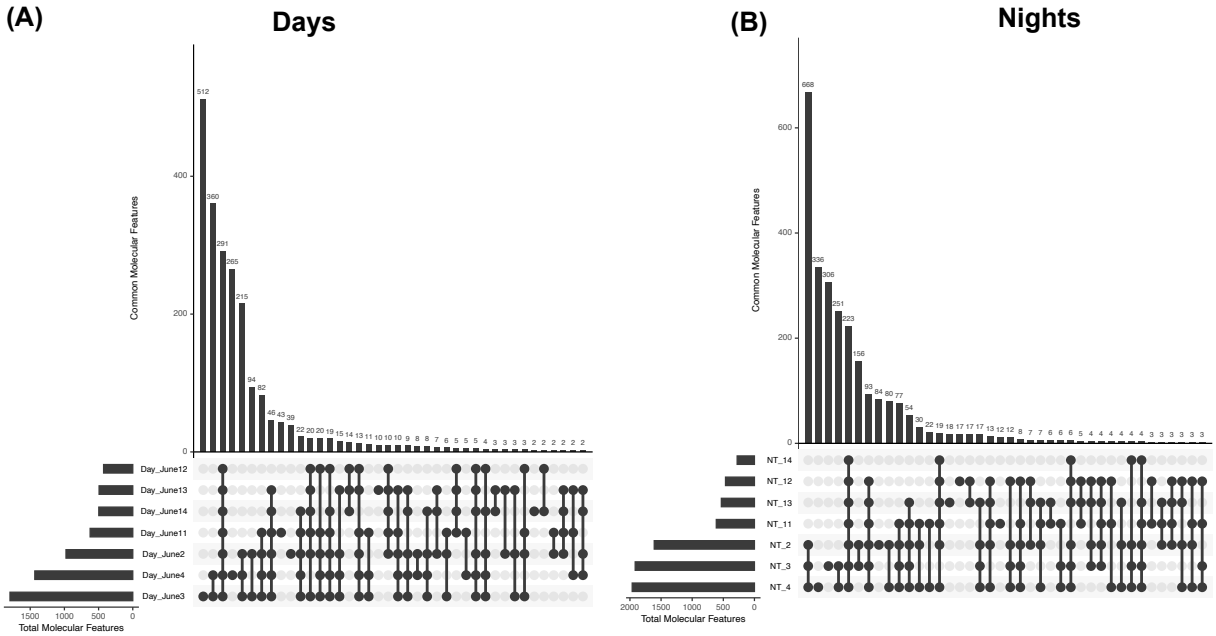

Figure C.11: UpSet plots corresponding to the pool of daytime (A) and nighttime (B) samples.

C.6.3 Organics Distribution across June-ACSM

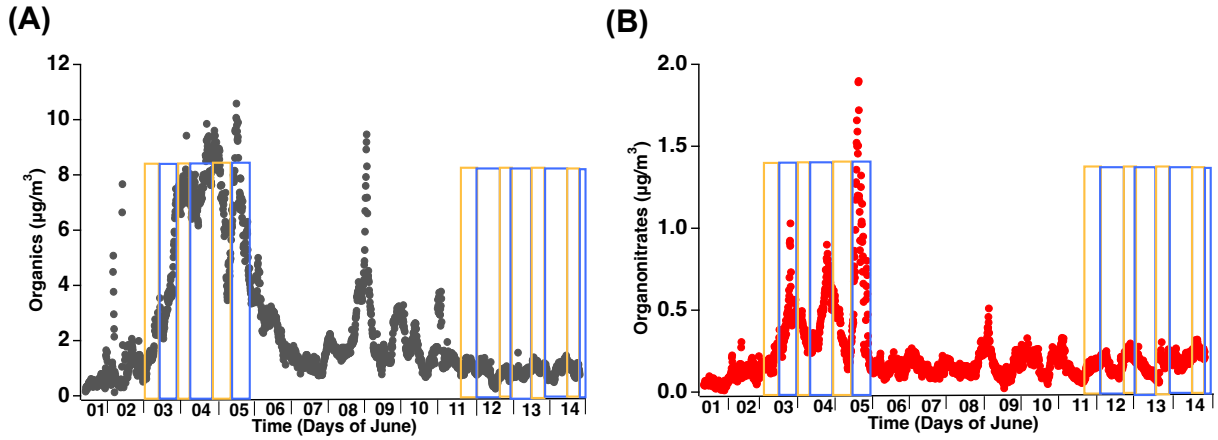

Figure C.12: Results from Aerosol Chemical Speciation Monitor (ACMS) at the S3 site across the sampling periods of June during TRACER-ARM campaign. Main results from June 1 to June 14 2022 demonstrating the distribution of mass concentration of organics (μg.m^{-3}) in (A) and CHNOs (μg.m^{-3}) in (B). The day and night time periods are indicated by yellow and blue colored boxes respectively.

C.6.4 Predicted Parameters for Sampling Periods

Table C.4: List of elemental ratios and predicted parameters for sampling periods across June 2022.

Group	**MF**	**H:C**	**O:C**	**O:N**	**O:S**	**OS_C**	**DBE**	**Average m/z**	
Daytime - June 2									
CHO	555	1.3±0.3	0.5±0.3	-	-	-0.3±0.6	5.8±2.1	0.2±0.2	282±69
CHNO	265	1.3±0.3	0.6±0.2	6.4±2.35	-	-0.6±0.5	5.2±1.5	0.2±0.2	264±68
CHOS	157	1.7±0.3	1.0±0.4	-	7.6±1.8	-0.6±0.6	2.3±1.2	0.3±1.3	270±60
CHNOS	0	-	-	-	-	-	-	-	-
total/average	977	1.5±0.3	0.7±0.7	-	-	-0.6±0.6	4.4±1.6	0.2±0.3	282±69
Nighttime - June 2									
CHO	821	1.3±0.3	0.5±0.2	-	-	-0.3±0.6	6.1±2.2	0.2±0.2	319±99
CHNO	476	1.6±0.2	0.6±0.2	8.2±2.9	-	-0.6±0.4	5.9±1.6	0.1±0.2	334±105
CHOS	225	1.7±0..3	0.98±0.37	-	8.25±2.10	-0.5±0.6	2.7±1.4	0.3±1.4	290±69
CHNOS	88	1.7±0.2	1.03±0.27	10.65±.47	10.65±1.47	-0.7±0.3	3.4±1.0	0.5±1.9	365±56
total/average	1610	1.5±0.2	0.7±0.2	-	-	-0.4±0.4	4.9±1.6	0.2±0.4	327±82
Daytime - June 3									
CHO	996	1.4±0.3	0.5±0.2	-	-	-0.3±0.6	5.8±2.1	0.2±0.2	339±116
CHNO	462	1.4±0.2	0.6±0.2	8.9±3.0	-	-0.5±0.4	5.6±1.5	0.1±0.2	353±110
CHOS	231	1.7 ±0.3	1.0±0.4	-	8.39±2.17	-0.5±0.6	2.7±1.4	0.2±1.1	295±70
CHNOS	107	1.7±0.1	1.0±0.3	11.2±2.0	11.2±2.0	-0.7±0.3	3.6±1.2	0.5±1.8	390±85

Table C.4 continued from previous page

Group	**MF**	**H:C**	**O:C**	**O:N**	**O:S**	**OS_C**	**DBE**	**AImod**	**Average m/z**
total/average	1796	1.5±0.2	0.8±0.3	-	-	-0.5±0.4	4.4±1.6	0.2±0.8	344±95
Nighttime - June 3									
CHO	931	1.4±0.3	0.6±0.2	-	-	-0.2±0.6	5.8±2.1	0.2±0.2	356±120
CHNO	568	1.3±0.3	0.6±0.2	9.2±3.4	-	-0.5±0.3	6.3±1.8	0.2±0.2	359±118
CHOS	296	1.7±0.3	1.0±0.3	-	9.3±2.8	-0.5±0.5	3.0±1.6	0.2±1.0	327±94
CHNOS	121	1.7±0.2	1.0±0.3	11.4±2.0	11.4±2.0	-0.7±0.3	3.7±1.2	0.4±1.7	395±78
total/average	1916	1.5±0.2	0.8±0.3	-	-	-0.5±0.4	4.7±1.7	0.2±0.8	359±103
Daytime- June 4									
CHO	643	1.3±0.3	0.6±0.3	-	-	-0.2±0.6	5.5±2.0	0.2±0.2	289±82
CHNO	222	1.3±0.2	0.7±0.2	7.2±2.1	-	-0.5±0.4	5.3±1.5	0.2±0.2	276±59
CHOS	380	1.7±0.3	0.9±0.3	-	9.2±2.6	-0.5±0.6	3.2±1.6	0.2±1.1	334±90
CHNOS	188	1.7±0.2	1.0±0.3	10.6±2.0	10.6±2.0	-0.8±0.4	3.4±1.3	0.5±1.6	372±77
total/average	1433	1.4±0.2	0.8±.3	-	-	-0.5±0.5	4.3±1.6	0.3±0.8	318±77
Nighttime - June 4									
CHO	1019	1.2±0.3	0.5±0.3	-	-	-0.2±0.5	6.6±22.7	0.3±0.2	309±106
CHNO	454	1.2±0.3	0.6±0.2	7.7±2.9	-	-0.4±0.4	6.5±2.1	0.2±0.2	307±93
CHOS	322	1.6±0.3	1.0±0.3	-	9.2±2.7	-0.4±0.6	3.1±1.7	0.2±1.2	318±87

Table C.4 continued from previous page

Group	**MF**	**H:C**	**O:C**	**O:N**	**O:S**	**OS_C**	**DBE**	**AImod**	**Average m/z**
CHNOS	169	1.7±0.2	1.0±0.3	10.6±2.1	10.6±2.1	-0.7±0.4	3.5±1.2	0.5±1.7	365±74
total/average	1964	1.4±0.3	0.8±0.3	-	-	-0.4±0.5	4.9±1.9	0.3±0.8	325±90
Daytime - June 11									
CHO	451	1.3±0.4	0.5±0.3	-	-	-0.2±0.6	5.9±2.5	0.3±0.2	289±65
CHNO	70	1.2±0.2	0.6±0.2	5.1±1.6	-	-0.6±0.4	4.9±1.4	0.3±0.2	207±43
CHOS	103	1.8±0.3	1.1±0.4	-	7.5±1.7	-0.5±0.6	1.9±0.1.1	0.5±1.6	252±52
CHNOS	0	-	-	-	-	-	-	-	-
total/average	624	1.4±0.3	0.8±0.3	-	-	-0.4±0.5	4.2±1.6	0.3±0.3	249±40
Nighttime - June 11									
CHO	386	1.2±0.3	0.6±0.3	-	-	-	6.0±2.2	0.3±0.2	272±60
CHNO	139	1.2±0.3	0.7±0.2	5.8±2.0	-	-0.5±0.5	5.3±1.6	0.3±0.2	227±53
CHOS	88	1.7±0.3	1.2±0.4	-	7.8±1.4	-0.2±0.6	2.1±1.1	0.7±1.9	249±43
CHNOS	0	-	-	-	-	-	-	-	-
total/average	613	1.4±0.3	0.8±0.3	-	-	-0.2±0.6	4.5±1.6	0.4±0.8	249±52
Daytime - June 12									
CHO	306	1.4±0.3	0.5±0.3	-	-	-0.4±0.7	4.9±1.2	0.2±0.2	278±64
CHNO	25	1.3±0.2	0.6±0.2	4.0±1.3	-	-0.8±0.4	4.1±0.9	0.3±0.2	170±30

Table C.4 continued from previous page

Group	**MF**	**H:C**	**O:C**	**O:N**	**O:S**	**OS_C**	**DBE**	**AImod**	**Average m/z**
CHOS	96	1.8±0.3	1.1±0.4	-	7.0±1.5	-0.6±0.7	1.7±1.0	0.6±1.7	237±45
CHNOS	0	-	-	-	-	-	-	-	-
total/average	427	1.5±0.3	0.7±0.3		-	-0.6±0.6	3.6±1.2	0.3±0.7	228±46
Nighttime - June 12									
CHO	294	1.3±0.3	0.5±0.3	-	-	-0.30±0.75	5.3±1.8	0.3±0.2	268±60
CHNO	82	1.1±0.2	0.6±0.3	4.3±2.1	-	-0.75±0.67	5.2±1.3	0.4±0.3	192±45
CHOS	89	1.7±0.3	1.2±0.4	-	7.2±1.5	-0.6±0.6	2.0±1.1	0.6±1.7	239±46
total/average	465	1.4±0.3	0.8±0.3	-	-	-0.5±0.3	4.1±1.4	0.4±0.3	233±50
Daytime - June 13									
CHO	324	1.3±0.3	0.5±0.3	-	-	-0.3±0.7	5.2±1.9	0.2±0.2	275±63
CHNO	90	1.2±0.2	0.6±0.2	5.0±1.9	-	-0.60±0.5	5.2±1.4	0.3±0.2	210±49
CHOS	79	1.8±0.3	1.1±0.4	-	6.7±1.5	-0.6±0.7	1.7±0.9	0.7±1.8	229±43
total/average	493	1.4±0.3	0.7±0.3	-	-	-0.5±0.6	4.1±1.4	0.4±0.7	238±52
Nighttime - June 13									
CHO	360	1.3±0.3	0.5±0.3	-	-	-0.3±0.8	5.2±1.8	0.3±0.2	278±61
CHNO	91	1.3±0.3	0.6±0.2	5.0±1.9	-	-0.7±0.5	4.7±1.3	0.4±0.3	202±45
CHOS	81	1.7±0.3	1.2±0.4	-	7.5±1.5	-0.4±0.7	2.0±1.1	0.6±1.7	246±42

Table C.4 continued from previous page

Group	**MF**	**H:C**	**O:C**	**O:N**	**O:S**	**OS_C**	**DBE**	**AImod**	**Average m/z**
total/average	532	1.4±0.3	0.8±0.3	-	-	-0.4±0.7	4.0±1.4	0.4±0.7	242±50
Daytime - June 14									
CHO	334	1.3±0.3	0.5±0.3	-	-	-0.3±0.8	5.3±1.9	0.2±0.2	278±62
CHNO	74	1.2±0.2	0.6±0.2	5.0±1.9	-	-0.6±0.5	5.1±1.3	0.3±0.2	204±46
CHOS	89	1.8±0.3	1.1±0.4	-	7.4±1.5	-0.4±0.7	1.9±1.1	0.6±1.7	246±41
total/average	497	1.4±0.2	0.8±0.2	-	-	-0.4±0.5	4.1±1.1	0.4±0.5	243±50
Nighttime - June 14									
CHO	195	1.3±0.3	0.5±0.3	-	-	-0.2±0.7	5.2±1.8	0.3±0.2	273±60
CHNO	13	1.1±0.2	0.6±0.2	3.7±1.3	-	-0.8±0.7	4.7±1.3	0.4±0.3	164±27
CHOS	70	1.7±0.3	1.1±0.4	-	7.2±1.5	-0.5±0.6	2.0±1.1	0.6±1.7	244±41
total/average	278	1.4±0.2	0.7±0.3	-	-	-0.5±0.7	4.0±1.2	0.4±0.6	227±43
Unique to daytime June 3 (subset day-night comparison)									
CHO	184	1.3±0.3	0.3±0.2	-	-	-0.6±0.5	6.8±2.2	0.3±0.2	339±116
CHNO	62	1.6±0.2	0.5±0.2	7.9±2.6	-	-0.9±0.5	5.0±1.8	0.1±0.1	353±110
CHOS	12	1.4±0.2	0.8±0.3	-	8.8±1.5	-0.3±0.5	4.7±1.1	-	295±70
CHNOS	19	1.6±0.1	0.9±0.4	11.6±2.5	11.6±2.5	-0.7±0.5	4.3±1.3	0.1±0.4	390±85
total/average	277	1.5±0.2	0.6±0.2	-	-	-0.7±0.5	5.2±1.6	0.12±0.2	344±95

Table C.4 continued from previous page

Group	**MF**	**H:C**	**O:C**	**O:N**	**O:S**	**OS_C**	**DBE**	**AImod**	**Average m/z**
Unique to nighttime June 3 (subset day-night comparison)									
CHO	119	1.4±0.3	0.70±0.2	-	-	-	6.8±2.7	0.1±0.2	356±120
CHNO	168	1.2±0.3	0.6±0.2	9.3±4.1	-	-0.4±0.4	7.5±1.8	0.3±0.2	359±118
CHOS	77	1.6±0.2	0.9±0.2	-	12.0±2.4	-0.4±0.4	4.2±1.6	-	327±94
CHNOS	33	1.6±0.2	0.9±0.2	12.2±2.0	12.2±2.0	-0.6±0.3	4.1±1.3	0.2±0.9	395±78
total/average	397	1.5±0.3	0.8±0.2	-	-	-0.3±0.4	5.6±1.9	0.1±0.3	359±103
Unique to daytime June 4 (subset day-night comparison)									
CHO	32	1.6±0.3	0.5±0.3	-	-	-0.6±0.6	4.7±2.1	0.1±0.2	289±82
CHNO	8	1.5±0.2	0.8±0.2	9.6±2.0	-	-0.3±0.4	4.6±1.4	-	276±59
CHOS	89	1.7±0.2	0.6±0.1	-	9.5±2.5	-0.9±0.4	3.6±1.6	-	334±90
CHNOS	52	1.7±0.2	0.8±0.3	10.8±2.2	10.8±2.2	-1.0±0.4	3.5±1.6	0.1±0.6	372±77
total/average	181	1.6±0.2	0.7±0.2	-	-	-0.7±0.4	4.1±1.7	0.1±0.2	318±77
Unique to nighttime June 4 (subset day-night comparison)									
CHO	408	1.1±0.3	0.5±0.2	-	-	-0.2±0.5	8.2±2.7	0.4±0.2	309±106
CHNO	240	1.2±0.3	0.6±0.2	8.1±3.4	-	-0.4±0.4	7.5±2.1	0.3±0.3	307±93
CHOS	31	1.5±0.4	1.08±0.3	-	11.1±3.2	-	4.0±2.2	0.1±0.7	318±87
CHNOS	33	1.5±0.2	0.9±0.3	10.9±3.0	10.9±3.0	-0.7±0.5	4.5±1.0	0.1±0.5	365±74

Table C.4 continued from previous page

Group	**MF**	**H:C**	**O:C**	**O:N**	**O:S**	**OS_C**	**DBE**	**AImod**	**Average m/z**
total/average	712	1.3±0.3	0.8±0.3	-	-	-0.3±0.5	6.0±2.0	0.2±0.4	325±90
Unique to daytime June 3 (subset-all daytimes)									
CHO (54%)[a]	278	1.5±0.2	0.5±0.2	-	-	-0.5±0.4	6.6±2.1	0.1±0.1	434±128
CHNO (44%)[a]	223	1.5±0.2	0.6±0.2	10.8±2.7	-	-0.6±0.4	6.2±1.5	-	433±89
Unique to nighttime June 3 (subset-all nighttimes)									
CHO (52%)[b]	160	1.5±0.2	0.6±0.2	-	-	-0.4±0.4	6.4±2.5	0.1±0.1	485±88
CHNO (32%)[b]	98	1.5±0.2	0.7±0.2	13.2±2.7	-	-0.3±0.3	6.8±1.9	-	487±103
Unique to daytime June 4 (subset-all daytimes)									
CHOS (54%)[a]	144	1.6±0.2	0.8±0.3	-	10.4±2.7	-0.6±0.6	4.0±1.6	0.1±1.1	399±81
CHNOS (34%)[a]	91	1.7±0.2	1.0±0.4	10.3±2.1	10.3±2.1	-0.9±0.5	3.3±1.5	0.4±1.4	368±79
Unique to nighttime June 4 (subset-all nighttimes)									
CHO (54%)[b]	181	1.0±0.3	0.4±0.2	-	-	-0.2±0.5	9.1±2.8	0.5±0.2	363±82
CHNO (17%)[b]	56	1.0±0.2	0.5±0.2	6.9±3.1	-	-0.4±0.4	9.2±1.1	0.5±0.19	345±82

[a] Percent representation of MFs from number based subset of MFs in daytime sample pool.
[b] Percent representation of MFs from number based subset of MFs in nighttime sample pool.

C.6.5 Van Krevelen diagrams and Mass Spectra

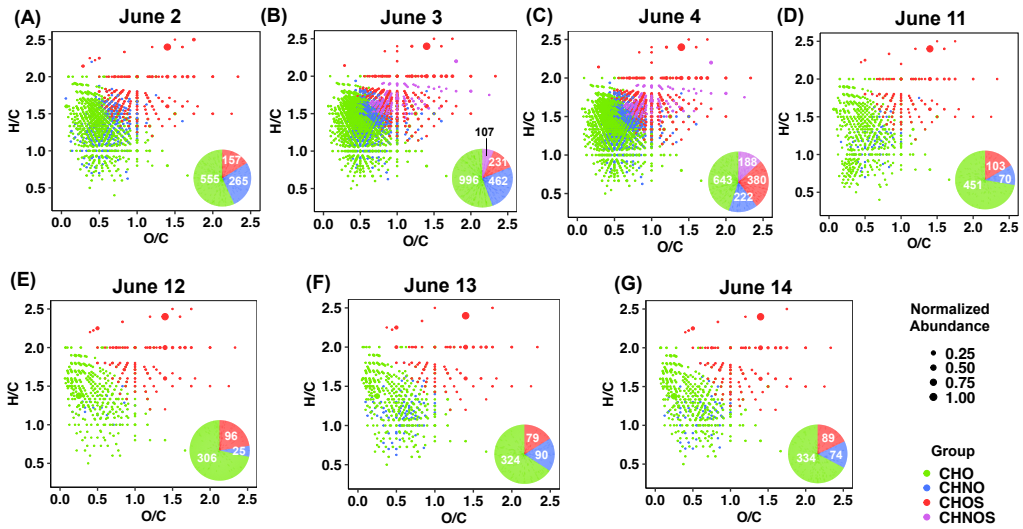

Figure C.13: Van Krevelen diagrams for daytime June Sampling periods (June 2 to June 14). The inset pie chart reflects the number based molecular distribution of functional groups found in each daytime sample.

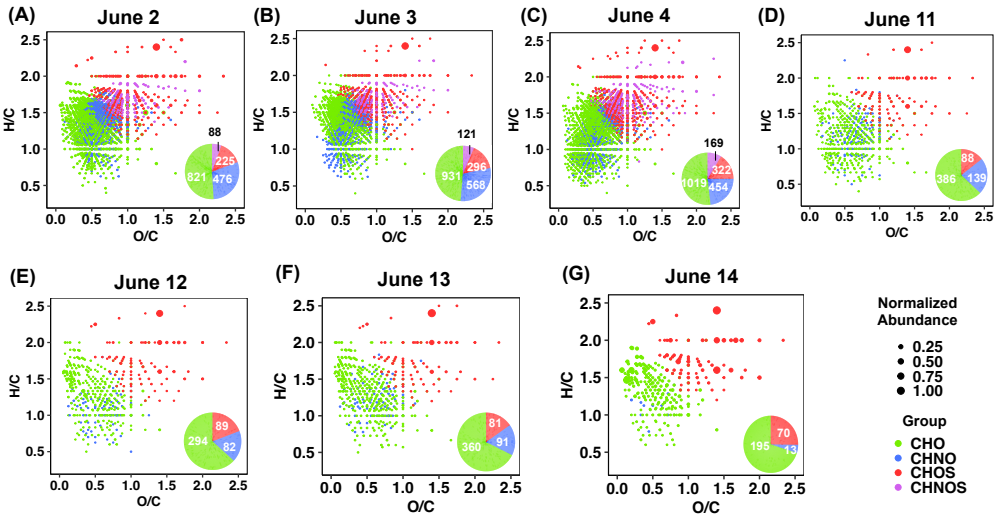

Figure C.14: Van Krevelen diagrams for nighttime June Sampling periods (June 2 to June 14). The inset pie chart reflects the number based molecular distribution of functional groups found in each night time sample.

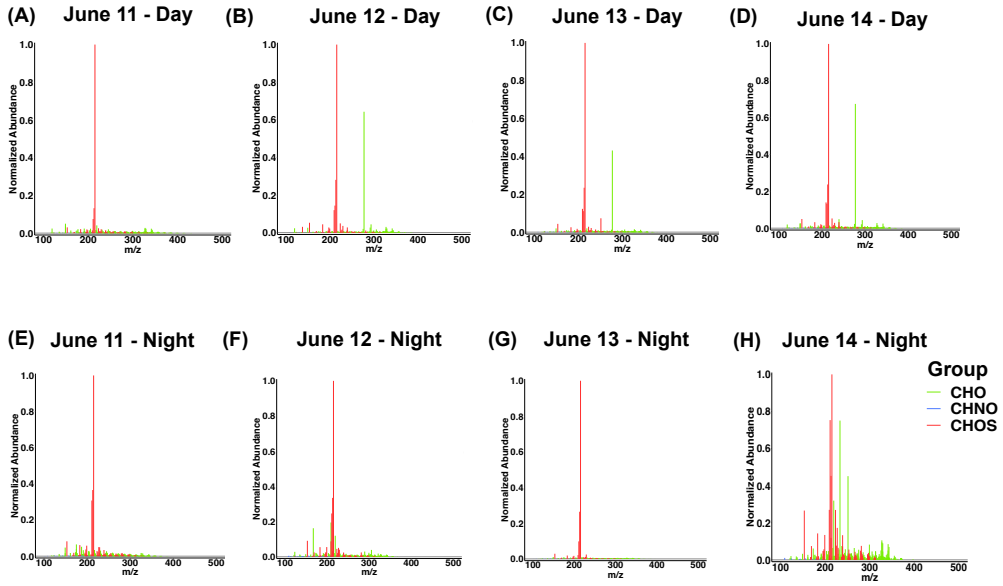

Figure C.15: Mass spectra for daytime and nighttime samples from June 11 (A) and (E), June 12 (B) and (F), June 13 (C) and (G), June 14 (D) and (H) respectively is shown as normalized abundance with respect to mass to charge ratio (m/z).

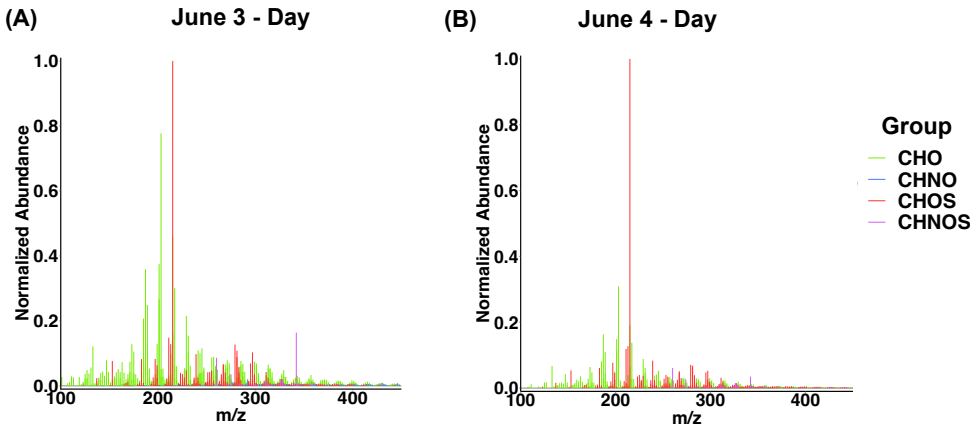

Figure C.16: Mass spectra for two of the daytime sampling periods: June 3 (A) and June 4 (B) are shown. The abundance of observed molecular functional groups is normalized.

C.7 Literature and Experimentally Reported CHOS, CHNOS and CHNO

Table C.5: List of identified CHOS, CHNOS and CHNO during daytime comparison of samples

m/z	Molecular Formula (M)	Reference	Sample	VOC precursor
			CHOS	
152.9864	$C_3H_6O_5S$	a,n	June 2 to June 14	Îś-pinene
194.9968	$C_5H_8O_6S$	a,m	June 2 to June 14	isoprene
197.0125	$C_5H_{10}O_6S$	a,m	June 2 to June 14	isoprene
210.9919	$C_5H_8O_7S$	a,m	June 2 to June 14	isoprene
213.0076	$C_5H_{10}O_7S$	a,m	June 2 to June 14	isoprene
215.0231	$C_5H_{12}O_7S$	a,i,m	June 2 to June 14	isoprene
239.0231	$C_7H_{12}O_7S$	a,b,m	June 2 to June 14	d-limonene,isoprene
223.0282	$C_7H_{12}O_6S$	a,b,m	June 2 to June 14	Îś-pinene
237.0438	$C_8H_{14}O_6S$	a,b,n	June 2 to June 14	Îś-pinene
281.0702	$C_{10}H_{18}O_7S$	a,b	June 2 to June 14	Îś-pinene
251.0596	$C_9H_{16}O_6S$	a,b	June 2 to June 14	d-limonene
265.0388	$C_9H_{14}O_7S$	a,m	June 2 to June 14	isoprene
267.0544	$C_9H_{16}O_7S$	a,b	June 2 to June 14	d-limonene, Decalin/cyclodecane
279.0546	$C_{10}H_{16}O_7S$	a,b	June 2 to June 14	d-limonene
281.0702	$C_{10}H_{18}O_7S$	a,b,m	June 2 to June 14	d-limonene,Îś-terpinene,Îś-pinene
311.0442	$C_{10}H_{16}O_9S$	a,b	June 2 to June 14	Decalin

Table C.5 continued from previous page

m/z	Molecular Formula (M)	Reference	Sample	VOC precursor
211.0645	$C_7H_{16}O_5S$	b,f	June 4	unknown
363.1483	$C_{16}H_{28}O_7S$	h	June 4	Sesquiterpene
423.0964	$C_{16}H_{24}O_{11}S$	a,b	June 4	d-limonene, Observed in cloud water samples
441.1070	$C_{16}H_{26}O_{12}S$	a,b	June 4	d-limonene, Observed in cloud water samples
457.1022	$C_{16}H_{26}O_{13}S$	a,b	June 4	d-limonene, Observed in cloud water samples
439.1278	$C_{17}H_{28}O_{11}S$	a,b	June 4	d-limonene, Observed in cloud water samples
455.1228	$C_{17}H_{28}O_{12}S$	a,b	June 4	d-limonene, Observed in cloud water samples
469.1020	$C_{17}H_{26}O_{13}S$	a,b	June 4	d-limonene, Observed in cloud water samples
471.1175	$C_{17}H_{28}O_{13}S$	a,b	June 4	d-limonene, Observed in cloud water samples
451.1280	$C_{18}H_{28}O_{11}S$	a,b	June 4	d-limonene, Observed in cloud water samples
465.1072	$C_{18}H_{26}O_{12}S$	a,b	June 4	d-limonene, Observed in cloud water samples
467.1231	$C_{18}H_{28}O_{12}S$	a,b	June 4	d-limonene, Observed in cloud water samples
			CHNOS	
294.0653	$C_{10}H_{17}NO_7S$	b,c,f,a	June 3 and 4	Îś-pinene, observed in rain water samples
342.0502	$C_{10}H_{17}NO_{10}S$	b,c,a	June 3 and 4	Îś/Îš-Pinene, Îś/Îş-Terpinene, observed in rain water samples
312.0759	$C_{10}H_{19}NO_8S$	b,d,a	June 3 and 4	unknown
300.0760	$C_9H_{19}NO_8S$	b,e,a	June 4	possibly monoterpenes

Table C.5 continued from previous page

m/z	Molecular Formula (M)	Reference	Sample	VOC precursor
			CHNO	
220.0462	$C_7H_{11}NO_7$	b,g,a,k	June 3	Îś-pinene, d-limonene
194.0459	$C_9H_9NO_4$	a,l	June 3	cellulose Salicylamide acetic acid
230.0670	$C_9H_{13}NO_6$	b,g,a,k	June 3 and 4	Îś-pinene, d-limonene
246.0619	$C_9H_{13}NO_7$	b.g,a	June 3 and 4	Îś-pinene, monoterpenes
406.1355	$C_{16}H_{25}NO_{11}$	b,g,a	June 3	Îś-pinene
418.1357	$C_{17}H_{25}NO_{11}$	b,g,a	June 3	Îś-pinene
436.1460	$C_{17}H_{27}NO_{12}$	b,g,a	June 3	Îś-pinene
432.1511	$C_{18}H_{27}NO_{11}$	b,g,a	June 3	Îś-pinene
464.1047	$C_{17}H_{23}NO_{14}$	a,k	June 3	d-limonene
504.1360	$C_{20}H_{27}NO_{14}$	a,k	June 3	d-limonene
520.1310	$C_{20}H_{27}NO_{15}$	a,k	June 3	d-limonene

[a] this study [b] Cook et al[501] [c] Alteiri et al[61] [d] Stone et al[424] [e] Ning et al[432] [f] Cai et al[613] [g] Sun et al[614] [h] Pratt et al[409] [i] Surratt et al 2007 and Surratt et al 2008[56, 615] [j] Chan et al 2007[485] [k] Faxon et al 2007[505] [l] Kong et al 2007[616] [m] Huang et al 2007[506] [n] Ma et al 2007[422]

C.8 Measurements for Cloud Formation

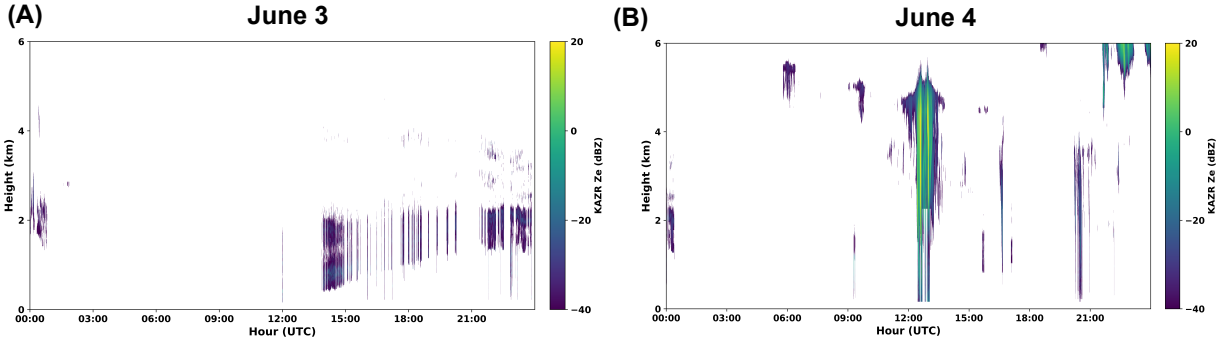

Figure C.17: Doppler-lidar measurements for daytime periods of (A) June 3 and (B) June 4. Scattered cloud was observed for June 3 and convective cloud event was observed for June 4.[617, 618]